

AD-A166 699

COAST OF CALIFORNIA STORM AND TIDAL WAVES STUDY
SOUTHERN CALIFORNIA COAST. (U) ARMY ENGINEER DISTRICT
LOS ANGELES CA COASTAL RESOURCES BRANC

1/7

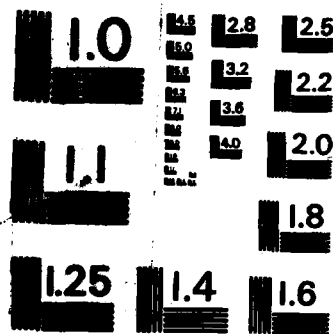
UNCLASSIFIED

D L INMAN ET AL. FEB 86 CCSTWS-86-1

F/G 8/3

NL





MICROCOPY RESOLUTION TEST CHART
NATIONAL BUREAU OF STANDARDS - 1963 - A



US Army Corps
of Engineers
Los Angeles District

COAST OF CALIFORNIA
STORM AND TIDAL WAVES STUDY

11

SOUTHERN CALIFORNIA COASTAL PROCESSES DATA SUMMARY

DTIC
ELECTE
APR 10 1986
S D

AD-A166 699

DTIC FILE COPY



Approved for public release
Distribution Unlimited

CCSTWS 86-1
February 1986

86 4 14 049

region, not a review of the nearshore processes literature. Interested readers should consult the extensive coastal engineering and nearshore processes literature for a historical perspective of the topics discussed. Because of space constraints, some topics are only scantily covered.

REPORT DOCUMENTATION PAGE		READ INSTRUCTIONS BEFORE COMPLETING FORM
1. REPORT NUMBER CCSTWS 86-1	2. GOVT ACCESSION NO. AD-A166 697	3. RECIPIENT'S CATALOG NUMBER
4. TITLE (and Subtitle) SOUTHERN CALIFORNIA COASTAL PROCESSES DATA SUMMARY		5. TYPE OF REPORT & PERIOD COVERED
		6. PERFORMING ORG. REPORT NUMBER
7. AUTHOR(s) INMAN, D.L., R.T. GUZA, D.W. SKELLY, T.E. WHITE		8. CONTRACT OR GRANT NUMBER(s)
9. PERFORMING ORGANIZATION NAME AND ADDRESS JAYKIM ENGINEERS		10. PROGRAM ELEMENT, PROJECT, TASK AREA & WORK UNIT NUMBERS
11. CONTROLLING OFFICE NAME AND ADDRESS COASTAL RESOURCES BRANCH/PLANNING DIVISION LOS ANGELES DISTRICT, COE P.O. BOX 2711, LA. CA. 90053		12. REPORT DATE FEBRUARY 1986
14. MONITORING AGENCY NAME & ADDRESS (if different from Controlling Office)		13. NUMBER OF PAGES
		15. SECURITY CLASS. (of this report) UNCLASSIFIED
		15a. DECLASSIFICATION/DOWNGRADING SCHEDULE
16. DISTRIBUTION STATEMENT (of this Report) Approved for public release; distribution unlimited		
17. DISTRIBUTION STATEMENT (of the abstract entered in Block 20, if different from Report)		
18. SUPPLEMENTARY NOTES Copies obtainable from the National Technical Information Service, Springfield, VA. 22151		
19. KEY WORDS (Continue on reverse side if necessary and identify by block number) Coast of California Storm and Tidal Wave Study, Coastal Processes		
20. ABSTRACT (Continue on reverse side if necessary and identify by block number) The intent of this report is to provide a broad picture of the physical, mechanical and geological processes pertaining to coastal engineering along the shorelines of southern California, and to give references to data sources. The references were selected predominantly on the basis of perceived direct engineering application to the study area. Space and time constraints did not allow a review of the engineering and/or scientific background necessary to fully interpret the data presented. Citation to the originators of concepts, theories, etc. are not always given because this is a data summary for the		

**SOUTHERN CALIFORNIA
COASTAL PROCESSES DATA SUMMARY
Ref. No. CCSTWS 86-1**

Coast of California Storm and Tidal Waves Study

**U.S. Army Corps of Engineers
Los Angeles District, Planning Division
Coastal Resources Branch
P.O. Box 2711
Los Angeles, California 90053**

FEBRUARY 1986

prepared by

**Jaykim Engineers
Douglas L. Inman
Robert T. Guza
David W. Skelly
Thomas E. White**

CONTENTS

Purpose of Report

Acknowledgements

1. PHYSIOGRAPHY AND REGIONAL DESCRIPTION 2

1.1 Geologic Setting 2

- Plate tectonics 3
- Seismicity 5
- Sea-level change and paleoclimate 5

1.2 Littoral Cells 8

- Big Sur Group of Cells 11
- Santa Maria Cell 11
- Santa Barbara Cell 13
- Santa Monica Cell 14
- San Pedro Cell 14
- Oceanside Cell 15
- Mission Bay - Sub-Cell 15
- Silver Strand Cell 16

2. COASTAL PROCESSES (General for Southern California) 18

2.1 Wave-cut Terraces and Sea Cliffs 18

2.2 Formation of Beaches 18

2.3 Beach Cycles 24

2.4 Littoral Transport 27

- Instantaneous longshore transport 28
- Rhythmic beach forms and cusps 31

2.5 Sediment Transport by Rivers and Streams 37

- Erosion-rate method 38
- Sediment rating curves 38
- Total load transport 39

2.6 Transport by wind 43

2.7 Weather, Waves and Extreme Events 45

- El Nino/Southern Oscillation 50
- Climate 52



Accession For	
NTIS	CRA&I <input checked="" type="checkbox"/>
DTIC	TAB <input type="checkbox"/>
Unannounced <input type="checkbox"/>	
Justification	
By _____	
Distribution/	
Availability Codes	
Dist A-1	Avail and/or Special 1

- Historical storm tracks	52
- Episodicity and the budget of sediment	55
3. REGIONAL OCEANOGRAPHY	57
3.1 Shelf Currents	57
3.1.1 - Brief description of major, large-scale coastal currents (i.e. California, Davidsen, etc.)	
3.1.2 - Fluctuating (tidal and wind driven) currents	
3.2 Deepwater waves (unsheltered by islands)	77
3.2.1 - Generation by tropical and northern and southern hemisphere storms.	77
3.2.2 - Wave climate; data sources, statistics, and measurements	85
3.2.3 - Recent Storms	123
3.3 Coastal Waves and Associated Currents	128
3.3.1 - General patterns of spatial variability including effects of island sheltering.	128
3.3.2 - Wave climate: Data sources (ongoing measurements, historical data, and hindcasts)	
3.3.3 - Generation of longshore currents by incident wind waves (general discussion of principals)	145
3.3.4 - Infragravity and other long waves (periods < 12 hours)	152
3.4 Astronomical Tides and other Sea Level Fluctuations	159
3.4.1 - General description of tidal patterns (ranges, extreme and other tidal statistics)	159
3.4.2 - Extreme elevations	169
- Storm surge	171
- Tsunamis	178
3.4.3 - Interannual effects	183
3.4.4 - Long-term sea level changes	184
4. BIG SUR GROUP OF LITTORAL CELLS	189

4.0 Introduction (description of cell, previous studies)	
4.1 Coastal Erosion Problems	189
- Natural	
- Man Made	
4.2 Shoreline Changes	191
- Patterns, short-term and seasonal, long-term	
- Existing surveys, mapping studies, aerial photographs (Table 4.2-1)	
4.3 Nearshore Waves	192
- Transformation of deep water waves to the nearshore	
- Local sea wave generation	
- Summary of available data	
4.4 Nearshore Currents	200
- Wave driven currents	
- Wind driven currents	
- Tidal currents	
4.5 Sediment Sources	204
4.5.1 Cliff erosion and relict dunes	
- Case studies, petrology and grain size	
- Average and episodic input rates	
4.5.2 Sediment discharge from rivers and streams	
- Drainage basin and areas	
- Sediment types	
- Gaging stations, sediment discharge estimates	
- Impact of sand and gravel mining	
4.5.3 Artificial beach nourishment	
- Nourishment projects	
- Source material and size matching	
4.6 Sediment Transport Modes	206
4.6.1 Cross-shore transport	206
- Case studies	
- Trends and seasonal patterns	

- Long-term losses and gains	
4.6.2 Longshore transport	206
- Case studies (measured vs. wave potential)	
- Trends and seasonal patterns (up and down-coast)	
- Wind wave transport vs. swell	
4.6.3 Wind Transport	206
- Augmenting and opposing longshore transport	
4.7 Sediment Sinks	208
4.7.1 Submarine canyons	208
- Case studies, average and episodic rates of loss	
4.7.2 Entrapment by harbors, bays and estuaries	208
- Case studies, average and episodic rates	
- Dredging and bypassing	
4.7.3 Littoral Barriers	210
- Headlands, groins, jetties, breakwaters and inlets	
- Average and episodic rates	
4.7.4 Wind Transport	210
- Dunes and transport paths	
- Case studies and rates	
4.7.5 Berm Overwash and Offshore Loss	210
- Estimates and potential rates	
4.8 Budget of Sediment	210
- Case studies	
- Summary of: (4.5) sources; (4.6) transport paths; and (4.7) sinks. Budget of sediment.	
5. SANTA MARIA LITTORAL CELL*	212
6. SANTA BARBARA LITTORAL CELL*	232
7. SANTA MONICA LITTORAL CELL (incl. Dume Sub-Cells)*	303
8. SAN PEDRO LITTORAL CELL (incl. Palos Verde Sub-Cells)*	313

9. OCEANSIDE LITTORAL CELL (incl. Laguna Sub-Cells)*	378
10. MISSION BAY LITTORAL SUB-CELL*	468
11. SILVER STRAND LITTORAL CELL*	499
12. REFERENCES	538

* Subsections .0 through .8 listed under Chapter 4 also apply to Chapters 5 through 11.

ACKNOWLEDGEMENT

↓
The intent of this report is to provide a broad picture of the physical, mechanical and geological processes pertaining to coastal engineering along the shorelines of southern California. and to give references to data sources. The references were selected predominantly on the basis of perceived direct engineering application to the study area. Space and time constraints did not allow a review of the engineering and/or scientific background necessary to fully interpret the data presented. ↘ Citation to the originators of concepts, theories, etc. are not always given because this is a data summary for the region, not a review of the nearshore processes literature. Interested readers should consult the extensive coastal engineering and nearshore processes literature for a historical perspective of the topics discussed. Because of space constraints, some topics are only scantily covered.

Chapters 1 and 2 and portions of the following chapters were written by Douglas L. Inman. Chapter 3 and the sections on nearshore waves and currents for each cell described in Chapters 4 through 11 were written by Robert T. Guza. For Chapters 4 through 11 the sections on coastal erosion, shoreline changes, sediment sources and the budget of sediment were written by David W. Skelly; while the sections on sediment transport modes and sediment sinks were written by Thomas E. White. Unpublished notes provided by Dr. Reinhard Flick were used for the preparation of Chapter 3.4 on tides and sea level fluctuations. Barbara Pinkston and Joan Semler typed the manuscript. ↑

1. PHYSIOGRAPHY AND REGIONAL DESCRIPTION

The present physiography of the coast of California is the result of coastal processes modifying a continental margin that has been subject to complex tectonic motions, large sea level changes, and significant fluctuations in climate. The continuing movements of the earth's plates and continents gradually modify the position of land and water on time scales of millennia and longer. The present relatively long stillstand in sea level has produced coastlines that are unique in this millenium and probably for the entire Pleistocene Epoch. The sea level has been relatively high during the past 3 to 6 thousand years, accentuating the broad shelves carved into the continental platform during this and previous high stands. As a consequence, stream valleys cut at lower sea level are filling, streams near the coast are "at grade," and coastlines in their present natural state typically have long continuous beaches of sand (Inman, 1983).

1.1 *Geologic Setting*

A number of worldwide geological phenomena have a fundamental bearing on the morphology and present configuration of the world's coastal zones. The most important of these are plate tectonics, climate, sea level, and the adjustment of the earth to changes in the distribution of masses of ice and water. The movement of oceanic plates and adjacent continental mass determines the type of coast and its exposure to waves and currents. While worldwide climate affects marine and terrestrial organisms and terrestrial erosion, its principal coastal impact is on sea level. Sea level determines the position of the coastline.

Summaries of the physiography and geology of coastal southern California are given in Inman (1954), Oakeshott (1971), Ernst (1981), Inman (1983), and Inman and Jenkins (1983).

Plate Tectonics

The west coasts of the Americas are collision coasts. Collision coasts are those that occur along a plate margin where the two plates are in collision or impinging upon each other (Figure 1.1-1). Tectonically this is an area of crustal compression and consumption. These coasts are characterized by narrow continental shelves bordered by deep basins and ocean trenches. Submarine canyons cut across the narrow shelves and enter deep water. The shore is often rugged and backed by sea cliffs and coastal mountain ranges, and earthquakes and volcanism are common. The sea cliffs and mountains often contain elevated sea terraces representing former relations between the level of the sea and the land. Typical examples of collision coasts include the western coasts of North, South and Central America (Inman and Nordstrom, 1971).

In contrast, the eastern coasts of North and South America are examples of mature trailing-edge coasts that occur on the "trailing-edge" of a land mass that moves with the plate and are thus situated upon the stable portion of the plate away from the plate margins (Figure 1.1-1). These coasts typically have broad continental shelves that slope into deeper water without a bordering trench. The coastal plain is also typically wide and low-lying and usually contains lagoons and barrier islands as on the east coasts of the Americas.

Southern California tectonics is complex because the spreading center has passed the southern California coastline and is now in the Gulf of California. The Gulf of California spreading center is joined to the Gorda spreading center (off Eureka, California) by the San Andreas transform fault. Yet because of the Markovian nature of geological processes (i.e. their present manifestation depend upon past events), the California coast still retains most of the attributes of a collision coast - narrow shelves cut by submarine canyons, offshore residual trench, coastal mountains and uplifted coastal terraces - all remnants from its tectonic history as a collision coast. Accordingly, the west coast of the United States is a "California-type" collision coast (Dickinson, 1981; Inman, 1983).

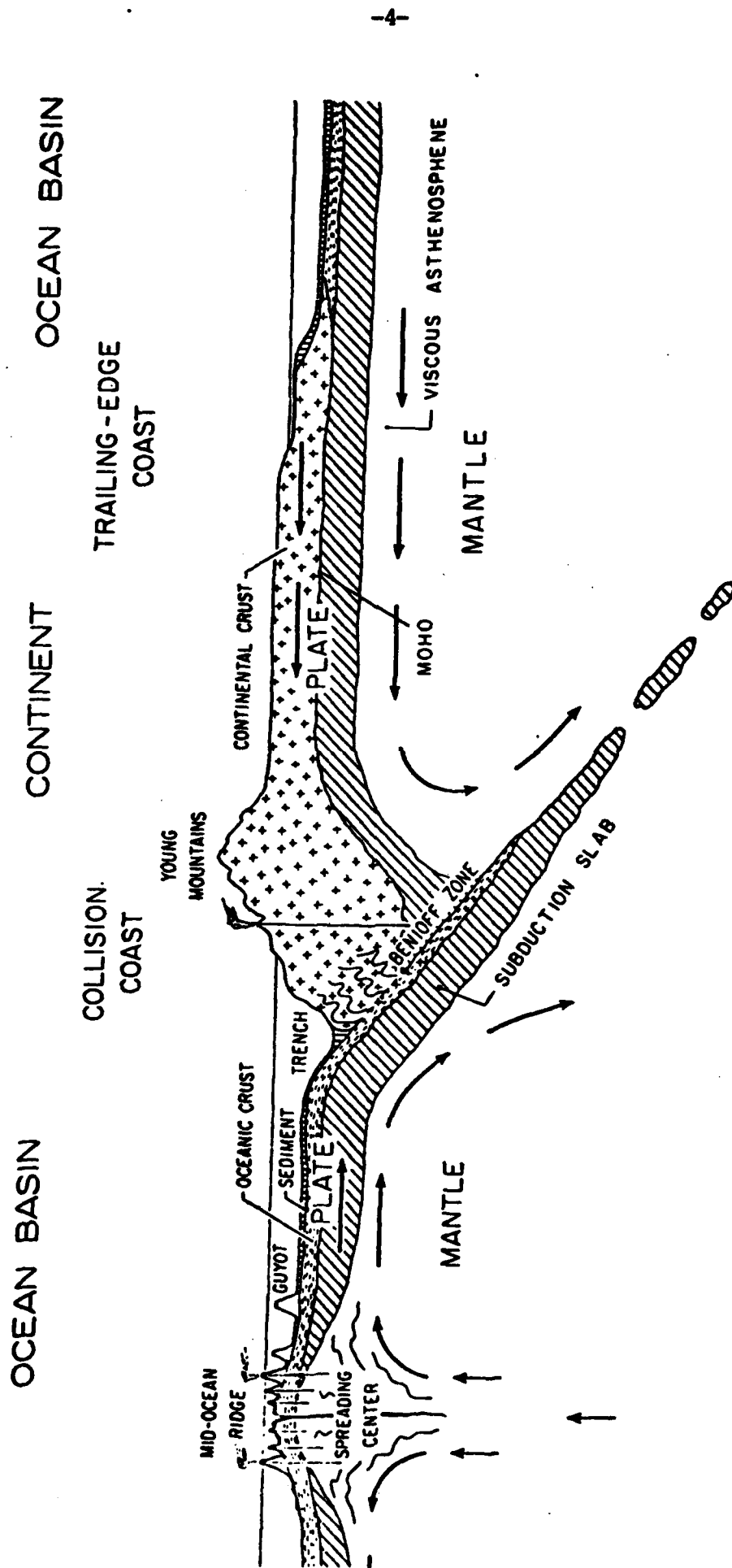


Figure 1.1-1. Schematic illustration of the formation of a collision coast and a trailing-edge coast. New crust is formed at the mid-ocean ridge, while crust is consumed in the subduction zone (Benioff Zone) where it plunges into the mantle. Arrows indicate direction of relative motion. Representative of section from the East Pacific Rise (spreading center) through the Peru-Chile trench off South America at 35° South Latitude (from Inman and Nordstrom, 1971).

It is important to note that in the long term geologic sense, collision coasts are erosional while trailing-edge coasts are depositional. However, as we shall see, both types of coast may be erosional during rising sea level and during long periods of relative still-stand in sea level.

Seismicity

Coastal California has a complicated structural setting that includes plate collision followed by continental over-riding of the spreading center, and the development of transform faulting. The combination of plate collision and transform faulting led to the complex wrench-fault structure of the continental borderland. This results in a variety of geologic structures and faults that are seismically active (e.g. Crouch, 1981; Hagstrum, et al., 1985).

The seismicity occurs in three major swarms of epicenters (Figure 1.1-2). The largest swarm covers the Long Beach, Los Angeles, Santa Monica area. Next in size is one near Santa Barbara, and the third is in the Santa Monica Mountains extending along the coast from Point Dume to Point Mugu. However, it should be noted that earthquake centers of various magnitudes occur throughout southern California and the Continental Borderland (e.g. Hileman et al, 1973; Legg, 1980).

Sea-Level Change and Paleoclimate

A generalized sea-level curve applicable to the coast of southern California over the past 40,000 years is shown in Figure 1.1-3. Sea level rose rapidly about 1 m per century from about 16,000 years BP (before present) to about 6,000 years BP, followed by a more gradual rise of about 10 cm per century from 6,000 BP to the present. The "generalized" sea-level curve in Figure 1.1-3 is typical for the central and southern coasts of the United States, Gulfs of Mexico and California, the Netherlands, the north of France, and southeastern Australia (e.g. Bloom, 1977).

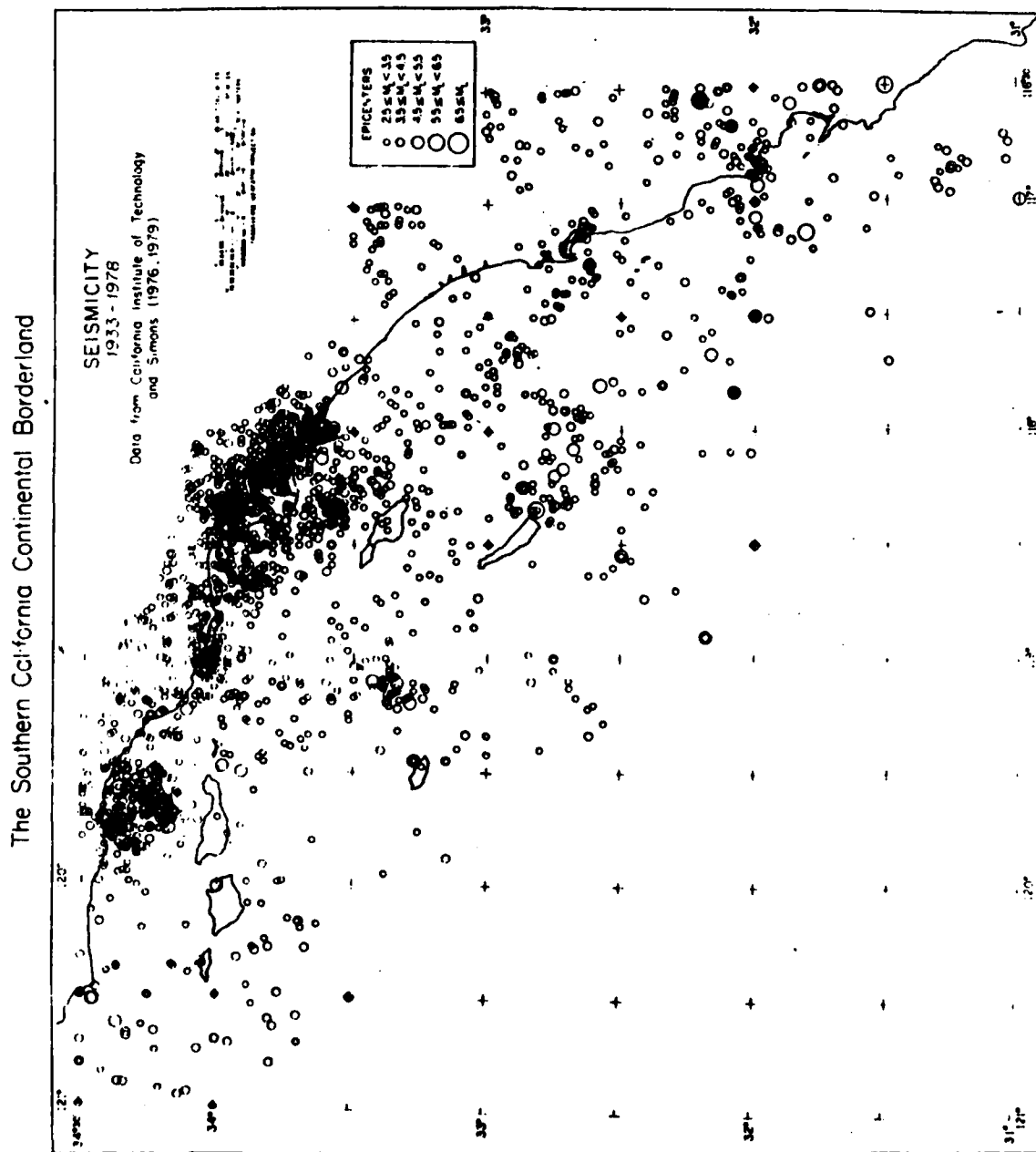


Figure 1.1-2. Distribution of earthquake epicenters in southern California and the continental borderland. Data from California Institute of Technology, catalog of earthquakes, modified from Simons (1977; 1979) and Legg (1980).

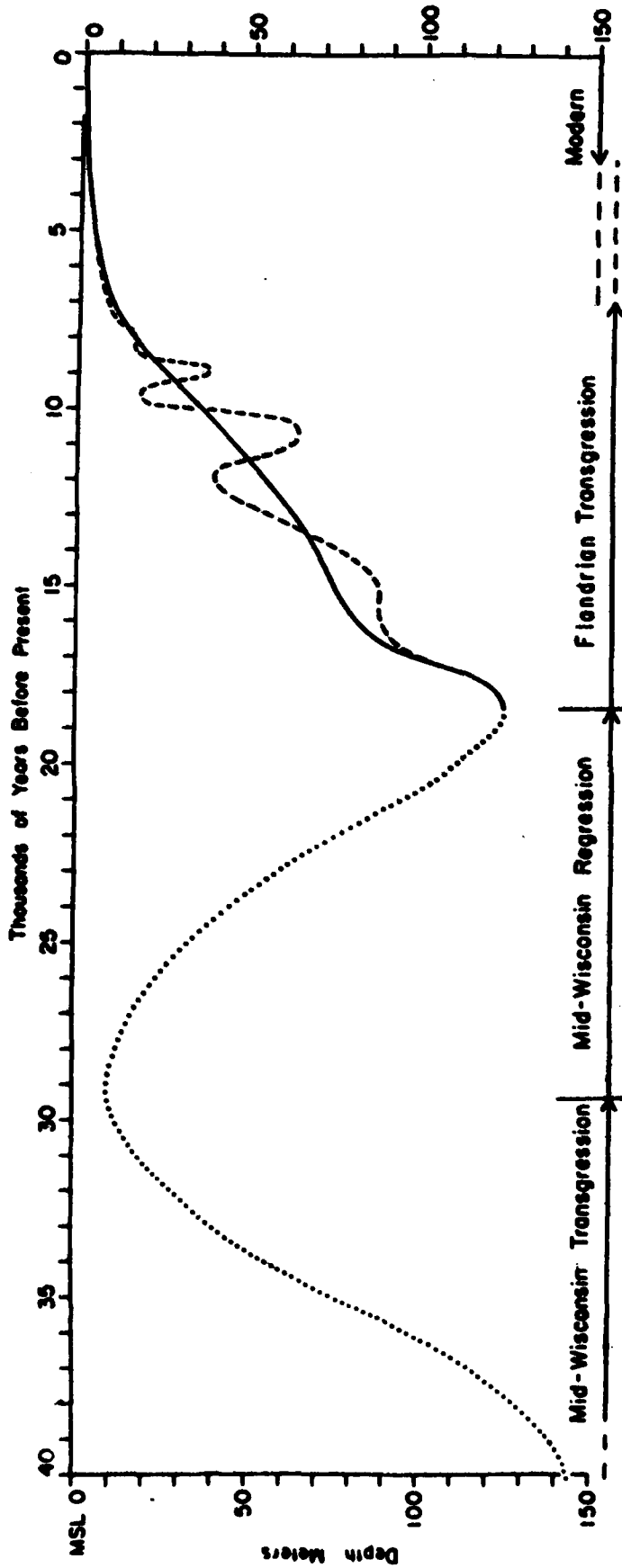


Figure 1.1-3. Late Quaternary fluctuations in sea level. Solid line is the "generalized" sea level curve (from Curray, 1965); dashed line is detailed curve for northwestern Gulf of Mexico (from Curray, 1960; 1961).

In passing, it should be noted that tide gauge records show that sea level is still rising on a worldwide basis at a rate of about 23 cm (3/4 ft) per century since the early 1900's (Barnett, 1984). Using the eigenmodes in a covariance analysis of tide gage records Barnett (1984) finds a rise in sea level of 17.4 cm (0.57 ft) per century at La Jolla (Scripps Pier), 23.5 cm (0.77 ft) per century at Santa Monica, and an anomalously low value of 4.6 cm (0.15 ft) per century at Los Angeles (also see Hicks, 1981; Hicks et al., 1983). There is the distinct possibility of an increased rate of rise due to the greenhouse effect of carbon dioxide released by man in coming years (e.g. Emery, 1980). This continuing rise in sea level increases sea cliff erosion and produces a gradual retreat of beaches in California and on a worldwide basis.

1.2 LITTORAL CELLS

A littoral cell is a coastal compartment or physiographic unit that contains a complete cycle of littoral sedimentation including sources, transport paths and sediment sinks. Within a littoral cell the principle of the conservation of mass may be applied to the evaluation and interpretation of coastal sedimentation. The procedure, sometimes referred to as the "budget of sediment", consists of assessing the sedimentary contributions (credits) and losses (debits) and equating these to the net gain or loss (balance) of sediment within a given coastal segment (Inman and Chamberlain, 1960; Inman and Frautschy, 1965; Inman and Brush, 1973).

In general, a littoral cell is a large, continuous coastal segment that includes the sediment source areas, usually drainage basins, and the sediment transport paths, usually rivers, beaches and submarine canyons. There is generally little transport of sediment from cell to cell. Some large cells may contain a number of pronounced physiographic features, such as headlands, that constitute logical boundaries for sediment balance within the cell. In this case the subdivisions of the cell are referred to as "sub-cells". Also, each pocket and crescent beach separated by headlands is a sub-cell. Significant transports of sediment may occur between sub-cells.

The concept of the littoral cell and its budget of sediment was based on four cells in southern California that had rivers as sources, beaches as transport paths and submarine canyons as sinks. These were the Santa Barbara, Santa Monica, San Pedro and Oceanside Littoral Cells (Inman and Chamberlain, 1960; Inman and Frautschy, 1965). The concept was extended to include cells with other kinds of sinks, such as the Silver Strand Cell with offshore deposition from an ebb tide jet (Inman et al., 1974), deposition in offshore shoals such as Diamond Shoal off Cape Hatteras (Inman, 1985a) and in dune fields (Bowen and Inman, 1966). The Nile Littoral cell in the eastern Mediterranean is the largest cell studied in detail (Inman and Jenkins, 1984).

Determination of the boundaries of littoral cells requires identification of the sediment sources, transport paths and sinks, and assessment of the budget of sediment within the cell. In cases where the boundaries of littoral cells have not been established, it is convenient to refer to the coastal segment in question as a "group of cells" if it is large and appears to contain more than one cell. The "Big Sur Group of Cells" that extend from Point Lobos to Point Buchon is an example (Figure 1.2-1). If the coastal segment is small and consists principally of "pocket" beaches, as off headlands, it is referred to as a group of sub-cells or simply as "sub-cells". Examples in this study are the Dume, Palos Verde and Laguna Sub-Cells. A useful graphic summary of littoral transport paths along the California coast and of possible cell boundaries is found in the "Assessment and Atlas of Shoreline Erosion Along the California Coast" (California, 1977a).

For purposes of this study, the coast of southern California is divided into eleven segments consisting of one "group" of littoral cells, six littoral cells and four groups of sub-cells. The cells from Point Lobos to Point Buchon are grouped into a single "Big Sur Group of Cells" because of the limited information available for defining individual cells within the group. Ragged Point (3 mi. south of the Monterey-San Luis Obispo County line) which is the northern boundary of this

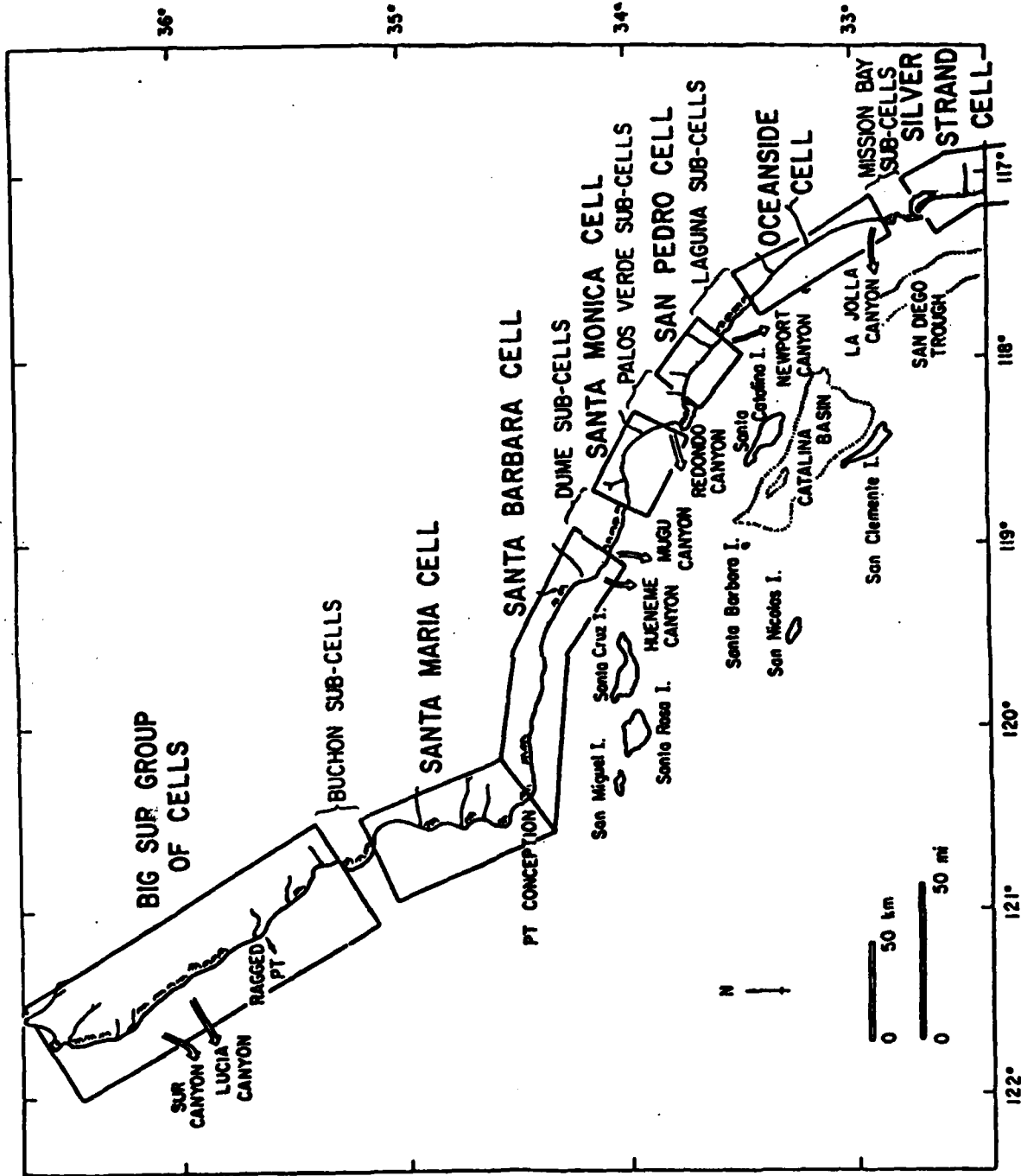


Figure 1.2-1. Littoral cells and sub-cells in southern California. See Table 1.2-1 for coastal length and chapter.

study is the center of this group of cells (Figure 1.2-1). The six littoral cells include Santa Maria, Santa Barbara, Santa Monica, San Pedro, Oceanside and Silver Strand. The four groups of sub-cells, Dume, Palos Verde, Laguna and Mission Bay are mostly associated with pocket beaches along rocky headlands. In this report, except for Mission Bay Sub-Cell, all their descriptions are included as part of an "extended," down-coast, littoral cell: Santa Monica, San Pedro and Oceanside Cells respectively (compare Figure 1.2-1 and Table 1.2-1). This subdivision of the coast of southern California provides for a continuous, uninterrupted series of sub-cells, cells and extended cells without the problem of having coastal gaps in coverage or of having separate general descriptions for the many sub-cells.

Big Sur Group of Cells

This is a poorly defined group of cells and sub-cells extending from Point Lobos south of Carmel to Point Buchon, a distance of 133 miles, 55 of which are south of Ragged Point, the northern boundary of this review. This is the rugged, picturesque, mountainous coastline of the Big Sur country of California. It consists mostly of rocky coast with pocket beaches and a few crescent beaches. The number and size of beaches gradually increase to the south. The nine miles of beach along Estero Bay, six miles of which is the Morro Bay sand spit, is the longest sandy coastline in the group. The 55 miles of coast from Ragged Point to Point Buchon was designated as the Morro Bay Cell in the Assessment and Atlas of Shoreline Erosion (California 1977a).

Santa Maria Cell

Including the Buchon Sub-Cell, this littoral cell extends for 82 miles from Point Buchon to Point Conception. It was first studied in detail by Bowen and Inman (1966). For purposes of balancing the budget of sand, they divided the cell into four sub-cells based on the natural headlands of Point Sal, Purisima Point, Point Arguello and Point Conception. With the

TABLE 1.2-1. Littoral Cells and Groups of Sub-Cells in southern California
(north to south)

	<u>Length (miles)</u>	<u>Chapter</u>
<u>Big Sur Group of Cells:</u> Pt. Lobos - Pt. Buchon (including Pt. Sur, Big Sur, Partington, Ragged Pt., San Simeon, Estero Bay)	133	4
<u>Santa Maria Cell:</u> Pt. San Luis - Pt. Conception (extended cell includes Buchon Sub-Cells: Pt. Buchon - Pt. San Luis)	68 <u>14</u> 82	5
<u>Santa Barbara Cell:</u> Pt. Conception - Pt. Mugu	96	6
<u>Santa Monica Cell:</u> Pt. Dume - Palos Verdes Pt. (extended cell includes Dume Sub-Cells: Pt. Mugu-Pt. Dume)	40 <u>9</u> 49	7
<u>San Pedro Cell:</u> Pt. Fermin - Corona del Mar (extended cell includes Palos Verde Sub-Cells: Palos Verde Pt. - Pt. Fermin)	31 <u>12</u> 43	8
<u>Oceanside Cell:</u> Dana Pt - Pt. La Jolla (extended cell includes Laguna Sub-Cells: Corona del Mar - Dana Pt.)	56 <u>14</u> 70	9
<u>Mission Bay Sub-Cell:</u> Pt. La Jolla - Pt. Loma (including La Jolla headland, Mission Bay, Pt. Loma)	15	10
<u>Silver Strand Cell:</u> Pt. Loma - Baja, Calif., Mexico	16(in U.S.)	11

exception of the Buchon Sub-Cell which consists of the northern 14 miles of rocky coast extending from Point Buchon to Point San Luis, this cell has the longest sandy beach in southern California. Pismo Beach is over 16 miles long and is backed by some of the largest, most extensive sand dunes in California.

These beaches receive the highest fluxes of wave energy of the long beaches of California. Yet because the shoreline is aligned nearly normal to the prevailing waves, the net longshore transport of sand is relatively small, averaging about 60,000 yd³ per year to the south between sub-cells (Bowen and Inman, 1965).

Santa Barbara Cell

This cell extends for 96 miles from Point Conception to Point Mugu. It is the longest littoral cell in southern California and includes a variety of coastal types and shoreline orientations. The east-west trending beaches near Point Conception are narrow and backed by high seacliffs. Beaches between Ventura and Port Hueneme trend southeast and are generally wide and backed by the low-lying Oxnard Plain.

This is one of the original four littoral cells defined by Inman and Frautschy (1965) and was the first cell to have a well established net littoral transport. The channel islands provide considerable protection from wave action from the south. Even so, construction of the Santa Barbara Breakwater in 1927/28 emphasized the importance of the longshore transport of sand in littoral systems. By 1937 the breakwater had trapped nearly 2,000,000 yd³ of sand. Dredging between 1938 and 1951 established that the net easterly longshore transport of sand trapped by the harbor was 280,000 yd³ per year (Johnson, 1953; 1957). The role of Hueneme and Mugu Submarine Canyons as sediment sinks and the effect of the Port Hueneme jetties in channeling additional sand down Hueneme Canyon and starving the downcoast beaches was first described by Inman (1950a).

Santa Monica Cell

This cell extends for 40 miles from Point Dume to Palos Verde Point. Including the nine miles of pocket beaches and rocky cliffs in the Dume Sub-Cell, the entire length of the extended cell is 49 miles. The Santa Monica Bay shoreline includes 19-1/2 miles of sandy beaches extending from Pacific Palisades to Malaga Cove. Most of the Santa Monica Bay beaches were naturally backed by extensive fields of sand dunes. The extended cell had two natural sinks, Dume and Redondo Submarine Canyons. Some sand bypasses Dume Canyon and is transported into the Santa Monica Cell.

Man's intervention in the form of coastal structures has been extensive in the Santa Monica Cell and the San Pedro Cell to the south. Santa Monica Bay has so many structures impeding longshore sand transport that the entire coast of the bay is essentially "stabilized". Kings Harbor (Redondo Breakwater) prevents sand from entering Redondo Submarine Canyon from the north, so that the canyon is virtually "dead" in the sense of a sand sink.

San Pedro Cell

This littoral cell extends for 31 miles from Point Fermin to the City of Corona del Mar just southeast of Newport Submarine Canyon. Including the 12 miles of rocky coast of the Palos Verde headland extending from Palos Verde Point to Point Fermin, the extended San Pedro Cell has a coastal length of 43 miles. Under natural conditions the Los Angeles, San Gabriel and Santa Ana Rivers, collectively draining the largest area in southern California, supplied the sediment for the cell. The sink for this sediment was down Newport Submarine Canyon.

The San Pedro Cell has been extensively modified by man. Dams on the rivers intercept much of the sediment (Brownlie and Taylor, 1981). The breakwater for the Los Angeles Outer Harbor protect most of the sandy coast from ocean waves, so that there is relatively little longshore transport of sand. As a consequence Newport Submarine Canyon appears to be inactive as a sink for littoral sand.

Oceanside Cell

This cell extends for 56 miles from Dana Point to Point La Jolla. Including the 14 miles of cove and pocket beaches of the Laguna Sub-Cells extending from Corona Del Mar to Dana Point, the extended cell has a length of 70 miles. The coast from Dana Point to La Jolla consists of relatively narrow, semi-continuous sandy beaches backed by wave-cut seacliffs. Some of the seacliffs are over 300 feet high, as along Torrey Pines State Reserve, and present some of the most spectacular sea scapes in the world.

The extended cell includes two harbors for small craft, Dana Point Harbor and Oceanside Harbor. Dana Harbor located between the sub-cells and the main littoral cell is essentially free of siltation problems. Oceanside Harbor is in the center of the "river of sand" for the littoral cell, as is Santa Barbara Harbor to the north, and as a consequence is a major trap for littoral sand.

Portions of the Oceanside Littoral Cell are the most studied coastal segments in southern California. This was the first coastal area where a submarine canyon was identified as a sediment sink (Shepard, 1951; Chamberlain, 1964). The source and nature of the beach sediment is known (Inman, 1953), and the seasonal changes in beach profile have been extensively studied (e.g. Nordstrom and Inman, 1975; Winant et al., 1975; Aubrey et al., 1980). The budget of sediment for previous natural and for present conditions has been studied, and the effect of dams on the rivers assessed (e.g. Brownlie and Taylor, 1981; Inman and Jenkins, 1983, Inman 1985a). The geology and tectonics of the southern portion of the cell have been studied, and it has been possible to re-establish the paleocoastlines of former times (Inman, 1983a).

Mission Bay Sub-Cell

This coastal compartment extends along the coast for 15 miles from Point La Jolla to Point Loma. It includes four miles of picturesque pocket beaches along the La Jolla headland

and six and one-half miles of rocky cliffs along the Point Loma headland. Four and one-half miles of sandy beach, extending from False Point to the Municipal Pier at Ocean Beach, are situated along the Mission Bay sand spit. This coastal compartment is best described as a sub-cell.

The natural source of sediment for this sub-cell was the San Diego River which flowed alternately to either side of the Point Loma headland; sometimes into Mission Bay (False Bay) and sometimes into San Diego Bay (Brooks et al., 1948). During significant floods the river flowed through Mission bay depositing some material in the ocean. There, ebb-tidal currents from Mission Bay and ocean currents transported some sand south along the rocky coast of Point Loma. Under such conditions some material probably "leaked" around Point Loma and into the Silver Strand Littoral Cell. In 1906 the U.S. Army Corps of Engineers built a dike that permanently channeled the river flow into Mission Bay. However, the many dams on the San Diego River may prevent it from being a source of sediment (Brownlie and Taylor, 1981).

Silver Strand Cell

This littoral cell extends for 16 miles from Point Loma to the United States/Mexico Boundary, and for many miles along the coast of Baja California, Mexico. With the exception of two miles of rocky coast at Point Loma, the cell includes 14 miles of sandy beach extending from Zuniga Jetty at the entrance to San Diego Bay to the border. The Mexico portion of the cell appears to extend about 20 miles below the border to Punta El Descanso, or farther. This portion of the cell consists of sandy beaches backed by seacliffs.

This is one of the few cells with a significant northerly transport of sand, caused by the wave shadow in the lee of Point Loma. Under natural conditions the principal source of sediment was the Tijuana River which brought material to the coast just north of the border. Northerly transport of sediment from the delta of the Tijuana River built the primordial Silver Strand, and northerly transport has continued to supply its beaches with sand. Construction of

the Zuniga Jetty in 1898 extended the ebb-tide jet from the bay, causing the tidal delta to move into deeper water, creating an artificial sink for sediment (Inman et al., 1974). Construction of the Rodriguez Dam in Mexico and Morena and Barrett Dams in the United States has eliminated the Tijuana River as a significant source of sediment for the cell. This has resulted in serious erosion in the vicinity of Imperial Beach.

2. COASTAL PROCESSES

Structures placed along the coast and on rivers have had a major impact on the natural coastal processes that mold the world's shorelines. And conversely, coastal processes often make coastal structures less effective than designed, causing costly modifications.

The processes of primary interest here are action of waves in eroding and terracing the land and in transporting sediment along the coast; the tractive forces of streams in eroding, transporting and depositing sediments; the effect of changing sea level on beach erosion; and finally, the influence of tides and streams in the maintenance and filling of coastal lagoons. The cumulative effect and interaction of these dynamic coastal processes are considered in the context of the sources and sinks of sediment and their balance in the littoral cell. Historically, the principal sources of sediment for the cell were the coastal streams; waves transport the sediment along the coast; while the main sink for sediments were the submarine canyons.

Waves and the currents that they generate are the single most important factors in the erosion, transportation and deposition of nearshore sediments. Waves mold beaches forming typical "summer" beach profiles in response to low waves and "winter" profiles in response to storm waves (Figure 2.0-1). Waves erode sea-cliffs and cut terraces (e.g. Inman, 1983). When sediment is available, waves are effective in moving material along the bottom and in placing it in suspension for weaker currents to transport.

Parts of the Oceanside Littoral Cell are the most studied coastal sections in southern California. For this reason many of the examples of coastal processes used in this chapter of the report will be taken from this cell (e.g. Inman and Jenkins, 1983).

2.1 WAVE-CUT TERRACES AND SEA CLIFFS

In the absence of beaches fronting sea cliffs, the direct force of the breaking waves erodes cliffs and forms coastal terraces. The rising and lowering sea levels during the Pleistocene epoch caused the seas to transgress and regress across the land both eroding and depositing material

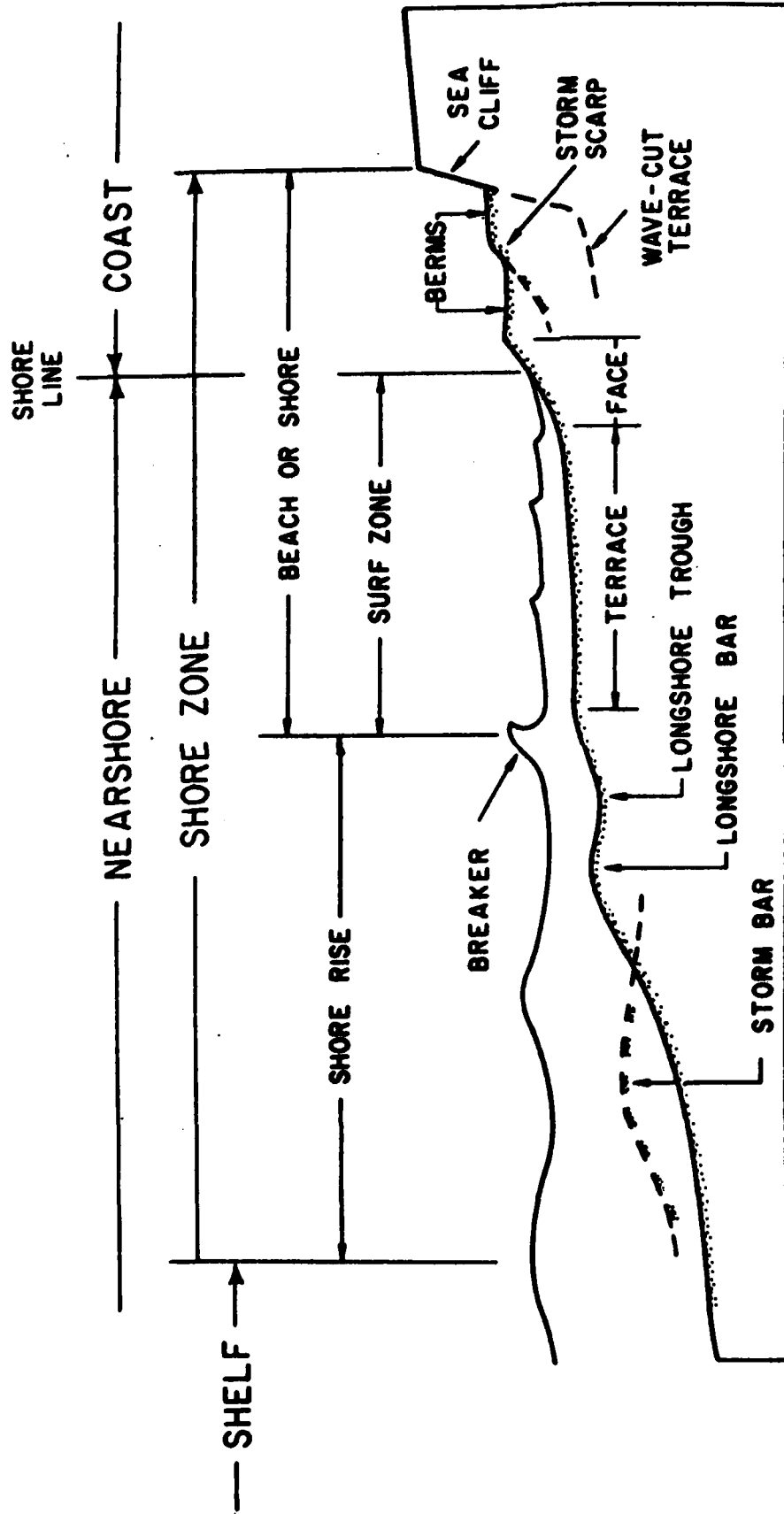


Figure 2.0-1. Nomenclature and schematic diagram for the summer profile of the shore zone of coasts with sea cliffs. Storms modify the beach profile as shown by the storm bar and storm scarp. The shore rise during storms is seaward of the storm bar (after Inman, 1971).

(Inman, 1983). Erosion is most pronounced during relative stillstands or pauses in the transgressive/regressive cycles. The signature for the sea's presence at a relative stillstand is usually in the form of a wave-cut terrace on gently sloping terrain, backed by sea cliffs when the near stillstand has been long, as at present.

Active cliff erosion still occurs during severe winter wave conditions at many locations along the southern California coast. And, in the absence of beaches, the erosion products from sea cliffs supplies sand to the cell. Shepard and Grant (1947) found that wave erosion of the consolidated rocky coasts of southern California has been negligible during the preceding 50 years. On the other hand they found a retreat of as much as a foot a year in unconsolidated formations. Based on a comparison of old maps, Kuhn and Shepard (1984) claim that the sea cliff at Encinitas retreated more than 600 feet between 1883 and 1891.

The wave-cut terrace associated with the sea cliffing at La Jolla is shown in cross-section in Figure 2.1-1. The decrease to one degree in slope of the wave-cut terrace, beginning about 200 meters (650 ft) seaward of the sea cliff and at a terrace depth of 4 to 5 meters (13 to 16 ft) below mean sea level, probably represents the terracing that began about 6,000 yrs BP at the beginning of the slow (15 cm/century) rise to present sea level.

Borings show that a wave-cut terrace also occurs at the base of the sea cliff and under the modern beach sand at many coastal locations (e.g. Figure 2.1-1). At Oceanside the sea cliff is about 11 meters (35 ft) high and occurs just seaward of Pacific Street (Artim, 1981). Within the past two centuries, and during times of intense wave action and little sediment discharge from rivers, the beach was eroded back to the sea cliffs. Following periods of major flooding, the sandy deltas of the Santa Margarita and San Luis Rey Rivers built the beach seaward forming a wide backshore area between the sea cliff and the beach berm. Photographs taken in 1916 show the sand delta of the San Luis Rey River extending out almost a pier length beyond the sea cliffs (Figure 2.1-2).

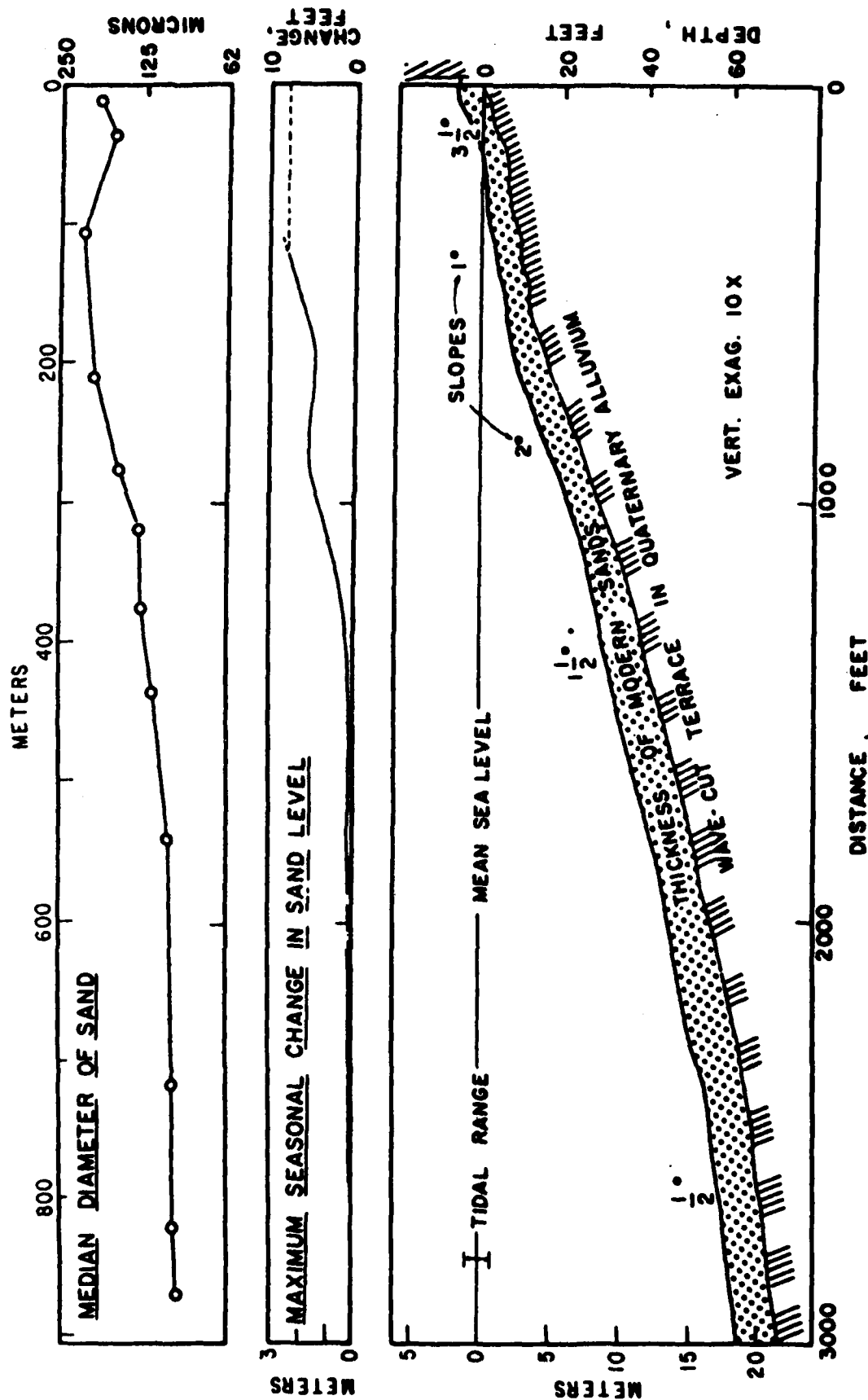


Figure 2.1-1. Profile of a fine sand beach at La Jolla, California, showing the median sand size, the maximum seasonal change in the level of the sand associated with winter and summer waves, and the thickness of the modern nearshore sand over the wave-cut terrace. The recent slow rise in sea level that began 6,000 years BP produced the gently sloping terrace beginning 200 m seaward of the cliff (from Inman and Bagnold, 1963).

DELTA OF THE SAN LUIS REY RIVER



Figure 2.1-2. Oceanside Pier and flood delta of the San Luis Rey River. Photographed in 1916 after the flood. Note driftwood on beach (from Inman and Jenkins, 1983).

2.2 FORMATION OF BEACHES

Wherever there are waves and an adequate supply of sand or coarser sediment, beaches form. Even man-made beach fills are effectively eroded and reformed by the waves. The initial and most characteristic event in the formation of a new beach from a heterogeneous sediment is the sorting out of the material, with coarse material remaining on the beach and fine material being washed away. Concurrent with the sorting action, the material is rearranged, some being piled high above the water level by the run-up of the waves to form the beach berm, some moved back and forth by the swash to form the beach face, some carried back down the face to form the terrace that is characteristic of beach surf zones (Figure 2.0-1). In a relatively short time, the beach assumes a profile which is in dynamic equilibrium with the wave forces generating it as shown by the beach profile of modern sands over the wave-cut terrace in Figure 2.1-1.

The oscillatory motion of waves in shallow water produces stresses on the bottom that place sand in motion. The interaction of the oscillatory water motion with the bottom also induces a net boundary current flowing in the direction of wave travel. The most rapidly moving layer of water is near the bed, and for waves traveling over a nearly horizontal bed the interaction of wave stresses and the boundary current produces a net transport of sand in the direction of wave travel. Thus waves traveling toward the shore exert a net shoreward stress on the bottom sediments that tends to contain sand and cobbles against the shore (e.g. Inman, 1971).

The action of waves on an inclined bed of sand eventually produces a beach profile that is in dynamic equilibrium with the energy dissipation associated with the oscillatory motion of the waves over the sand bottom. When a beach slope exceeds the natural equilibrium slope, an offshore transport of sand results and the beach slope flattens. Conversely, if a slope is less than the natural equilibrium slope, a shoreward transport of sand will result, and the beach slope will

steepen. A dynamic equilibrium slope is attained when the up-slope and down-slope transports are equal (Inman and Frautschy, 1965).

Many factors such as rip currents, presence of structures and promontories, etc., affect local beach slopes. However, in general on long beaches composed of fine or medium-size sand, the following general description of the beach profile applies. The equilibrium beach slope steepens with the increasing onshore-directed bottom stress that is associated with shoaling waves. The slope is usually gentle in deeper water over the shelf and steepens into the characteristic "shore-rise" where the onshore stress is greatest just before the wave breaks. The slope decreases at the break point and is gentle over the terrace and longshore bar. The bore from the breaking wave traverses the gentle outer terrace, causing it to gradually steepen until it reaches the beach face where the remaining energy from the breaking wave is dissipated in the swash and backwash. The beach face is the steepest portion of the beach profile (Winant et al, 1975).

2.3 BEACH CYCLES

Changes in the character and direction of approach of the waves causes a migration of sand between the beaches and deeper water. In general, the beaches build seaward during the low steepness waves of summer and are cut back by higher, steeper winter storm waves (Figures 2.0-1, 2.1-1 and 2.3-1). There are also shorter cycles of cut and fill associated with spring and neap tides and with nonseasonal waves and storms. Bottom surveys indicate that most offshore-onshore interchange of sand occurs in depths less than about 10 meters (33 feet) but that some effects may extend to depths of 30 meters (100 feet) or more (Nordstrom and Inman, 1975).

Shepard and LaFond (1940) made the first systematic attempts to document the seasonal changes in beaches by measuring beach profiles from the ocean pier at the Scripps Institution of Oceanography, La Jolla, California. They were able to document the cutting back of the beach

TORREY PINES BEACH - NORTH RANGE

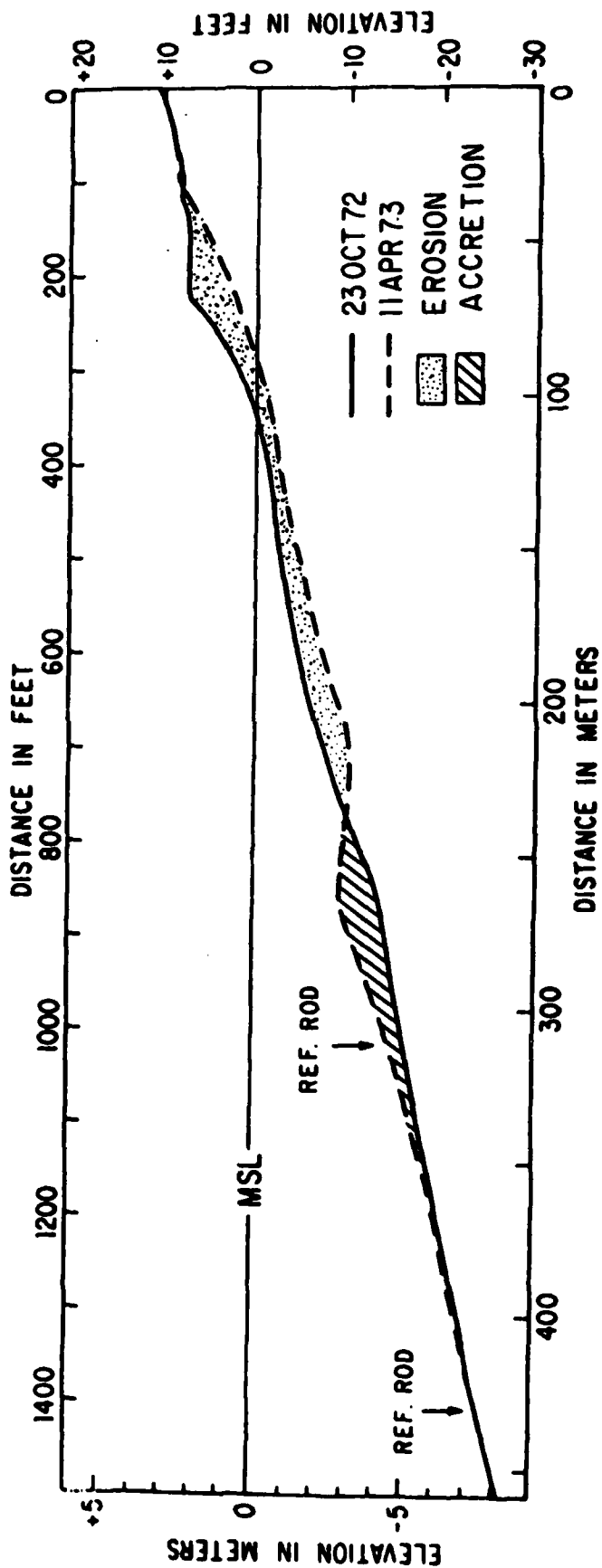


Figure 2.3-1. Comparison of beach profiles measured at North Range showing seasonal changes in beach configuration 1972-73. The profile measured on 11 April 1973 shows the winter configuration during the winter of 1972-1973. Arrows indicate the positions of reference rod stations (from Nordstrom and Inman, 1975).

by storm waves, as well as the gross seasonal changes associated with longer periods of low waves of summer and the higher waves of winter. However, their measurements did not extend beyond the pier, and the quantitative aspects of the data were questionable because of the influence of the pier pilings. Accurate profiles of the beach and nearshore bottom were made by Inman and Rusnak (1956) using standard survey techniques across the beach and corrected fathogram records offshore. The fathograms were corrected to give accurate depth changes by referring them to diverse measurements of changes in the length of "reference rods" that protruded above the bottom. These measurements showed that systematic seasonal changes of beach profile were observed to depths of over 10 meters, while measurable bottom changes were observed in depths of 25 meters (Figure 2.1-1).

More extensive measurements extending over periods of several years, using the technique of fathometer corrections from bottom reference rods have been made off Torrey Pines Beach, California (Nordstrom and Inman, 1975; Winant, et al., 1975). The Torrey Pines profiles were measured monthly from June 1972 through April 1974, and intermittently through December 1978 (Inman et al., 1980). These measurements clearly show seasonal changes. The more gentle beach face slope that occurs for fully developed winter profiles is in contrast with the wider berm and steeper beach face of the summer profiles (Figure 2.3-1).

A statistical analysis of the Torrey Pines beach profiles that separates the spatial and temporal dependence of the profile changes is given in Winant et al (1975). This analysis showed that most of the variations in profile configuration can be accounted for by three eigenfunctions corresponding to the three largest eigenvalues. The largest eigenvalue corresponds to the "mean beach function" which represents an average beach profile (see Figure 9.6-6). The major seasonal cross-shore changes were associated with the second eigenfunction, the "bar-berm function" which has a maximum at the location of the winter bar. The cross shore pivotal point lies between at a depth of 6 to 9 feet. A correlation of these cross-shore

beach changes with waves and tides was demonstrated by Aubrey et al (1976) and Aubrey (1979). At Torrey Pines Beach the average net change in profile from summer to winter is an erosion of the beach face and foreshore of about 92 cubic meters per meter of beach length (110 yd³ per yd). This material is deposited offshore in winter and redeposited on the beach face every summer when the beach is in a dynamic equilibrium state (refer to Table 9.6-1).

2.4 LITTORAL TRANSPORT

The littoral transport of sand along ocean beaches has been evaluated in a number of ways. These include natural and artificial tracer studies, estimates of accretion and erosion near coastal structures, and estimates based on the potential for waves to transport sand. Traditionally, the amount of material trapped by coastal structures, such as jetties and breakwaters, divided by the time of trapping has been used to estimate the transport rate. In this case it must be recognized that there may be both up and downcoast transports with rates indicated by Q_u and Q_d respectively. Their sum is the gross transport rate Q_g and their difference is the net transport rate Q_l ;

$$\text{gross } Q_g = Q_d + Q_u \quad (2.4-1a)$$

$$\text{net } Q_l = Q_d - Q_u \quad (2.4-1b)$$

Further, these rates may change with season and with the time interval used to establish the rate. But in general at Santa Barbara Harbor the east to west transport dominates to the extent that over periods of a year or more the net and gross transport rates are essentially equal (Johnson, 1953; Dean and Seymour, in press). At Oceanside the annual downcoast rate is about twice the upcoast rate, and Q_g equals about $3Q_l$ (Inman and Jenkins, 1983). Also some structures act as efficient sand traps, providing a good measure of the gross transport, while others may bypass significant portions of the littoral transport. Finally, the rate at which the

structure retains sand usually differs for up and downcoast transports, and this retention rate will change with time as the structure fills with sand. These factors have complicated the interpretation of littoral transport rates from trapping by structures, leading to wide differences in opinion (e.g. compare Weggel and Clark (1983) with Inman and Jenkins, 1983).

Instantaneous Longshore Transport

An increasingly important method for estimating littoral transport rates is that based on the flux of the radiation stress of the waves that drive the transport process. This "stress-flux" is obtained from "instantaneous" measurements of the wave energy flux and direction over periods of about 20 minutes which is then related to the resulting "instantaneous" transport of sand. The littoral transport rates for longer periods such as for a season or a year is obtained by summing the wave measurements by intensity and direction over the appropriate time intervals. Estimates of longshore transport obtained in this way are sometimes referred to as "potential" transport.

When waves approach at an angle to the shoreline they transport sand along the beach. This longshore transport results from the combined effect of the breaking waves which place sand in motion and the presence of a longshore current in the surf zone which aids in the movement of sand along the beach. Theory and field measurements of waves and the resulting longshore transport of sand, show that the immersed weight sand transport rate I_l , is proportional to the stress-flux factor, P_l (e.g. Komar and Inman, 1970; Inman et al., 1980).

$$\begin{aligned} I_l &= KP_l = K[P \sin \alpha \cos \alpha]_b \\ &= K[C'S_{yx}]_b \end{aligned} \quad (2.4-2)$$

where $K \approx 0.8$ is a dimensionless constant. A similar relation but using significant waves, is given as equation (4-48) in the Shore Protection Manual (USACE CERC, 1984). Relation (2.4-2) may be calculated in either metric or American units; however the energy density from wave

arrays is usually given in metric units. Accordingly, $P = EC_n$ is the energy flux of the waves (watts/m), E is the wave energy per unit area (joules/m), C is the wave phase velocity (m/sec), C_n is the group velocity, $S_{yx} = E_n \sin \alpha \cos \alpha$ is the longshore component of the radiation stress, α is the angle the breaking wave makes with the shoreline, and the subscript b indicates that all properties are measured at or calculated for the breakpoint of the waves.

In the above relation I_1 is the immersed weight longshore transport rate (newtons/sec) and may be expressed in terms of the "at rest" volume transport rate Q_1 (m^3/sec)

$$Q_1 = I_1 / [(\rho_s - \rho)gN_o] \quad (2.4-3)$$

where ρ_s and ρ are the densities of the solid grains and the water respectively, g is the acceleration of gravity, and N_o is the volume concentration of sand, equal to about 0.6 for well sorted sand at rest (e.g. Inman and Bagnold, 1963). For quartz sand ($\rho_s = 2.65 \times 10^3 \text{ kg/m}^3$) transported in sea water at 15°C ($\rho = 1.026 \times 10^3 \text{ kg/m}^3$) with $N_o = 0.6$ the bracketed quantity in equation (2.4-3) equals $9.55 \times 10^3 \text{ newton/m}^3$. For this case

$$Q_1 = 1.05 \times 10^{-4} I_1 \quad (2.4-3a)$$

where Q_1 is in m^3/sec and I_1 is in newton/sec = watt/m. For ease of calculation in the above equation wave height in feet is usually converted to meters (1 ft = 0.3048 m). When desired, the volume transport is converted to cubic yards per second ($yd^3/sec = 0.765m^3/sec$).

Equations 2.4-2,3 show that the weight and volume of sand transported along the beach is directly proportional to the stress-flux of the waves. Thus it is apparent that the potential longshore transport of sediment along a sandy coast can be estimated if the budget of wave energy (that is, the wave climate) is known.

The above principle would also apply to the transport of larger particles such as cobbles. But they would travel at a much slower rate because the wave-induced shear stress required to

move gravel or cobbles increases in direct proportion to the diameter of the particle. Therefore equation (2.4-2) would be expected to apply to cobbles. but the constant K, which is a form of efficiency, would be reduced.

Evaluation of K

Recent experiments by White and Inman (in press,b) together with the data from Inman et al (1980) show that the value of K in equation 2.4-2 is a function of beach slope and breaker type. It is found that K varies as a form of the dimensionless "surf similarity parameter" of Battjes (1974), here given in the form of a reflection coefficient following Inman and Guza (1976):

$$\begin{aligned} c_{rb} &= |2g \tan^2 \beta| / H_b \sigma^2 \\ &= |L_\infty \tan^2 \beta| / \pi H_b \end{aligned} \quad (2.4-4)$$

where β is the slope of the beach, $\sigma = 2\pi/T$ is the radian frequency of the incident waves, and L_∞ is the deep-water wavelength. The relation has been used successfully for surf similarity proposed by Bowen et al (1968), Galvin (1972), Guza and Inman (1975), and Munk and Wimbush (1969).

White and Inman (in press) use least-squared methods to show that

$$K = 2.2 \sqrt{c_{rb}}, \text{ for } 0.02 < c_{rb} < 0.42 \quad (2.4-5)$$

This relation shows that steepening the beach profile increases K and thus increases the longshore transport rate of sand.

The studies of longshore transport by Inman et al (1968) and Komar and Inman (1970) were made using fluorescent dyed sand injected on the beach. Since there were no measurements of suspended load, it was assumed that most of the sand traveled as bedload. The coefficient K was found to equal 0.77. Later studies by Inman et al (1980), White and

Inman (in press), and Zampol and Inman (in press) included separate measures of bedload and suspended load. As before, the bedload was obtained from the distribution of tracers injected on the beach. The suspended load was obtained from in situ measurements of the water column in the surf zone (Zampol and Inman, in press). The total load was taken as the sum of the bedload and the suspended load.

Data from the earlier studies and the more recent studies are plotted in Figure 2.4-1. The more recent data from Torrey Pines and Santa Barbara used two different tracer techniques referred to as temporal and spatial sampling. Following tracer injection, samples are taken continuously along a fixed range downcoast for temporal sampling. This procedure has only been used at Torrey Pines and Santa Barbara. In spatial sampling, a grid extending over the expected area of tracer movement is sampled at a fixed time after injection (Inman and Hanes, 1980; White and Inman, in press,a).

The mean values of the coefficients for the more recent experiments are found (White and Inman, in press,b) to be: $K_b = 0.67$ for bedload; $K_s = 0.11$ for suspended load, and $K = 0.78$ for total load. It is of interest to note that the earlier studies using only bedload ($K_b = 0.77$) are in agreement with the total load ($K=0.78$) of the later studies. This is probably because most of the earlier studies were performed on steep beaches, which from relation (2.4-5) give larger values of K .

Rhythmic Beach Forms and Swash Cusps.

Rhythmic topography is the consistent repetition along a beach of wavy topographic forms. They may occur along the shoreline or be submerged. Rhythmic shoreline forms include swash cusps, surfzone cusps, and cusped spits that usually occur inside elongated lagoons. Submerged rhythmic features include crescentic bars and transverse bars.

Beach cusps are genetically of two types, "surfzone" cusps and "swash" cusps. The former are formed in the surfzone by the nearshore circulation system, and have wavelengths that may

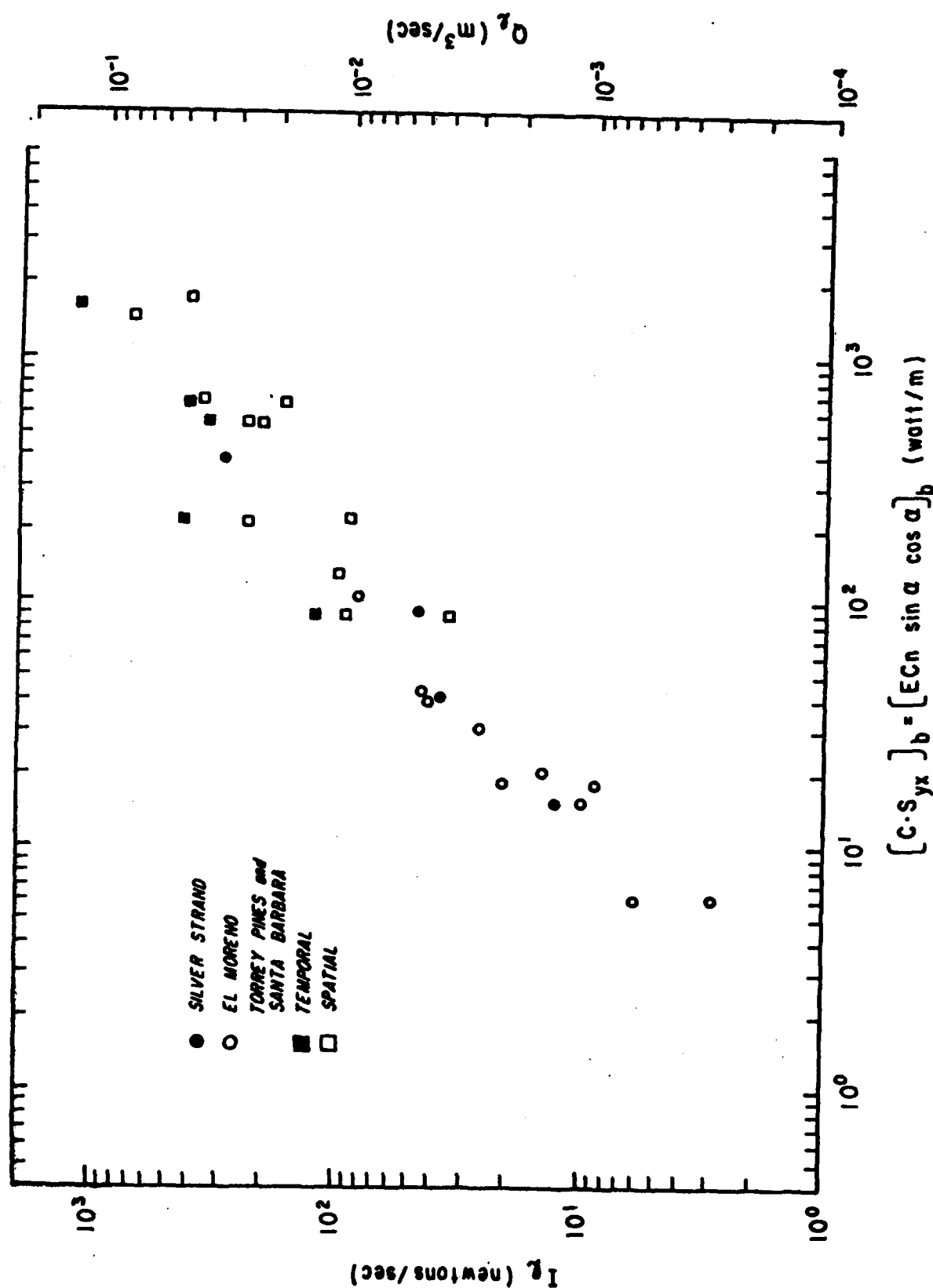


Figure 2.4-1.

Field measurements of total immersed-weight longshore transport rate I_I vs the flux of radiation stress $C \cdot S_{yx}$ as described by equation (2.4-2). I_I is converted to volume transport rate Q_I using equation (2.4-3a). Data for circles are from Inman et al (1968), and Komar and Inman (1970); squares are from Inman et al (1980) and "best fit" data of White and Inman (in press, b). See text for temporal and spatial sampling techniques.

range up to hundreds of meters. Swash cusps are formed by the swash and backwash acting directly on the beachface and berm (Inman and Guza, 1982). Our concern here is with the occurrence of swash cusps and their effect on the longshore transport of sand.

Swash cusps are formed by the swash and backwash acting directly on the beachface and berm. They scallop the beach into regular forms with wavelengths typically ranging from a few centimeters to about 75 m, but otherwise do not change the overall alignment of the beach. They are most common on steep reflective beaches, where the incident waves produce a substantial surge of swash up the beachface.

There are many explanations for the formation of swash cusps (reviewed by Guza and Inman, 1975; Sallenger, 1979) but several works suggest that edge waves are involved (e.g. Galvin, 1964; Bowen and Inman, 1969; Guza and Bowen, 1981). Edge waves are longshore periodic gravity waves which can be excited by wind-generated waves impinging on a beach. This excitation has been observed in the laboratory (e.g. Galvin, 1964; Harris, 1967; Bowen and Inman, 1969) and explained theoretically (Guza and Davis, 1974). The longshore wavelength, L_e , and period, T_e , of edge waves are related by Eckart (1951):

$$L_e = \frac{g}{2\pi} (2n + 1) \tan\beta \quad (2.4-6)$$

where g is gravity and $n = 0, 1, 2$, etc., is the mode number. The most easily excited edge wave, and the one with the largest amplitude, is of mode zero ($n = 0$) and is a subharmonic of the incident wave, i.e., the edge wave has a period twice that of the incident wave, $T_e = 2T_i$, where T_i is the incident wave period.

Inman and Guza (1982) hypothesizes that the superposition of swash from incoming waves with the motion of sub-harmonic edge waves produces a systematic variation in run-up height along the beachface, which in turn produces periodic circulation and erosional perturbations. The initial perturbation in circulation of the swash and backwash over the cusp form are basic

to the formation of swash cusps and their development into mature forms. The swash runs up the beachface to the cusp apex where it divides, half of its flow swinging into a longshore direction and flowing as backwash into the cusp valley, where it and its sediment load flow seaward as small but intense rip currents. Once the rip current reaches the water the sediment load is deposited forming a small delta off the cusp valley. This swash circulation is responsible for enlarging the initially small edge wave induced topographic perturbations and maintains the mature cusp form.

Thus it appears that the edge wave is necessary to initiate the formation of cusps, but that edge-wave persistence is not required for cusp growth. Once the bedform perturbation is initiated, then the incident waves alone force the bedform perturbations to grow until the cusp reaches maturity and a maximum steepness. Further, the strong bedform feedback tends to eliminate the edge wave because its nodal point, with the requirement for longshore orbital velocities (e.g. Bowen and Inman, 1971) cannot exist in the presence of strong offshore rip currents in the cusp valley, nor in the presence of the seaward protruding delta off the cusp valley.

Inman and Guza (1982) show that the longshore wavelength of swash cusps λ_c are in agreement with the wavelength of subharmonic edge waves (Figure 2.4-2). They also find that the maximum cusp height η_c , as measured from cusp apex to valley is approximately equal to the significant run-up height of the waves. They show that the relation for the cusp height reduces to

$$\eta_c \leq 0.24 \lambda_c \tan \beta$$

as shown in Figure 2.4-3.

Swash cusps tend to occur on steep beaches. This is in agreement with experiments showing that the excitation of subharmonic edge waves occur only when the incident waves are

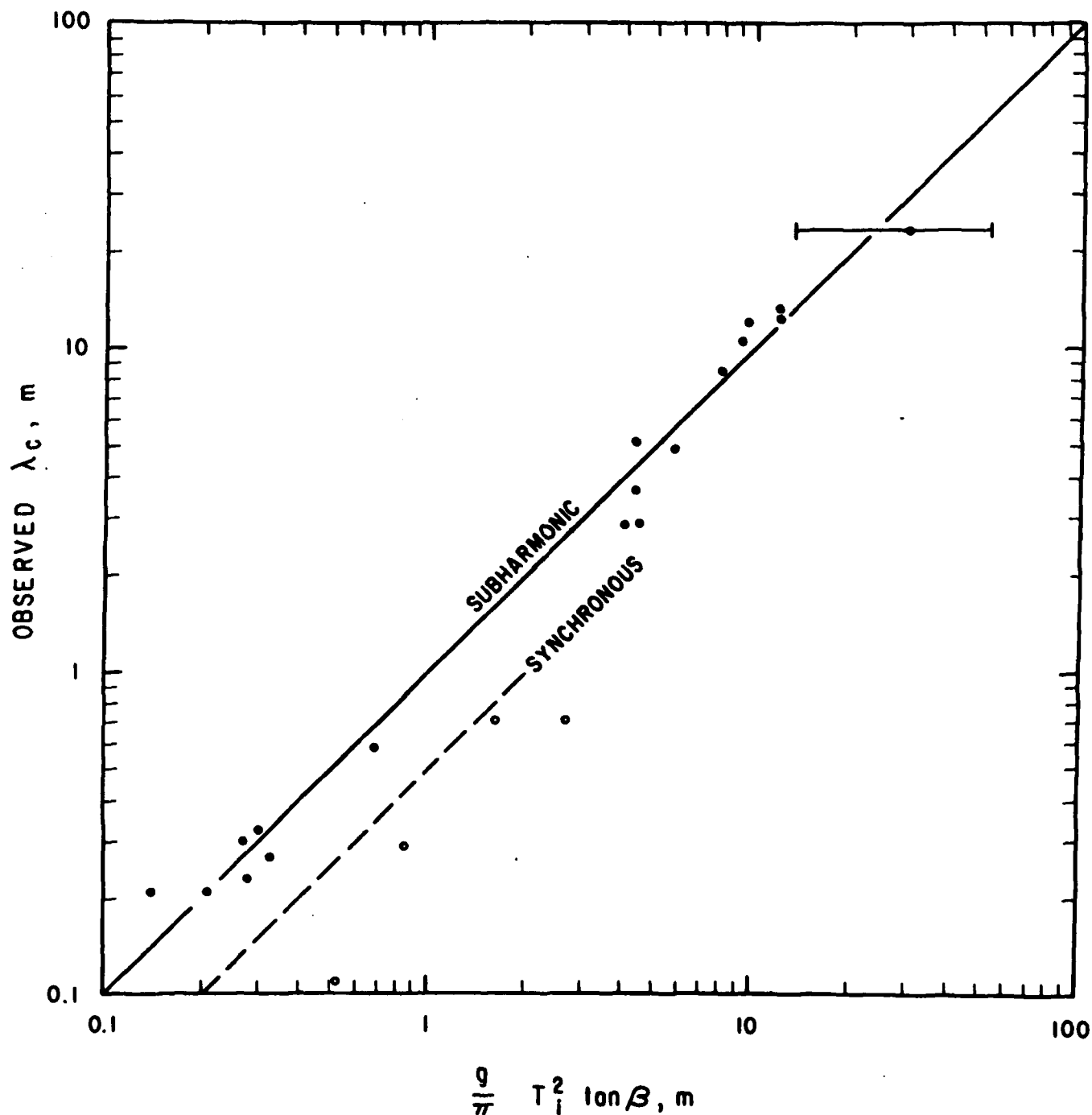


Figure 2.4-2. Observed longshore wavelengths of swash cusps vs. $(g/w) T_i^2 \tan \beta$. Solid line at 45° is perfect agreement for subharmonic edge waves, and dashed line is agreement for synchronous edge waves (from Inman and Guza, 1982).

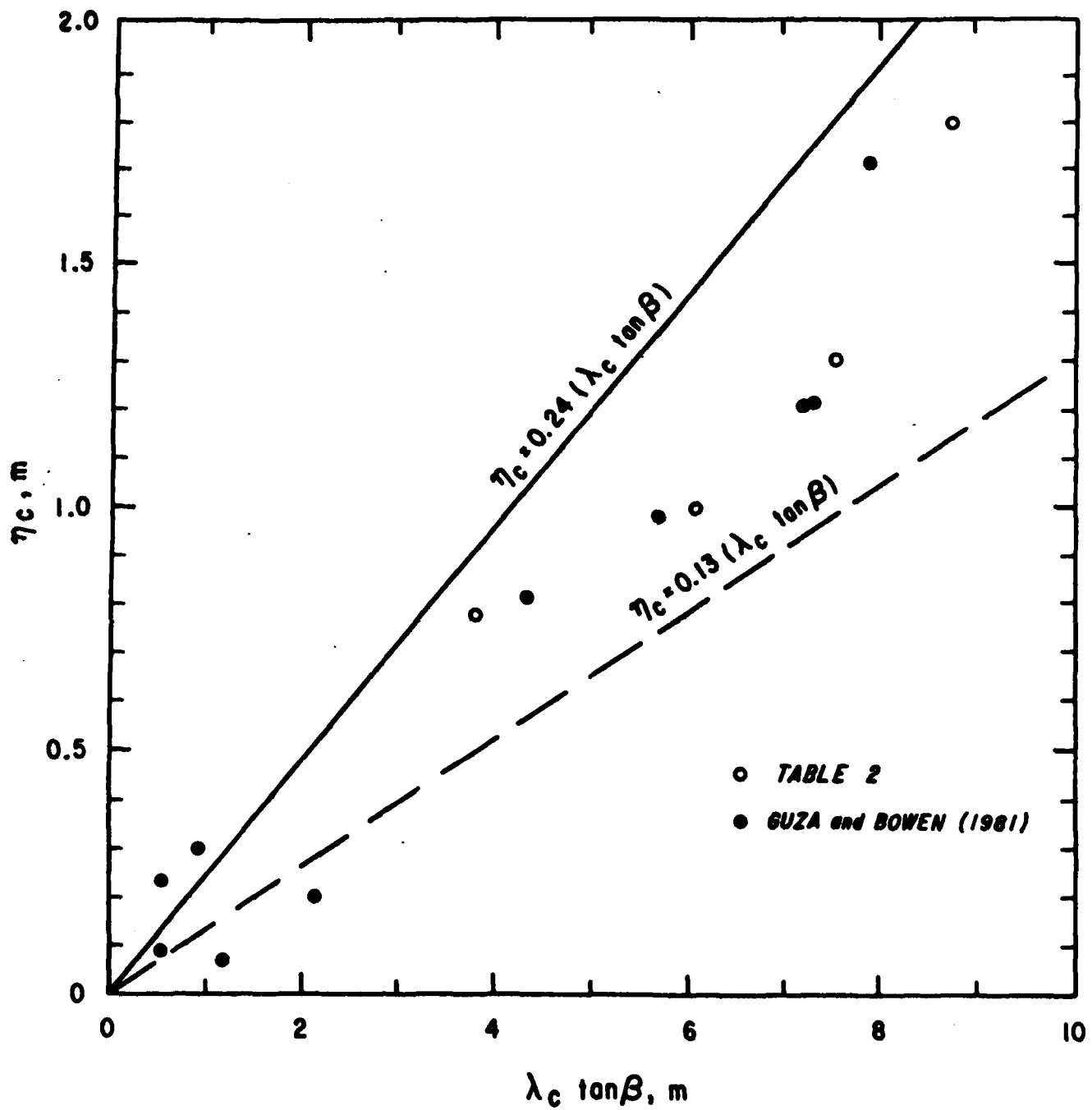


Figure 2.4-3. Observed cusp height, η_c versus λ_c is the observed wavelength of swash cusp (from Inman and Guza, 1982).

strongly reflected, such that the reflection coefficient $c_{rb} \geq 1/3$ in equation (2.4-4) (Guza and Bowen, 1976). Also it was shown in the previous section that the factor K in the stress-flux relation for longshore transport increases with increasing beach slope. Thus there is an apparent paradox, since well-developed, mature cusps clearly inhibit longshore transport.

The resolution of this paradox appears to be as follows. Increasing c_{rb} increases the longshore transport potential and increases wave reflection. If the longshore transport rate is not excessive, the reflected waves may excite edgewaves and cusps will form. If later the potential for longshore transport increases, the cusps will be destroyed or remain as remnants. In this case, the presence of the remnant cusp form does increase the longshore transport rate. This was shown to be true in two experiments at Santa Barbara by White and Inman (in press,b).

2.5 SEDIMENT TRANSPORT BY RIVERS AND STREAMS

A number of procedures have been used to estimate the yield of sediment to the coast from erosion of the land. These include estimates based on the erosion rate of the land in the drainage basin, estimates from sediment rating curves, and estimates from theoretical relations for the transport capacity of a flow. The more common theoretical relations include those of Meyer-Peter et al. (1934), Einstein (1942; 1950), and Bagnold (1966). Theoretical relations are useful in cases where stream data is insufficient for determining sediment rating curves, and in cases where high stream discharge rates greatly exceed the data leading to rating curves. The theoretical relations will not be discussed further here, but interested readers may refer to the original references or to texts on river hydraulics (e.g. Raudkivi, 1976; Richards, 1982).

Studies of river sedimentation have given rise to a number of terms for the description of the material and its transport mode. Classic treatments of the subject define *suspended load* as that portion of the total load that is supported by fluid turbulence, while *bedload* is material that is placed in motion by the tangential shear stress of the fluid over the bottom and has a

vertical dispersion of particles that is maintained by grain-to-grain contact and lift forces over the bed. Bedload includes transport by rolling, sliding and saltation. Total load is the sum of bedload and suspended load. *Wash load* consists of the fine material not present in the stream bed material. It is essentially the fine portion of the suspended load, sometimes referred to as *suspended fines*.

Erosion-Rate Method

A long term estimate of sediment yield in common use by geomorphologists is based on the erosion rate of the land. In this procedure, referred to as the "erosion-rate method," the total sediment yield is calculated as the average erosion rate per unit area of land multiplied by the area of the drainage basin. The erosion rate is usually established by measuring the amount of material trapped in dams and reservoirs. Schumm (1977) shows that the yield of sediment from erosion is a function of climate and the size and topographic relief in the drainage basin. Longbein and Schumm (1958) showed that the sediment yield was a maximum for semi-arid climates, where the annual rainfall was about 30 cm (1 ft) This explains why the rivers in southern California produce large volumes of sand.

Sediment Rating Curves

For streams with gaging stations, the discharge of suspended sediment can be related to the water discharge by a *sediment rating curve*. There are a number of types of rating curves, the most common being the instantaneous and the annual sediment rating curves. Instantaneous sediment discharge is usually predicted from a relation of the form

$$Q_{ss} = aQ^b \quad (2.5-1)$$

obtained from simultaneous measurements of the suspended sediment discharge (Q_{ss}) and the water discharge (Q). The constants a and b are usually obtained from the measured data

points in the rating relation using a simple linear regression analysis when the rating relation is expressed in the form, $\log Q_{ss} = b \log Q + \log a$ (Figure 2.5-1).

An annual rating curve relates the annual sediment yield from a stream to the annual runoff of water. This is obtained from the instantaneous rating curve by summarizing the sediment discharges over the hydrograph (flow vs time) for each water event such as a storm. Then the sums of the sediment discharges for the year are plotted against the sums of the water discharges. Again, this gives a sediment rating curve of the form

$$V_{ss} = AV^B \quad (2.5-2)$$

where V_{ss} is the predicted annual suspended sediment yield, V is the annual water discharge, and A and B are constants determined from the data (Figure 2.5-2).

From Table 2.5-1 it is observed that for southern California rivers the exponent b in equation 2.5-1 has an average value of 1.6 and ranges from 1.2 to 1.8 for instantaneous suspended load discharge. From Table 2.5-2 the exponent B from equation (2.5-2) for the annual suspended sediment discharge averages 1.5 and ranges from 1.2 to 1.6.

Total Load Transport and Sediment Yield

Sediment rating curves are the most reliable method of estimating the suspended yield of sediment from a river. The problem is to determine the best estimate for total load transport. Although bedload transport can be satisfactorily measured under some stream conditions using tracers, in practice there is no routine procedure for obtaining bedload. This means that it is usually taken to be a certain percentage of the suspended load, an entirely unsatisfactory procedure.

In their study of southern California rivers, Brownlie and Taylor (1981) assumed that the bedload was 10% of the suspended load. This criterion appears to be based on their more extensive experience with northern California rivers. Ten-percent appears to be too low for the

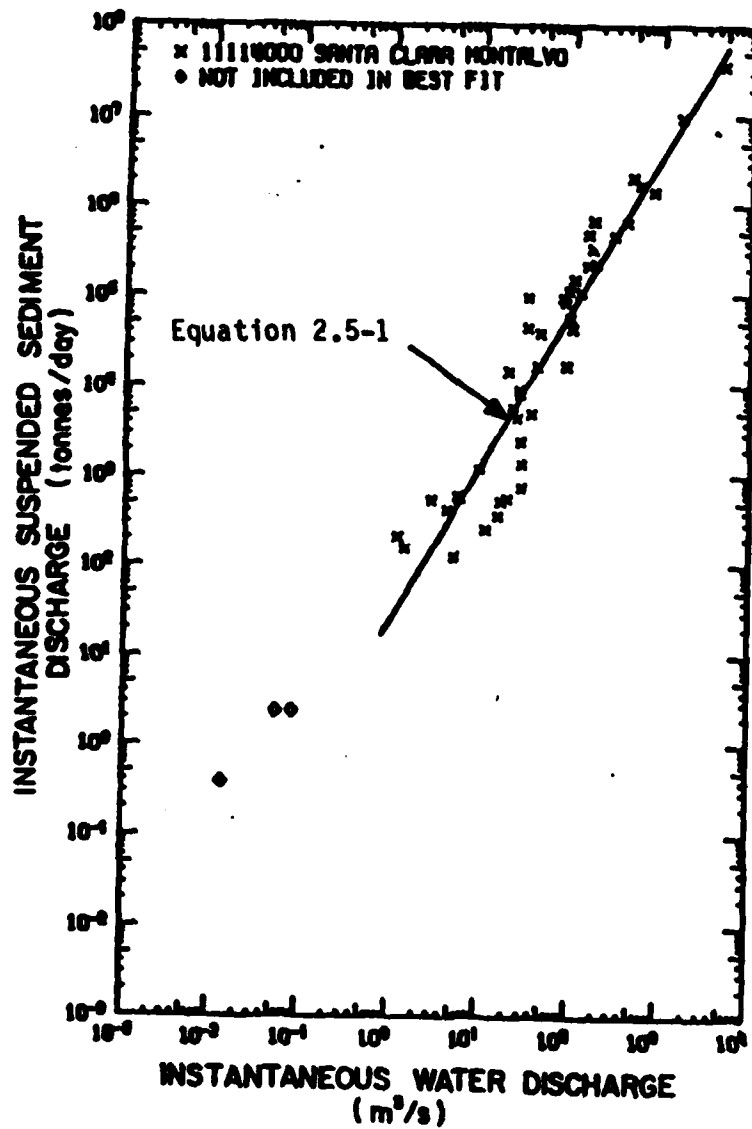


Figure 2.5-1. Relation of instantaneous sediment discharge to water discharge at Santa Clara River station 11114000, 1969-76 (from Brownlie and Taylor, 1981).

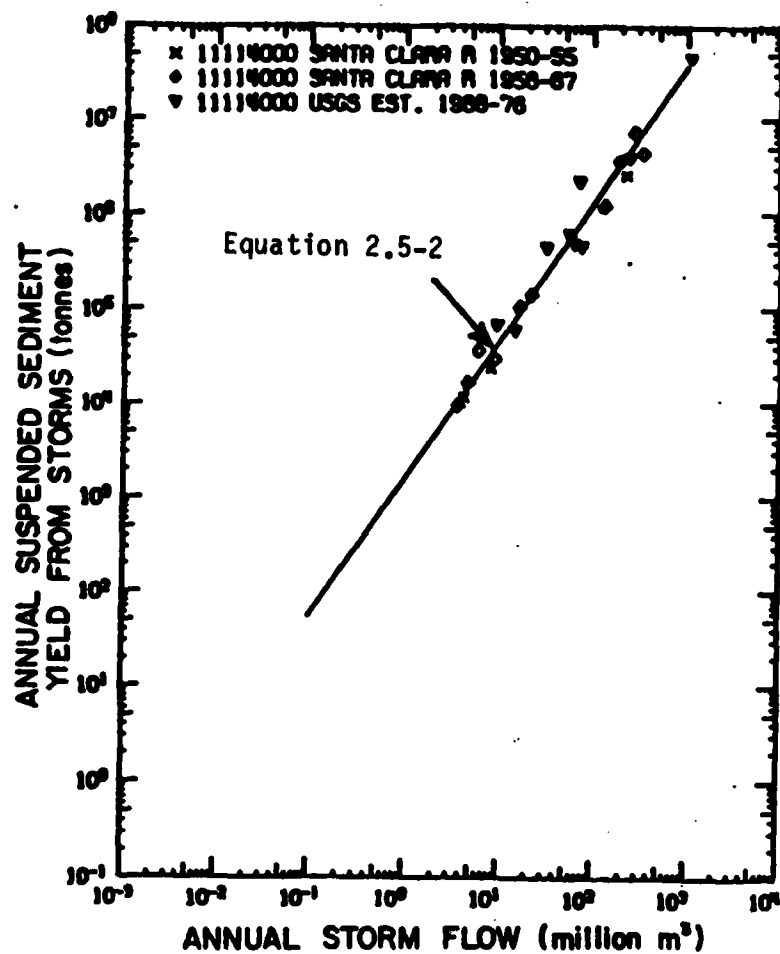


Figure 2.5-2.

Relation of annual suspended sediment delivered by storms to annual storm flow at Santa Clara River station 11114000, 1950-76 (from Brownlie and Taylor, 1981).

Table 2.5-1

Instantaneous Sediment Rating Curves

USGS Station	River	No. of Samples	Highest Discharge (m ³ /s)	Correlation Coeff. of Logarithms	Coefficient, ^a	Exponent, ^b
11118500	Ventura	49	555	0.978	14.2	1.83
11114000	Santa Clara	46	4,620	0.942	24.4	1.73
11046000	Santa Margarita	25	527	0.951	8.90	1.66
11042000	San Luis Rey	18	81.8	0.985	26.0	1.78
11022500	San Diego	27	33.4	0.970	8.73	1.58
11013500	Tijuana	43	3.23	0.951	255	1.22

Avg. 1.63

* Rating curve is of the form $Q_{ss} = aQ^b$ where Q_{ss} is the predicted instantaneous suspended sediment discharge, in tonnes/day, and Q is the instantaneous water discharge, in m³/s (from Brownlie and Taylor, 1981).

-42-

Table 2.5-2

Annual Storm Sediment Rating Curves

USGS Station	River	Number of Samples		Correlation Coeff. of Logarithms	Coefficient ^{**} A	Exponent ^{**} B
		Predicted [*]	USGS Est. Total			
11118500	Ventura	35	7	0.978	588	1.52
11114000	Santa Clara	16	10	0.990	938	1.53
11046000	Santa Margarita	29	--	0.976	132	1.58
11042000	San Luis Rey	23	--	0.971	544	1.54
11022500	San Diego	47	7	0.988	139	1.43
11013500	Tijuana	27	6	0.996	3120	1.15

* Predictions based on daily streamflow data and instantaneous rating curves.

Avg. 1.46

** Rating curve has the form $V_{ss}(\text{storm}) = A[V(\text{storm})]^B$, where $V_{ss}(\text{storm})$ is the predicted annual suspended sediment yield delivered by storms, in tonnes, and $V(\text{storm})$ is the annual storm flow, in million m³ (from Brownlie and Taylor, 1981).

drier, sandier southern California rivers. Schumm (1977, p. 110) shows that bedload increases for drier climates and for wider, shallower streams. Richards (1982, p. 106) concludes that for large rivers, bedload is normally less than 10% of the total load, but in mountain streams may reach 70%. Inman (1963, Table 8) using data from Colby and Hembree (1955) shows that the bedload was 40% of the total load (67% of the suspended load) for the sandy Niobrara River.

In the absence of reliable bedload measurements for southern California rivers, the above considerations led Inman and Jenkins (1983) to conclude that bedload equal to 20% of the suspended load was a more reliable estimate. Accordingly they used 20% in their estimates for the bedload and total load yield of the Santa Margarita and San Luis Rey Rivers (Inman and Jenkins, 1983, Table 3.4.3). This may be compared with estimates using 10% for the same rivers in Brownlie and Taylor (1981, Tables C6-5, C7-5).

2.6 TRANSPORT BY WIND

The relations for the transport of windblown sand were developed by Bagnold (1941) in his classic study, "The physics of blown sand and desert dunes." The relations have been verified over horizontal beds in laboratory experiments by Kadib (1963) and Belly (1964). Several studies have evaluated Bagnold's relations in the field. Kadib (1964) evaluated the relation for sand transport by wind on natural beaches. Finkel (1959) measured the rates of migration of dunes in Peru, and Inman et al (1966) evaluated the relation for a coastal dune field.

The wind transport relation is formulated in a manner similar to that for bedload in a stream. The rate of transport (discharge) of granular bed material by a fluid is directly proportional to the power expended by the fluid in transporting it. If the total power available by fluid action per unit area of bed is ω , then a portion, $K\omega$, of this power is available for transporting sand, and the transport rate becomes

$$i = K\omega \quad (2.6-1)$$

where i is the immersed weight of sediment transported across unit width of bed in unit time. The immersed weight transport rate is converted to dry mass transport per unit time and unit width by the relation

$$j = i\rho_s/(\rho_s - \rho)g \quad (2.6-2)$$

and to bulk-volume transport per unit time and width q_s by a relation similar to (2.4-3),

$$q_s = i/(\rho_s - \rho)gN_o = j/\rho_s N_o \quad (2.6-3)$$

Since the density of air, ρ , is very small compared to that of the grains, ρ_s , the relation for the dry-mass transport per unit time and width becomes

$$j = i/g = K\omega/g \quad (2.6-4)$$

where g is gravity. The power is given by $\omega = \tau u_*$ where τ is the stress and u_* is the friction velocity obtained from the von Karman-Prandtl relation for flow over an aerodynamically rough surface. Experiments show that the coefficient of proportionality K in equation (2.6-4) varies with sand size and sorting. Bagnold (1941, p. 67) showed that

$$K = C\sqrt{D/250} \quad (2.6-5)$$

where D is the grain diameter in μ and C is an empirical coefficient having the following values: 1.5 for a nearly uniform size sand; 1.8 for naturally sorted sands such as dunes; and 2.5 for a sand with a very wide range of grain size.

Bagnold shows that for "driving sand" the wind velocity follows the logarithmic velocity profile, and further, the profiles for all winds converge on the same point near the bed, referred to as the "Focus". Experiments by Zingg (1953), Belly (1964), and Johnson (1965) verify the existence of the focus but show that its values differ with size and sorting of the sand.

The occurrence of a focal point in the velocity distribution profiles permits the friction velocity u_* , and hence the discharge j , to be calculated from a single measurement of wind velocity u_2 at height z_2 , i.e., the data from the wind recorder.

For quartz sand of 200μ diameter, the focus z_1 will be about 0.5 cm and u_1 about 2 m sec^{-1} . Then, taking z_2 as 10 m, and computing K from (2.6-5) to be 1.61, the transport relation of (2.6-4) becomes

$$i = gj = 2.9 \times 10^{-4} (u_2 - 2.0)^3$$

or

(2.6-6)

$$j = 2.95 \times 10^{-5} (u_2 - 2.0)^3$$

where i is in newton $\text{sec}^{-1} \text{ m}^{-1}$, j is in $\text{kg sec}^{-1} \text{ m}^{-1}$, u_2 is in m sec^{-1} and the coefficients are dimensional.

The dry mass discharge j is converted to volume discharge using relation (2.6-3). A more complete derivation of the transport relation and the method for converting wind anemometer measurements to transport rates is given in Bagnold (1941) and Inman et al (1966).

2.7 WEATHER, WAVES AND EXTREME EVENTS

The wave climate of a coastal section is manifest principally by the amount of the seasonal fluxes of wave energy and the direction from which the energy comes. Wave climate is a direct response to the fetch, duration and velocity of distant winds blowing over large ocean areas that generate swell waves along the coast; supplemented by local intense winds that generate wind waves. Although there is a correlation between wave climate and rainfall (and other weather patterns as well), the correlation is far from perfect, being mostly related to wind waves and rainfall which is associated with the frequency of frontal systems and cyclonic disturbances that pass locally.

Our knowledge of wave climate has been principally based on wave hindcast/forecast techniques developed during World War II and applied to the world oceans during the 30-year period between 1945 and 1975. Wave measuring techniques were mostly developed during the two decades of the 1950's and 1960's. Thus our knowledge of wave climate is mostly based on the unusually mild thirty year period between the mid 1940's and 1970's. Recent events suggest that these wave statistics may prove to be anomalously low in wave intensity and erroneous in wave direction (e.g. Seymour et al., 1984).

There are periods of many years and sometimes decades, when weather is climatologically stable and there are few strongly anomalous years. Such a period of climatological stable weather occurred during the 30 years between the mid-1940's and mid-1970's. Along the Pacific coast winters were moderate with low rainfall (Figure 2.7-1). Winds were moderate and predominantly from the west-northwest as shown by a wind rose for Oceanside, California (Figure 2.7-2). The principal wave energy was from Aleutian lows whose storm tracks, for the most part, did not reach southern California. Summers were mild and dry with principal wave energy coming from the southern hemisphere. There were no tropical storms during the summer and fall along the west coast. Yet there were many tropical storms in the years preceeding 1942 (Figure 2.7-3). The largest waves ever observed off this coast were from the tropical storms of September 1939 (Horrer, 1950).

We now appear to be entering a period of more variable climate with more extreme weather events (Namias, 1980; Karl et al., 1984; Seymour et al., 1984). Some years have been mild, others relatively severe. For example, the winter of 1976/77 was mild and dry along the west coast of the United States because the storm tracks missed the southwestern coast. However, there were major freezes in the eastern United States. The winter of 1977/78 was much wetter with flooding along the west coast. The winter of 1978/79 was very mild, as were the winters of 1980/81 and 1981/82. In contrast there was flooding along the west coast during

SAN DIEGO

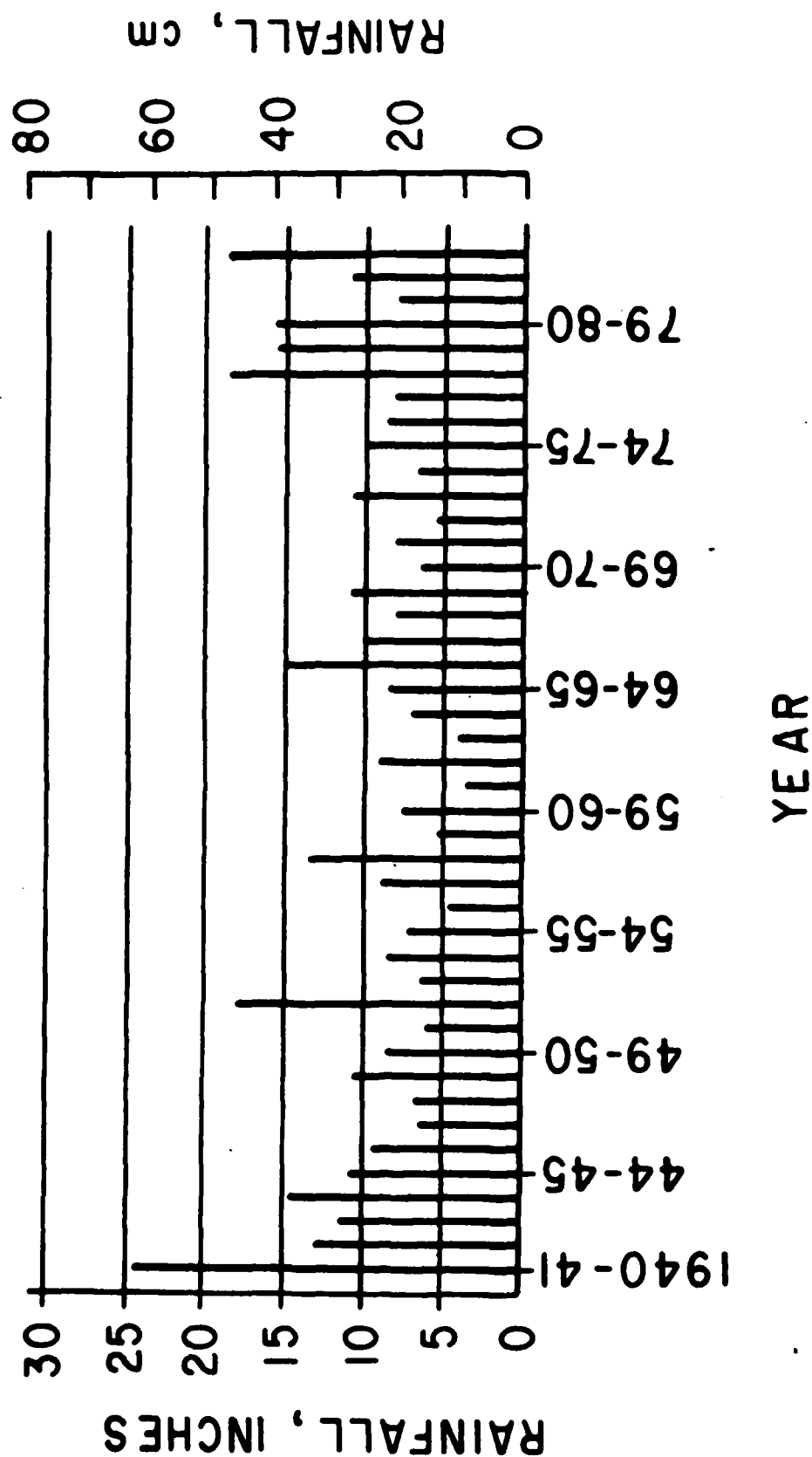


Figure 2.7-1. Annual rainfall at San Diego. Note the relatively low rainfall from 1945 to 1976/77 (from Inman and Jenkins, 1983).

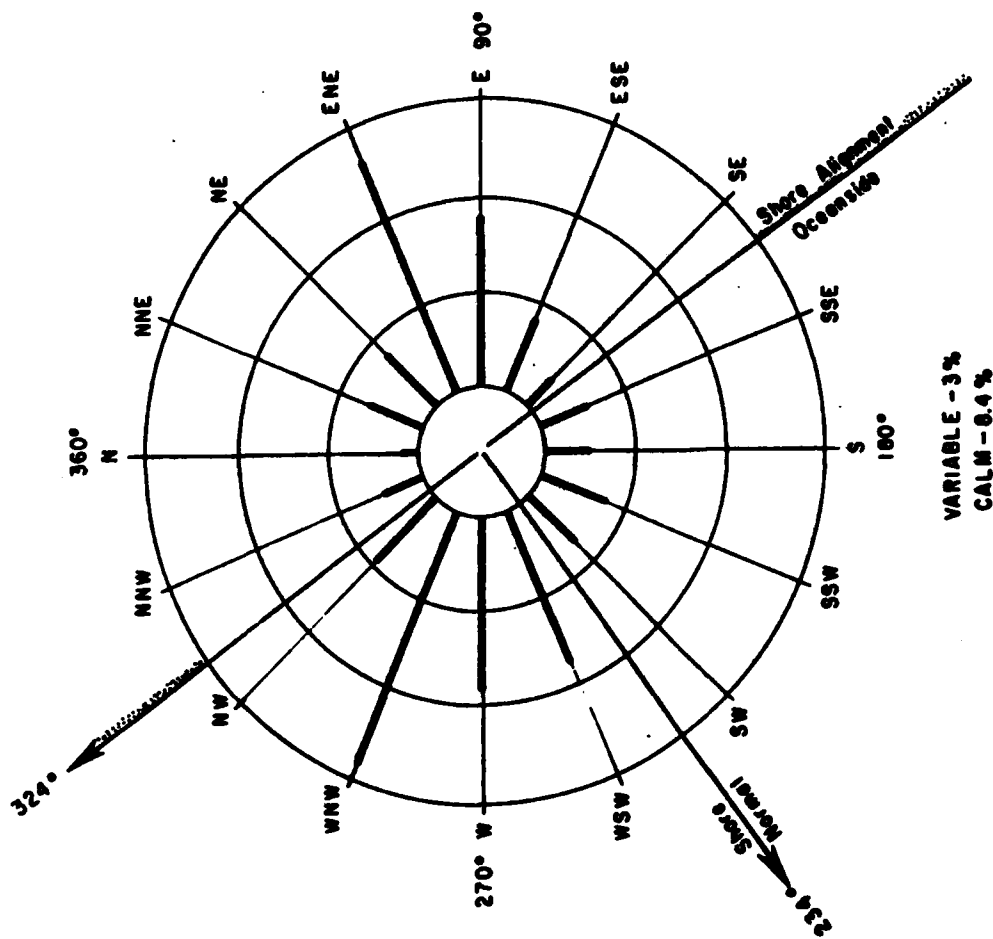


Figure 2.7-2. Wind rose at Oceanside (from U.S. Marine Corps, Camp Pendleton for years 1952-1961).

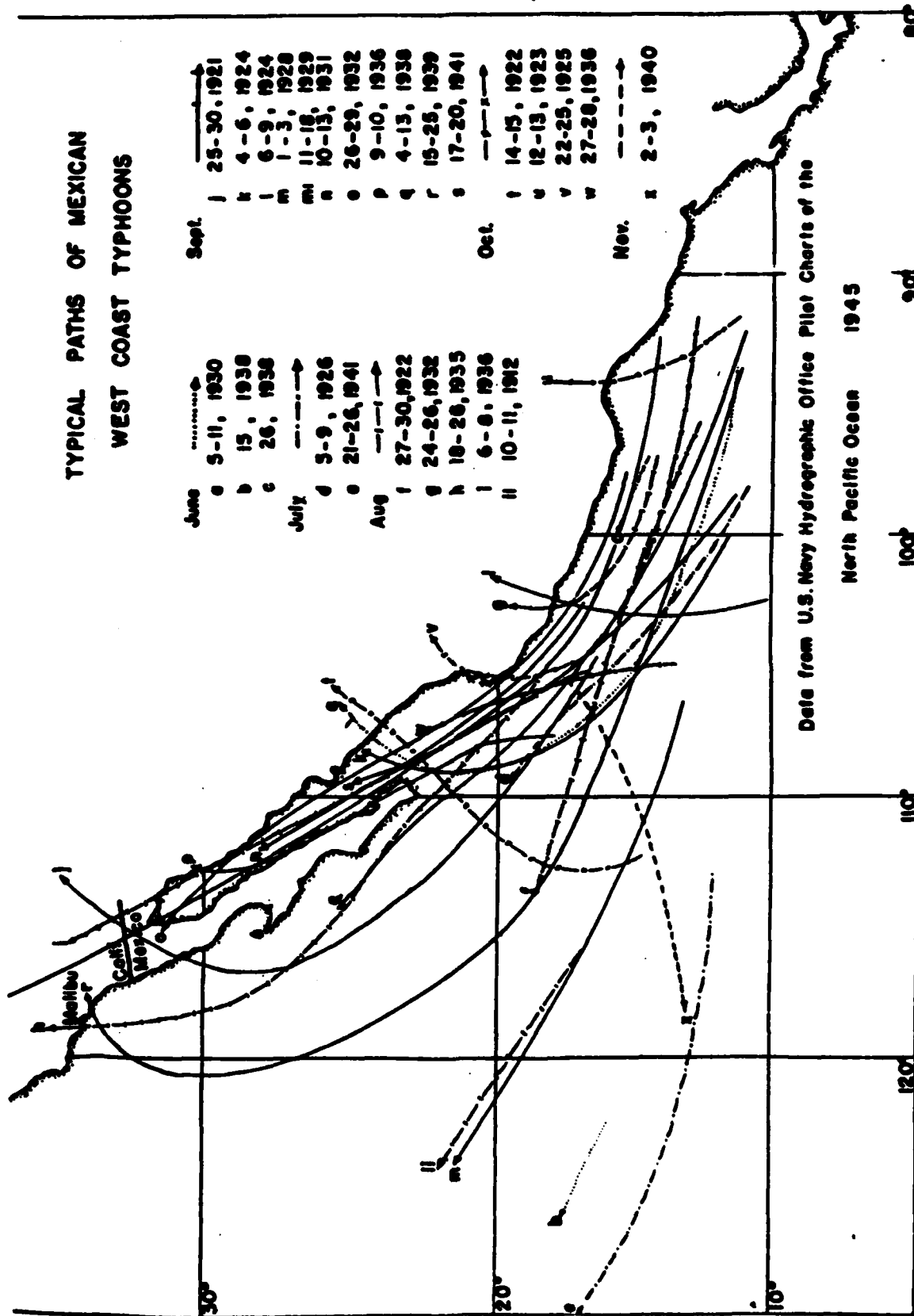


Figure 2.7-3. Typical storm tracks of west coast tropical cyclones. None in the Pacific have traveled north of about 25° latitude since 1941.

the winters of 1979/80 and 1982/83, and the Aleutian storm tracks traveled far to the south before approaching the west coast from the west-southwest (Figure 2.7-4). The two winters following the severe winter of 1982/83 were again quite mild. Addressing the unusual weather across the United States in recent years, Karl et al. (1984) find that statistically (Monte Carlo simulation) that the return period of occurrence is 1164 years. They conclude that "the recent variability is either a moderately rare event in a reasonably stationary climate, or it represents climate change."

This return to a more variable weather is the reason that the National Climate Act was passed with NOAA responsible for monitoring weather. Also, the National Research Council publication, "Storms, Floods and Debris Flows in Southern California and Arizona, 1978 and 1980" (487 pp.), was written to document the severe flooding during the winters of 1977/78 and 1979/80.

El Niño/Southern Oscillation

Large scale atmospheric/oceanic interactions drive climate changes with temporal scales of years that result in significant modifications of wave climate along the world's coasts. The "Southern Oscillation" is one of the best known, but not yet fully understood, phenomena of this type. It is an oscillatory exchange of atmospheric mass, as manifest by sea surface pressure, between the tropical east Pacific (centered near Easter Island) and the tropical Indian Ocean (centered near Djakarta). Associated with this exchange of mass are changes in the trade winds, the monsoons, ocean currents and sea surface temperatures that result in alternate periods of warm, wet (El Niño) low pressure areas off the tropical and temperate portions of the west coasts of the Americas (Julian and Chervin, 1978).

The southern oscillation phenomena have a spatial scale that extends nearly around the globe and from the tropics into temperate latitudes, and a temporal scale of 2 to 7 years with strongest coherence for reoccurrences with periods of 2.8 to 3.5 years (Julian and Chervin, 1978,

1200Z 16 Feb. 1980

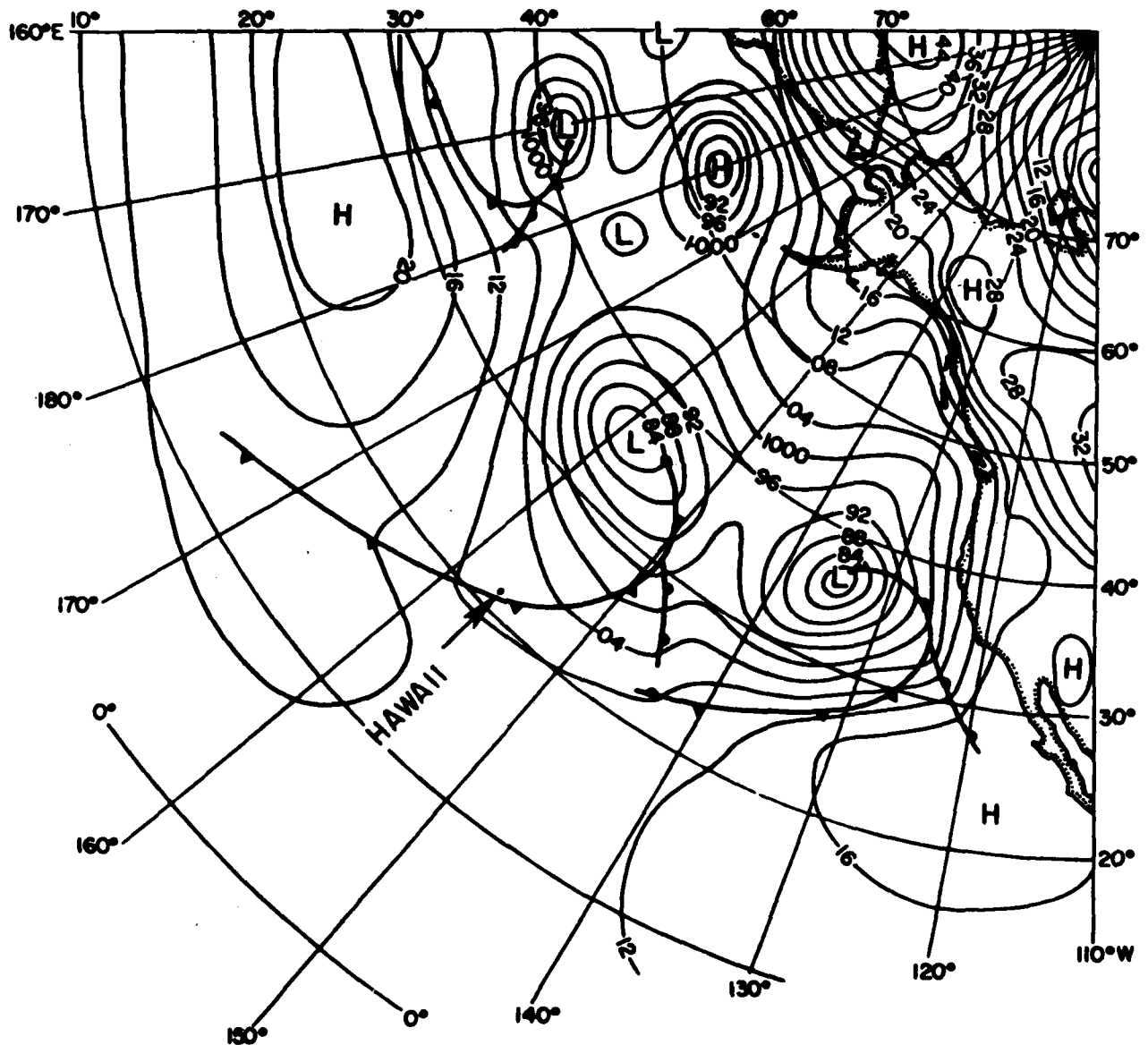


Figure 2.7-4. Surface pressure map showing a train of Hawaiian extra-tropical storms moving towards the coast of southern California in February 1980. Note that the front from the second low is passing over Hawaii.

Figure 2). The evidence suggests that the southern oscillation is periodic and accounts for most of the wet years during the 30 years of mild, dry climate from the mid 1940's through the mid 1970's along the west coast of the Americas (e.g. winters of 1951/52, 1957/58, 1965/66, 1968/69, 1972/73.) However, it would appear that the long periods of drought are terminated by unusually pronounced El Niño epochs as in 1977/78 and 1982/83.

The severe winter of 1982/83 was caused by an El Niño. The El Niño of 1982/83 was the greatest atmospheric/oceanic disturbance that has ever been recorded. The surface westerly trade winds actually reversed direction in some areas towards the end of 1982 (Kerr, 1983) while the winds aloft were abnormally strong and reversed (Winston, 1982). The change in the westerlies and the recession of the normal high pressure ridge caused abnormally warm water and high sea levels to occur along the west coast. Sea level was 20 cm higher in November 1982 than the average sea level for the preceeding 57 years from 1925-1981 as shown in Figure 2.7-5 (University of California, San Diego, 1985).

Climate

Southern California has a semi-arid Mediterranean type climate maintained by the relatively cool waters of the California current. Winters are mild, and rainfall along the coast is typically about 10 to 20 inches per year (Figure 2.7-1). Rainfall increases inland, attaining values of 20 to 60 inches per year at times in the coastal mountains.

Historical Storm Tracks

For the exposed harbors in the Southern California Bight, the wave statistics vary seasonally in response to winter storms from the Gulf of Alaska, and sub-tropical cyclone or southern hemisphere swell in summer. This observation is substantiated by spectral measurements due to Pawka et al (1976) and Seymour et al (1980; 1984). The winter waves generally have a net energy flux component to the south because they were generated by north

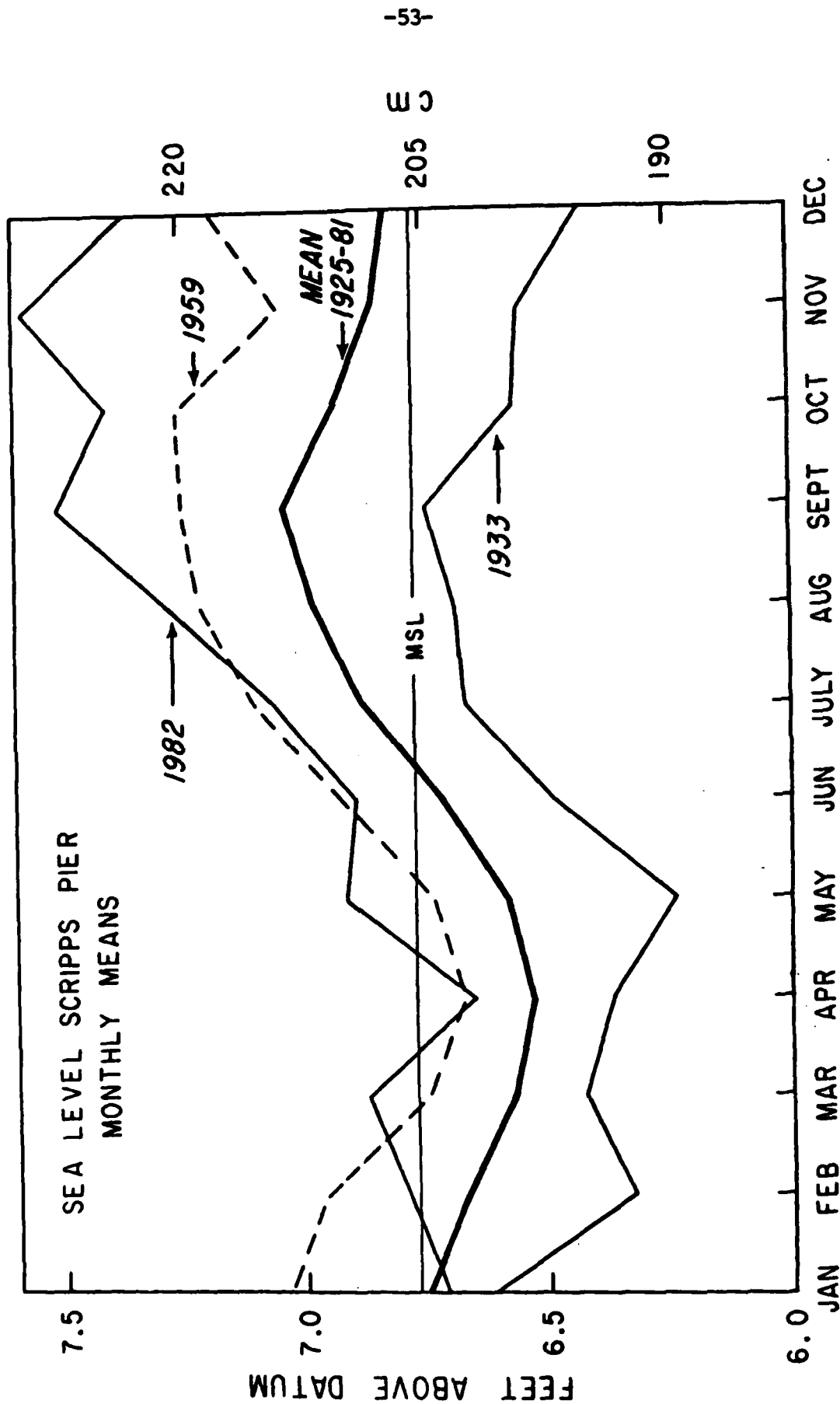


Figure 2.7-5. Monthly mean sea level at Scripps Pier, La Jolla, showing the mean annual fluctuation of ± 7.5 cm (heavy line) around mean sea level (MSL) averaged from 1925-1981. The curves of 1959 and 1982 show elevated sea level associated with El Nino epochs. Data from National Ocean Survey, NOAA, based on arbitrary datum.

Pacific storm-fronts passing close to southern California. Conversely the summer waves often show a net energy flux to the north from more distant storm sources, either southwest of Acapulco or from near Antarctica (Snodgrass et al., 1966). Therefore the net annual longshore component of wave energy flux determining the net littoral drift is the net of two competing seasonal sources. It is the overall climate trends of the hemisphere which determine which of these wave sources will dominate the wave climate for any particular year.

Comparing observations of Sverdrup and Munk (1947), Weigel (1959), Pawka et al (1976), Seymour et al (1984), it is apparent that wave statistics have greatly varied from year to year. Interestingly, this variability has accompanied a shift in characteristic weather patterns over the past 35 years. From 1945 until 1977 the Southern California Bight has experienced a temperate drought under the influence of a semi-permanent high pressure ridge, the Sierra High (Douglas and Fritz, 1972). The ridge remained strong and overdeveloped for more than 30 years preventing subtropical cyclones from tracking near enough into the southern window to have a dominant effect on the waves. Consequently the North Pacific storms dominated this period causing a net littoral drift to the south as evidenced in the skewness of sand spits, fillet beaches and lagoon entrances toward the south.

During the previous century there was a similar series of alternate periods of drought and wet. There appears to have been a wet period from about 1830 to 1841, followed by a period of drought from 1842 to 1883. Richard Henry Dana's (1909) very detailed accounts of wind and waves while sailing off this coast in the brig Pilgrim during 1834/35 make it clear that this was a wet period with local storms arriving abruptly from the southwest to southeast. Twenty four years later in 1859 he comments (p. 384) "the climate has altered;...the southeasters are no longer the bane of the coast." The long drought in the 19th century was ended by a protracted wet period (1884-1891) so intense that it has been remembered as "Noah's Deluge."

In fact, 30 year drought cycles are evidenced in tree rings of the bristle cone pine in southern California over the previous 800 years. Each of these droughts has been flanked by flood periods when the Sierra High was broken down allowing sub-tropical disturbances to travel into the Southern California Bight. The (1945-1977) drought was preceeded by a flood period of 1934-45 and was ended by another wet period 1978-1980 which caused the worst flooding in California history. The moisture in these transitional wet periods came from subtropical cyclones advancing up from the south as shown in Figure 2.7-3. The wind waves due to these violent warm storms cause reversals of the net littoral drift, shifting sand spits and reopening lagoon inlets to the north. However, because the transitional wet periods persist in time only briefly in comparison to the protracted droughts, the net littoral drift in the long term still appears to be to the south. However, these conclusions need to be quantified in greater detail by analysis of the available historical data. The very detailed measurements of Pawka et al (1976) and Seymour et al (1980) do not contain sufficient time histories to answer these questions of longer term climatic effects on the wave climate and net littoral drift.

Episodicity and the Budget of Sediment

As described earlier in Section 1.2, the concept of the budget of sand within the confines of a littoral cell is a useful aid in the interpretation of sources and transport paths in the cell. However to be valid, the episodicity in supply and wave-induced transport must be carefully considered.

The apparent inconsistency between the episodic nature of the supply of coarse sediment by rivers and the concept of a littoral "river of sand" that moves frequently and with some regularity along the coast, is resolved when the proper time scales are considered. Similarly, in computing sediment budgets, the usefulness of a mean annual sediment supply and a mean annual longshore transport rate is also resolved when averaged over the appropriate time scales. The "annual mean" situation may probably never occur because the dynamics of the wave-

induced littoral systems are more frequent than annual, while the occurrence of major coarse sediment supply by rivers is usually less frequent. The annual rates simply represent a middle ground between the longshore transport rates on beaches, which are individually calculated in mass or volume per second, and that of deposition at river mouths which is usually in volume per flood. As a rate, the latter may be more descriptively stated in terms of decades or centuries.

The concept of a budget of sediment that has differing spatial and temporal scales in supply, transport rates and sinks, is placed in proper perspective when considered in terms of the "littoral cell." Spatially, a littoral cell includes a complete cycle of littoral transportation and deposition including all sources, transport paths and rates, and sediment sinks (e.g. Inman and Frautschy, 1965). Temporally, the budget of sediment for a littoral cell must be averaged over sufficiently long time spans to be meaningful in terms of episodic events within the cell as well as fluctuations and trends in sediment amounts in sources, paths and sinks.

The occurrence and magnitude of river floods that bring sediment to the coast, and the changes in magnitude and trend of the littoral forcing functions (waves and winds) that transport the sediments along the coast, are both integrally related to changes in climate, as are local and regional changes in sea level. Thus the budget of sediment for a given littoral cell may be quite different from one decade or century to another, making the budget of sediments that is of interest to coastal dynamicists, coastal planners and engineers, and geomorphologists quite different in time span, magnitude, and to some extent in the kind of source, transport path, and sink.

3. REGIONAL OCEANOGRAPHY

3.1 SHELF CURRENTS

The purpose of this section is to provide an extremely brief overview of (1) major, large-scale coastal currents (i.e. California, Davidson, etc.) which constitute the "mean" seasonal circulation, and (2) tidal and "event scale" fluctuations (time scales 3 to 10 days) which are expected to be superimposed on the "mean" seasonal circulations.

3.1.1 *Seasonal mean currents*

Estimates of mean coastal currents based on hydrographic measurements, surface drifters, ship drift and the mean wind field constitute the "classical" picture of the California current. A thorough review of this literature is given by Hickey (1979) and Newberger (1982). Newberger (1982), which deals exclusively with the physical oceanography of the continental shelf, is a synthesis of several other summary reports (Maloney and Chan, 1974; Winzler and Kelly, 1977; Williams et al, 1981, Godshall and Williams, 1981). Each of these summaries reviews hundreds of scientific papers dealing with California shelf marine geology, chemistry, biology, climatology and physical oceanography. Extensive hydrographic surveys by the California Cooperative Fisheries Investigations group (CALCOFI) of the California current system are summarized in the atlas by Wyllie (1966). The rest of Section 3.1.1 is taken, with only minor editorial changes and comments, directly from Newberger (1982).

GENERAL DESCRIPTION OF THE REGIONAL CIRCULATION

The California current system is the eastern limb of the North Pacific gyre. It is driven primarily by the wind stress patterns over the North Pacific Ocean. Variability in ocean circulation in the California Current system is controlled primarily by interactions between the subtropical high pressure cell over the North Pacific Ocean and the atmospheric thermal low located over California/Nevada. Current flow is primarily southward in spring and summer in

response to southward-directed wind stress. Associated Ekman transport results in a circulation away from the coast in the near-surface layers, with concomitant upwelling of cold, salty water from below. This pattern of circulation with southward-directed flow and coastal upwelling is often called the "upwelling season" during the strongest period of upwelling in spring, and the "oceanic season" during the weaker upwelling of late summer and early fall (Skogsberg, 1936).

In late fall and early winter, northerly winds weaken and winds are at times from the southwest. This atmospheric wind regime produces a northward flow along the coast, the Davidson Current, hence, giving rise to a "Davidson Current Season" (Skogsberg, 1936). Offshore, the mean flow continues southward. The onset of this period is often rapid, accompanied by a rise in surface temperature and a deepened mixed layer (Winzler and Kelly, 1977). The end of the Davidson Current period and the onset of upwelling can also occur suddenly (Huyer et al, 1979). Along the coast, an undercurrent flows northward at depths below 200 m. When upwelling weakens or ceases, the core of the undercurrent propagates upward toward the surface, occasionally allowing northward flow to reach the surface (Sverdrup et al, 1942). When southward winds relax along the coast during fall, the undercurrent surfaces to form the Davidson Current. Some investigators believe that this undercurrent is a major flow component of the Davidson Current (e.g., Hickey, 1979).

In the Southern California Bight, a cyclonic eddy is often found, which includes a countercurrent along the coast and a split in flow at Point Conception, where one branch flows southwest joining with the California Current to form the western part of the eddy, and one branch flows northward along the coast as a narrow countercurrent.

There is much variation in nomenclature in the literature for these flows. In her comprehensive monograph on the California Current system, Hickey (1979) defines the constituents of the system as follows:

The California Current - The equatorward flow of water off the coast.

The California Undercurrent - A subsurface northward flow that occurs below the main pycnocline and seaward of the continental shelf.

The Davidson Current - A northward flowing nearshore current associated with winter wind patterns north of Point Conception.

The Southern California Countercurrent (also called the Southern California Eddy) - A northward flow in the Southern California Bight south of Point Conception and inshore of the Channel Islands.

THE CALIFORNIA CURRENT

The California Current is a wide, sluggish body of water characterized by relatively low temperature and salinity. It is about 600-1000 km in width, and 100-500 m deep (Wooster and Reid, 1963). Estimates of the transport are on the order of $10-12 \times 10^6 \text{ m}^3/\text{sec}$. The mean speed is about 12.5-25 cm/sec, although speeds as high as 50 cm/sec have been observed, primarily within eddies or meanders (Schwartzlose and Reid, 1972).

Peak velocities in the current occur in summer, following several months of persistent northwesterly winds (Schwartzlose and Reid, 1972). In the spring, the current moves closer to the coast, resulting in the disappearance of the Davidson Current, and sometimes even the counter-current (Wyllie, 1966).

In winter, the California Current moves farther offshore, as the Davidson Current develops along the coast. The flow in the California Current is not uniform, but rather is characterized by streaks of relatively high velocity interspersed with very slowly moving water. For example, off Cape Mendocino, two southward flows are formed: one about 125 km off the coast during February through October; the second, a broader flow located about 475 km offshore from February through September, when it is strongest (Hickey, 1979). This offshore flow tends to merge with the inshore flow in winter. Off Point Conception, a southward nearshore maximum

is found during April and May. Hickey (1979) has presented numerous cross sections of flow perpendicular to the coast which document these streaks from Cape San Lazaro to Washington.

THE CALIFORNIA UNDERCURRENT

The California Undercurrent flows inshore of the California Current northward along the continental slope. This current is not often continuous along the entire California Coast, but is particularly well developed in summer, with a width of 40-50 km (Winzler and Kelly, 1977). Mean speeds are low, on the order of 5-10 cm/sec (Schwarzlose and Reid, 1972). The Undercurrent region is characterized by high temperature and salinity, since it is a northward movement of equatorial water.

Wooster and Jones (1970) observed the Undercurrent off Baja California and noted that it could be distinguished from surrounding water by a high salinity maximum (34.3 ppt) occurring at temperatures between 8° and 11°C. Farther north, the high salinity core thinned to a narrow band just seaward of the 200 m isobath. Wickham (1975) determined that off Monterey, streaks of equatorial water occur between 200 and 500 m, interspersed with California Current water. These filaments are 10-20 km in width, maybe 50 km in length and may have speeds as high as 20-40 cm/sec toward the north, inshore of the California Current. These northward flowing filaments must be part of the Undercurrent.

THE DAVIDSON CURRENT

The Davidson Current is probably the surface expression of the Undercurrent north of Point Conception. The Davidson Current is found off California from mid-November to mid-February, when southerly winds occur along the coast. During the period of persistent northwesterly winds in spring and summer, northward flow is usually confined to deep water over the continental shelf, continental slope, and farther offshore.

Most of the evidence for this current comes from drift bottle data, as geostrophic currents are difficult to calculate nearshore. From the drift bottle records, Schwartzlose and Reid (1972) found that the Davidson Current attained speeds as high as 15-30 cm/sec. These drift bottle studies revealed that the Davidson Current is usually a continuous feature along the West Coast of the United States in winter, and not merely a succession of eddies. Off Point Conception, the Davidson Current has a width of about 80 km and widens to the north (Tsuchiya, 1975).

SOUTHERN CALIFORNIA COUNTERCURRENT/SOUTHERN CALIFORNIA EDDY

The Southern California Countercurrent is the inshore part of a large semi-permanent eddy which rotates cyclonically in the Southern California Bight south of Point Conception. The eddy is formed as the Countercurrent diverges at Point Conception, with flows moving toward the north and to the southwest. Geostrophic current measurements show that the Countercurrent occurs in all seasons, although it appears best developed in winter (Maloney and Chan, 1974).

Geostrophic speeds in the Countercurrent were determined to be on the order of 12-18 cm/sec (Sverdrup and Fleming, 1941). Schwartzlose (1963) found the eddy to occur during all months except March through May. Velocity maxima in the Countercurrent during winter as high as 35 to 40 cm/sec have been observed (Maloney and Chan, 1974).

Tsuchiya (1980) has noted that the circulation in this region is more complex than anywhere else off California. He notes that inshore of a line connecting Point Conception and Cortes Bank, the flow is northerly, to the west it is southerly. This line, then, roughly delineates the center of the Eddy. Shoreward of the Countercurrent, southeast flow is often present. However, Tsuchiya (1980) notes the following complications in the flow pattern:

The large Eddy contains smaller eddies of varying scale (Schwartzlose, 1963).

The California Current moves inshore in April and May, often eliminating the Countercurrent. In other months, the Countercurrent may increase in intensity and displace the California Current offshore.

SEASONAL TRANSITIONS

Huyer et al (1979) noted that the 1973 and 1975 transitions from the winter ("Davidson season") to the summer flow ("upwelling season") regimes occurred within a period of days off Oregon, due to strong equatorward wind stress events. Thus, off the California coast, the transition from winter to spring circulation patterns could also be abrupt. Huyer et al (1979) also noted that during these two years, adjusted coastal sea level was a good indicator of the time of this transition, as a rapid drop in sea level accompanied the onset of upwelling circulation. Although they did not discuss it, their data showed a sharp increase in adjusted coastal sea level in late October, 1973 which apparently signaled the transition to winter circulation (the onset of the Davidson Current) and which was forced by a strong poleward wind stress event. They unfortunately did not have accompanying current meter data during this transition to determine if a large increase in poleward flow accompanied this sea level change, but it is probably a safe assumption that it did. Williams et al (1981) used time series of adjusted coastal sea level to estimate the times of both spring and fall transitions for four locations on the California coast (Table 3.1.1). Most transitions were marked by sharp changes in sea level, and the week number of the transition could easily be estimated. In a few cases, no transition time was detectable at all. The mean and standard deviation of the transition time, in weeks, is given in Table 3.1.1-1. Both transition times occur earlier in the year going southward along the California coast. The spring transition actually occurs in winter off the southern California coast. Thus, nearshore southward flow begins earlier in the year in the Southern California Bight. This conclusion is supported by equatorward-traveling drifters (Appendix D in Newberger, 1982). The fall transition actually occurs in summer in the

Table 3.1.1-1 Approximate times of occurrence of the spring and fall transitions at four locations along the California coast, 1970 through 1978 (Williams et al, 1981).

Year	Station Pair	Spring Transition	Fall Transition
1970	Arcata/Crescent City San Francisco/San Francisco Pt. Mugu/Rincon Is. Imperial Beach/San Diego	Early Apr. Early Apr. Mid-Apr. (Late 1969)	Late Oct. Early Nov. Mid-Aug. Early Oct.
1971	Arcata/Crescent City San Francisco/San Francisco Pt. Mugu/Rincon Is. Imperial Beach/San Diego	Late Jan. Mid-Feb. Early Feb. Early Dec. (1970)	Early Dec. Early Sep. Mid-July Late July
1972	Arcata/Crescent City San Francisco/San Francisco Pt. Mugu/Rincon Is. Imperial Beach/San Diego	Late Apr. Early Apr. Early Mar. Late Nov. (1971)	Early June Mid-July Late July Mid-July
1973	Arcata/Crescent City San Francisco/San Francisco Pt. Mugu/Rincon Is. Imperial Beach/San Diego	Late Mar. Mid-Mar. Late Mar. Late Mar.	Mid-Nov. Mid-Dec. (none) (none)
1974	Arcata/Crescent City San Francisco/San Francisco Pt. Mugu/Rincon Is. Imperial Beach/San Diego	Mid-Apr. Early May (none) (none)	Late Nov. Mid-Sep. Late July Early Aug.
1975	Arcata/Crescent City San Francisco/San Francisco Pt. Mugu/Rincon Is. Imperial Beach/San Diego	Late Mar. Late Mar. Mid-Jan. Mid-Jan.	Mid-Jan. (1976) Mid-Jan. (1976) (none) Early Aug.
1976	Arcata/Crescent City San Francisco/San Francisco Pt. Mugu/Rincon Is. Imperial Beach/San Diego	Mid-Mar. Early Mar. (none) Mid-Feb.	Late Sep. Late July Early July Late June
1977	Arcata/Crescent City San Francisco/San Francisco Pt. Mugu/Rincon Is. Imperial Beach/San Diego	Mid-Mar. Mid-Mar. Early Mar. Early Mar.	Early Oct. Mid-Sep. Mid-Aug. Late July
1978	Arcata/Crescent City San Francisco/San Francisco Pt. Mugu/Rincon Is. Imperial Beach/San Diego	Early May Early May Late Mar. Late Mar.	Early Oct. Late Sep. Mid-Aug. Mid-Aug.
1970- 1978 Mean	Arcata/Crescent City San Francisco/San Francisco Pt. Mugu/Rincon Is. Imperial Beach/San Diego	Late Mar. Late Mar. Early Mar. Late Jan.	Late Oct. Late Sep. Late July Late July
1970- 1978 Standard Deviation (weeks)	Arcata/Crescent City San Francisco/San Francisco Pt. Mugu/Rincon Is. Imperial Beach/San Diego	9 8 3 3	4 4 4 7

Southern California Bight. Most surface drifters released nearshore in the Bight from July through September traveled poleward.

The standard deviation of the spring transition time decreased from about nine weeks off Northern and Central California to about four weeks off Southern California. The standard deviation of the fall transition time was four weeks from northern California southward to near Point Conception, and seven weeks near San Diego. Thus, significant interannual variability exists in the time of both transitions.

ESTIMATES OF SEASONAL MEAN CURRENTS

One objective of Williams et al (1981) was the production of maps of mean current vectors on a regular grid for application in pollutant spill trajectory models. Inputs to the preparation of these maps include the currents computed from ship drift, geostrophic currents, wind drift currents derived from the mean wind stress, and currents from surface drifters.

Examination of these data sets show that insufficient observations of any one type exist to prepare reliable circulation charts on a monthly basis. Hence, the data was combined according to the distinct circulation seasons, after Skogsberg (1936), as follows: The Davidson Current Period, December-January; The Upwelling Period, May-June-July; The Oceanic Period, September-October. Transition months which may fall into one of two seasons are not included in the average as they increase the "noise" in the data fields. Considerable semi-empirical adjustments had to be made to the calculated (from mean wind stress and geostrophy) mean flows in order to obtain even rough agreement with ship drift and previous observations (Williams et al, 1981). Calculated mean surface currents (speed and bearing are shown in Figures 3.1.2-1,2,3. During December-January (Figure 3.1.3-1) mean currents are everywhere less than 0.3 kt (.15 m per sec) and in most locations less than 0.2 kt (.10 m per sec). Between Cape Mendocino and Point Conception, the flow is highly variable, but in most areas exhibits a component of flow toward the coast. This variability agrees with the low persistence seen in the

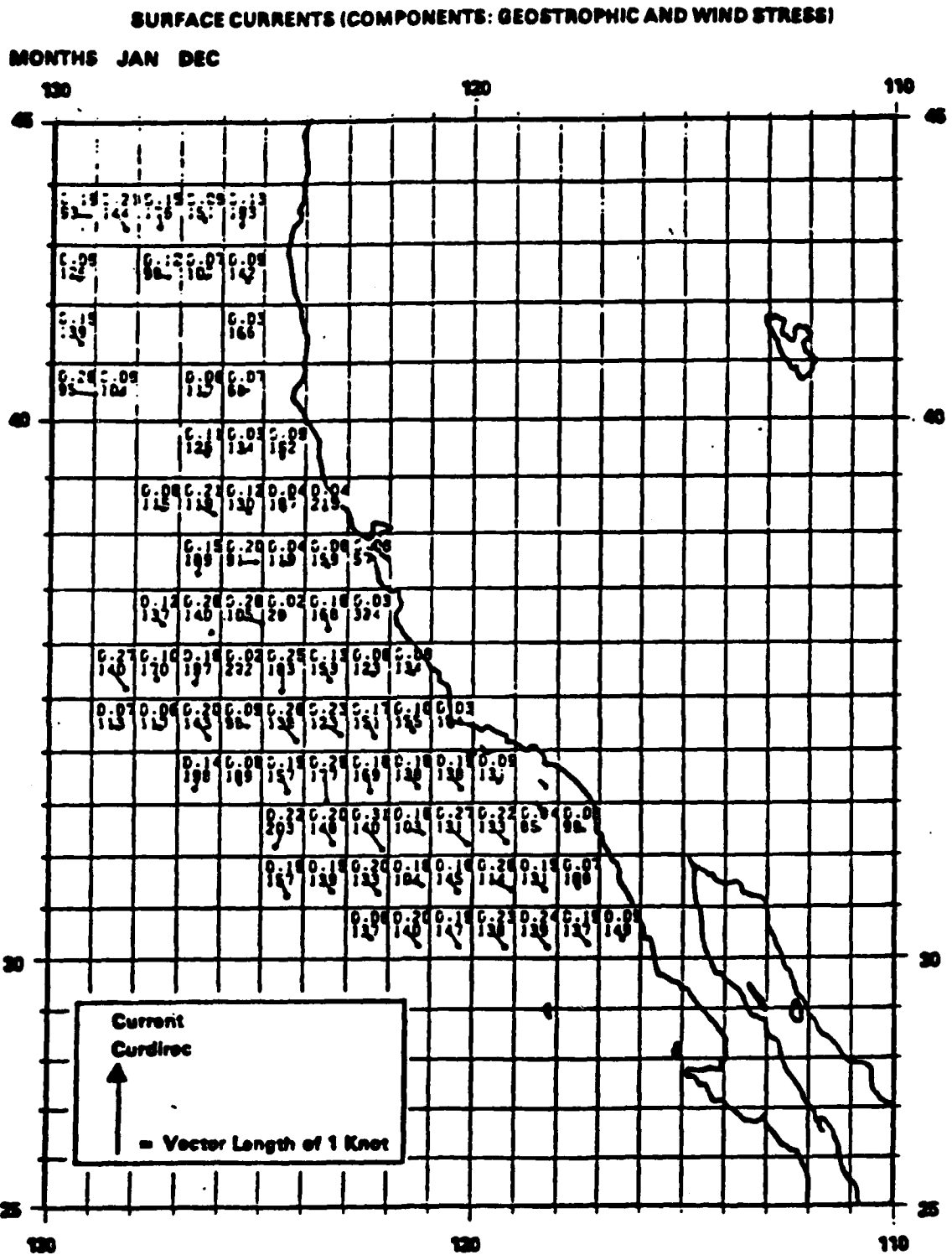


Figure 3.1.1-1 Surface currents during Dec-Jan (Components: Geostrophic and Wind Stress) (Williams et al. 1981)

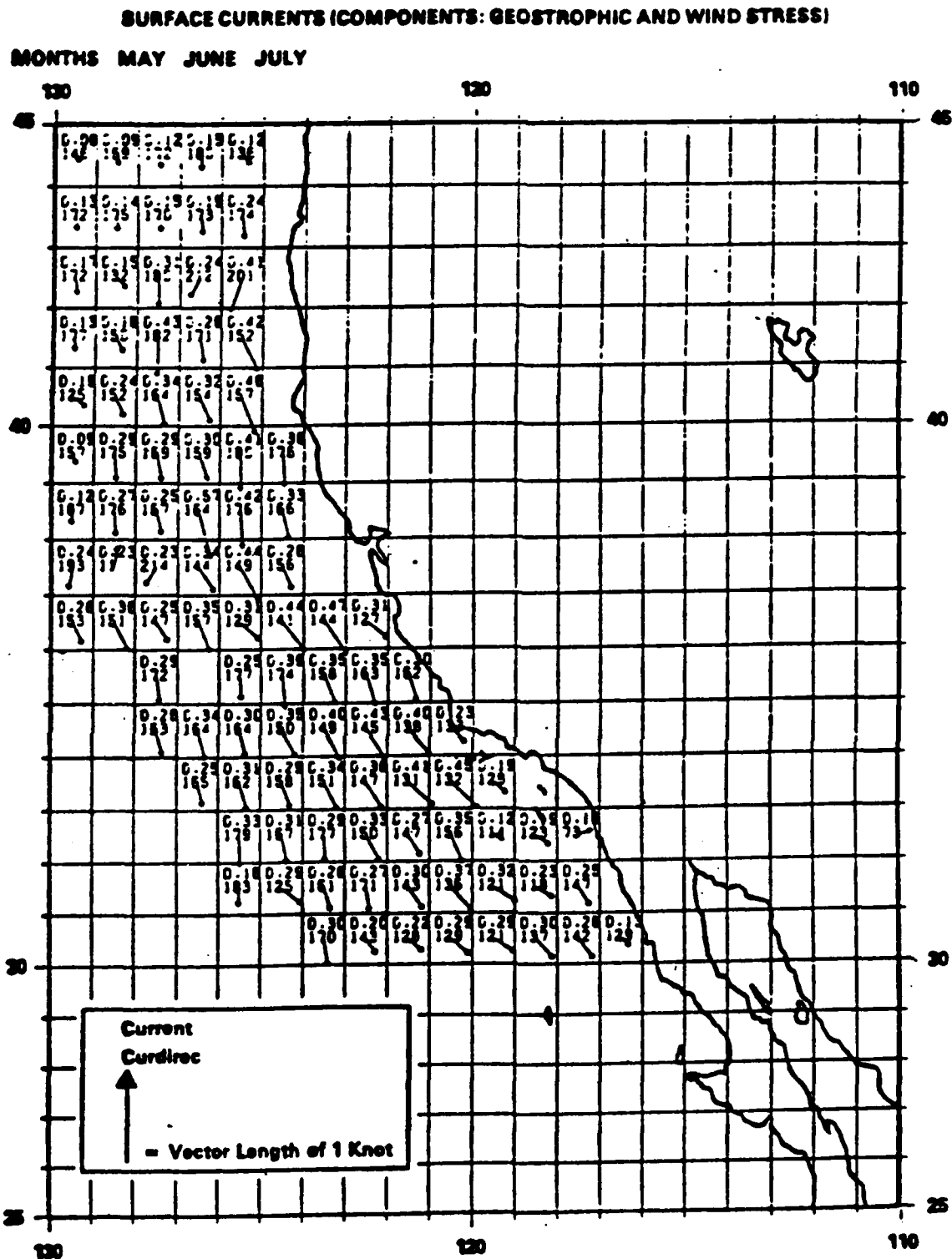


Figure 3.1.1-2 Surface Currents during May-July (Components: Geostrophic and Wind Stress) (Williams et al, 1981)

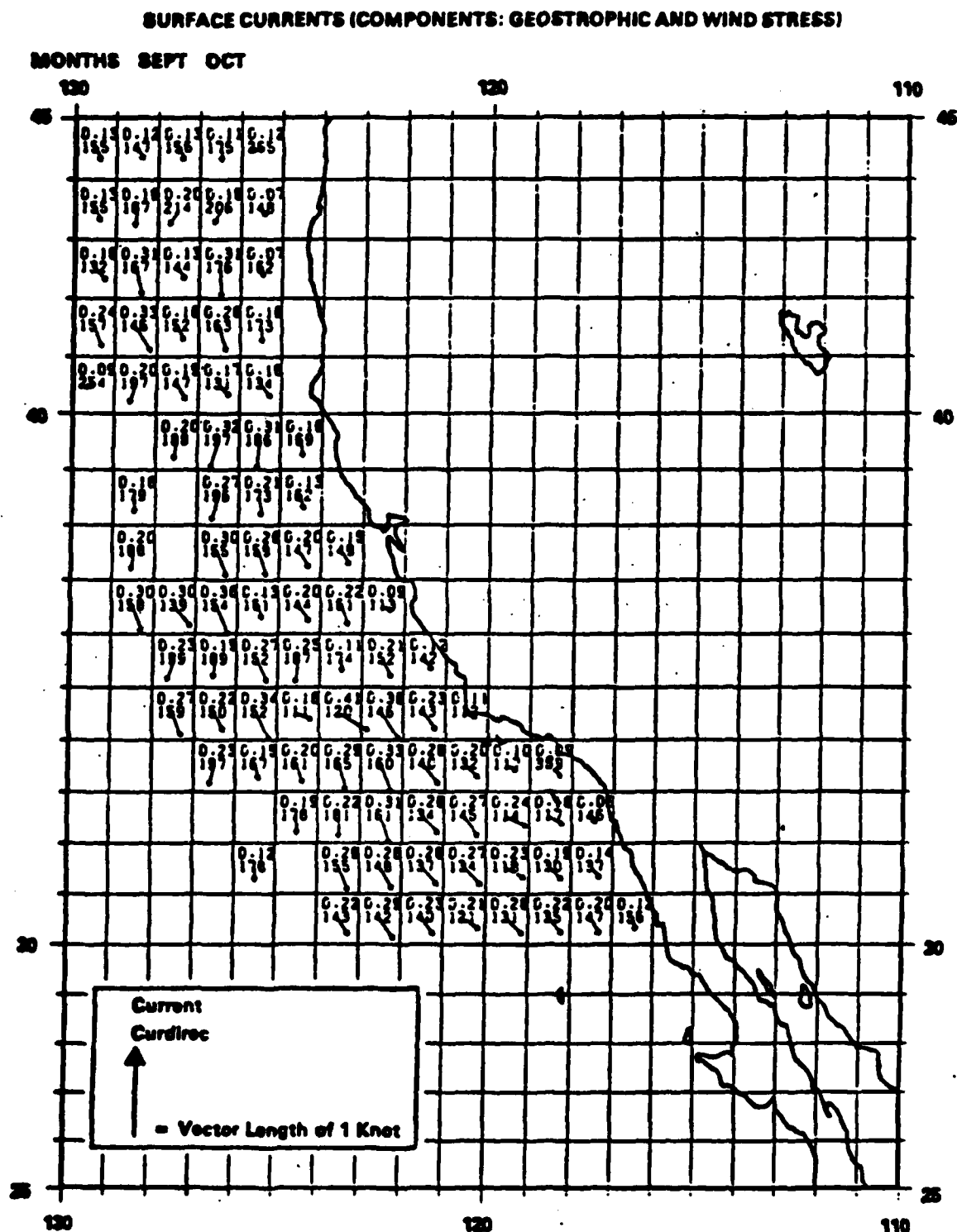


Figure 3.1.1-3 Surface Currents during Sep-Oct (Components: Geostrophic and Wind Stress) (Williams et al, 1981)

ship drift charts for this region. South of Point Conception, a fairly coherent mean flow to the southeast prevails. This procedure for 1° square summary areas does not resolve the Davidson or Countercurrent Systems; yet there is some indication on the chart of mean northward flow off San Francisco.

In May, June, and July, the geostrophic/wind stress current chart (Figure 3.1.3-2) indicates strong southward flow with an average speed of roughly 0.3 kts (.15 m per sec). There is a suggestion of the turn-in of current off San Diego, forming the lower half of the Southern California Eddy. The ship drift current chart for this period shows general agreement in speed and direction although the flow field from the ship drift exhibits a larger cross isobath angle away from the coast.

The geostrophic/wind stress current chart for September-October (Figure 3.1.3-3) indicates flow generally toward the southeast, and weaker than May-July, but stronger than December-January. Northward flow is indicated along the coast in the Southern California Bight. The ship drift chart shows similar patterns.

Hickey (1979) compared the above classical picture with recent current meter observations. The greatest difficulty in comparing the different types of data stems from their vastly different spatial and temporal scales. Current meter arrays give excellent temporal resolution, but poor spatial coverage. Hydrographic and drift methods yield infrequent snapshots of the currents (Winant, 1979). Within the limitations imposed by such problems, Hickey (1979) finds general agreement in the long-term mean circulation deduced from the two methods. An additional important conclusion of Hickey (1979) is that seasonal large-scale current fluctuations are correlated with seasonal fluctuations in the longshore component of wind stress and wind stress curl.

3.1.2 *Fluctuating (tidal and wind-driven) currents*

Time series from moored current meters show that fluctuations from the mean are almost always larger than the mean itself. There are also very substantial variations in the fluctuating field measured with sensors separated in either the vertical or horizontal directions. The mean fields described above could only appear in moored current meter records which have a great deal of temporal (and perhaps spatial) averaging. A typical example of inner shelf fluctuating currents and their vertical variation is shown in Figure 3.1.2-1. This data (hourly averages) was collected from a vertical string of current meters deployed in 70 m of water due west of Point Conception (Brink et al, 1985). Removal of currents at tidal frequencies (and higher) still leaves a time series with relatively large fluctuations about the mean (Figure 3.1.2-2). There is, of course, a large and growing literature which attempts to relate these current (and also temperature) fluctuations to meteorological forcing (primarily wind) and other quantities of dynamical significance (e.g. pressure gradients associated with a sloping sea surface). Recent review articles with emphasis on the west coast include Allen (1980) and Winant (1979, 1980).

TIDAL CURRENTS

Currents in the tidal band (12-24 hr) typically contribute a substantial fraction of the total observed variance (not including surface gravity waves). Typical shelf tidal currents have peak longshore velocities of roughly 20 cm/sec, although considerable amplification occurs near larger bays. Although tidal elevations are very well predicted, tidal currents are not. This has been shown in the transition zone between oceanic and southern California coastal waters (Munk et al, 1970) and also at various locations on a transect across the southern California shelf (Winant and Bratkovich, 1981). This result has been ascribed to baroclinic effects. However, even vertically averaged tidal currents (which should filter baroclinic effects) do not show high correlation with tidal elevations (Figure 3.1.2-3). The distinct fortnightly beat in the sea level fluctuations is not present in the currents.

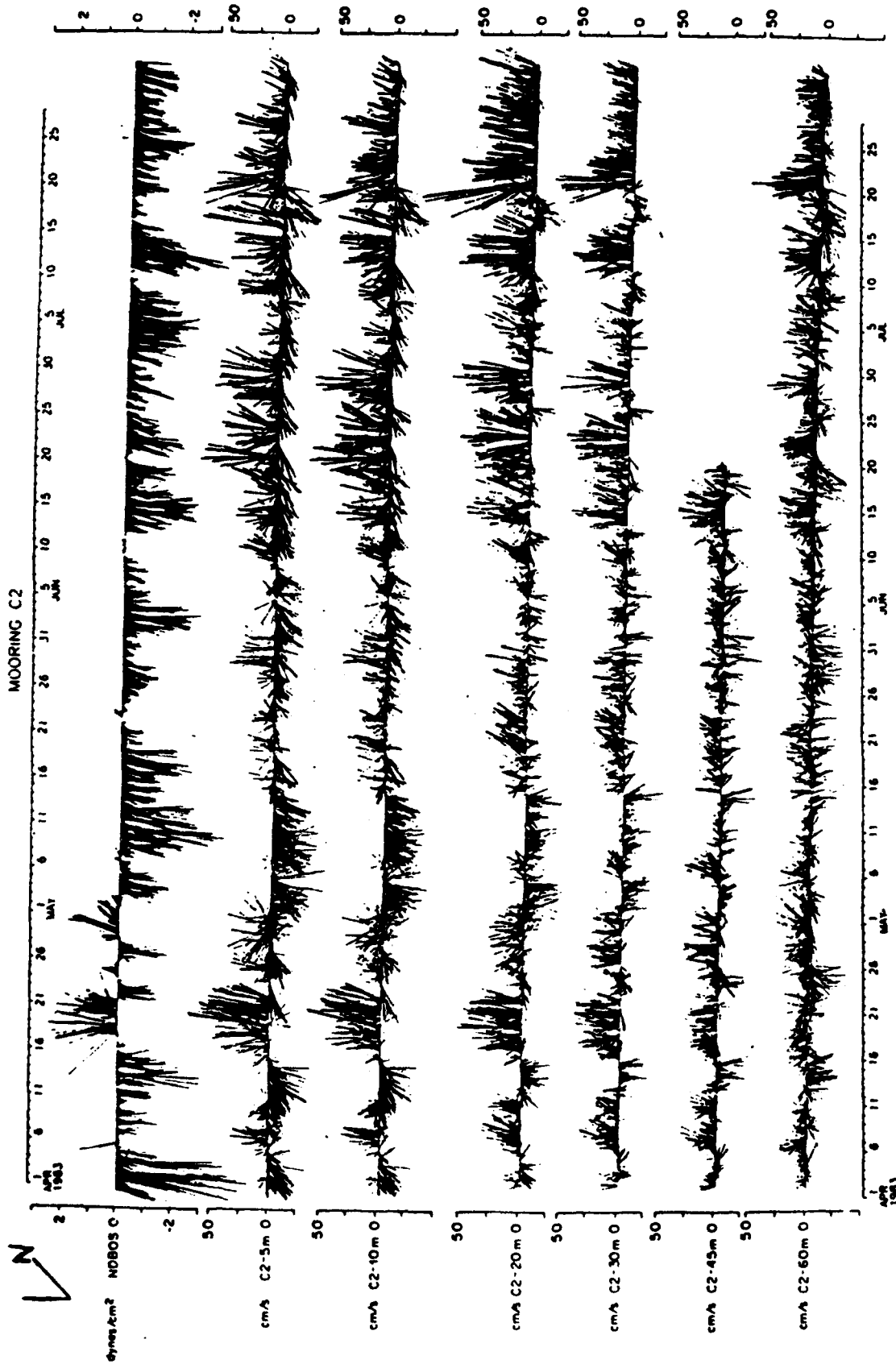


Figure 3.1.2-1 Hourly wind stress (upper panel) and currents (water depth 70 m, instrument location in water column indicated) due west of Point Conception (Brink et al, 1985).

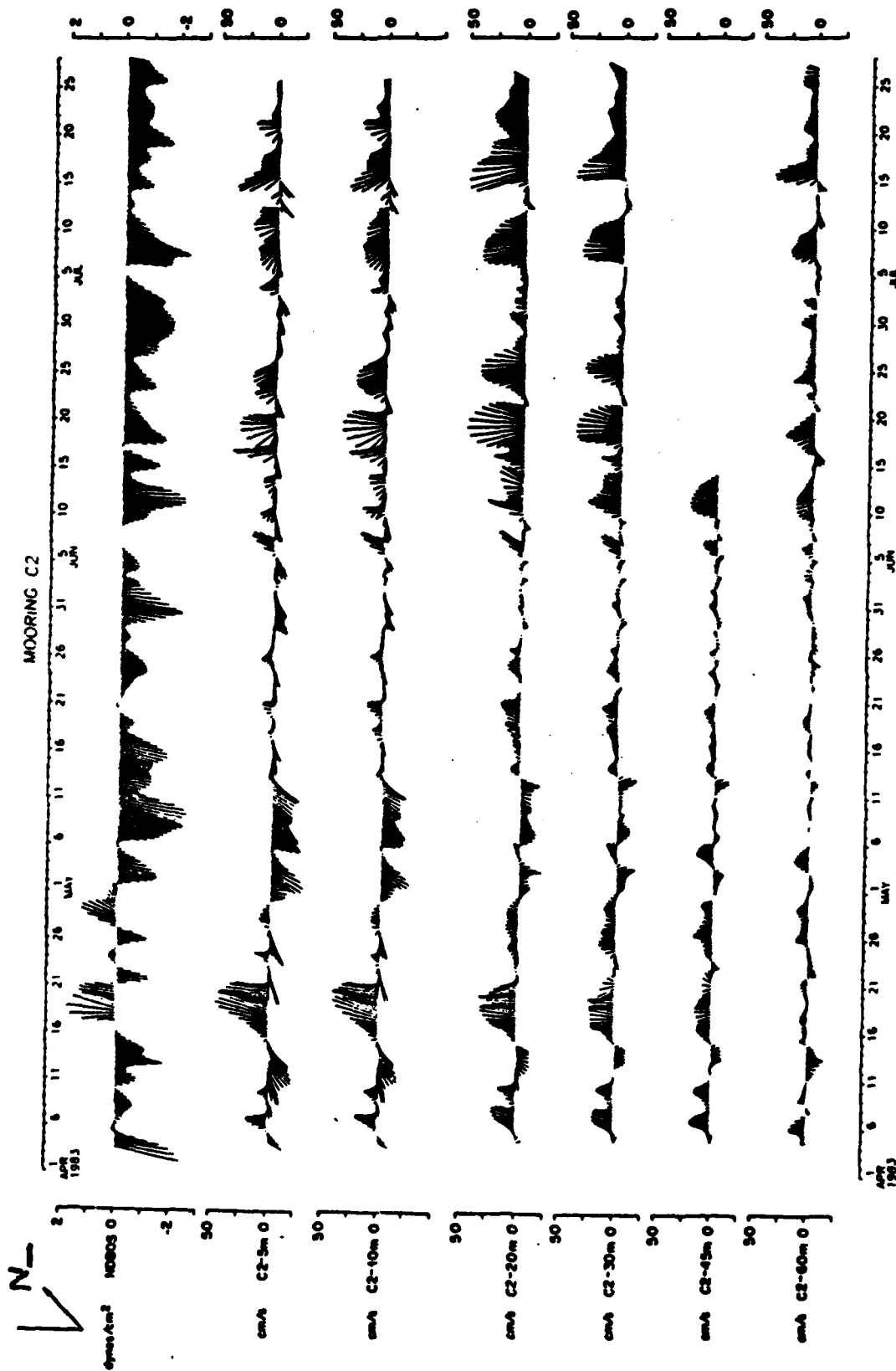


Figure 3.1.2.2 Low-passed (subtidal) version of Figure 3.2.1-1 (Brink et al, 1985)

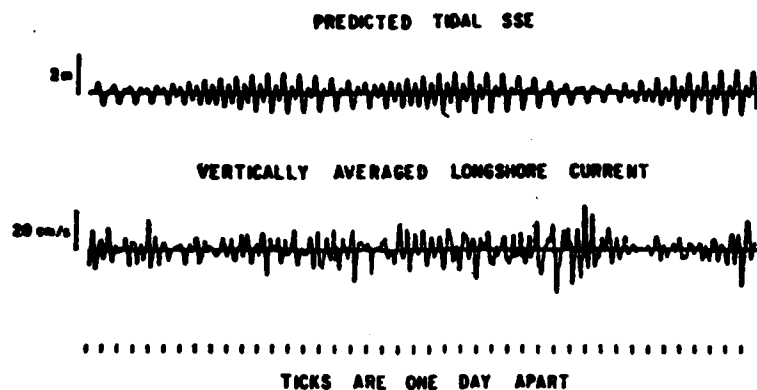


Figure 3.1.2-3 Comparison of predicted tidal sea surface elevation and tidal frequency band vertically averaged longshore currents, 21 October-3 December 1978 off Del Mar, California (Winant and Bratkovich, 1981).

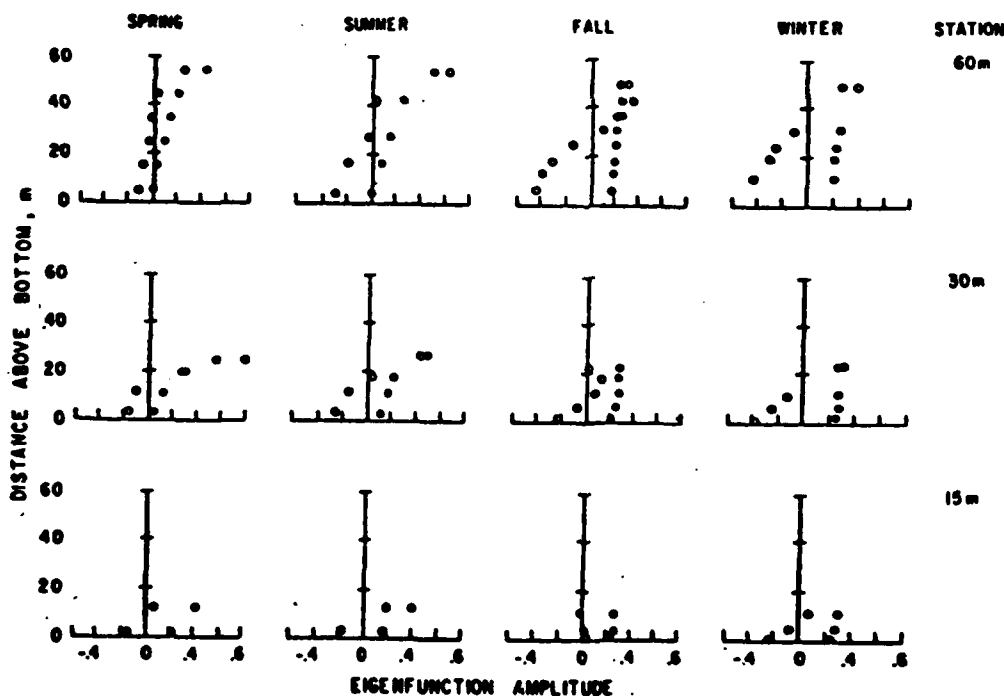


Figure 3.1.2-4 Distribution of the amplitude of the largest eigenvectors of the longshore (●) and cross-shelf (○) tidal-band (periods between 36 and 4 h) currents off Del Mar, California (Winant and Bratkovich, 1981).

The vertical structure of tidal currents, and the seasonal variability of the structure was investigated by Winant and Bratkovich (1981). They used data from current meter strings deployed off Del Mar in depths of 60, 30 and 15 m; with about 7, 5, 2 instruments on each string, respectively. Figure 3.1.2-4 shows the distribution of the amplitudes of the largest eigenvector for both longshore and cross-shore velocity components. In oversimplified terms, the largest eigenvector structure represents a coherent spatial pattern which, when multiplied by some function of time, reproduces the maximum possible amount of the original time series variance. The longshore current is barotropic (no sign reversals) during all seasons and shelf locations, although there is substantial vertical shear during spring and summer. The cross-shore flow is always baroclinic; flows near top and bottom of the water column have opposite signs. Longshore current variance in the tidal band does not vary significantly as a function of season, but the cross-shelf variance does, reaching a minimum in the winter when stratification is weak (Winant and Bratkovich, 1981). Although these measurements were obtained off Del Mar (very southern California) they are probably valid qualitative descriptions of inner shelf, open coast tidal flow elsewhere in the study region.

EVENT SCALE WIND FORCED CURRENTS

Allen (1980) discusses similarities and differences between flows observed on various continental shelves. Although significant differences exist, a feature common to most shelf flows is a response of currents to longshore directed coastal winds. A strong correlation between longshore winds and longshore currents is obvious in Figure 3.1.2-5. Some correlation is also apparent in the first half of the record shown in 3.1.2-2. Event scale currents tend to be very strongly polarized with currents following local bathymetric contours in shallow water. The polarization is less strong with increasing offshore distance (Figure 3.1.2-6). Such polarization is almost always observed. Note that sea level can also fluctuate substantially (~ 20 cm) and coherently with wind events (Figure 3.1.2-5). As soon as longshore motions develop, sea level

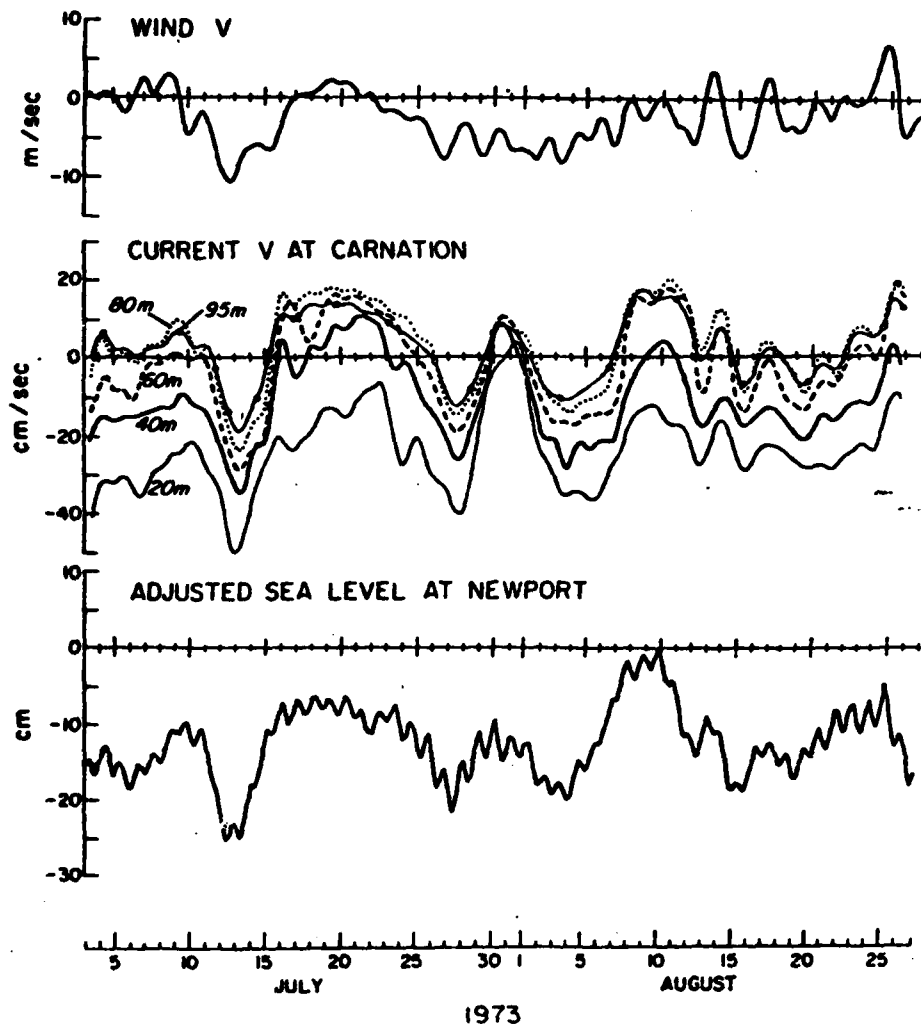


Figure 3.1.2-5 Low-pass-filtered north-south (alongshore) component of wind and currents, and adjusted sea level off Oregon during July and August 1973 (Kundu et al, 1975). The currents were measured at 45° 16'N, water depth 100 m, at the depths indicated (Allen, 1980).

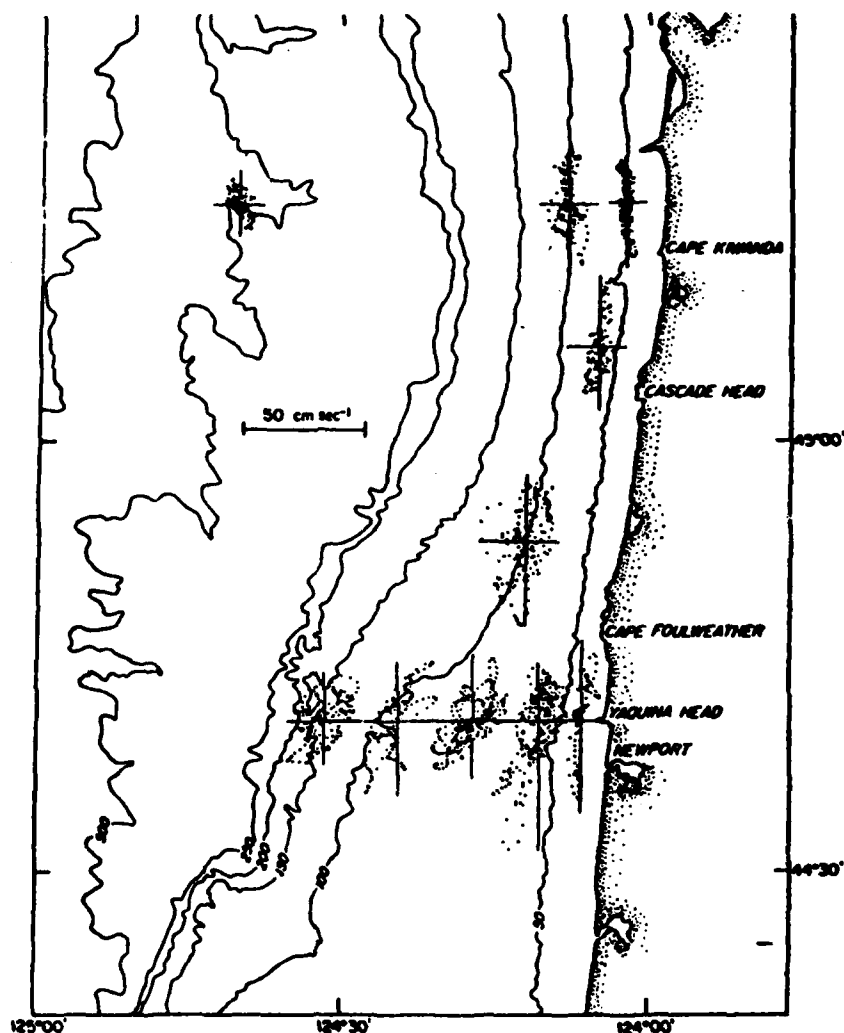


Figure 3.1.2-6

Scatter diagrams of horizontal velocity fluctuations (mean values subtracted) superimposed on a bathymetric contour map, with the origin of the diagram at the horizontal location of the measurements (Kundu and Allen, 1976). The currents were measured at about 40 m depth during the summer of 1972 (the six southern diagrams) and during the summer of 1973 (the four northern diagrams). The low-pass-filtered current fluctuations are plotted as a point every six hours. Depths are in meters (Allen, 1980).

fluctuations are induced which create cross-shore pressure gradients to balance the cross-shore Coriolis forces arising in the cross-shore momentum balance (Winant, 1980).

Lentz (1984) presents a detailed analysis of event scale (sub-tidal) longshore flows observed off Del Mar. The inner shelf is primarily wind driven while the outer shelf is primarily driven by longshore gradients in sea level. In both cases the driving term is apparently balanced by bottom friction. The Southern California Bight is a region of relatively light winds. North of Point Conception winds are stronger and may dominate (Figure 3.1.2-5). Allen and Smith (1981) find that off Oregon the flow is primarily wind driven. There are also some suggestions that event scale waves may propagate northward along the west coast, so that both local and remote winds can play roles in generating currents.

Perhaps the most important points here are that wind-driven (event scale) shelf flows are quite energetic (50 cm/sec is commonly attained in the upper portion of the water column), can have either sign, and are not predictable. The dynamics vary according to the strength of the winds relative to other effects.

Shelf currents clearly are strong enough to transport very large amounts of sediment, but meaningful transport estimates require a much fuller understanding of the complicated bottom boundary layers which occur under the combined influence of oscillating gravity waves and longer time scale wind-forced events.

Very significant advances in both the quantity and quality of observations of California shelf flows are being made. The amount of effort and money expended on recent California shelf dynamics experiments (e.g. OPUS, CODE, etc.) equals or exceeds that spent on nearshore processes experiments and monitoring programs. Existing summary reports such as Newberger (1982), Williams et al (1981), Winzler and Kelly (1977) are largely concerned with the "classical" seasonal mean flows. Unfortunately it is beyond the scope of the present work to review the many recent observational and theoretical studies concerning shelf flows in the study area.

3.2 DEEPWATER WAVES (UNSHELTERED BY ISLANDS)

3.2.1 Generation

Ocean waves off the coast of southern California fall into three main categories: northern hemisphere swell, consisting of waves generated in the northern hemisphere but which arrive in southern California waters after leaving the generating area; southern hemisphere swell, consisting of similar waves generated south of the equator; and sea, consisting of waves generated within the local area (Munk and Traylor, 1947; Scripps, 1947).

Northern Hemisphere Swell

Winds which produce northern hemisphere swell are usually associated with one of the following meteorological situations (Marine Advisers, 1961a):

1. Japanese-Aleutian storms, which move from west to east across the North Pacific in relatively high latitudes, often stagnating in the Gulf of Alaska. Waves generated by these storms reach most of California but usually decrease in energy southward along the coast. Occasionally, especially during winter and spring, this storm track shifts southward and the maximum wave heights occur at central or southern California latitudes. These extratropical cyclones are the most important source of severe waves reaching the California coast.
2. Hawaiian storms, which move from west to east in middle latitudes, generally originating in the vicinity of the Hawaiian Islands. These occur less frequently than the Japanese-Aleutian storms.
3. Typhoons in the western North Pacific. Swell from these storms usually is not significant at the California coast.
4. Tropical hurricanes which commonly develop off the west coast of Mexico, move in a westerly direction at first, and then usually recurve to the north and northeast. These occur almost exclusively during the months of July through October. The resulting swell rarely exceeds 2 m, but a strong tropical storm will occasionally move far enough north to cause

destructively high waves in the area under consideration. The storm of September 1939, which passed directly over southern California and caused very high waves, is an example, although the maximum waves of that system should be classed as "sea" rather than "swell" since they occurred when the generating wind system was active over southern California waters.

5. Steep pressure gradients around the Pacific high pressure cell. Such gradients can cause very strong and persistent north and northwest winds over the extreme eastern Pacific. This prevailing wind pattern is particularly important to the summer wave climate.

Southern Hemisphere Swell

The probable importance of waves generated in the Southern Ocean to the coastal southern California wave climate was first emphasized by Munk and Traylor (1947) and Scripps (1947). O'Brien (1950) used refraction diagrams to show that an unusual and destructive wave focusing at the tip of the Long Beach breakwater was consistent with long southern swell. Wiegel and Kimberly (1950) used visual observations at Camp Pendleton, California to infer that southern swell dominates the littoral processes of southern California during the southern hemisphere winter. At the time of these studies, weather maps of the southern oceans were not adequate for a detailed correlation between California waves and southern hemisphere storms.

Munk and Snodgrass (1957) used wave energy spectra at Guadalupe Island (located at an exposed site off the coast of Baja, Mexico) and San Clemente Island to infer southern hemisphere sources for long period (14-25 sec) swell detected at all of the 24 southern California wave stations described by Munk et al, (1959). Munk and Snodgrass (1957) showed that the appearance of a very low frequency swell peak, which over a period of days gradually shifts to higher frequencies, is consistent with dispersive arrivals from distant (10,000 km) storms in the South Pacific and Indian Oceans. This "dispersive arrival" method had previously been used by Barber and Ursell (1948) to associate wave events off Britain with Atlantic storms in both hemispheres. Munk and Snodgrass (1957) considered their results "not conclusive" because of

incomplete weather maps and a lack of measured wave directions. Both these shortcomings were overcome in Munk et al, (1963). A three element triangular pressure sensor array was deployed in 100 m depth off the western shore of San Clemente Island (Figure 3.2.1), from May-October 1959. The measured directions of low frequency swell were in quantitative agreement with directions inferred from the dispersive arrival method of Barber and Ursell (1948), both indicated southern hemisphere sources. Energetic south swell at San Clemente Island could in every case be associated with a southern hemisphere storm, although not every storm appeared to generate a detectable swell signal. Munk et al, (1963) suggest three major source areas: the Ross Sea, the New Zealand-Australia-Antarctic sector, and the Indian Ocean near the antipole. Figure 3.2.1-1 shows the Tasman (230° - 234°) and South New Zealand (206° - 225°) windows open to the Indian Ocean. However, the Tongan Islands interfere with directions north of 232° ; the Taumotu and Society Islands with directions east of 216° . The south New Zealand window is also limited by the Antarctic ice pack. Figure 3.2.1-2 shows an example of a typical wave shadow cast by the Taumotu group. The number of islands and percentage of the sectors blocked are shown in Figure 3.2.1-3. The least blocked path to the Indian Ocean is through the south New Zealand window (the sector 225° - 234° is blocked by New Zealand). The Indian Ocean source is then north of Kerguelen Island, in the stormiest latitude belt on earth. The southern ocean source areas, and the importance of sheltering by island chains, were verified by Snodgrass et al (1966). This classic study used an array of stations stretching from New Zealand to Alaska, and included directional stations at Honolulu and FLIP (Figure 3.2.1-4). At frequencies above about .07 hz ($T < 14$ sec) individual storm events were difficult to identify in the chain of wave stations. These higher frequencies are maintained at relatively steady energy levels and are the result of moderate storms which occur frequently, and perhaps simultaneously at several locations. Lower wave frequencies are the result of severe storms which occur intermittently at intervals large compared to a storm

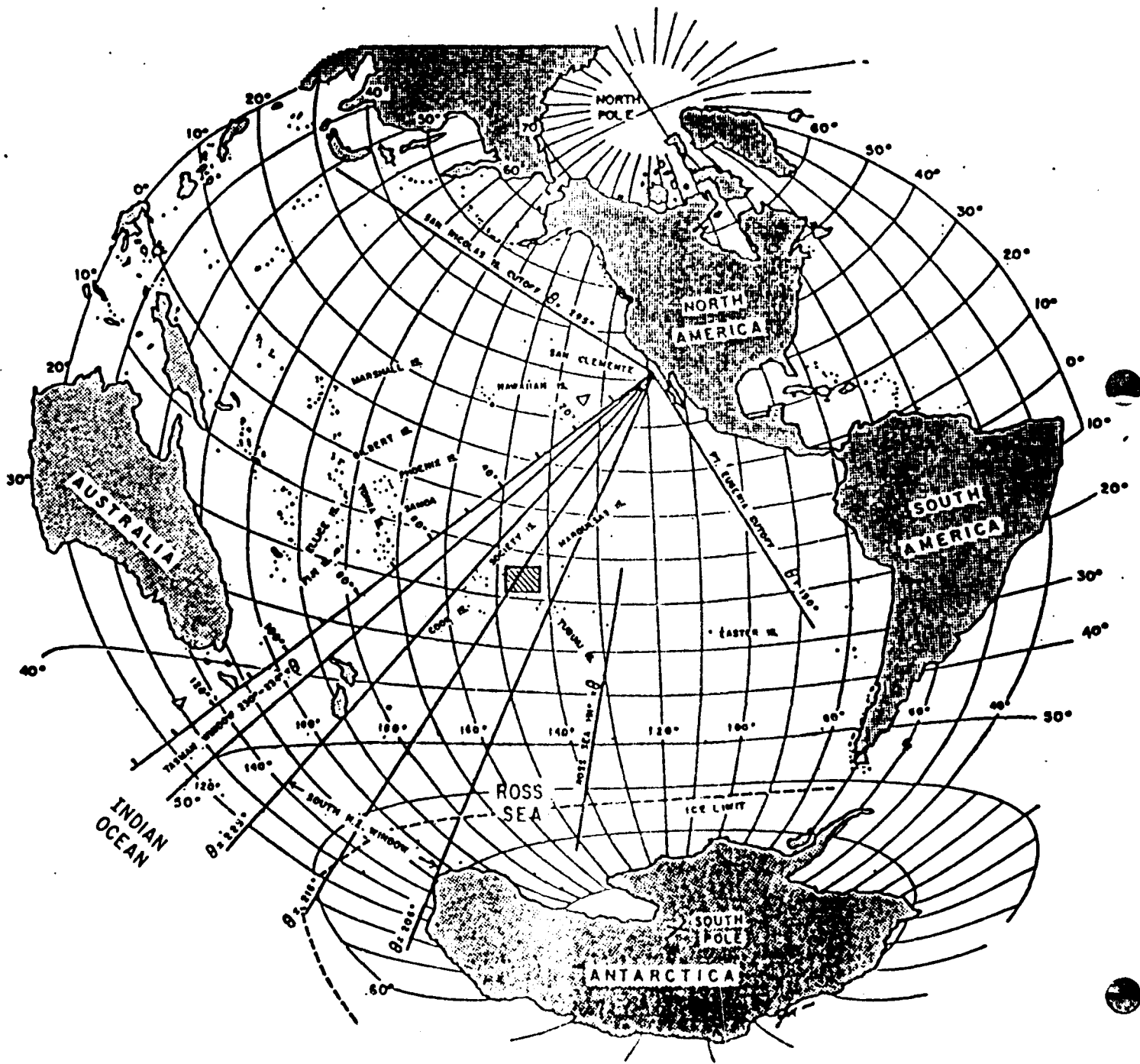


Figure 3.2.1-1

Azimuthal equidistant projection centered on San Diego, California. Some great-circle routes ($\theta = \text{constant}$) are indicated. The Tasman Sea and the region south of New Zealand provide two windows into the Indian Ocean, and these are partially obstructed by the Tongan and Taumotu island groups, respectively. The hatched area is shown on Figure 3.2.1-2 on an enlarged scale. (Munk et al. 1963).

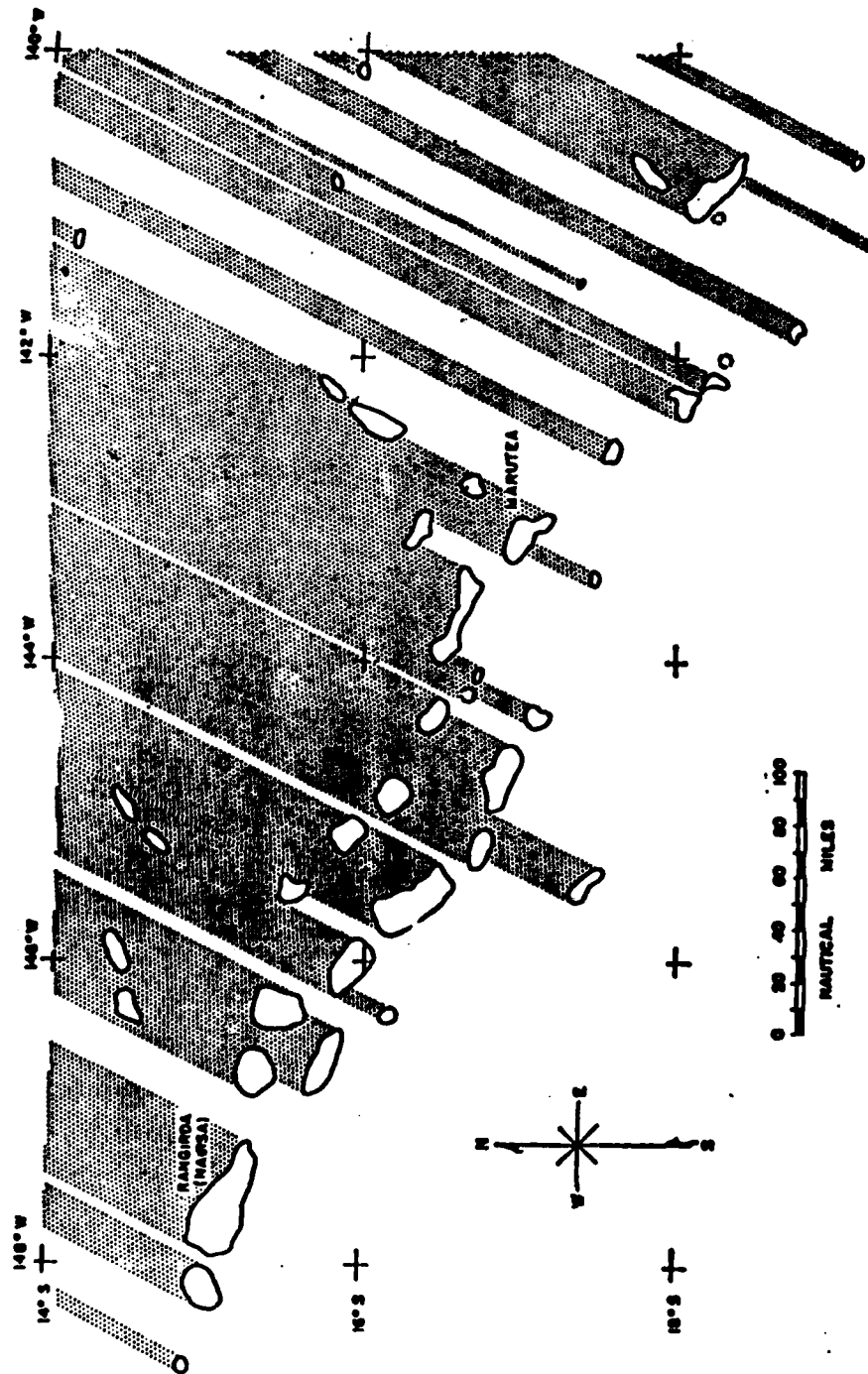


Figure 3.2.1-2 The wave 'shadow' cast by a portion of the Taumotu group for waves from 0 = 216° travelling towards San Clemente Island (Munk et al, 1963).

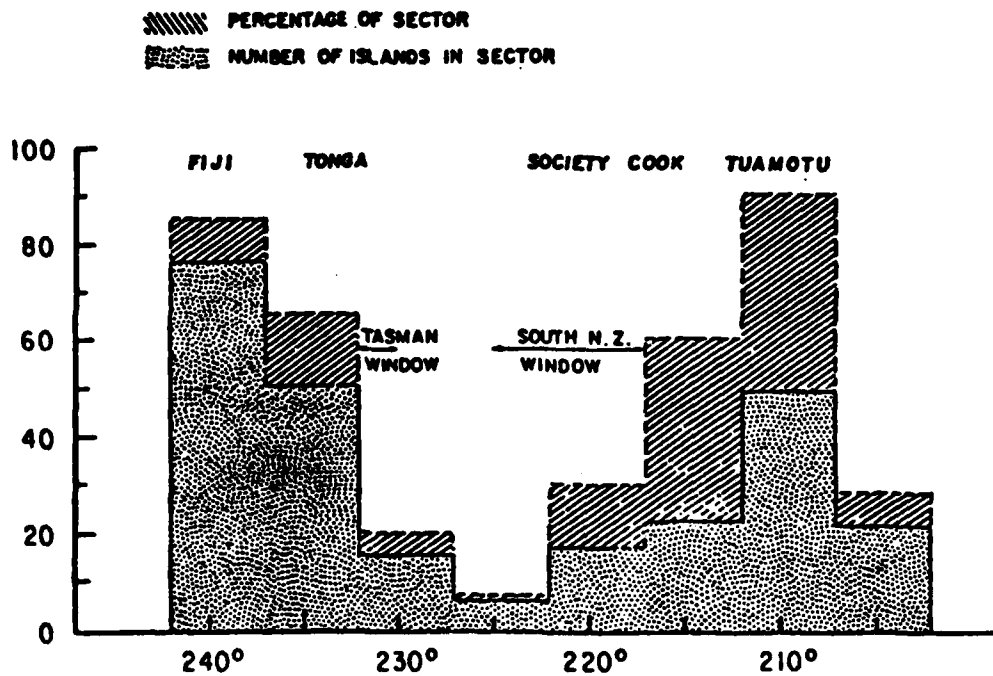


Figure 3.2.1-3

Numbers of islands north of 25° S in 5° sectors subtended at San Clemente Island, and the percentage of the sectors blocked by these islands (Munk et al, 1963).

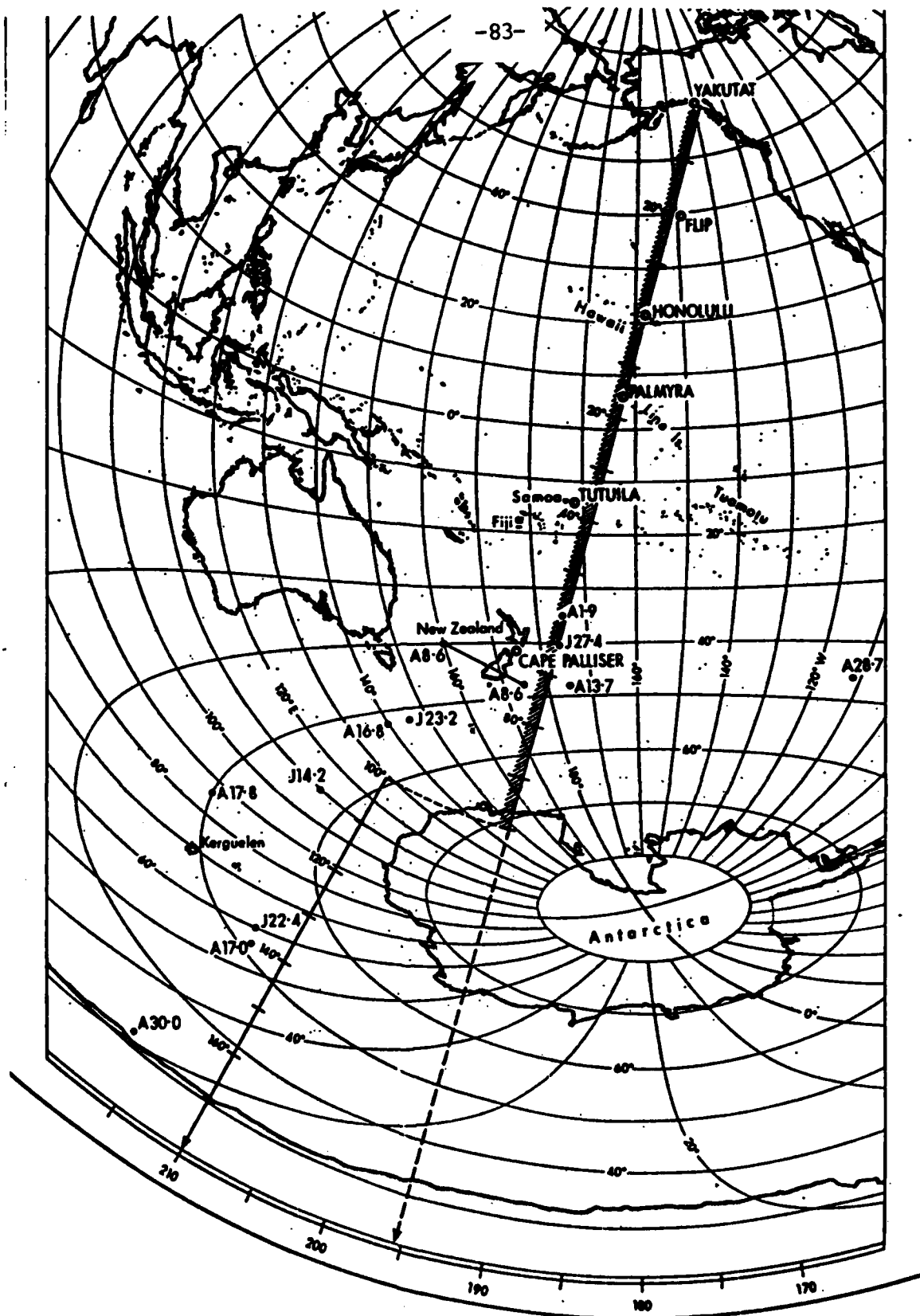


Figure 3.2.1-4

Great-circle chart based on Honolulu showing the location of the six wave instruments and of the principal storm sources. The 'reference great-circle' is in the direction 195.5° T from Honolulu; the Tasman window into the Indian Ocean bears 210° T. Distances from Honolulu are in degrees (1° = 50 nautical miles). Each storm is marked by a dot and its fractional date (J27.4 means 27 July, 9.6 h G.M.T.). (Snodgrass et al, 1966).

duration, and thus have a pronounced effect on energy levels. Once or twice a week a wave train associated with a severe southern storm leads to an identifiable event that can be traced across the entire Pacific Ocean. Averaged over many storms, and accounting for island chain blocking, the low frequency swell attenuation rates are vanishingly small. Although relative simple overall patterns of southern swell propagation emerge from considering two months of data, "individual events do not fit easily into a generalized pattern" (Snodgrass et al, 1966). Observed event spectra fluctuate by factors of ± 4 between stations even after island shadowing effects are accounted for. These fluctuations are thought to be associated with nonlinear interactions and the complexity of propagation through dense island chains.

The South Pacific is of such a large area, and the wave travel times to California span a sufficiently long time (several days between the arrivals of the longest period forerunners to the higher frequency swell), that waves from several southern storms commonly reach southern California simultaneously (Munk et al, 1963; Snodgrass et al, 1966). Although they only measured in a single year, Munk et al (1963) reasonably conclude that southern swell will be most important during the southern winter (April-September) with north Pacific events dominating the remainder of the year. They specifically comment on the importance of southern swell to littoral transport in southern California and refer to the "sensitive balance between this northward transport during.....the southern winter and a southward transport associated with waves from Alaskan cyclones during the remaining year."

Sea

Sea is the term applied to short, steep waves which are still in or near the area in which they were generated, as distinguished from swell, which refers to longer, flatter waves which have left the generating area and have begun to change their physical characteristics through the processes of sorting and decay. In order to forecast sea it is necessary to have data representative of the winds over the water area immediately to windward of the forecast

location, winds which in this case are associated either with storms that have invaded southern California, with strong pressure gradients over the area, or with the daytime sea breeze. Wind conditions vary greatly as one moves offshore from the southern California coast, changing from relatively mild winds over the inner channels to strong, gusty winds outside the islands (Marine Advisers, 1961a). The transition zone extends southeastward from Point Conception in a direction which corresponds roughly to the orientation of the central California coastline (Figure 3.2.1-5).

Santa Ana winds are a fairly common local wind event in southern California, and are caused by the formation of a high pressure system over inland areas, creating a flow of warm dry air down through mountain passes and out over the coast. The Santa Ana wind speed can reach 25 m/s and extend to 160 km seaward of the coast (Figure 3.2.1-6). These local wind conditions result in the generation of wind waves.

3.2.2 Wave Climate

There are relatively few in situ long-term measurements of the deep ocean (i.e. unaffected by the channel islands and/or coastal bathymetry) wave field for the study region. Deployments for several months (Munk et al, 1963) are too short to establish meaningful wave climate parameters and were not intended for that purpose. In the literature reviewed, the principal source of long-term in situ measurements is the Coastal Data Information Program (Seymour and Sessions, 1976), which has reported statistics for nondirectional buoys (1) at Begg Rock (Figure 3.2.2-1) in 110 m depth, a site fully exposed to deep ocean waves from the directional range 180°-320°, and (2) in unsheltered waters off Point Arguello in the depth range 80-220 m.

Seasonal height data for the 2 years (1983-84) of Begg Rock data, and the 2 years (1979, 1982) with the most (9 mo/yr) Point Arguello data, are shown in Figures 3.2.2-2 to 3.2.2-5. At both these sites, significant wave heights exceed 3 m at least 15% of the time during the winter

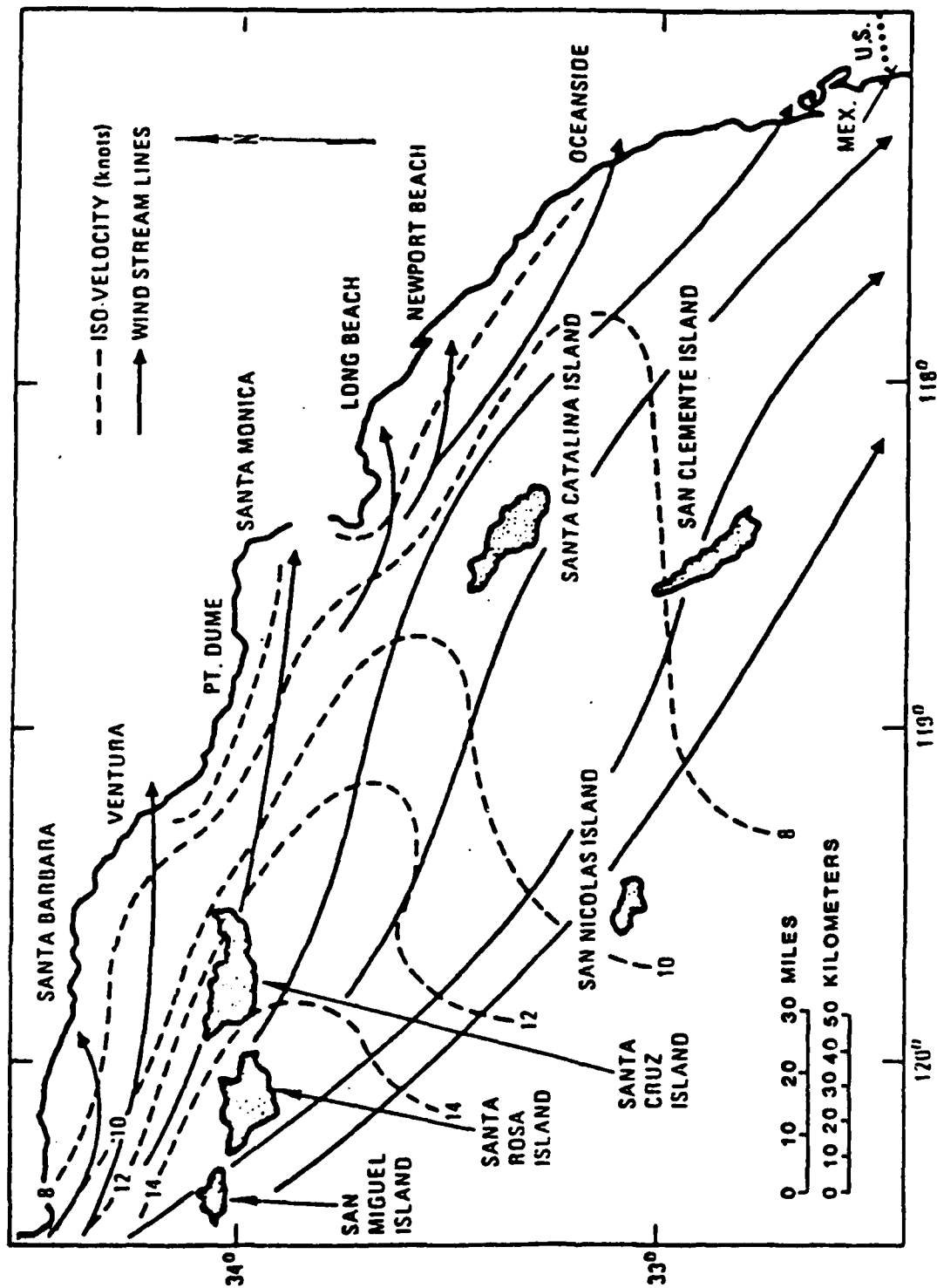


Figure 3.2.1-5 Average wind field offshore southern California (Allan Hancock Foundation, 1965).

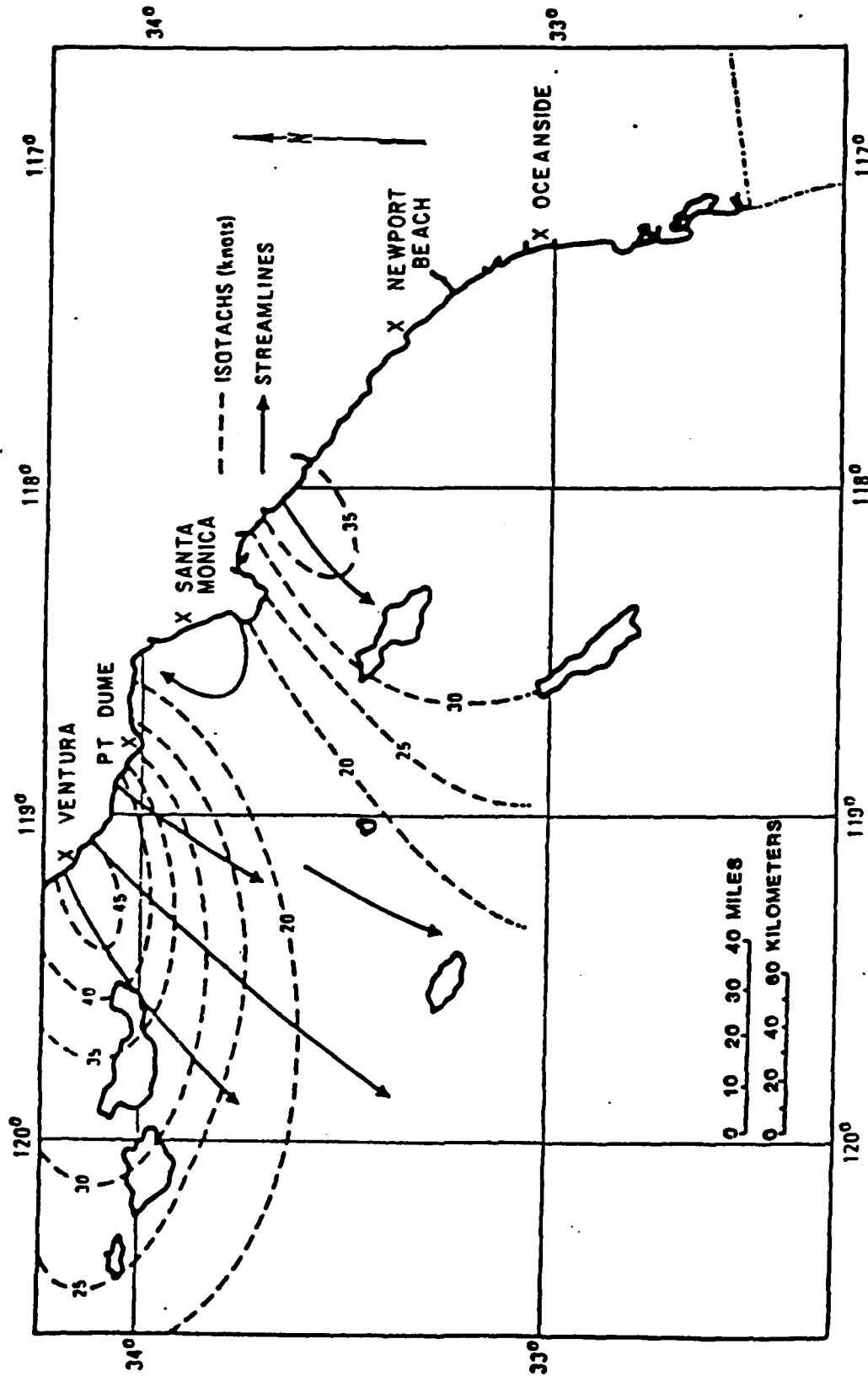


Figure 3.2.1-6 Santa Ana wind condition offshore southern California (The Aerospace Corporation, 1977; after Strange, 1975).

AD-A166 699

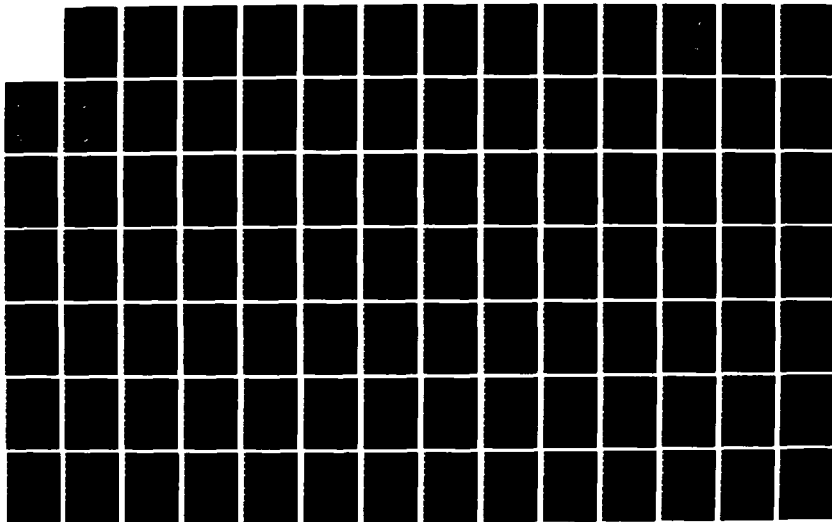
COAST OF CALIFORNIA STORM AND TIDAL WAVES STUDY
SOUTHERN CALIFORNIA COAST (U) ARMY ENGINEER DISTRICT
LOS ANGELES CA COASTAL RESOURCES BRANC.
D L INMAN ET AL FEB 86 CCSTW5-86-1

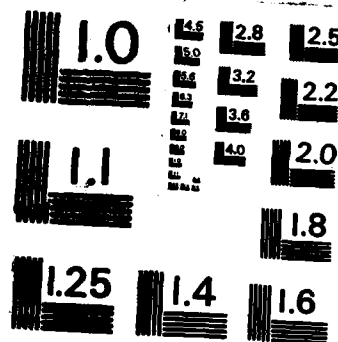
2/7

UNCLASSIFIED

F/G 8/3

NL





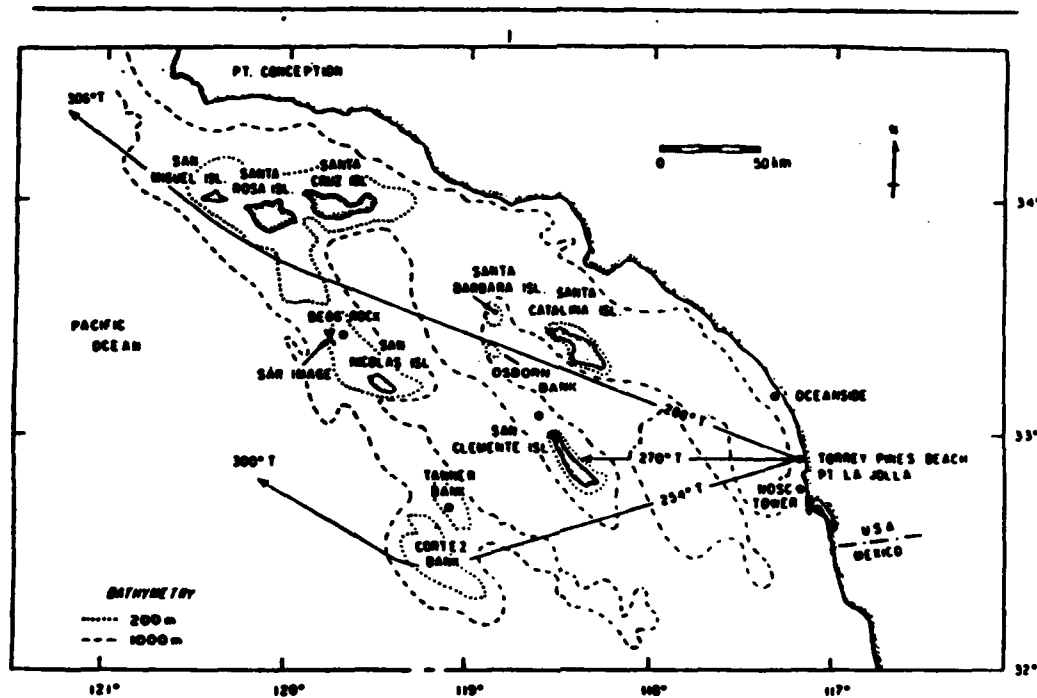
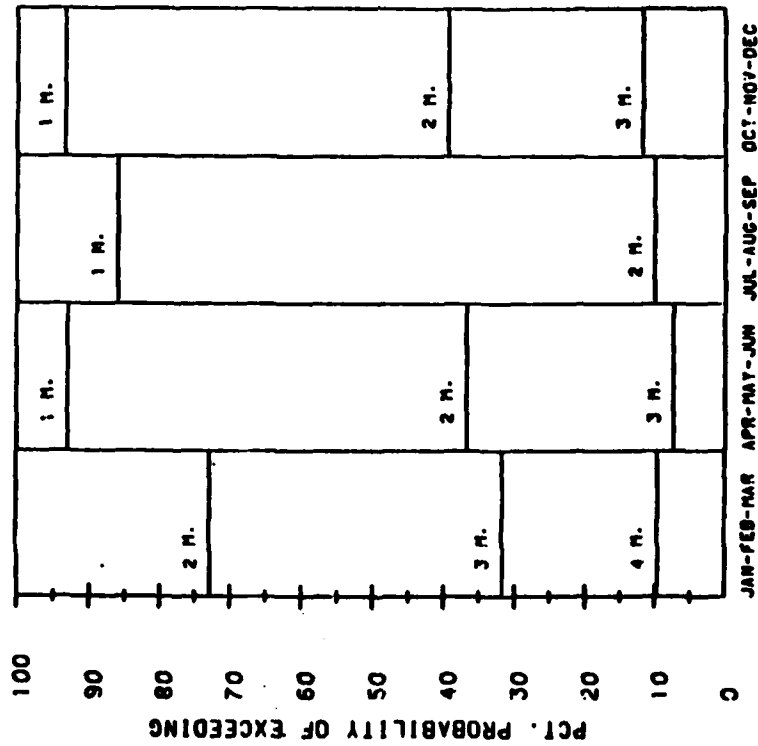


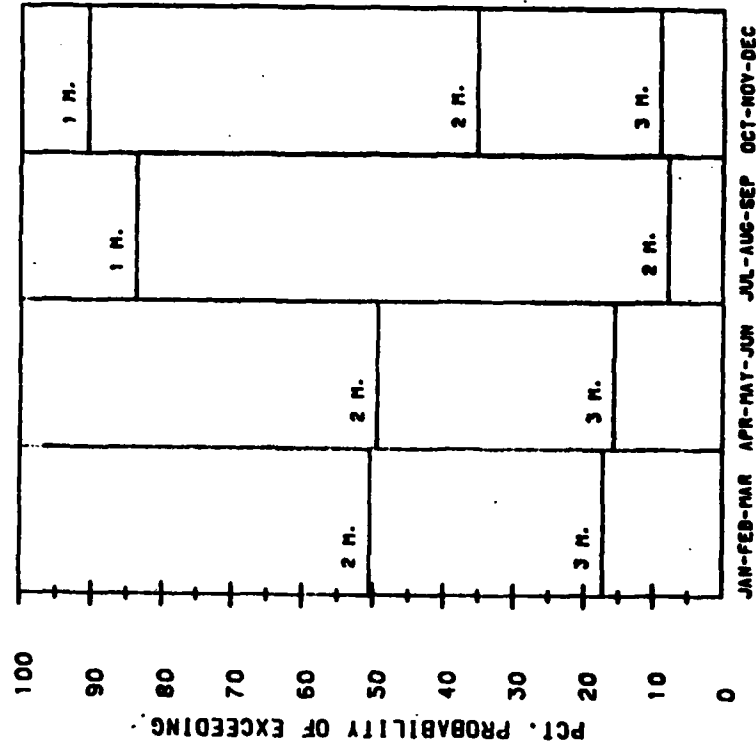
Figure 3.2.2-1 Schematic map of the southern California borderland. The surface sensor sites (dots) and location of the 'deep ocean' SAR images (X) are from the experiments of Pawka et al (1984) discussed in Section 3.3.1. Also shown are three rays for 0.059 Hz waves incident to Torrey Pines Beach.

SEASONAL PROBABILITY OF EXCEEDING
VARIOUS SIGNIFICANT WAVE HEIGHTS

1983



1984



BEGG ROCK BUOY

Figure 3.2.2-2

1983 CDIP seasonal heights for Begg Rock
(Seymour et al, 1983).

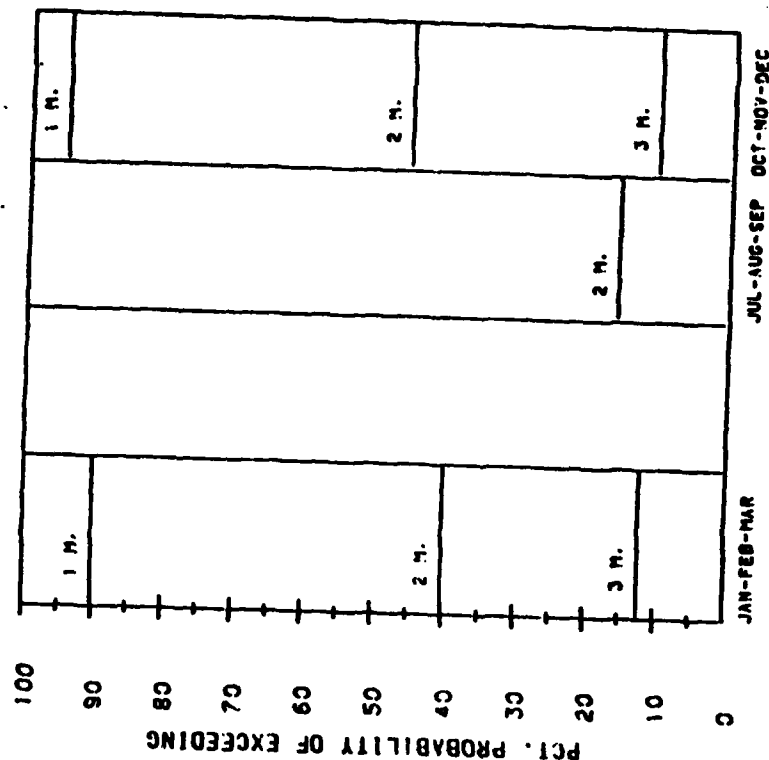
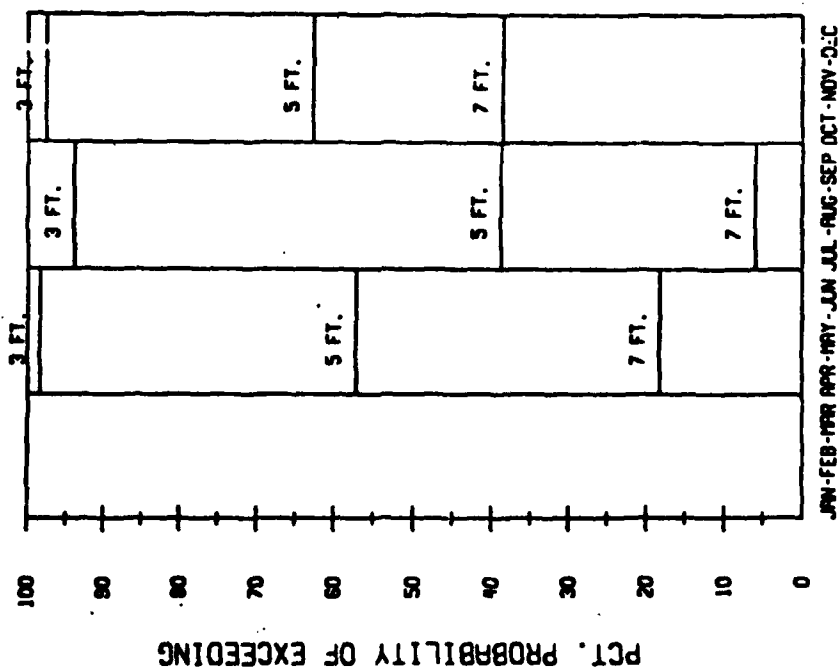
Figure 3.2.2-3

1984 CDIP seasonal heights for Begg Rock
(Seymour et al, 1984).

SEASONAL PROBABILITY OF EXCEEDING VARIOUS SIGNIFICANT WAVE HEIGHTS

1979

1982



PT ARGUELLO BUOY

Figure 3.2.2-4 1979 CDIP seasonal heights for Point Arguello (Seymour et al, 1979).

Figure 3.2.2-5 1982 CDIP seasonal heights for Point Arguello (Seymour et al, 1982).

months (October-March). More detailed statistical summaries (height distribution functions, joint distributions of significant wave height, etc.) are given in the monthly and annual reports of the Coastal Data Information Program (for example, Seymour et al, 1985). The Point Arguello buoy was reactivated in February, 1985, and the Begg Rock data collection is ongoing. A directional NOAA buoy was deployed due south of San Nicholas Island and west of San Clemente Island (Figure 3.2.2-1) in April 1984 for a period of 18 months. This site is open to virtually all important wave directions and could potentially provide very important information about the directional characteristics of waves outside the channel islands (CCSTWS, 1985). However, the absolute accuracy of moored directional buoys is not well known. Comparisons with a three-wavestaff array suggest an accuracy of about $\pm 10^\circ$ (Burdette and Howard, 1982). A 10° difference in deep water direction can sharply alter the expected coastal response (compare 280° with 290° in Figure 3.3.1-6). Subsequent modifications are reported to have improved buoy directional accuracy to better than 5° (Steele, 1982, 1984) although this apparently has not been confirmed by further intercomparison studies. As discussed below, the wave transformation through the channel islands is so sensitive to the details of the deep water directional spectrum that both very accurate instrumentation and high resolution estimator techniques (Hasselmann et al, 1980; Lawson and Long, 1983; Oltman-Shay and Guza, 1985) are required if the deep ocean data is to be quantitatively related to coastal conditions.

The most extensive deep water ocean data is not directly measured, but is inferred from the wind field, which is usually inferred from maps of barometric pressure. It is clear that the quality of these wave hindcasts is limited in accuracy by the quality of the initial barometric pressure fields, and the subsequent models for the wind fields and wave generation-propagation. Each of these sources of error can be substantial.

There are several hindcast studies for deep water locations in the study region. The oldest (UCSD, 1947) is based on daily wind maps of the North Pacific for the 3-year period (1936-1938) inclusive. The wind fields are based on ship observations which were sparsely spaced. Subjective judgments as to the fetch, wind speed, etc. entered to a "considerable degree." The formulas of Sverdrup and Munk (1947) were used to predict the waves, given the wind field. Because of the poor wind data base, and subsequent improvements in wave generation models, this hindcast study is rarely used in recent studies.

Marine Advisers (1961a) has generated hindcasts estimates for three southern California sites (A, B, C, in Figure 3.2.2-6). Station A is approximately 65 nautical miles southwest seawards of San Clemente Island, while B, C are highly sheltered and are discussed primarily in Sections 4 through 11.

Different procedures were used for estimating waves from storms in the northern and southern hemispheres, and for locally generated seas. A common element was the use of Bretschneider's (1957) modified form of the Sverdrup-Munk formula for wave generation, given the wind field. Wind fields for swell generation in both hemispheres were deduced from daily U.S. Weather Bureau maps. Northern hemisphere swell was hindcast for 1956-58, and southern hemisphere swell for 1948-50. The southern hemisphere swell hindcasts also use observations at Huntington Beach and El Segundo as a critical element. Huntington Beach is exposed principally to swell from 155° - 198° while El Segundo is more affected by that from 195° - 235° . Since the directional variability of waves from a distant southern hemisphere source is small, swell which is significant at one location often will be small at the other. The method used to combine the coastal observations and (poor quality) southern hemisphere weather maps to yield the deep ocean southern swell climate is very briefly described in Marine Advisers (1961a). Apparently the measured coastal swell was crudely transformed backwards over the local topography and through the islands. Presumably directions inferred from the southern swell

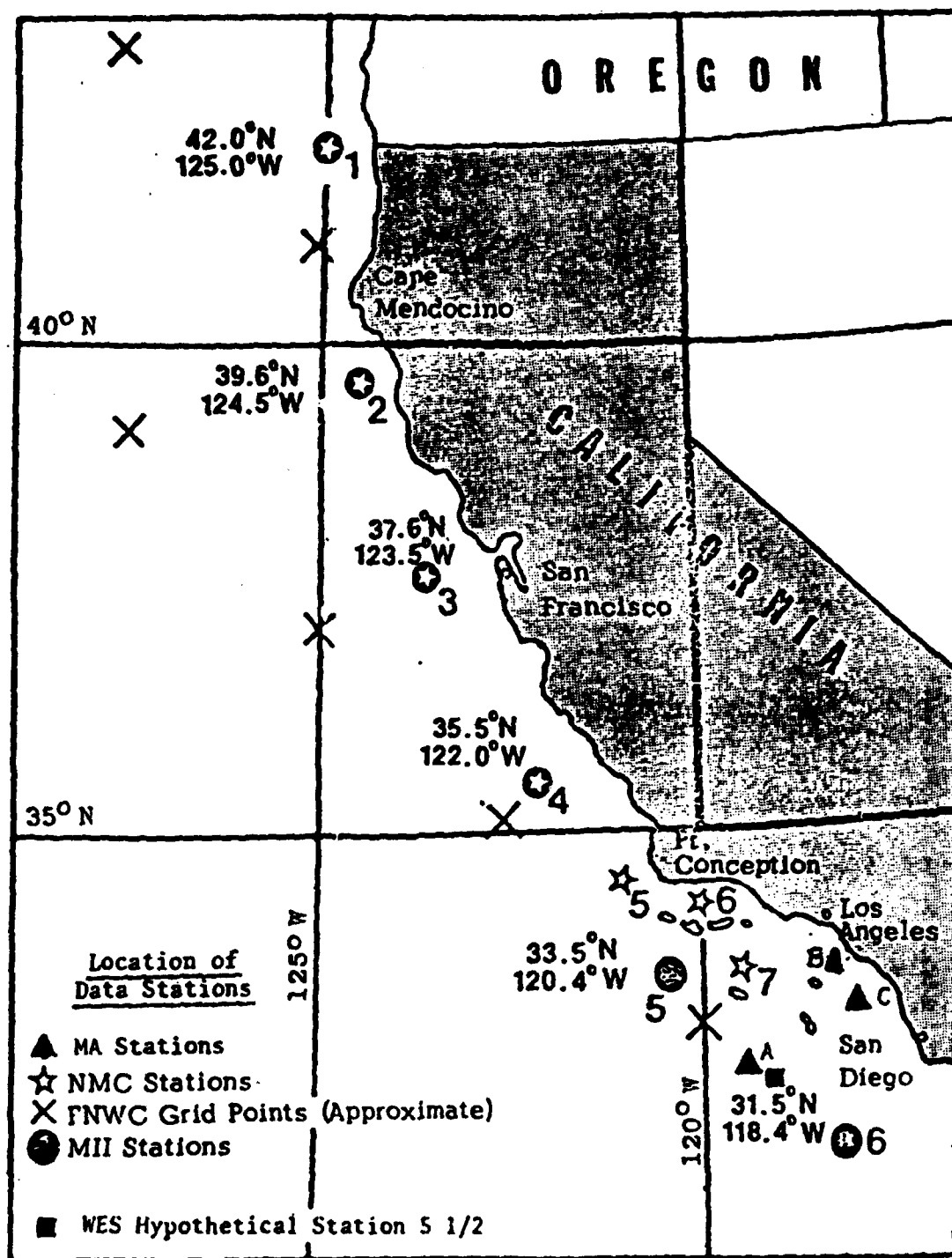


Figure 3.2.2-6 Location of deep water wave statistical stations off the coast of California by National Marine Consultants, Marine Advisers, and Meteorology International, Inc. (after Meteorology International, Inc., 1978).

weather maps were used to guide the exact angles assumed for the measured El Segundo and Huntington Beach waves. As detailed in Section 3.2.1, extensive studies on southern swell (Munk et al, 1963; Snodgrass et al, 1966) point out the extreme difficulty of making good southern swell hindcasts. Furthermore, Thompson (1977) has shown that the pre-1972 data (pen and ink traces collected for 7 minutes, 4 times daily) at Huntington Beach were corrupted by instrumental inaccuracies and faulty analysis methods (it is not clear whether Marine Advisers (1961a) used the same faulty Beach Erosion Board analysis method discussed by Thompson). At any rate, the Huntington Beach records must be considered suspect. Of course, Marine Advisers (1961a) did not have the benefit of subsequent work by Snodgrass et al (1966) and Thompson (1977). Possible refinements that they were aware of were "beyond the scope of this project." Marine Advisers (1961a) considered their southern swell hindcast to be of use "in determining characteristics of harbor entrances and in qualitative calculations of the littoral drift of sediments."

Marine Advisers (1961a) also showed differences of a factor of 2.0 between measured Huntington Beach wave energies for 1948-50 (the period hindcast for southern swell) and 1956-58 (the period hindcast for northern swell). The average energy for 1956-58 was greater. "Consideration was given to the advisability of altering the 1948-50 data so that it would represent waves having energy comparable to those of 1956-58, but the idea was rejected in favor of simply informing potential users of the difference so that they could make modifications themselves if it proved desirable. Actually we are unable at this time to say whether the recorded Southern Hemisphere Swell was more typical in 1948-50 or in 1956-58." It seems clear that at least a factor of 2 in energy (1.4 in wave height) variability in the southern swell hindcast is associated with the relatively short time span covered by Marine Advisers (1961a), and that additional unknown (and substantial) errors are associated with the analysis method. The above discussion is not intended as a criticism of the southern swell hindcast of Marine

Advisers (1961a). They made ingenuous use of a very limited data set and relied heavily on experienced forecasters. The point here is that the southern swell hindcast, which has been very extensively used for quantitative calculations (of littoral drift for example) was never intended for this purpose. No other hindcast studies reviewed here give any climatology for southern swell.

Due to the relatively sparse (in both space and time) nature of the available weather information, a considerable degree of subjectivity was involved in deducing the northern hemisphere large-scale wind fields (Marine Advisers, 1961a). The relatively fine scale wind fields necessary for the calculation of locally generated seas could not be calculated because the required information on the barometric pressure field was not available. Consequently, wind observations from San Nicolas Island (50 miles north of location A, Figure 3.2.2-6) were used for sea hindcasts. San Nicolas wind data was not available for the 1956-58 time period used for the northern hemisphere swell prediction, and it is unclear what time period was actually used. Winds for hindcasts of local seas at the coastal stations B, C (Figure 3.2.2-6, and discussed further below) were measured at Oceanside during the period 1934-1938. Note that wind speeds are spatially variable over the Southern California Bight (Figure 3.2.1-5). It seems that the use of any single wind station cannot give more than a qualitative estimate of wind wave generation which occurs over the whole bight. Thus, at least three different time periods were used for the hindcasts of different components of the wave field. It is therefore not possible to reconstruct the total wave field (i.e. the sum of sea and northern and southern swell) at any particular time. In fact, if more than one wave train of a particular type (for example, 2 northern hemisphere swell wave trains from 2 different storms) would occur simultaneously, the effect of the earlier arriving train is assumed to end with the arrival of the 2nd wave train. This assumption leads to considerable computational simplification, but is also very nonphysical. Clearly the arrival of a small second wave train should reinforce an already existing large wave train, rather than

drastically decreasing the wave height. This shortcoming was appreciated by Marine Advisers (MA, 1961a), but analyzing each storm event in enough detail to determine the duration of individual wave trains was "beyond the scope" of that study. Authors that use the Marine Adviser (1961a) hindcasts should acknowledge the qualitative nature of the data.

Monthly and annual statistics of the probability of occurrence (according to wave height, period and direction) are tabulated separately for swell from each hemisphere and sea. This information is compactly expressed in wave roses, Figures 3.2.2-7,8,9. The radiating bars represent direction classifications, and the concentric circles which intersect them form a frequency scale which is in percentage of the average total number of hours in a year (8766 hours). The alternating shaded and white segments are successive wave height classes, each segment being of length commensurate with the percentage frequency of its height class. For example, in Figure 3.2.2-7 the longest bar represents all northern hemisphere swell approaching Station A from between 300 and 310°. The inner segment, out to the numeral 1, gives the frequency of waves from that direction in the 0.1-0.9 foot height group. It measures approximately 6.9%, which indicates that waves of this classification can be expected for a total of $.069 \times 8766 =$ approximately 605 hours per year. The next segment, out to the numeral 2, gives 7.2% as the frequency of waves in the 1-1.9 foot height group. The total bar length gives the total frequency (25.6%) of all northern hemisphere swell from between 300° and 310° at Station A. According to these wave roses, the largest and most frequently occurring waves at Station A are northern swell in the directional range 290-310°, and sea in the range 304-326°. Note that maximum south swell heights are only about 25% as large as north swell heights.

The hindcast study by National Marine Consultants (NMC, 1960b) covers the years 1956-58, and includes 7 deep water sites off California (Figure 3.2.2-6). Four of these sites (4, 5, 6, 7) are in the present study area. Waves at Station 6, in the Santa Barbara Channel, are heavily influenced by Point Conception and are discussed in Section 6. Station 7 (33.5° N, 119.5° W) is

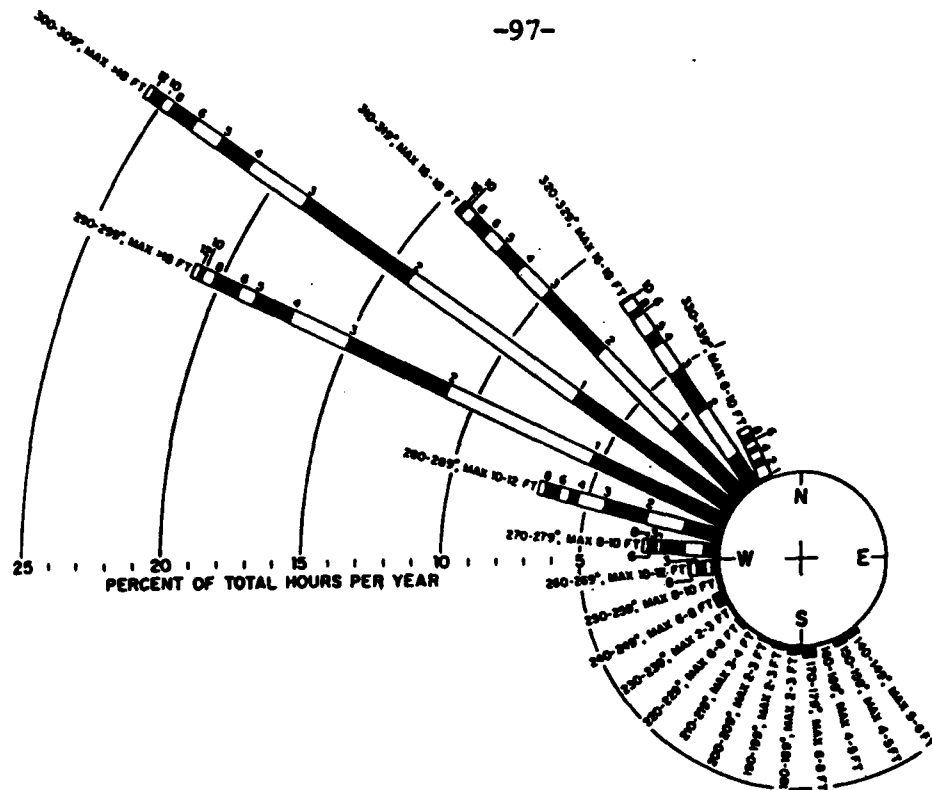


Figure 3.2.2-7 Wave rose, Station A, annual average (1956-58) northern hemisphere swell (Marine Advisers, 1961).

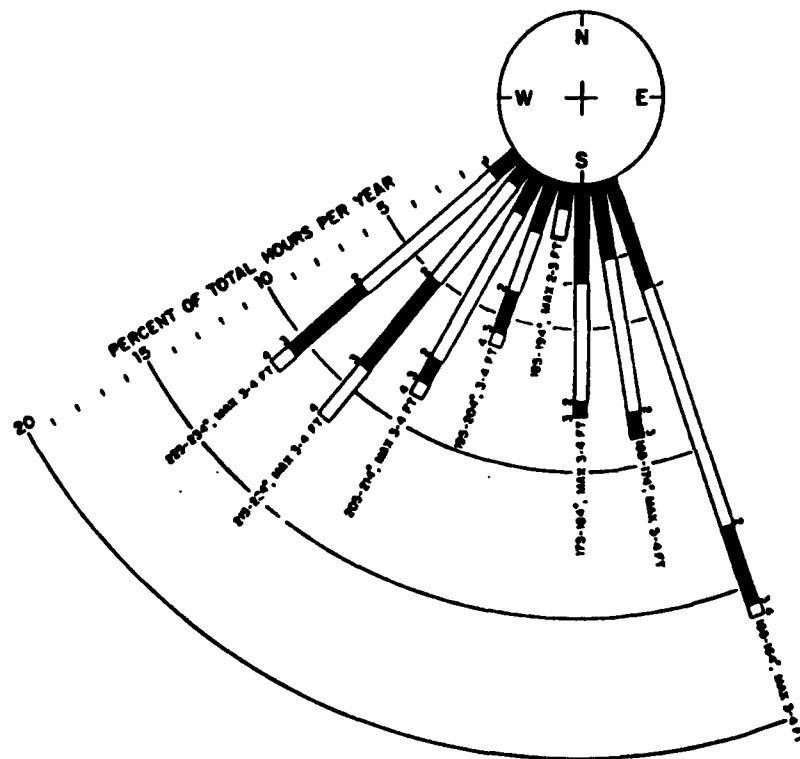


Figure 3.2.2-8 Wave rose, Station A, annual average (1948-50) southern hemisphere swell (Marine Advisers, 1961).



located in a region of submerged banks (slightly east of Begg Rock, Figure 3.2.2-1) and swell waves at this site are in reality somewhat affected by the local topography. However, these topographic effects are apparently not included in the NMC (1960b) calculations, so the Station 7 hindcasts are more properly considered as deep water conditions incident to the banks region. The Meteorology International Inc hindcast study (MII, 1977) discussed below replaces the NMC Stations 5, 6, 7 with two true deep water locations (MII Stations 5 and 6, Figure 3.2.2-6) to avoid difficulties associated with banks and islands.

The NMC (1960b) hindcast study used 4 times daily U.S. Weather Bureau synoptic weather charts to deduce the wind field. The Piersen Neumann and James (1953) generation theory is used to calculate the wave field, given the winds. Generation in the southern hemisphere is not considered. Unlike the MA (1960b) study, many wave trains were allowed to exist simultaneously and their energies added for calculation of wave heights. Results of the hindcasts are given as average monthly and annual significant height-period-direction frequency distributions. Annual wave roses for NMC Stations 5 and 7 are shown in Figures 3.2.2-10,11. As would be expected, because of their close physical proximity, the roses from MA (1961a) Station A (Figures 3.2.2-7,9) and NMC (1960b) Station 7 (Figure 3.2.2-11) are qualitatively similar. Both show sea having a predominantly NW direction and maximum heights of approximately 15 feet. Northern hemisphere swell is generally NW to W, also with a maximum height of approximately 15 feet. Differences are expected, of course, because of differences in the hindcast years and hindcast methodologies. It is likely that the differences would be larger except for the fact that both hindcasts involved subjective judgments by personnel having much experience with the California wave climate. That is, the studies were constrained to give results generally consistent with observations. There are, however, important differences, the absence of any south swell in NMC (1960b) being the most obvious example. On the other hand, the NE sea apparent at NMC Station 7 (Figure 3.2.2-11) is totally absent at MA Station

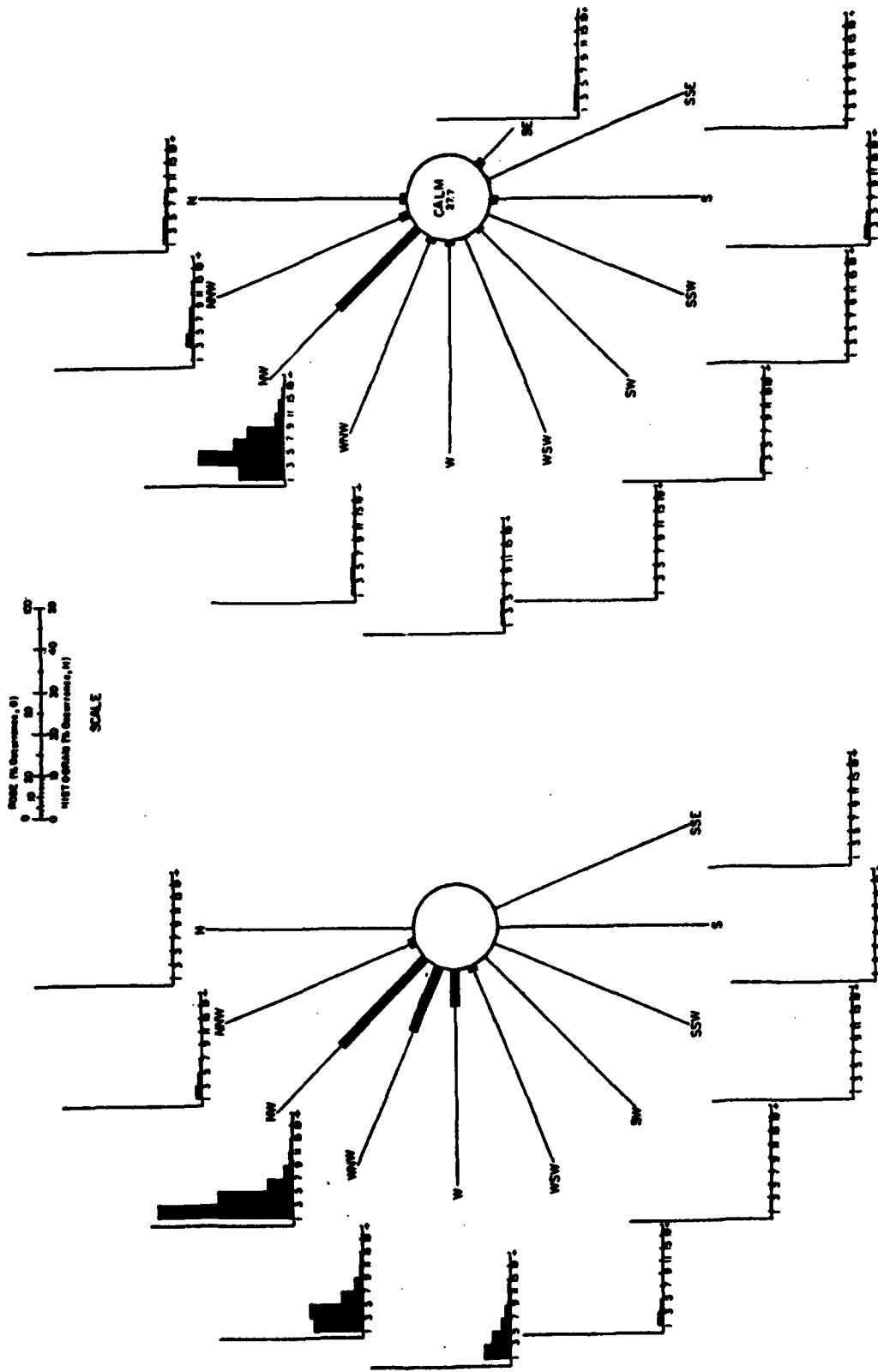


Figure 3.2.2-10 Average annual (1956-58) swell (left) and sea (right) roses for NMC Station 5 (NMC, 1960).

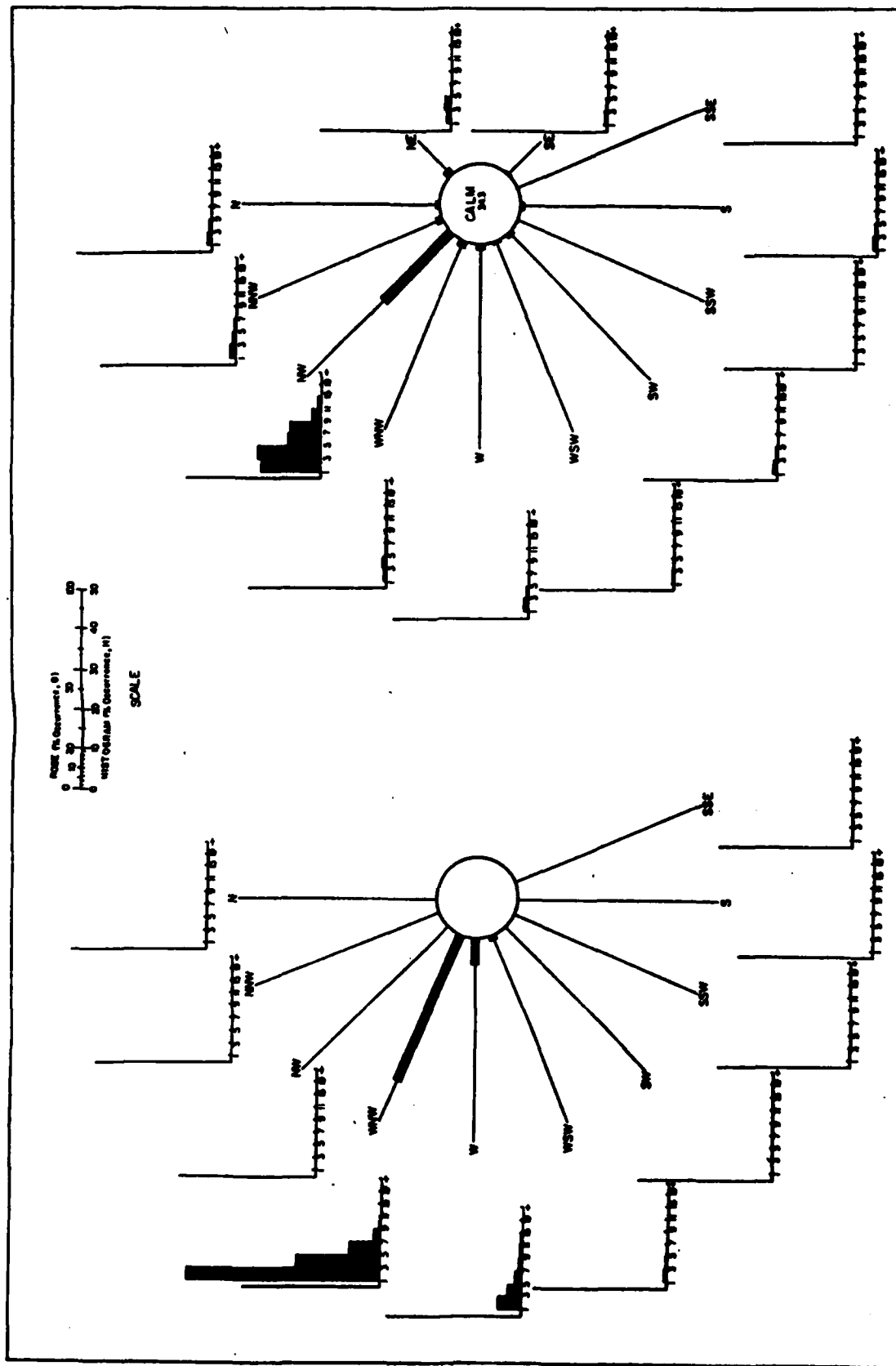


Figure 3.2.2-11 Average annual (1956-58) swell (left) and sea (right) roses for NMC Station 7 (NMC, 1960).

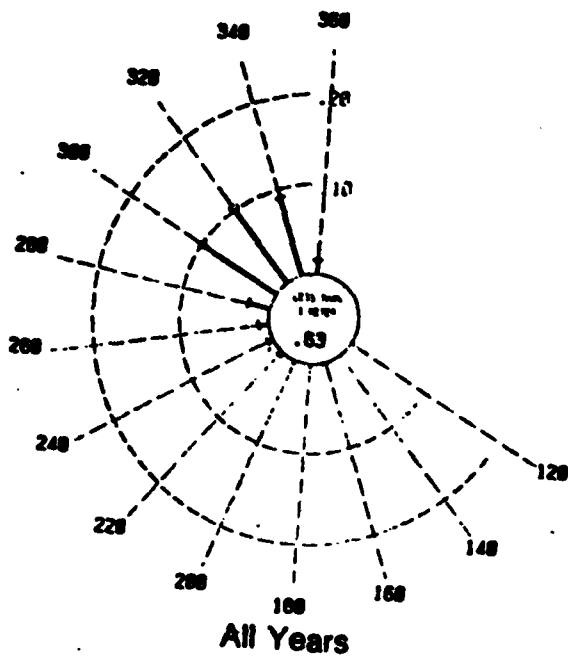
A (Figure 3.2.2-9). This NE sea is due to Santa Ana winds (Figure 3.2.1-5) which occur principally in November and December. In fact, the December statistics for sea at Station 7 show that NE sea accounts for about 1/3 of the non-calm December conditions (NMC Table 7.12). NE sea is entirely absent in the MA December statistics (MA Table 12). Santa Ana winds also generate SE seas important in the Santa Barbara channel (NMC Station 6, see Section 6). Comparison of NMC Stations 5 and 7 (Figures 3.2.2-10,11) show them to be qualitatively similar. The chief difference is the presence of NW swell at Station 5, a direction which is shadowed at Station 7 by Point Conception. NMC Station 4 (not shown) is similar to NMC Station 5.

Johnson et al (1971) present summaries of annual wave *power* for ten deep water stations along the west coast. The locations and basic wave statistics are the NMC (1960b) hindcast discussed above. The motivation for the study is that "Basic to an appraisal of the *characteristics of shore processes in a given locality is adequate information on the wave climate.*" (Johnson et al, 1971). While this statement is true, the understanding of coastal wave climate is not meaningfully advanced by simple conversion to deep water power statistics such as is done in this report. This report is very rarely, if ever, used.

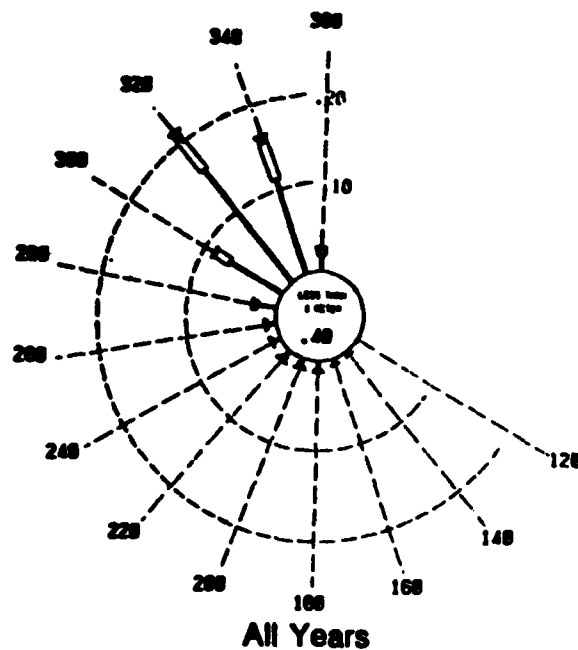
Modern computers provided the opportunity to perform systematic hindcasts for many years. The Meteorology International Inc (MII, 1977) hindcast covers 1951-1974, using a standardized procedure. There are far fewer subjective decisions than in the previous hindcasts (this may or may not improve the results, see below), the time period covered is greatly increased, and the directional resolution is finer. Daily barometric pressure maps yielded wind fields which in turn were coupled with the Fleet Numerical Weather Central (FNWC) wave generation model (Hubert and Mendenhall, 1970). Of the 6 California station locations, 3 are in the study area (MII Stations 4, 5, 6; Figure 3.2.2-6). All these stations are seawards of islands and banks, although Stations 5 and 6 are sheltered from northerly waves by the continent. The

FNWC model allows multiple wave trains to coexist. The initial FNWC analysis yielded wind and wave parameters at grid points (Figure 3.2.2-6) which do not correspond to the station locations. Swell at the station locations was estimated from the nearest grid point, while sea was calculated from an interpolated wind field. No southern swell, tropical cyclones, or offshore (Santa Ana) wind waves are included in this study.

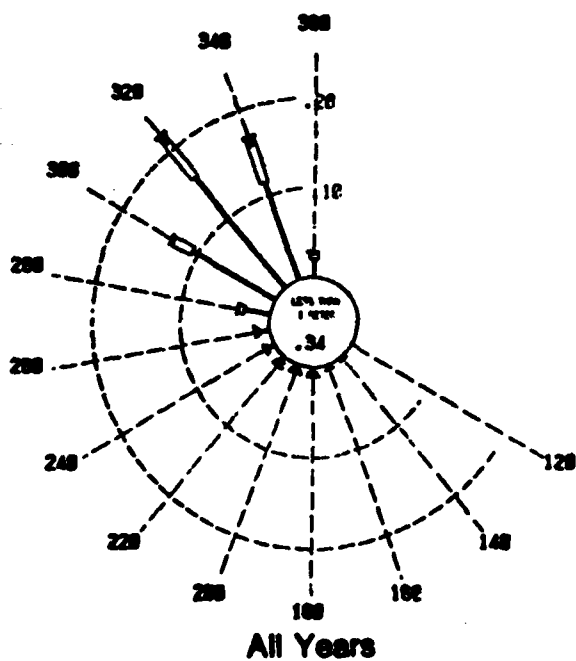
The hindcast data is presented in a variety of graphs and tables, including (1) monthly and yearly average wave roses for sea and swell separately, and combined, (2) wave height duration bar graphs by year and month, (3) direction-period-height frequency of occurrence, both monthly and yearly averages, (4) monthly mean wave heights by year, (5) direction-period-height frequency distributions, for each month with the highest and lowest combined wave heights (i.e. for the period 1951-1974, the statistics for the January with the lowest waves are listed without averaging, similar tables given for February, March, etc.), and (6) listings of extreme events. There are approximately 250 pages of hindcast statistics for each station. Average yearly wave roses for swell, sea and combined sea/swell are given in Figures 3.2.2-12, 13, 14 for Stations 4, 5, and 6 respectively. The principal difference in the directional wave rose characteristics between MII Stations 4, 5, and 6 is the reduced occurrence of NNW (340°) sea and swell at Station 6 because of shadowing by the continent. Averaged (over all years) monthly combined sea/swell significant wave heights show a maximum, at all 3 stations, in (surprisingly) May-June (Tables 3.2.2-1,2,3). This is due to the consistent occurrence of strong local winds and seas from about 320° . The combined sea/swell wave heights averaged over all months and years, are 1.34, 1.42, 1.5 m for Stations 4, 5, and 6 respectively, showing (surprisingly) a slight increase in heights towards the southernmost station. This increase is associated with highly energetic local seas at Station 6. Swell energy (not shown) increases very slightly from south to north. The largest and most frequent extreme events occur at Station 4 (Table 3.2.2-4). Many of these events are swell from the NNW, a partially sheltered direction



SWELL



SEA



COMBINED SEA/SWELL

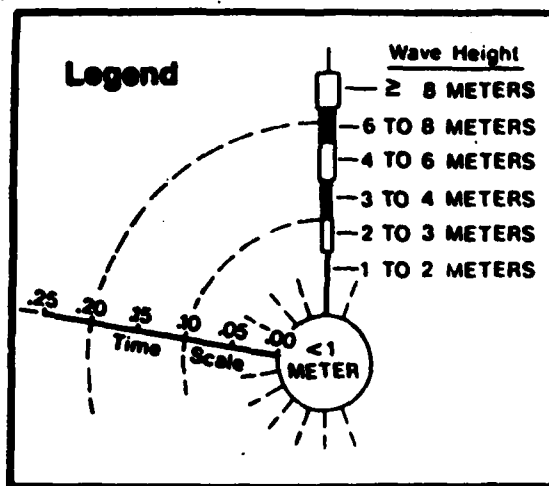
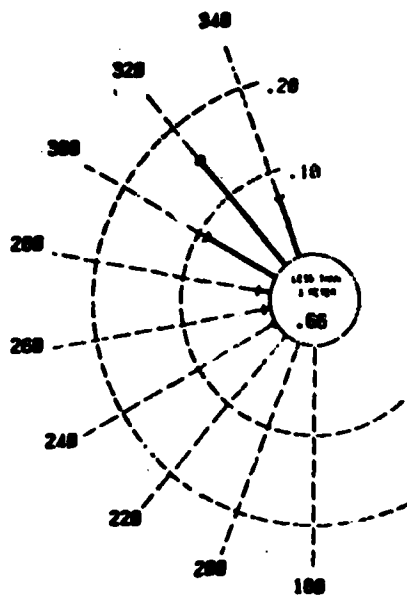
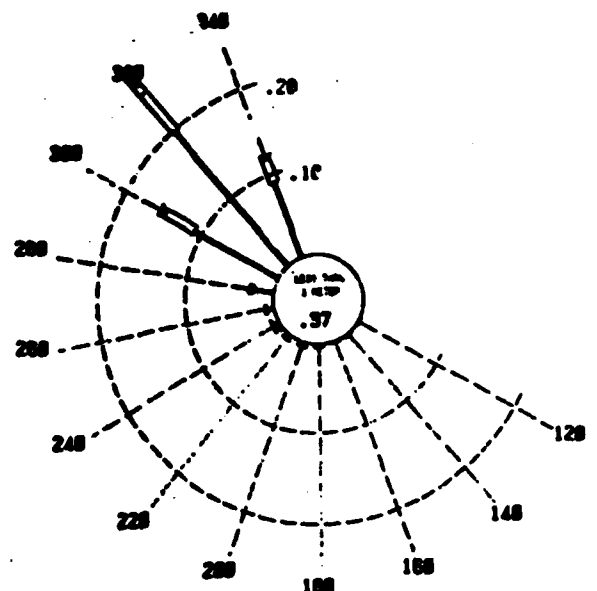


Figure 3.2.2-12 Average annual (1951-74) swell, sea and combined sea/swell roses for MII Station 4 (MII, 1977).



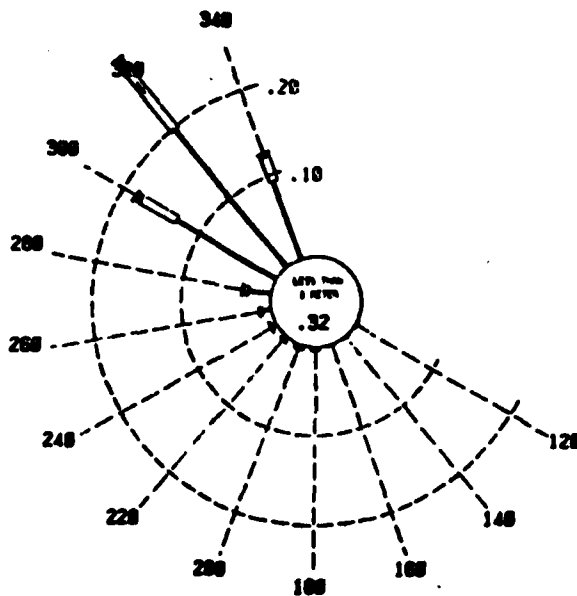
All Years

SWELL



All Years

SEA



All Years

COMBINED SEA/SWELL

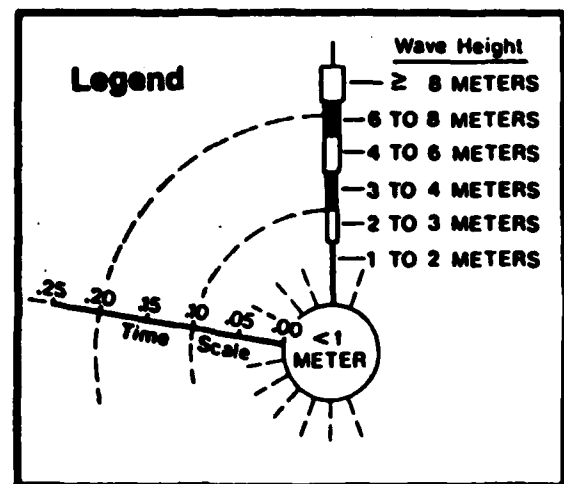
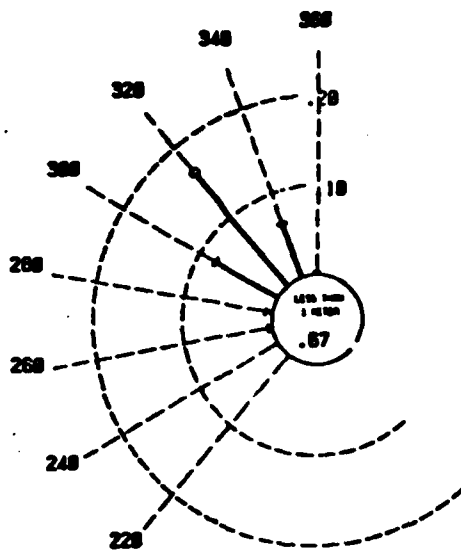
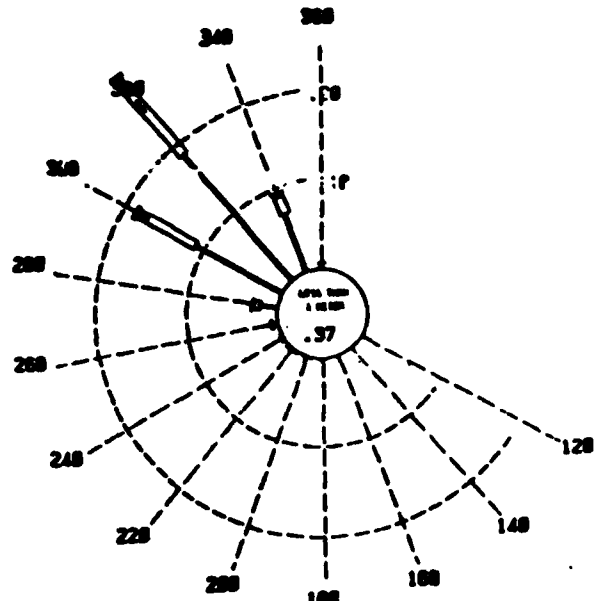


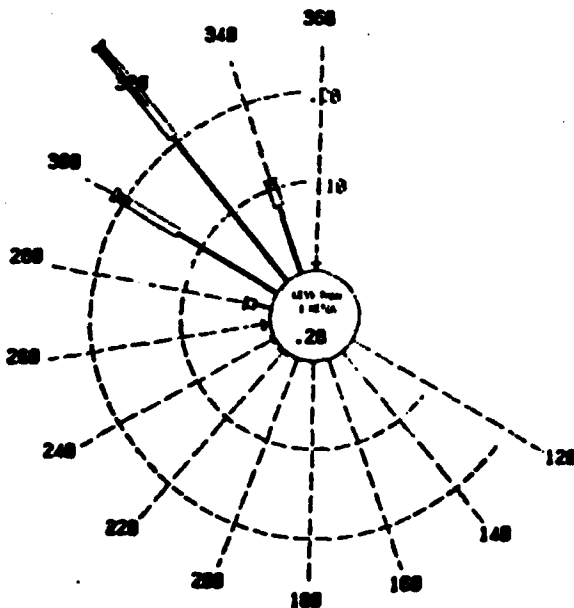
Figure 3.2.2-13 Average annual (1951-74) swell, sea and combined sea/swell roses for MII Station 5 (MII, 1977).



All Years
SWELL



All Years
SEA



All Years

COMBINED SEA/SWELL

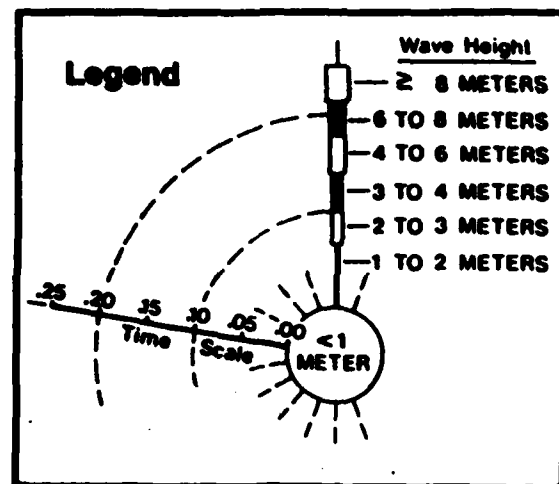


Figure 3.2.2-14 Average annual (1951-74) swell, sea and combined sea/swell roses for MII Station 6 (MII, 1977).

Table 3.2.2-1 MII Station 4 hindcast (1951-74) statistics (MII, 1977)

STATION 4
(35.5N 122.0W)
MEAN WAVE HEIGHTS(METERS)
COMBINED SEA/SWELL

	JAN	FEB	MAR	APR	MAY	JUN	JUL	AUG	SEP	OCT	NOV	DEC
1951	1.4	1.2	1.7	1.3	1.7	1.5	1.8	1.5	1.1	1.0	1.2	1.2
1952	1.7	1.3	2.0	1.4	1.8	1.8	1.3	1.4	1.9	1.5	1.2	1.0
1953	1.3	1.3	1.3	1.7	1.7	2.1	1.3	1.0	1.2	1.0	1.2	1.0
1954	1.3	1.3	1.3	1.3	1.8	1.8	1.4	1.4	1.2	1.0	1.2	1.0
1955	1.3	1.3	1.3	1.3	1.8	2.0	1.4	1.4	1.2	1.0	1.2	1.0
1956	1.1	1.2	1.3	1.3	1.4	1.9	1.5	1.5	1.2	1.2	1.2	1.0
1957	1.1	1.2	1.3	1.3	1.4	1.9	1.5	1.5	1.2	1.2	1.2	1.0
1958	1.1	1.2	1.3	1.3	1.4	1.9	1.5	1.5	1.2	1.2	1.2	1.0
1959	1.1	1.2	1.3	1.3	1.4	1.9	1.5	1.5	1.2	1.2	1.2	1.0
1960	1.1	1.2	1.3	1.3	1.4	1.9	1.5	1.5	1.2	1.2	1.2	1.0
1961	1.1	1.2	1.3	1.3	1.4	1.9	1.5	1.5	1.2	1.2	1.2	1.0
1962	1.1	1.2	1.3	1.3	1.4	1.9	1.5	1.5	1.2	1.2	1.2	1.0
1963	1.1	1.2	1.3	1.3	1.4	1.9	1.5	1.5	1.2	1.2	1.2	1.0
1964	1.1	1.2	1.3	1.3	1.4	1.9	1.5	1.5	1.2	1.2	1.2	1.0
1965	1.1	1.2	1.3	1.3	1.4	1.9	1.5	1.5	1.2	1.2	1.2	1.0
1966	1.1	1.2	1.3	1.3	1.4	1.9	1.5	1.5	1.2	1.2	1.2	1.0
1967	1.1	1.2	1.3	1.3	1.4	1.9	1.5	1.5	1.2	1.2	1.2	1.0
1968	1.1	1.2	1.3	1.3	1.4	1.9	1.5	1.5	1.2	1.2	1.2	1.0
1969	1.1	1.2	1.3	1.3	1.4	1.9	1.5	1.5	1.2	1.2	1.2	1.0
1970	1.1	1.2	1.3	1.3	1.4	1.9	1.5	1.5	1.2	1.2	1.2	1.0
1971	1.1	1.2	1.3	1.3	1.4	1.9	1.5	1.5	1.2	1.2	1.2	1.0
1972	1.1	1.2	1.3	1.3	1.4	1.9	1.5	1.5	1.2	1.2	1.2	1.0
1973	1.1	1.2	1.3	1.3	1.4	1.9	1.5	1.5	1.2	1.2	1.2	1.0
1974	1.1	1.2	1.3	1.3	1.4	1.9	1.5	1.5	1.2	1.2	1.2	1.0
ALL-YEARS	1.3	1.3	1.5	1.5	1.7	1.6	1.5	1.4	1.0	1.0	1.1	1.2
MAXIMUM	2.1	2.1	2.1	2.1	2.2	2.2	2.2	2.0	1.4	1.4	1.4	1.2
MINIMUM	1.0	1.0	1.2	1.1	1.1	1.2	1.0	1.0	1.0	1.0	1.0	1.0

Table 3.2.2-2 MII Station 5 hindcast (1951-74) statistics (MII, 1977)

STATION 5
(55.5N 130.4W)
MEAN WAVE HEIGHTS (METERS)
COMBINED SEA/SWELL

	JAN	FEB	MAR	APR	MAY	JUN	JUL	AUG	SEP	OCT	NOV	DEC
1951	1.3	1.2	1.4	1.3	2.0	1.7	1.4	1.3	1.2	1.1	1.1	1.1
1952	1.4	1.1	1.8	1.4	1.9	1.9	1.1	1.7	1.2	1.1	1.1	1.1
1953	1.1	1.6	1.9	2.0	2.1	2.3	1.4	1.3	1.9	1.0	1.3	1.1
1954	1.3	1.1	1.5	1.3	2.0	2.1	1.4	1.3	1.7	1.0	1.3	1.1
1955	1.3	1.2	1.3	1.7	2.1	2.4	1.9	2.1	1.7	1.3	1.3	1.1
1956	1.2	1.4	1.5	1.7	1.8	2.3	1.7	2.0	1.1	1.1	1.3	1.1
1957	1.0	1.0	1.2	1.6	1.6	2.0	1.7	1.7	1.1	1.1	1.3	1.1
1958	1.4	1.5	1.7	1.9	1.5	2.1	1.8	1.3	1.2	1.2	1.0	1.1
1959	1.2	1.3	1.7	1.4	1.5	2.1	1.1	1.3	1.5	1.3	1.3	1.1
1960	1.3	1.4	1.4	1.7	2.2	2.3	1.1	1.3	1.3	1.3	1.3	1.1
1961	1.0	1.1	1.4	1.7	2.2	1.5	1.1	1.4	1.3	1.3	1.3	1.1
1962	1.1	1.6	1.8	1.8	2.4	1.7	1.2	1.3	1.3	1.3	1.2	1.1
1963	1.2	1.1	1.5	1.3	2.0	1.7	1.3	1.2	1.3	1.3	1.2	1.1
1964	1.2	1.1	1.7	1.9	2.0	1.9	1.5	1.2	1.2	1.2	1.1	1.1
1965	1.2	1.1	1.7	1.9	2.0	2.2	1.2	1.2	1.2	1.2	1.1	1.1
1966	1.2	1.1	1.7	1.9	2.0	2.2	1.2	1.2	1.2	1.2	1.1	1.1
1967	1.2	1.1	1.7	1.9	2.0	2.2	1.2	1.2	1.2	1.2	1.1	1.1
1968	1.0	1.9	1.2	1.1	1.5	1.6	1.1	1.3	1.0	1.1	1.1	1.1
1969	1.0	1.0	1.2	1.3	1.4	1.7	1.1	1.4	1.0	1.1	1.1	1.1
1970	1.3	1.3	1.3	1.7	1.8	1.7	1.7	1.4	1.4	1.0	1.1	1.1
1971	1.1	1.0	1.4	2.0	2.4	2.0	2.3	1.9	1.7	1.2	1.1	1.1
1972	1.7	1.2	1.4	1.7	1.7	1.9	1.8	1.8	1.4	1.2	1.3	1.1
1973	1.1	1.1	1.3	1.9	2.0	2.1	1.8	2.0	1.3	1.4	1.3	1.1
1974	1.1	1.9	1.1	1.5	1.9	1.5	1.2	1.1	1.9	1.0	1.1	1.1
ALL-YEARS	1.2	1.2	1.5	1.6	1.9	1.9	1.4	1.5	1.2	1.0	1.1	1.1
MAXIMUM	1.7	1.6	1.9	2.0	2.4	2.4	2.3	2.1	1.7	1.4	1.3	1.1
MINIMUM	1.0	1.0	1.1	1.0	1.5	1.5	1.1	1.1	1.0	1.0	1.0	1.0

Table 3.2.2-3 MII Station 6 hindcast (1951-74) statistics (MII, 1977)

STATION 6
(31.5N 118.4W)

MEAN WAVE HEIGHTS(METERS)
COMBINED SEA/SWELL

	JAN	FEB	MAR	APR	MAY	JUN	JUL	AUG	SEP	OCT	NOV	DEC
1951	1.4	1.3	1.4	1.3	2.1	1.9	1.6	1.4	1.3	1.3	1.0	1.2
1952	1.3	1.1	1.3	1.3	2.0	1.8	1.1	1.4	1.3	1.3	1.2	1.2
1953	1.0	1.0	1.0	1.0	2.4	2.2	1.1	1.7	1.5	1.3	1.4	1.1
1954	1.4	1.4	1.4	1.8	2.1	2.2	1.3	2.2	1.7	1.4	1.2	1.1
1955	1.1	1.2	1.3	1.0	2.2	2.3	2.0	1.5	1.7	1.6	1.2	1.2
1956	1.2	1.3	2.0	1.7	2.1	2.3	1.7	2.0	1.2	1.2	1.2	1.2
1957	1.4	1.6	1.7	1.7	2.0	2.4	2.0	1.3	1.5	1.4	1.1	1.1
1958	1.1	1.3	1.6	1.5	2.2	2.4	1.3	1.3	1.3	1.1	1.1	1.1
1959	1.1	1.3	1.6	1.7	2.4	2.4	1.3	1.3	1.3	1.1	1.1	1.1
1960	1.1	1.3	1.6	1.7	2.4	2.4	1.3	1.3	1.3	1.1	1.1	1.1
1961	1.1	1.3	1.6	1.7	2.4	2.4	1.3	1.3	1.3	1.1	1.1	1.1
1962	1.1	1.3	1.6	1.7	2.4	2.4	1.3	1.3	1.3	1.1	1.1	1.1
1963	1.1	1.3	1.6	1.7	2.4	2.4	1.3	1.3	1.3	1.1	1.1	1.1
1964	1.1	1.3	1.6	1.7	2.4	2.4	1.3	1.3	1.3	1.1	1.1	1.1
1965	1.1	1.3	1.6	1.7	2.4	2.4	1.3	1.3	1.3	1.1	1.1	1.1
1966	1.1	1.3	1.6	1.7	2.4	2.4	1.3	1.3	1.3	1.1	1.1	1.1
1967	1.1	1.3	1.6	1.7	2.4	2.4	1.3	1.3	1.3	1.1	1.1	1.1
1968	1.1	1.3	1.6	1.7	2.4	2.4	1.3	1.3	1.3	1.1	1.1	1.1
1969	1.1	1.3	1.6	1.7	2.4	2.4	1.3	1.3	1.3	1.1	1.1	1.1
1970	1.1	1.3	1.6	1.7	2.4	2.4	1.3	1.3	1.3	1.1	1.1	1.1
1971	1.1	1.3	1.6	1.7	2.4	2.4	1.3	1.3	1.3	1.1	1.1	1.1
1972	1.1	1.3	1.6	1.7	2.4	2.4	1.3	1.3	1.3	1.1	1.1	1.1
1973	1.1	1.3	1.6	1.7	2.4	2.4	1.3	1.3	1.3	1.1	1.1	1.1
1974	1.1	1.3	1.6	1.7	2.4	2.4	1.3	1.3	1.3	1.1	1.1	1.1
ALL-YEARS	1.1	1.2	1.4	1.7	2.1	2.2	1.7	1.4	1.4	1.2	1.1	1.1
MAXIMUM	1.0	2.0	2.2	2.5	2.0	2.0	2.7	2.5	2.2	1.8	1.4	1.4
MINIMUM	1.0	1.0	1.1	1.2	1.7	1.0	1.1	1.2	1.0	1.0	1.0	1.0

Table 3.2.2-4 Extreme events at MII Stations 4,5,6 (MII, 1977)

STATION 4 (33.5N 122.0W)			
EXTREME WAVE EVENT LISTING			
COMBINED SEA/SWELL ~ 5 METERS			
COMPILED FROM ONCE-DAILY WAVE COMPUTATION 1951-1974			
DATE	HEIGHT	PERIOD	DIRECTION
23 DEC 55	7.5	12	222
12 AUG 60	6.8	12	351
02 APR 56	6.4	10	235
18 JAN 73	6.0	11	207
18 APR 73	5.5	10	343
21 MAR 60	5.3	10	334
28 MAR 73	5.3	10	332
09 FEB 60	5.3	10	289
24 MAY 67	5.3	10	342
22 APR 60	5.3	10	325
08 FEB 53	5.0	10	348
28 DEC 65	5.0	10	187
05 JUL 69	5.0	10	324
07 MAR 64	5.0	10	325
19 APR 73	5.0	10	336

STATION 5 (33.5N 120.4W)			
EXTREME WAVE EVENT LISTING			
COMBINED SEA/SWELL ~ 5 METERS			
COMPILED FROM ONCE-DAILY WAVE COMPUTATION 1951-1974			
DATE	HEIGHT	PERIOD	DIRECTION
06 MAR 56	5.6	11	339
14 MAY 55	5.5	10	331
08 FEB 53	5.1	10	341
07 MAY 70	5.0	10	323

STATION 6 (31.5N 119.8W)			
EXTREME WAVE EVENT LISTING			
COMBINED SEA/SWELL ~ 5 METERS			
COMPILED FROM ONCE-DAILY WAVE COMPUTATIONS 1951-1974			
DATE	HEIGHT	PERIOD	DIRECTION
06 MAR 56	6.7	11	344
29 FEB 72	6.6	11	321
24 DEC 64	5.8	11	311
29 MAR 53	5.7	10	310
08 JUN 64	5.6	10	298
20 APR 62	5.4	10	327
26 MAY 67	5.3	10	329
07 MAY 70	5.1	9	320
04 MAY 69	5.1	9	273
05 MAY 68	5.0	10	298

at Station 6.

Although the MII hindcasts are the most systematic and comprehensive, their accuracy has been questioned (Cross, 1980; Hales, 1978a,b; Walker et al, 1984). Cross (1980) compared wave height estimates from shipboard observations (SSMO, 1976), the Fleet Numerical Weather Central (FNWC) hindcasts which form the basis of the MII (1977) tabulations, and NMC (1960). The location of the comparisons is MII and NMC station 3 (Figure 3.2.2-6), offshore and slightly south of San Francisco. As shown in Figure 3.2.2-15, the FNWC (and MII) hindcasted wave heights exceed 5 feet much less often than both SSMO and NMC. There is also a disparity in storm wave direction, with the FNWC hindcasts showing more southwesterly events than NMC. Cross (1980) suggests that the once daily (0400 PST) sampling of wave heights in MII may miss or underestimate conditions detected by the 4 times daily NMC hindcasts. The 0400 PST sampling may also underestimate wind waves generated by strong summer onshore winds which are strongest during the day (Cross, 1980). More extensive evidence of the gross underestimation of wave height by the singular model is given by Lazanoff and Stevenson (1975). They compare FNWC singular and spectral model predictions for several severe storm events to wave heights measured by the oceanographic research vessel, *Flip*, and a specially instrumented Canadian weather ship. The singular model underpredicted the direct observations and the spectral model height predictions by nearly a factor of two. Lazanoff and Stevenson (1975) explicitly point out that the singular model did a particularly bad job of predicting very large waves. Hales (1978a,b), citing a personal communication from R. R. Strange, reports that "known (wave) events failed to show up at all" in the FNWC hindcasts. Walker et al (1984) point out that at MII Station 5, only 4 storms in 24 years have hindcast significant heights greater than 5 m (Table 3.2.2-4). Two of these are in May, not in the storm season, and none of several well-documented high wave episodes are hindcast. Walker et al (1984) state that "results of this (FNWC/II) hindcast have been studied in detail with the

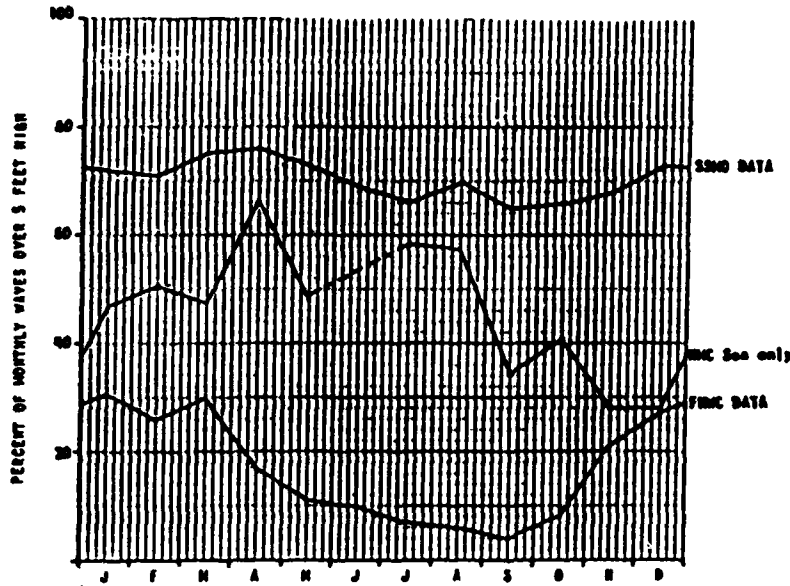


Figure 3.2.2-15 Percentage each month of waves exceeding 5 ft off San Francisco; upper line is shipboard observations, middle is NMC sea only hindcast, lower is FNWC hindcast (Cross, 1980).

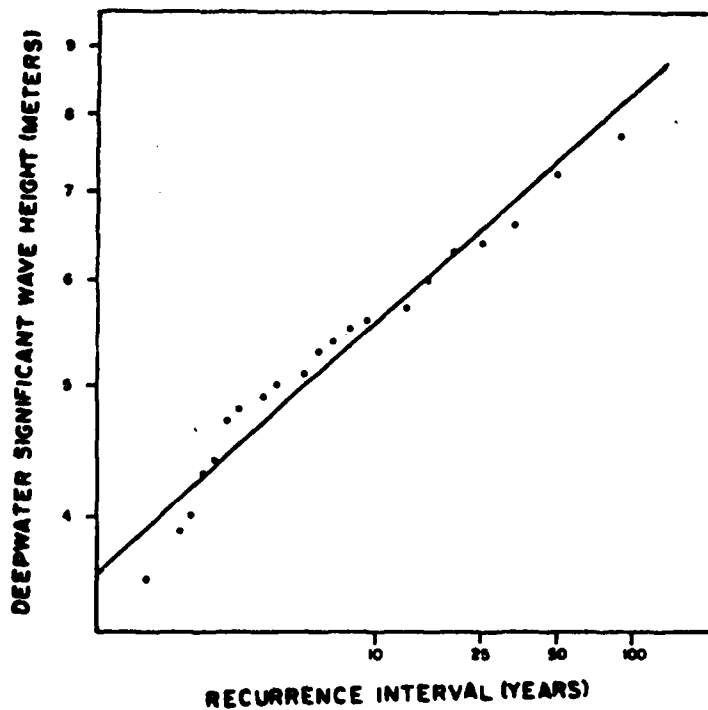


Figure 3.2.2-16 Recurrence intervals based on a 1900-83 hindcast (Tables 3.2.2-5,6) for a location seawards of the Channel Islands (Walker et al, 1984).

conclusion that there are major problems with the methods employed." On the other hand, Appendix T in Williams et al (1981) shows several good comparisons between FNWC hindcasts and ship observations. It is unclear whether the MII (1977) statistics at all stations are generally in error, or whether it is only at certain positions and/or the extreme wave conditions (i.e. Figure 3.2.2-15) which are inaccurately hindcast. The southerly station wave roses of MA (1961a), NMC (1960b) and MII (1977) are qualitatively similar (Figures 3.2.2-7 to 3.2.2-14).

Walker et al (1984) present extreme wave statistics from two sources: (1) Marine Advisers (MA, 1960a) for 1900-1957 for an unsheltered location seawards of Oceanside (Table 3.2.2-5), (2) Pacific Weather Analysis (1983) for 1958-1983 seawards of the channel islands in southern California (Table 3.2.2-6). The hindcasts are not directly comparable because of different hindcast years and methodologies, poor wind data in the early years, and other factors. No southern hemisphere swell is included in either study. The extreme wave statistics presented in Tables 3.2.2-5,6 have waves from extratropical and tropical storms. The most frequent and severe waves are due to the extratropical storms. However, the largest hindcasted wave event of record was the 1939 tropical storm that made landfall in southern California. The three maximum tropical storm swells in Table 3.2.2-6 (1958-83) are included for comparison with the 1939 event. The winter of 1983 was very stormy, and is discussed further in Section 3.2.3. Significant height recurrence intervals, based on all the hindcasts (1900-1983, except the 1939 tropical storm) are shown in Figure 3.2.2-16 (Walker et al, 1984). The 100-year recurrence interval wave height is 8.3 meters, compared to 6.6 m for the period 1900-1957. The 1983 storms contribute substantially to this increase.

Seymour et al (1984) present a storm wave hindcast for the period 1900-1984, using a single methodology (which is not described but implied to be spectral) throughout. The hindcast location is near 35° N, somewhat further north than Tables 3.2.2-5,6. Only waves with deep water approach directions between SW and WNW are considered. Tables 3.2.2-7,8 give

Table 3.2.2-5 Hindcast (1900-57) statistics for an unsheltered location off Oceanside (Marine Advisers, 1960)

Hindcasted Maximum Significant Wave Characteristics
in Deep Water for 1900 to 1957

<u>Date</u>	<u>H^a (Feet)</u>	<u>T (Seconds)</u>	<u>Azimuth (Degrees)</u>
9-10 Mar 1904	17.9	12.0	225
8-10 Mar 1912	17.5	11.5	270
16-17 Dec 1914	13.0	9.9	180
28-30 Jan 1915	16.3	11.8	205
1-3 Feb 1915	16.5	12.4	280
26-28 Jan 1916	14.0	9.6	250
1-2 Feb 1926	12.6	16.0	260
6-8 Apr 1926	11.8	13.8	270
6-12 Dec 1937	11.6	16.4	270
15-25 Sep 1939 ^a	26.9	14.0	205
20-23 Jan 1943	16.2	10.8	180
13-14 Mar 1952	11.7	11.7 ^b	250
6-8 Jan 1953	16.0	19.2 ^b	260

^atropical storm

^b15.0 to 15.8 seconds was recorded at Camp Pendleton

Table 3.2.2-6 Hindcast (1958-83) statistics for a location seawards of the Channel Islands
(Walker et al, 1984)

Hindcasted Maximum Significant Wave Characteristics
in Deep Water for 1958 to 1983

<u>Date</u>	<u>Classification</u>	<u>H (Feet)</u>	<u>T (Seconds)</u>	<u>Arimuth (Degrees)</u>
Jan 1958	sea	9.0	9-10	280
	swell	15.2	13-14	270
	summation	18.1	13-14	-
Apr 1958	sea	7.4	8-9	280
	swell	20.0	17-18	293
	summation	25.1	17-18	-
Feb 1960	sea	14.2	11-12	290
	swell	15.3	18-19	294
	summation	18.3	18-19	-
Feb 1963	sea	11.8	10-11	150
	swell	15.9	14-15	269
	summation	19.5	13-14	-
Sept 1963 ^a	swell	10.3	14-15	167
Feb 1969	sea	7.5	8-9	280
	swell	14.3	14-15	284
	summation	15.6	14-15	-
Dec 1969	swell	14.4	20-21	276
Aug 1972 ^a	swell	11.6	17-18	156
Jan 1978	sea	5.1	7-8	290
	swell	16.6	16-17	284
	summation	18.6	16-17	-
Feb 1980	sea	10.3	9-10	220
	swell	15.3	13-14	255
	summation	15.6	14-15	-
Jan 1981	swell	15.4	17-18	265
Jan 1981	sea	4.8	6-7	210
	swell	21.1	15-16	269
	summation	21.5	15-16	-
Sept 1982 ^a	swell	10.1	17-18	158
Nov 1982	sea	17.1	12-13	290
	swell	17.6	14-15	293
	summation	20.4	10-11	-
Jan 1983	sea	7.3	8-9	160
	swell	19.7	20-21	283
	summation	21.0	20-21	-
Feb 1983	sea	3.5	5-6	320-340
	swell	16.7	16-17	275
	summation	17.1	16-17	-
Mar 1983	sea	12.6	11-12	160
	swell	22.3	18-19	263
	summation	23.6	18-19	-

^atropical storm

Table 3.2.2-7 Hindcast (1900-84) waves exceeding 3 m height near 35° N (Seymour et al, 1984)

EXTREME WAVE EPISODES EXCEEDING 3 M. (BASIC SERIES) 1900 - 1984			
DATE	SIG. HT. (m)	MAX. PERIOD	DIRECTION
13 MAR 05	8.8	15	247
17 NOV 05	3.3	17	286
31 DEC 07	5.3	16	282
12 MAR 12	3.2	12	220
26 JAN 14	5.8	13	223
03 FEB 15	7.5	14	235
01 JAN 18	3.7	16	280
12 FEB 19	5.3	12	299
20 DEC 20	4.7	13	301
15 OCT 23	3.7	16	296
01 FEB 26	6.9	15	257
03 JAN 27	5.8	20	287
06 NOV 28	4.0	17	294
01 JAN 31	3.9	16	276
28 DEC 31	7.4	18	288
19 DEC 35	4.7	16	267
13 DEC 37	4.5	16	272
06 JAN 39	7.9	19	285
25 SEP 39	4.5	15	205
24 JAN 40	4.3	16	267
25 DEC 40	5.7	16	270
20 OCT 41	3.3	17	294
30 DEC 45	3.9	19	285
13 FEB 47	3.9	16	265
04 NOV 48	4.7	18	300
15 NOV 53	5.7	17	269
15 JAN 58	3.1	22	280
26 JAN 58	6.8	14	259
05 APR 58	7.7	18	289
16 FEB 59	5.1	14	244
09 FEB 60	8.1	19	295
22 DEC 60	3.4	17	276
31 JAN 63	4.2	16	260
10 FEB 63	5.9	15	256
19 NOV 65	4.0	15	277
07 DEC 67	4.0	15	298
06 FEB 69	4.7	13	222
04 DEC 69	3.6	17	278
06 DEC 69	4.9	22	274
14 DEC 69	5.7	17	290
19 DEC 69	4.7	18	281
26 DEC 72	4.1	15	289
21 FEB 77	5.2	18	280
29 OCT 77	5.5	20	299
16 JAN 78	6.0	13	240
01 JAN 80	4.7	20	272
17 FEB 80	6.1	18	249
22 JAN 81	4.3	20	258
28 JAN 81	7.0	17	262
13 NOV 81	4.9	18	284
01 DEC 82	6.4	14	295
18 DEC 82	6.4	20	288
25 JAN 83	6.1	17	278
27 JAN 83	7.3	22	279
10 FEB 83	6.7	25	281
13 FEB 83	4.9	17	268
01 MAR 83	8.2	20	258
14 NOV 83	5.8	17	290
03 DEC 83	7.0	17	285
25 FEB 84	6.4	17	300

Table 3.2.2-8 Hindcast (1900-84) waves exceeding 6 m height near 35° N (Seymour et al, 1984)

EXTREME WAVE EPISODES EXCEEDING 6 M.
1900 - 1984

DATE	SIG. HT. (m)	MAX. PERIOD	DIRECTION
13 MAR 05	8.8	15	247
03 FEB 15	7.5	14	235
01 FEB 26	6.9	15	257
28 DEC 31	7.4	18	288
06 JAN 39	7.9	19	285
26 JAN 58	6.8	14	259
05 APR 58	7.7	18	289
09 FEB 60	8.1	19	295
17 FEB 80	6.1	18	249
28 JAN 81	7.0	17	262
01 DEC 82	6.4	14	295
18 DEC 82	6.4	20	288
25 JAN 83	6.1	17	278
27 JAN 83	7.3	22	279
10 FEB 83	6.7	25	281
01 MAR 83	8.2	20	258
03 DEC 83	7.0	17	285
25 FEB 84	6.4	17	300

wave characteristics for the storm events with significant heights exceeding 3 and 6 m respectively. The post 1958 hindcasts in Walker et al (1984) and those in Seymour et al (1984) were both calculated by R. R. Strange of Pacific Weather Analysis, presumably using the same methodology. Thus, because of their close proximity, many of the storm waves in Table 3.2.2-6 differ by only small amounts from Table 3.2.2-7. Seymour et al (1984) point out that the most commonly occurring wave direction in the 84 year hindcast is about 280° , somewhat more westerly than the traditionally assumed northwest approach (Figures 3.2.2-7,10,12). The periods of extreme wave events are also longer than conventional hindcasts; most of the periods in Table 3.2.2-7 are greater than 15 sec, while all the MII (Table 3.2.2-4) and most of the Marine Advisor (Table 3.2.2-5) periods are less than 15 seconds. The longer periods are consistent with buoy observations. Particularly long periods are associated with the most severe storm waves; none of the > 6 m wave heights (Table 3.2.2-8) have periods less than 14 seconds.

All of the above hindcasts (with the exception of Walker et al (1984) and Seymour et al (1984)) are based on singular wave models rather than spectral wave models. In singular models, only a single swell train (1 period and 1 direction) is considered to be generated at a given time by a particular storm. In spectral models, the generated waves have a distribution in both frequency and direction. Most modern hindcast schemes are spectral. For example, the singular FNWC model (Hubert and Mendenhall, 1970), used in MII (1977), was replaced in 1974 with a spectral (FNWC) wave model. The development of spectral generation models is ongoing. Several large experiments (i.e. JONSWAP, GATE) have carefully monitored winds and the wave response. Discussions of these experiments and the general wave generation problem (Hasselmann et al, 1976; Foristall et al, 1978; Mitsuyasu and Rikiishi, 1978; Gunther et al, 1980; Cardone et al, 1981; Lawson and Long, 1983; Komen et al, 1985, and others), is beyond the scope of this report. It is true, however, that the deep water California hindcasts discussed above (with the noted exceptions) are based on outdated theories and are only qualitatively

correct, at best. Given the suggested inadequacies of the MII (1977) hindcast, the NMC (1960b) and Marine Advisers (1961a) seem best for applications. As part of its Wave Information Study, the Army Corps of Engineers is developing a spectral wave generation model for calculating a 20-year wave hindcast for the study region. This model will undoubtedly improve hindcasts for waves generated in the northern hemisphere, in part because of the availability of in situ measurements with which to "tune" the hindcasts. Other numerical models (Forristal et al, 1978) that have been developed and calibrated specifically for hurricanes can yield wave height predictions with errors of only about 30 percent. This accuracy cannot necessarily be expected for a hindcast in the present area, even using a spectral model, because of a lack of detailed wind observations for historical southern hemisphere and tropical storms. The accurate predictions of wave spectra during Hurricane Delia (Forristal et al, 1978) were generated using a model that had been calibrated previously with measured frequency spectra for Gulf of Mexico hurricanes (Cardone et al, 1976). Such calibration had not been done for the singular model. Furthermore, the calibration of models for coastal sites may be more difficult than for hurricanes or general open ocean sites.

There are two major aspects to the wave hindcasting model: the wind field description and the wave prediction technique. The importance of the wind field description cannot be overemphasized. For hurricanes, it is possible to use a model storm approach, since the similarity of hurricane pressure fields allows their description with relatively few parameters. This is fortunate, since the sparseness of measurements in most hurricanes precludes the use of standard synoptic meteorological analysis techniques. (Forristal et al, 1978).

Some very recent wind observations by Friehe and Winant in an area 105 km (65 mi) long and extending 40 km (24 mi) offshore of the Bodega Bay area in northern California, "revealed several interesting features of the coastal mesoscale structure which are very important in their relation to the wind-driven coastal processes. The existence of the low-level strong wind jet and spatial inhomogeneity of the surface wind are features that are not predictable from present synoptic or boundary layer analysis" (Friehe and Winant, 1982). The average wind speed

during these observations was 35 kn, with gusts to 50 kn. The large spatial fluctuations in the coastal wind field could certainly influence the local wave field. Local wind effects may also be quite important in the Santa Barbara Channel (Hales, 1978a,b). The point is that the quality of results from a wave generation model may be limited by knowledge of the wind field. This limitation may be important both in hindcasts of past major storms and present day conditions which are the result of anomalous local wind effects.

We note in passing that there is an extensive body of wave data based on visual observations from ships commonly referred to as SSMO (Synoptic Shipboard Meteorological Observations). These data are largely restricted to shipping lanes, are very qualitative, and may not reflect the most severe storms because ship routes are altered to avoid such conditions.

3.2.3 *Recent Storms*

The constantly increasing development of the coast has led to increasing damage from storm events. Particularly destructive storms occurred in the winters 1977-1978 and 1982-1983. The purpose of this section is to review the general characteristics of those storm events and the associated damages.

Winter 1977-1978

The coincidence of high waves, local storm surges, and high tides resulted in extensive erosion and damage to coastal structures in the winter of 1977-1978. Armstrong (1980) estimates the damages at \$18,000,000, split approximately equally between northern and southern California. This was the most expensive storm in decades.

During the 1977-78 winter storm period a large high-pressure system over Alaska and western Canada caused storm centers to be moved 1,000 to 1,500 miles due west of central California, further south than their normal locations. As a result extra-tropical cyclones followed a more southerly course than normal. As storms approached the coast, pre-frontal

southerly winds with speeds of 30-40 knots were recorded. These winds created large westerly and southwesterly swells which attacked beaches sheltered from north swell (for example, Point Dume to Santa Monica, Armstrong, 1980). Representative offshore wind and wave data is given in Table 3.2.3-1.

The most important characteristic of the 1977-78 winter storms was their persistence. Virtually every storm generated in the North Pacific hit the California coast (Armstrong, 1980). Figure 3.2.3-1 shows a comparison of wave power for three winter seasons, on a logarithmic scale (Dormurat, 1978). Waves in the winter of 1977-1978 consistently had roughly an order of magnitude more power than the preceeding two years.

The strong winds associated with these frequent storms caused superelevations of sea level (storm surges) that approached 2 ft at some locations. High spring tides in January and February coincided with storm arrivals. The repeated wave attacks, coupled with large water level superelevations due to storm surge and tides, eroded and lowered the beaches by 10 to 15 ft in elevation. This extreme loss of protective beach made all coastal structures vulnerable to the high-energy waves breaking at the base of or directly on the structures (Armstrong, 1980).

Winter 1982-1983 - An El Niño event?

The period December 1982 - March 1983 "was a period of intense storminess in the North Pacific. The coast of California was subjected to a number of events of extraordinarily large waves. During the storms of late January, the astronomical tides were very large (ranges of about 10 feet). During the entire winter, the El Niño climatic anomaly resulted in a slowing of the California Current and a general rise of sea level of about 8 inches along the coast. Strong winds accompanied many of the intense wave events and the wind stress probably elevated the surface by another foot. The combination of the astronomical and storm tides, plus the general rise in sea level, caused the already destructive waves to inflict a very substantial amount of structural damage, flooding and sand wash-over. Piers, jetties and breakwaters, which are

Table 3.2.3-1 **Wind (NOAA station at Farallon Island) and storm wave (60 miles west of Golden Gate) data for Jan-Feb 1978 (Armstrong, 1980)**

Date	Wind		Significant Wave		
	Speed (knots)	Direction	Height (ft)	Period (sec)	Direction
Jan. 9	35	SW	14	18	SSW
Jan. 13	35	SW	21	14	S
Jan. 16	50	SW	18	16	WSW
Feb. 9	45	S	20	16	SSW
Feb. 10	40	WNW	16	12	SSW
Feb. 13	40	NW	17	16	SSW

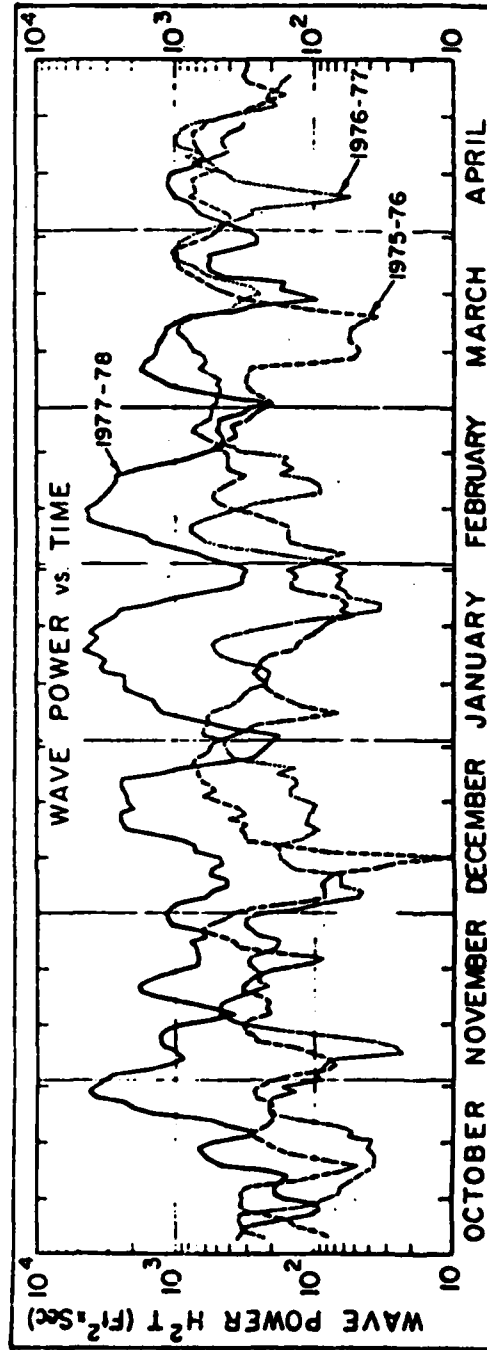


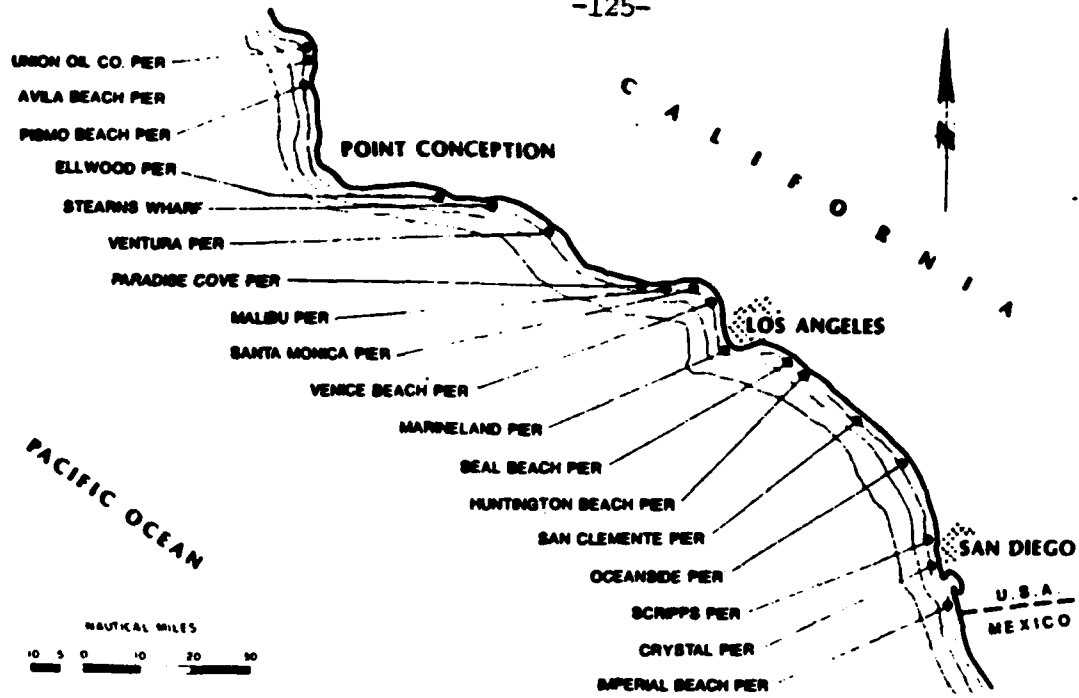
Figure 3.2.3-1 Five-day moving average of wave power offshore in deep water from San Francisco, California during the seven-month period of the winters of 1975-76, 1976-77, and 1977-78 (Dormurat, 1978).

particularly sensitive to superelevations of sea level, were damaged all along the coast during this winter." (Seymour, 1983b). The California coastal damage from these storms is estimated as \$118,000,000 (USACE LAD, 1984), about 6 times the damage of the 1977-1978 storms. Detailed estimates of damage, broken down according to county, type of damage, etc. are given in USACE LAD (1984). Figure 3.2.3-2 shows locations of pier and jetty damage in California (Walker et al, 1984).

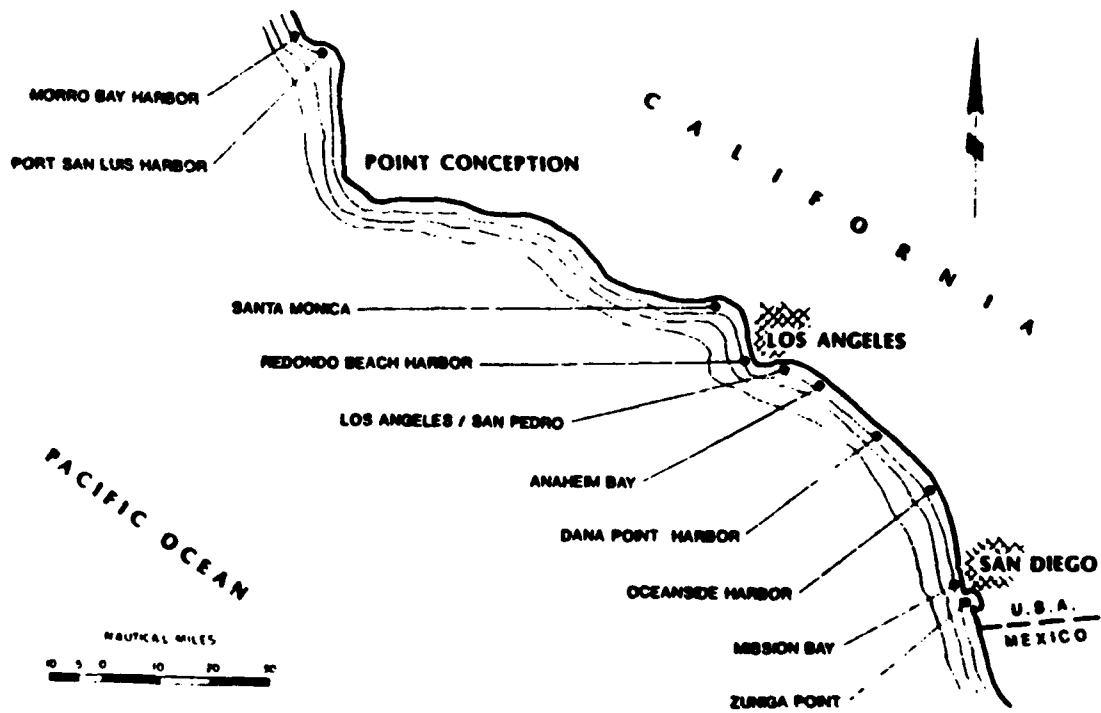
Table 3.2.3-2 (after Seymour, 1983b) lists the maximum heights and largest periods (at which spectra were peaked) in any of the wave station records of the CDIP operating at that time. The largest waves were almost always at the North Monterey Bay buoy, with only slightly smaller waves at Begg Rock. The longest periods were also at these locations. There were eight storms in 1983 with significant wave heights above 14 feet, and only seven such wave events in the preceeding 3 years. The highest significant wave recorded during 1980-1982 was 18 feet compared to 24 feet in 1983. Note also the very long periods found in the 1983 storms. All eight storms had peak periods of 17-22 seconds. In the previous three years, only one storm exceeded a 17-second peak period. An 84-year hindcast discussed above (Table 3.2.2-7,8) suggests that the 1982-1983 waves were among the most energetic in this century.

Measurements (NOAA buoy) and subsequent *spectral* hindcasts (Pacific Weather Analysis) show the storm waves to have much longer periods than previously thought. Prior to the recent storms, typical design waves had periods of 10 to 14 seconds. Some previously used hindcasted data sets indicated that waves of 14 seconds or more existed only as low forerunners. The buoy data indicate that rarely is there a high wave episode with peak energy periods below 14 seconds (Walker et al, 1984).

Seymour et al (1984) investigated the possible connection between the El Niño climatic anomaly and the occurrence of large waves in southern California. They summarize the meteorological conditions during the 1982-1983 winter El Niño; an unusually strong Gulf of



Pier Damage



Breakwater and Jetty Damage

Figure 3.2.3-2 Location of pier, breakwater and jetty damage from 1977-78 winter storms (Walker et al, 1984).

Table 3.2.3-2 Major storms, Jan-Mar during 1980-83 (Seymour, 1983)

YEAR	INCLUSIVE DATES	MAX. SIGNIFICANT WAVE HEIGHT (FT)	MAX. PEAK PERIOD (SEC)
1980	13 JAN	11	12
"	17-21 FEB	18	15
"	27-28 FEB	12	13
"	18 MAR	11	10
1981	21-22 JAN	16	20
"	27-28 JAN	18	14
"	24 FEB	11	14
"	4-5 MAR	12	13
1982	2-4 JAN	17	14
"	18-19 JAN	13	15
"	28-29 JAN	14	16
"	22-23 FEB	13	12
"	2 MAR	15	14
"	14-15 MAR	13	15
"	29-30 MAR	15	15
1983	18-20 JAN	16	17
"	23-25 JAN	18	20
"	26-29 JAN	24	20
"	12-14 FEB	18	22
"	18-21 FEB	15	18
"	28 FEB - 2 MAR	23	21
"	8 MAR	16	18
"	17-18 MAR	14	20

Alaska - Aleutian low pressure center which was generally large and displaced eastward enough to affect California. This pressure pattern spawned frequent and severe storms which propagated across the central North Pacific and struck California. The usual storm track has a more northerly landfall. Using historical records, Seymour et al (1984) demonstrated a strong correlation between moderate and strong El Niño events and large wave events in California. They also show a statistically significant correlation between non-El Niño winters and an absence of large waves. For example, considering a 3 m threshold for a wave event (Table 3.2.2-7), there was an average of .71 events per year over all 84 years, 1.58 events per year for the 19 moderate and strong El Niño years, and .45 events per non-El Niño years. Seymour et al (1984) also suggest that the pronounced warming of the surface waters along the California coast during a strong El Niño condition allows tropical cyclones to penetrate further northward than in non-El Niño years. They could not pursue this hypothesis with wave hindcast data, because tropical cyclones are of such small spatial extent that they are not described in detail sufficient for hindcasts on pre-satellite weather maps. It is true, however, that of 9 tropical cyclones which made landfalls in southern California during this century (85 years), 5 occurred in the 19 El Niño years.

3.3 COASTAL WAVES AND ASSOCIATED CURRENTS

Coastal wave conditions can be studied with direct measurements or by transforming the deep ocean hindcasts discussed above to coastal locations. The transformation models are very useful for gaining an understanding of the physical processes modifying deep ocean waves as they traverse the topographically complex Southern California Bight. Transformation models have also been used to infer wave conditions at sites where direct measurements are not available. Direct, in situ measurements obviously provide the most reliable information about the waves at a particular location. However, the measurements must be conducted for a long enough time to encounter the variety of conditions which may occur, and such measurements clearly cannot be made at every location where wave information may be needed. Below, transformation models are used to discuss possible general patterns of coastal wave spatial variability. Sources of in situ coastal wave data are then discussed, with detailed discussion of individual sites deferred to Sections 4-11. Section 3.3 is concluded with a general discussion of the surf zone longshore currents which are associated with the breaking and dissipation of waves on a beach.

3.3.1 *Patterns of coastal wave spatial variability*

The topographic setting of the study area has a profound effect on the swell and wave climate. The Channel Islands and coastline orientation provide locations south of Point Conception with significant shelter from the deep ocean wave regime. A full understanding of the wave climate in this coastal region will ultimately require a complete knowledge of the island sheltering processes. Wave processes such as refraction and scattering by bathymetry, local wind generation, diffraction, nonlinear interactions, and wave-current interactions may all play roles in determining the nature of the island shadows. An experimentally verified model incorporating these effects is not available. It follows that, in the absence of long-term in situ measurements, coastal wave conditions south of Point Conception can only be approximated (with an unknown accuracy), from the wave field outside the islands, which is itself generally

not well known.

Pawka and Guza (1983) give a rather detailed discussion of the islands' effects on waves between Dana Point and the Mexican border (Figure 3.3.1-1). Their transformation model was based on a theoretical calculation which relates the coastal wave conditions (in deep water ~ 2 km from shore) to the deep ocean (outside of the islands) wave field. Wave refraction by shoals in the island vicinity and blocking by the islands are numerically evaluated by the coastal wave transformation model. The method of refraction of a continuous directional spectrum, described in detail by Collins (1972), was employed. The wave rays were drawn with a numerical model developed by Dobson (1967). The model neglects diffraction, focusing at caustics, and bottom dissipation. Pawka (1982) discusses these processes and indicates that they may be neglected for most wave conditions in this transformation model. Local wind generation of waves is also neglected although this process is occasionally important at higher wave frequencies. The effects of nonlinearities of the wave field are unknown. The details of the ray theory, bathymetry grids, etc. are discussed by Pawka (1982).

Several directional spectrum transformations for 17.0 second waves incident to local deep water at Torrey Pines Beach (Figure 3.3.1-1) are shown in Figure 3.3.1-2. The coastal "responses" show the effect of blocking of San Clemente Island ($\alpha \geq 270^\circ T$ in panel b) and Point Conception-Santa Rosa-Santa Cruz Islands ($\alpha \geq 290^\circ T$ in panel a), (Figure 3.3.1-1). Also evident is the strong refraction effects associated with the shoals in the directional ranges $250-260^\circ T$ and $280-290^\circ T$. Of particular importance are the Cortez and Tanner Banks ($250-260^\circ T$) which refract energy to this coastal site in response to a wide range of deep ocean conditions. Thus, at this coastal site there is (theoretically) incident wave energy at $250-260^\circ$ for both southerly, west and northern deep ocean swell peaks (Figure 3.3.1-2). In fact, the banks provide a relatively narrow southerly peak at Torrey Pines Beach in response to high angle north swell in the deep ocean (Figure 3.3.1-2a)! The location of these banks, and

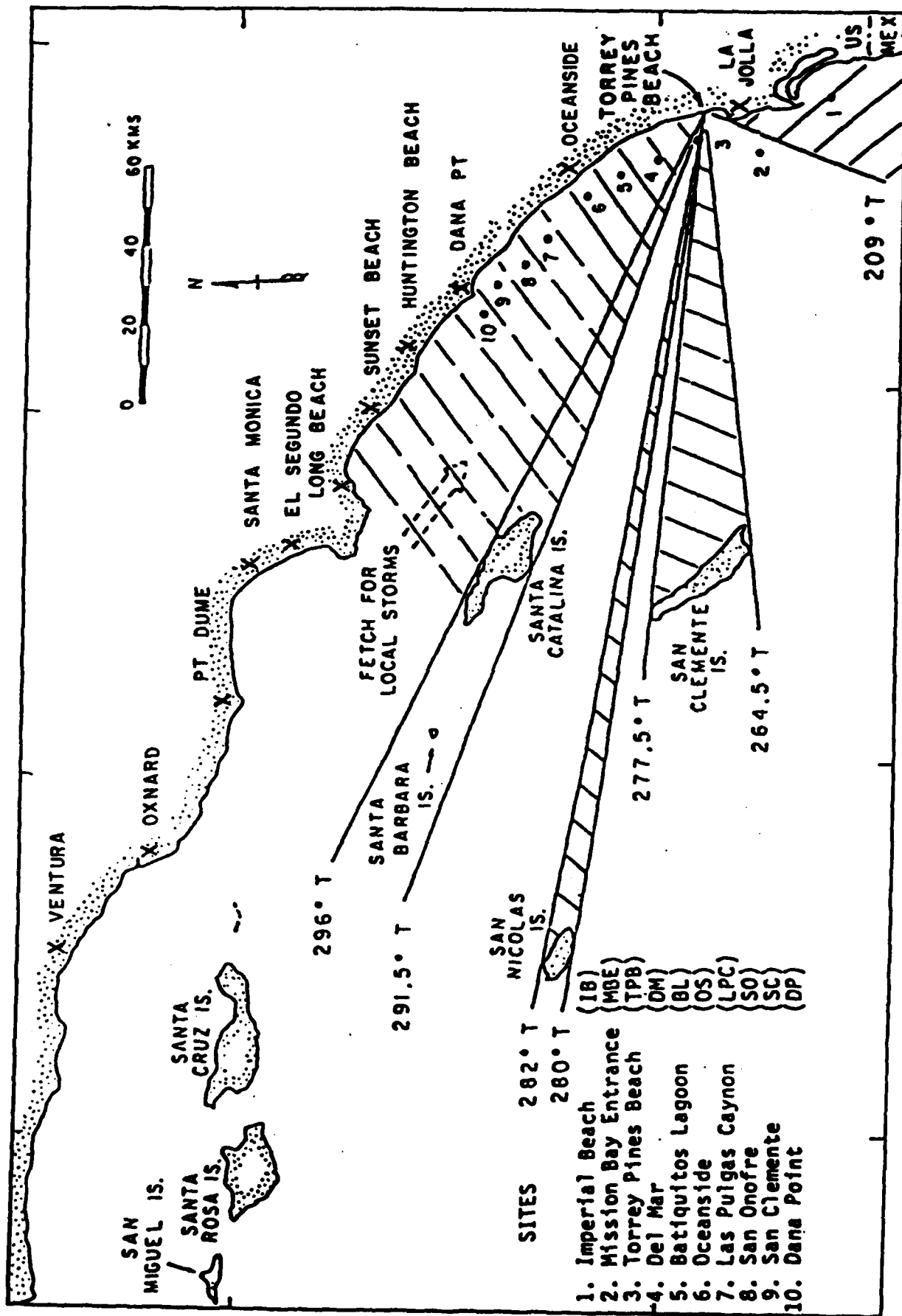


Figure 3.3.1-1

Map of southern California coastline with approximate sites (numbered) for the wave field analysis of Pawka and Guza (1983). The sites are in approximate "deep water."

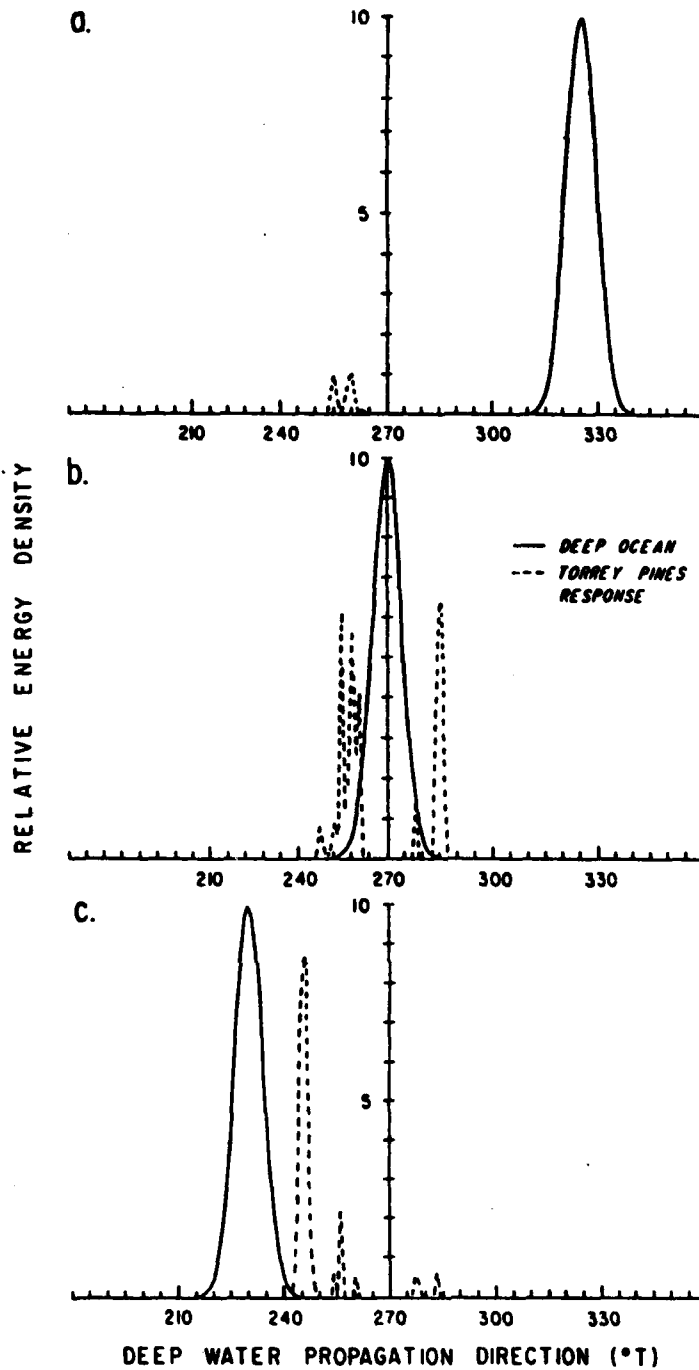


Figure 3.3.1-2

Theoretical directional response at Torrey Pines Beach (local deep water) for 0.059 Hz waves and several deep ocean spectrum forms. The transformations were computed using the coastal wave transformation model. Low energy density is predicted for the shadowed quadrants (for example, the San Clemente Island shadow centered on about 270°T). (Pawka and Guza, 1983).

schematic rays, are shown in Figure 3.2.2-1. Figure 3.3.1-3 shows directional spectra offshore of Torrey Pines Beach, based on 64 hours of data collected during March 1977 with a high resolution linear array (Pawka, 1983). The San Clemente Island shadow at 270° is very clear. Pawka et al (1984) show, using a synthetic aperture radar (SAR) to measure northerly swell at Begg Rock (seawards of the islands, Figure 3.2.2-1) that the secondary peak with direction 255° (Figure 3.3.1-3) is indeed a refractive peak associated with the effects of Cortez and Tanner Banks on north swell. Pawka (1982) and Pawka et al (1984) contain detailed quantitative comparisons of predicted and observed island shadows at Torrey Pines Beach. Their conclusion is that a refraction-blocking transformation model contains much of the essential physics of the island sheltering process at Torrey Pines Beach, for the frequency range .082 - .114 hz (periods 8-12 seconds). At lower frequencies the offshore wave field contained substantial southerly, as well as northerly, components and the offshore SAR measurements were not sufficiently accurate to provide quantitative deep water wave inputs to the transformation model. On days thought to be predominantly north swell, the low frequency coastal observations are in agreement with the model (Pawka et al, 1984). At high frequencies ($f > .12$ hz, $T < 8$ sec), comparisons were difficult because of local generation (i.e. inside the islands). Comparable, detailed verification studies have not been done at any other locations in the study area. Nevertheless, the above studies (and much other work not done in the study area) give some confidence in transformation models.

The directionally integrated frequency responses at Torrey Pines Beach and Oceanside versus deep ocean direction are shown in Figure 3.3.1-4. The responses are calculated by integrating the coastal response over all directions for 5° rectangular spreads in deep ocean energy. The strong variation of the curves with frequency is due to the wavelength dependence of the refraction process. The "windows" to the deep ocean are sharpest at the higher wave frequencies. Refraction effects, which tend to fill in the shadows, are relatively strong at Torrey

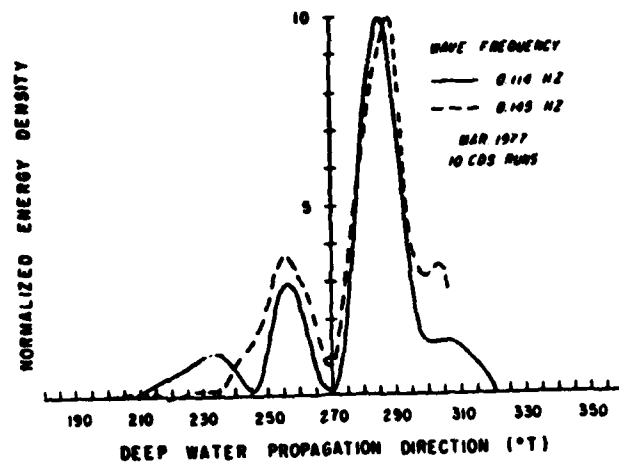


Figure 3.3.1-3 Measured directional spectra at Torrey Pines Beach (refracted into local deep water) for the 10 sample days. The data runs have a cumulative length of roughly 64 hours (Pawka, 1983).

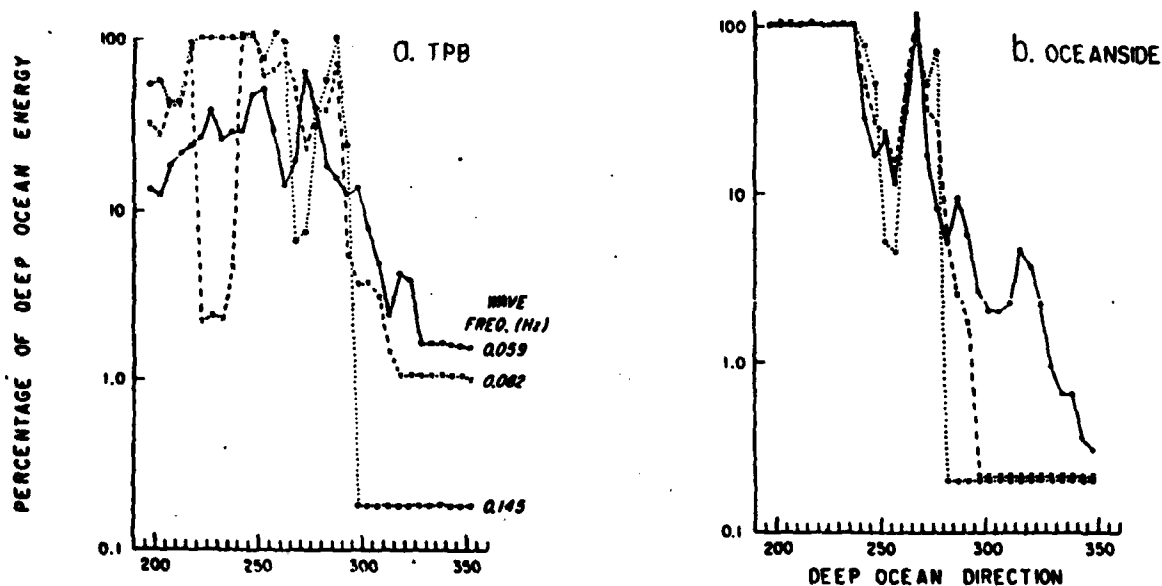


Figure 3.3.1-4 Calculated wave energy response at a) Torrey Pines Beach and b) Oceanside (local deep water) versus deep ocean direction. The values given are the wave energy ratio coastal/deep ocean for 5° rectangular spreads in deep ocean directions (Pawka and Guza, 1983).

Pines Beach due to its exposure to a large cross-section of Cortez and Tanner Banks. The exposure to these banks at Oceanside is partially shielded by San Clemente Island ($\alpha \sim 250^\circ$). Note that for all wave frequencies at both sites a 10° shift in deep ocean mode direction can radically alter the predicted coastal energy.

Wave transformations similar to those discussed above were performed for 10 coastal locations between Dana Point and the Mexican border (Figure 3.3.1-1), for wave periods of 17.0 and 12.2 seconds (Pawka and Guza, 1983). The sites are roughly evenly spaced, with a mean separation of 13 km, and are in approximate "deep water" 2 km offshore. Further refraction would be necessary to bring the waves into shallow coastal areas. In addition to the analysis for the two wave periods, the case of no refractive effects (i.e. only shadowing by the subaerial islands is considered), appropriate for wave periods less than about 7 seconds, was calculated for each site. The structure of the coastal response displayed by this model for the shorter periods ($T \leq 7.0$ second) will be altered by local generation when local winds are energetic.

The directional structure of the climatic north and south swell was obtained from hindcast data (Marine Advisers, 1961a). The directional distribution of the climatic north swell energy is smooth with a mode of roughly $305^\circ T$ and a width (full width at half maximum, FWHM) of 40° . The FWHM is a measure of the narrowness of a directional distribution. More specifically, it is the angular separation between the shoulders (half power points). The climatic south swell is somewhat broader ($FWHM = 50^\circ$) with a mode direction of $225^\circ T$. The energetic responses to the climatic conditions as a function of coastline position are shown in Figure 3.3.1-5. The north response is very smooth with a rough "V" shape. The rise in the response north of Oceanside is due to a window opening between Santa Catalina and Santa Rosa Islands (Figure 3.3.1-1). Neglecting Torrey Pines Beach, the south swell response is very smooth with a monotonic decrease in energy upcoast. Torrey Pines Beach is locally sheltered from south swell by Point La Jolla (Figure 3.3.1-1).

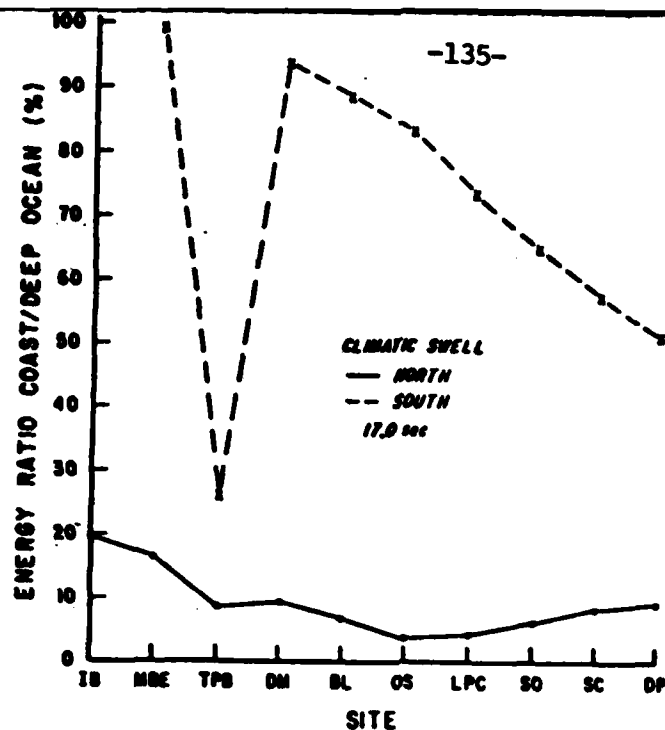


Figure 3.3.1-5

Coastal response to climatic offshore wave conditions obtained from Marine Advisors (1961) and described in the text. The symbols for the sites are defined in Figure 3.3.1-1. The anomalous response to south swell at Torrey Pines Beach (TPB) is due to local sheltering by Point La Jolla (Pawka and Guza, 1983).

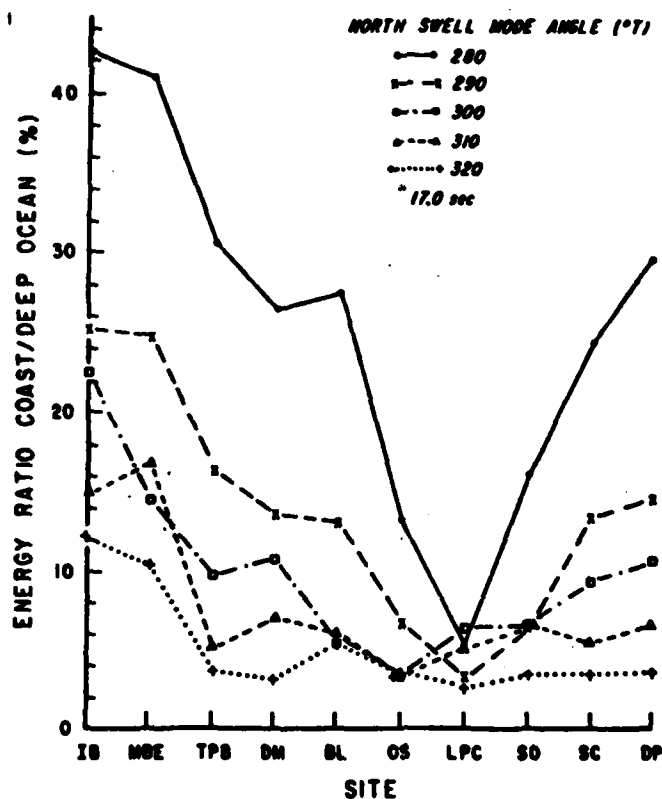


Figure 3.3.1-6

Coastal response to north swell events. The directional distributions of the deep ocean events are all 20° wide (full width at half maximum). The site symbols are defined in Figure 3.3.1-1 (Pawka and Guza, 1983).

The coastal energy response to typical individual north swell events (i.e. relatively narrow directional beam) are shown in Figure 3.3.1-6. The assumed directional width of these events ($\text{FWHM} = 20^\circ$) was typical of spectra sampled in the deep ocean during the West Coast Experiment (Pawka, 1982; Pawka et al, 1984). Although some of the responses are much more dramatically varying than the climatic responses (Figure 3.3.1-5) the basic "V" shape is preserved. The "V" consistently bottoms out in energy in the vicinity of Oceanside and Las Pulgas Canyon. Note that a change in 10° of the mode angle of these events can sharply alter the expected coastal response (compare 280° with 290° in Figure 3.3.1-6).

The south swell event responses are shown in Figure 3.3.1-7. Because of the large distances to southern hemispheric storms, the directional spectra of these events is expected to be narrower ($\text{FWHM} = 10^\circ$) than the north swell. There is nearly full exposure, neglecting Imperial Beach and Torrey Pines Beach, for mode angles in the range $190\text{--}210^\circ\text{T}$. Note that southerly sites (Mission Bay, Del Mar, Batiquitos, Oceanside) receive 100% of the deep ocean energy from south swell with directions $190\text{--}230^\circ$, but less than 25% of the deep ocean energy from north swell with angles $290\text{--}320^\circ$ (Figure 3.3.1-6). This sheltering is responsible for the fact that south swell is very important to the southernmost areas of California, even though it is much less energetic than north swell seawards of the islands (compare heights on Figures 3.2.2-7,8). Note that the south swell response at Imperial Beach (IB) is not given on Figure 3.3.1-7. The relatively broad and shallow Coronado Platform south of IB introduces very complex patterns of refraction, including many caustics, and standard refraction calculations may not be suitable. San Clemente Island interferes with the south swell events $220\text{--}240^\circ\text{T}$ incident to the northern stations (Figure 3.3.1-7). The region of most rapid variation of south swell energy is from Oceanside north to Dana Point.

Wave refraction due to shoals in the island vicinity is important in the north swell responses. The variation with wave period, which is illustrative of the refraction effects, of one

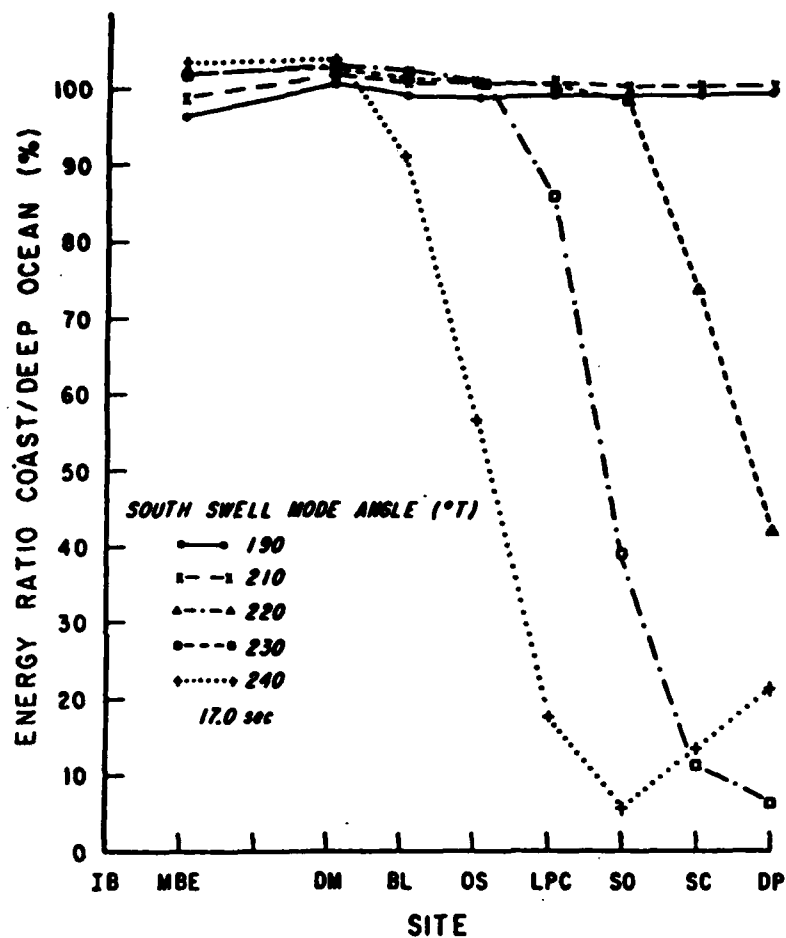


Figure 3.3.1-7

Coastal response to south swell events. The directional distributions of the deep ocean events are all 10° wide (full width at half maximum). The site symbols are defined in Figure 3.3.1-1 (Pawka and Guza, 1983).

of the dramatically varying response functions (290° , Figure 3.3.1-6) is shown in Figure 3.3.1-8. Because refraction tends to blur the edges of the island shadow, the decrease in refractive effects with decreasing wave period sharpens the response functions, and the sharpest shadows occur at $T < 7.0$ sec. Still, no dramatic small scale (order of 10 km) features appear at short periods. Furthermore, the shorter period response function will be smoothed during periods of local generation. The effects of refraction on the south swell response (Figure 3.3.1-9) are much less evident. This is due primarily to the fact that San Clemente Island blocks exposure to the refractively important Cortez and Tanner Banks at the more northern coastal sites. The northern shelf of San Clemente Island, which is relatively small in cross-section, is the major bathymetry which interferes with south swell incident to the northern part of the Pawka and Guza (1983) study region. The central points of Pawka and Guza (1983) are that the southernmost California coastal response to offshore waves is: (1) strongly influenced by the shadows of offshore islands and refraction by submerged island margins and offshore banks (particularly important for swell), (2) highly sensitive to the directional characteristics of the offshore waves, and (3) significantly sheltered to north swell, but largely exposed to south swell.

Arthur (1951) did theoretical calculations concerning the general effects of islands on waves and compared these results to visual observations of the effect of San Clemente and Santa Catalina Islands on south swell at coastal locations. Important theoretical results are that refraction of waves by subaerial island topography, and variability in incident wave direction are important factors in determining the extent of the wave shadow behind an island. Refraction of swell by steady currents, and diffraction, were found to be generally unimportant, at least theoretically. Arthur (1951) considered two sets of visual observations of breaker height between Point Dume and Oceanside. In both cases the deep water waves were south swell with deep water approach angles of about 190° .

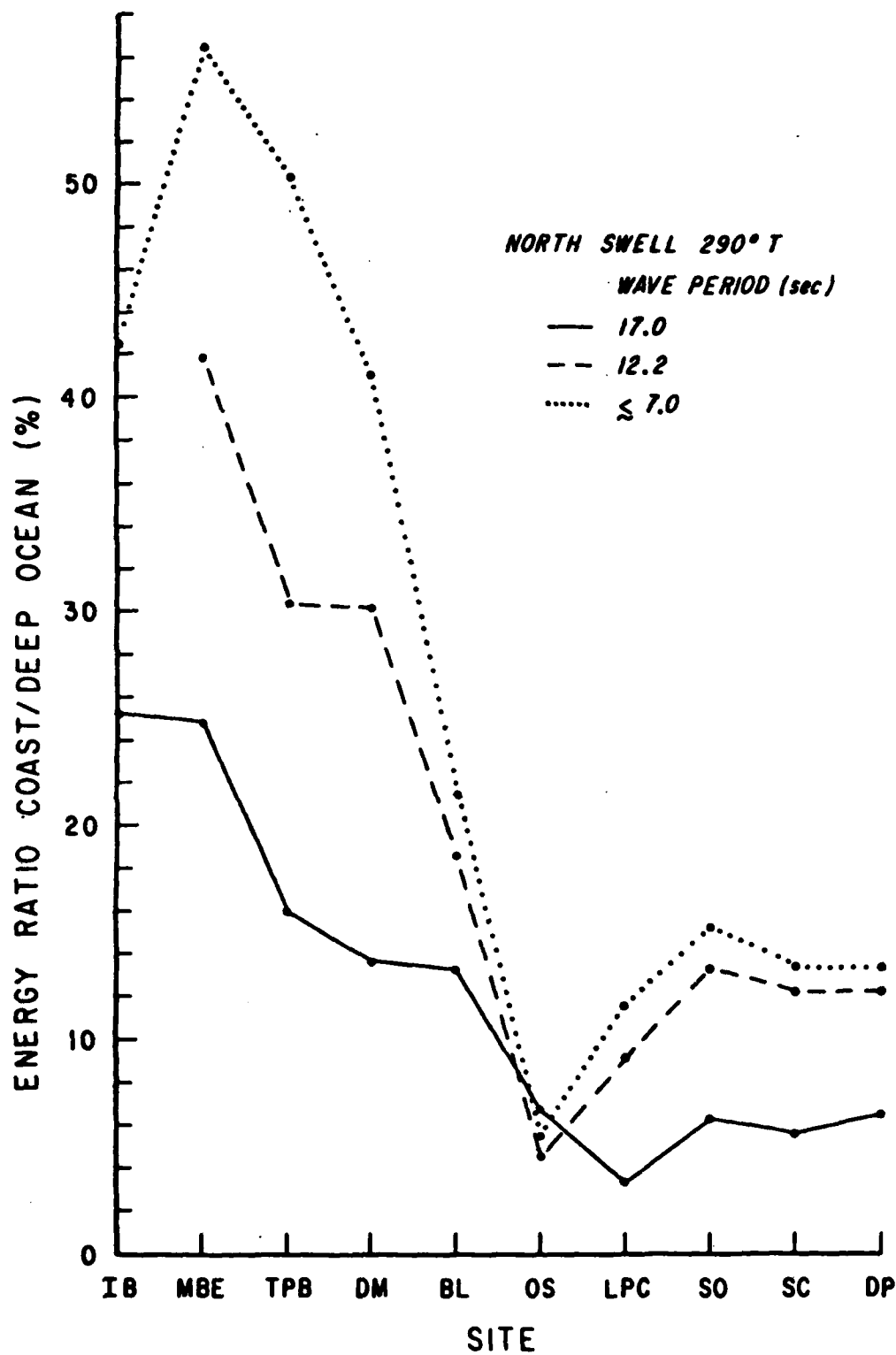


Figure 3.3.1-8

Coastal response to a north swell event from 290° T with various wave periods. The site symbols are defined in Figure 3.3.1-1 (Pawka and Guza, 1983).

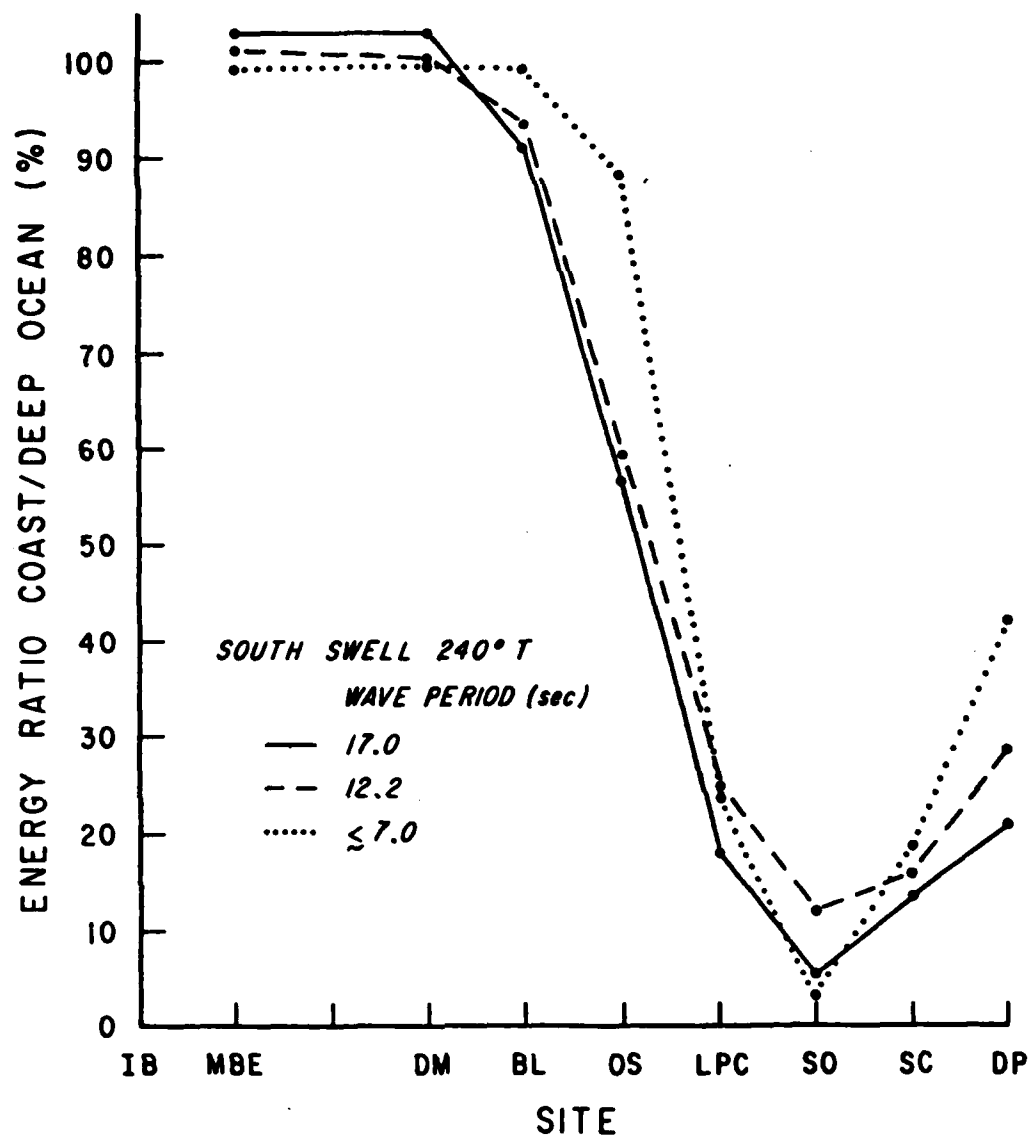


Figure 3.3.1-9 Coastal response to a south swell event from 240° T with various wave periods. The site symbols are defined in Figure 3.3.1-1 (Pawka and Guza, 1983).

With swell approaching from 190° , the islands cast a wave shadow on the coast from Santa Monica to Sunset Beach (Figure 3.3.1-1). The observations show the shadow clearly, but it is not complete; swell is not entirely eliminated from this stretch of coast, but rather there is a general decrease of breaker height from either edge of the shadow toward the center. This decrease is not altogether regular, there being important effects of the bottom topography immediately offshore, but the over-all tendency of the change in breaker height is toward a decrease.

Since swell from a very distant generating area has a relatively small variability in direction, the southerly swell may be expected to have the least directional variability of any swell reaching the southern California coast. Wiegel and Kimberley (1950) find, by using the observed decrease of period with time of trains of southern swell at Camp Pendleton and the storm-tracking methods developed by Munk (1947), that the decay distance is approximately 5,000 nautical miles. If the swell is assumed to travel a great-circle route, then a fetch width of 600 nautical miles, which is relatively large, is associated with a variability in direction of $\pm 5^\circ$ after a decay of 5,000 nautical miles. The effect of such a variability on the wave pattern beyond San Clemente and Santa Catalina islands is not great, since Catalina Island is only 20 nautical miles from the coast in the direction of the wave advance. The effect is roughly that of rotating the refraction patterns by 5° about the extremities of Santa Catalina Island, and the alteration is still not in agreement with observations. Arthur's (1951) calculations for the effect of refraction around the west end of Santa Catalina, and the southeast extremities of San Clemente and Santa Catalina, show that the magnitude and trend of the refraction factors are in agreement with the observations of breaker heights. Thus, Arthur (1951) concludes that in the particular case of long south swell, it is refraction rather than variability in direction, which fill in the island shadows.

Vesecky et al (1980) used a high frequency radar to measure the shadowing of 7 sec waves travelling from San Clemente Island to the town of San Clemente, California (Figure 3.3.1-1). Although the shadow was clearly evident, there was more energy in the shadow than predicted by refraction and diffraction effects. Vesecky et al (1980) suggest that nonlinear interactions (as opposed to the refractive effects suggested by Arthur (1951)) play a major role in filling in shadows. Both may be correct; Arthur (1951) was considering long swell and Vesecky (1980) short seas. Pawka (1982) suggests that different processes are indeed important for high and low frequencies.

The coastal waves discussed by Arthur (1951) are in response to a south swell from 190° . There are different responses to other swell directions. For example, Huntington Beach is exposed principally to swell from $155-198^{\circ}$ while El Segundo is more affected by that from $195-235^{\circ}$ (Figure 3.3.1-1). Since the directional variability of waves from southern hemisphere sources is small, swell which is significant at one location often will be of little consequence at the other (Marine Advisers, 1961). Between Ventura and Point Conception, south swell is almost completely blocked by the channel islands.

Although detailed coastal response calculations for north swell only cover the region from the border to Dana Point, inspection of Figure 3.3.1-1 suggests that locations between Long Beach and Point Conception are increasingly highly sheltered from north swell by the general coastline orientation. Thus, only a narrow window to the west allows open ocean waves (both north and south swell) to reach the north shore of the Santa Barbara Channel. Coastal locations north of Point Conception are completely exposed to north swell, so the coastal wave climate is radically different in this region.

3.3.2 Coastal Wave Measurements

The principal source of tabulated and published long-term coastal wave measurements is the Coastal Data Information Program (CDIP). Two different types of wave measurements are

made; nondirectional (i.e. energy) and directional. The nondirectional measurements are made with either a bottom mounted pressure sensor or waverider buoy. The directional measurements are made with a slope array (Seymour and Higgins, 1977) which yields directional information similar to a pitch and roll buoy. In both cases, data runs at typically 1024 seconds (17 minutes) long, with 4 runs per day. Table 3.3.2-1 gives some information about the stations which are in the yearly CDIP reports. Some of the stations were initially nondirectional, and later upgraded to arrays; these are listed as arrays. In other cases, sensor positions varied somewhat between years. The CDIP reports should be consulted for detailed information about any particular station.

The CDIP reports present a variety of wave statistics in tabular and graphical form. These include tables of wave height exceedance probabilities, plots of wave height and peak period exceedance times, seasonal wave height exceedance plots (for example, Figures 3.2.2-2,3,4,5), plots of the time variation of sea and swell significant heights, and tabulated joint distributions for wave height and period. For the directional stations, the wave information is used to estimate quantities related to sediment transport.

An earlier coastal wave monitoring program (Thompson, 1977, 1980) made measurements at 4 locations in the study area: south of Point Conception, Port Hueneme, Venice and Huntington Beach. The data are plagued with a host of problems including: (1) using a variety of analysis techniques which yield wave heights differing from each other and from conventional methods, (2) record lengths commonly only 7 minutes long and as short as 4 minutes, (3) use of a step-resistance wave gauge which differs substantially from other sensors (pressure and continuous wire gauge) particularly at significant wave heights less than 2 feet (see Figure 7 in Thompson, 1977), (4) difficulties in instrument maintenance, (5) improper correction for depth attenuation of pressure signals (Thompson, 1977). It is very difficult to determine the magnitude of errors likely to be present from these several sources. Only the data collected at

Table 3.3.2-1. Coastal Station Summary for Coastal Data Information Program

Station Name	Location		Type* (m)	Depth	Years (19__)
	N. Lat.	W. Long.			
Imperial Beach	32 35.0'	117 08.2'	Array	10.2	77-78, 83-84
Ocean Beach	-	-	-	-	77-78
Mission Bay Ent.	32 45.4'	117 15.7'	Array	10	78-83
Mission Bay	32 45.9'	117 22.5'	Buoy	168	81-83
Scripps Pier	32 52.0'	117 15.4'	S.P.	8.0	77-84
Del Mar	32 57.4'	117 16.7'	Array	10.7	83-84
Oceanside	33 11.4'	117 23.4'	Array	9.2	77-81, 83-84
San Clemente	33 24.9'	117 37.8'	Array	10.2	83-84
Sunset Beach	33 42.5'	118 04.2'	Array	8.2	80-83
Santa Cruz Is.	33 58.3'	119 38.5'	Buoy	54.8	83-84
San Pedro Chan.	33 35.0'	118 14.9'	Buoy	117	81-82
Santa Monica Bay	33 53.0'	118 38.0'	Buoy	185	81-82
Point Mugu	34 05.4'	119 06.8'	Buoy	18.0	82-83
Channel Is.	34 10.0'	119 14.2'	S.P.	6.0	77-83
Santa Barbara	34 24.1'	119.41.5'	Array	9.0	80-83
Point Conception	-	-	Buoy	-	79
Point Arguello	34 40.0'	120 50.5'	Buoy	80-220	79-82
Point Arguello	34 33.3'	120 36.5'	S.P.	3.0	79-80
Diablo Canyon	35 12.5'	120 51.7'	Buoy	22.9	84

* Buoy = WAVERIDER accelerometer buoy for deepwater wave energy.
 Array = 4-gauge slope array for nearshore direction and energy.
 S.P. = single point gauge for nearshore wave energy.

Point Mugu (1972) and Huntington Beach (1972, 1974-77), with a continuous wire gauge, and standard spectral analysis of 17 minute records will be discussed below.

Several of the reviewed reports present additional wave measurements at specific coastal sites. Other site specific studies transform (unsheltered) deep ocean hindcasts to shore locations, similar to Pawka and Guza (1983) discussed above. These data are considered in Sections 4-11, as is the CDIP data.

3.3.3 *Generation of longshore currents by incident wind waves*

It is well known that wind and swell waves which break on a beach can generate quasi-steady longshore currents in the surf zone. These currents can transport large quantities of sand. Below, some of the earliest nearshore current studies are reviewed. The observations were made primarily in the southern California study area, and also illustrate the principals which apply in general.

Shortly after World War II, systematic observations of currents in the surf zone were begun. These early observations generally used triplanes and floats for tracking mean current patterns, and visual observations of wave height and direction. Shepard and Inman (1950, 1951b) measured currents at Scripps Beach, inshore of a complex offshore topography containing deep submarine canyons. Munk and Traylor (1947) had previously constructed refraction diagrams for this area, showing a divergence over the canyon head and a convergence between them for typical 14 sec WNW swell (Figure 3.3.3-1). Visual observations of breaker heights at 12 longshore locations, averaged over 7 days of observations with approximately the same dominant wave period (12-14 sec) and direction (WNW), were in very good agreement with the predicted pattern of spatial variation (Figure 3.3.3-2).

Shepard and Inman (1950) discuss the Scripps Beach nearshore circulation occurring with a variety of incident wave conditions. For long period waves, effects of the canyon refraction result in very large wave height gradients in the longshore direction. The longshore currents

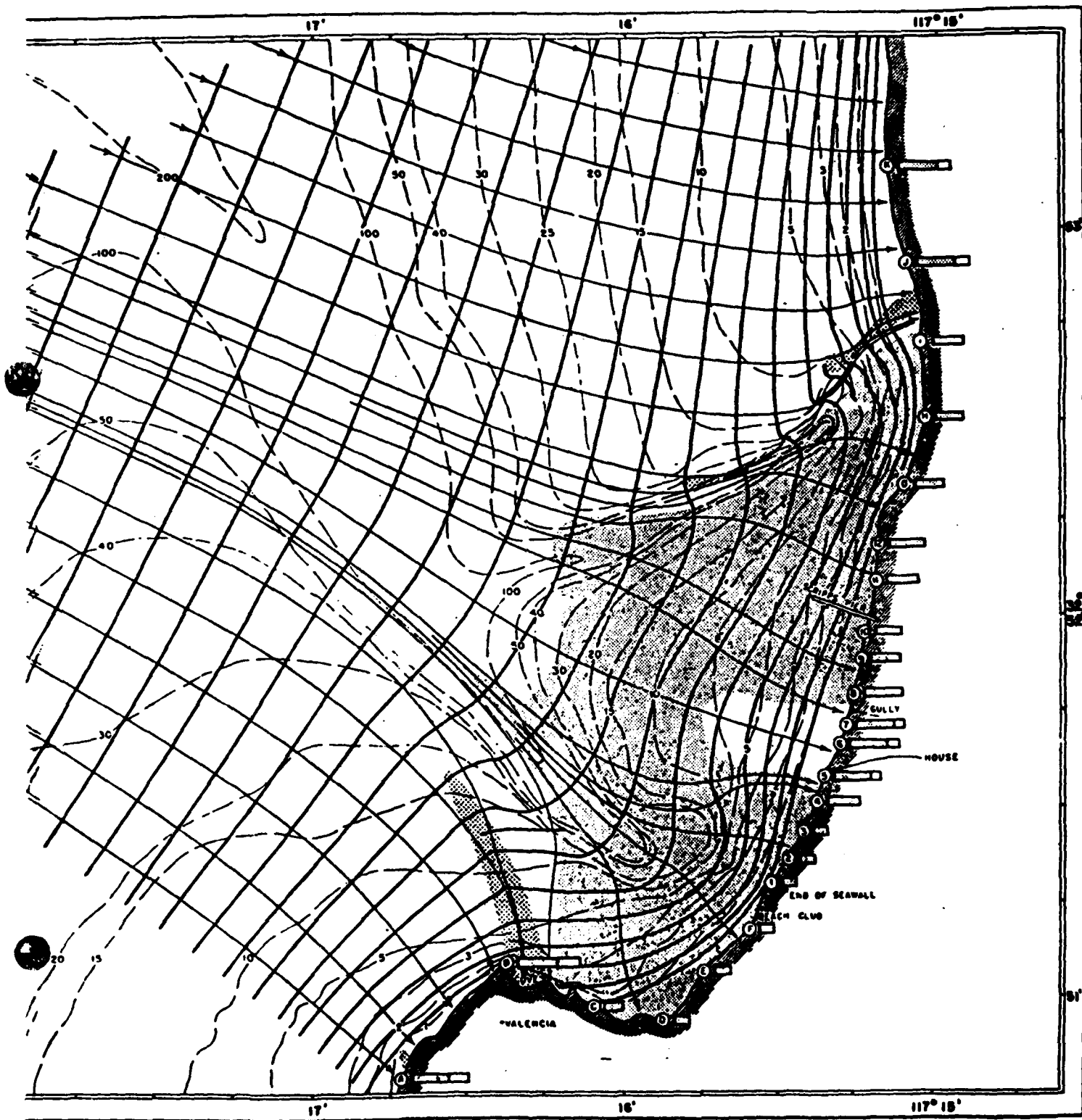


Figure 3.3.3-1

Wave refraction diagram for 14 sec waves from WNW at Scripps Beach. Heavy solid lines are wave crests, solid lines with arrowheads are orthogonals, dashed lines are depth contours. Cross hatched (shaded) regions are convergences (divergences). Length of rectangles opposite shore stations are proportional to wave height (Munk and Traylor, 1947).

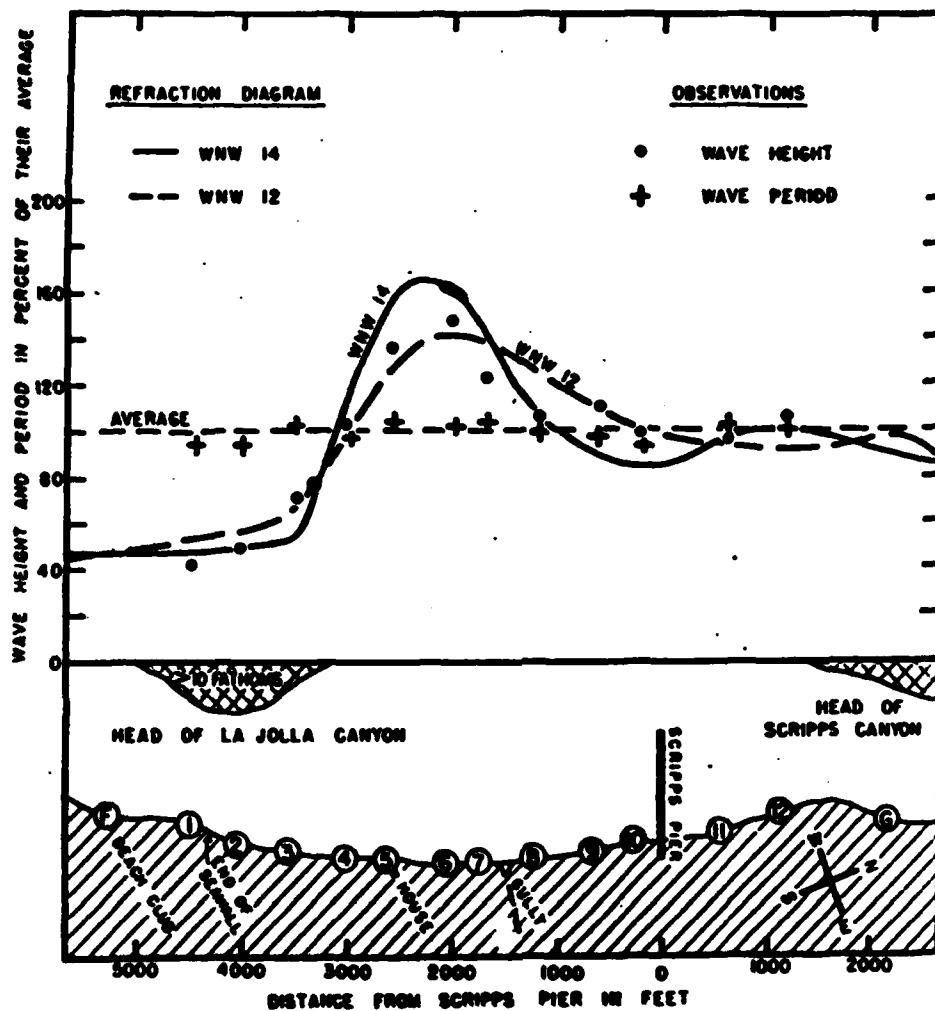
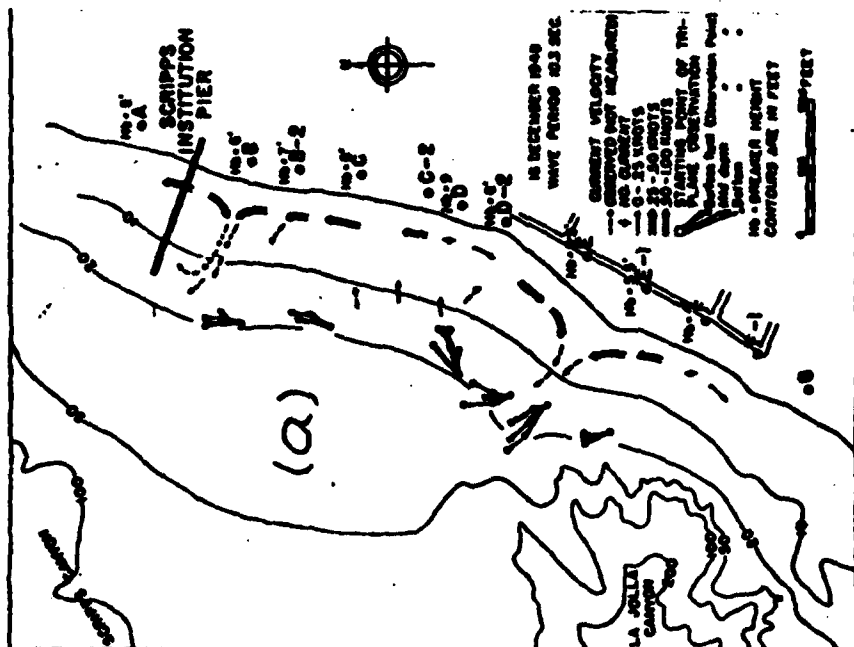
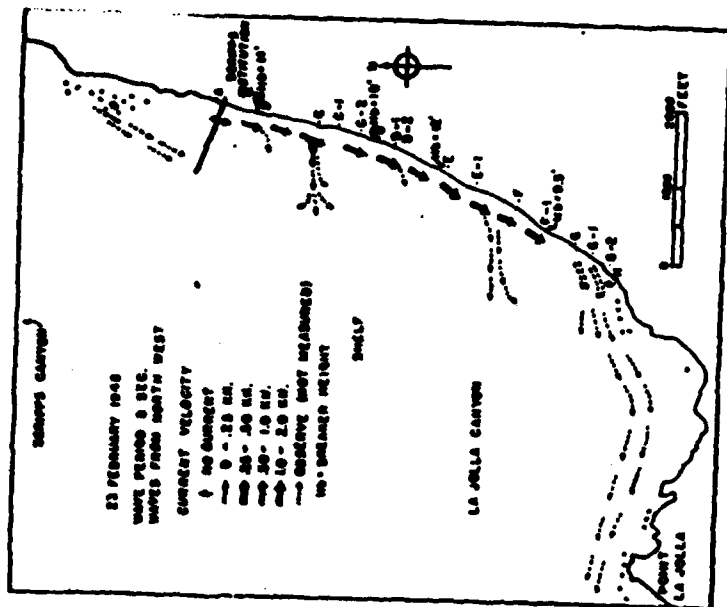


Figure 3.3.3-2 Observed and theoretical changes in wave height along Scripps Beach (Munk and Traylor, 1947).

flow away from the zone of highest waves (Station D in Figure 3.3.3-3a, approximately Station 6 in Figure 3.3.3-2). Shepard and Inman (1950) explained this effect as due to the larger piling up of water (10 years later termed set-up) in the zone of high waves, and a consequent "downhill" flow of water under the resulting hydrostatic pressure head. At various distances from the convergence, the longshore currents turn seaward as rip currents. Shepard and Inman (1950) point out that the extreme longshore wave height variations at Scripps are unusual. The hydrostatic driving force associated with wave height variations can be so strong that steady currents flowing away from the high wave zone actually move opposite to the direction of wave approach. Short period incident waves are less effected by the offshore canyons (they do not feel bottom until the water is shallow) and consequently do not show the large longshore variation in breaker height associated with longer waves. Currents generated by short waves were found to be controlled by the direction of wave approach (Figure 3.3.3-3b) as was known to be the case on beaches with relatively uniform topography in the longshore direction (e.g. Torrey Pines Beach, 3 miles northward (Shepard and Inman, 1951b; Inman and Quinn, 1952), Oceanside Beach, about 15 miles northward (Putnam et al, 1949), and Pacific Beach (Inman and Quinn, 1952)). Inman (1950a) observed similar opposition of the mean current and wave direction in the vicinity of Mugu Canyon. Thus, although crude by today's standards, these measurements revealed that "the direction of the longshore current is primarily dependent on two factors: (1) the direction of wave propagation; and, (2) the rise in water level.....which is greatest in the zones of highest breakers along a beach (wave convergence zones). The longshore currents commonly flow away from these zones of highest waves" (Shepard and Inman, 1951b). Observations throughout southern California (Putnam et al, 1949; Shepard, 1950; Shepard and Inman, 1950, 1951b; Shepard and Saylor, 1953) established that the wave-driven longshore current is confined to the surf zone. Inman and Quinn (1952) point out that the significant spatial and temporal variability of longshore currents (which occurs even on



(a)



(b)

Figure 3.3.3.3 Typical nearshore circulation patterns at Scripps Beach (a) left panel; long period waves ($T > 10$ sec) (b) right panel; short waves from northwest (Shepard and Inman, 1950).

relative planar topography) requires that considerable averaging be done to obtain a mean value representative of the beach as a whole. Inman et al (1971) studied the mixing and advection of the incident wave-longshore current-rip current system. Observations at Scripps Beach and Silver Strand Beach (near Point Loma) show that the surf zone longshore currents advect a tracer much faster than any cross-shore or outside the surf zone processes.

Currents outside the surf zone are not wave driven and can be in a direction opposite to the surf currents. Shepard and Saylor (1953) measured near surface currents by tracking dye patches from the Scripps pier. Their 5-year study (800 observations) showed currents to almost always be stronger in the surf zone than just outside the surf zone or at the pier end (depth 8 m). Considering only the cases in which measurable longshore currents existed both in the surf zone and at the pier end, they found these currents to oppose each other about 1/3 of the time.

Subsequent work has provided theoretical models which quantify the relationship between longshore currents and beach slope, longshore gradients of wave height, and the approach angle, period and height of the incident waves. Longshore current generation is one of the most studied topics in nearshore process. Galvin's (1967) review comments on the existence of "at least 12 different equations to predict velocity and at least 352 published field and laboratory observations." A comprehensive review of the post-1967 surf zone current literature (Basco, 1982) is 240 pages long, and contains a separate volume for the bibliography. Longshore current theories depend critically on many subareas of nearshore hydrodynamics; e.g. the breaking and subsequent decay of wind and swell waves, the nature of bottom drag in a turbulent flow containing both oscillating and steady components, and turbulent momentum transfer in a setting in which few turbulence measurements have been made. It is manifestly apparent that a discussion of recent theories is beyond the scope of this work. An elementary introduction to longshore current theory, and a useful discussion of simple approximate formulas based largely on observations, are given in Komar (1976a,b). Another widely available text book (Mei, 1983)

gives a more rigorous mathematical discussion, and provides references to recent numerical models which consider the influence of structures, wave-current interactions, etc. on nearshore circulation. There are several reviews of longshore currents and nearshore circulation, the most recent and comprehensive is Basco (1982).

Two multi-investigator nearshore processes experiments were recently conducted in southern California as part of the Nearshore Sediment Transport Study (Seymour, 1983a). These experiments are not discussed in the above references. Extensive arrays of pressure sensors, current meters, and sediment monitoring devices were deployed at Torrey Pines Beach in November 1978, and at Santa Barbara during February 1980. Descriptions of the study sites, instrumentation and data collected are given in Gable (1979, 1981). Guza and Thornton (1980) and Thornton and Guza (1983) show that the utility of the Torrey Pines experiments to longshore current studies is severely limited by the near normal approach direction of the incident waves. Small sensor alignment errors result in relatively large errors in the measured value of S_{yx} , the off axis component of the radiation stress which is the key quantity in modern longshore current theories. In contrast, in the Santa Barbara experiments, the waves had relatively large approach angles and reasonably accurate measurements of S_{yx} were possible. Wu et al (1985) show that the observed currents are well described by a numerical model which is an extension of classical radiation stress formulations. These observations are considered in more detail in Section 6, the Santa Barbara cell. The point here is that recent measurements on relatively straight beaches confirm the validity of radiation stress based theories, and provide additional field calibration for the unknown parameters in those models. There is very little quantitative data for longshore currents near jetties or breakwaters. Numerical models (Mei, 1983) suggest that these structures have a profound effect on the nearshore circulation, similar in some ways to the canyon effects discussed above.

3.3.4 *Infragravity and other long period waves*

The vast majority of ocean wave energy is contained in 2 period ranges, ordinary surface gravity waves (roughly 1-30 sec period) and tides (primarily 12 and 24 hours). This section briefly discusses waves with periods between these energetic bands. Although of low height in deep water, these waves may have engineering importance if they are amplified by resonance. For example, a harbor with a natural period of oscillation of a few minutes may develop substantial surges in response to only very small inputs of energy from the open ocean (Munk, 1951). The role of low frequency waves in sediment transport is unclear.

The infragravity (also known as surf beat) period band is roughly 30-300 sec for typical Pacific beaches. These oscillations have been observed to contain a substantial portion of total variance of surf zone elevation and current fluctuations. There is general agreement that wave breaking decreases the energy of swell and wind waves as the shoreline is approached, while surf beat energy levels increase. This is evident from visual inspection of time series from 3 locations across the surf zone (Figure 3.3.4-1). At the deepest station ($h = 1.8$ m), the most energetic waves are steep-faced bores with periods of approximately 8 seconds. At the shallowest station ($h = .75$ m), the wind waves are decreased in height by breaking, and are riding upon energetic surf of much longer period. Figure 3.3.4-2 shows the shoreward decay of wind and swell waves. Surf beat energy levels do not decrease in the shoreward direction, becoming progressively more important in shallow water (Figure 3.3.4-3). An offshore decrease of surf beat energy seems to be a general result. Figure 3.3.4-4 shows such a decay on two California beaches, for both elevation and velocity fluctuations at surf beat periods.

Numerous observations (see Guza and Thornton (1985) for a review) suggest that surf beat energy levels increase as the height of incident wind and swell waves increases. Figure 3.3.4-5 plots significant surf beat cross-shore velocities observed between 1. and 2. m depth ($U_s^{1,2}$) against the significant height of wind and swell waves (H_s). U_s is defined as 4 times the rms velocity, analogous to the definition of H_s as 4 times the rms sea surface displacement. It is

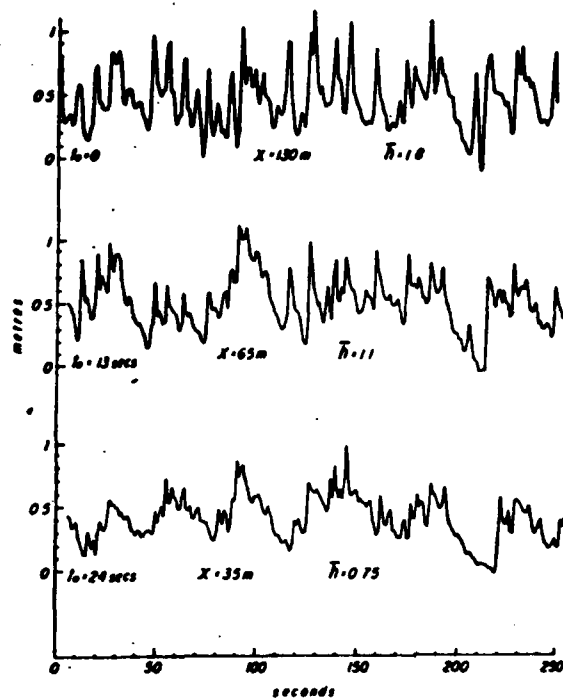


Figure 3.3.4-1

Time series of pressure from 3 locations (h = depth, x = distance from shore) across a very wide Australian surf zone (Wright et al, 1982).

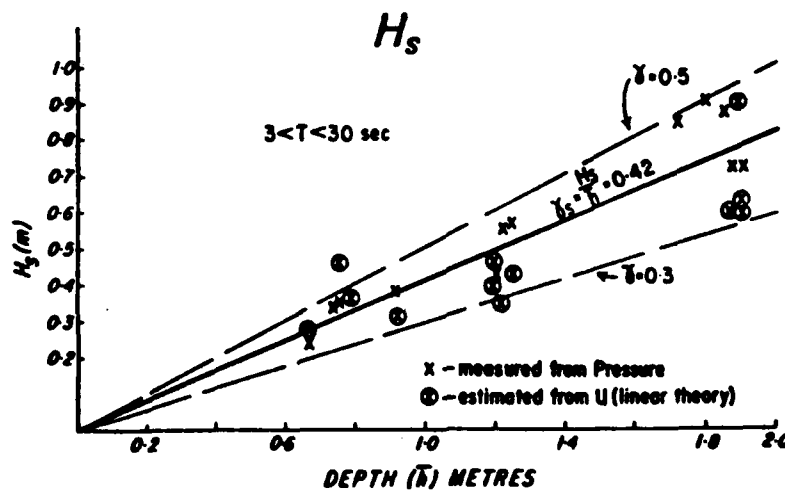


Figure 3.3.4-2

Significant bore heights, H_s (as computed from pressure and current time series plotted against local water depth h (Wright et al, 1982).

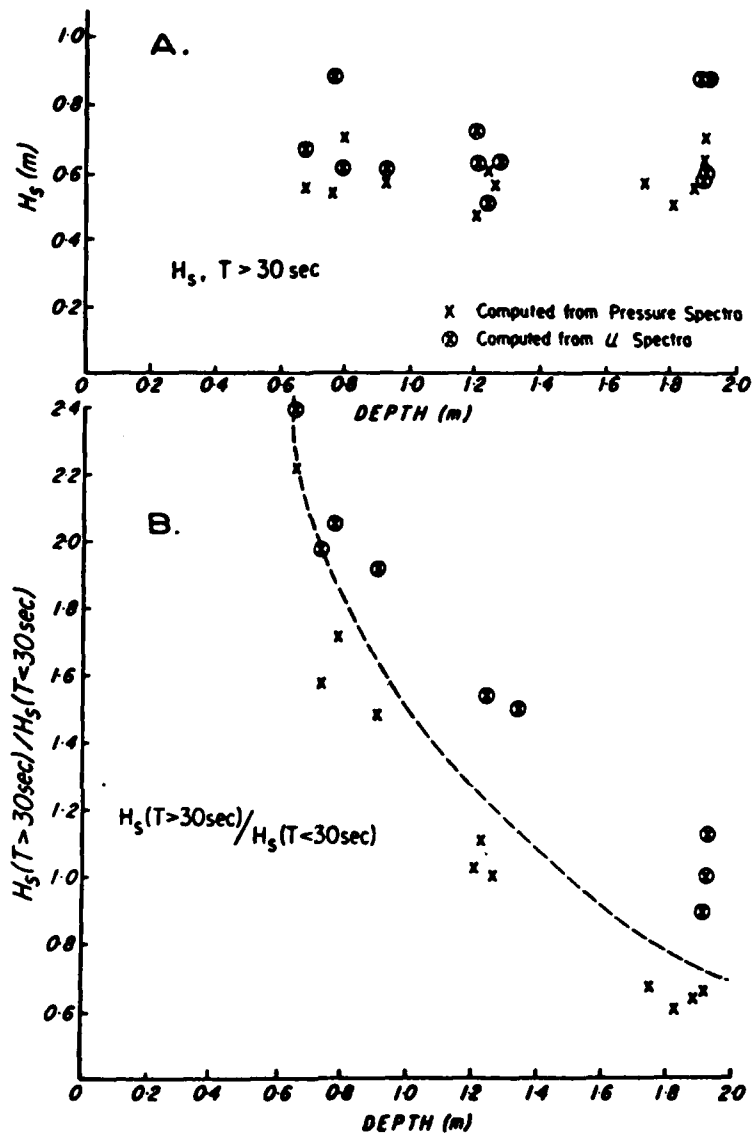


Figure 3.3.4-3

Significant height of surf beat (all periods greater than 30 sec) at different depths across the surf zone. A. significant surf beat height. B. Significant surf beat height ($T > 30 \text{ sec}$) expressed as a ratio relative to the significant wind wave and swell height ($T < 30 \text{ sec}$). (Wright et al, 1982).

TORREY PINES

SANTA BARBARA

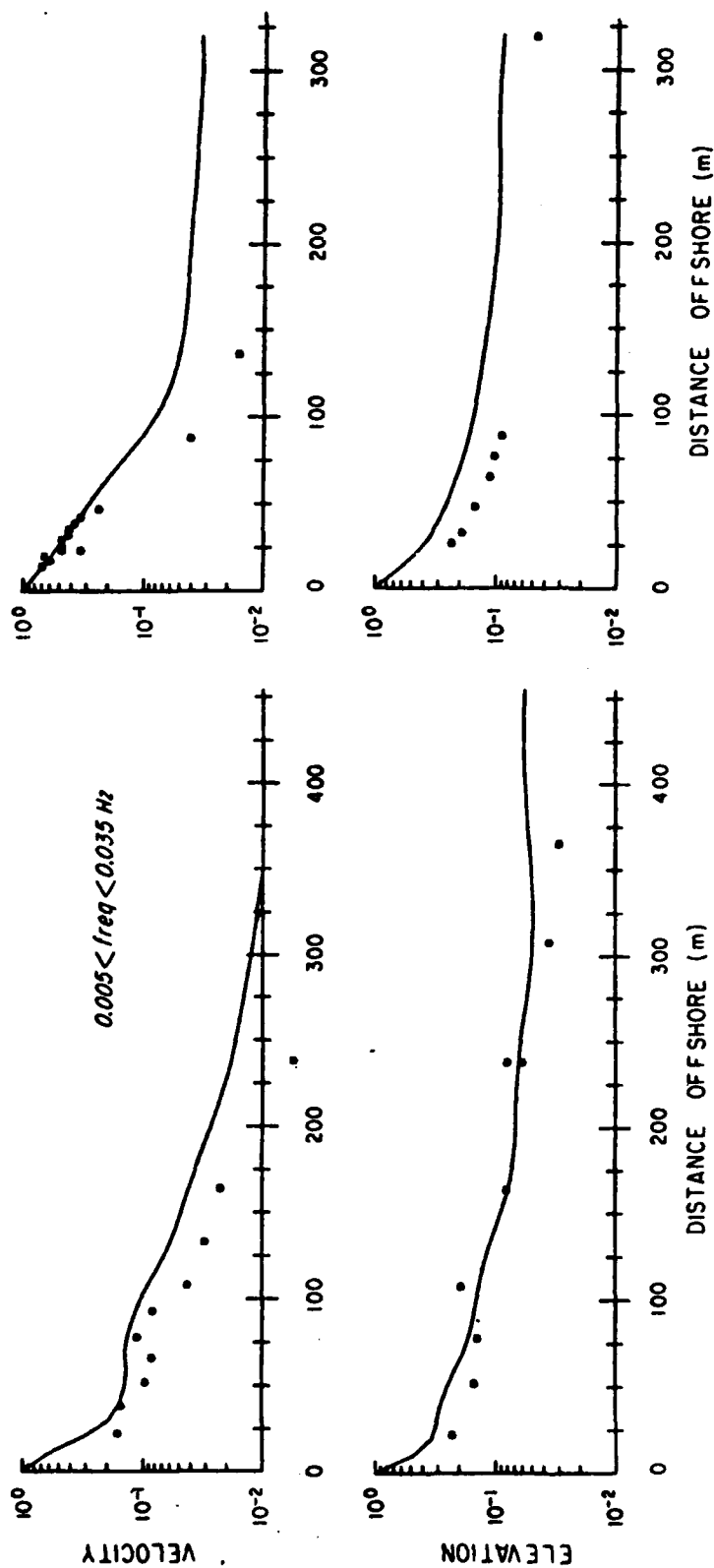


Figure 3.3.4-4 Predicted (solid lines) and observed (asterisks) variance in the frequency range .005-.035 hz (periods 30-200 sec). Upper panels are velocity; lower panels are elevation. Prediction based on measured run-up spectra and a standing wave model (Guza and Thornton, 1985).

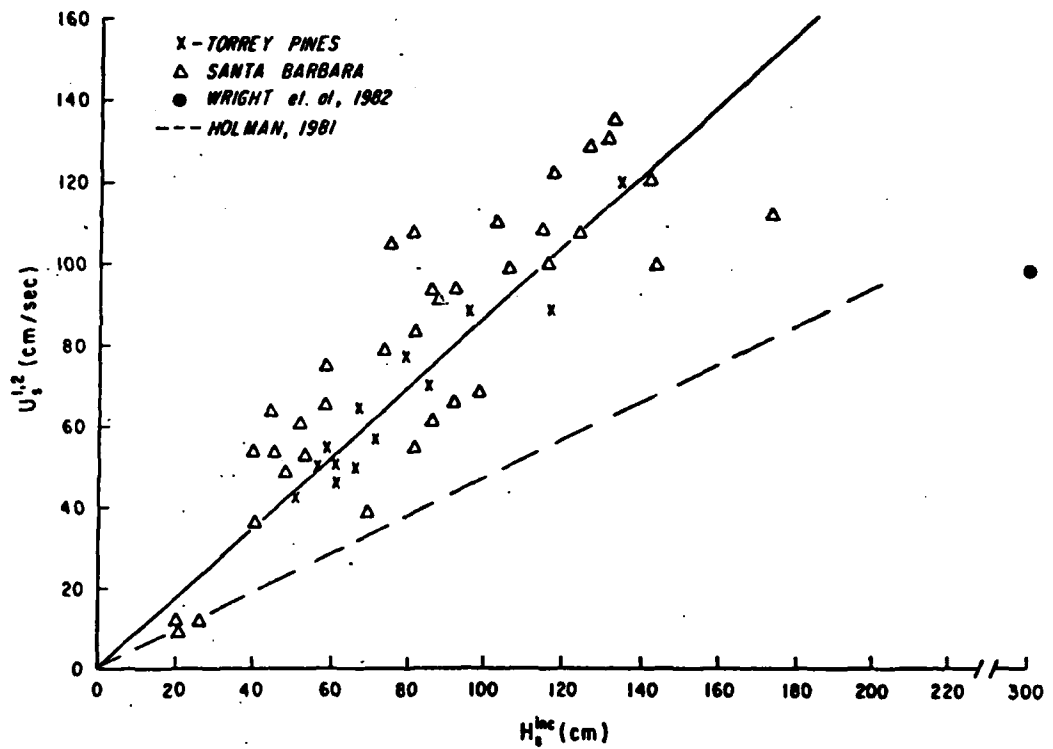


Figure 3.3.4-5

Average significant velocity in depths between 1. and 2. m ($U_{1,2}$) versus offshore significant wave height (H_0^{inc}). The dashed line is a visual fit to the data of Holman (1981). Solid line is the best fit straight line constrained to pass through the origin, $U_{1,2}(\text{cm/s}) = 0.92 s^{-1} H_0^{inc}(\text{cm})$. Triangles and crosses are from Guza and Thornton (1985).

clear that surf beat can have large orbital velocities.

The swash can be completely dominated by surf beat. Huntley et al (1977) use run-up data from Scripps beach and elsewhere to support their hypothesis for a saturated region of the run-up spectra. That is, wind and swell waves are thought to be depth limited in very shallow water, so the amount of wind and swell wave reaching the shoreline is independent of offshore conditions. Guza and Thornton (1982) suggest that because wind and swell wave heights are limited by breaking in very shallow water, and surf beat energy levels at the shoreline increase with increasing incident wave height, the principal beach face and swash zone manifestation of large offshore waves is energetic surf beat. Indeed, Wright et al (1982) show time series of swash zone suspended sediment concentrations which are dominated by fluctuations at surf beat periods.

It has been further hypothesized that edge waves contribute substantially to the surf beat velocity field, and that these edge waves are responsible for crescentic bar formation (Bowen and Inman, 1971). Huntley et al (1981) used a 520 m long array of current meters, deployed in approximately 1 m depth at Torrey Pines Beach, to determine the longshore wavenumber of velocity fluctuations at surf beat periods. The longshore velocity fluctuations were clearly dominated by low mode edge waves, while the cross-shore velocities gave no clear result. The surf beat generation mechanism, and the relative importance of edge waves, are subjects of ongoing scientific research. It is widely believed that surf beat is generated by nonlinear interactions in the incident wave field, but the detailed dynamics remain obscure. At the present time, surf beat does not explicitly enter into coastal design procedures or sediment transport models.

Sea level fluctuations in the period band between surf beat (infragravity) and the tides are not much studied, presumably because of the generally very low signal levels. Except for occasional tsunamis, this is a very quiet band with rms heights of a few centimeters (Munk et

al. 1959; Munk, 1962a,b). Snodgrass et al (1962) use simultaneous measurements at La Jolla and San Clemente to show that a variety of edge wave modes must be simultaneously present, but were unable to determine further details because of the fundamentally limited amount of information in a two-sensor experiment. Munk et al (1964) deployed a 39 km long array along the 7 m depth contour off Oceanside. They showed clearly that the band between surf beat and tides is dominated by low mode edge waves. Although of scientific interest, these long low waves do not appear to be of much importance to coastal structure design or sediment transport. They may influence harbor seiching.



3.4 ASTRONOMICAL TIDES AND OTHER SEA LEVEL FLUCTUATIONS

This 5-part section discusses the fluctuations of sea level which may have engineering significance. The discussion is general and applies to the entire coast of California. The first part deals with the sea level fluctuations which are included in the official NOAA tide predictions. The following sections deal with the short (storm surge and tsunamis) and long (interannual and secular changes) time scale deviations from the largely predictable tides.

3.4.1 *Tides - General Description and Prediction*

The astronomical tides are responsible for the largest portion of the sea level variability with time scales less than millenia. The tides are also one of the very few important geophysical quantities that are accurately predictable. It is very important to note, however, that the tide is only one component of the total sea level fluctuation. The effects of wind, atmospheric pressure, waves, ocean temperature and currents and long-term secular trends must be added to the tide to obtain instantaneous sea level. Unfortunately, "tide level" or "tide height" is often used interchangeably with "sea level".

Tidal fluctuations in the sea level are due to the periodic orbital changes in position of the moon and the sun relative to the earth. The resulting variations in gravitational attraction on the waters of the earth cause both currents and changes in sea elevation. Since the astronomical motions are very regular, the tides are quite accurately predictable, provided a sufficiently long and accurate series of observations exists at any particular location. The observations are necessary (even without contributions to the sea level record by the other factors just mentioned) because the uneven topography of the ocean floor and the presence of the continental land masses significantly alter the local response of the ocean to the gravitational tide-producing forces. In effect, the combination of local setting and ocean basin characteristics selectively responds to some of the many tidal forcing harmonic constituents in preference to others, and the precise response varies from place to place. This is particularly true at the coast

making the usual coastal tide gauge measurements less useful for solution of the deep sea, global tide problem.

Tides along the California coast are of the "mixed" type; greater than 90% of the total tidal variance is at frequencies of 2 cycles per day (semidiurnal) and 1 cycle per day (diurnal) and these are of the same order of magnitude. Tidal forcing at monthly and fortnightly periods is so small it is generally neglected in the official NOAA predictions. Annual and semi-annual contributions due to both astronomical effects and cyclical changes in solar heating are included in NOAA predictions, and amount to about 10% of the tide signal.

The "state of the art" of tidal prediction is reviewed by Zetler (1982). The harmonic method of prediction is used by NOAA for the official tide forecasts at reference stations in the United States. The method was essentially perfected by the late 1800's and except for advances in the technology of bigger and better tide predicting mechanical machines, no revolutionary strides were made until digital computers became available and economical in the 1960's. Zetler (1982) finds it ironic that one of the few fields of geophysics, tides, where perfectly acceptable prediction methods already existed, would undergo such significant improvement. The improvements include:

1. Capability to analyze large data sets of observations; in particular to simultaneously compute many harmonic coefficients by least-squares;
2. New methods of tidal analysis based on advances in geophysical understanding such as response analysis and extended harmonic analysis enabling eventual improvement in predictions;
3. Tidal measurements offshore in the coastal transition zone and in the deep sea to better understand the effects of solid earth yielding under the ocean tides and the important problem of tidal dissipation;
4. Global numerical modeling of tides which will for the first time allow experimentation on realistic worldwide tide models. Engineering applications include the study of effects of

extracting energy from areas with large tides such as the Bay of Fundy (Garrett, 1977).

Except for the use of digital computers to analyze records for tide constituents, most of the advances listed have not been exploited for improved tide predictions. This is not a factor with major consequences for coastal engineering, since as already noted, the coastal tide predictions have been adequate for over 100 years. In the present NOAA system, a fit of the constituents to the observations is used to calculate the local response and then the known future astronomical inputs are used to make tidal predictions.

Daily predictions of high and low tide are given in Table 1., U.S. Department of Commerce, Tide Tables 1985, West Coast of North and South America. Predictions are listed for San Diego (Bay), Los Angeles (Outer Harbor), San Francisco (Golden Gate) and Humboldt Bay (North Spit), California. Sea level measurements are also made at these and some other stations along the coast. The locations with relatively long records along with representative statistics for each station, including length of available record, monthly mean data and trend of sea level rise, are listed in Hicks et al (1983). The longest record in the U.S. is from San Francisco, starting in 1854. Other records and their starting years are San Diego - 1906; La Jolla - 1925; Los Angeles - 1924; Alameda - 1940; Crescent City - 1933.

Standard NOAA data products beside the tide predictions, consist of tabulations of observed daily high and low water level, and tabulations of monthly mean sea level and extreme high and low readings. These are available for the stations listed above and for Newport Bay, Santa Monica, Port San Luis, Rincon Island, Monterey and Pt. Reyes.

MEAN RANGES

The mean ranges of tide are given in Table 2, U.S. Department of Commerce, Tide Tables 1985, West Coast of North and South America. The range and other tidal characteristics for most of the 201 locations (except for the four reference stations) listed for the California coast

are interpolated or derived from short series of measurements by the "method of simultaneous comparison." Application of modeling results or response analysis to predictions for areas with significant local perturbations (harbors and large estuarine systems) may have future benefits. For example, the use of large, expensive, floating dry docks requires precise knowledge of water elevations and rates of change during the day of ship loading and unloading.

Two ranges are listed in the Tide Table for coastal locations (including the major bays and estuaries) from Point Loma to Crescent City. The "mean range", defined as the difference between mean high water and mean low water, varies from about 3.7 ft in the south to about 5.0 ft at the California-Oregon border. The "diurnal range", defined as the difference between mean higher-high water and mean lower-low water is more descriptive of California's mixed tide regime with its pronounced daily inequality. The mean diurnal range also increases smoothly from south to north with a value of about 5.3 ft at Pt. Loma to almost 7.0 feet at the California-Oregon border.

Both mean ranges are observed to be amplified by the major harbors along the coast. San Diego Bay shows about 10% amplification of tide amplitude compared with adjacent coastal areas; Long Beach shows about 6%. Locations within harbors can also show wide variability of tide ranges. San Francisco Bay shows a wide range of amplification leading to mean ranges from 4.1 - 7.4 ft and diurnal ranges from 5.8 - 9.2 ft compared with about 4.0 ft and 6.0 ft respectively on the adjacent coast.

Extreme Ranges

Since the extreme events cause damage and hence dictate design criteria, the extreme ranges of coastal water level are of obvious coastal engineering importance. However, most studies have concentrated on mean sea levels and relatively few (Disney, 1955; Smith and Leffler, 1980) have described the statistics (let alone the processes) of extreme events on the California coast. As is the case with instantaneous levels of the sea, the largest contribution to

the maxima (as a fraction of the departure from mean sea level, say) in California can be attributed to the astronomical tides.

Extreme low water events cause some coastal engineering difficulties; exposing intake pipes and increasing the pumping head loss, or decreasing navigation channel depths causing hazardous boating conditions (Shore Protection Manual, USACE CERC, 1977). However, these problems are relatively minor compared with the destructive potential of extreme high water events. Therefore this discussion will be focused on extreme highs.

Zetler and Flick (1985a, b) used the harmonic prediction approach and tabulated the predicted extreme high tide for each month between 1983-2000 for the four California reference stations, San Diego, Los Angeles, San Francisco and Humboldt. The predictions are shown in Tables 3.4.1-1,2,3,4. These tables are useful for design purposes with the caution that they do not account for storm surge, wave set-up or other non-tidal sea level effects, including the cumulative effects of sea level rise.

The maximum predicted extreme ranges between 1983 and 2000 are: San Diego, 10.0 ft in December 1986 and December 1990; Los Angeles, 9.2 ft in December 1986 and December 1990; San Francisco, 9.2 ft in December 1986; Humboldt, 10.9 ft in December 1985, June and December 1986 and December 1990.

Three important features stand out in a graph of these extreme tides (Figure 3.4.1-1) aside from the fact that the curve for each of the ports is very similar. First, the peak tides in California always occur in summer and winter, with lower extremes (and ranges) in spring and fall. There is as much as two feet seasonal fluctuation in predicted extreme high tides. Second, there is a distinct 4.4 year beating that raises the extremes about 1/2 foot, for example, in 1986-87 and 1990-91 compared with the years in between. Third, the influence of the 18.6 year lunar node cycle causes tides enhanced by a few tenths of a foot in the years 1986-90 compared with 9 years later. Extreme low tides accompany the extreme highs shown in Figure 3.4.1-1,

Table 3.4.1-1 San Diego predicted extreme high tides, 1983-2000 (Zetler and Flick, 1985b).

Year (1)	January (2)	February (3)	March (4)	April (5)	May (6)	June (7)	July (8)	August (9)	September (10)	October (11)	November (12)	December (13)	Annual Maximum	
													Height (14)	Date (15)
1983	7.6	7.2	6.4	6.4	6.6	7.2	7.6	7.7	7.4	6.7	7.0	7.2	7.7	August 7, 8
1984	7.5	7.3	6.8	6.6	7.0	7.1	7.4	7.4	6.9	7.3	7.5	7.4	7.5	January 18, November 22, 23
1985	7.0	7.1	6.8	6.6	7.1	7.4	7.5	7.1	6.8	7.1	7.6	7.7	7.7	December 11, 12
1986	7.5	7.1	6.5	6.9	7.3	7.7	7.7	7.5	6.8	6.7	7.3	7.8	7.8	December 31
1987	7.6	7.0	6.2	6.4	6.9	7.4	7.7	7.8	7.3	6.8	7.2	7.5	7.8	August 8
1988	7.6	7.3	6.6	6.7	6.9	7.3	7.6	7.4	7.0	7.4	7.4	7.2	7.6	January 19, July 28
1989	7.2	7.2	6.7	6.8	7.2	7.3	7.3	7.1	6.8	7.4	7.7	7.7	7.7	November 13, December 12
1990	7.4	6.9	6.6	7.1	7.5	7.6	7.6	7.2	6.5	7.0	7.5	7.8	7.8	December 2, 31
1991	7.7	6.7	6.1	6.6	7.1	7.6	7.8	7.6	7.0	6.9	7.4	7.6	7.8	July 11
1992	7.6	7.2	6.4	6.6	6.9	7.5	7.6	7.3	7.0	7.3	7.3	7.1	7.6	January 19, July 28, 29
1993	7.3	7.2	6.6	6.8	7.1	7.2	7.1	7.1	6.9	7.4	7.6	7.5	7.6	November 13, 14
1994	7.1	6.6	6.6	7.0	7.4	7.5	7.3	6.9	6.5	7.0	7.5	7.7	7.7	December 2, 3
1995	7.6	6.5	6.2	6.6	7.1	7.5	7.6	7.4	6.8	7.0	7.4	7.6	7.6	January 1, July 11, December 21, 22
1996	7.5	7.0	6.3	6.3	6.9	7.5	7.6	7.3	6.7	7.0	7.0	7.2	7.6	July 29
1997	7.4	7.3	6.7	6.5	6.8	6.9	7.3	7.3	6.9	7.1	7.3	7.3	7.4	January 9
1998	7.0	6.8	6.4	6.9	7.2	7.3	7.2	7.0	6.9	6.9	7.3	7.6	7.6	December 3
1999	7.5	6.7	6.4	6.5	7.1	7.5	7.6	7.4	6.8	7.0	7.5	7.7	7.7	December 22
2000	7.6	7.1	6.4	6.0	6.8	7.5	7.7	7.4	6.7	6.7	7.4	7.0	7.7	July 30

In feet above chart datum.

Note: Highest = 7.8 ft in 1986, 1987, 1990, 1991; for 1983-1984, datum below mean sea level by 2.93 ft; for 1985-2000, datum below mean sea level by 2.94 ft.

Table 3.4.1-2 Los Angeles predicted extreme high tides, 1983-2000 (Zetler and Flick, 1985b).

Year (1)	January (2)	February (3)	March (4)	April (5)	May (6)	June (7)	July (8)	August (9)	September (10)	October (11)	November (12)	December (13)	Annual Maximum	
													Height (14)	Date (15)
1983	7.1	6.7	5.9	5.9	6.1	6.7	7.1	7.2	6.9	6.2	6.5	6.7	7.2	August 8
1984	6.9	6.8	6.3	6.1	6.4	6.6	6.9	6.9	6.5	6.7	7.0	6.9	7.0	November 23
1985	6.5	6.6	6.3	6.1	6.6	6.9	7.0	6.6	6.4	6.6	7.1	7.2	7.2	December 11, 12
1986	7.1	6.6	6.0	6.4	6.8	7.2	7.2	7.0	6.4	6.2	6.8	7.3	7.3	December 31
1987	7.1	6.6	5.7	5.9	6.4	6.9	7.2	7.3	6.8	6.3	6.7	7.0	7.3	August 8
1988	7.1	6.8	6.2	6.2	6.4	6.8	7.1	6.9	6.5	6.9	7.0	6.8	7.1	January 19, July 28
1989	6.7	6.7	6.3	6.3	6.7	6.8	6.8	6.7	6.3	6.9	7.2	7.2	7.2	November 13, December 12
1990	6.9	6.4	6.1	6.6	7.0	7.1	7.1	6.7	6.1	6.5	7.0	7.3	7.3	December 2, 31
1991	7.2	6.2	5.6	6.1	6.6	7.0	7.2	7.1	6.5	6.5	6.9	7.1	7.2	January 1, July 10, 11
1992	7.1	6.7	5.9	6.1	6.5	6.9	7.0	6.8	6.5	6.8	6.8	6.7	7.1	January 19
1993	6.8	6.7	6.1	6.3	6.6	6.7	6.7	6.7	6.4	6.9	7.1	7.0	7.1	November 13, 14
1994	6.7	6.2	6.1	6.5	6.9	7.0	6.8	6.4	6.1	6.6	7.0	7.2	7.2	December 2, 3
1995	7.1	6.0	5.7	6.1	6.6	7.0	7.1	6.9	6.3	6.5	6.9	7.1	7.1	January 1, July 11, December 21, 22
1996	7.0	6.5	5.8	5.8	6.4	7.0	7.1	6.8	6.2	6.5	6.5	6.7	7.1	July 29
1997	6.9	6.8	6.3	6.0	6.3	6.5	6.8	6.8	6.5	6.6	6.8	6.8	6.9	January 9
1998	6.6	6.3	5.9	6.3	6.7	6.8	6.7	6.5	6.4	6.4	6.8	7.1	7.1	December 3
1999	7.0	6.3	6.0	6.1	6.6	7.0	7.1	6.9	6.4	6.5	7.0	7.2	7.2	December 22
2000	7.1	6.6	5.9	5.6	6.3	7.0	7.2	6.9	6.3	6.2	6.5	6.9	7.2	July 30

In feet above chart datum.

Note: Highest = 7.3 ft in 1986, 1987, 1990; for 1983-1984, datum below mean sea level by 2.81 ft; for 1985-2000, datum below mean sea level by 2.84 ft.

Table 3.4.1-3 San Francisco predicted extreme high tides, 1983-2000 (Zetler and Flick, 1985b).

Year (1)	January (2)	February (3)	March (4)	April (5)	May (6)	June (7)	July (8)	August (9)	September (10)	October (11)	November (12)	December (13)	Annual Maximum	
													Height (14)	Date (15)
1983	7.1	6.6	5.9	5.8	6.0	6.5	6.9	7.0	6.6	6.8	6.4	6.8	7.1	January 27, 28
1984	7.0	6.8	6.2	6.0	6.3	6.5	6.7	6.6	6.2	6.5	6.8	7.0	7.0	January 18, December 21
1985	6.9	6.7	6.3	6.2	6.5	7.0	7.0	6.5	6.3	6.6	7.0	7.3	7.3	December 11, 12
1986	7.3	6.9	6.2	6.4	6.8	7.1	7.2	6.9	6.3	6.3	6.8	7.4	7.4	December 30, 31
1987	7.2	6.6	5.8	6.0	6.4	6.9	7.2	7.1	6.6	6.3	6.7	7.1	7.2	January 1, 28, 29 July 10
1988	7.2	6.9	6.1	6.1	6.3	6.8	6.9	6.7	6.4	6.7	6.9	7.0	7.2	January 18
1989	6.8	6.7	6.2	6.4	6.6	6.9	6.9	6.5	6.5	6.8	7.1	7.3	7.3	December 12
1990	7.1	6.7	6.3	6.6	6.9	7.1	7.1	6.7	6.3	6.6	7.0	7.4	7.4	December 31
1991	7.2	6.4	6.0	6.2	6.6	7.0	7.1	7.0	6.4	6.5	6.9	7.2	7.2	January 1, December 21, 22
1992	7.2	6.7	6.0	6.1	6.4	6.8	6.9	6.6	6.4	6.7	6.8	6.8	7.2	January 19
1993	6.9	6.7	6.2	6.3	6.5	6.7	6.7	6.5	6.5	6.8	7.0	7.2	7.2	December 12
1994	7.0	6.5	6.3	6.5	6.8	6.9	6.9	6.5	6.3	6.6	6.9	7.3	7.3	December 31
1995	7.2	6.3	6.0	6.2	6.6	6.9	7.0	6.9	6.3	6.5	6.9	7.2	7.2	January 1, December 21, 22
1996	7.1	6.7	6.0	5.9	6.4	6.9	6.9	6.6	6.2	6.4	6.6	6.8	7.1	January 19, 20
1997	7.0	6.8	6.3	6.0	6.2	6.5	6.7	6.7	6.3	6.5	6.8	6.9	7.0	January 8, 9
1998	6.8	6.4	6.1	6.3	6.6	6.8	6.8	6.5	6.2	6.4	6.8	7.1	7.1	December 3, 31
1999	7.1	6.4	6.1	6.2	6.5	6.9	7.0	6.9	6.4	6.5	7.0	7.2	7.2	December 22, 23
2000	7.2	6.8	6.1	5.8	6.3	7.0	7.1	6.8	6.2	6.1	6.5	7.0	7.2	January 20

*In feet above chart datum.

Note: Highest = 7.4 ft in 1986, 1990; for 1983-1984, datum below mean sea level by 3.05 ft; for 1985-2000, datum below mean sea level by 3.13 ft.

Table 3.4.1-4 Humboldt Bay predicted extreme high tides, 1983-2000 (Zetler and Flick, 1985b).

Year (1)	January (2)	February (3)	March (4)	April (5)	May (6)	June (7)	July (8)	August (9)	September (10)	October (11)	November (12)	December (13)	Annual Maximum	
													Height (14)	Date (15)
1983	8.1	7.6	6.6	6.6	6.9	7.3	7.6	7.6	7.2	6.9	7.3	7.8	8.1	January 28, 29
1984	8.0	7.8	7.1	7.0	7.1	7.2	7.4	7.2	7.0	7.4	7.8	7.9	8.0	January 18, 19
1985	7.8	7.8	7.6	8.0	8.3	8.4	8.3	7.5	7.6	8.1	8.5	8.6	8.6	December 11, 12
1986	8.3	7.9	7.7	8.1	8.5	8.6	8.4	7.9	7.3	7.7	8.2	8.6	8.6	June 21, December 30, 31
1987	8.4	7.8	7.3	7.7	8.1	8.4	8.4	8.2	7.7	7.6	8.0	8.3	8.4	January 1, June 12, July 10, 11
1988	8.4	8.0	7.7	7.9	8.0	8.1	8.1	7.8	7.9	8.2	8.3	8.1	8.4	January 19
1989	8.0	7.9	7.8	8.1	8.3	8.3	8.1	7.6	7.9	8.3	8.5	8.5	8.5	November 13, 14 December 11, 12
1990	8.1	7.6	7.9	8.3	8.5	8.5	8.2	7.7	7.5	7.9	8.4	8.6	8.6	December 2, 3, 31
1991	8.4	7.5	7.5	7.9	8.2	8.5	8.4	8.1	7.4	7.8	8.2	8.4	8.5	June 12
1992	8.3	7.9	7.6	7.8	7.9	8.2	8.1	7.7	7.9	8.1	8.1	7.9	8.3	January 19
1993	8.0	7.9	7.8	8.0	8.2	8.1	7.9	7.6	7.9	8.2	8.4	8.4	8.4	November 13, 14 December 12
1994	8.0	7.4	7.9	8.3	8.4	8.3	8.0	7.4	7.5	8.0	8.4	8.5	8.5	December 2, 3
1995	8.3	7.3	7.5	7.9	8.2	8.4	8.3	7.9	7.4	7.9	8.3	8.4	8.4	June 12, 13 December 21, 22
1996	8.3	7.9	7.3	7.5	7.9	8.3	8.2	7.8	7.5	7.7	7.8	8.0	8.3	January 19, 20 June 30
1997	8.2	8.1	7.6	7.7	7.9	7.9	7.9	7.8	7.6	7.9	8.1	8.1	8.2	January 9
1998	7.8	7.7	7.7	8.0	8.2	8.2	7.9	7.5	7.4	7.8	8.2	8.4	8.4	December 3, 4
1999	8.3	7.6	7.4	7.9	8.2	8.4	8.3	7.9	7.4	7.9	8.4	8.5	8.5	December 22, 23
2000	8.4	7.9	7.2	7.4	7.9	8.4	8.5	7.9	7.2	7.4	7.9	8.3	8.5	July 1

*In feet above chart datum.

Note: Highest = 8.6 ft in 1985, 1986, 1990; for 1983-1984 for South Jetty (40° 45' N, 124° 14' W), datum below mean sea level by 3.45 ft; for 1985-2000 for North Spit (40° 46' N, 124° 13' W), datum below mean sea level by 3.70 ft.

PREDICTED EXTREME HIGH TIDES

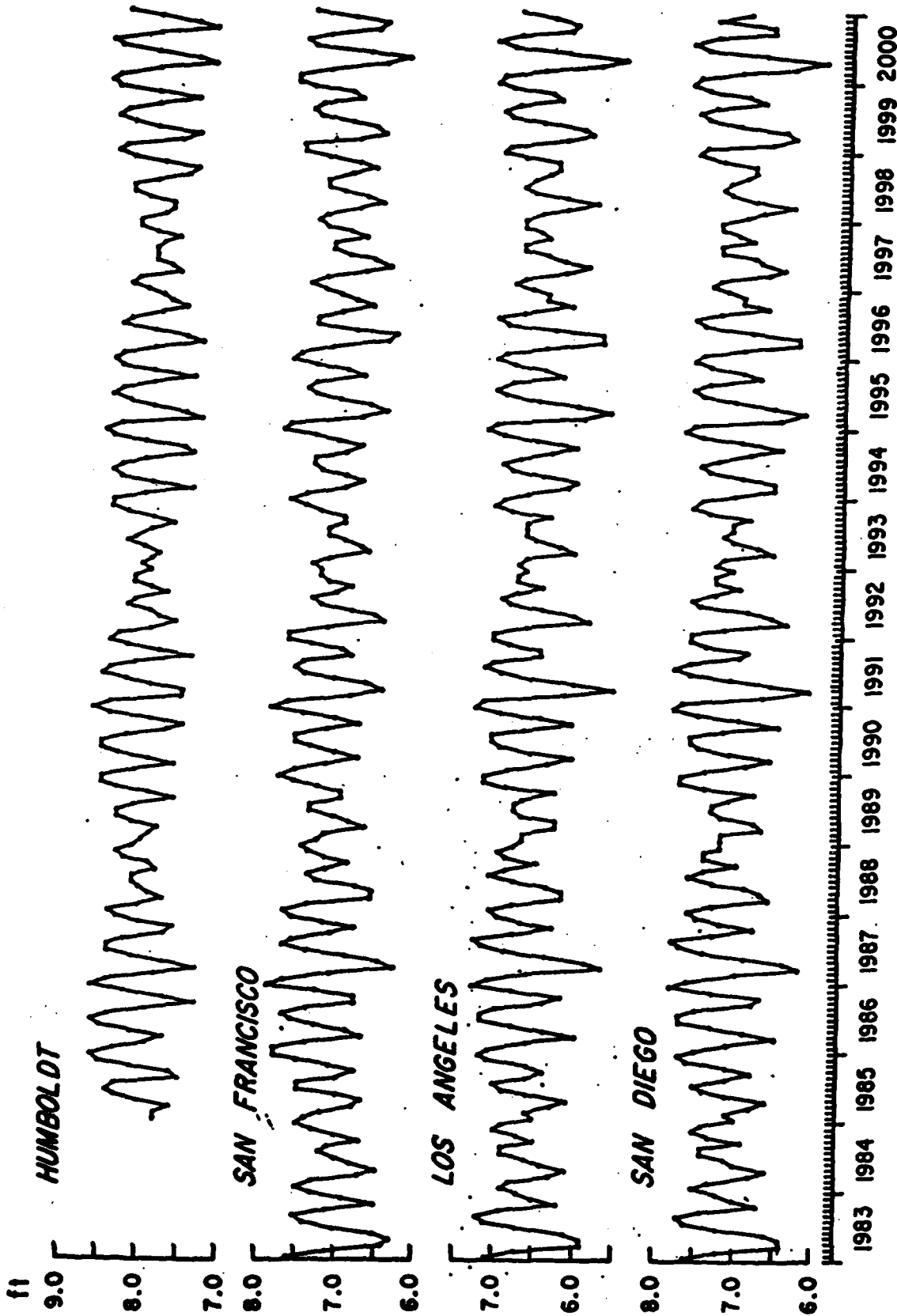


Figure 3.4.1-1 Predicted monthly extreme high tides for four California reference stations for the period 1983-2000 (Flick and Zetler, 1985b).

and exhibit the same beating. The fact that semi-annual peaks in extreme tides occur in winter (usually December or January) greatly increases the chance that large tides will coincide with winter storm events, resulting in coastal damages (Wood, 1978; Walker et al, 1984; Flick and Cayan, 1984).

Since adequate tide prediction capability exists, future extremes can be extracted from standard predictions, at least over the reasonably short periods in Figure 3.4.1-1. Wood (1978) implies a criticism of this method by listing a myriad of astronomical coincidences to "explain" occurrences of high tides and high tidal currents (Wood, 1981). Wood (1978, 1981) cites such things as unusually close approaches of the moon, coincidence of the length of anomalistic and synodic months and close coincidence of declination angles of moon and sun implying that there may be astronomical phenomena with no corresponding prediction constituents. However, no definitive suggestions for improvement of the harmonic method based on these phenomena have been published, nor has there been a systematic, quantitative comparison with measured sea levels. Alarming forecasts of much higher future tides appearing in the media during the severe winter of 1982-83 stem from the erroneous conclusion that large tidal events are necessarily associated with these astronomical coincidences.

Seasonal Effects

Annual and semi-annual variations in *mean* sea level due mainly to cyclical changes in solar heating are included in the standard predictions as the "solar annual" (S_a) and "solar semi-annual" (S_{sa}) coefficients. Seasonal variations in mean sea level are often displayed using monthly mean sea levels routinely computed by NOAA for their tide gauge network and widely distributed as a standard data product. Monthly mean values are the most thoroughly studied sea level statistic. Figure 3.4.1-2 shows the monthly mean value from the tide station in San Diego computed over the 19-year tidal epoch from 1960-78. There is a clear seasonal variation of about 15 cm with low water levels in the spring, and high levels in the fall. The large

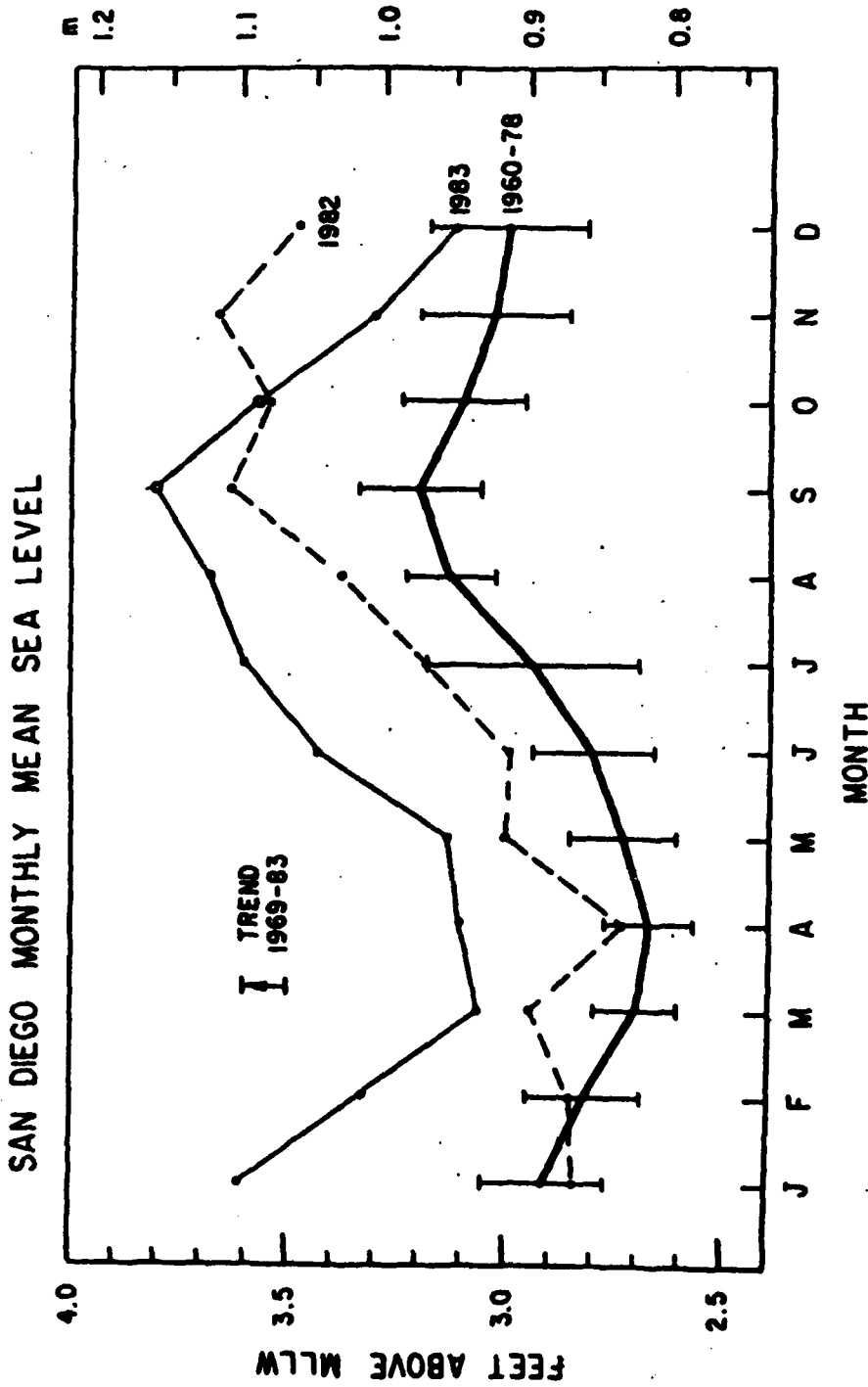


Figure 3.4.1-2 Seasonal variability of monthly mean sea level at San Diego. Heavy curve shows 1960-78 average. Vertical bars indicate ± 1 standard deviation. Lines marked 1982 and 1983 show large deviation from average during these years (Flick and Cayan, 1984).

variation (several standard deviations) during 1982-83 are discussed in Section 3.4.4, Interannual Effects.

The seasonal pattern in Figure 3.4.1-2 is fairly typical of all stations south of San Francisco. It can be explained as largely a consequence of seasonal ocean heating and cooling with a smaller adjustment due to changes in atmospheric pressure and minor dependence on mean offshore currents (Reid and Mantyla, 1976). On the average, the water temperature is coolest in spring, leading to lower mean sea levels, and warmest in autumn, leading to higher levels. The secondary peak in January is not explainable as a temperature effect. Note that these seasonal effects do not much influence the extreme and mean *ranges* discussed above, but do impact the maximum *elevations* discussed below.

3.4.2 Extreme Elevations

The maximum observed water level in absolute terms, relative to fixed bench marks on land, occurred during the winter of 1982-83 and were due to a combination of extreme tides, a strong and persistent El Niño event which raised sea level, and severe storms. Table 3.4.2-1 shows that the sea level generally peaked on the morning of 27 January 1983, although Newport reached its maximum the following day. The previous extreme had been reached in January 1973 at San Francisco (Smith and Leffler, 1980), and in various other years at other stations (see table). The fact that all stations between San Diego and San Francisco reached their all-time high during essentially the same time, and the fact that November 1982 to March 1983 showed several record-breaking events underscores the severe nature of this particular winter season (USACE LAD, 1984a). The years 1986-87 and 1990-91 are the next windows with peak predicted tides a few tenths of a foot higher than those of 1982-83. It is, of course, not known whether meteorological and other factors will combine to produce similar high water.

Smith and Leffler (1980) show frequency distributions of the month of occurrence of each year's peak water level for the period 1933-1977 at San Diego, Los Angeles, San Francisco and

Table 3.4.2-1 Maximum Observed Water Levels*

Location	Ft Above Local (1960-78)		Time	Date	Previous Max** Ft Above (1960-78)		Date
	MLLW	MHHW			MLLW	MHHW	
San Diego (1906)	8.3	2.6	0730	27 Jan 83	8.2	2.5	20 Dec 68
SIO Pier (1925)	7.8 (7.7)	2.4 (2.3)	—	8 Aug 83 (29 Jan 83)	7.6	2.2	19,20 Dec 68 22 Nov 72
Newport	7.9	2.5	0806	28 Jan 83	7.5	2.1	8 Jan 74 22 Nov 76
Los Angeles (1924)	8.0	2.5	0712	27 Jan 83	7.8	2.3	8 Jan 74
Port San Luis Avila (1945)	7.7	2.3	0754	27 Jan 83	7.8	2.4	18 Jan 73
San Francisco (1855)	8.9	3.1	0930	27 Jan 83	8.3	2.5	16,18 Jan 73

** Includes tides and other effects.

* Prior to 1982-83, which produced a cluster of record breaking maxima.

Crescent City. There is a distinct seasonal pattern, with 40-50% of the peak yearly levels occurring in December or January. A secondary peak occurs in the summer. In light of the strong semi-annual tidal monthly maxima displayed in Figure 3.4.1-1, this result is not surprising. Since the tidal contribution to the yearly peak can be easily removed (or added back in for estimates of total height), it is instructive to calculate statistics of the anomalies of monthly extremes (Smith and Leffler, 1980; Flick and Cayan, 1984). In other words, the absolute maximum water level combines all possible effects and is valuable for "design" water level values, but is less useful for understanding the contributing factors. The anomaly calculations systematically account for the variation in tide range between stations provided the proper constituents are used. The resulting anomaly will still display the secular trend which can also be removed.

Smith and Leffler (1980) follow this approach for a short segment of hourly data from 14-17 January 1973. Their chief conclusion is that the 2 foot high anomaly observed is strongly correlated with low atmospheric pressure (15 mb below January means) and strong southerly winds. Figure 3.4.2-1 shows similar data from Flick and Cayan (1984) for San Diego during winter 1982-83. Many sea level anomaly (computed in various ways) studies show this "inverse barometer effect" and seemingly strong, visual correlation with coastal winds, among other factors (Chelton and Davis, 1982; Noble and Butman, 1979; Saur, 1962; Emery and Hamilton, 1985; to name only a few). Severe fluctuations of sea level due to wind and barometric effects is the definition of "storm surge". While the contribution to the extreme heights has been noted, a fuller discussion follows.

Storm Surge

Storm surge is the fluctuation of sea level at a coast associated with wind and atmospheric pressure. For the present discussion, storm surge will be defined to have time scales on the order of 1 to 3 days (LeBlond and Mysak, 1978). Typical surge heights on the California coast

SAN DIEGO DAILY OBSERVATIONS

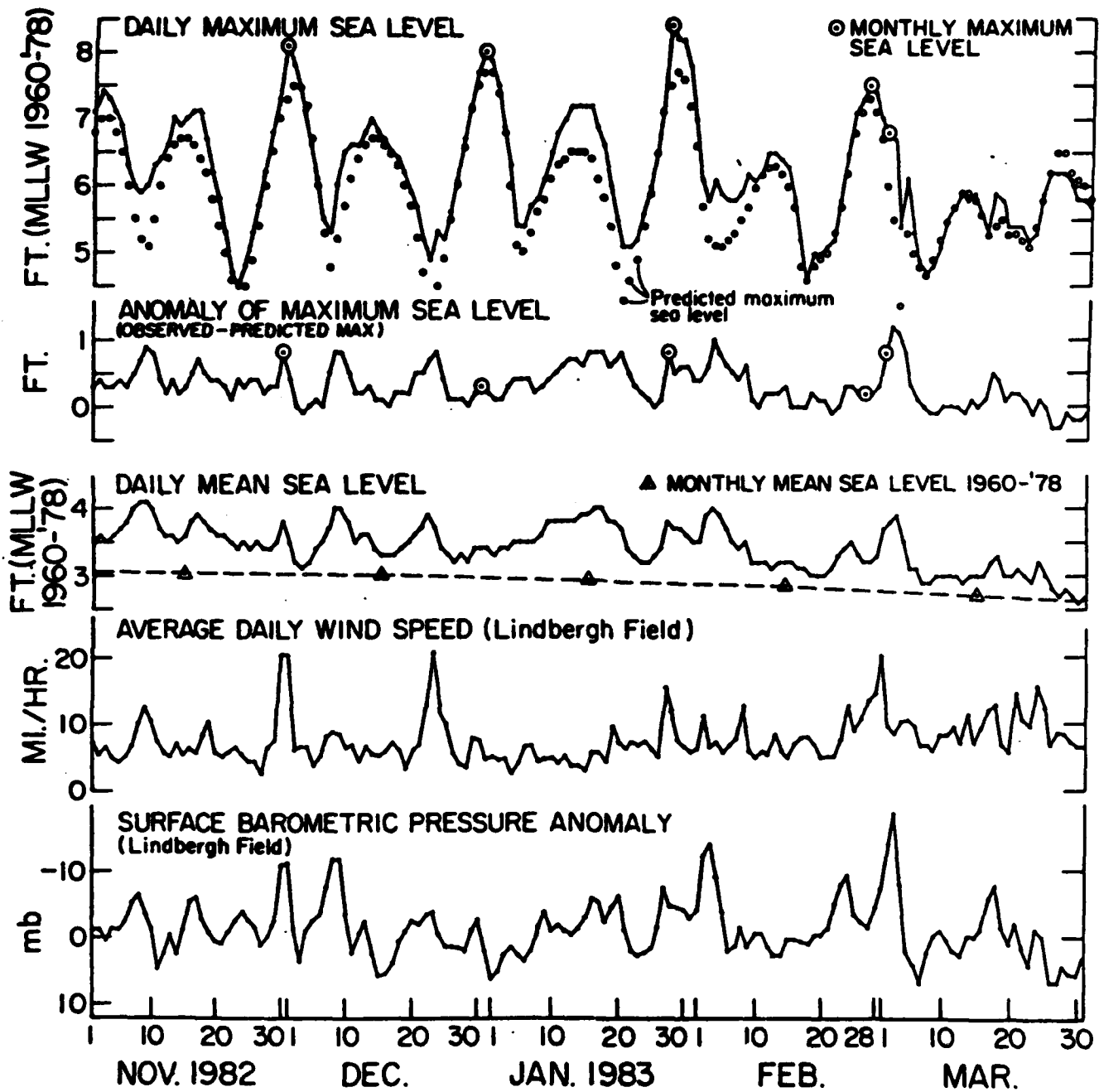


Figure 3.4.2-1 Daily sea level, atmospheric observations, and maximum predicted tide during winter 1982-1983 (Flick and Cayan, 1984).

are 1-3 ft. The 2 ft surge discussed by Smith and Leffler (1980) is a classic west coast example. Storm surge heights on the California coast are small compared to those on the east and Gulf coasts where extreme heights of 2-10 ft are more typical, and a peak 25 ft was documented for Hurricane Camille in 1969 (Shore Protection Manual). This is mainly due to the narrow continental shelf and the absence of tropical storms and hurricanes in California. Consequently, numerical storm surge models have reached a relatively high degree of sophistication for east and Gulf coast applications, but relatively little effort has gone to surge prediction on the California coast (Jelesnianski, 1972).

Solution of storm surge equations for any configuration resembling realistic bottom topography and atmospheric forcing conditions generally requires digital computer integrations. The Shore Protection Manual, however, does outline a recipe for hand calculations of surface elevation using greatly simplified storm surge equations proposed by Freeman et al (1957). Crease (1956) suggested theoretically that storm wind systems generate wavelike motions at near inertial periods that decay with distance from the generation area. Heaps (1965) and many others have extended this work to include effects of barometric pressure (inverse barometer effect), bottom stress and more realistic boundary conditions at the edge of the computational area. Heaps (1965) was able to achieve remarkable agreement between calculated and observed storm surge heights for a particular case in England (LeBlond and Mysak, 1978).

A large literature of wind-driven circulation and associated sea level fluctuations over the continental shelf of the west coast has appeared over the past 10 years. While this work is not specifically addressed to the "storm surge" question directly, the results are clearly relevant. However, detailed discussion of this work is beyond the scope of this report and the reader is referred to recent reviews such as Winant (1980), Mysak (1980) or Allen (1980).

Besides the dynamical approaches mentioned above, considerable effort has been applied to develop statistical relationships between wind and pressure forcing of sea level (Groves and

Hannan, 1968; Wunsch, 1972; Garrett and Toulany, 1982; Chelton, 1983). If the dynamics are linear, it can be shown that statistical linear regression coefficients are the best estimate of the dynamical coupling coefficients and the statistical and dynamical methods are essentially identical (Chelton, 1983).

The standard statistical method for displaying the relationship of sea level to atmospheric pressure and two wind components, for example, is to compute multiple linear regression coefficients as a function of frequency from the cross spectral quantities. Results show that sea level is inversely related to atmospheric pressure in the sub-tidal, storm surge band with a regression coefficient near 1 cm/mb. The relationship between sea level and wind is more site and setting specific. In general, higher correlations of sea level are found with longshore wind fluctuations than with on-offshore wind in this band (Lentz, 1984).

Extensive storm surge statistics are not available for the study area. Typical storm surge anomalies at San Diego, during the very stormy winter of 1982-83, were approximately 1/2 foot (i.e. the sea level anomaly events on Figure 3.4.2-1).

Flick and Cayan (1984) and Cayan and Flick (1985) have calculated anomaly statistics for *monthly extremes* at San Diego Bay. Figure 3.4.2-2 shows the median anomaly as a function of month of year for the period 1940-1983. There is a clear seasonal variation with larger than normal anomalies in December through April, with median values around 0.1 to 0.15 foot. During the summer and in October and November, the median of the highest monthly sea levels are very close to the predicted tides with median anomalies not significantly different from zero. In September, there is a significant peak, with median anomalies over 0.1 foot higher than predicted tides at maximum sea level. Inspection of weather maps corresponding to selected, strong cases suggests this feature is attributable to extra-tropical low pressure systems that are frequently observed offshore of San Diego in September. These systems may cause depressions in atmospheric pressure of at least 5-10 mb compared with seasonal normals at San Diego, and

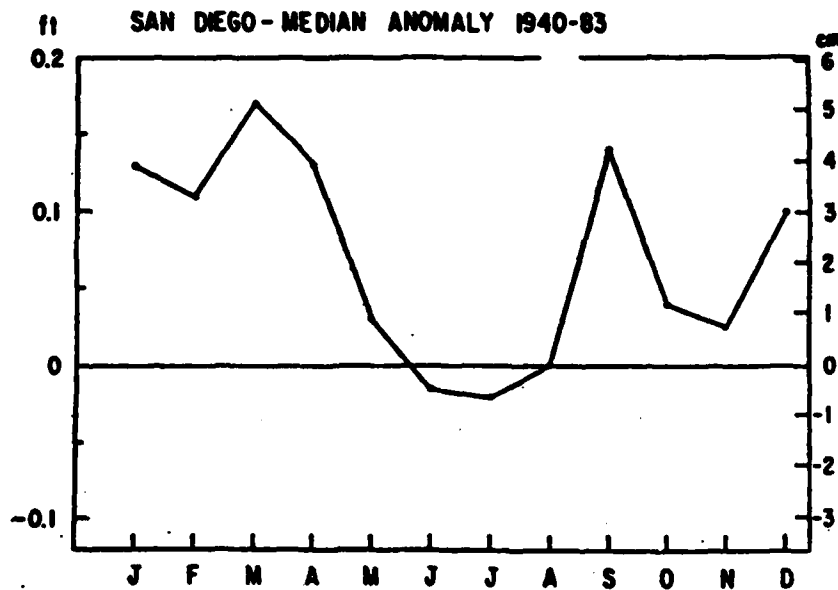


Figure 3.4.2-2 Median adjusted (linear trend removed) anomaly, 1940-1983 showing seasonal cycle. From Cayan and Flick (1985).

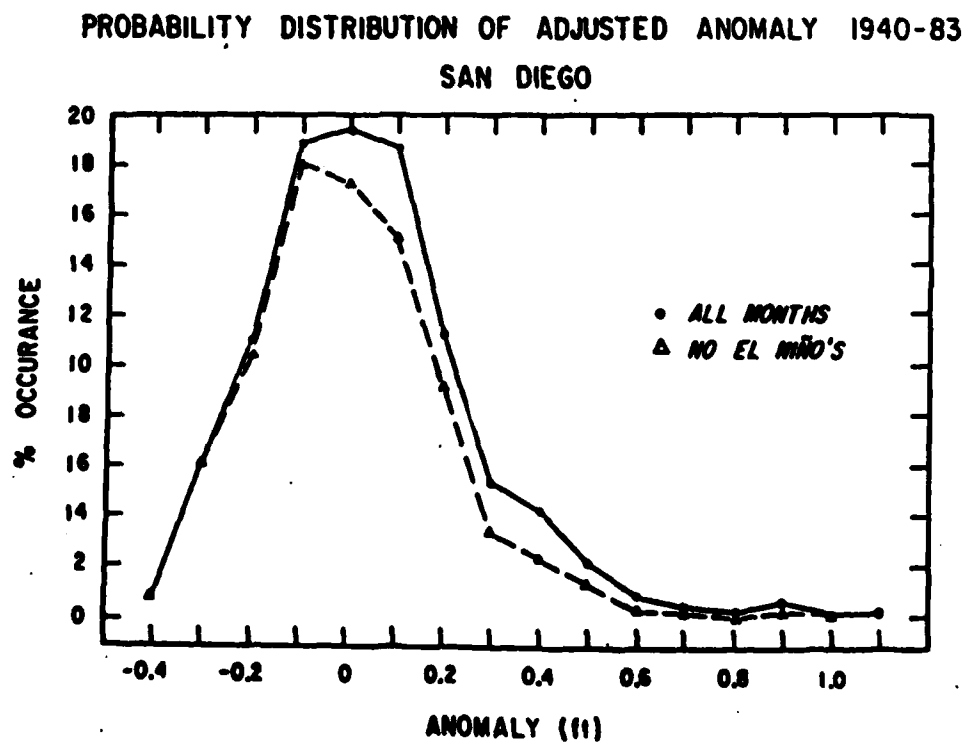


Figure 3.4.2-3 Probability distribution of adjusted (linear trend removed) San Diego sea level anomalies at maximum monthly sea level from 1940-1983, with and without El Niño months (Cayan and Flick, 1985).

this roughly accounts for the magnitude of the anomalies (Cayan and Flick, 1985). In other words, storms and storm surge at San Diego occur primarily during December through April, and in September. The median anomalies are small (0.1 ft) compared to individual surge events (.5 ft) because many of the monthly extremes do not coincide with storms.

Figure 3.4.2-3 shows the probability distributions of the adjusted anomalies (a) including all data from 1940-1983, and (b) excluding data from the major El Niño periods of 1940-41, 1958-1959 and 1982-1983. The mode (peak) of the distribution is very near zero anomaly, but it has a strong skewness toward higher values. This is consistent with expectations, since this particular sample of anomalies represents exceedances *at the time of maximum observed sea level* and the distributions thus contain a bias toward positive anomalies.

Cumulative probability distributions corresponding to the above data samples are shown in Figure 3.4.2-4. The exceedance interval for both positive and negative anomalies corresponding to the observed cumulative statistics are shown along the top margin of the figure. The larger (in absolute value) the specified magnitude, the longer the interval. Since only 44 years of data have been analyzed, not enough large events have been observed to place much confidence in the accuracy of the longer intervals and larger anomalies. Hence, the estimated exceedance intervals for anomalies greater than about 0.5 foot are in some doubt. It does seem fair to assume however, that up to 0.3 foot anomalies will recur at times of maximum observed level (on the average) every year. Note, however, that since certain extreme years, such as 1982-1983, have a propensity for frequent positive sea level anomalies, this recurrence interval is somewhat deceptive. This non-uniform spacing in time is well exemplified by winter of 1982-1983, in which all five monthly maximum sea level days had anomalies in excess of 0.3 feet.

It is not known how representative these San Diego statistics are for the rest of the coast. Similar analysis could be undertaken using data readily available from other stations. The crucial aspect of the analysis is removing the predictable, tide (and radiational) portion of the

SAN DIEGO - CUMULATIVE ANOMALY DISTRIBUTION

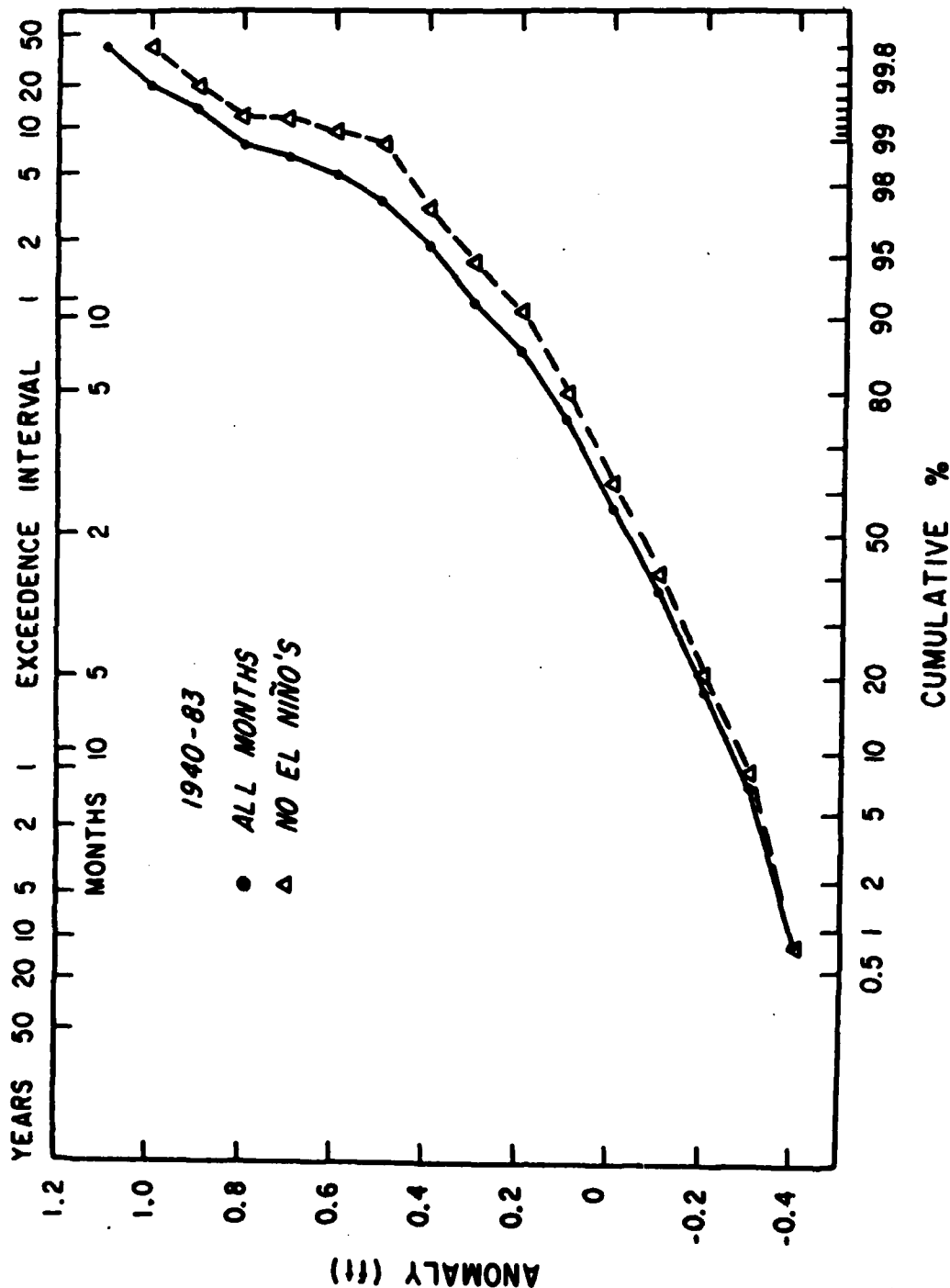


Figure 3.4.2-4 Cumulative distribution of San Diego adjusted sea level anomalies (linear trend removed), 1940-1983 at maximum monthly sea level, with and without El Niño months (Cayan and Flick, 1985).

fluctuations to expose the more random, atmospheric and ocean-driven fluctuations.

TSUNAMIS

Tsunamis are long (compared to the ocean depth) gravity waves generated by sudden movements of the ocean bottom during submarine earthquakes, landslides or volcanic activity. Tsunami effects are of interest to coastal engineering because of their large destructive potential in shallow water. The Pacific Ocean rim is highly tectonically active, so most of the world's tsunamis are found in the Pacific. Two source regions are primarily responsible for tsunamis potentially damaging to California: the Peru-Chili Trench and the Aleutian Trench (Houston, 1980; Houston and Garcia, 1978). Southern California, south of Point Conception, is much less susceptible to severe tsunami elevations than areas to the north owing to the orientations of these coasts relative to the Aleutian Trench (see maps in Houston, 1980). Three events caused major damage to the United States coasts in modern times: the 1946 Aleutian tsunami, the 1960 Chilean tsunami and the 1964 Alaska tsunami (Houston, 1980). Rapidly changing water levels associated with tsunamis on the California coast have been observed to generate strong currents that are largely responsible for the damage to boats, aquatic structures and inundated landside developments (Magoon, 1965).

For purposes of coastal design and planning it is desirable to have accurate estimates of possible tsunami inundation levels as a function of coastal location, and the associated recurrence intervals. Several factors make this a difficult task for southern California. First, tsunamis are so infrequent here that detailed, well-documented accounts of coastal water elevations exist for only a few events. Actual measurements are confined to several tide gauge records and a few fortuitous measurements at La Jolla during the 1960 event (Miller et al, 1962). Scarcity of observations precludes any direct statistical recurrence calculations. Second, the coastal response during the initial period of an event is highly variable. Offshore topography, location and orientation of the source and details of its motion (such as area and

type of fault involved and the intensity of the associated earthquake) all cause variations in coastal response. These difficulties dictate relatively sophisticated numerical methods to produce estimates of coastal water levels. The requirements of 100-year and 500-year recurrence interval inundation levels by the Federal Emergency Management Agency (FEMA) spurred the recent work by Houston and co-workers at WES. The numerical simulation models used are fairly involved and require a number of assumptions to be viable. The scheme consists of several distinct steps:

1. Probability estimation of tsunami intensity from observations in the source region.
2. Assuming a relationship of tsunami intensity and actual submarine ground motion.
3. Modelling the initial sea surface disturbance based on the assumed ground deformation.
4. Propagation of the disturbances across the Pacific Ocean to shallow water areas using a coarse grid finite difference model.
5. Propagation of the oceanic forcing (from 500 m depth) over local continental shelf topography to shore.
6. Inclusion of tidal effects important in southern California where tide heights generally exceed expected tsunami elevations.
7. Calibration and verification of intermediate and final results with observations.

Very encouraging model verification was possible by comparing predicted and measured time series of ocean elevation at several locations in southern California for the 1964 Alaska event. The amplitude and shape of the response varied considerably between the 7 tide stations located from Point Conception to San Diego operating at the time (Houston, 1980). The amplitude of the signal was generally 2-4 ft peak-to-peak, with an 8 ft peak-to-peak maximum at Santa Monica. Figure 3.4.2-5 shows predicted and observed elevations at Santa Monica and San Diego.

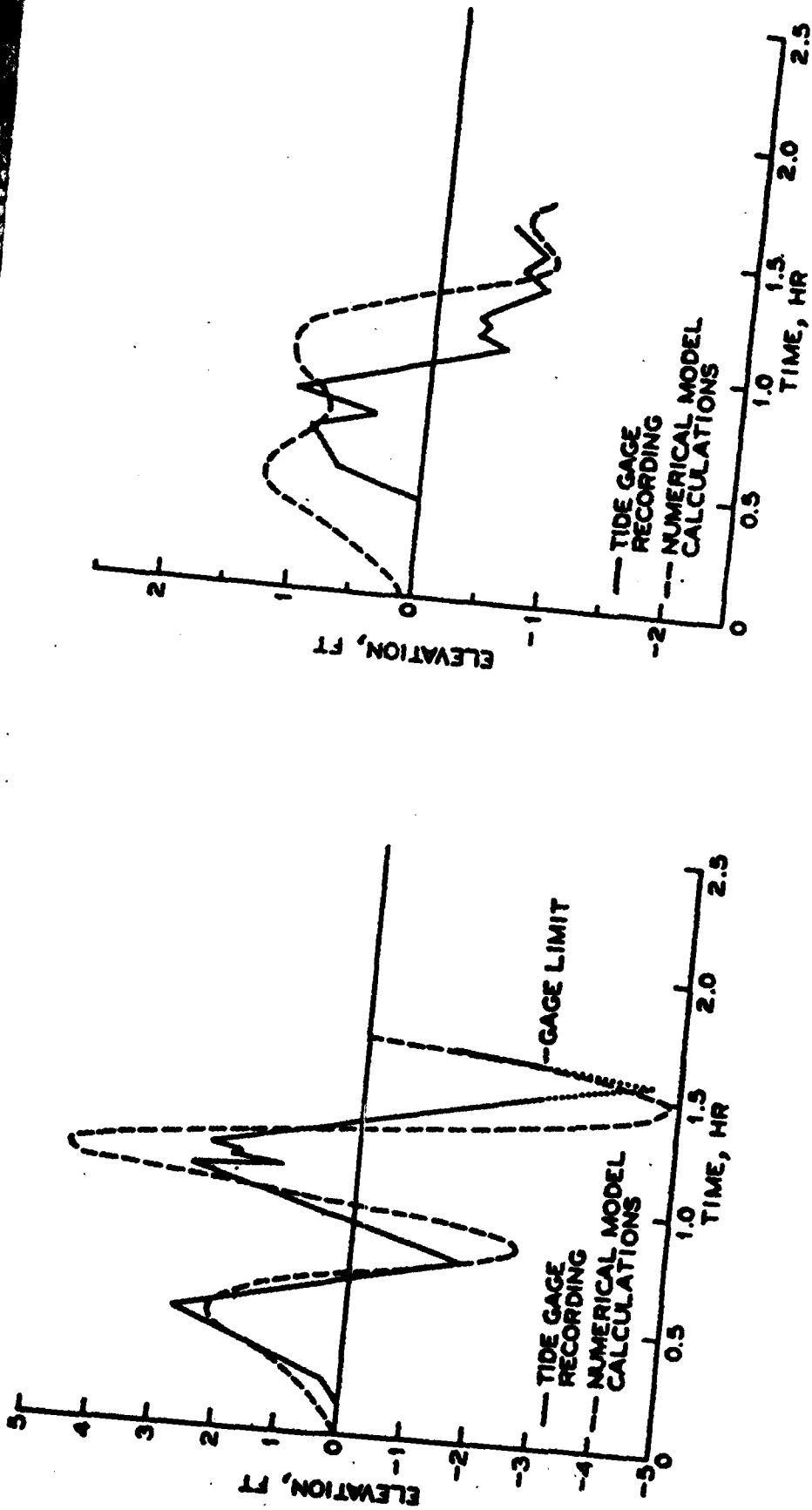


Figure 3.4.2-5 Comparison of observed and predicted sea level elevation at Santa Monica (left) and San Diego (right) during the 1964 tsunami (Houston, 1980).

The verified model was then used to predict tsunami run-up heights as a function of location for 100-year and 500-year events. Houston (1980) gives these run-up heights for 240 locations between Santa Barbara and the Mexican border. Typical heights are 4-6 ft (100-year recurrence) to 5-8 ft (500-year recurrence) over most of the reach. Several areas, however, show local amplification: Ventura, 6 ft (100 yr) to 13 ft (500 yr); Santa Monica, 7 ft (100 yr) to 14 ft (500 yr); and Long Beach, 6 ft (100 yr) to 12 ft (500 yr).

North of Point Conception (about $34^{\circ}30'N$) there is a higher degree of variability of probable tsunami run-up as a function of position. Figure 3.4.2-6 shows the predicted run-up as a function of 100-year or 500-year recurrence interval and latitude. The model predictions in this region have been verified against available tide gauge records and field measurements from Crescent City following the 1964 event. This tsunami caused heavy damage in Crescent City when 3 or 4 waves about 20 ft above MLLW inundated the city over a 2 hour period on the night of 27-28 March 1964 (Magoon, 1965). The wave events were described as rapid rises of water level at rates of about 1-2 ft/min. These caused large ebb and flood currents which swept boats and other facilities from their moorings and battered structures with large logs and other floating debris (Magoon, 1965).

Pressure gauge instruments were installed off Scripps Pier as part of another experiment during the less severe Chilean Tsunami of May 1960. Miller et al (1962) report on these measurements, and in particular discuss the temporal decay of tsunami energy on the continental shelf off the La Jolla area. These measurements are better suited to comparisons with numerical model results than are tide gauge measurements, because tide gauges are intended to filter waves of much higher frequency than the tides. A substantial amount of energy in tsunamis exists at periods shorter than 12 min, about the Nyquist period of a typical tide gauge. The measurements of Miller et al (1962) showed that the tsunami energy decayed by $1/e$ approximately every 12 hours. Oscillations remained above the "background" for about 1

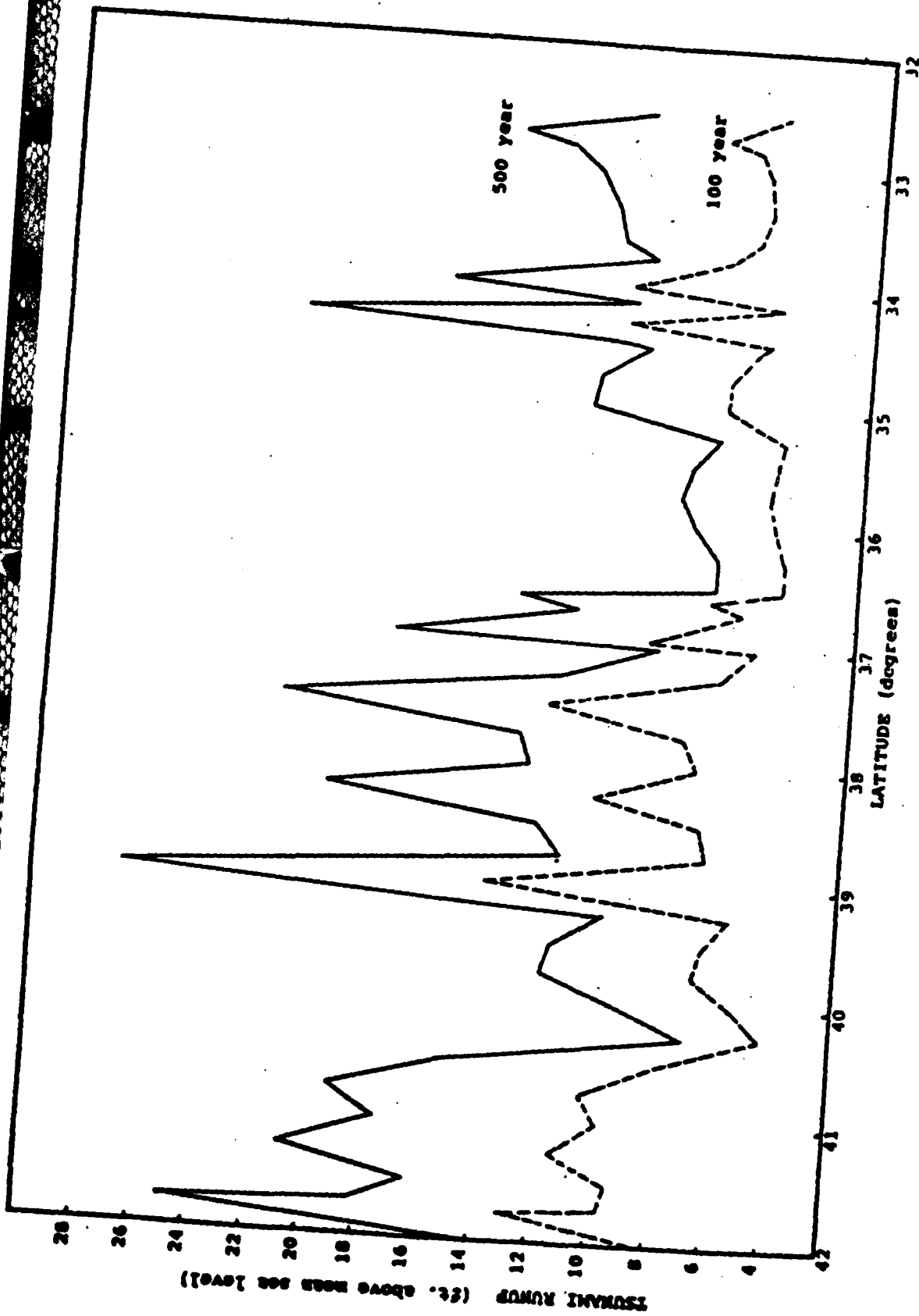


Figure 3.4.2-6 Tsunami runup as a function of recurrence interval and latitude along the California coast (Williams et al. 1981).

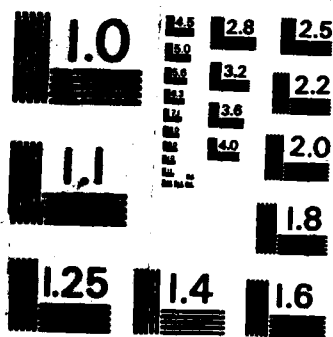
UNCLASSIFIED

D L INMAN ET AL. FEB 86 CCSTWS-86-1

NL

F/G 8/3

NL



MICROCOPY RESOLUTION TEST CHART
NATIONAL BUREAU OF STANDARDS-1963-A

week after the initial disturbance reached La Jolla.

3.4.3 *Interannual Effects*

As an example of extreme interannual variability at San Diego, Figure 3.4.1-2 shows the monthly average sea levels for 1982 and 1983. The warm water and other conditions conducive to higher than normal sea levels started with the onset of El Niño in spring of 1982. By late 1982 and through most of 1983, monthly means were 15 cm (2 or 3 standard deviations) above normal. It is interesting to note that the typical seasonal signal is conserved in both extreme years, only amplified by a factor of about 2 and displaced by about 15 cm. This steady superelevation clearly contributed to the record-breaking maximum elevations shown in Figure 3.4.2-1; tides and storm surge events were superposed on an already elevated surface.

There is overwhelming evidence that interannual variability of sea level on the west coast is associated with large-scale, Pacific Ocean basin wide fluctuations in wind, pressure and mixed layer temperature. Namias and Huang (1972) show a "decadal" fluctuation using data from San Diego that produced winter (December-February) sea level averages 5.6 cm higher between 1958-69, compared with 1948-57. They indicate that the change came comparatively suddenly, around 1957-58, suggesting a shift between different winter patterns of wind, pressure and ocean temperature. After independently computing the effects of other possible causes (including the negligible contributions of long period tides, local runoff and changes in bathymetry), they conclude that the largest contribution (3.7 cm) was due to thermal expansion of the offshore waters. Changes in current circulation and the cumulative secular rise contributed about 1. cm each, while lowered atmospheric pressure added another 0.6 cm. The total, independently calculated rise of 6.3 cm thus compared favorably with the 5.6 cm observed.

Namias and Huang (1972) show that the offshore warming was associated with lower than normal north to south wind stress resulting in less southward flow in the California current during the later period. Sea level atmospheric pressure differences between the two periods

indicate a coherent, anomalous pattern extending from the west coast to the date line (180° W) and from the Gulf of Alaska (60° N) to 20° N. Coherent patterns of sea surface temperature anomaly cover a similar extent. These patterns are attributed to a strengthened trough (low pressure) over the central North Pacific during the 1958-69 period. More recent research suggests that this troughing is also associated with heightened storm activity, and related sea level anomalies, on the west coast, particularly during El Niño events (Namias and Cayan, 1984). However, the exact position of the low pressure system is highly variable from one event to another. Since the path of extratropical storms is greatly influenced by the position of this system, not all El Niño's display severe storms in southern California. During the 1976-77 El Niño storm tracks veered sharply north and California experienced the height of a prolonged drought. In contrast, the 1982-83 event, with the low farther eastward, was one of the stormiest winters on record. The sea level effects of El Niño events in the last century are qualitatively illustrated in Figure 3.4.4-1. Further discussion of the global scale climate effects associated with interannual variability is beyond the scope of this work.

3.4.4 Long-Term Changes

Much recent attention has been focused on long-term, secular trends in sea level because of heightened awareness and concern over the so-called "greenhouse effect". Preponderance of scientific opinion holds that continued buildup of carbon dioxide and other gases (methane, nitrous oxide and chloro-fluorocarbons) will cause a substantial warming of the earth and consequent sea level rise by increasing melting of land-bound ice mass and by direct thermal expansion of the ocean (Hoffman et al, 1983). Even a modest increase of 15 cm would greatly increase seasonal beach and cliff erosion and storm flooding in the study area. The unlikely collapse of the west Antarctic ice sheet could result in a 5-6 m increase in sea level (Gornitz et al, 1982) with catastrophic consequences unparalleled in modern history. Leaving aside the more radical scenarios, which will be obvious enough if they occur, the more subtle, steady

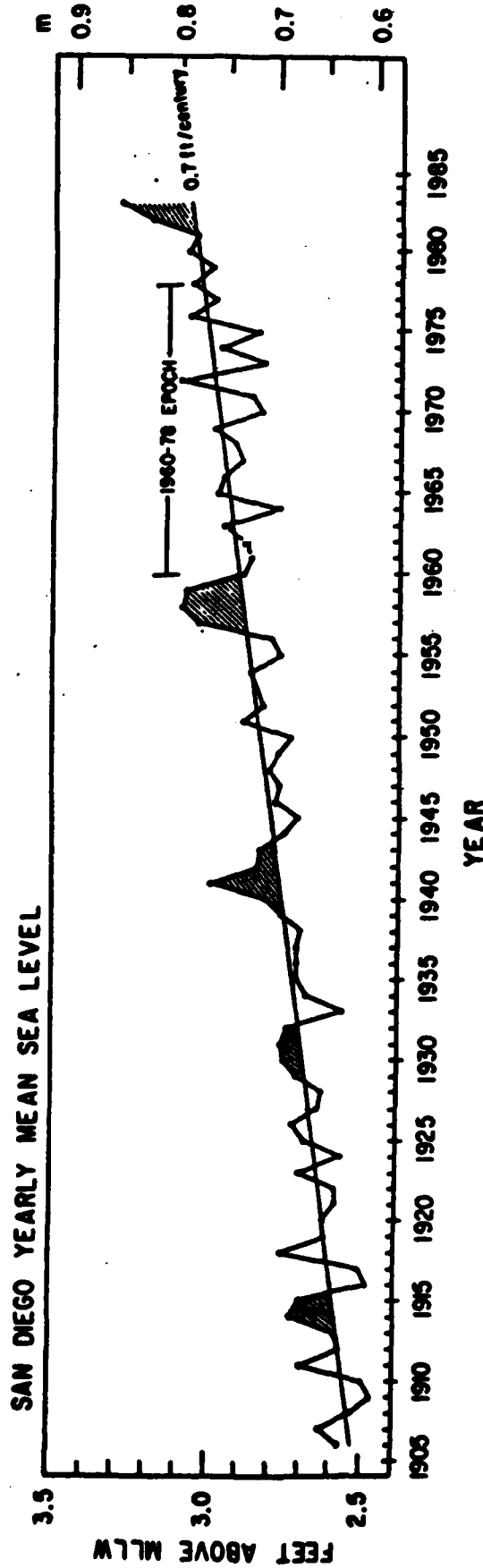


Figure 3.4.4-1 Yearly mean sea level above 1960-78 MLLW datum. Straight line shows secular increase of 0.7 foot/century, comparable to global sea level rise. Shaded areas are coincident or near in time to major El Niño episodes (Flick and Cayan, 1984).

increases are very difficult to quantify in the very noisy sea level record. They are even harder to estimate by applying models of sea level rise to the scant ocean temperature records or from estimates of global ice mass decrease.

The only geophysical time series long enough to study the history of sea level rise and its spatial pattern are the tide gauge records. Tide gauges are mostly located at continental coastlines and measure the relative elevation of land and sea. Thus geologic (tectonic and isostatic) motions of the earth's crust as well as meteorologic and oceanographic processes contaminate the data. Very few tide stations have continuous records over 50 years old, and by far the most stations are in the industrialized nations of the Northern Hemisphere (U.S., Europe and Japan). The importance of the problem (extracting a "global" rise separable from the regional patterns) and the noisy data set call for very sophisticated tide gauge data analysis methods and more modelling work.

Gornitz et al (1982), like many similar studies, separated the available stations into 14 regions on the basis of proximity and similarity of geological behavior. They culled the stations with record lengths less than 20 years and those in tectonically active, or rapidly subsiding locations. Least squares fits to the remaining series and averaging over the regions produced a global rise of 12 cm/century over the past century. This is very similar to other estimates (see Linitzin, 1974; Barnett, 1983a) but smaller than Emery (1980). More recent work (Barnett, 1983a; Aubrey and Emery, 1983) has used sophisticated normal mode analysis to objectively separate the complicated spatial and time behavior of the tide gauge data and thus avoids some of the subjectivity of previous studies. However, the basic problem of short time series with poor spatial distribution remains and no analysis can reduce these fundamental shortcomings. As a result, separating and quantifying the various causes of sea level rise is highly speculative and controversial (Barnett, 1983b; Lambeck and Nakibogler, 1984).

For engineering and coastal protection purposes, it is a reasonable assumption that sea levels will continue to rise at at least their previous rate (15 cm/century) and more likely at about twice that rate in the study area (Gornitz et al, 1982; Flick and Cayan, 1984). Table 3.4.4-1 summarizes the observed sea level trends for stations in California according to Hicks et al (1983). Figure 3.4.4-1 shows yearly mean values for San Diego. The linear least square fit includes data from 1981-83, resulting in a slightly higher estimate than Hicks et al (1983). The table shows mean rates of rise in cm/century and associated error for 6 stations (1st column) with reasonably long records. The rates are generally stable, within the error bounds, for the period 1940-80 (2nd column) or for each entire available record (3rd column). There is no convincing evidence in Table 3.4.4-1 or in Gornitz et al (1982) that sea level rise is accelerating in the study area, although some interpretations of data for all U.S. coasts and the world suggest this may be the case (Aubrey and Emery, 1983).

Table 3.4.4-1 Sea level increase (cm/century) at west coast tidal stations (compiled from Hicks et al, 1983).

	1940-80	Entire Record	Period
San Diego	16 ± 4	19 ± 1	1906-1980
La Jolla	15 ± 4	17 ± 2	1925-1980
Los Angeles	-1 ± 4	6 ± 2	1924-1980
San Francisco	15 ± 4	12 ± 1	1855-1980
Alameda	1 ± 5	1 ± 5	1940-1980
Crescent City	-16 ± 4	-0 ± 3	1933-1980

4. BIG SUR GROUP OF CELLS

The Big Sur Group of Cells extends from Point Lobos, south of Carmel, to Point Buchon. The group of cells cover a distance of 133 miles, 55 of which are south of Ragged Point, the northern boundary of this review (see Figure 1.2-1). The coastline is very rugged and rocky with small pocket beaches and a few crescent beaches. The number and sizes of beaches gradually increase to the south.

4.1 COASTAL EROSION PROBLEMS, NATURAL AND MAN-MADE

USACE LAD (1970) discusses the general shoreline conditions in San Luis Obispo County. They report no noticable erosion of public beaches during the three year report period. USACE SPD (1971) reports on the coastal characteristics related primarily to erosion produced by waves or other coastal phenomena (Figure 4.2-1). The majority of this county's coastline is privately owned and is undeveloped. California (1977a) is a report and atlas that presents an assessment of the erosion that is occurring along the ocean shoreline of the State. The report-atlas identifies the shoreline characteristics of the entire coastline and shows two areas, San Simeon and just south of Cayucos, where critical erosion occurs. Now critical erosion occurs along most of this coastline. The report is based on a mile-by-mile review of the conditions as they existed in 1977.

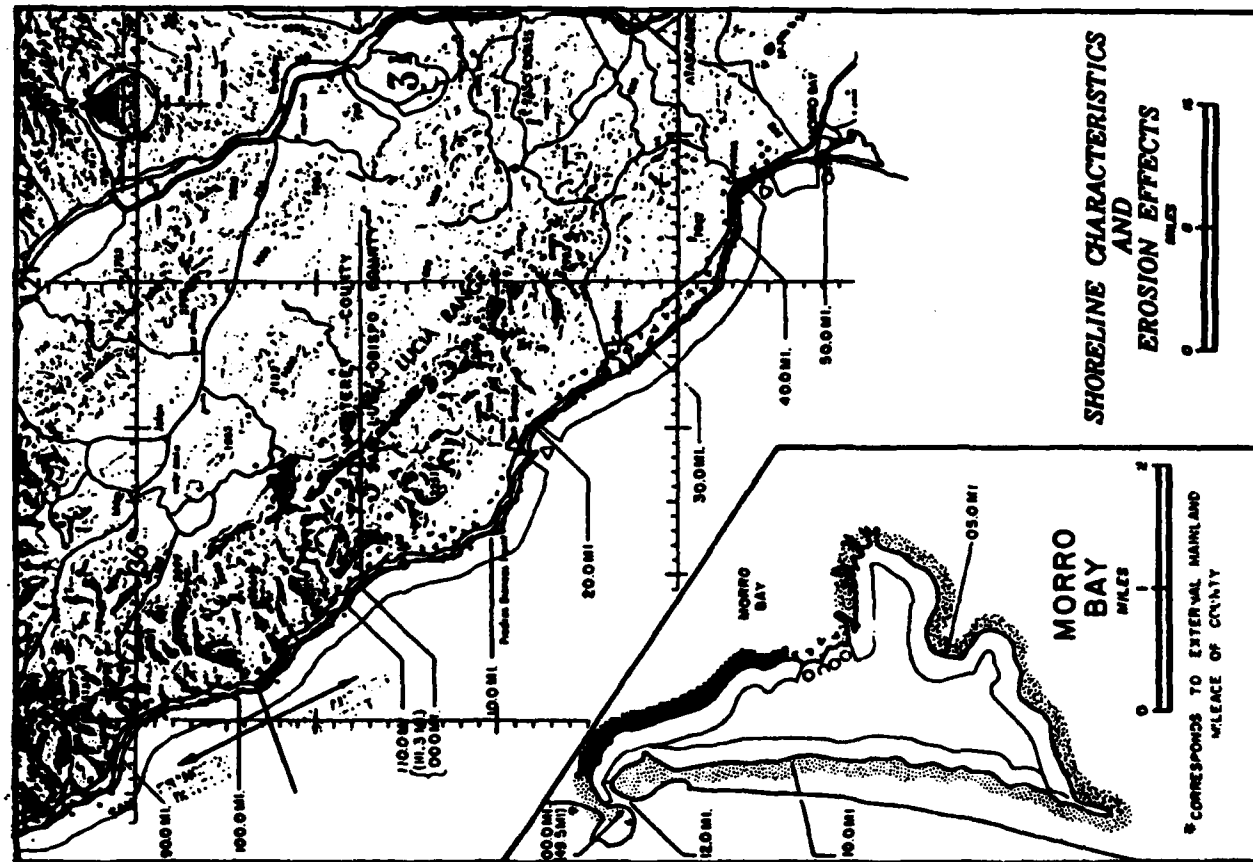


Figure 4.2-1. Shoreline characteristics and erosion effects (from USACE SPD, 1971).

4.2 SHORELINE CHANGES

There are very few reports reviewed for this study concerning shoreline changes in the Big Sur group of littoral cells. USACE LAD (1969) contains two hydrographic surveys of Morro Bay Harbor, one in 1965 and the other in 1966. It also includes a summary of aerial photographs taken along the coast but the photographs are not included in the report. USACE LAD (1970) contains an additional list of ground and aerial photographs of this coastline. Figure 4.2-1, from USACE SPD (1971), summarizes the shoreline changes from Lucia to Morro Bay.

4.3 NEARSHORE WAVES

As discussed in Section 3.3, the coastal wave climates north and south of Point Conception are radically different. The southern region is sheltered from northwest swell by the shape of the coastline and the Channel Islands (Figure 3.2.2-1). In addition, coastal wind speeds are higher in the northern region. As a result, coastal swell and sea are most energetic north of Point Conception.

Because there are no island shadows, deep ocean wave statistics can be applied without modification to the (deep) waters directly off the coast of the cell. The CDIP buoys at North Monterey Bay, Point Arguello and Begg Rock (see Section 3.2.2) provide relatively nearby and readily accessible in situ statistics (Figures 3.2.2-2,3,4,5) which are probably illustrative of conditions offshore of this cell. However, Begg Rock is in a region of offshore banks and is somewhat sheltered from angles greater than 320° (Figure 3.2.2-1), and some of the Point Arguello data was collected in depths as shallow as 80 m. The North Monterey Bay buoy ($36^\circ 55', 122^\circ 19.5'$) is in deep water (320 m) but is sheltered from very high angle north swell by the Farrallon Islands. The importance of these local effects is not known but is thought to be relatively small. The distance of the buoys from the cell is probably not an important factor because the deep ocean wave climate is generally homogeneous over that length scale. Seymour (1983) calculated significant height return periods for the Monterey Bay buoy (Figure 4.3-1); there was insufficient data at the other buoys. The 10-year return period significant wave height is about 27 feet, with one observation of 24 feet.

SSMO (1970) observations are qualitative estimates made by observers on ships of opportunity on a 2° spread of latitude centered at Point Sal. Furthermore, "these data are based upon observations made by ships in passage. Such ships tend to avoid bad weather, thus biasing the data toward good weather samples" (SSMO, 1970). It is important to note also that the SSMO data supposedly include "only sea waves generated by local winds in the vicinity of

N. MONTEREY BAY BUOY

27 OCT.1979 TO 20 APR.1983

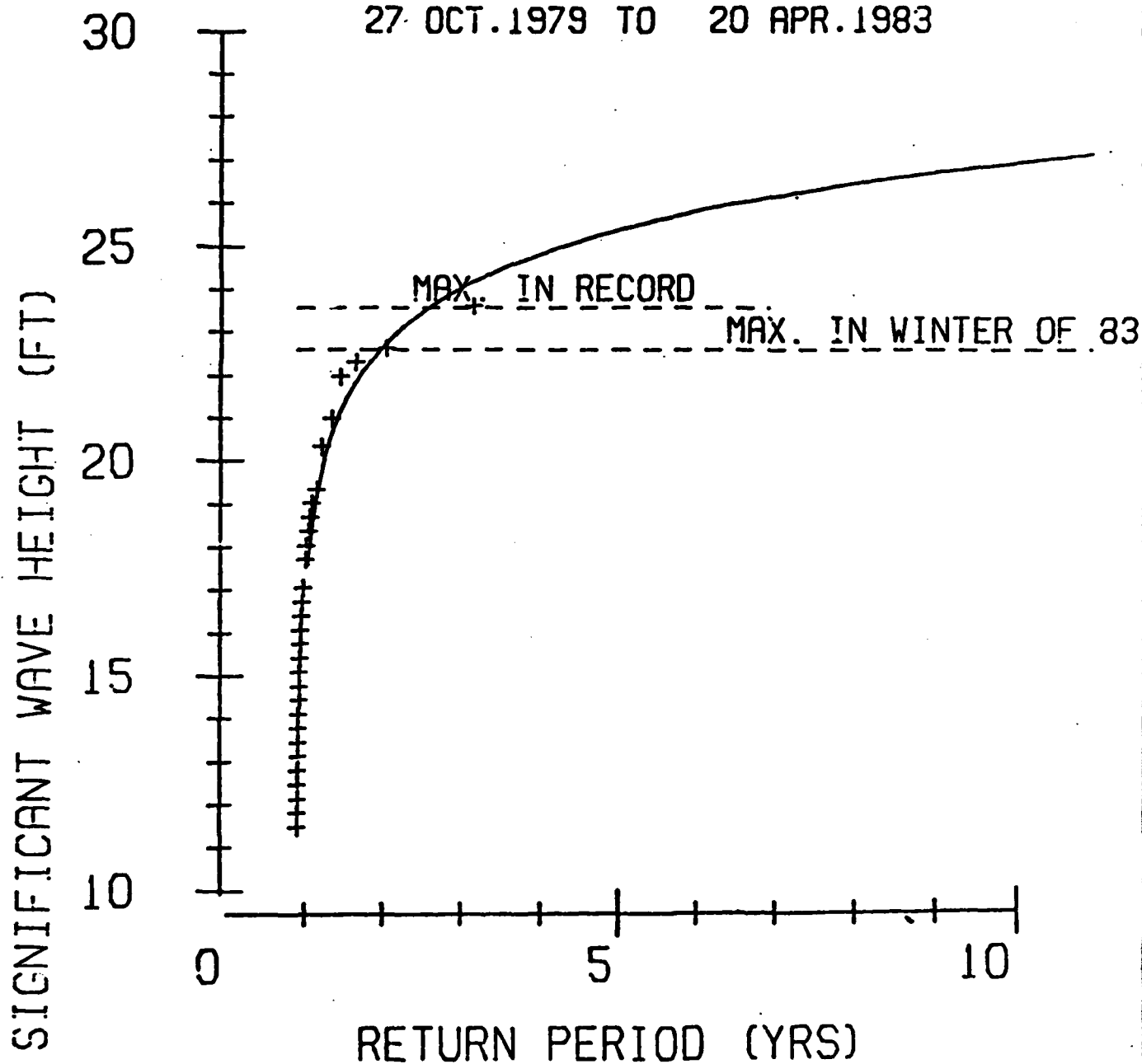


Figure 4.3-1

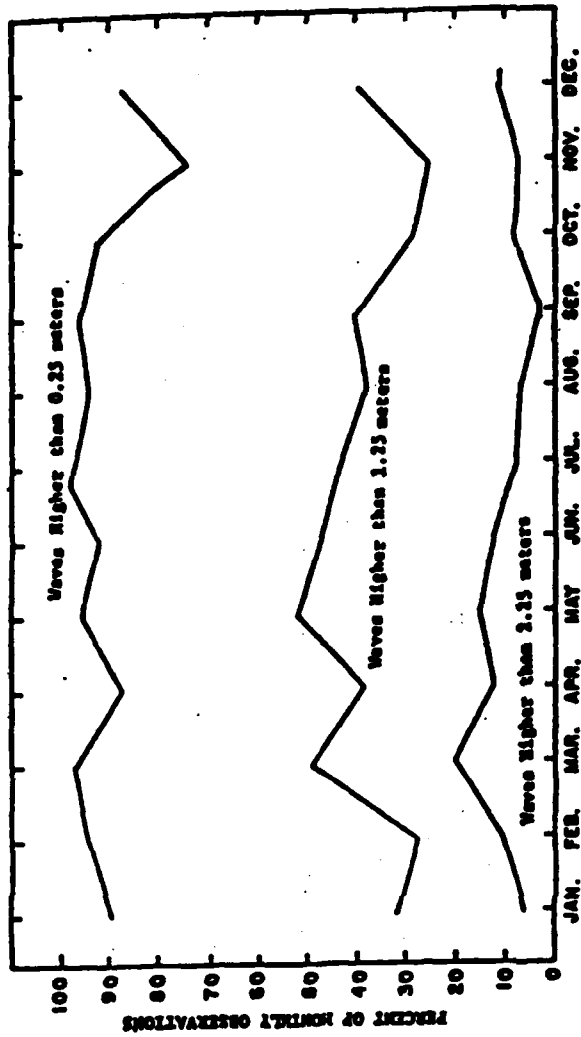
Significant height return periods at the North Monterey Bay Buoy (Seymour, 1983).

the observer." Tetra Tech (1976) summarized the SSMO (1970) wave height data; this summary and their annual offshore wave rose is shown in Figure 4.3-2. The most prominent features are the dominance of waves from the northwest and the relatively small monthly changes in wave height statistics. The figure shows also the frequency of occurrence of wave heights for the period 1963 to 1968.

The Point Arguello waverider significant height data exceeded 2.75 m (9 ft) only 2.2 percent of the time during May through September, and November-December 1978; not at all during January-February and July-August 1979; and for 49 percent of January through March 1980. Averaged over this 14-month period, significant heights exceeded 2.75 m (9 ft) for 11.6 percent of the time, compared to 8.1 percent in the SSMO data (Figure 4.3-2). It should be noted that the waverider statistics are given in terms of significant height, a statistical quantity defined as the average height of the highest one-third of all waves. The SSMO (1970) shipboard observations do not really define wave height; for example, it could be the average height or the maximum height. Nevertheless, the SSMO observations are qualitatively consistent with the significant height from direct waverider measurements.

During the 14 months of Point Arguello buoy data considered here, the maximum Hsig was 5.4 m (17 ft) on 17 February 1980. This implies that the average of the highest 1/100 of all waves on 17 February 1980 was roughly 9 m (30 ft), based on the statistical theory of Longuet-Higgins (1952). Note that this 14-month period contained an episode lasting at least 2 months when the significant wave height exceeded 2.75 m (9 ft) 50 percent of the time. During February and March 1980, there were not 2 days in a row with significant wave heights less than 1.8 m (6 ft), and there were at most only 3 days in a row with significant heights less than 2.75 m (9 ft). There is one 18-m (60-ft) height observation in the SSMO data.

Hindcast data for deepwater waves offshore of this cell are available from several sources. UCSD (1947) gives statistics for 35°N, 121°W (offshore of Point Sal). Using the hindcast



Shipboard Observations of Percent-Frequency of Wave Height (m)

Height:	<0.75	0.75-1.75	1.75-2.75	2.75-3.75	3.75-4.75	4.75-6.75	> 6.75
Percent:	22.3	47.8	21.9	6.3	1.4	0.3	0.06

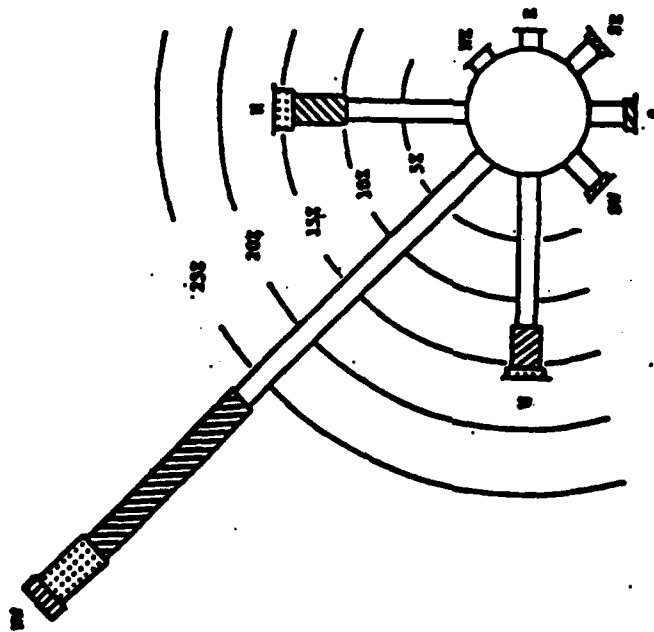


Figure 4.3-2 Wave height statistics based on shipboard observations (SSMO, 1970) summarized in Tetra Tech (1976).

years 1936-1959b, NMC (1959) generated a hindcast at a deepwater location adjacent to Morro Bay. Offshore significant wave heights exceeded 12 feet at least once every year. Further statistics dealt with deepwater waves in the sector 190° - 310° because the specific coastal site studied (Morro Bay) is sheltered from very high angle wave directions (Figure 4.3-3). Considering only this sector, there were 32 hindcast (deepwater) wave events with significant heights greater than 14 ft (Table 4.3-1). MII (1977) extreme events for 1951-74 (Table 3.2.2-4) have shorter wave periods (10-12 sec) than the NMC (1959b) events (typically 11-14 sec, Table 4.3-1), but roughly comparable magnitudes (heights 15-21 ft).

Hindcast statistics for 35° N (Station 4 on Figure 3.2.2-6) are given by NMC (1960b) and MII (1977) (see Section 3.2.2 for a discussion of hindcast methods). The yearly NMC (1960b) and MII (1977) yearly waves roses (Figures 4.3-4 and 3.2.2-12 respectively) both show a predominantly NW approach direction for both sea and swell, but considerable differences in heights. Swell heights rarely exceed 2 m in MII (Figure 3.2.2-12), but are greater than 7 ft about 10% of the time in NMC (Table 4.13 in NMC, 1960b). The 10% exceedance of 7 ft (NMC, 1960) is qualitatively consistent with the 8% exceedance of 9 ft in SSMO (1970) (Figure 4.3-2). As discussed in Section 3.2.2, the MII (1977) hindcasts may consistently underestimate wave heights (Hales, 1978a,b; Cross, 1980; Walker et al, 1984) and the NMC hindcast only considers 3 years of data and uses the rather primitive forecasting methods available at that time.

Hindcasts of storm events (1900-1984) using more modern techniques (Seymour et al, 1984) indicate much longer periods (14-20 seconds, Table 3.2.2-7,8), and somewhat larger waves. Table 3.2.2-8 shows 7 events with significant heights over 20 ft during 1900-1958, while Tables 4.3-1 and 3.2.2-4 (Station 4) show only 1 and 3 events respectively. The Seymour et al (1984) hindcasts are reported to compare favorably with recent buoy measurements, and are probably the most reliable storm event hindcasts.

Table 4.3-1 Hindcast (1899-1959) significant wave height-period (in parenthesis)-direction distribution for a deepwater site offshore Morro Bay (NMC, 1959).

Significant wave height	Direction					Total
	SSW	SW	WSW	W	WNW	
Feet						
14			(11)	(10,12,12,12,15)	(11, 14)	8
15	(9)	(14)	(11, 12)		(13, 14)	6
16		(11)	(11)	(12, 14, 14)	(12, 13, 15)	8
17		(13, 14)		(13, 15)		4
18		(13, 14)	(14)	(13)		4
19			(13)			1
20						0
21				(14)		1
Total...	1	6	6	12	7	32

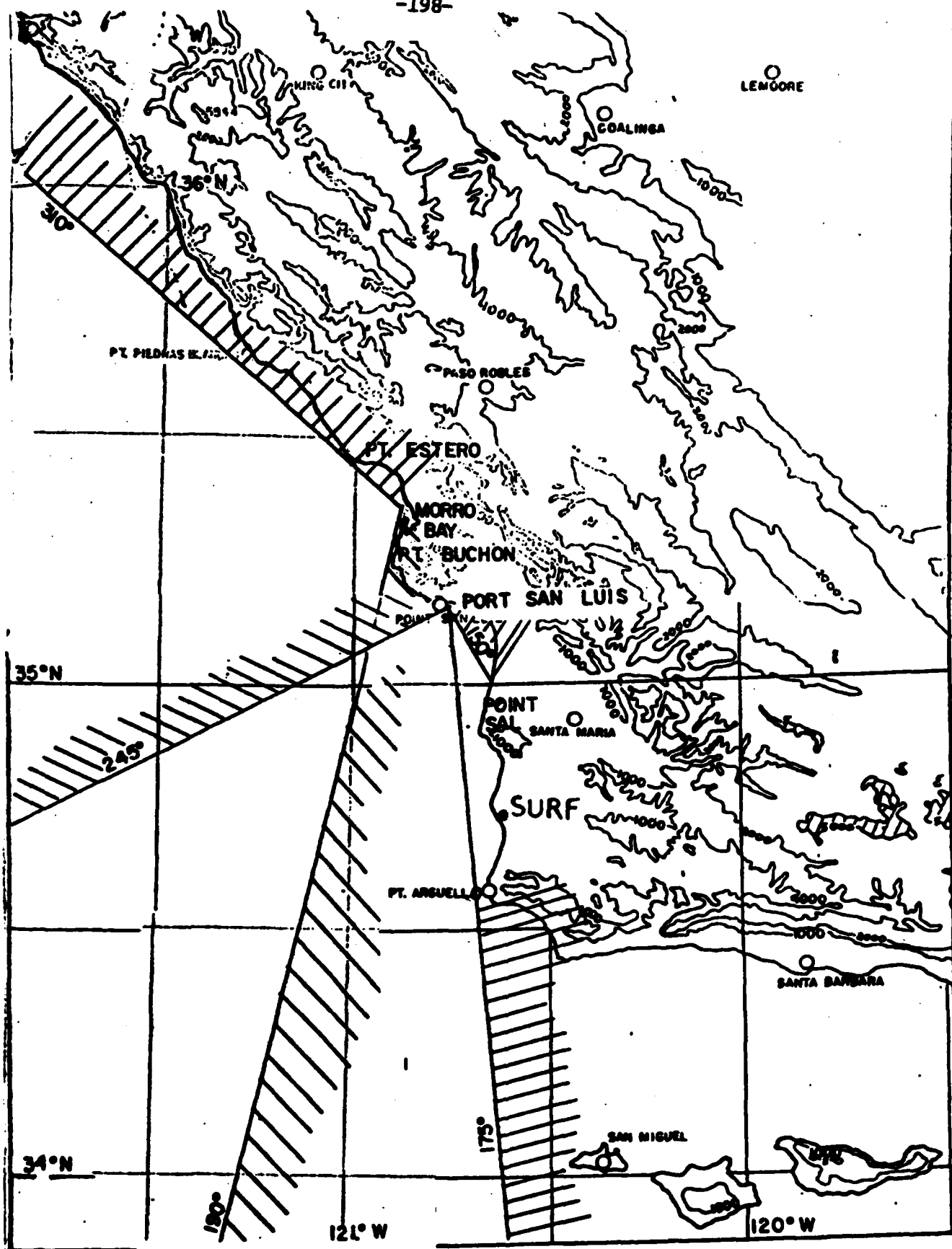


Figure 4.3-3

Open wave windows at Morro Bay (190°-310°) and Port San Luis (175°-245°).

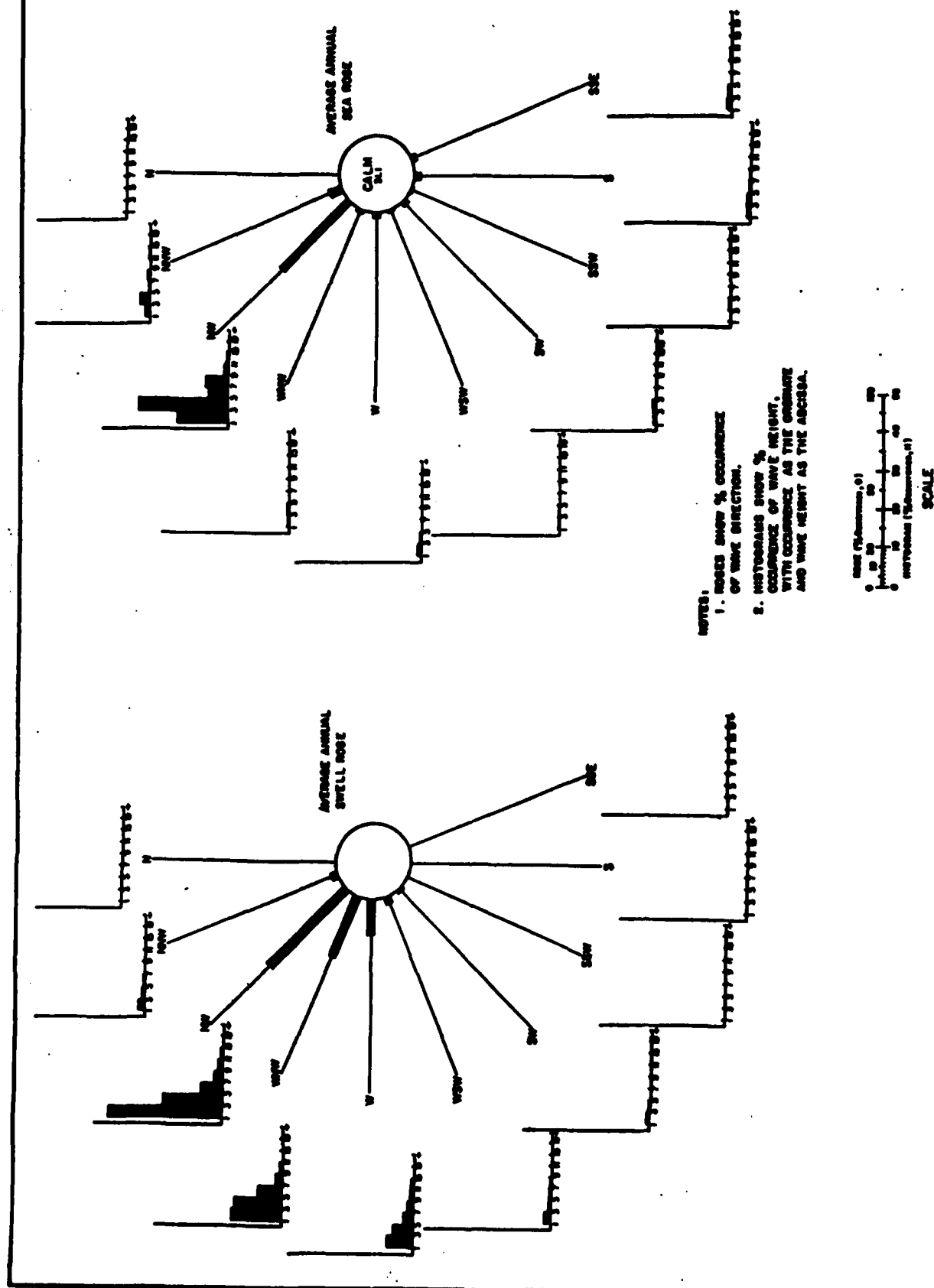


Figure 4.3-4 Hindcast average annual (1956-1958) swell (left) and sea (right) for NMC Station 4 (NMC, 1960).

Recurrence intervals based on the Seymour et al (1984) hindcasts are shown in Figure 3.2.2-16. The 100-year recurrence interval is about 8 m, comparable to the wave height for a 10-year recurrence interval using 4 years of buoy data (Figure 4.3-1). The apparent contradiction arises from the fact that the buoy data spans a very stormy time period. Of the 18 storm events exceeding 6 m significant height in this century (Table 3.2.2-8), 8 events occurred within the 4 years of buoy data. This suggests that the buoy recurrence intervals are based on a nonrepresentative time period.

There are no long-term in situ shallow water wave measurements for this cell. NMC (1959a) present 19 refraction diagrams, spanning a range of wave periods and directions, for the region between Point Buchon and Point Estero (Figure 4.3-3). Figure 4.3-5 shows a portion of the refraction pattern for 18-second swell from the west, typical of the extreme events in Table 3.2.2-7 (Seymour et al, 1984). NMC (1959b) used the refraction diagrams and hindcast storm waves (Table 4.3-1) to develop design wave heights for Morro Bay.

Hales (1978a,b) used the MII (1977) hindcast statistics, and extensive refraction calculations, to develop a coastal wave climatology for a site ($35^{\circ}11'$) near Point Buchon. However, Hales (1978a,b) believes the basic MII (1977) statistics to be biased very low (see Section 3.2.2), and unsuitable except for comparisons between sites (i.e. relative wave heights). Given this disclaimer, none of the statistics in Hales (1978a,b) are presented here. The refraction diagrams and tables of refraction coefficients are not corrupted by any shortcomings of the MII statistics, and may be of use when coupled with more reliable hindcasts (Hales, 1978a,b).

4.4 NEARSHORE CURRENTS

The surf zone currents in this cell would be expected to be predominantly from north to south, in response to the waves which approach the coast almost exclusively from north of west (Figures 4.3-4 and 3.2.2-12). Of course, the direction of surf zone currents can be reversed by

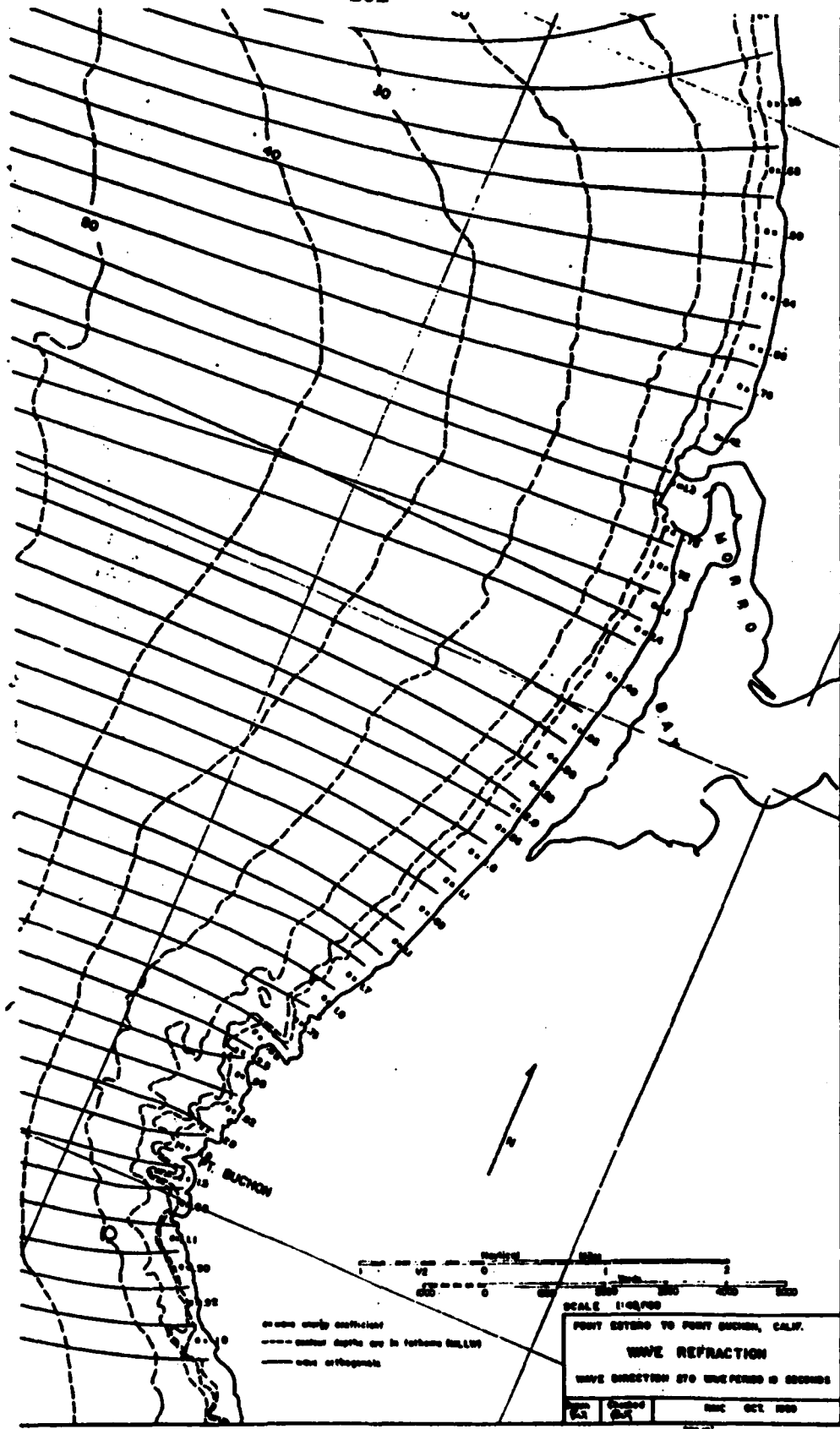


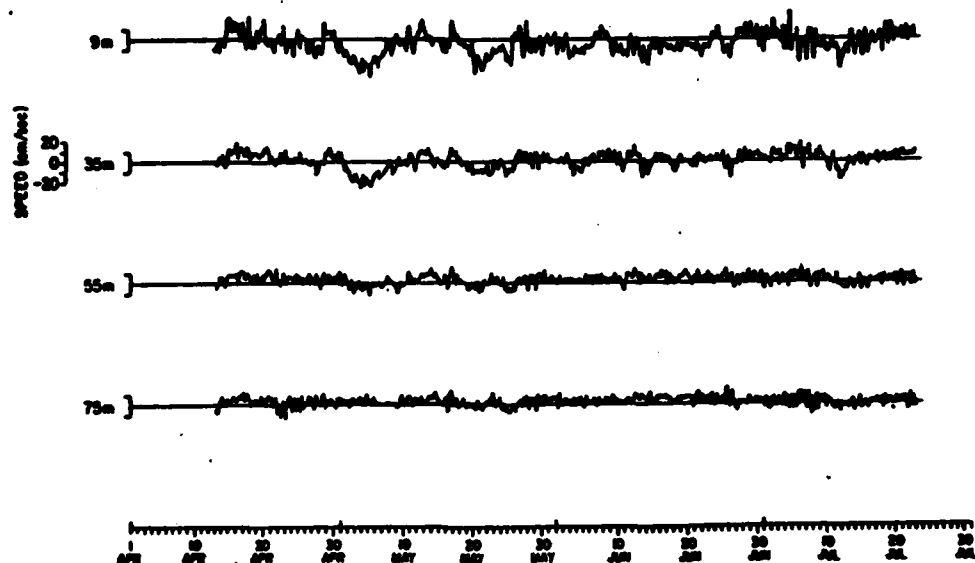
Figure 4.3-5

Refraction diagram for 18 second waves from 270°, in the vicinity of Morro Bay. Values listed as e are refraction coefficients (NMC, 1959).

very local topographic effects.

There are few direct measurements of shelf currents in this cell. The long-term, mean (seasonal) circulation is discussed in Section 3.1.1. The tidal and wind-driven fluctuating currents are expected to be qualitatively similar to those observed in the CODE region north of San Francisco. Hourly averages from a 4-month deployment (1981) of a string of current meters in 90 m depth, roughly midway between Point Reyes and Point Arena ($38^{\circ}20'$) are shown in Figure 4.4-1 (Rosenfeldt, 1983). Notable features which would be expected to also occur in the Big Sur cell are rather weak tidal currents (peak values of roughly 10 cm/sec), strong polarization in the longshore direction (with the exception of the uppermost current meter), substantial fluctuations at 'event' (2-10 day) scales, and means (less than 5 cm/sec for all cases in Figure 4.3-2) which are far smaller than the fluctuations.

R3: CROSS-SHELF CURRENT



R3: ALONG-SHELF CURRENT

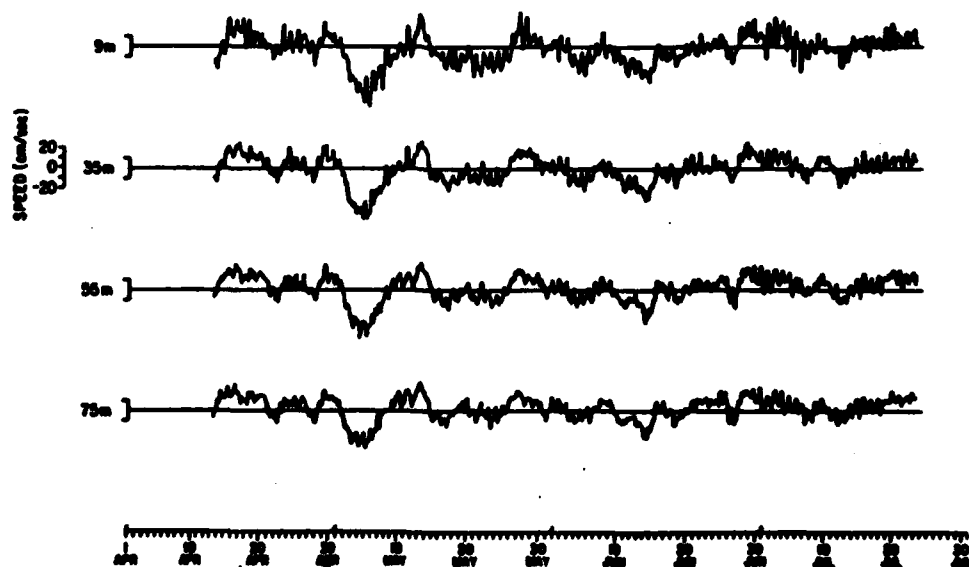


Figure 4.4-1

Hourly averaged currents from mooring R3 in the CODE-1 pilot study (Rosenfeldt, 1983).

4.5 SEDIMENT SOURCES

4.5.1 *Cliff Erosion and Relict Dunes*

Zeller (1962) inventories the coastal dunes in this group of littoral cells. These small dunes are not considered as a source of sand to the littoral cell. There were no additional reports reviewed for this study concerning cliff erosion or relict dunes as a sediment source.

4.5.2 *Sediment Discharge From Streams and Rivers*

Judge (1970) estimates the drainage area and average discharge of the Big Sur River and Arroyo de la Cruz (Table 4.5-1). Pollard (1979) contains grain size distribution plots for samples taken at Morro Strand Beach, Pico Creek and Hearst State Park. There were no additional reports reviewed for this study concerning sediment discharge from streams and rivers.

4.5.3 *Artificial Beach Nourishment*

No reports concerning artificial beach nourishment were reviewed for this study.

Table 4.5-1

River Discharge and Drainage Area

<i>Stream</i>	<i>Average Discharge</i> (acre-feet per year)	<i>Drainage Area</i> (square miles)
Big Sur River	69,570	47
Arroyo de la Cruz	36,560	41

Data from topographic maps and U.S. Geological Survey Water Supply Paper 1735.

Discharges are averages of available years at every station, but more than five years as a minimum. Areas are by planimetric determinations to nearest 10 square miles.

4.6 SEDIMENT TRANSPORT MODES

4.6.1 *Cross-shore Transport*

In Shepard's (1950a) examination of beach cycles in southern California, he included two beaches from this cell: Carmel and Pt. Sur. The typical seasonal cross-sectional changes shown in Figure 4.6-1 for these two beaches give some idea of the large seasonal changes possible in this high-energy environment.

The only other measure of cross-shore transport in the articles reviewed for study in this cell comes from bathymetric surveys at Morro Bay. Since these changes are induced by the breakwaters and harbor, they are covered in Section 4.7.2 of this report.

We are unaware of any quantitative studies of net and seasonal cross-shore transport in this group of cells.

4.6.2 *Longshore Transport*

Judge (1970) performed grain-size and mineralogy analyses at three beaches in this cell: Carmel River at the northern edge of the cell; San Simeon; and Atascadero, just north of Morro bay. He concluded from grain size changes, southward decrease of hornblende and augite, and the heavy mineral content, that net longshore transport must be to the south.

No other articles reviewed for this study quantify longshore transport rates in this group of cells.

4.6.3 *Wind Transport*

The only area in these cells where wind transport is likely to be important is in Morro Bay. There is an eight mile long, wide sandy beach there; the central three miles of the beach just south of the harbor are backed by large dune fields. No articles included in this report attempt to quantify wind transport there. For estimates of wind transport in similar dune fields, see Bowen and Inman's (1966) estimates in Section 5.6.3 of this report.

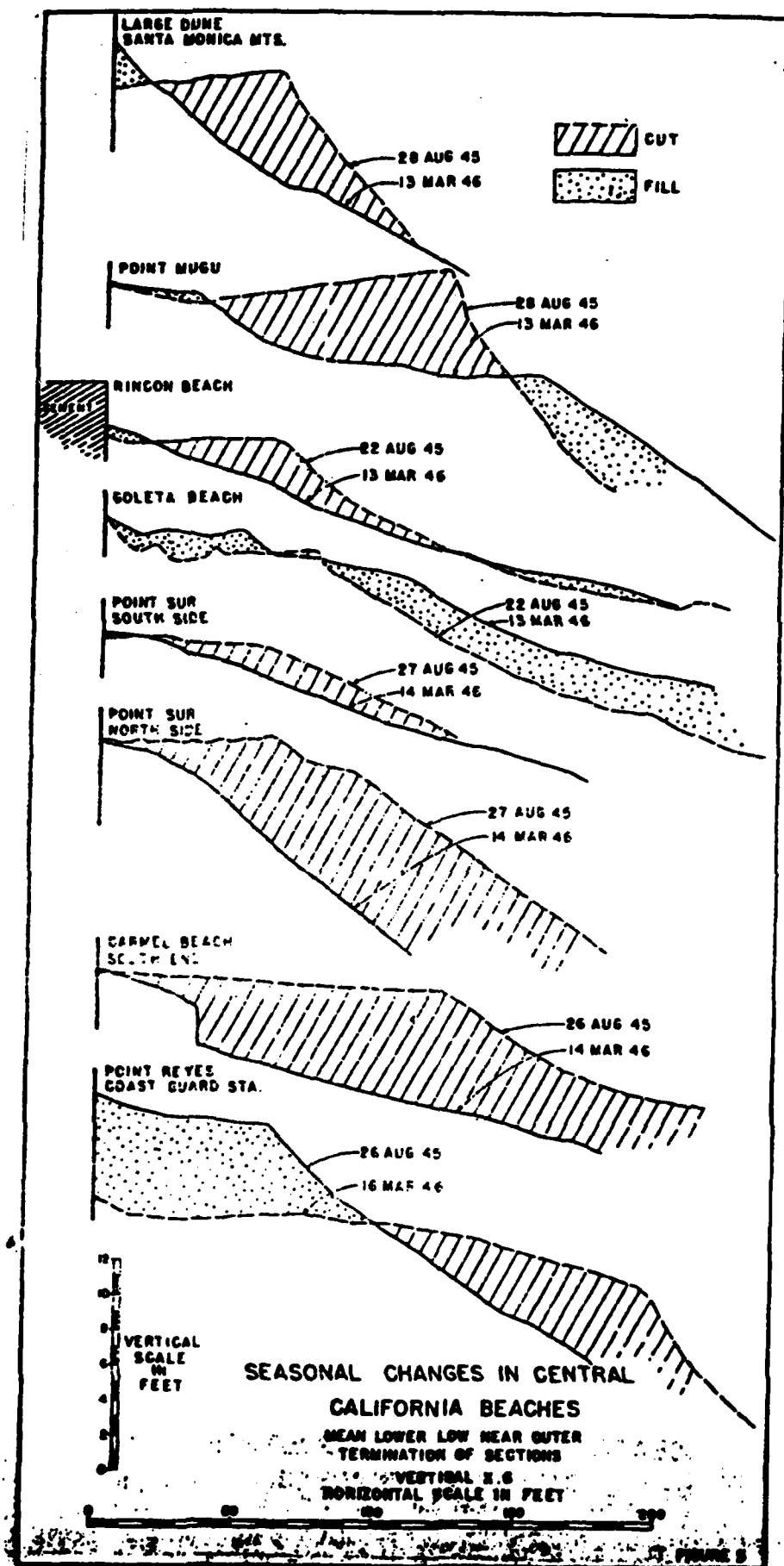


Figure 4.6-1. Seasonal changes in central California beaches, as measured by rod-and-level profiling (from Shepard, 1950c).

4.7 SEDIMENT SINKS

4.7.1 *Submarine Canyons*

Carmel Submarine canyon is to the north and outside of these cells. It approaches close enough to shore to have an effect on transport, but does not effect this cell since it is north of Pt. Lobos.

It is not yet clear whether Lucia and Sur (via Partington, its southern head) act as sediment sinks. Some of their tributary heads have significant depths in waters less than three miles from shore. Future investigation is required to resolve their role.

4.7.2 *Entrapment by Harbors, Bays and Estuaries*

Just north of Cayucos State Beach is a small harbor protected by a rock breakwater, 42 miles south of the Monterey County line (California, 1977a). Since this is an area of rocky headlands and small pocket beaches, the breakwater's effect on transport is negligible.

At the northern end of Morro Bay there are two 0.3-mile-long stone breakwaters protecting the entrance channel to the bay (Figure 4.7-1). Bathymetric surveys were performed in and near the harbor in 1943 and 1958. Based on the differences between these two surveys, USACE LAD (1960c) made several conclusions regarding sand transport. A total of $2731 \times 10^3 \text{ yd}^3$ was dredged from the harbor during this period and placed on the beach to the south, of which $951 \times 10^3 \text{ yd}^3$ remained on the beach in 1958. This represents a loss of $119 \times 10^3 \text{ yd}^3/\text{yr}$ into the bay due to tidal currents and wind transport. The actual accretion in the bay was $144 \times 10^3 \text{ yd}^3/\text{yr}$. The difference of $25 \times 10^3 \text{ yd}^3/\text{yr}$ ($144-119$) must be the transport from harbor to bay. Additionally $31 \times 10^3 \text{ yd}^3/\text{yr}$ was lost in areas near the harbor. Thus a total of $56 \times 10^3 \text{ yd}^3/\text{yr}$ ($25 + 31$) must have moved from the beaches and Charro Creek into the bay. The amount which is of interest for this report is the transport loss into the harbor, $25 \times 10^3 \text{ yd}^3/\text{yr}$.



Figure 4.7-1. Aerial photograph of Morro Bay (from USACE LAD, 1960c).

4.7.3 *Littoral Barriers*

The effects of harbor breakwaters on transport were discussed in Section 4.7.2. The only other shore-normal structure in these cells, according to California (1977a), is a pier at an oil storage facility just south of Morro Strand State Beach and 45.5 miles south of the Monterey County line. Locations of seawalls and revetments may be found in California (1977a).

4.7.4 *Wind Transport*

The only extensive dune field in these cells is at Morro Bay. USACE LAD (1960c) estimates total loss from the beach due to both tidal currents in the bay and wind transport is $119 \times 10^3 \text{ yd}^3/\text{yr}$. They are unable to discern how much of this is due to which transport mode, although it is probable that most is transported by tidal currents.

Bowen and Inman's (1966) study of wind transport loss in Santa Maria Cell dune fields may be qualitatively applicable to this site. (See Section 5.7.4 of this report.)

4.7.5 *Berm Overwash and Offshore Loss*

Berm overwash loss of sand is unlikely to be important in these cells since most beaches are pocket beaches backed by high cliffs. Overwash is possible at the Morro Bay State Park Beach, although the sand may later return to the beach via wind transport from the dune field behind the beach.

The rate of permanent offshore loss of sand on beaches such as those in these cells is unknown.

No data are available on either of these sinks in this area.

4.8 BUDGET OF SEDIMENT

There is insufficient information to compile a budget of sediment for these cells. In fact, there is no informational basis for sub-divisions of this group of cells into individual littoral cells. There were no case studies of the budget of sediment reviewed for this study. There were no reports reviewed that were directly concerned with the sources of sediment in this group of

littoral cells. However, Judge (1970) contains average annual water discharge estimates for Big Sur River and Arroyo de la Cruz (see Table 4.5-1). Judge also concludes that the longshore transport, just north of Morro Bay, must be to the south because of the longshore distribution of heavy minerals. He does not make estimates for longshore transport rates.

The submarine canyons in the group of cells, Sur and Lucia Submarine Canyons, are too far offshore to intercept the longshore movement of sand. USACE LAD (1960c) discusses the accretion of sand in the Morro Bay Harbor. They estimate the harbor traps about 119×10^3 yd³/yr. The report also discusses the wind transport for the dune field at Morro Bay. However, the report does not estimate that amount actually transported by winds.

5. SANTA MARIA CELL

The Santa Maria Cell extends for 82 miles from Point Buchon to Point Conception (see Figures 1.2-1 and 5.6-1). This cell has the longest sandy beaches in southern California. Pismo Beach is over 16 miles long and is backed by some of the most extensive sand dunes in California. These long beaches receive the highest fluxes of wave energy, but because the shoreline is nearly normal to the prevailing waves, the net longshore transport of sand is relatively small. The cell was first studied by Bowen and Inman (1966), and their study is still the most detailed study of the Santa Maria Littoral Cell.

5.1 COASTAL EROSION PROBLEMS, NATURAL AND MAN-MADE

In an effort to compile information on the problem of erosion for development of policies, the California Dept. of Boating and Waterways, formerly the Dept. of Navigation and Ocean Development, published the Assessment and Atlas of Shoreline Erosion along the California Coast (California, 1977a). The atlas shows few erosion problems in the Santa Maria Littoral Cell. USACE LAD (1970) summarizes the shoreline conditions from Point Buchon in San Luis Obispo County to Point Conception in Santa Barbara County. These summaries contain some information on local erosion problems occurring during the late 1960's. Very little erosion was observed during this period. occurring during the late 1960's. USACE SPD (1971) is an inventory of shoreline characteristics related primarily to erosion. Figure 5.1-1 shows no critical erosion areas from Point Buchon to Point Arguello. Asquith (1983) studied cliff retreat in the vicinity of Pismo Beach. He calculates a maximum retreat of 1.1 ft/yr and predicts a 100-year edge of cliff position (see Figure 5.1-2).

5.2 SHORELINE CHANGES

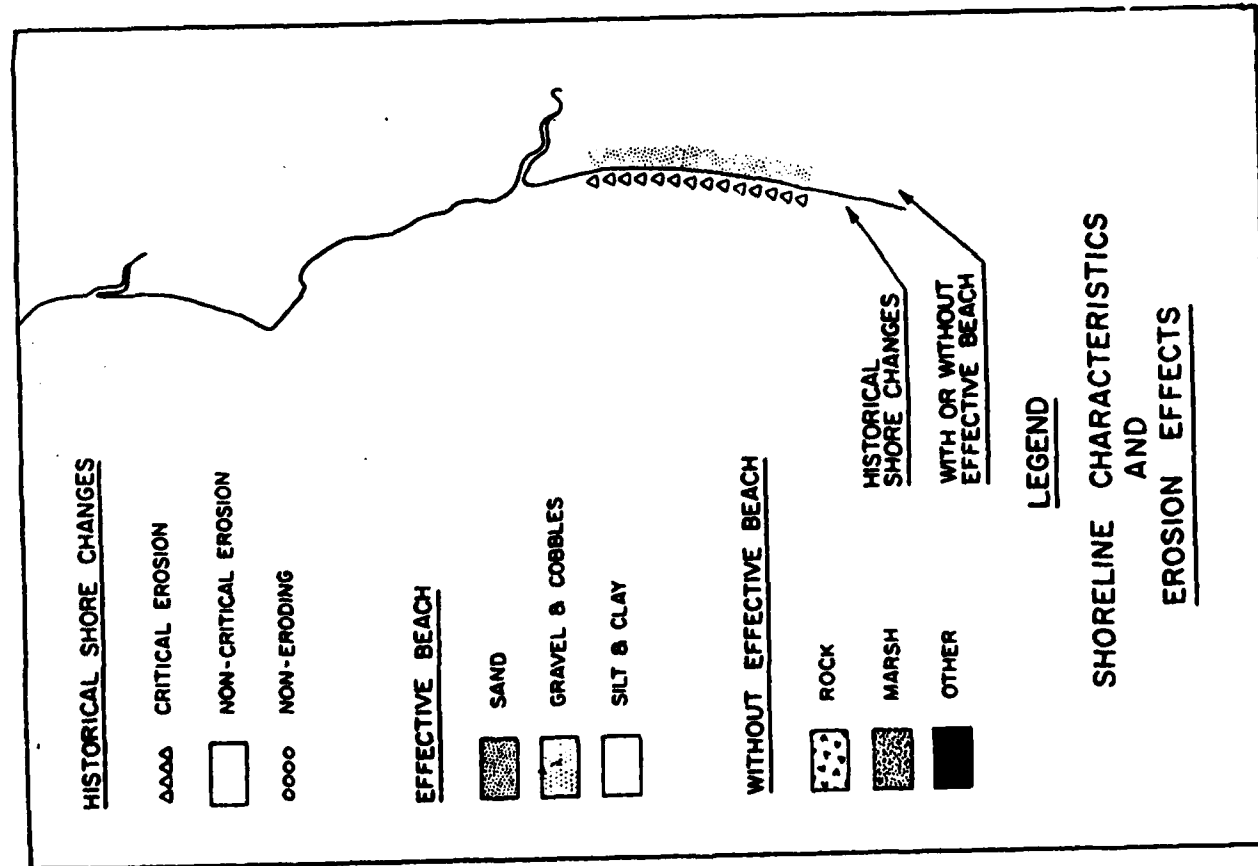
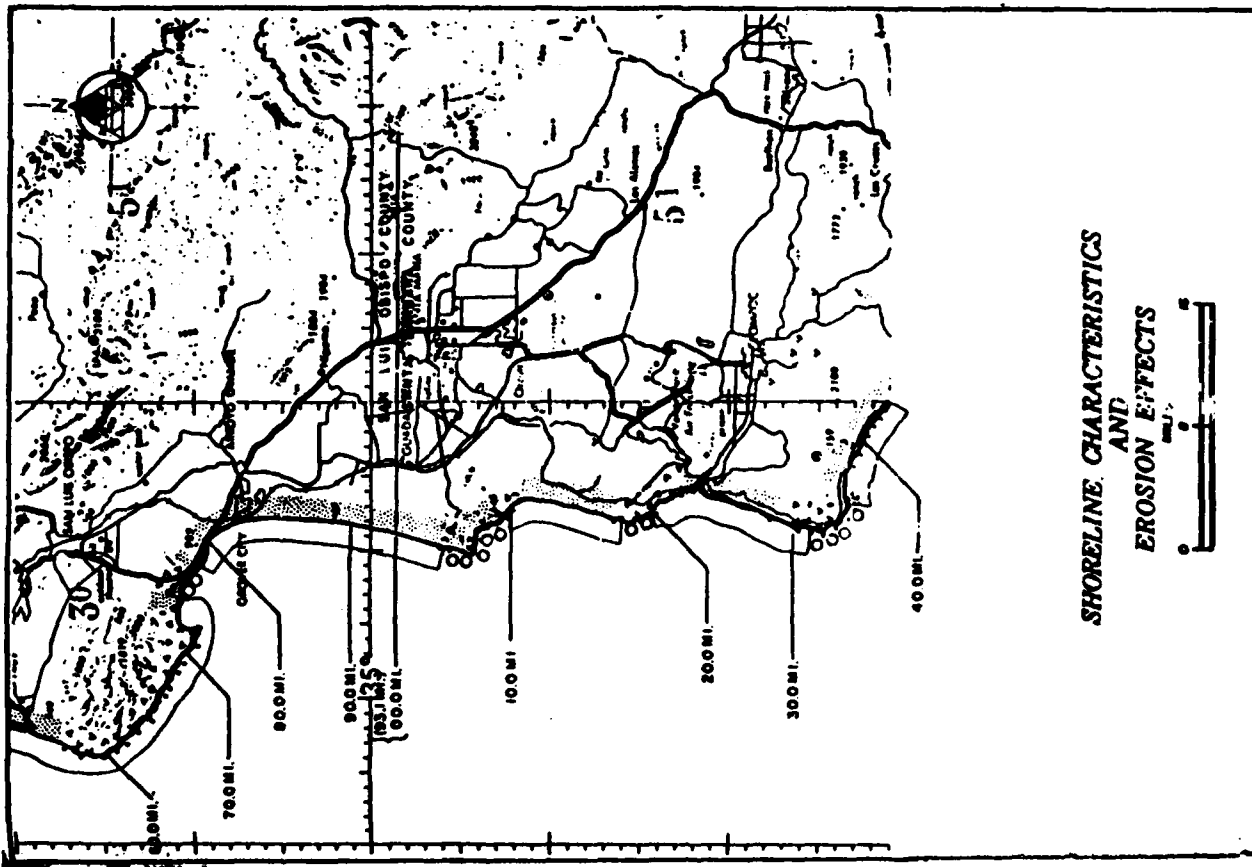


Figure 5.1-1. Shoreline characteristics and erosion effects (from USACE SPD, 1971).

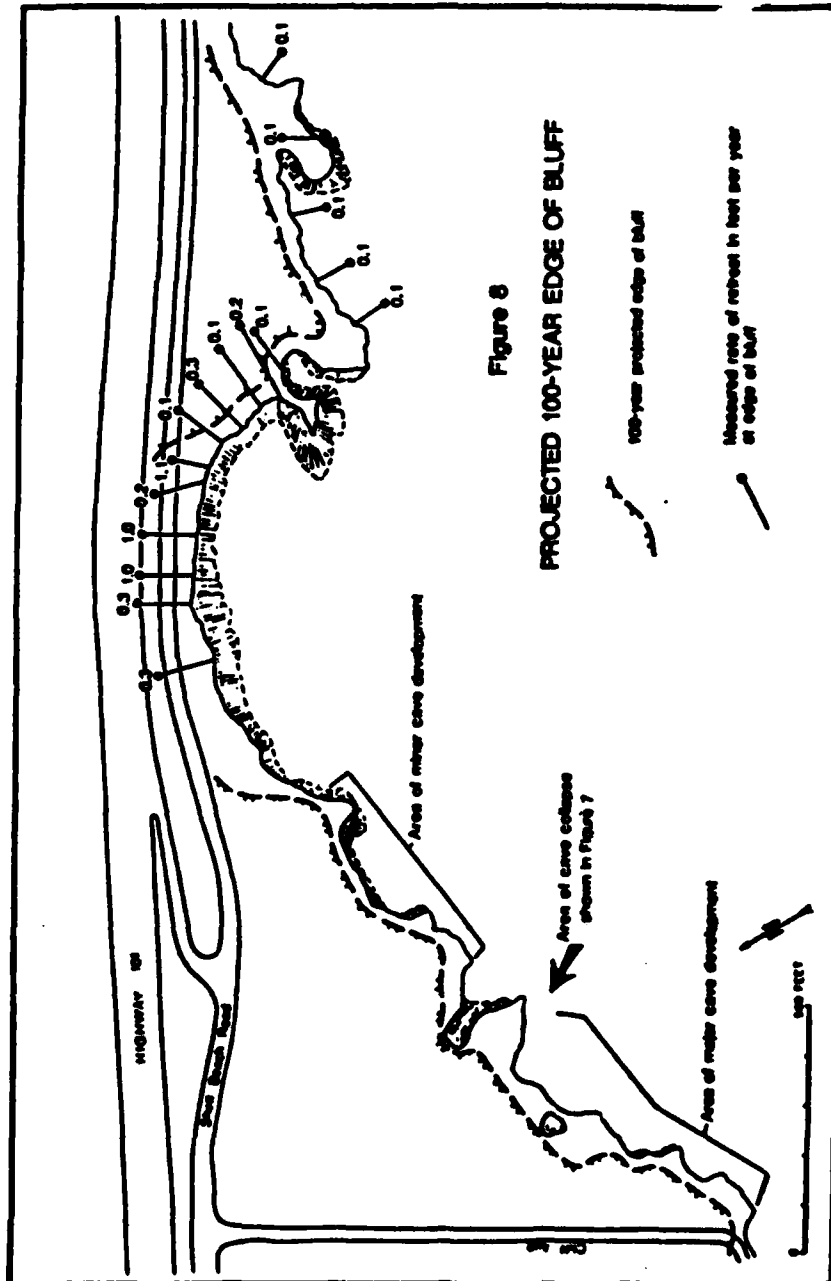


Figure 5.1-2. Project 100-year edge of cliff at Shell Beach, north of Pismo Beach (from Asquith, 1983).

Bowen and Inman (1966) give a geological description of the area in the vicinity of Point Arguello. The report includes 1966 aerial photographs of: Point Arguello, Pismo Beach sand dunes, Mussel Point, sand dunes north of San Antonio Creek, Purisima Point, the mouth of the Santa Ynez River, and the cliffs between Point Arguello and Point Conception. The report also includes beach profiles in the coastal segments: Pismo Beach to Point Sal; Point Sal to Point Arguello; Point Arguello to Point Conception; and Point Conception to Saint Augustin (in the Santa Barbara Cell). USACE LAD (1969a) contains a 1966 hydrographic survey of the Port of San Luis. USACE LAD (1969b) is a design memorandum for the general design of the Port of San Luis. This memorandum contains an offshore contour map and some descriptive information on the local shoreline. USACE LAD (1970) lists aerial photographs, historical ground photographs, hydrographic surveys, and beach profiles taken in San Luis Obispo County and Santa Barbara County, but does not include the photographs or survey/profile data. USACE SPD (1971) briefly discusses shoreline changes along this littoral cell (see Figure 5.1-1). Asquith (1983) uses aerial photographs to map cliff retreat, but the report does not contain the actual photographs (see Figure 5.1-2).

5.3 NEARSHORE WAVES

The offshore (deep water) wave statistics in the parts of this cell north of Point Arguello should not differ significantly from the Big Sur cell (Section 4.3). See that section for reference to appropriate tables.

NMC (1959a) developed hindcast statistics for breakwater design at Port San Luis (Figure 4.3-3). Because of sheltering by Point Buchon and Point Arguello they only consider storm waves with approach directions between 175° - 245° (Figure 4.3-3). The exclusion of sources from directions greater than 245° substantially reduces the frequency of occurrence of severe storm waves. NMC (1959a) hindcasts 22 storms with wave heights greater than 10 feet in the period 1899-1958, compared with 32 storms greater than 14 feet in the sector 190° - 310° for Morro Bay (see Section 4.3). It is clear from Figure 4.3-3 that a great deal of spatial variation of wave height may be associated with sheltering by points and headlands in this cell. For example, COE (1958) contains three years of visual observations of wave height, period and direction at the Point Arguello lighthouse. The relatively small wave heights (rarely more than 6 ft) and the almost total absence of directions north of west suggests that the observations are from an area locally sheltered from the dominant NW waves.

In addition to developing design wave statistics for Port San Luis, NMC (1959a) gives 19 refraction diagrams (for a variety of wave parameters) for a 20-mile reach centered on the port. USACE LAD (1969b, 1976) uses the same NMC (1959a, 1960b) wave hindcasts discussed above for design wave calculations at Port San Luis.

Marine Advisers (1964) develops a deep water wave climatology for this cell using a variety of sources: UCSD (1947), NMC (1960b), and 4 years of visual observations from scientific vessels for northern swell; Huntington Beach wave records (5/48 - 1/52), El Segundo wave records (7/48 - 1/52), and southern hemisphere weather maps (7/48 - 12/50) for southern swell (see Section 3.2.2). These are apparently the only hindcast statistics which include southern

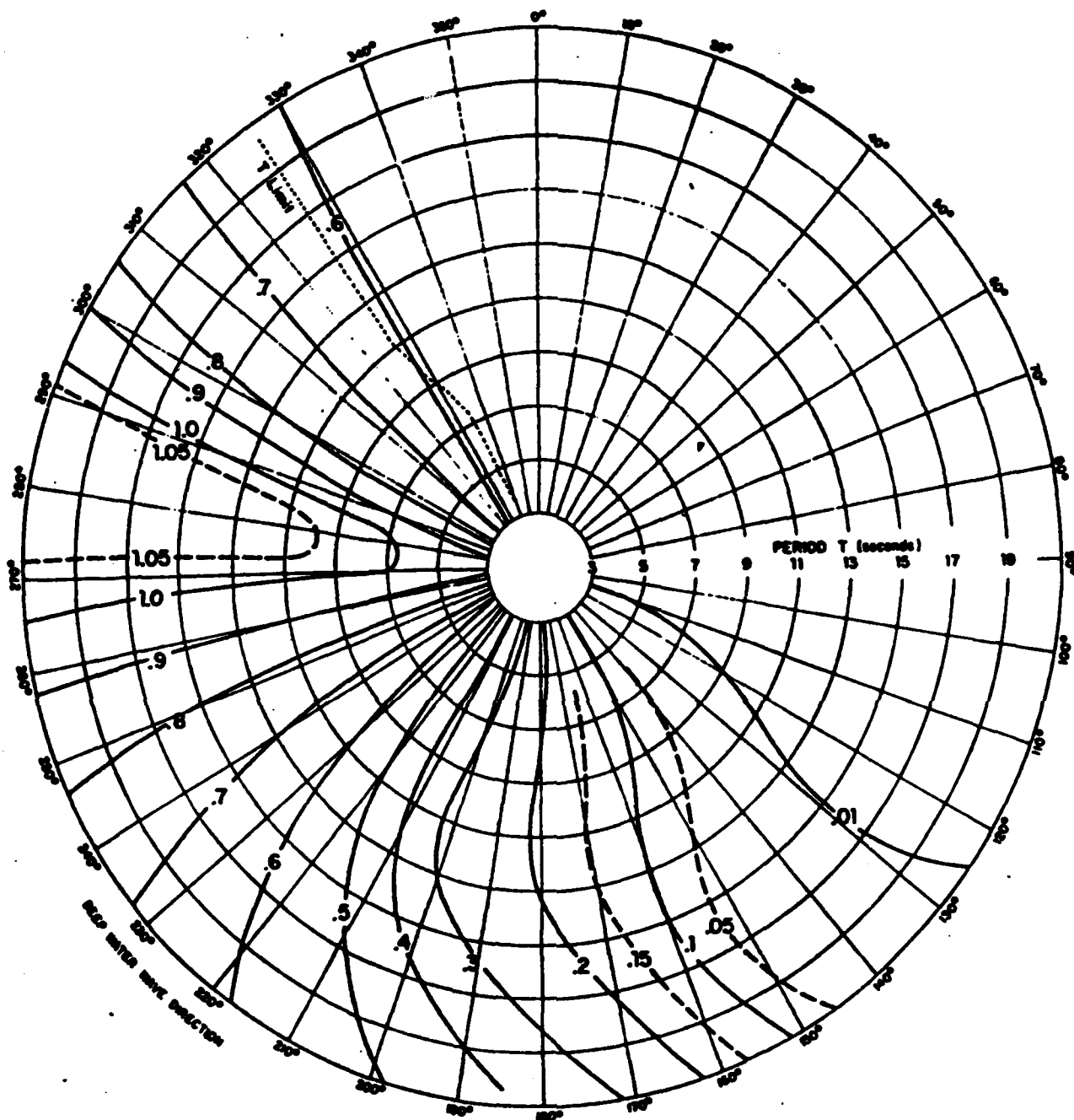


Figure 5.3-1

Contours of refraction coefficients, for varying wave period and deep water direction, at Surf, California (Marine Advisers, 1964).

swell. The frequency of occurrence of deep water significant height, period and direction are tabulated by season, but unfortunately no simple summary statistics are given. Marine Advisers (1964) also presented refraction summaries for the breaker region at three locations in this cell (Santa Maria River just north of Point Sal, and San Antonio Creek and Surf, California, located between Point Sal and Point Arguello (Figure 4.3-3). The refraction summary for Surf (Figure 5.3-1) shows the open wave window to span approximately 160° - 330° , wider than either Morro Bay or Port San Luis (Figure 4.3-3). The refraction diagrams and offshore wave statistics were combined to yield seasonal estimates of the longshore component of wave power at each of three coastal locations in this cell. This data was used by Bowen and Inman (1966) to estimate the longshore transport of sand.

5.4 NEARSHORE CURRENTS

The surf zone and shelf currents north of Point Arguello are probably qualitatively similar to those in the Big Sur cell (Section 4.4). The shelf circulation in the vicinity of Point Conception is briefly discussed in Section 6.4 (see Figures 3.1.2-1,2 and 6.4-1,2,3).

5.5 SEDIMENT SOURCES

5.5.1 *Cliff Erosion and Relict Dunes*

Zeller (1962) describes the sand dunes from Pismo Beach to Point Sal, and the dunes at Purisma Point and Point Penderales North. This report is a general reconnaissance, descriptive in nature, and does not directly discuss the dunes as a sediment source or sink. Bowen and Inman (1966) discuss cliff erosion in the Santa Maria cell. They estimate that cliff erosion of the Orcutt sandstones from north of Mussel Point to south of Point Sal yields about 40,000 yd³/yr.

5.5.2 *Sediment Discharge from Rivers and Streams*

Bowen and Inman (1966) performed a detailed study of the budget of littoral sands in the vicinity of Point Arguello. The report discusses and presents tables detailing the drainage areas and sand discharge from the Santa Ynez River and from streams between Pismo Beach and Santa Barbara (see Section 5.8). The report also contains grain-size analysis of samples taken in the study area. Judge (1970) studied the heavy minerals in beach and stream sediments. He lists the average discharge and drainage area of the Arroyo Grande, Santa Maria River, San Antonio Creek and the Santa Ynez River (see Table 5.5-1). Pollard (1979) contains grain-size distributions for 10 beach sand samples taken throughout this littoral cell.

5.5.2 *Artificial Beach Nourishment*

No data on artificial beach nourishment for this littoral cell was contained in the reports reviewed for this study.

5.6 SEDIMENT TRANSPORT MODES

5.6.1 *Cross-shore Transport*

Table 5.5-1

River Discharge and Drainage Area

<i>Stream</i>	<i>Average Discharge</i> (acre-foot per year)	<i>Drainage Area</i> (square miles)
Arroyo Grande	15,570	106
Santa Maria River	26,790	1763
San Antonio Creek	4,720	134
Santa Ynez River	37,070	900

Data from topographic maps and U.S. Geological Survey Water Supply Paper 1735 (from Judge, 1970)..

Discharges are averages of available years at every station, but more than five years as a minimum. Areas are by planimetric determinations to the nearest 10 square miles.

Bowen and Inman (1966) computed a complete budget of sand for the Santa Maria Cell. They divided the region into five sub-cells, four of which are in the Santa Maria Cell (Figure 5.6-1). They had access to bathymetric surveys which detailed the long-term changes (1933-1964) both offshore and on the beach. However, most of this change was probably due to seasonal cycles. They used two sets of profiles detailing seasonal changes in 1964 to subtract out the seasonal changes from the long-term measurements. The only region where the remaining changes exceeded the errors in measurement was sub-cell I (Figure 5.6-1). From these data they estimated mean net annual onshore transport as $100 \times 10^3 \text{ yd}^3/\text{yr}$ in sub-cell I and negligible in sub-cells II and III. Data were not available north of sub-cell I or south of sub-cell III. However, these areas are primarily rocky rather than sandy. Net onshore or offshore transport in such areas must be small.

Quantitative data on seasonal cross-shore transport are not listed in any other reports reviewed for this report.

5.6.2 Longshore Transport

Net longshore transport rates for this cell are summarized in Table 5.6-1. "Estimated" rates are obtained from application of the standard "stress-flux" (equation 2.4-2) with wave data as inputs. Both volume transport Q_l (yd^3/yr) and immersed-weight transport I_l (newtons/second) are listed. In converting between the two measures, it was assumed that solids concentration $N_o = 0.6$ (porosity = 0.4) and sand density $\rho_s = 2.65 \text{ g/cm}^3$, using equation (2.4-3a). Positive values represent transport to the south, negative to the north.

Trask (1955) performed mineralogy studies on sand from Surf (middle of sub-cell III, Figure 5.6-1) to Pt. Conception. He did not quantify longshore transport but made several qualitative observations: surfzone transport was interrupted at promontories, the transport in the "active zone" (< 30 ft deep) was significantly affected by promontories, the 30-60 ft zone

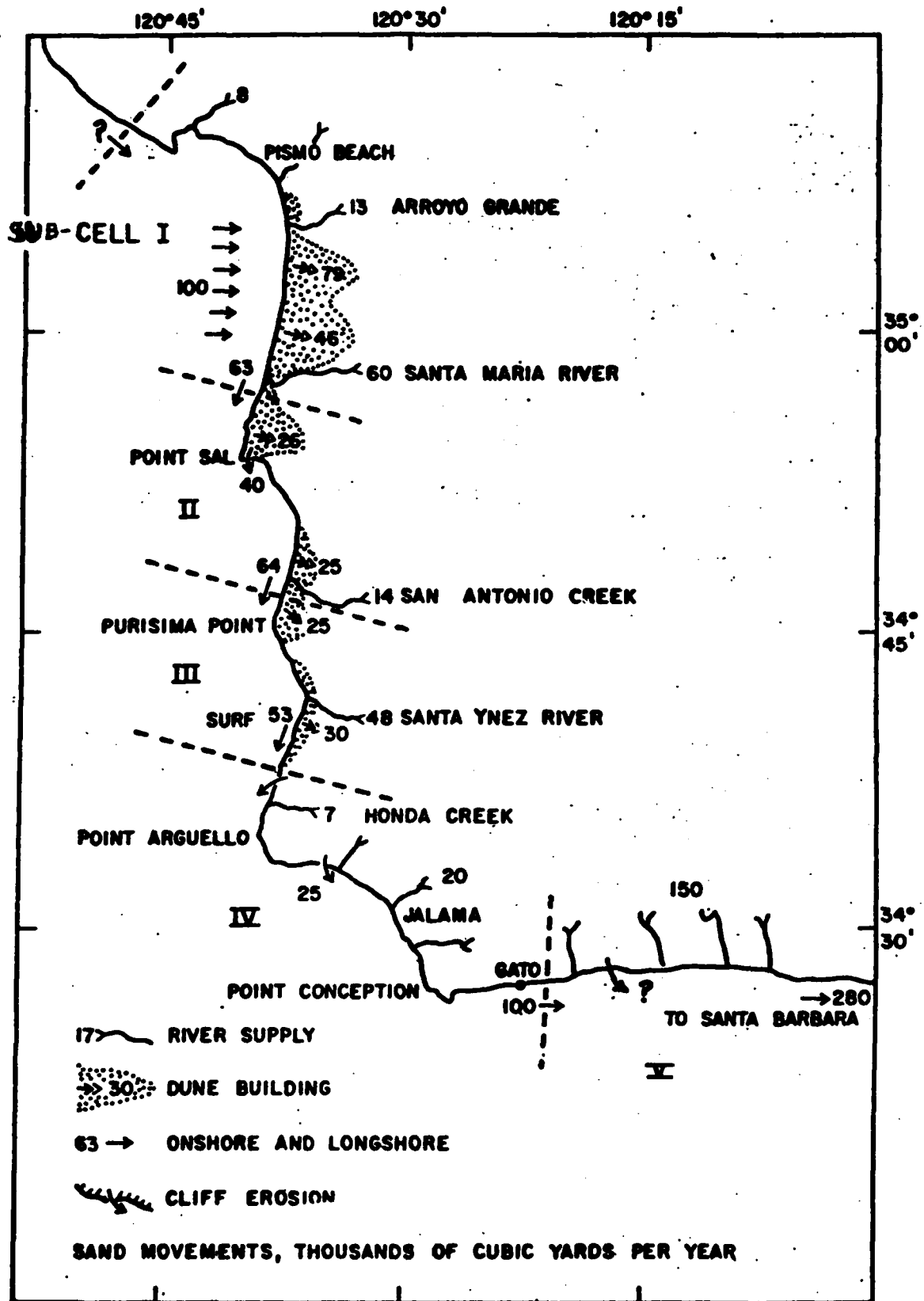


Figure 5.6-1. Schematic diagram of the budget of littoral sands (from Bowen and Inman, 1966).

Table 5.6-1 . Longshore Transport Rates
(Positive values indicate transport to the south, negative to the north)

Location	Notes	Reference	Potential Transport (Wave Refraction Studies)		Gross Transport (Trapping Studies)		Instantaneous Net Transport (Sand Tracer Studies)	
			Q_1 ($10^3 \text{ yd}^3/\text{yr}$)	I_1 (N/sec)	Q_1 ($10^3 \text{ yd}^3/\text{yr}$)	I_1 (N/sec)	Q_1 ($10^3 \text{ yd}^3/\text{yr}$)	I_1 (N/sec)
*Santa Maria River		Bowen and Inman (1966)	62	15				
*Point Sal		Bowen and Inman (1966)	40	9				
*San Antonio Creek		Bowen and Inman (1966)	64	15				
*Surf		Bowen and Inman (1966)	53	12				
Surf	Sand mineralogy study	Bowen and Inman (1966)					65	15
Surf	Faulty lab model	Garcia and Perry (1976)	214	50				

* "Best" estimate at that location.

was unaffected by promontories, and there was no transport deeper than 60 ft.

Bowen and Inman (1966) used two methods to estimate longshore transport in this cell. They were able to use the distribution of augite in sand samples from Trask's (1955) study along with reliable estimates of transport at the total sand trap at Santa Barbara to compute a net transport rate of $65 \times 10^3 \text{ yd}^3/\text{yr}$ to the south at Surf.

Bowen and Inman (1966) also applied the stress-flux transport equation using wave data and bathymetric surveys from Marine Advisors (1964). Their results for gross transport during winter, transition, and summer months, total gross transport, and net transport are listed in Table 5.6-2. There is a general trend of slightly northward net transport in the winter and strong southerly net transport in the transition and summer months.

Duane and Judge (1969) performed a radioisotope sand-tracer experiment at Pt. Conception in order to determine transport rates around that point. They found that there was no transport around that point, either because there really is no transport there or because their experimental methods were faulty. They list several problems encountered with their methods. Not least of which is the difficulty of performing accurate field experiments in this environment of high-energy waves. Judge (1970) examined the sand mineralogy along the coast, with special attention near Pt. Conception. He concluded there was strong downcoast transport well to the east and west of Pt. Conception and that longshore transport was only partially blocked at Pt. Conception.

Garcia and Perry (1976) modelled longshore transport in the Surf area (sub-cell III) with an empirical model based on laboratory data. Their study's limitations and faulty assumptions render their results suspect. Limitations include: application of laboratory data to the field, spherical sand grains assumed, no suspended load, and bedload only two grain diameters thick. They obtained a southerly net transport of $214 \times 10^3 \text{ yd}^3/\text{yr}$.

5.6.3 Wind Transport

Table 5.6-2. Estimate of the longshore transport of sand based on the longshore component of wave energy (thousands of cubic yards)

	<u>Winter (DJFM)</u>	<u>Transition (AMON)</u>	<u>Summer (JJAS)</u>	<u>Annual Total</u>	<u>Annual Net</u>
Santa Maria River					
Toward upcoast	95	51	68	214	-
" downcoast	83	95	98	276	62
San Antonio Creek					
Toward upcoast	119	64	80	263	-
" downcoast	97	109	121	327	64
Surf					
Toward upcoast	109	59	86	254	-
" downcoast	92	103	112	307	53
Gato					
Toward upcoast	17	2	0.4	19.4	-
" downcoast	41	26	52	119	100

Because of the extensive dune fields in this cell, wind transport is probably more important here than anywhere else in southern California. The best documentation on wind transport is available for this cell. Bowen and Inman (1966) used measures of dune advance rates and aerial photographs of dune extent to estimate wind transport in the five large dune fields of this cell. The length of dune fields, transport rates, and volume transports are listed in Table 5.6-3. The transport losses for each sub-cell are illustrated in Figure 5.6-1.

Bowen and Inman (1966) used wind-velocity records in a relation of the form of Equation 2.6-6 to estimate that the offshore transport rate (dunes to beach) is about 5% of the onshore rate.

Effects of wind transport in areas of the cell outside the five dune fields in Figure 5.6-1 must be relatively small. The only other dune field is a small one near Pt. Conception (Bowen and Inman, 1966).

5.7 SEDIMENT SINKS

5.7.1 *Submarine Canyons*

There are no submarine canyons with heads in the nearshore in this cell. Arguello and other submarine canyons appear to be too far offshore to influence the budget of sediment. However, this matter requires additional study.

5.7.2 *Entrapment by Harbors, Bays and Estuaries*

Except for Port San Luis, there are no harbors in this cell. Bays are each immediately downcoast of a headland dividing the sub-cells (Figure 5.6-1) and will be discussed in Section 5.7.3 as headland effects. Small estuaries are present at the mouths of the rivers. However, the only time when they could act as significant longshore-transport sinks would be just after a flood has washed the estuary sediment onto the beach, clearing the river mouth of sand.

Table 5.6-3. Estimate of the sand transport by wind from the beaches to the dunes.

<u>Section of Coastline</u>	<u>Length Feet</u>	<u>Average Transport Rate* Ft³/Ft/Day</u>	<u>Total Annual Transport Rate Yd³/Yr</u>
Pismo Beach Pier to	39,000	0.15	79,000
Oso Flaco Creek to	22,500	.15	46,000
Santa Maria River to	13,900	.15	26,000
Mussel Point Schuman Canyon to	37,000	.10**	50,000
Purisima Point Canada Tortuga Creek to	22,000	.10**	<u>30,000</u>
Bear Valley		Total	231,000

*Based on an angle of repose of 30°

**Assume 1/3 of area occupied by vegetation-covered ridges.

5.7.3 *Littoral Barriers*

In the geologic sense, the headlands that form Points Sal, Purisma and Arguello are major littoral barriers. These points are east-west trending structures associated with the faults in the transverse range system that form the major headland of Point Arguello/Conception (refer to Section 1.1 Plate Tectonics/Seismicity). Streams such as the Santa Maria and Santa Ynez Rivers and San Antonio Creek supply sediments that have built the coast seaward to its present position. The three beaches between the points are aligned normal to the prevailing waves. The rocky headlands at the southern end of each sub-cell act as a pivot point with beaches forming to the north perpendicular to the prevailing angle of wave attack.

The coast from Pt. Buchon to Pt. San Luis is rocky with only small pocket beaches, thus there is little sand motion to be blocked. At mile 64 south of the Monterey County Line is a small breakwater for the Diablo Canyon nuclear power plant intake structure (California, 1977a). This breakwater appears to have little effect on sand transport on this rocky coastline.

At Pt. San Luis there is a half-mile long breakwater. Since potential transport is to the south here, and there are only small pocket beaches to the north, the breakwater's effect on transport must be small. There are four piers along the next few miles of coastline: at 72.5, 73.8, 74.2, and 80.9 miles south of the Monterey County line (California, 1977a). These piers have little effect on transport.

Trask (1955) and Judge (1970) found some longshore transport at depth around rocky headlands, but were unable to quantify it. At the headlands there must be some trapping of sand. However, there is also longshore motion offshore and increased cliff erosion at these points, to partially balance the trapping effect. The studies which have specifically addressed the sources, transports and sinks at each of these headlands have been either inconclusive (Duane and Judge, 1969) or not quantitative (Trask, 1955; Judge, 1970).

A Coast Guard boat landing at Pt. Arguello is protected by a small rock-rubble breakwater (California, 1977a). It has little effect on transport, since it is even smaller than the nearby natural rocky points.

5.7.4 *Wind Transport*

The methods of Bowen and Inman (1966) for estimating the significant wind-transport rates in this cell were detailed in Section 5.6.3. The losses to each of the five dune fields are listed in Table 5.6-3 and illustrated in Figure 5.6-1.

5.7.5 *Berm Overwash and Offshore Loss*

Any berm overwash at the five dune field sites (Figure 5.6-1) must be eventually incorporated into the dune fields by wind transport. Thus such losses are actually included in the numbers of Table 5.6-3 as wind loss. Berm overwash at the pocket beaches in the rest of the cell must be small, since they are backed by cliffs.

From the comparisons of bathymetric surveys by Bowen and Inman (1966), it is concluded that permanent offshore loss is probably negligible. In fact, in sub-cell I (Figure 5.6-1) the opposite occurs - there appears to be a significant onshore net transport.

5.8 SEDIMENT BUDGET

Bowen and Inman (1966) performed the first case study concerning the sediment budget for the Santa Maria Cell (see Table 5.8-1). Pollard (1979) used the methods and results of Bowen and Inman to re-summarize the sediment budget. There were no other reports reviewed for this study that directly address this subject. Figure 5.6-1 illustrates the budget of littoral sands and shows the quantities and sources of sediment. Judge (1970) provides estimates of the average discharge and drainage area of the major rivers and creeks in this cell. These estimates could then be used to calculate the sediment yield by the methods outlined in Section 2.5. The transport direction is primarily to the south at rates varying from $40-65 \times 10^3 \text{ yd}^3/\text{yr}$ (see Table

Table 5.8-1.
(from Bowen and Inman, 1966)

Budget of Littoral Sands In Thousands of Cubic Yards Per Year
(Refer to Figure 15)

Agency	CELL I			CELL II			CELL III			CELL IV			CELL V		
	Pismo Beach to Santa Maria River			Santa Maria River to San Antonio Creek			San Antonio Creek to Surf			Surf to Gato			Gato to Santa Barbara		
	In	Out	Net	In	Out	Net	In	Out	Net	In	Out	Net	In	Out	Net
River	8			14			48			7			150		
Transport	13						20								
	60		+81			+14			+48			+27			+150
Dune Building	79	46	-125	26	25	-1	25	30	-5	-	-	-	-	-	-
Cliff Erosion	-	-	-	40		+40	-	-	-	25		+25	some		
Longshore Transport	07	63	-63	63	64	-1	64	53	+11	53	100	-47	100	280	-180
Total	81	188	-107	117	115	+2	112	108	+4	105	100	+5	250+	280	-30

5.6-1). The primary sink for sands is the dune fields located between Pismo Beach to Point Arguello. These dune fields receive wind blown sands from the adjacent beaches at rates detailed in Table 5.6-3 and Bowen and Inman, (1966).

6. SANTA BARBARA CELL

The Santa Barbara Cell extends from Point Conception to Point Mugu, a distance of 96 miles (see Figure 1.2-1). This is the longest littoral cell in southern California and was first defined by Inman and Frautschy (1965). The cell includes a variety of coastal types and shoreline orientations. The beaches near Point Conception are east-west trending, narrow and backed by high sea cliffs. Beaches between Ventura and Port Hueneme are generally wide and trend southeast. The Hueneme and Mugu Submarine Canyons are active sediment sinks at the southern end of the littoral cell.

6.1 COASTAL EROSION PROBLEMS, NATURAL AND MAN-MADE

Johnson (1957) and Weigel (1959) describe how the breakwater constructed at Santa Barbara Harbor interrupts the littoral drift of sand. The man-made harbor fills with sand and the downcoast beaches are nearly completely stripped of sand, until sand is bypassed around the harbor. The net longshore transport rate at Santa Barbara was shown to be $280,000 \text{ yd}^3/\text{yr}$.

Inman (1950a;b) describes the erosion of downcoast beaches caused by construction of the breakwaters at Port Hueneme. The north breakwater directs sand into Hueneme Submarine Canyon, where it is lost from the littoral system. Herron and Harris (1966) also discusses the erosion downcoast from Port Hueneme. Surveys from 1940 to 1966 show a consistent annual rate of erosion of 1,200,000 cubic yards. USACE LAD (1970) describes the Channel Island Harbor sand trap, which is dredged every two years for downcoast beach nourishment.

USACE SPD (1971) presents an inventory of coastal shoreline characteristics related primarily to erosion produced by waves or other coastal phenomena. Figures 6.1-1 and 6.1-2 show the prevalence of critical and non-critical erosion along this littoral cell. Bruno (1977) examines the erosion problems due to man-made jetties and the construction of an offshore breakwater at Channel Island Harbor. The California Department of Boating and Waterways

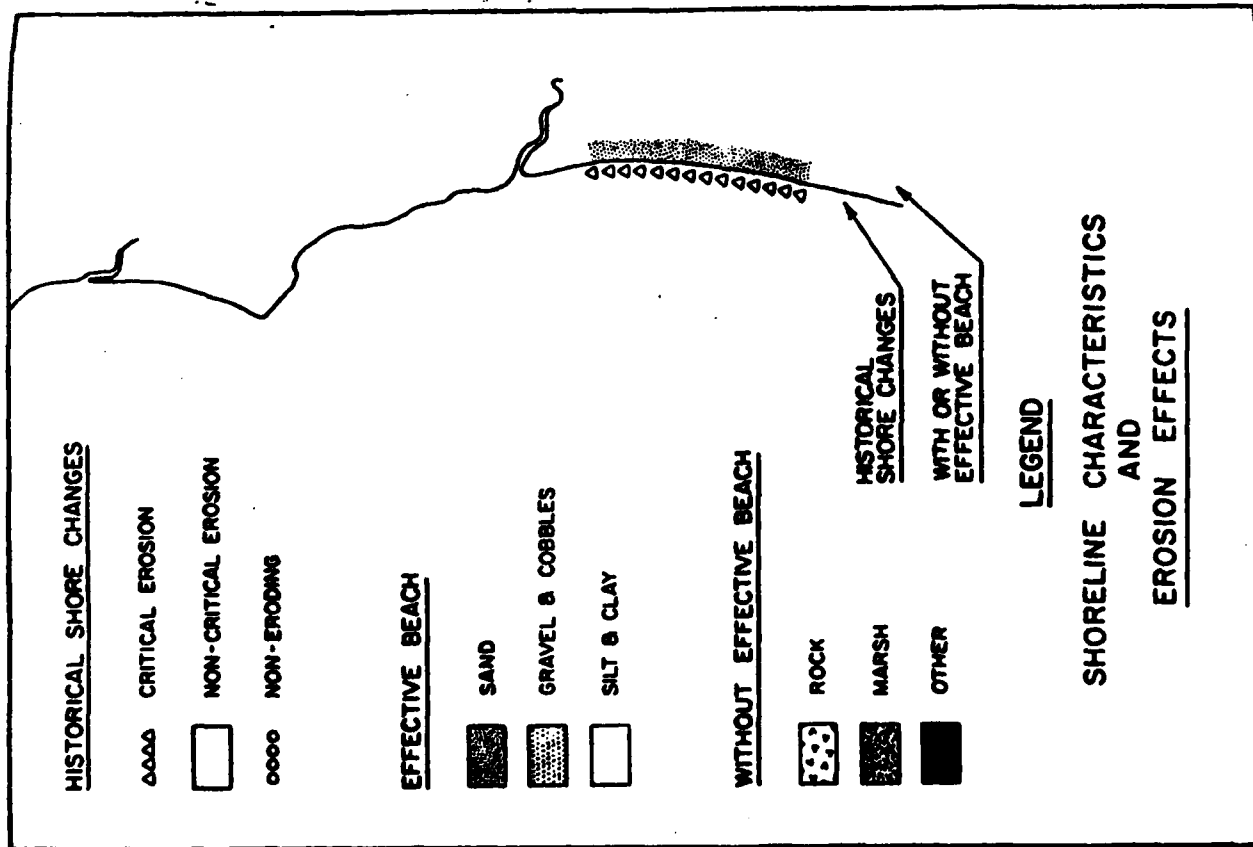


Figure 6.1-1. Shoreline characteristics and historical shore changes from Point Conception to Santa Barbara Harbor (from USACE SPD, 1971).

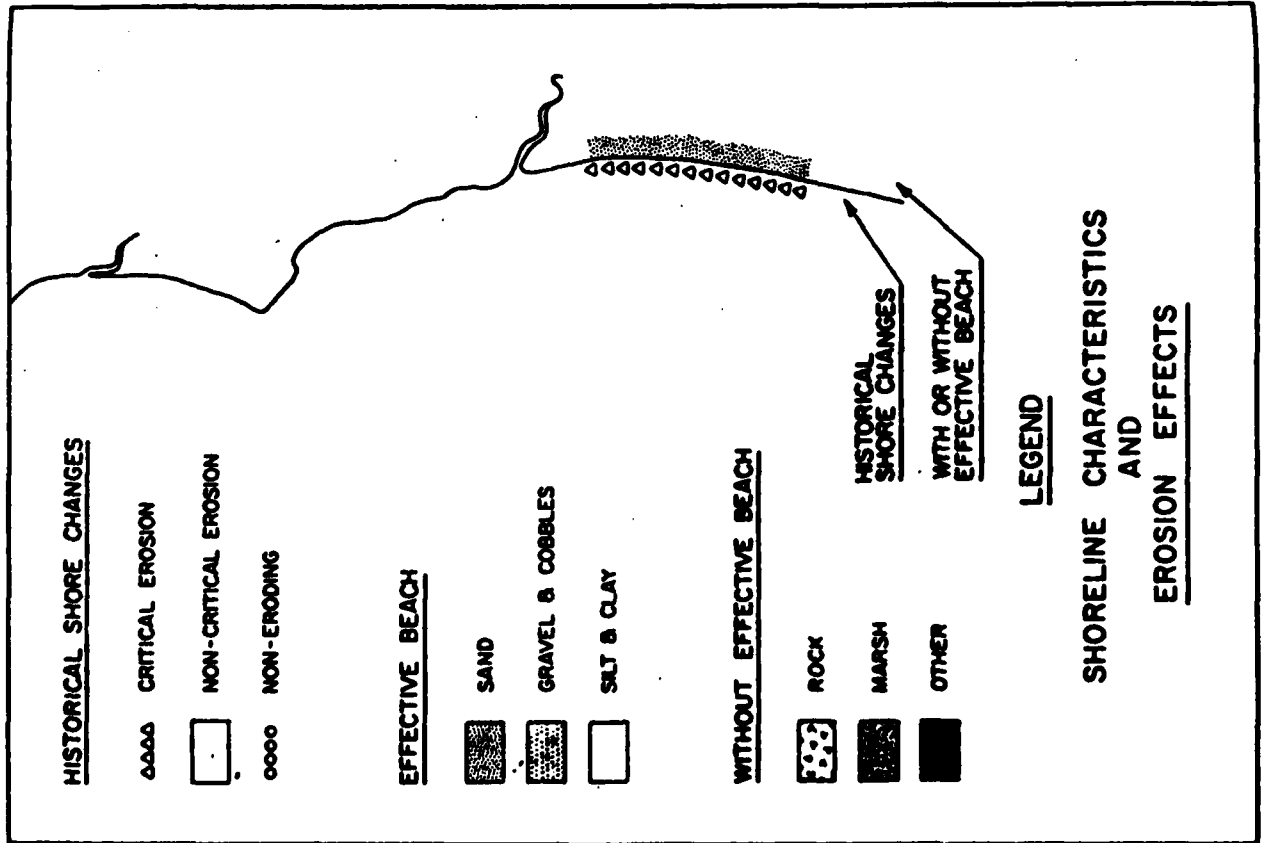


Figure 6.1-2 Shoreline characteristics and historical shore changes from Carpenteria to Point Dume (from

compiled an atlas and assessment of shoreline erosion along the California coast (California, 1977a). This report systematically proceeds through all the littoral cells describing shoreline features and conditions. Many of the beaches to the east of Santa Barbara have never fully recovered from the initial blockage of easterly sand movement by the construction of the Santa Barbara Harbor. Cramer and Pauly (1979) discuss shore processes at the man-made headland between Punta Gorda and Seacliff. The man-made headland was created by locating about 7,000 feet of Highway 101 on an offshore fill. They document the monitoring of the downcoast erosion at Seacliff.

USACE LAD (1979) discusses erosion problems in Ventura County from Mussel Shoals to County Line Beach. Rates of erosion are calculated (see Table 6.1-1) by comparing aerial photographs from the Fairchild collection (1929, 1943) and Corps of Engineers Los Angeles District file photographs (1974). Herron (1980) briefly addresses erosion problems in the Santa Barbara Littoral Cell. Inman (1981) reports that the average erosion for eleven beaches from Ventura to Point Mugu during the period from 1929-1974 was 0.6 feet per year. Orme and Brown (1983) give several explanations for the erosion problems in Ventura County. According to them the cause of the problem is not just the local rivers' inability to deliver sediment to the coast because of damming. They discuss five other important facts regulating the local sediment flux. These are:

1. The Santa Clara River contains a massive reservoir of sediment within its floodplain downstream from the dams, unprotected by levees and available for removal seaward during floods.
2. Despite dams and levees, the Ventura and Santa Clara rivers still yield on average a sand and gravel fraction (that part of the total yield most available for beach replenishment) of about $0.77 \times 10^6 \text{ m}^3/\text{yr}$. This approximates the volume of

Table 6.1-1

SUMMARY OF ANNUAL RATES OF EROSION

<u>Name</u>	<u>Rates/erosion</u> <u>(Ft/yr)</u>
Mussel Shoals	—
Faria Park	1.3
Faria Beach Colony	—
Solimar Beach	—
Emma Wood State Beach	0.6
31st Agricultural District Association	0.5
Surfer's Point	—
Ventura Marina Beach	—
McGrath State Beach	—
Mandalay Beach Park	1.5
Oxnard Shores	0.8
Hollywood Beach Park	—
Silver Strand Beach Park	—
Port Hueneme Beach	—
Ormond Beach	3.5
Pt. Mugu State Beach	—
Sycamore Beach	1.9
County Line Beach	0.9

Note: Erosion less than 0.5 ft/yr is considered insignificant and is not shown.

(from USACE LAD, 1979).

sediment estimated to move along the coast annually.

3. During major floods, much of the sediment available for beach replenishment is carried beyond the immediate shorezone and is thus denied, at least initially, to the beaches.

4. Whether or not this large offshore reservoir of sediment is made available to the beaches depends on the subtle coincidence of hydrodynamic forces and nearshore geometry.

5. Under appropriate combinations of high tides, high waves, and swift currents, coastal erosion forces will overwhelm the protection afforded by all but the most massive accumulations of beach sediments.

6.2 SHORELINE CHANGES

Table 6.2-1 is a summary of existing surveys, mapping studies, and photographs in the Santa Barbara Littoral Cell contained in the reports reviewed for this study. Inman (1950a) investigated beach processes in the vicinity of Mugu Lagoon. He discusses previous investigations, historical surveys, and beach profile changes in the lagoon area. Inman also includes several aerial photographs of the area. Inman (1950b) presents additional data on the Mugu Submarine Canyon. Johnson (1953; 1957) and Wiegel (1959) report on historical shoreline changes in the areas adjacent to the Santa Barbara Harbor. These papers contains historical data such as comparative beach profiles and short and long term depositional patterns in the harbor. USACE LAD (1960b) contains several beach profiles taken as early as 1937 along the coast from Santa Barbara to Port Hueneme.

USACE LAD (1961a) is concerned with the Ventura area. It summarizes historical shoreline changes and includes tables of volume changes and comparative beach and offshore

Table 6.2-1

EXISTING SURVEYS, MAPPING STUDIES, PHOTOGRAPHS

Author(s) Date	Type of Data	Location and Dates
Inman, 1950a	List of hydrographic charts/maps	Mugu Lagoon, 1856-1947
	Aerial photographs	Mugu Lagoon, 1947-1949
Wiegel, 1959	Beach profiles	Santa Barbara, 1930-1932
	Hydrographic survey	Santa Barbara, 1937
	Gain or loss of beach material	Santa Barbara 1942-1946
	Depositional patterns (comparison)	Santa Barbara, 1935-1952
USACE LAD, 1960b	Beach Profiles	Santa Barbara to Carpinteria, 1937, 1959
		Ventura, 1938, 1948, 1959
		Port Hueneme, 1938, 1948, 1953, 1959
USACE LAD, 1961a	Table of volume changes	Ventura area, 1938-1948, 1948-1959, 1938-1959
	Shoreline and offshore changes	Ventura area, 1855-1961
	Comparative profiles	Ventura area, 1938, 1948, 1959

Table 6.2-1 (cont'd)
EXISTING SURVEYS, MAPPING STUDIES, PHOTOGRAPHS

Author(s) Date	Type of Data	Location and Dates
USACE LAD 1962b	Beach profiles	El Capitan Beach, 1933-1960 Goleta Beach, 1933-1960 Refugio Beach, 1960
	Condition surveys	Ventura County Harbor, 1959, 1960, 1961
	Shoreline and offshore changes	Ventura County Harbor, 1959-1962
	Hydrographic survey	Santa Barbara Point to Carpinteria, 1960
Herron and Harris, 1966	Delta profiles	Ventura River, 1959, 1962
	Aerial photographs	Santa Clara River, 1938-1962 Port Hueneme, 1960
	Hydrographic surveys	Port Hueneme Sand Trap, 1963, 1965
	Comparative profiles	Channel Islands Harbor, 1938, 1960, 1966
USACE LAD, 1967	Hydrographic surveys	Rincon Point to Ventura, 1965

Table 6.2-1 (cont'd)
EXISTING SURVEYS, MAPPING STUDIES, PHOTOGRAPHS

Author(s) Date	Type of Data	Location and Dates
USACE LAD, 1967	Beach profiles/Shoreline offshore changes	Rincon Point to Ventura, 1969, 1933, 1965
	Hydrographic surveys	Ventura Pier point to Port Hueneme, 1962-1963
	Hydrographic survey	Santa Barbara Harbor, 1965
	Beach condition survey	Ventura to Port Hueneme, 1965, 1966
USACE LAD, 1969a	Aerial photographs	Santa Clara River Delta 1967, 1969
	Hydrographic survey	Gaviota, Refugio, El Capitan, 1968
	List of hydrographic surveys	Throughout the littoral cell
	Hydrographic surveys	Pt. Mugu to Channel Island Harbor, 1969, 1970
Bruno et al., 1977	Shoreline and offshore changes	Ventura County, 1967, 1968, 1969, 1970
	Hydrographic survey	Channel Island Harbor Sand Trap, 1943
	Bathymetric profiles	Channel Island Harbor Sand Trap, 1974, 1975

Table 6.2-1 (cont'd)
EXISTING SURVEYS, MAPPING STUDIES, PHOTOGRAPHS

Author(s)	Date	Type of Data	Location and Dates
Rod Lundin and Associates, 1978		Aerial photograph	Ventura Harbor, 1977
Cramer and Pauly, 1979		Aerial photographs	Seacliff, 1978 Hobson Park, 1976
Pollard, 1979		Deposition patterns/grain size	Santa Barbara Harbor (no date)
		Aerial and satellite photographs	Pt. Conception Area (various dates)
USACE LAD, 1979		Beach profiles	Ventura Pier/Port Hueneme Piers, 1977, 1978
		Ground and aerial photographs (comparative)	Rincon Point to Sequit Point, 1929, 1945, 1975
		Comparative contours	Emma Wood State Beach, 1965, 1978 Surfers Point, 1966, 1977 Ventura River Delta, 1975, 1976

Table 6.2-1 (cont'd.)
EXISTING SURVEYS, MAPPING STUDIES, PHOTOGRAPHS

Author(s) Date	Type of Data	Location and Dates
USACE LAD, 1980a	Beach profiles	Ventura Pier/Port Hueneme Piers, 1977, 1978
	Ground and aerial photographs (comparative)	Rincon Point to Sequit Point, 1929, 1945, 1975
	Comparative contours	Emma Wood State Beach, 1965, 1978
Gable, 1981		Surfers Point, 1966, 1977
		Ventura River Delta, 1975, 1976
	Ground and aerial photographs	Santa Barbara Harbor, 1928, 1929, 1930, 1932, 1933
Baillard and Jenkins, 1982	Beach Profiles	Carpinteria, 1981, 1982
	Aerial photographs	Santa Barbara Harbor, 1982

profiles. USACE LAD (1962b) contains several types of shoreline change data as shown in Table 6.2-1. The report includes a short discussion of historical shoreline changes. Herron and Harris (1966) plot comparative profiles, from 1938 through 1966, and hydrographic surveys at Channel Island Harbor and Port Hueneme. USACE LAD (1967) summarizes the existing shoreline conditions and includes hydrographic surveys and beach profiles throughout the littoral cell. USACE LAD (1969a) contains most of the same data as USACE LAD (1967) but includes some additional beach profile data taken in 1966.

USACE LAD (1970) is similar to the two previous Corps of Engineers reports. It summarizes the current shoreline conditions and includes additional hydrographic surveys and profile data taken along the Ventura County coastline. USACE SPD (1971) inventories the coastal shoreline characteristics related primarily to erosion produced by waves or other coastal phenomena. The report systematically proceeds downcoast discussing shoreline changes (see Figure 6.1-2). Bruno et al (1977) performed a 1.5 year study of the sedimentation patterns behind the Channel Island Harbor Sand Trap. They include hydrographic surveys/bathymetric profiles taken in that area from 1974 to 1975. Cramer and Pauly (1979) discuss the shoreline changes as a result of the construction of the Seacliff Interchange on offshore fill. Pollard (1979) addresses the source and distribution of sediments in Santa Barbara County. He includes several aerial and satellite photographs.

USACE LAD (1979) discusses shoreline conditions and changes in Ventura County. It includes monthly beach profiles at Ventura Pier and Port Hueneme. This report also includes some carefully scaled comparative aerial photographs which clearly illustrate shoreline changes. USACE LAD (1980a) is similar to the previous Corps of Engineers reports with some additional discussion of shoreline changes and erosion problems. Gable (1981) is a summary of the data taken during the 1980 National Sediment Transport Study Experiment at Leadbetter Beach. Profile data taken during the experiment is available on magnetic tape. Inman (1981) uses

comparative surveys to show that the 1959-61 shoreline is 650 feet seaward to the 1855 shoreline in the vicinity of Mandalay Beach. Brown (1983) contains beach profile data at eight locations on four Ventura beaches. The data is not presented in the standard profile manner but rather in a statistical manner. This makes the data rather difficult to compare with other data. Orme and Brown (1983) contains the same data as Brown (1983).

6.3 NEARSHORE WAVES

SHELF SITES

The topographic setting of this cell has a profound effect on the swell and wave climate. For example, there is only one narrow aperture, the west (240° - 275°) window in Figure 6.3-1, through which significant amounts of Pacific swell can reach Santa Barbara. Waves from the south to southeast also occur but are decidedly less frequent. These are the only directions that are exposed to a significant fetch. The distance between Santa Barbara and the Channel Islands is too short (50 km) for generation of all but the shortest wind waves. As discussed below, the angles of the open sectors depend strongly on the station position, both east-west and north-south.

There are no long-term direct measurements of deep water waves in the Santa Barbara Channel. NMC (1960a) gives hindcast data for 34.2° N, 120.0° W (NMC Station 6 in Figure 6.3-1). The annual average swell is highly directional with most of the energy from the west (Figure 6.3-2). Seas also are largely from this quadrant. However, sometimes very significant energy does come from the southeast. These southeast seas can be associated either with storms within the Southern California Bight or strong Santa Ana winds. Southeast seas tend to occur almost exclusively in the winter and spring months, so their importance is reduced in annual roses. Southeast seas contribute about 30% of the noncalm sea conditions in February (Table 6.2 in NMC, 1960). Hales (1978a,b) suggests that there are patterns of Santa Ana wind intensification in the Santa Barbara Channel which produce somewhat higher southeast seas than hindcast, particularly in the vicinity of Point Conception. Average annual period-height distributions, for essentially the same location as NMC (1960a) are given for a different hindcast (Strange and Graham, 1983) in Table 6.3-1. Hindcasts for several sites within the Channel Islands, and one site on the shelf (East Channel Shelf, Figure 6.3-3) are given by Hales (1978a,b). The East Channel site hindcast is a very slightly modified version of NMC Station 6

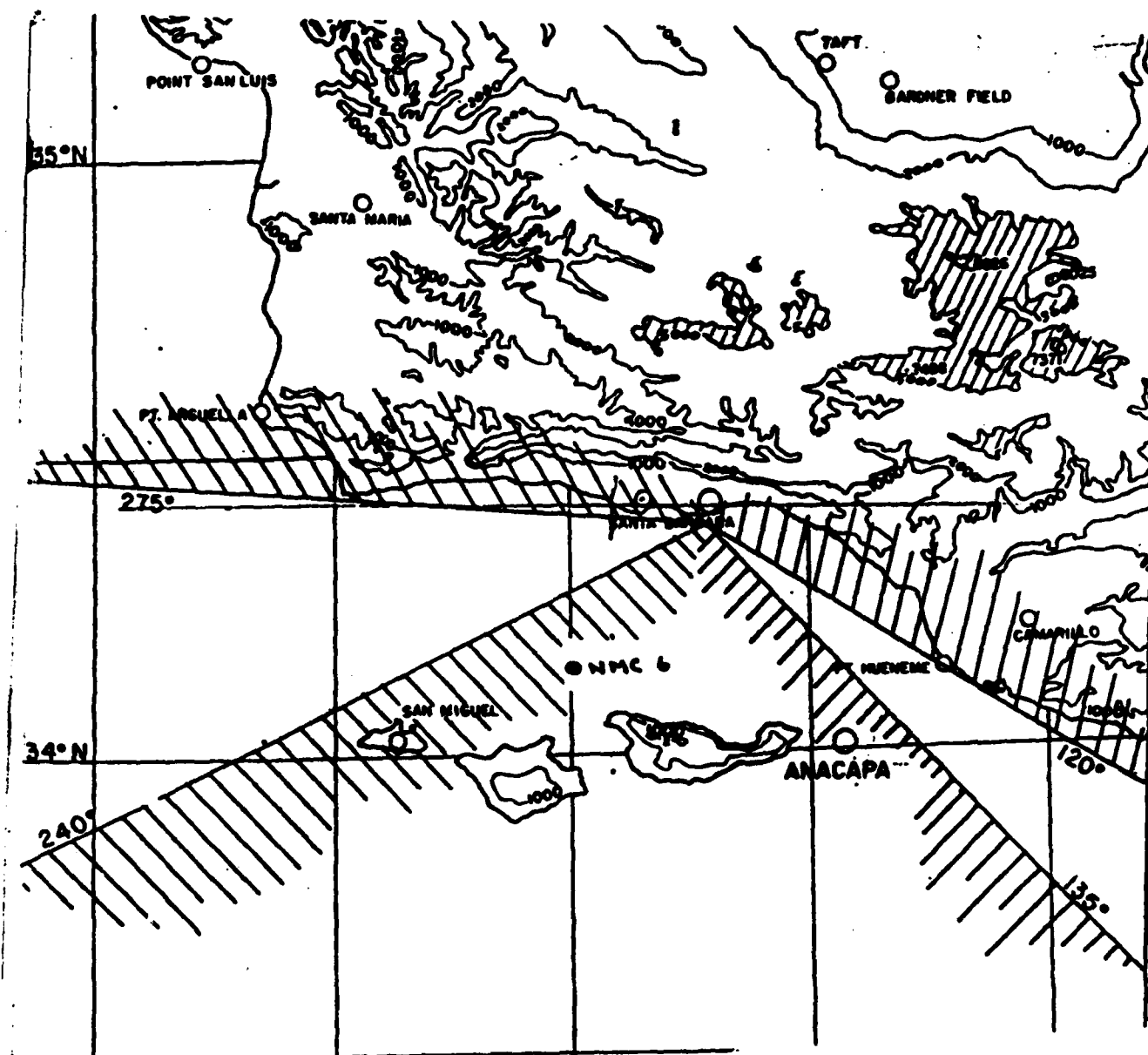
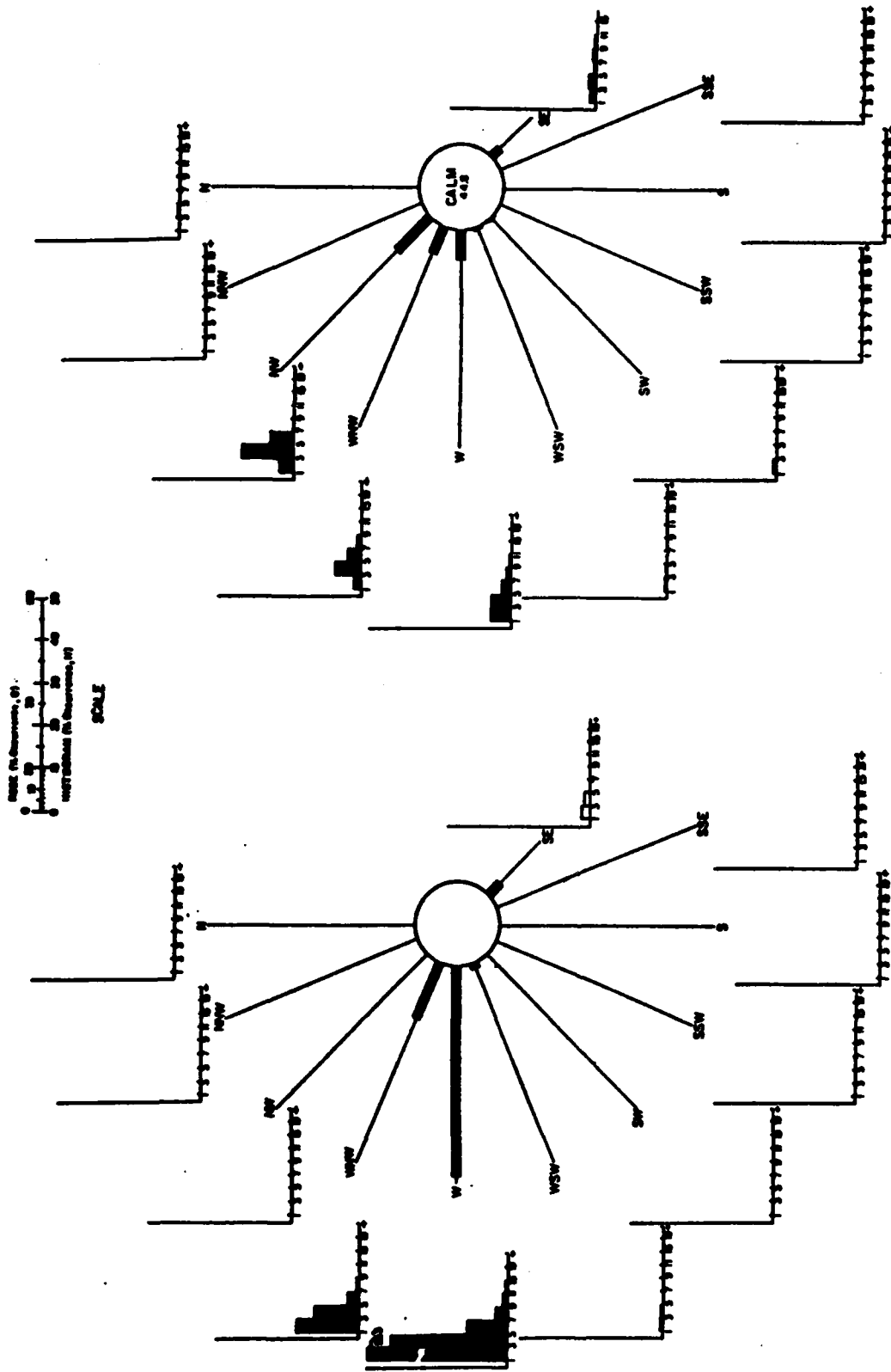


Figure 6.3-1

Schematic of directional sectors in which waves with significant energy can reach Santa Barbara (NMC, 1960).



AVERAGE ANNUAL SWELL ROSE FOR STATION 6

AVERAGE ANNUAL SEA ROSE FOR STATION 6

Figure 6.3-2 Hindcast (1956-1958) annual average swell and sea roses in the Santa Barbara Channel (NMC, 1960).

Table 6.3-1 Hindcast 1970-1978 wave statistics in the Santa Barbara Channel (Strange and Graham, 1983).

Santa Barbara Channel Wave Statistics (31° 21' 27" N, 120° 7' 14" W)

Average Annual Period (T _p)		Direction: All																		
5	6	7	8	9	10	11	12	13	14	15	16	17	18	19	20	Total				
Height (H _s) FT.																				
1	1.714	5.044	7.015	11.019	10.725	17.003	13.463	11.012	6.773	5.264	4.061	2.369	1.010	0.417	0.152	0.167	100.00			
2	1.406	4.426	7.381	10.403	8.533	12.157	0.720	7.105	4.547	3.527	2.730	1.443	0.742	0.320	0.120	0.135	74.14			
3	0.751	3.000	6.497	0.000	5.360	4.458	4.014	4.603	3.466	2.674	1.070	1.000	0.545	0.220	0.096	0.111	49.37			
4	0.308	1.524	4.705	5.051	3.142	3.450	2.501	2.500	2.345	1.700	1.160	0.664	0.300	0.165	0.064	0.064	20.20			
5	0.131	0.095	2.984	3.299	1.926	1.090	1.372	1.402	1.421	1.222	0.710	0.435	0.107	0.094	0.040	0.032	10.07			
6	0.040	0.261	1.563	1.997	1.121	1.066	0.662	0.014	0.750	0.723	0.434	0.277	0.134	0.047	0.024	0.000	9.03			
7	0.008	0.119	0.700	1.104	0.702	0.504	0.307	0.340	0.434	0.457	0.221	0.190	0.102	0.000			5.33			
8	0.000	0.040	0.147	0.607	0.403	0.300	0.140	0.174	0.220	0.244	0.095	0.005	0.047				2.03			
9		0.000	0.134	0.316	0.245	0.174	0.094	0.056	0.007	0.102	0.056	0.032	0.000				1.31			
10		0.095	0.095	0.142	0.134	0.127	0.055	0.024	0.040	0.030	0.024	0.016					0.70			
11		0.032		0.007	0.070	0.040	0.016	0.000	0.024								0.30			
12				0.040	0.024	0.040		0.000	0.016								0.13			
13				0.024	0.024	0.032		0.000	0.016								0.00			
14				0.000		0.024											0.03			
15				0.000		0.016											0.02			
16				0.000													0.01			
17				0.000													0.01			
18																	0.01			
19																	0.01			

(see Table B7a,b in Hales, 1978). Apparently no allowance is made for the increased width and fetch of the east window at the East Channel site compared to NMC Station 6 (Figure 6.3-3). Nevertheless, most waves come from the westerly sector, and the slight decrease (about 10%) in the heights of westerly waves predicted at East Channel relative to NMC 6 is qualitatively consistent with other refraction studies; for example, Figure 6.3-4 (ERT, 1984). Regardless of the exact location, Channel wave heights are markedly reduced relative to north of Point Conception. Shipboard observations in the Santa Barbara Channel give 3.8% exceedance of 8 ft (Hales, 1978) compared to an 8% exceedance of 9 ft off Point Sal.

OSI (1969, 1971) (in SAI, 1984) and Strange and Graham (1983) (in ERT, 1984) have used hindcast models to estimate wave conditions in the Santa Barbara Channel for historical storm events. Although there are differences in details of the model wave statistics, there is rough agreement about the significant height of waves for the 100-year storm. The Strange and Graham data predicts 26.3 ft (8 m) (ERT, 1984) compared to about 21 ft (6.4 m) for the OSI model (SAI, 1984). Table 6.3-2 shows the 10 most severe hindcast wave events, since 1958, on the shelf 7 miles SSE of Gaviota (ERT, 1984). There were only 10 storms in 25 years with significant heights greater than 10 ft (3 m). Eight of these events occurred in January or February, and one storm each occurred in February and April. The OSI hindcast study shows a similar clustering of storm events in winter. Note that there may be substantial variation of the wave field within the Santa Barbara Channel, even at mid-channel sites, so Table 6.3-2 cannot necessarily be directly applied to other locations.

Because of the oblique incidence of the prevalent westerly or northwesterly waves, the energy at coastal sites on the north shore of the Santa Barbara Channel is usually reduced relative to values directly offshore (Figure 6.3-4). On the other hand, southwest swell impinges almost directly on the western portion of the north shore of the Santa Barbara Channel and there is little reduction in height (Figure 6.3-5) relative to shelf sites. That is, the isolines of

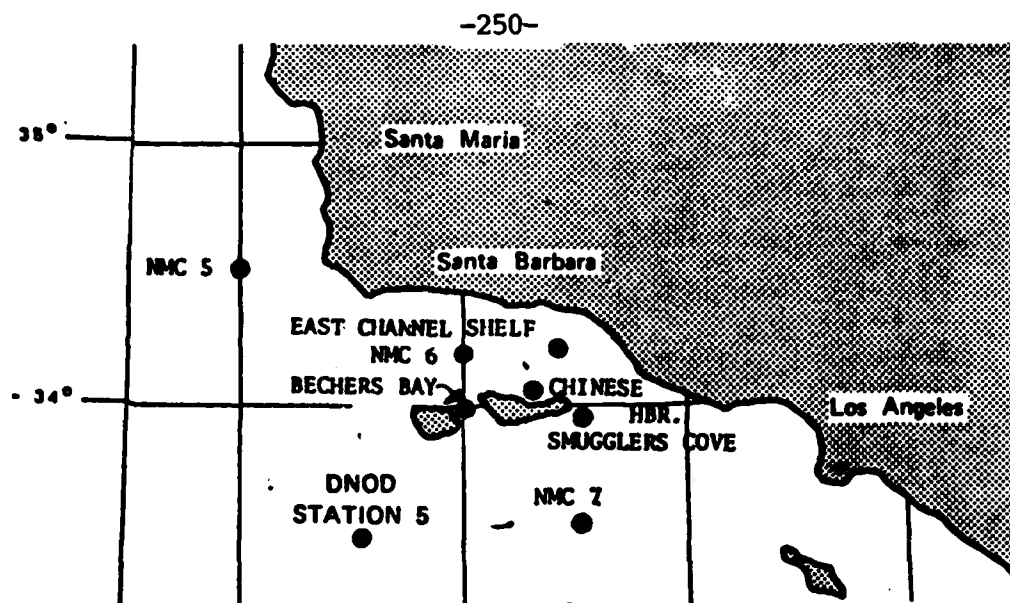


Figure 6.3-3 Santa Barbara Channel hindcast sites considered by Hales (1978).

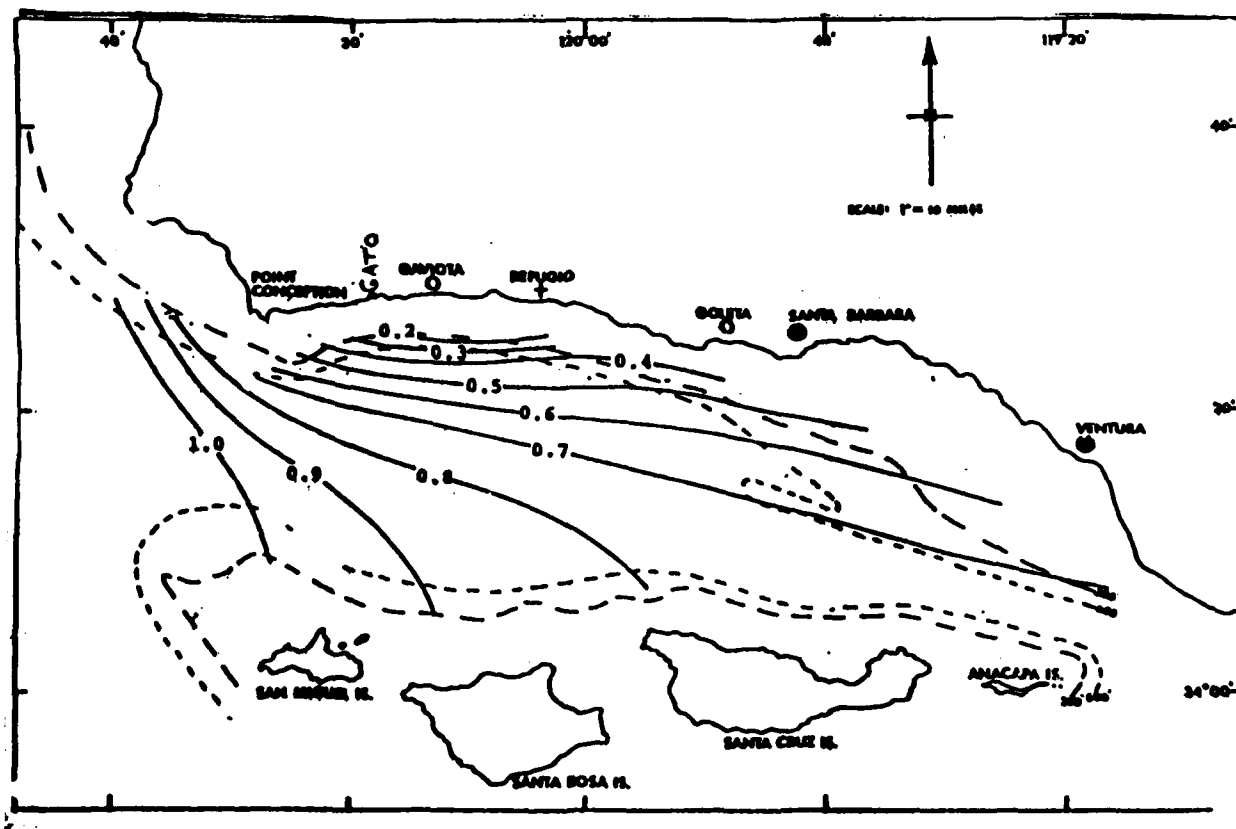


Figure 6.3-4 Lines of equal wave height for 9-12 sec northwesterly swell (EPT, 1984).

Table 6.3-2 Ten highest hindcast wave events (1958-1983) at a site 7 miles SSE of Gaviota (ERT, 1984).

DATE	SIGNIFICANT HEIGHT (FT)	PERIOD OF MAXIMUM ENERGY (SEC)
Feb 1983	24.3	18-19
Apr 1958	22.9	17-18
Feb 1980	20.4	15-16
Jan 1983	19.8	20-21
Jan 1981	18.8	14-15
Feb 1963	16.8	13-14
Feb 1959	15.9	9-10
Dec 1969	15.4	22-23
Jan 1981	15.4	20-21
Feb 1963	10.9	15-16

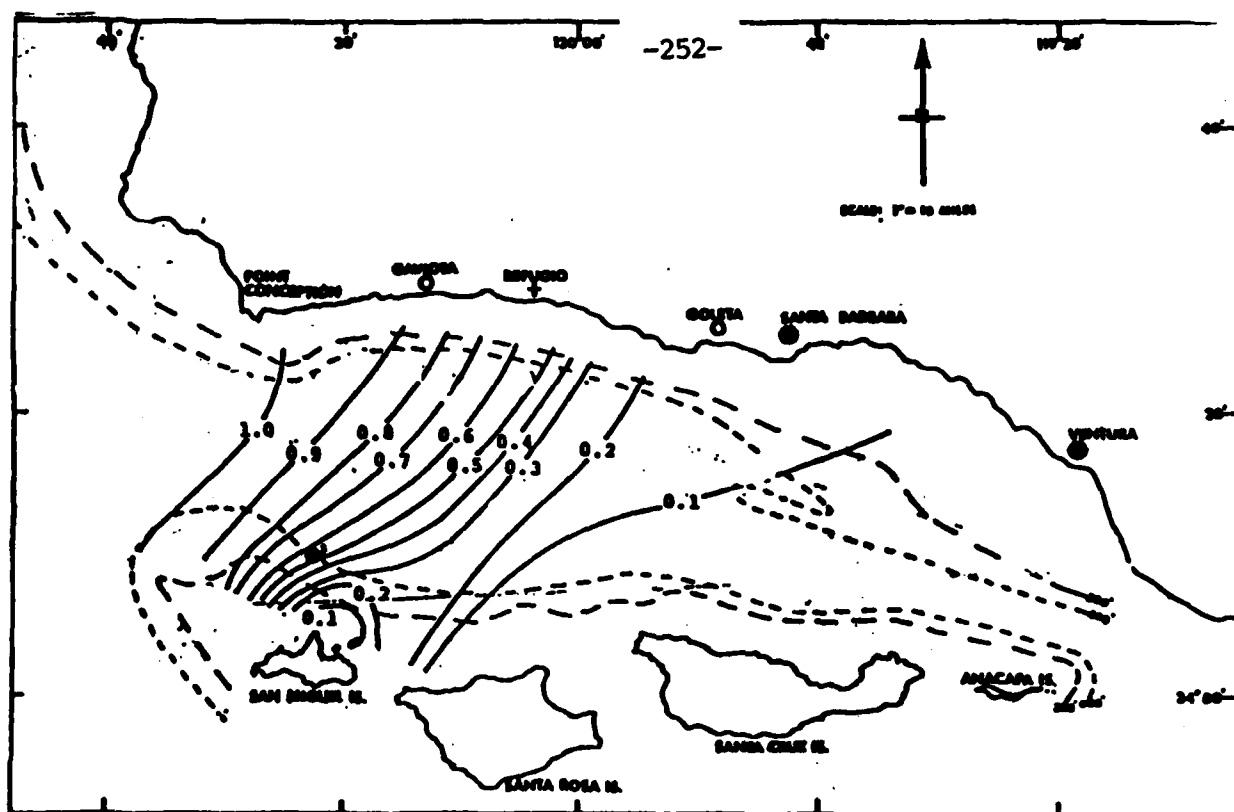


Figure 6.3-5 Lines of equal wave height for 9-12 second southwesterly swell (ERT, 1984).

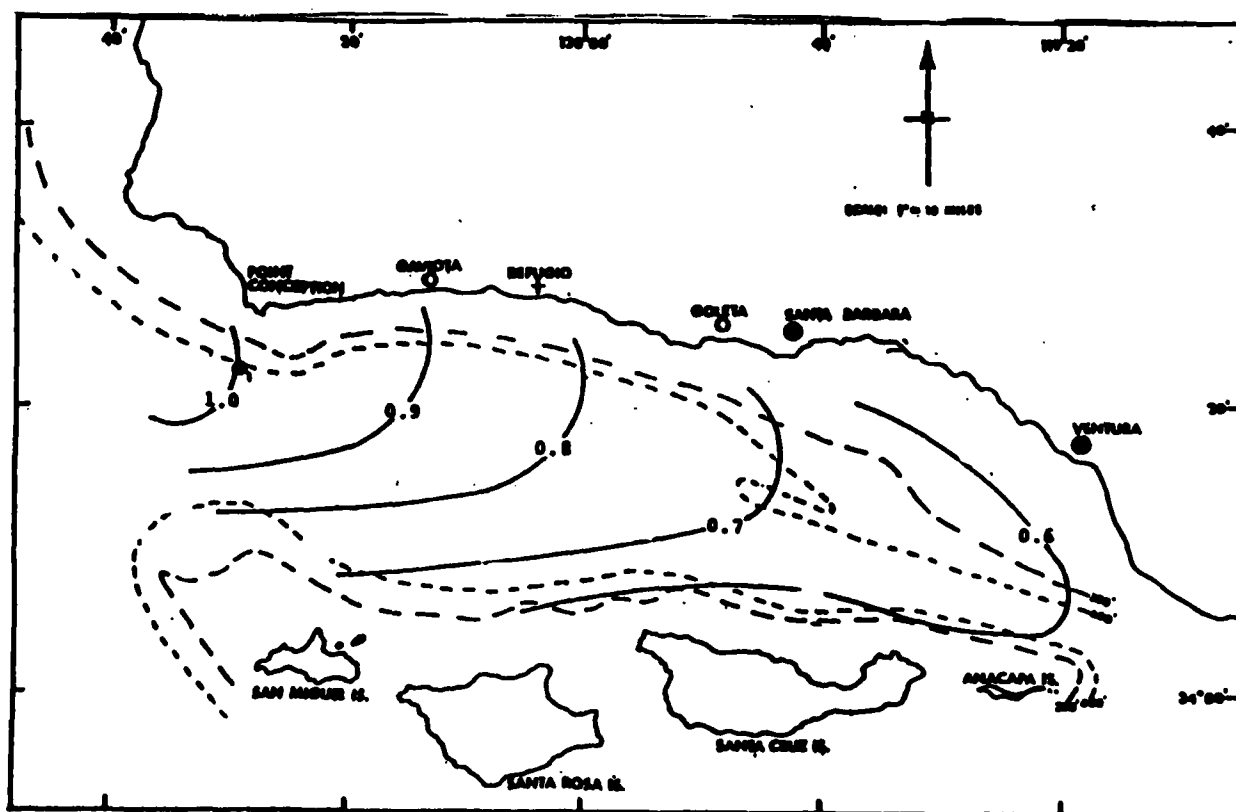


Figure 6.3-6 Lines of equal wave height for 7-9 sec east southeast sea (ERT, 1984).

equal wave height are nearly perpendicular to each other in Figures 6.3-4 and 6.3-5. According to these diagrams, there is strong longshore variation of north shore coastal wave height in response to southwest swell, and much weaker variation to northwest swell. Locally generated easterly (or ESE) show substantial down channel variations (Figure 6.3-7) associated with increasing fetch length.

Figures 6.3-4,5,6 suggest that mid-channel wave heights generally decrease from west to east. This is probably true at least as far east as Santa Barbara. However, deepwater sites at the far eastern end of the Santa Barbara Channel (i.e. east of Santa Cruz Island, offshore of Ventura and Point Mugu) are also exposed to waves from remote southerly sources, as well as locally generated waves from the entire southern sector (Figure 6.3-7). The literature reviewed does not contain tabulated hindcasts for this deepwater area.

COASTAL SITES

Wave statistics based on in situ shallow water (~ 7 m depth) measurements for this cell are available in the annual CDIP reports for Santa Barbara (1980-1982) and near Point Mugu (the Channel Islands station, 1978-1983). Yearly cumulative height probabilities, for 1980-1982, are given in Table 6.3-3. The waves at Santa Barbara are notably small; the 5% exceedance heights are roughly 85, 70, 70 cm for 1980-1982 respectively. The corresponding exceedances at Channel Islands are about 165, 170, 155 cm respectively. The much larger waves at Channel Islands are due to both increased exposure to south swell (Figure 6.3-7) and the more direct exposure of beaches near Ventura and Point Mugu to northwest swell propagating down the Santa Barbara Channel (Figure 6.3-4). Significant height return periods for these sites are given in Figure 6.3-8. Figure 6.3-9 shows a seasonal variation of wave heights typical of both CDIP sites in all years. The maximum wave heights occur between October and March. Note that during the stormy winter of 1980, significant heights exceeded 1.5 m about 25% of the time at Channel Islands. During this winter, the maximum significant height at the CDIP Santa

Table 6.3-3 Cumulative height probabilities (after CDIP).

CHANNEL ISLANDS

SANTA BARBARA

HEIGHT
(CM) PROBABILITY

HEIGHT
(CM) PROBABILITY

275 0.0000
265 0.0000
255 0.0008
245 0.0016
235 0.0024
225 0.0039
215 0.0071
205 0.0134
195 0.0213
185 0.0292
175 0.0426
165 0.0693
155 0.1040
145 0.1355
135 0.1749
125 0.2204
115 0.2821
105 0.3365
95 0.4338
85 0.5193
75 0.6281
65 0.7415
55 0.8452
45 0.9433
35 0.9992

1980

205 0.0000
195 0.0000
185 0.0000
175 0.0008
165 0.0024
155 0.0048
145 0.0097
135 0.0145
125 0.0265
115 0.0354
105 0.0386
95 0.0475
85 0.0555
75 0.0821
65 0.1078
55 0.2043
45 0.3870
35 0.6895
25 0.9566
15 0.9992
5 0.9992

310 0.0000
295 0.0000
280 0.0015
265 0.0029
250 0.0034
235 0.0065
220 0.0087
205 0.0175
190 0.0255
175 0.0444
160 0.0800
145 0.1258
130 0.1833
115 0.2625
100 0.4007
85 0.5702
70 0.7487
55 0.9328
40 0.9964

1981

175 0.0000
160 0.0000
145 0.0008
130 0.0023
115 0.0069
100 0.0116
85 0.0200
70 0.0555
55 0.2311
40 0.6957
25 0.9961
10 0.9992

325 0.0000
310 0.0007
295 0.0007
280 0.0028
265 0.0028
250 0.0077
235 0.0091
220 0.0126
205 0.0141
190 0.0210
175 0.0273
160 0.0399
145 0.0630
130 0.1057
115 0.1745
100 0.3123
85 0.4902
70 0.7304
55 0.9363
40 0.9963

1982

115 0.0000
100 0.0036
85 0.0173
70 0.0568
55 0.1662
40 0.6453
25 0.9957
10 0.9993

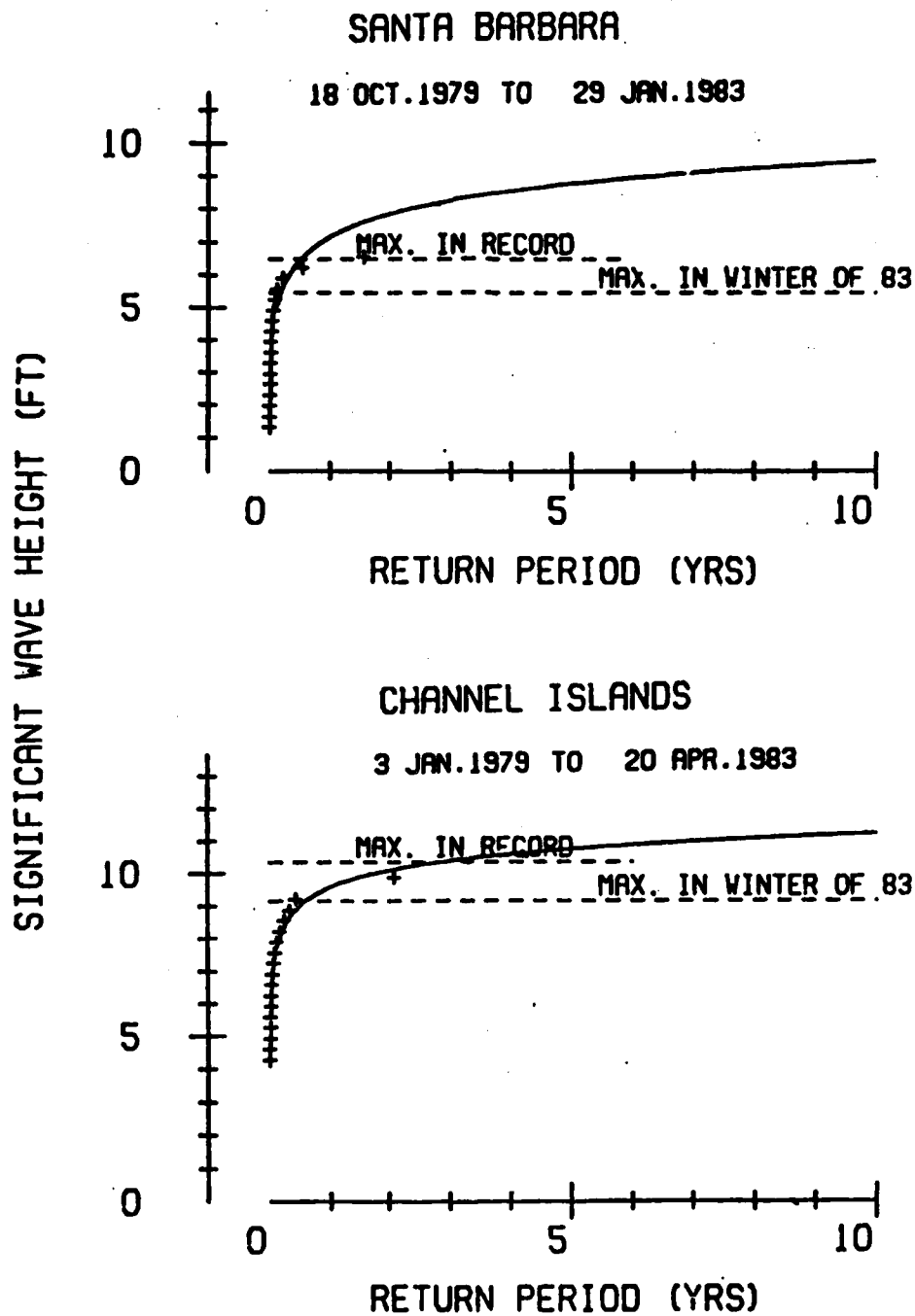
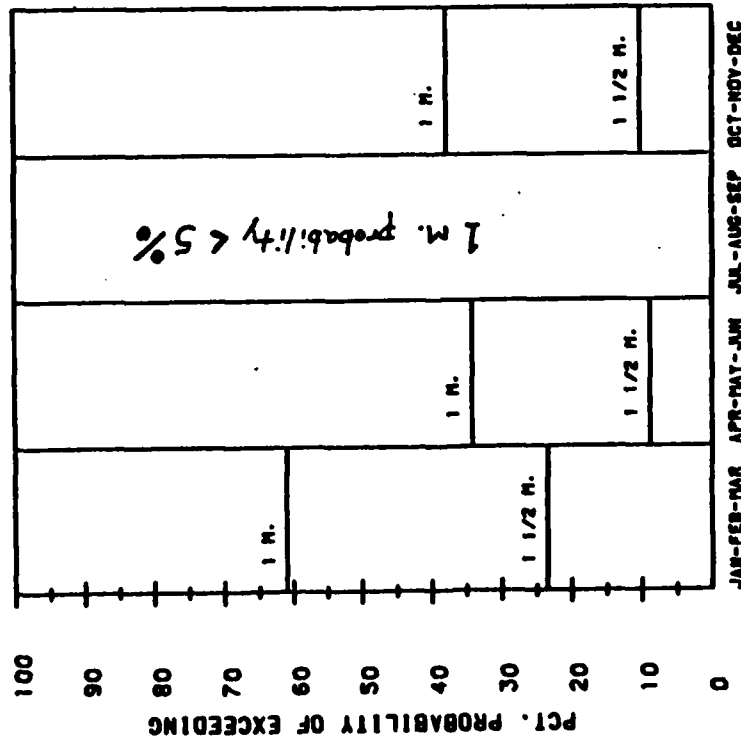


Figure 6.3-8

Significant height return periods at Santa Barbara and Channel Islands, based on about 4 years of data in 7 m depth (Seymour, 1983).

CHANNEL ISLANDS JAN-DEC 1980

SEASONAL PROBABILITY OF EXCEEDING
VARIOUS SIGNIFICANT WAVE HEIGHTS



CHANNEL ISLANDS JAN-DEC 1982

SEASONAL PROBABILITY OF EXCEEDING
VARIOUS SIGNIFICANT WAVE HEIGHTS

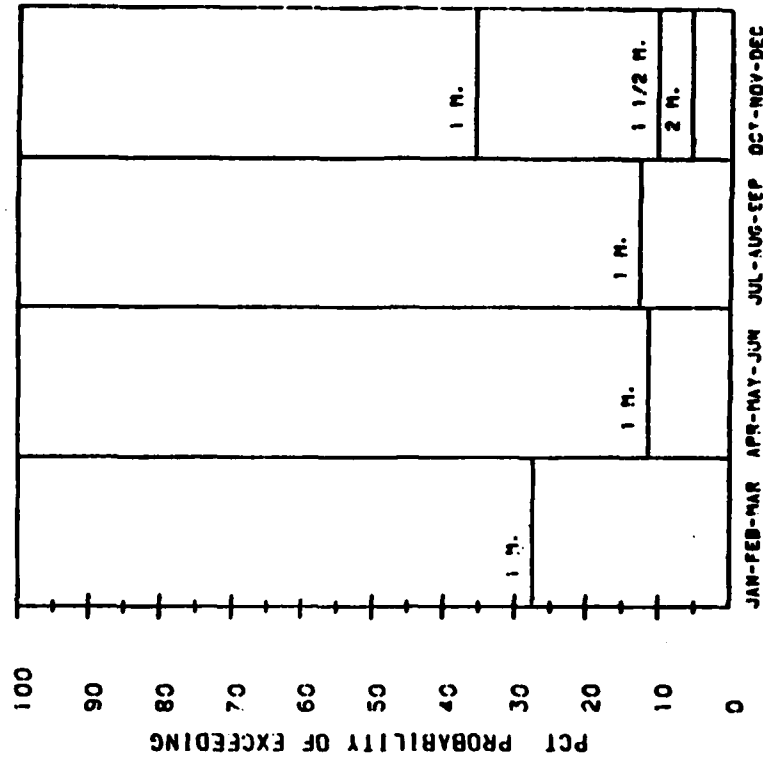


Figure 6.3-9 Seasonal probability of exceeding various significant wave heights (CDIP annual reports).

Barbara gauges was about 2 m. Note that individual breakers can be much larger than the CDIP significant height in 8 m depth. Visual estimates of 4 m breakers at Santa Barbara in February, 1980 are not inconsistent with the CDIP data.

Seasonal variability of wave heights similar to Figure 6.3-9 is apparent in two years (1975-1976) of LEO observations of wave height at several beaches in the Point Mugu area (USACE LAD, 1979, 1980b). Average visually observed breaker heights were maximum (about 3 ft) in February, and minimum (about 2 ft) in June-July. Schneider and Weggel (1980) compared 9 months of LEO waves observations and in situ (pressure sensor) data at Point Mugu. Although there is very significant scatter, the LEO and direct measurements yield wave heights which have comparable probability distributions. That is, over a long time period the distribution of wave heights observed and measured are similar. In contrast, the LEO wave periods appear to be nearly uncorrelated with the in situ data. LEO observers reported periods between 10-12 seconds almost independent of the measured period (Figure 7 in Schneider and Weggel, 1980). Additional in situ wave height measurements near Point Mugu are reported for 2/72 - 12/72 and 4/73 - 12/74 in Thompson (1977, 1980). Thompson (1980) gives an interesting discussion of the characteristics of the 1972 spectra.

Borgmann and Pannicker (1970) carefully designed a wave array for measuring directional characteristics of waves at Point Mugu. The selected array geometry was based on an analysis method which simultaneously uses all possible sensor pairs. They also mention 5 other plausible analysis schemes. This array was installed and operated for several years. Esteva (1977) analyzed the data and reached the conclusion that "accuracies no better than 20° can be expected for wave directions resulting from 3 gauge arrays." Since refraction limits the shallow water approach angles of 16 second waves to less than 22°, "the directional information provided by the array adds little to this and seems hardly cost effective." The statements are wrong. Munk et al (1963) and Snodgrass et al (1966) used 2 element arrays to obtain far better

than 20° accuracy. Others have successfully used arrays (see Figure 3.3.1-3). Esteva (1977) did not, in fact, use any of the six ^{analysis}schemes suggested by Borgmann and Pannicker (1970). The failure of the array is probably associated with the poor analysis methodologies employed.

A variety of nearshore wave and current measurements were made onshore of the CDIP station at Santa Barbara. The longshore currents are briefly discussed in Section 6.4. The application of high resolution, data adaptive directional estimators to the CDIP slope array is discussed in Oltman-Shay and Guza (1984). Directional wave energy is shown to be concentrated in the open windows (Figure 6.3-1). Nonlinear properties of the shoaling wave field are discussed in Elgar and Guza (1985a,b). Observations of surf beat (see Section 3.3.4) at Santa Barbara are described by Guza and Thornton (1985). Elgar et al (1984) discuss the grouping of high waves.

Several studies include hindcast and/or refraction diagrams for specific coastal locations. Using historical data and refraction diagrams, NMC (1960a) concluded that a shallow water (depth 32 ft) site at Santa Barbara is so highly sheltered from northwesterly swells (which may be large in the channel and small at coastal sites, Figure 6.3-4), that the design waves actually are from the southeast. Figure 6.3-10 shows isolines of K_r for the shallow water Santa Barbara site. NMC (1960a) hindcast waves from major storms (1879-1959) which generated waves propagating toward Santa Barbara with directions in the sector 120°-135°. They find 13 storms generating waves in excess of 10 ft with a maximum of 15.9 ft. Periods are between 7-9 seconds. As these waves are in the eastern sector, there is not much modification in going from deep to shallow water (Figure 6.3-10).

Bailard and Jenkins (1982) develop wave statistics for shallow water in the Carpinteria area (approximately mid-way between Santa Barbara and Ventura, Figure 6.3-4). A rather crude island blocking model is used: waves in windows defined as open are transmitted unaltered from deep water, waves in closed windows are totally blocked. No allowance is made

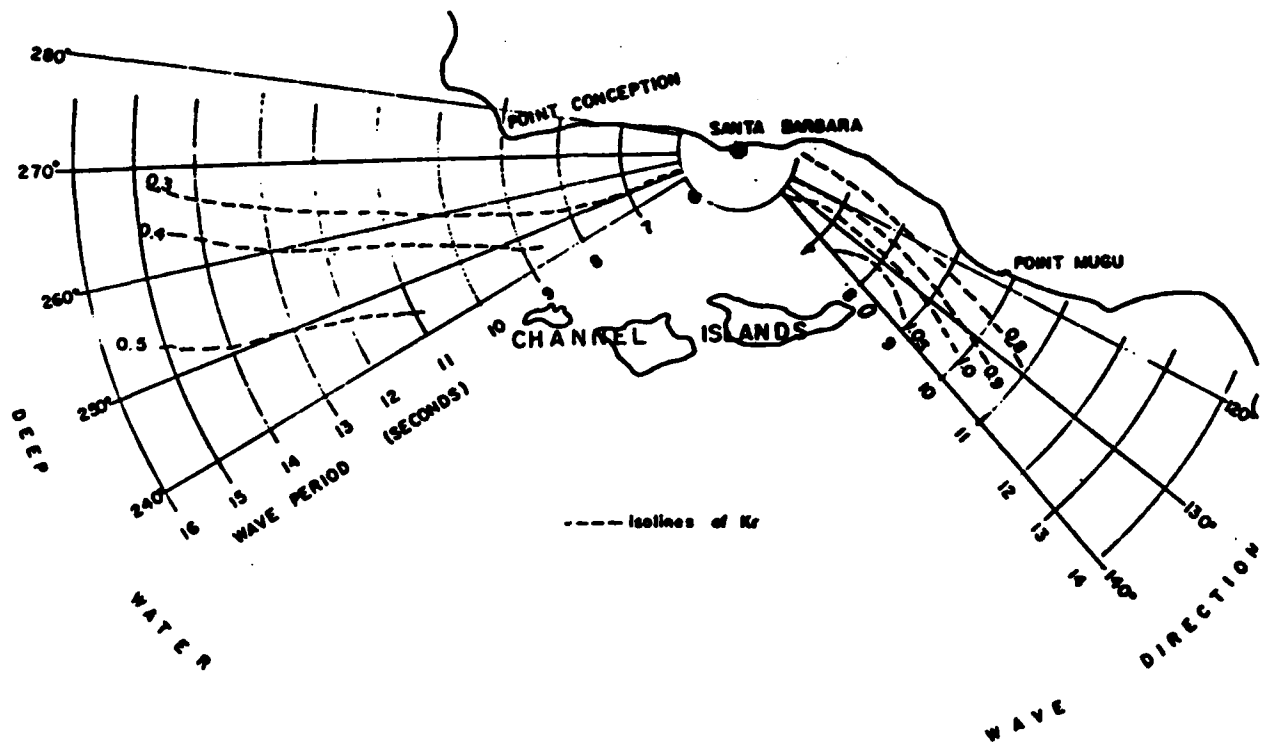


Figure 6.3-10

Isolines of refraction factor (K_r) for a site in 32 ft depth near the Santa Barbara breakwater (NMC, 1960).

for refraction by submerged banks which can steer waves towards or away from the study site (see Section 3.3.1). Using this model, they develop tables which give the breaker heights and angles near Carpinteria as a function of deep water height, direction, and period. These transformation tables are used to hindcast waves at Carpinteria, using both historical extreme events and the MII (1977) average yearly statistics at Station 5 (Figure 3.2.2-6).

Lundin (1978) use NMC Station 6 statistics (Figure 6.3-2) and refraction diagrams to estimate the wave climate at Ventura. Southerly waves which are blocked at NMC station 6 (Figure 6.3-1) but not at Ventura (Figure 6.3-7) are not considered. The conclusion that downcoast transport far exceeds the upcoast transport at Ventura may indeed be correct, but the wave statistics used to show this (Lundin, 1978) are incomplete. NMC (1960a) contains numerous refraction diagrams for Point Hueneme, as does Inman (1950a) for the Mugu Lagoon vicinity.

6.4 NEARSHORE CURRENTS

SHELF CURRENTS

Kolpack (1971) released 15,000 drift cards between June 1969 and February 1970. Based on the somewhat subjective interpretation of these data he inferred qualitative seasonal surface water circulation patterns. The surface water circulation pattern in the Santa Barbara Channel consists of a counter-clockwise cell in the western half of the channel and a northwesterly inflowing current in the eastern part of the channel (Figure 6.4-1). The flow into the eastern end is presumably the extension of the Southern California Countercurrent (see Section 3.1.1). Some of Kolpack's diagrams show substantial surface flow out of the eastern end of the Santa Barbara Channel while others do not. It is fair to say that water mass exchanges between the Santa Barbara Channel and adjacent areas is not well understood. The convergence of the western cyclonic eddy and the inflow from the east results in a complex pattern of eddies in the

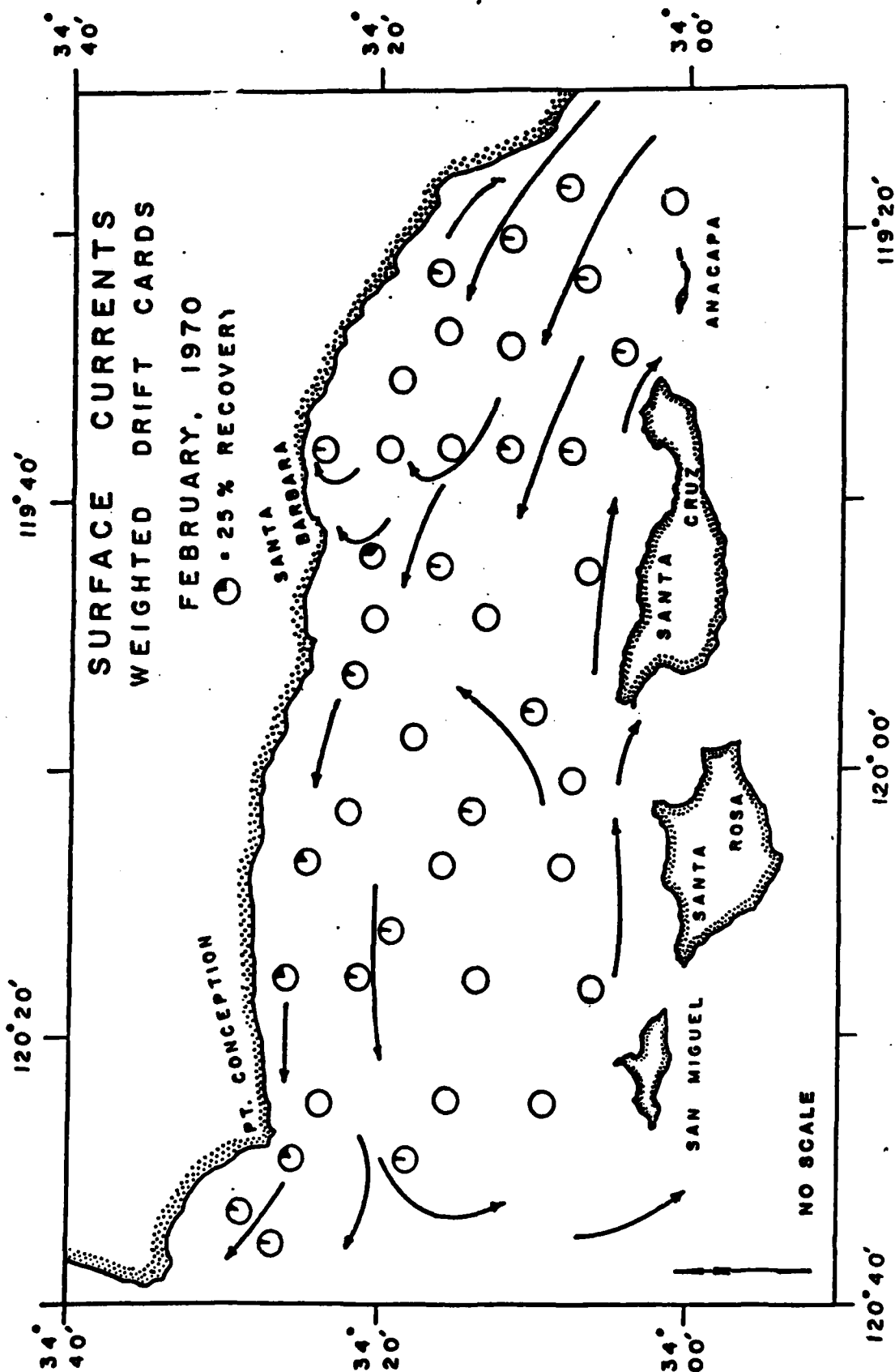


Figure 6.4-1 Winter surface water circulations inferred from drift cards (Kolpack, 1971).

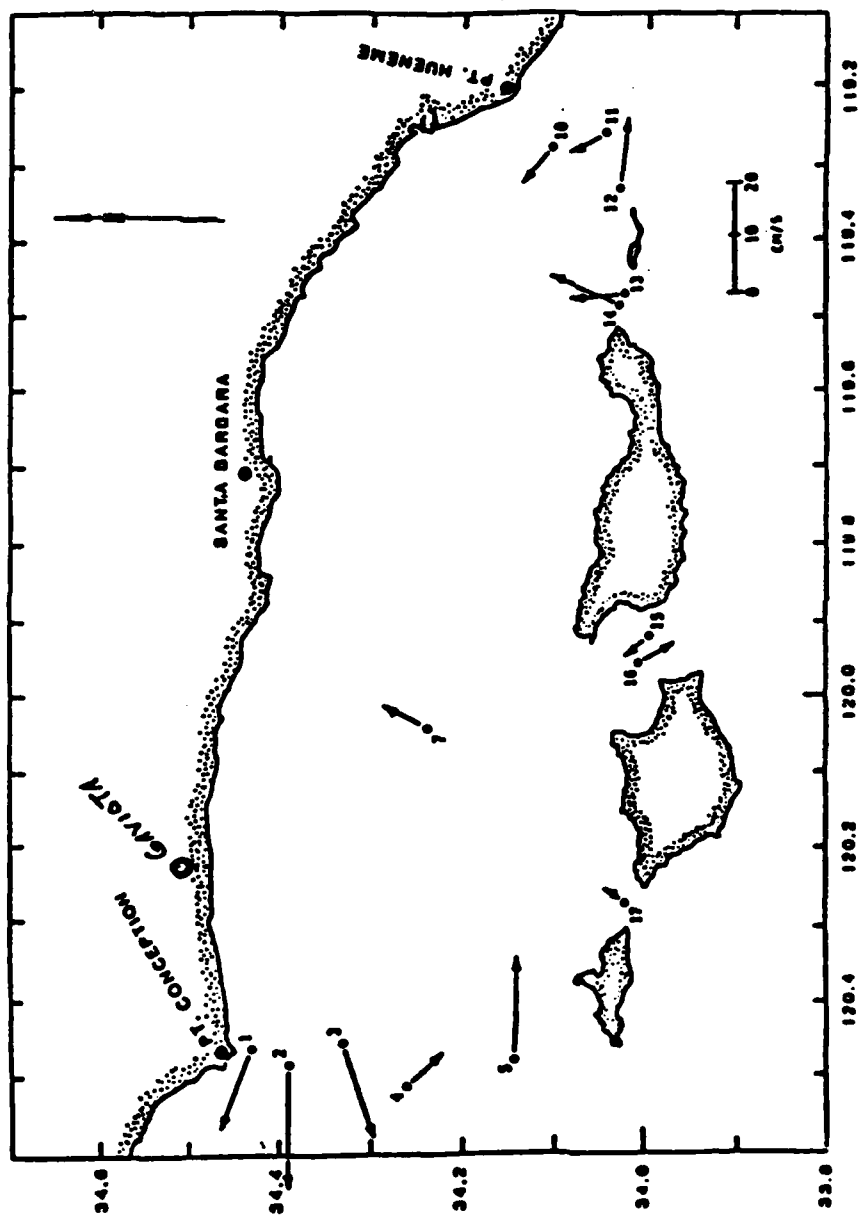
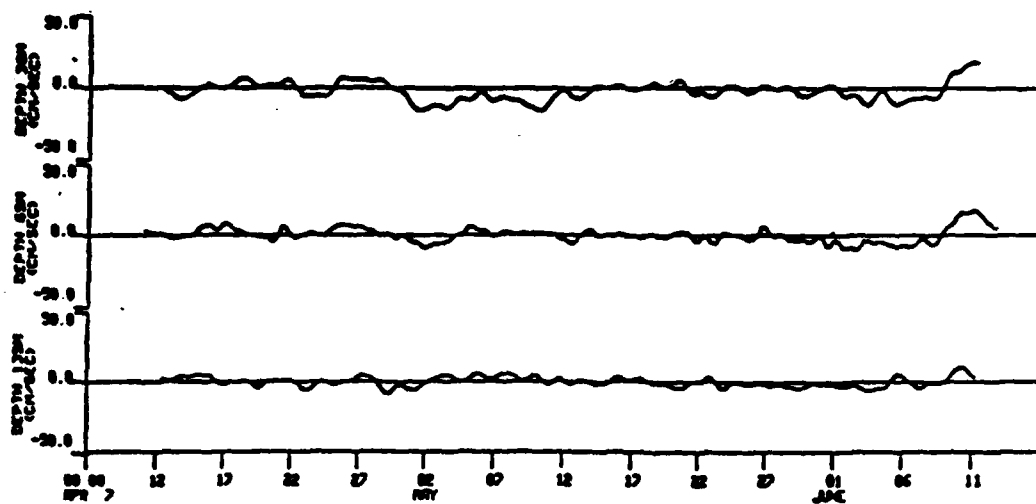


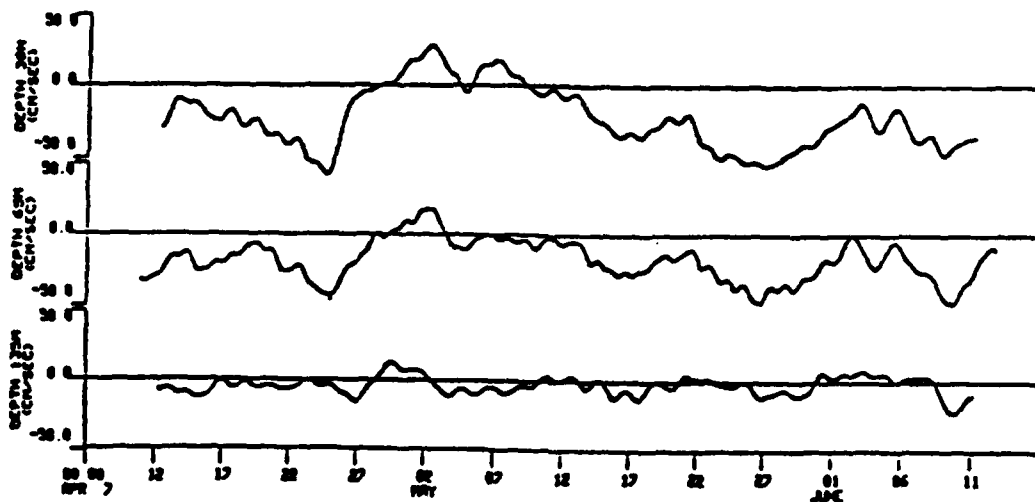
Figure 6.4-2 Vector average current speeds in the Santa Barbara Channel, April-July 1983 (SAI, 1984).

Table 6.4-1 Current meter statistics from MMS survey of Santa Barbara Channel, April-June 1983. Mooring locations shown in Figure 6.4-2 (SAL, 1984).

MOORING NO.	BOTTOM DEPTH (M)	METER DEPTH (M)	MEAN SPEED (CM/S)	MINIMUM SPEED (CM/S)	MAXIMUM SPEED (CM/S)	2-MONTH VECTOR AVERAGE SPEED (CM/S)	DIRECTION (°T)
1	71	30	23	0	74	16	290
		65	14	0	52	2	287
2	181	30	29	0	84	22	269
		-65	22	0	65	16	274
		135	13	0	43	3	292
3	366	30	30	3	85	18	252
		65	26	1	75	18	258
		100	21	0	54	15	255
		135	17	1	43	12	257
		205	11	0	48	6	249
		275	9	0	29	1	176
		350	8	0	37	2	117



N-S CURRENT SPEED, MOORING 2 - SANTA BARBARA CHANNEL



E-W CURRENT SPEED, MOORING 2 - SANTA BARBARA CHANNEL

Figure 6.4-3 Low-pass filtered (35 hr) shelf currents south of Point Conception (Mooring 2; MMS, 1983).

area between Santa Barbara and Santa Cruz Island. Other eddies along the eastern margin of the channel are reported to be produced by deflections resulting from current impingement near Santa Barbara and, to a lesser extent, the area between Santa Barbara and Ventura (Kolpack, 1971). Current magnitudes were not measured in this study.

The two-month long (4/83 - 6/83) MMS current meter study (Science Applications, SAI, 1984) gave results qualitatively consistent with the patterns suggested by Kolpack (1971). Vector averaged currents at the shallowest meter of each mooring show both the western cyclonic eddy and the inflow-recirculation at the eastern boundary (Figure 6.4-2). Some indication of the temporal and vertical variability of current magnitudes in the shelf currents (mooring numbers 1, 2, 3 in Figure (6.4-2) are given by Table 6.4-1. Maximum speeds greatly exceed the vector average speeds. Maximum and mean speeds both generally decrease with increasing current meter depth, on a single mooring. Currents were strongly polarized in the longshore direction, for example mooring 2 (Figure 6.4-3). These low-pass currents were generally westward with the exception of a reversal (eastward) of the current from 28 April to 10 May. Analysis of similar signals at the other mooring locations and concurrent temperature records suggest that this was a period of upwelling in the region (SAI, 1984).

Current measurements at 6 locations on the shelf due south of Gaviota, in depth between 60-200 m, are reported by Dames and Moore (1982). None of the deployments was longer than six weeks, and several were only two weeks. This is too short a duration to indicate anything other than the mean currents during that particular time period. Speeds were generally between 20 and 30 cm/sec, and rather variable in direction.

Similar short term current measurements with similar limitations in the western Santa Barbara Channel have been reported by Nekton (1984) and Marine Biological Consultants (1984). Nekton obtained current speed and directions during two one-month periods (May, August) at a depth of approximately 200 ft (60 m) at a site west of Dames and Moore's

measurements. Surface and bottom current speeds varied between 0-80 cm/sec and 0-50 cm/sec respectively and were principally longshore directed (between 240° - 300°). MBC collected current meter data between September and December 1983 at a site at 60 m depth in the same general vicinity as Dames and Moore's measurements and to the east of the Nekton site. Currents were essentially to the west (250°) with speeds ranging 0-51 cm/sec with an average speed of approximately 13 cm/sec. There are other current meter studies. Variability of speed, and direction to a lesser degree, are the common features. Seasonal variation in the speeds based on ship drift estimates (USGS, 1974) for summer (15 to 30 cm/s) and winter (25 to 34 cm/s) shows a slight increase in winter. This is consistent with the seasonal variation in wind speeds and (presumably) wind-generated currents.

SURF ZONE CURRENTS

When waves approach the beach at an angle, quasi-steady longshore currents are generated in the surf zone. The currents increase in strength with increasing wave height and deviation of the incident waves approach angle from normal incidence to the beach. The approach angle dependence is important because long Pacific swell entering the Santa Barbara Channel through the west window (Figure 6.3-1) has a large deep water approach angle relative to the beach normal. Breaker angles are therefore exceptionally large. Waves entering through the southeast window also have large breaker angles. Thus, surf zone longshore currents in the Santa Barbara Channel are surprisingly strong (Figure 6.4-4), considering the relatively small wave heights. The longshore currents on 5 Feb occurred with long low (significant height H_s about 50 cm) swell coming through the west window. Very small waves ($H_s = 21$ cm) from the southeast were associated with the weak currents of 31 January 1980, while larger southeast waves ($H_s = 80$ cm) drove the stronger currents on 13 February. The 13 February waves were generated by the first of several storms which hit the Santa Barbara Channel in late February 1980. Later storm-generated waves came through the west window, and mean currents exceeded 170 cm/sec.

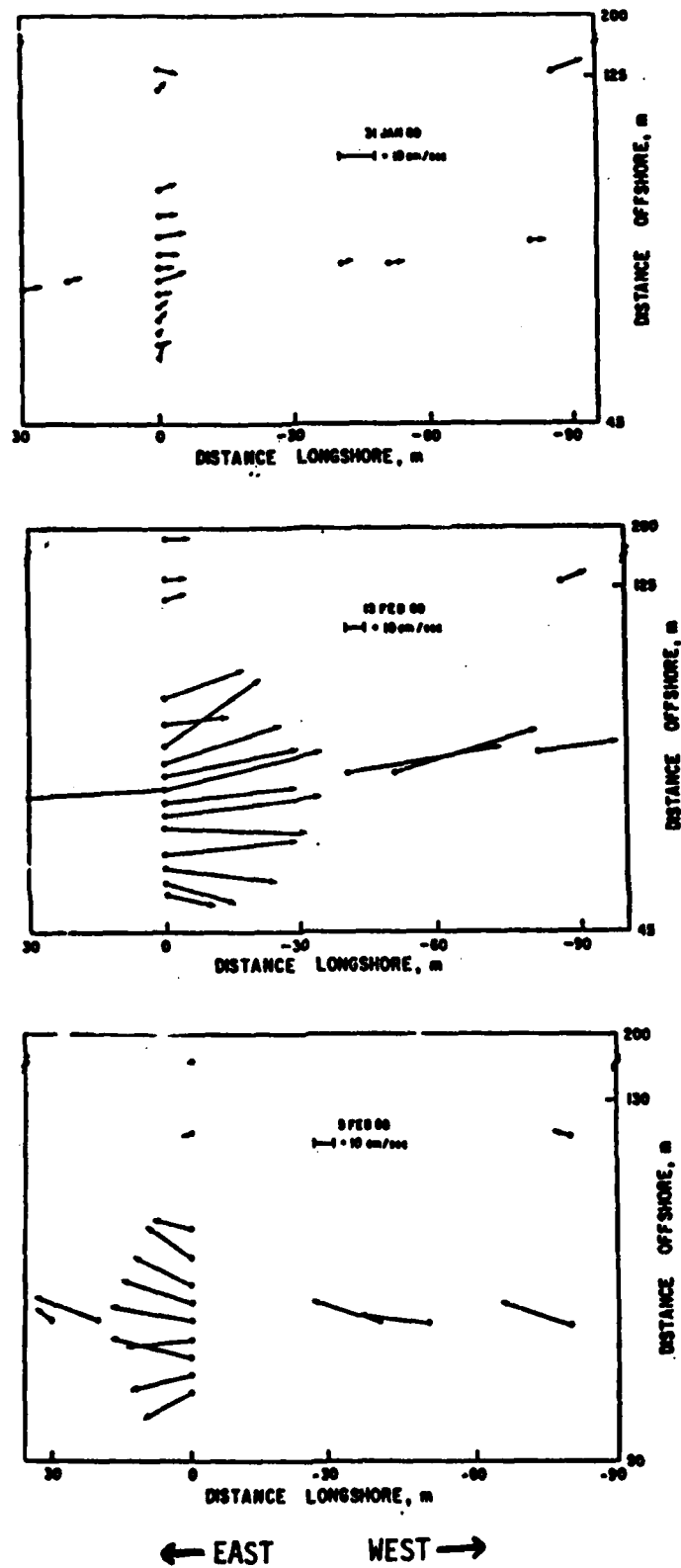


Figure 6.4-4 Vector average (17 minute) surf zone currents at Santa Barbara.

Longshore current observations in this experiment are compared with two different numerical models in Wu et al (1985) and Thornton and Guza (1985).

Longshore currents of similar magnitude probably occur on most beaches on the northern Santa Barbara Channel. Even stronger currents probably occur at locations west of Santa Barbara because incident wave heights are larger and the incidence angles are comparable. Using NMC (1960) hindcast data, Marine Advisers (1964) estimated the longshore components of wave power at Gato (between Point Conception and Gaviota). The eastward directed component is estimated to be 6 times larger than westward. Because the wave power is closely related to the off-axis component of the radiation stress tensor important to longshore currents, the Marine Adviser result implies that surf zone longshore currents will be predominantly from west to east at Gato. A similar situation would be expected on the north shore of the Santa Barbara Channel, at least as far east as Santa Barbara.

As discussed in Section 6.3, sites on the far eastern end of the Santa Barbara Channel (e.g. Ventura) are not shadowed from south swell by the Channel Islands (Figure 6.3-7). Wave-driven longshore currents respond to this change in wave climate. Balsillie (1975) compared one year (5/72 - 4/73) of surf zone longshore currents at Point Mugu measured (timing dye patches) and predicted using LEO observations of wave height, breaker angle and surf zone width as input to a crude model. Although there is large scatter when considering individual points, there is still a very significant correlation. In fact, the monthly averaged observed and predicted currents are in surprisingly good agreement (Figure 6.4-5). All three locations, both observed and predicted, show flow to the north from May-October in response to south swell (generated in the southern hemisphere winter, Section 3.2.1). During November-April the south swell is unimportant, and waves generated in the North Pacific drive surf zone currents to the south.

It is clear that meaningful estimates of the seasonal variability of longshore currents can be obtained from LEO observations, at least at Point Mugu. It is also worth noting that these

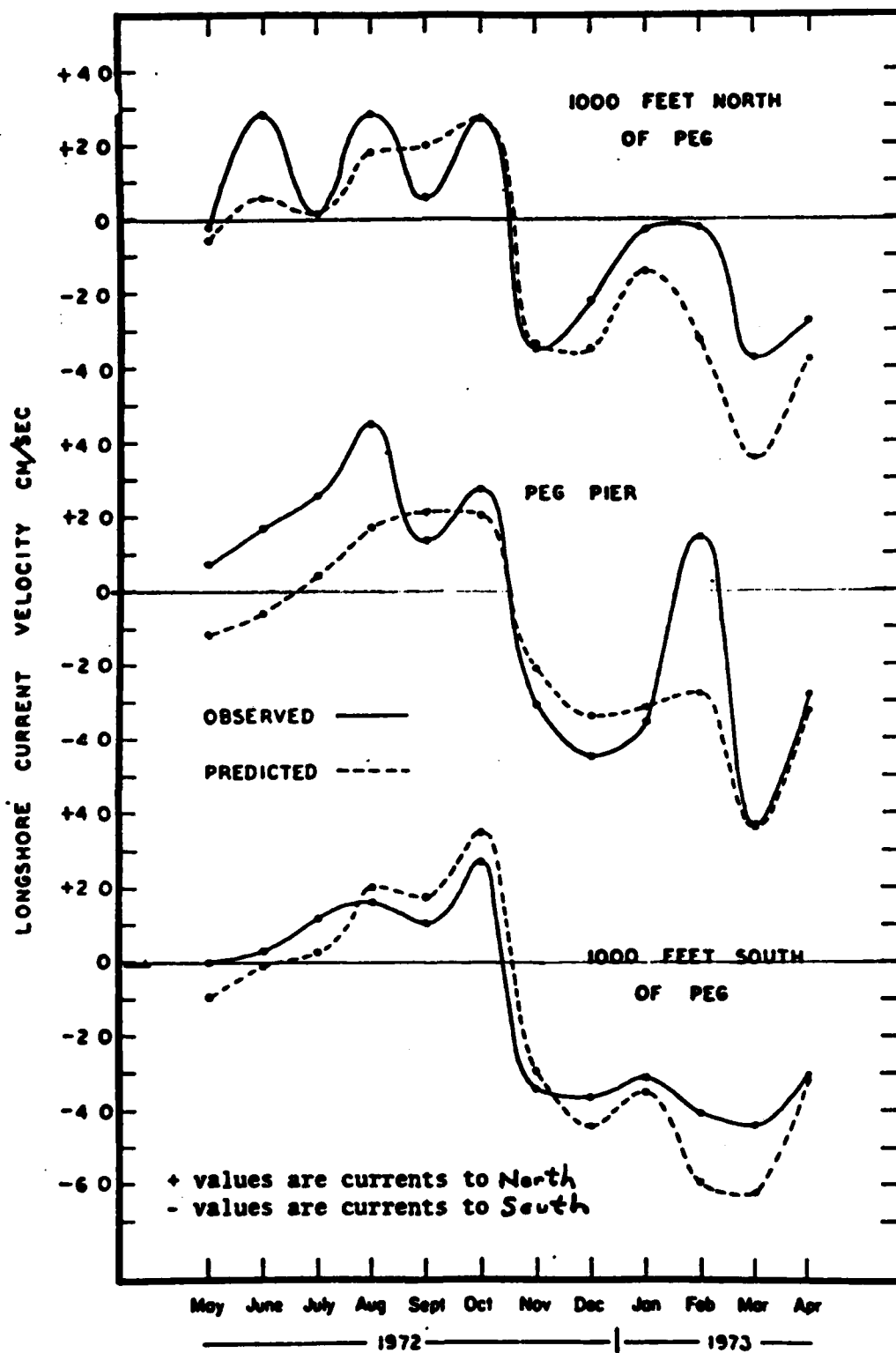


Figure 6.4-5

Time series plot of net monthly mean observed and predicted longshore currents at 3 locations near Point Mugu (Basille, 1975).

LEO observations (which are probably of very high quality relative to other LEO data sets) do not provide accurate estimates of the net *yearly* surf zone current. The average (over all values in Figure 6.4-5) observed and predicted longshore currents are -14 cm/sec and -8 cm/sec. Net yearly longshore transports calculated using these values would differ by roughly a factor of 2.

LEO data from 1975-1976 has also been used to calculate longshore drift near Port Hueneme (USACE-LAD, 1979, 1980a,b). That data shows the same seasonal variability as Figure 6.4-5; northward in summer and southward in winter.

Bruno et al (1981) compare LEO and in situ wave parameter observations at Point Mugu. They point out that sometimes LEO observers report the breaking wave height on an inner bar, rather than the desired larger breaker height on an outer bar. They caution against using LEO data which has not at least been spot-checked with in situ data. Presumably each individual observed should be "calibrated."

Brown (1983) made visual observations of breaker angle, wave height, wave period and longshore current (dye), at 4 beaches near Mugu Canyon. Figure 6.4-6, from Mandalay Beach (8 km north of Port Hueneme), shows the considerable variability of wave height, breaker angle (90° is offshore) and surf zone width observed at all 4 beaches. The strongest, and most frequent, longshore currents flow northwards, as expected during the summer months (Figure 6.4-5).

It seems worth noting (again) that local topographic effects can alter surf zone currents, sometimes causing flows opposed to the direction of wave approach (Section 3.3.3.) Such reversals have been observed in the vicinity of Mugu Canyon (Inman, 1950a), and would also be expected in the vicinity of headlands, groins, etc.

Mandalay Beach

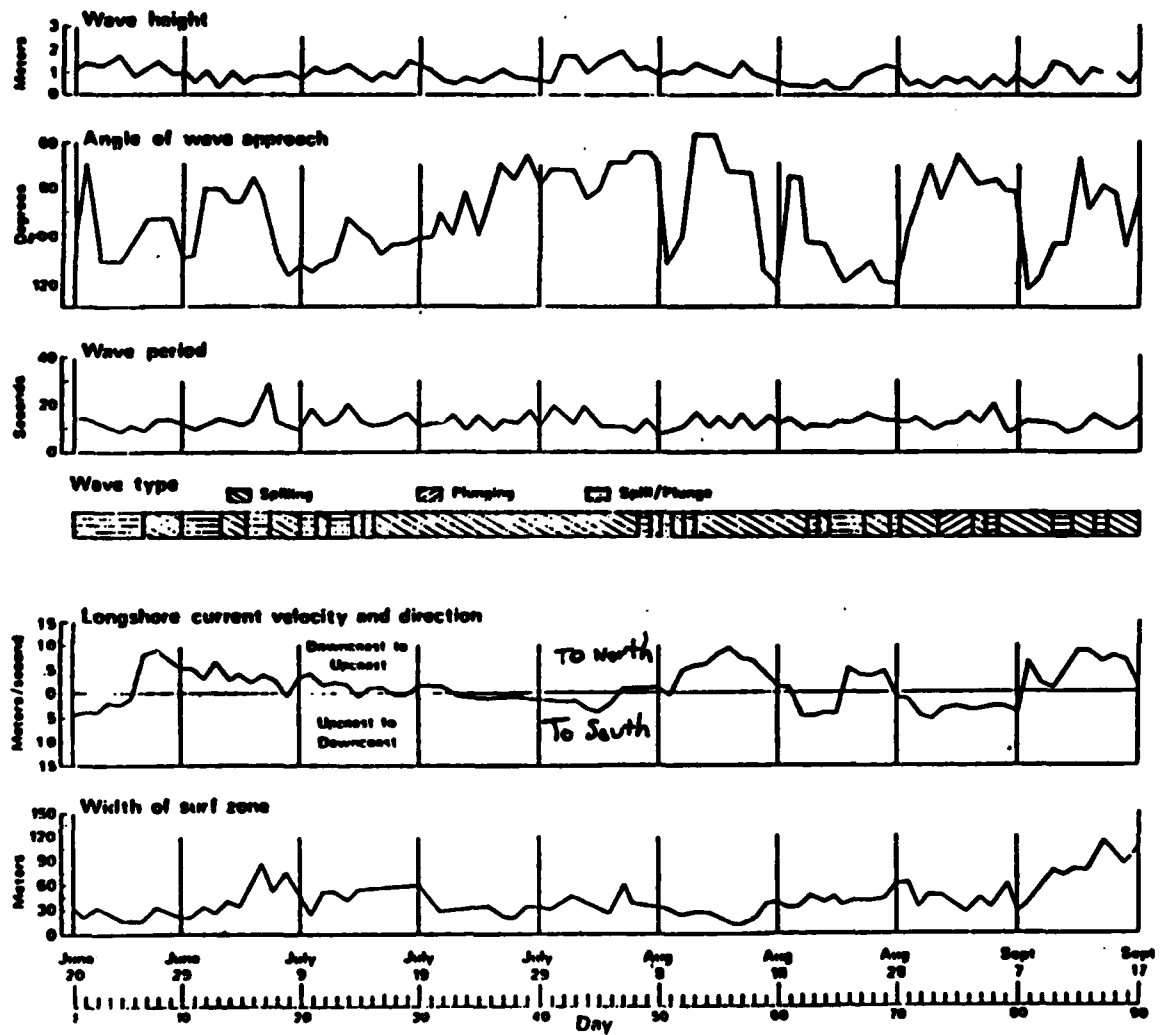


Figure 6.4-6 Surf zone wave and current parameters observed at Mandalay Beach (Brown, 1983).

6.5 SEDIMENT SOURCES

6.5.1 *Cliff Erosion and Relict Dunes*

Zeller (1962) discusses the coastal dunes of California. The dunes along this littoral cell are small and very sparse, and are located at Point Conception, Goleta Point and the Ventura River-Point Mugu area. Wiegel (1959) points out that the major source of sand for this littoral cell is from local streams feeding into the ocean. He states that sand from local dunes blown by wind is a relatively unimportant source of sand for the beaches. Pollard (1979) discusses cliff erosion and presents a table of average annual retreat rates for the cliffs located north of Santa Barbara. Inman (1981) discusses the beach and dune stability in the vicinity of Mandalay Beach.

6.5.2 *Sediment Discharge from Rivers and Streams*

Inman (1950a) discusses the nature of the beach material and plots grain size distribution for the Mugu Lagoon area. The sand on the beach foreshore near Mugu Lagoon had an average median diameter near 0.3 mm. Inman (1950b) discusses the petrology of the sediments found near the Mugu Submarine Canyon. Handin (1951) describes the streams and drainage basins that feed this littoral cell. He estimates the sediment discharge from the Ventura, Matilija and Coyote watersheds. He also discusses the sediment mineralogy and petrology, and includes sand grain size distribution data. Weigel (1959) briefly describes the sources of sediment for Santa Barbara Harbor and includes grain size versus beach slope plots for the harbor area. USACE LAD (1961a) details the tributary drainage and sediment yield for this littoral cell. It also describes the littoral materials and includes grain size distribution plots. USACE LAD (1962b) contains sand sample analysis for samples taken at Ventura County Harbor. Herron and Harris (1960) briefly describes the major sources of beach material for the southern half of this littoral cell. Judge (1970) discusses the heavy mineral content of local beach sediments, and estimates

average annual water discharge and drainage area of the Atascadero Creek, Carpinteria Creek, Ventura River and Santa Clara River (see Table 6.5-1). USACE LAD (1970) summarizes a study of the Santa Clara River Delta and includes sand size analysis for samples taken in Ventura County. Drake et al (1972) examines sediment transport on the Santa Barbara-Oxnard shelf. They include estimates of historical flood sediment yield from the Ventura and Santa Clara Rivers. Bruno et al (1977) contains a discussion of the sediment properties of sand samples taken from the Channel Island Harbor Sand Trap. California (1977b) examines the watershed hydrography and sediment production in this littoral cell.

Brownlie and Brown (1978) studied the effects of dams on the beach sand supply. They discuss the drainage areas and sediment yields, using a double-mass analysis, for both the Ventura and Santa Clara Rivers. Pollard (1979) summarizes the river and stream sediment transport and includes an extensive reference list on the subject. He also includes sand sample statistics for samples taken in Santa Barbara County. USACE LAD (1979 and 1980a) discuss the delivery of sediments to the Ventura and Santa Clara River Deltas. Brownlie and Taylor (1981) summarize water and sediment discharges for the Ventura River Basin, the Santa Clara River Basin, and the Calleguas Creek Basin (see Figures 6.5-1 and 6.5-2 and 6.5-3). They estimate sediment yield using sediment rating curves and by assuming the bedload to be 10% of the suspended load which may tend to underestimate the total yield (see Inman and Jenkins (1983) and Section 2.5 for discussions). Brown (1983) and Orme and Brown (1983) briefly discuss river flow, sediment yield and sediment properties for Ventura and Santa Clara Rivers.

6.5.3 *Artificial Beach Nourishment*

Johnson (1953;1957) and Wiegel (1959) discuss the dredging and sand bypassing at Santa Barbara Harbor, and the downcoast beach nourishment. Herron and Harris (1966) describe the sand traps at Port Hueneme and Channel Island Harbor and estimate the amount of beach material trapped and bypassed. These sand traps are also discussed in USACE LAD (1970).

Table 6.5-1

River Discharge and Drainage Area

<i>Stream</i>	<i>Average Discharge</i> (acre-feet per year)	<i>Drainage Area</i> (square miles)
Carpinteria Creek	1,240	15
Ventura River	43,220	210
Santa Clara River	132,630	1700
Calleguas Creek	1,090	250

Data from topographic maps and U.S. Geological Survey Water Supply Paper 1735 (from Judge, 1970).

Discharges are averages of available years at every station, but more than five years as a minimum. Areas are by planimetric determinations to the nearest 10 square miles.

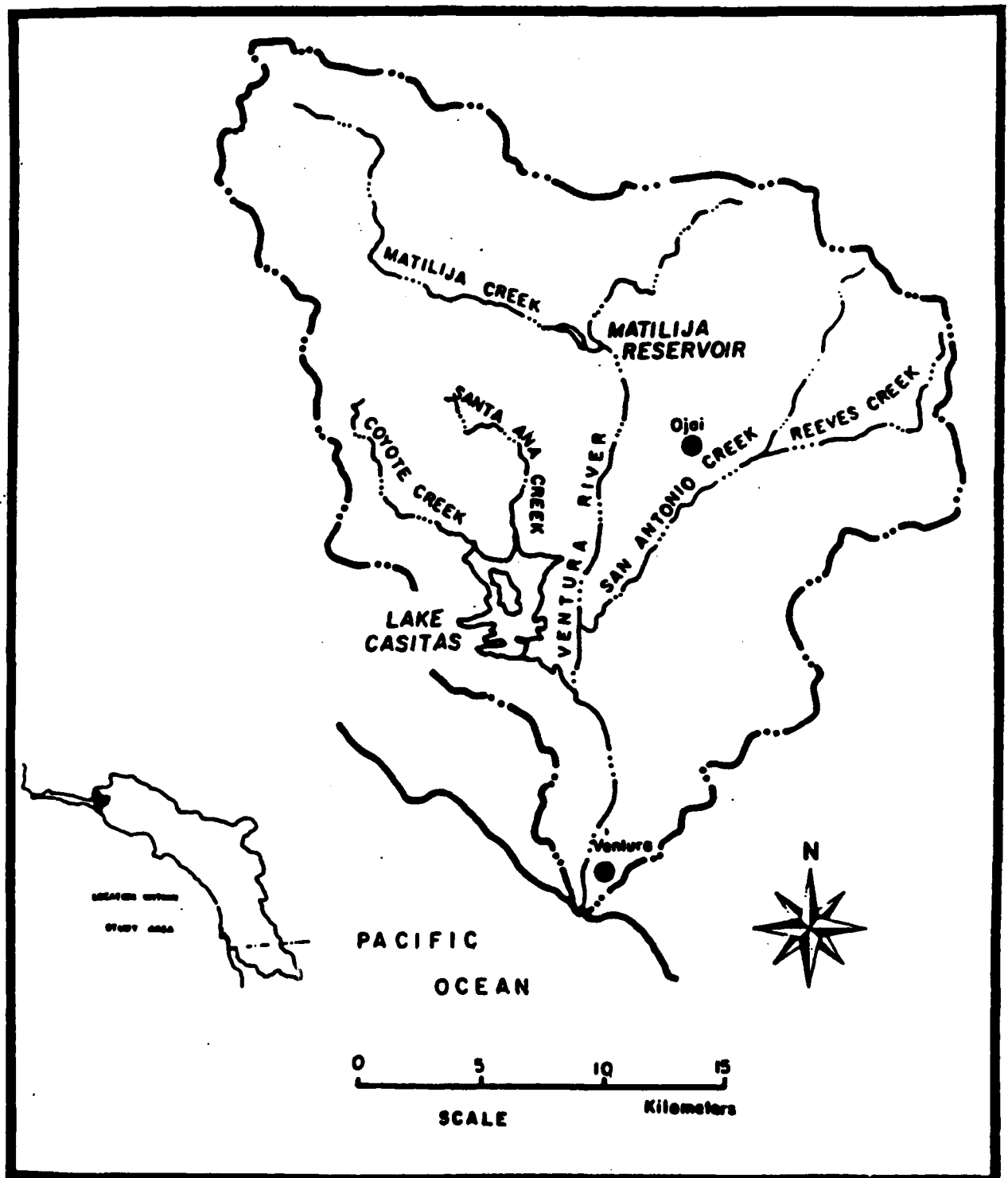


Figure 6.5-1. Ventura River Basin (from Brownlie and Taylor, 1981).

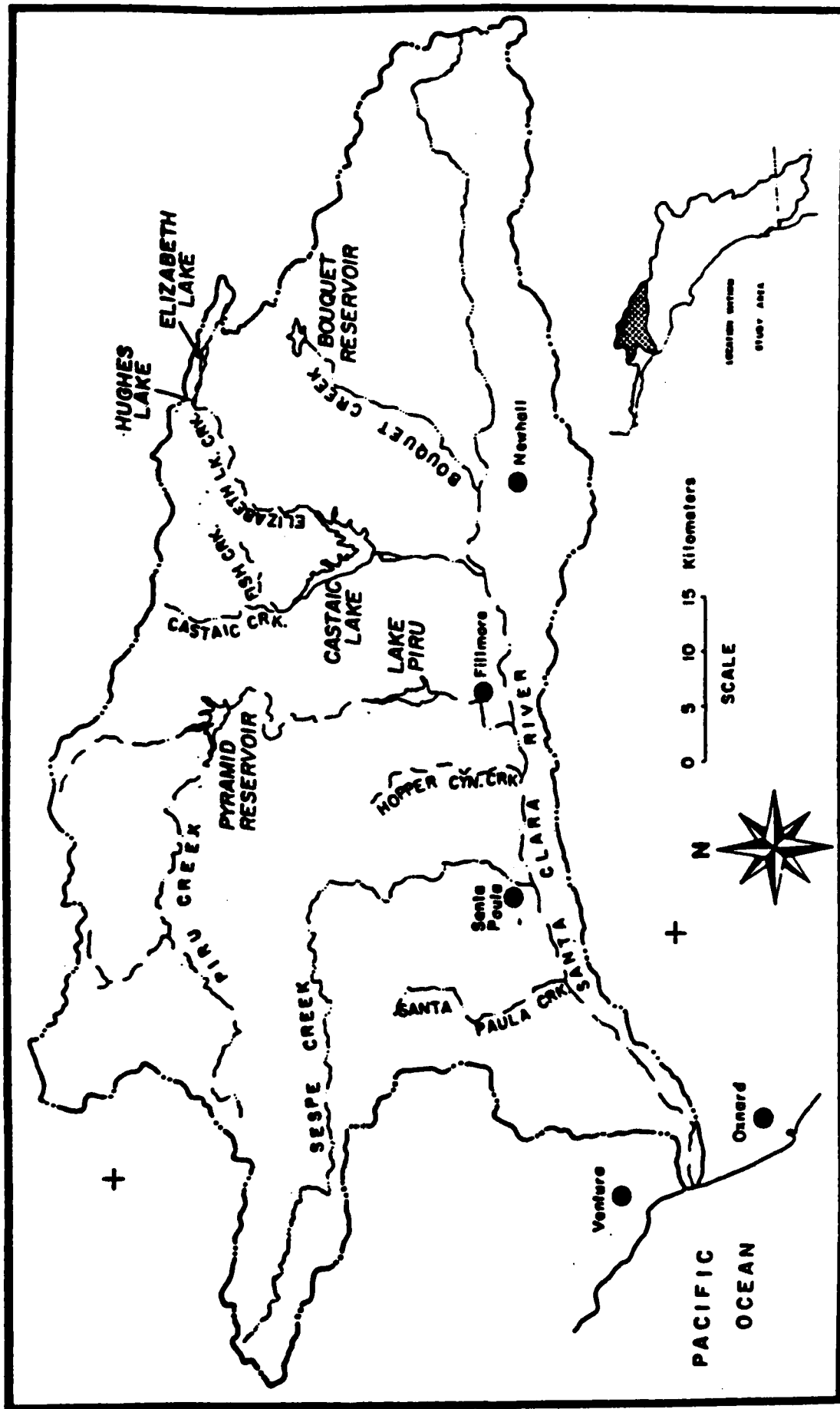


Figure 6.5-2. Santa Clara River basin (from Brownlie and Taylor, 1981).

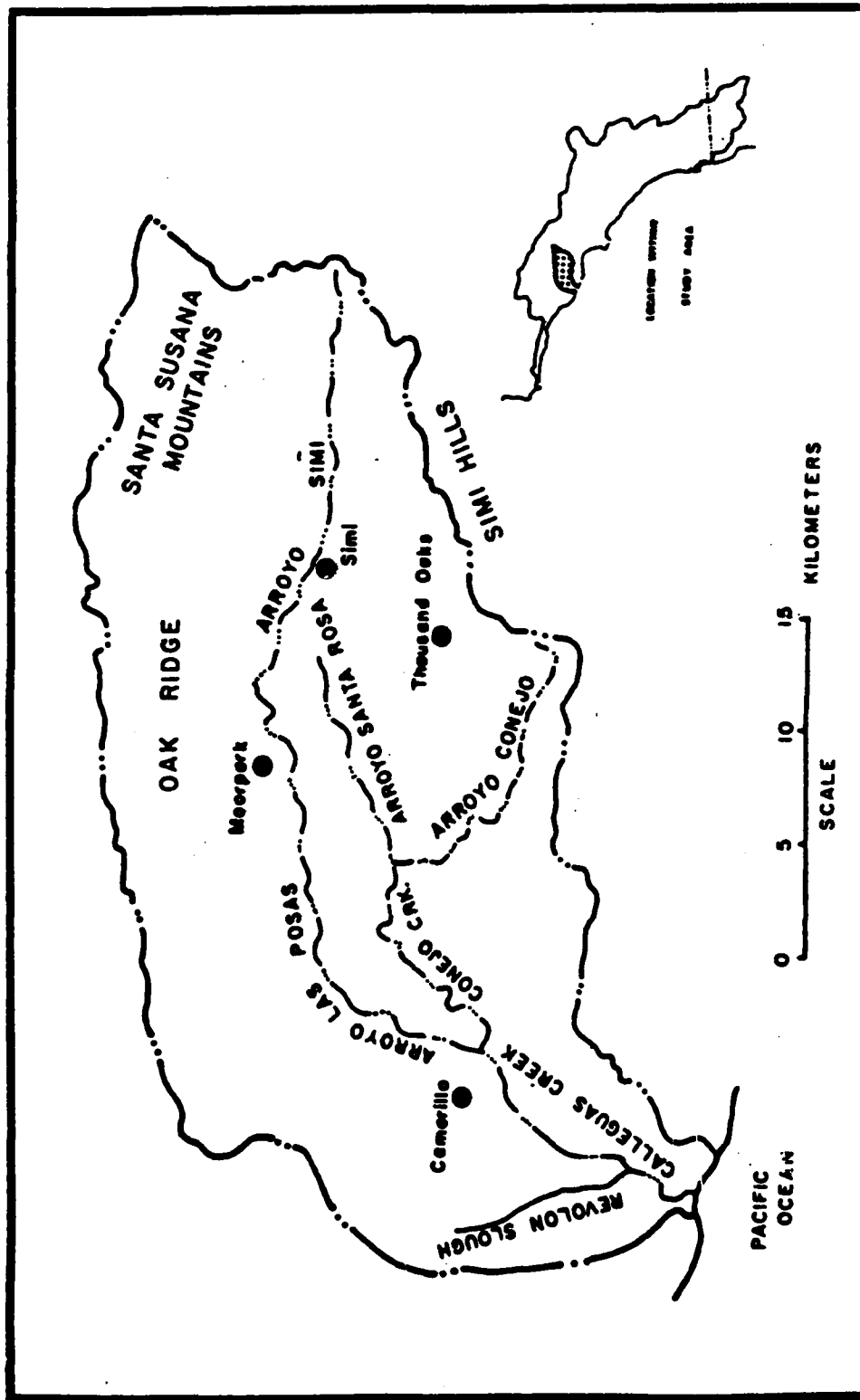


Figure 6.5-3 . Calleguas Creek basin (From Brownlie and Taylor, 1981).

NO-A166 699

COAST OF CALIFORNIA STORM AND TIDAL WAVES STUDY
SOUTHERN CALIFORNIA COAST (U) ARMY ENGINEER DISTRICT
LOS ANGELES CA COASTAL RESOURCES BRANC.

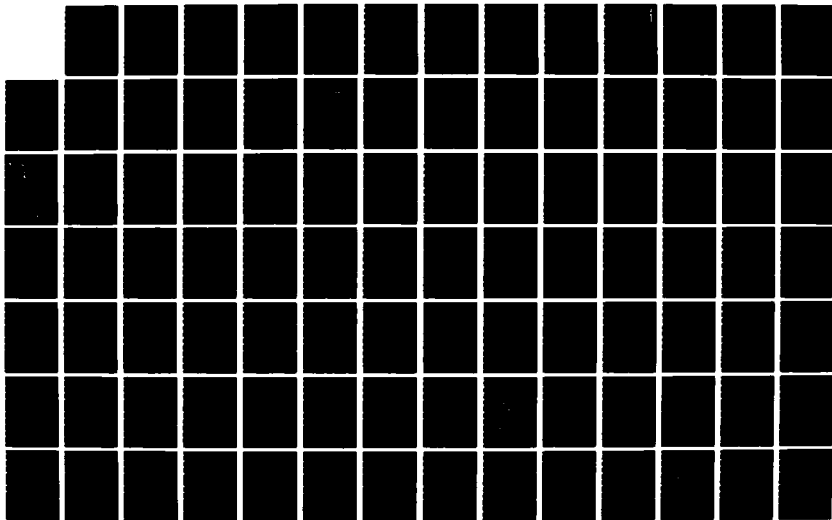
4/7

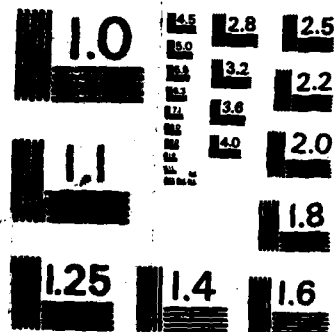
UNCLASSIFIED

D L INMAN ET AL FEB 86 CCSTWS-86-1

F/G 8/3

NL





California (1977b) is a compilation of information on sediment transport in coastal stream basins and beach nourishment. The findings provide order of magnitude estimates of sediment production and locations of abundant inland sources of material for beach nourishment. Herron (1980) describes the Santa Barbara Littoral Cell and discusses the erosion problem and artificial beach nourishment projects.

Shaw (1980) outlines artificial sediment transport in this littoral cell. The report includes a table showing fill location, source of material, volume of sand and date of nourishment. The report is very thorough and contains most of the basic facts available on beach nourishment projects in southern California. Hobson (1982) discusses the effectiveness of beach fill at the Channel Island Harbor area. Brown (1983) mentions that 535,000 m³ of material is dredged yearly from the Channel Island Harbor and is deposited on the south side of Port Hueneme to combat erosion problems at Port Hueneme and Oxnard Beaches.

6.6 SEDIMENT TRANSPORT MODES

6.6.1 *Cross-shore Transport*

Seasonal beach cycles were studied in Santa Barbara County as early as 1950 at Rincon and Goleta beaches (Shepard, 1950c, Figure 4.6-1). Gable (1981) describes an experiment performed at Leadbetter Beach in Santa Barbara in 1980. One of the tasks was to quantify seasonal and net cross-shore transport. Data used for this task included monthly beach profiles for a few years, daily profiles for one month, and wave and current measurements. The results are currently in press as the National Sediment Transport Study monograph. Bailard and Jenkins (1982) describe seasonal cross-shore transport at Carpinteria, east of Santa Barbara. They estimate the average seasonal shoreline excursion as 68 ft.

Net cross-shore transport is much more difficult to quantify, because it is usually so much smaller than seasonal changes. Bowen and Inman (1986) observed no evidence of net cross-

shore transport when comparing bathymetric profiles between Pt. Conception and Gaviota. Pollard (1979) found almost entirely clay and silt deposits on the Santa Barbara County shelf, indicating little offshore transport of sand from beaches. Offshore transport of river-borne silt and clay may be considerable, however (Drake, Kolpack and Fischer, 1972). Shaw (1982) reports dramatic offshore transport of $140 \text{ m}^3/\text{m}$ of beach during a 17-day period on a beach just upcoast of Santa Barbara Harbor. Investigators in the NSTS experiment (Dean et al., 1982) found that nearly all of this sediment returned either to the same beach or moved longshore into or past the harbor.

There is a long history of beach profiling in Ventura County, but few cases in which cross-shore transport rates have been computed. Inman (1950a) gives a detailed descriptive history of the cross-shore and longshore motions induced by the complicated topography near Mugu Lagoon. Volume changes on beach profiles in the Ventura area are listed in USACE LAD (1961a) from 1938 to 1959. However, it appears that seasonal and net changes have not been separated. Volume changes between 1960 and 1961 at Port Hueneme can be found in USACE LAD (1962b).

Drake, Kolpack and Fischer (1972) examined the process of offshore transport, primarily of river-borne sediments, past the surfzone and onto the shelf during floods. Most of the sediment was silt and clay from the Ventura and Santa Clara Rivers. They found that concentrations were highest in the middle of the water column rather than a density flow along the bottom. During a flood in 1969 they documented the flow of 50 million metric tons of silt and clay, more than 70% of which was initially deposited shallower than 30 ft. deep. Their report deals only with silt and clay, not sand-size material.

Brown (1983) performed statistical calculations of space and time relationships between profiles on Ventura County beaches. Data consisted of daily observations of profiles and waves. No attempt was made to compute transport rates, to separate long-term and short-term

changes, or to separate seasonal and net changes.

Orme and Brown (1983) detail seasonal cross-shore motions at Pt. Mugu. They document the seasonal migration of bars and troughs in the area. However, cross-shore transport rates are not computed.

6.6.2 Longshore Transport

Longshore transport rates for this cell are summarized in Table 6.6-1. "Potential" rates are obtained from application of the standard "stress-flux" equation (Section 2.4) with wave data as inputs. Both volume transport Q_l (yd³/yr) and immersed-weight transport I_l (newtons/second) are listed. In converting between the two measures, it was assumed that solids concentration $N_o = 0.6$ (porosity = 0.4) and sand density $\rho_s = 2.65$ g/cm³. Positive values represent downcoast transport to the east or south, negative values upcoast.

The longshore transport rate is not relatively uniform throughout this cell, as in some others (i.e., Oceanside). The general trend is an increasing rate as one proceeds downcoast (east). At the rocky cliff area at the west end of the cell transport is relatively small, increasing to hundreds of thousands of yd³/yr at Santa Barbara, and exceeding a million yd³/yr at the eastern end of the cell, largely due to the input of the Santa Clara River.

Sources, transport rates and sinks all generally increase from east to west. Because of this large geographical variance and the large number of reports on transport for this cell, transport rates will be discussed in each area in turn, from west to east: Pt. Conception to Goleta, Goleta area, Santa Barbara, Ventura/Oxnard, Hueneme/Channel Island Harbors, and Pt. Mugu.

Trask (1955) and Judge (1970) used sand mineralogy studies to give some evidence of transport around Pt. Conception but were unable to quantify it. Duane and Judge (1969) attempted to measure transport around Pt. Conception with radioactive sand tracer. They concluded there was no measurable transport but admitted their methods may have been faulty.

Table 6.6-1. Longshore Transport Rates
(Positive values indicate transport to the south, negative to the north)

Location	Notes	Reference	Potential Transport (Wave Refraction Studies)		Gross Transport (Trapping Studies)		Instantaneous Net Transport (Sand Tracer Studies)	
			Q_1 ($10^3 \text{ yd}^3/\text{yr}$)	I_1 (N/sec)	Q_1 ($10^3 \text{ yd}^3/\text{yr}$)	I_1 (N/sec)	Q_1 ($10^3 \text{ yd}^3/\text{yr}$)	I_1 (N/sec)
Gato	Insufficient sand supply for this potential rate	Bowen and Inman (1966)	100	24				
*Goleta Point	Average of several experiments	Ingle (1966)					259	61
*Santa Barbara	Harbor dredging	Johnson (1957)			280	66		
Santa Barbara	Harbor profiling	Dean et al (1982)			333	78		
Santa Barbara	No refraction < 10 m deep	Seymour and Castel (1984)	58	14				
Santa Barbara	Range of values for varying conditions	White and Inman (in press, b)					210 to 8700	50 to 2050
Santa Barbara	Harbor bypassing	Bailard and Jenkins (1982)			255	53		
*Carpenteria	Harbor bypassing plus creek yield	Bailard and Jenkins (1982)			255	60		

* "Best" estimate at that location

Table 6.6-1 . Longshore Transport Rates (Cont'd.)
(Positive values indicate transport to the south, negative to the north)

Location	Notes	Reference	Potential Transport (Wave Refraction Studies)		Gross Transport (Trapping Studies)		Instantaneous Net Transport (Sand Tracer Studies)	
			Q_1 ($10^3 \text{ yd}^3/\text{yr}$)	I_1 (N/sec)	Q_1 ($10^3 \text{ yd}^3/\text{yr}$)	I_1 (N/sec)	Q_1 ($10^3 \text{ yd}^3/\text{yr}$)	I_1 (N/sec)
Carpenteria		Baillard and Jenkins (1982)	269	63				
Punta Gorda	Visual wave data	USACE LAD (1979)	361	85				
Ventura	Harbor dredging	Rod Lundin (1978)			500	118		
Oxnard area	Harbor profiling	Bruno and Gable (1972)			210- 1710	49- 402		
*Oxnard area	Sand bypassing	Inman (1976)			1250	294		
Oxnard area	Harbor profiling	Hobson (1982)			600- 1260	141- 296		
Oxnard area	Visual wave data	USACE LAD (1979)	-165 to 950	-39 to 224				
Pt. Mugu	Visual wave data	USACE LAD (1979)	325	73				
Pt. Mugu	One day's rate	Duane and James (1980)					3160	744

* "Best" estimate at that location

Pollard (1979) performed statistical tests on much of Judge's (1970) data and found several conclusions to be statistically unjustified or faulty. In particular, Pollard (1979) found that the augite distribution heavily relied on by Trask (1955) and Judge (1970) to be incorrect. For this reason and insufficient sand supply, he also cautions that the $100 \times 10^3 \text{ yd}^3/\text{yr}$ longshore transport rate at Gato reported by Bowen and Inman (1966) must be considered a potential rate, not actual transport. Bowen and Inman (1966) obtained their estimate of $100 \times 10^3 \text{ yd}^3/\text{yr}$ easterly transport at Gato (Figure 5.6-1) from wave data and the stress-flux equation. Seasonal variation of the transport is listed in Table 5.6-2. Transport is strongly to the east in all seasons, but with occasional westerly transport in the winter.

Ingle (1962, 1966) performed fluorescent sand tracer studies at Goleta Point, about 10 miles west of Santa Barbara. The sand velocities and transport rates are reported in Ingle (1966). He reported an active transport thickness of 0.064 in (0.16 cm), grain velocities in the range of 7-23 ft/min (3-6 cm/s), and transport rates ranging from 80 to 2700 yd^3/day ($29\text{-}985 \times 10^3 \text{ yd}^3/\text{yr}$). The mean measured transport was $259 \times 10^3 \text{ yd}^3/\text{yr}$.

Ever since construction of the Santa Barbara Harbor in 1927, periodic dredging and beach profiling have provided estimates of longshore transport at this total trap. Johnson (1957) reported easterly net transport of $280 \times 10^3 \text{ yd}^3/\text{yr}$, probably the only transport estimate in his report which has not subsequently been altered by man's intervention on the coast. Trask (1955) points out that this transport is somewhat more uniform from year-to-year than variation in sand supply sources might suggest. He explains that the floods which bring large quantities of sand to the coast deposit most of the sand offshore at up to 10 m deep. These offshore sand reservoirs then act as a source for longshore transport over several years.

Gable (1981) reports on the tasks involved in a multi-faceted study of transport rates at Santa Barbara in January-February 1980, the National Sediment Transport Study. Measurements were made of beach profiles, suspended load, bedload, currents and waves.

Independent measures of transport included a sand-tracer study (White and Inman, in press.b), volumetric suspension sampling (Zampol and Inman, in press), optical backscatter of suspended load (Sternberg, Shi and Downing, 1984), and harbor profiling (Dean et al., 1982).

Dean et al's (1982) profiling study of the harbor yielded a measure of $253 \times 10^3 \text{ m}^3/\text{yr}$ net annual transport for 1979-80. Because their last survey period extended their measurements beyond one year, we obtained the estimate of $253 \times 10^3 \text{ m}^3/\text{yr}$ by adding the values for the remaining intersurvey periods.

The radiation stress was measured at two nearshore sites at Santa Barbara by pressure-sensor arrays. Castel and Seymour (1982) applied the stress-flux equation and obtained estimates of 38 and $47 \times 10^3 \text{ m}^3/\text{yr}$ (50 and $62 \times 10^3 \text{ yd}^3/\text{yr}$) annual easterly transport for 1980 and 1981. Seymour and Castel (1984a) added the value of $46 \times 10^3 \text{ m}^3/\text{yr}$ ($61 \times 10^3 \text{ yd}^3/\text{yr}$) for 1982. The waves used in these studies were not refracted into the beach from the sensors at 9 m depth. They assumed for the purpose of these calculations that topography was straight and parallel shoreward of the sensors, which was often not the case. Thus their transport estimates (columns 2 and 3 of Table 9.6-6) may not be reliable. However, their measures of variability and episodicity of transport (columns 4 and 5 of Table 9.6-6) are useful, since they are relative measures. Note that daily transport can be as large as 3-8% of the total annual transport. Also 50% of the year's transport can occur during only 10-18% of the days. Thus transport during storm periods can be much larger than might be assumed merely from knowledge of the annual rate. White and Inman (in press,b) measured the transport with sand tracer on days with wave conditions ranging from some of the lowest to the highest ever encountered at Santa Barbara. Their measures of total transport (sand-tracer bedload plus volumetric suspension sampling) ranged from 50 to 2050 N/s ($213\text{-}8713 \times 10^3 \text{ yd}^3/\text{yr}$). These measures give an idea as to the amount by which transport can vary day-to-day. Daily transport of $25 \times 10^3 \text{ yd}^3$ is possible during storms.

Sternberg, Shi and Downing (1984) measured suspended load with optical backscatter sensors. Their measure of the portion of total transport represented by suspended load above 10 cm from the bed (15-20% of total load) agrees with data obtained from volumetric sampling (Inman et al., 1980; Zampol and Inman, in press). But they obtain large values of suspension close to the bed. It is unclear whether this transport is bedload, suspended load or sand entrained by turbulence around their instrument. Their measures of suspended transport, including the values close to the bed, ranged from 44 to 520 N/s ($187-2210 \times 10^3 \text{ yd}^3/\text{yr}$). Bailard and Jenkins (1982) estimated longshore transport at Carpinteria, about 10 miles east of Santa Barbara. Their wave-refraction study, utilizing the radiation-stress equation, estimates annual transport as $314 \times 10^3 \text{ yd}^3/\text{yr}$ to the east, $45 \times 10^3 \text{ yd}^3/\text{yr}$ to the west, with a net easterly transport of $269 \times 10^3 \text{ yd}^3/\text{yr}$. They compare this value with $255 \times 10^3 \text{ yd}^3/\text{yr}$ obtained by adding the recent Santa Barbara bypassing rate ($225 \times 10^3 \text{ yd}^3/\text{yr}$) to the estimated yield from creeks between the two sites ($30 \times 10^3 \text{ yd}^3/\text{yr}$).

Longshore transport has been estimated at several sites in Ventura County by USACE LAD (1979). Unfortunately, their estimates are all based on visual (LEO) wave observations, and thus are subject to great error. The sites at which observations were made, and transport computed with the radiation-stress equation, are shown in Figure 6.6-1. The transport estimates are listed in Table 6.6-1 as averages over the 3-4 years of data. Note that not only do the values disagree with data from traps, but even the sign (upcoast vs. downcoast) is sometimes wrong. Rod Lundin and Associates (1978) use dredging records to point out that dredging at Ventura Harbor averages to $500 \times 10^3 \text{ yd}^3/\text{yr}$.

Several estimates of longshore transport are available in the area of Oxnard, Channel Islands Harbor and Port Hueneme. Bruno and Gable (1976) and Bruno et al (1978) use 18 months of profiling records from Channel Islands Harbor to record southerly transport rates ranging from 160 to $1300 \times 10^3 \text{ yd}^3/\text{yr}$. For purposes of comparison, they computed estimated

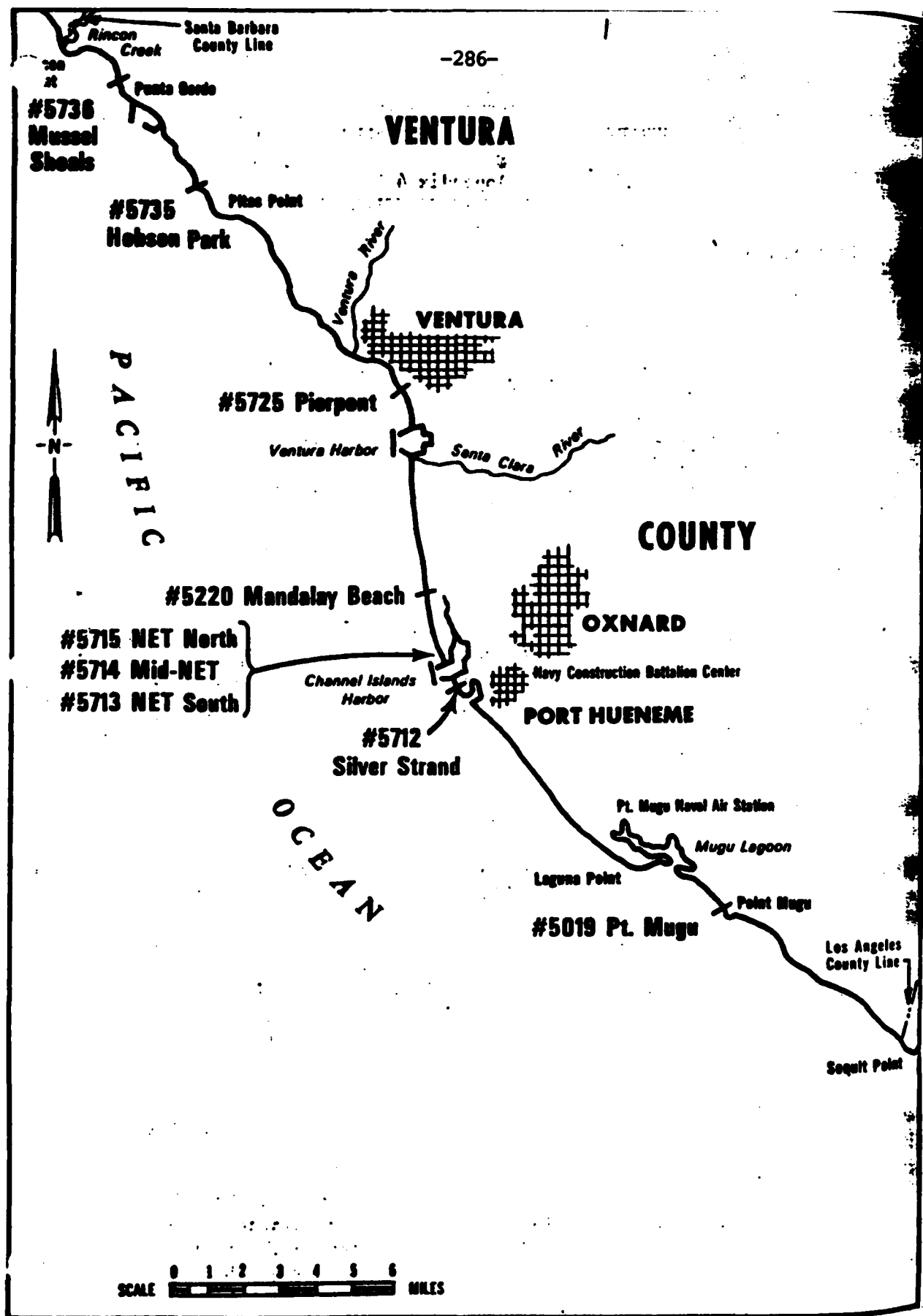


Figure 6.6-1. Location map for LEO visual wave observation sites in Ventura County (from USACE LAD, 1979).

transport from visual (LEO) observations and obtained estimates only half as large as the measured rates. Both the USACE LAD (1979) and Bruno and Gable (1976) studies seem to underestimate transport when using LEO visual wave data.

Inman (1976) sums all the upcoast sediment contributions and arrives at a sediment supply of $1230 \times 10^3 \text{ yd}^3/\text{yr}$ for the Oxnard area. He estimates transport from the Channel Islands bypassing as $1250 \times 10^3 \text{ yd}^3/\text{yr}$. Inman (1981) also points out that another estimate of transport could be the $800 \times 10^3 \text{ yd}^3/\text{yr}$ sum of bypassing around Ventura Marina and erosion from the Santa Clara River delta, each about $400 \times 10^3 \text{ yd}^3/\text{yr}$. Hobson's (1982) bathymetric measurements of trapping at Channel Island Harbor yielded transport rates of $460\text{-}960 \times 10^3 \text{ yd}^3/\text{yr}$.

Duane and James (1980) performed a sand tracer experiment just upcoast from Pt. Mugu. They measured transport over a one-day period at $2400 \times 10^3 \text{ yd}^3/\text{yr}$. This is not necessarily the annual average rate.

In conclusion, transport in the cell is from west to east, with only small intermittent, usually wintertime, transport to the west. Net transport is about $280 \times 10^3 \text{ yd}^3/\text{yr}$ at Santa Barbara and about $1250 \times 10^3 \text{ yd}^3/\text{yr}$ along the Oxnard Plain at the east end of the cell.

6.6.3 *Wind Transport*

Inman (1950a) reports that wind velocities are sufficiently high in the Ventura-Oxnard area to allow wind transport both onshore and offshore. He points out the extensive dunes behind the beach, extending from the Santa Clara River mouth to Mugu Lagoon. Northwest of Hueneme the dunes are aligned, such that a net southeast onshore wind transport is indicated. He also observed a large dune two miles east of Pt. Mugu where sand has blown across a highway and formed a dune several hundred feet high. During a one-day period, Inman (1950a) also observed net offshore wind transport. One inch of sand was lost from the berm during winds of 12 mph with gusts to 25 mph.

Bascom's (1951) observations on beaches near Santa Barbara indicate that wind is relatively unimportant at the western end of the cell. However, there are some west-facing beaches where active dune building is taking place (Pollard, 1979). On these beaches, wind blows onshore 68% of the time and offshore 3% of the time. Pollard (1979) used measured wind speeds in the Santa Barbara area and wind-transport equations to estimate that the offshore wind transport rate is 7.5% of the onshore rate, in good agreement with Bowen and Inman's 5% estimate.

Inman (1976) suggests that net onshore transport by wind and subsequent dune building may be smaller in the Oxnard area than it was in the past. It appeared that the sand supply exceeded the longshore transport potential before man's intervention in the area. Excess sand was then carried inland by the wind. After damming of the rivers, the excess supply was cut off, so dunes may no longer be actively forming.

Inman (1981) details the extensive problems encountered and special steps that must be taken to prevent dune erosion, motion and possible burial of structures when construction in these dune areas is contemplated.

6.7 SEDIMENT SINKS

6.7.1 *Submarine Canyons*

There are two submarine canyons in this cell, Hueneme and Mugu (Figure 6.7-1). Hueneme Canyon terminates about one mile from the beach. Mugu Canyon extends to the surfzone. Its two branches are located 2000 ft east and 1000 ft west of Mugu Pier (Inman, 1950b). In order to illustrate loss of sand down Mugu Canyon, Inman (1950b) examined sediment samples in the area. He found that the sand in the canyon head differs from continental shelf sand. The canyon sand is less sorted and has an asymmetrical size distribution, indicative of a mixture of coarse beach sand and fine shelf sand.

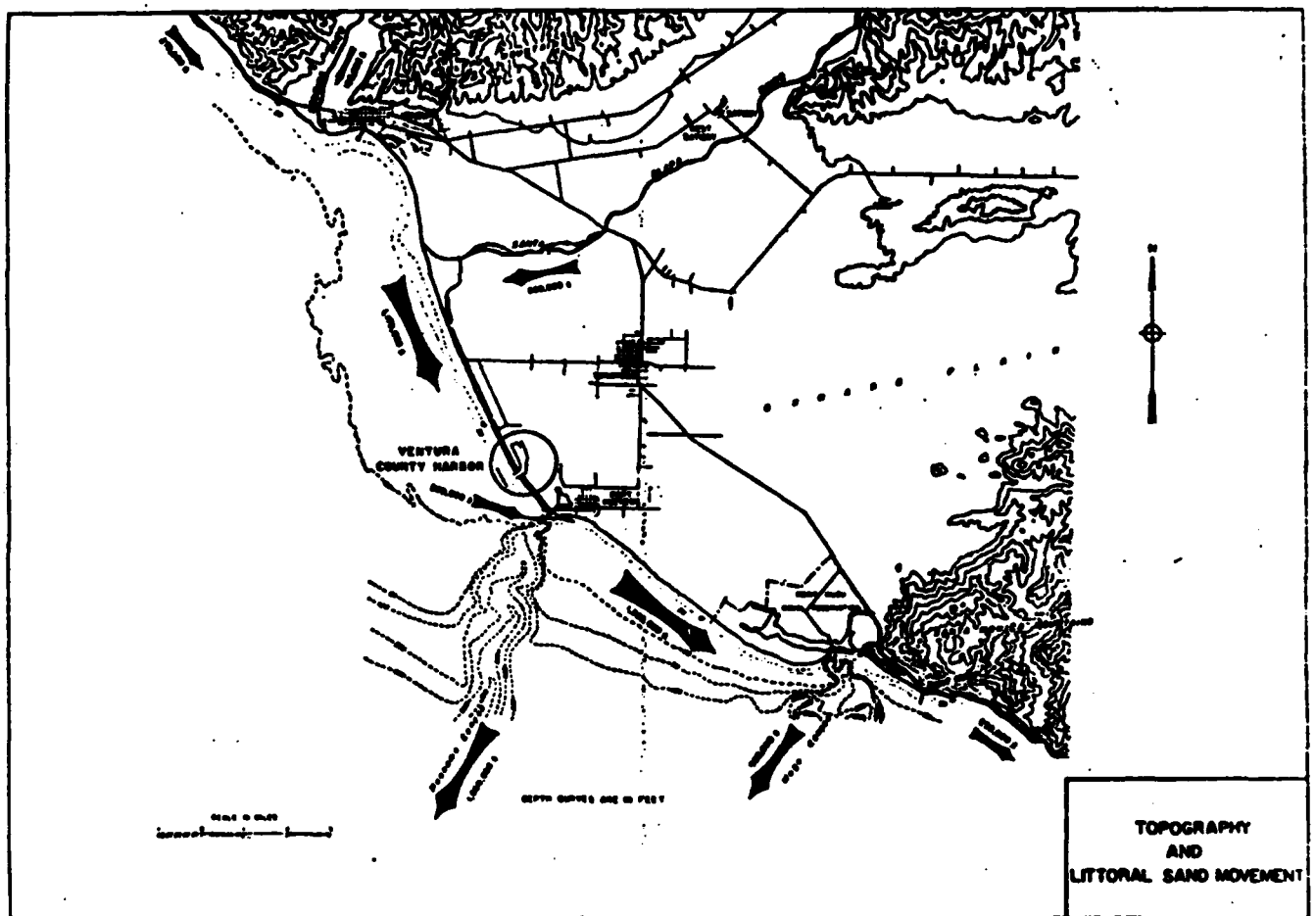


Figure 6.7-1. Location map for Hueneme and Mugu Submarine Canyons (from Herron and Harris, 1966).

Herron and Harris (1966) used a simple sand budget of the area (Figure 6.7-1) to conclude that loss down each of the canyons is about one million yd^3/yr . However, these figures are now out of date because of the effects of new coastal structures (Inman, 1976). Inman points to three different transport/sink scenarios in recent history. Prior to construction of Channel Islands and Port Hueneme Harbors, most of the sand was transported along the beach past Hueneme Canyon, which is far from the beach. Most sand was lost down Mugu Canyon, with some continuing along the coast to the next cell. The second scenario began with the construction of the Port Hueneme harbor jetties, which diverted sand down Hueneme Submarine Canyon at a rate of $1 \times 10^6 \text{ yd}^3/\text{yr}$, based on erosion rates to the south. The third and current transport scenario began with the impoundment and bypassing at Channel Islands Harbor and Port Hueneme. The bypassed sand is now transported south, where most enters Mugu Submarine Canyon (about $1 \times 10^6 \text{ yd}^3/\text{yr}$) and the relatively small remainder continues into the next cell.

6.7.2 *Entrapment by Harbors, Bays and Estuaries*

The structures now at Santa Barbara Harbor (Figure 6.7-2) include a 6970 m concrete breakwater, a 30 m groin, and a wharf. The original 1927-29 breakwater left a 180 m open section at the shore end. This resulted in sand accumulation there, and the open section was built over in 1930 (Shaw, 1980). The result of harbor construction has been upcoast sand accumulation forming Leadbetter Beach, continued shoaling of the harbor channel, and downcoast erosion. With the original breakwater construction, a wave of erosion proceeded downcoast. Various authors have observed different parts of this scenario. Their comments will now be detailed.

Wiegel (1959) reports on the dredging and bypassing history up to that date. In 1935, $200 \times 10^3 \text{ yd}^3$ of sand was dredged from the harbor and placed one mile east at 22 ft depth. It was expected that this material would move onshore to help alleviate erosion, but it stayed in place,

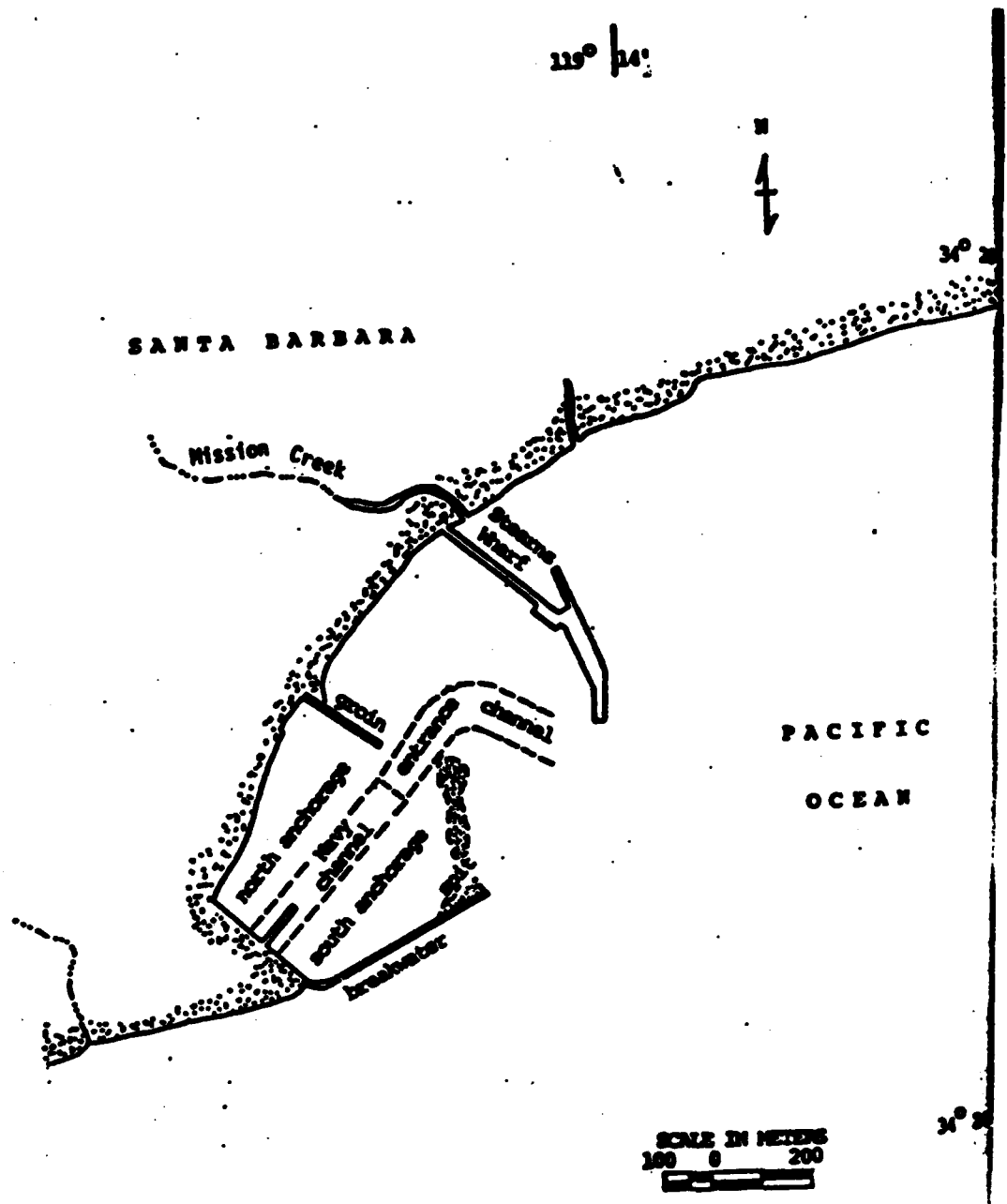


Figure 6.7-2. Santa Barbara Harbor (from Shaw, 1980).

according to bathymetric surveys (Wiegel, 1959). During the 1934-52 period, sand was bypassed with a pipeline dredge on a biannual basis. Harbor profiling, dredging records and bypassing records combine to give a measure of $270 \times 10^3 \text{ yd}^3/\text{yr}$ for the net annual transport (Wiegel, 1959).

A detailed historical summary of Santa Barbara Harbor may be found in Pollard (1979). The wave of erosion initiated by the breakwater construction is described. The biannual bypassing since 1934 apparently halted further erosion, but did not counteract the original erosion wave. In 1955 the city decided to dredge on a continual basis, in order to maintain the sand spit at the breakwater end, for protection against waves from the southeast. Despite two Marine Consultant reports advising continual dredging, the dredging program was abandoned in 1972. Periodic dredging is still employed to alleviate continual harbor shoaling. Dredging history from 1972 to 1980 may be found in Shaw (1980), with more recent dredging and profiling in Dean et al (1982). In 1973 an 850 ft timber bulkhead was constructed along the sand spit to protect the harbor from southeasterly waves, with reasonable success (Pollard, 1979).

Bailard and Jenkins (1982) present the most complete description to date of harbor effects, dredging, profiling, erosion and accretion. They estimate gross transports of $325 \times 10^3 \text{ yd}^3/\text{yr}$ to the east, $100 \times 10^3 \text{ yd}^3/\text{yr}$ to the west, and thus net easterly transport of $225 \times 10^3 \text{ yd}^3/\text{yr}$.

The next harbor along this coastline is the Ventura Marina (Figure 6.7-3). The three breakwaters were built in 1963. The breakwaters severely interrupted the flow of sand, causing immediate upcoast accretion and downcoast erosion. Inman (1981) expressed concern as to why structures which would nearly totally block longshore transport were built on a section of coastline which was widely known to have one of the highest longshore transport rates in southern California.

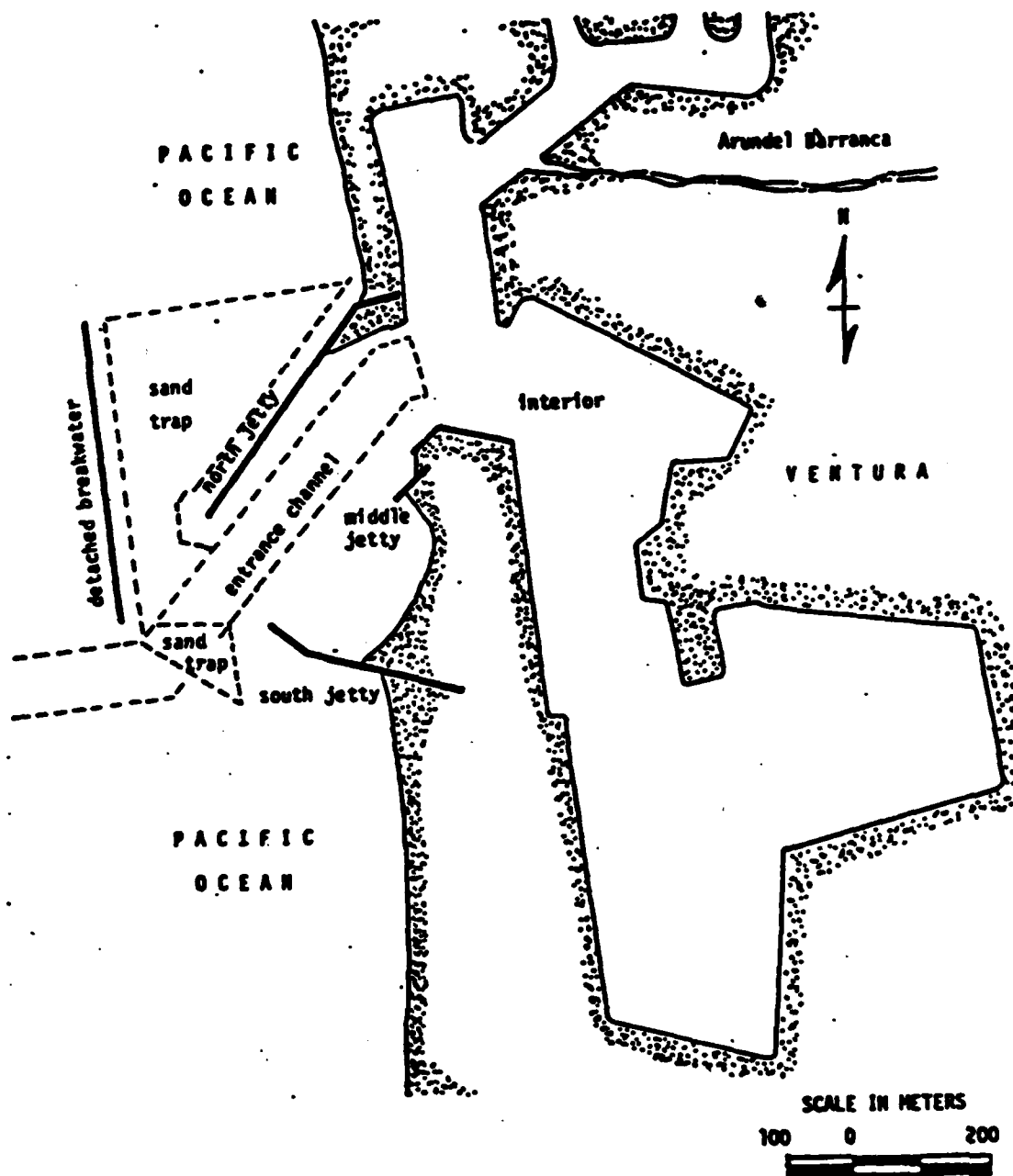


Figure 6.7-3. Ventura Marina (from Shaw, 1980).

USACE LAD (1979, 1980a) present construction details for the marina along with the history of the 452 m detached breakwater/sand trap system completed in 1972. Periodic dredging is now used to transfer sand from the trap to beaches to the south. It has been proposed to introduce a continual bypass system, the details of which are in Rod Lunden and Associates (1978).

Dredging and beach-fill histories for Ventura Marina may be found in Shaw (1980). Unfortunately, inadequate beach profiling prevents good estimates of longshore transport from the marina sand trap and jetties.

Channel Islands Harbor and Port Hueneme Harbor have had considerable effect on downcoast beaches and on loss of sand down submarine canyons, as detailed in section 6.7.1. Channel Islands Harbor consists of two 400 m jetties and a 700 m detached breakwater completed in 1960 (Figure 6.7-4). It was constructed as a small-craft harbor. The breakwater is intended to trap sand for bypassing. Port Hueneme Harbor shore structures consist of two approximately 300 m-long jetties constructed in 1940, with a small groin and a pier near the west jetty (Figure 6.7-5). It was originally a small boat harbor but was taken over and expanded by the Navy in 1942.

Herron and Harris (1966) give a detailed history of the two harbors and their effects on the beaches. They report a fairly constant downcoast erosion rate of $1.2 \times 10^6 \text{ yd}^3/\text{yr}$, a measure of the longshore transport in this area. The dredging history for Channel Islands Harbor may be found in USACE LAD (1970). Inman (1976) also reports the $1.2 \times 10^6 \text{ yd}^3/\text{yr}$ transport rate and gives a description of the interrelationship of construction impacts along this section of coastline; possible solutions to the problems caused by the harbors are presented.

Bruno and Gable (1976) present a short-term dredging and profile history for Channel Islands Harbor during 1974-75, by which they estimate transport rates. Bruno et al (1977) add grain size data to the study and also compare measured shoreline changes due to the breakwater

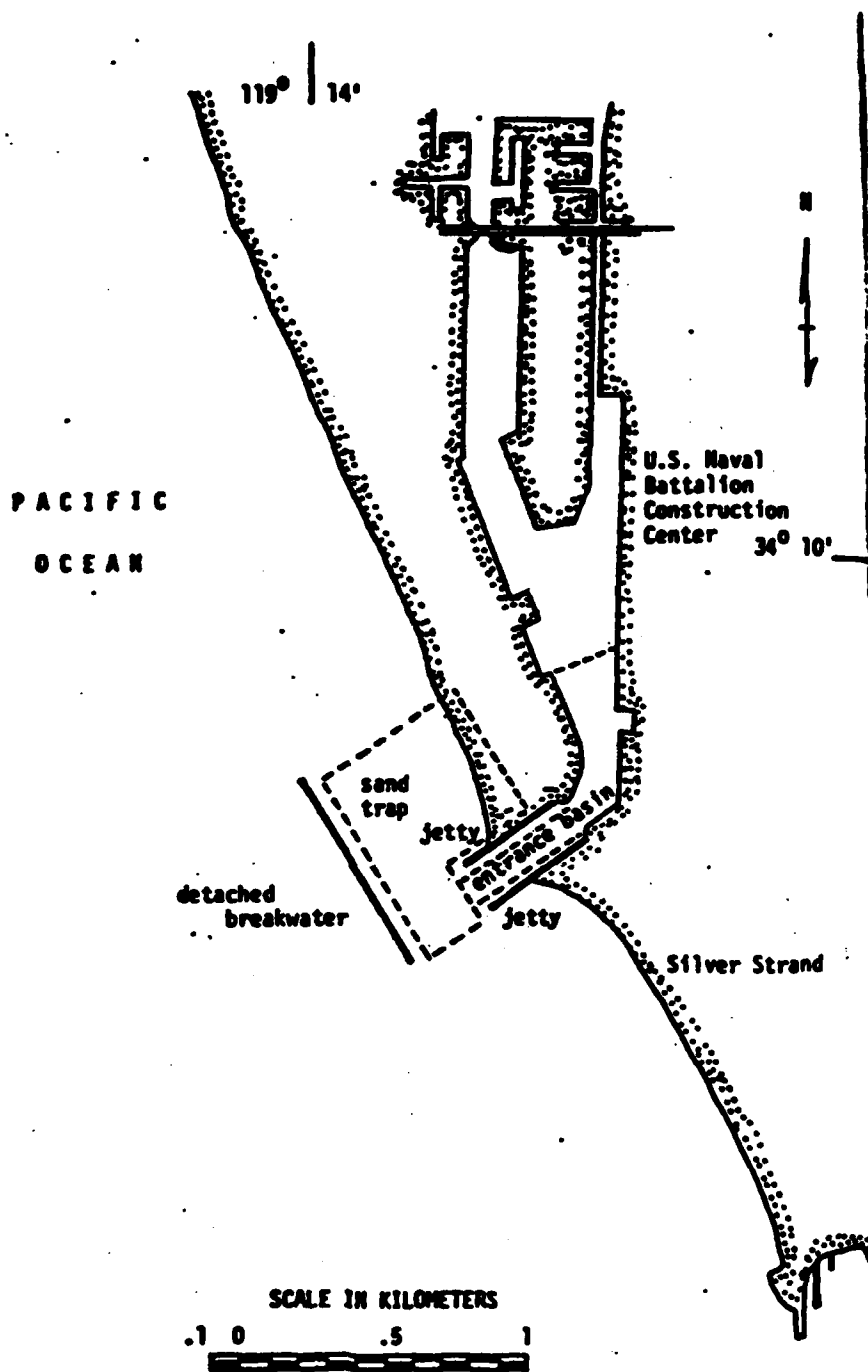


Figure 6.7-4. Channel Islands Harbor (from Shaw, 1980).

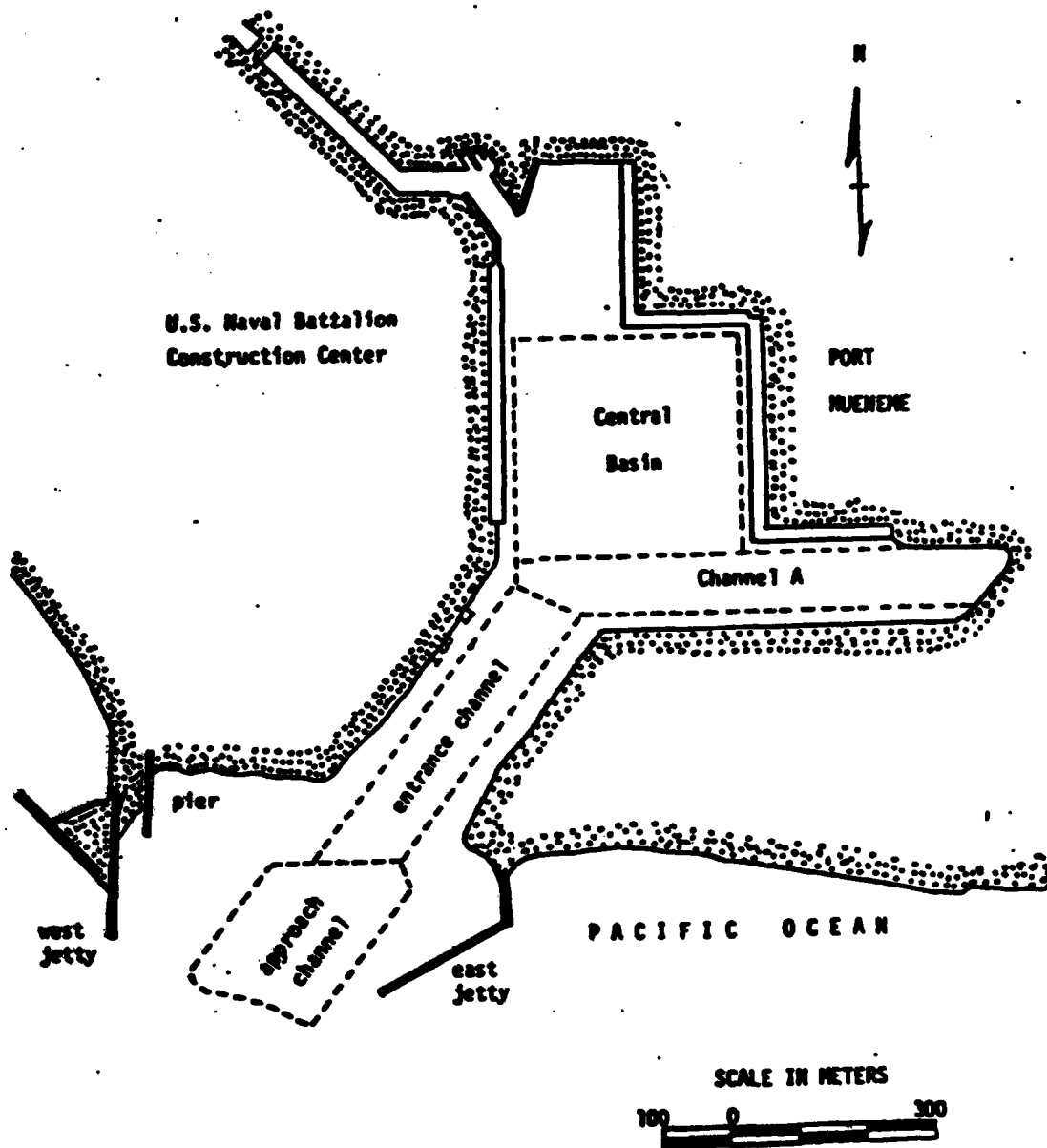


Figure 6.7-5. Port Hueneme (from Shaw, 1980).

construction with predicted changes. Bruno et al (1981) add wave-gauge data to this ongoing study of transport relations. The validity of the previous reports had been severely hampered by the availability of only visual wave data.

A detailed dredging and beach-fill history of both Channel Islands and Port Hueneme Harbors is presented in Shaw (1980). A descriptive history of Channel Islands Harbor may be found in Hobson (1982).

Perlin and Dean (1983) test a model intended to simulate the effects of the Channel Islands breakwater. Inputs to the model include wave and topography measurements and the structure design. The model includes such effects as refraction and diffraction, but uses linear waves, simplified spectra, and laboratory-generated cross-shore distribution of longshore transport. Nevertheless, it appears useful for prediction of first-order effects. It correctly predicted general areas of accretion and erosion at the breakwater.

A descriptive history of the interaction between longshore transport and the behavior of Mugu Lagoon inlet (Figure 6.6-1) may be found in Inman (1950a).

6.7.3 *Littoral Barriers*

The effects of the structures associated with this cell's four harbors were discussed in Section 6.7.2. The remaining shore-normal structures consist of headlands, several piers, three groin fields and an experimental groin.

Santa Barbara County has a pier at Carpinteria. Ventura County piers may be located on Figure 6.6-1. There are four piers at Punta Gorda, one at Ventura, and one at Pt. Mugu between the branches of Mugu Submarine Canyon (Shaw, 1980). The piers in this cell have not been found to have any effect on longshore transport (Simison et al., 1978).

In 1931 four 50 m groins were constructed a few miles east of Santa Barbara Harbor (Shaw, 1980). This attempt to halt the progress of the erosion wave caused by the harbor was unsuccessful, because the erosion continued downcoast past Carpinteria (Bailard and Jenkins,

1982; Pollard, 1979).

Cramer and Pauly (1979) report on the effects of a manmade headland at Seacliff, halfway between Punta Gorda and Pitas Point. Beach profiles and aerial photographs were used to monitor the behavior of this 500-ft wide fill. This area was undergoing continual erosion, which continued on both sides of the fill. Effects of the fill on the area are described but not quantified.

Natural headlands are present primarily at the western end of this cell. Effects of these headlands on transport have not been quantified.

USACE LAD (1961a) report on a proposed groin field at Ventura to counteract erosion. The seven 121 to 164 m long groins were constructed between 1962 and 1967 (Figure 6.7-6). The subsequent accretion is documented by USACE LAD's (1970) measure of shoreline motion.

In 1961 three groins were built along the spit north of Laguna Point (Figure 6.6-1) in order to counteract erosion in the area caused by construction of Port Hueneme Harbor. Beach profiles at the groin field showing slight accretion may be found in Orme and Brown (1983). A 212 m experimental groin with removable side panels was built at the same site in 1969. Panels are periodically removed or added in order to determine effects of different configurations on the beach. Resulting beach profiles are in Orme and Brown (1983).

6.7.4 *Wind Transport*

Inman (1950a), Bascom (1951), Inman (1976), Pollard (1979), and Inman (1981) have described wind transport in various parts of this cell as detailed in Section 6.6.3, but they have not quantified loss to the sand budget due to wind transport. In general it can be concluded that wind transport is not an important sink in the western part of the cell where there are no dune fields.

The large dune fields in the Ventura-Oxnard area indicate significant onshore and even offshore wind-induced loss (Inman, 1950a). Mason (1950) reports a loss to the area of 50×10^3

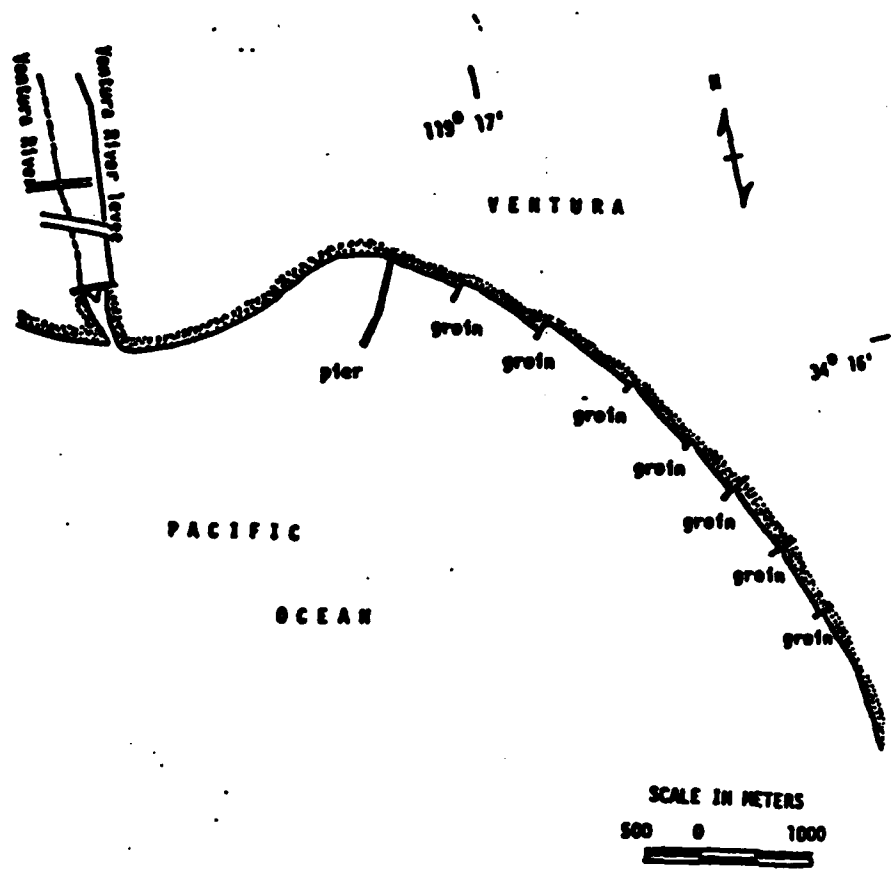


Figure 6.7-6. Ventura River and groin system (from Shaw, 1980).

yd³/yr by wind transport, but since no data are presented, we must assume the value is a guess. However, the longshore transport rate by waves in this area is quite large. In the absence of quantitative wind-induced losses, we may generally conclude that wind does not greatly affect longshore transport, but may represent a significant portion of net cross-shore transport and loss.

6.7.5 *Berm Overwash and Offshore Loss*

No quantitative data exist on either of these sinks for this cell. Berm overwash would be expected to be important only rarely, i.e., storm and high-tide coincidence. Offshore loss (except at submarine canyons) is generally assumed to be small, especially in comparison to this cell's large longshore transport rates. If offshore loss were quite significant, presumably it would show up in extensive beach profile studies such as those of Orme and Brown (1983), which it has not.

6.8 BUDGET OF SEDIMENTS

There are no existing reports that directly address the budget of sediments for the entire Santa Barbara Cell. However, Inman (1981) provides a rational interpretation of the sediment budget in terms of transport rates for the sub-cell from Ventura to the Hueneme Submarine Canyon (see Table 6.8-1). There are several reports that discuss separately the sediment sources, sinks and transport pathways as summarized in Sections 6.5, 6.6 and 6.7, respectively. There is very limited data on cliff retreat as a source of sediment. Handin (1951) estimates the small streams entering the ocean from Point Conception to Ventura contribute 350,000 yd³/yr, while the Ventura River contributes 300,000 yd³/yr, and the Santa Clara River 150,000 yd³/yr.

Results for studies of longshore transport rates and pathways are summarized in Table 6.6-1. The longshore transport is primarily to the south at an estimated rate of 280,000 yd³/yr (Johnson, 1957). The major sinks for sands are the Hueneme and Mugu Submarine Canyons,

Table 6.8-1. Transport rates for the sub-cell from
Ventura to Hueneme Canyon (from Inman,
1981).

a)	Bypassed around Ventura Marina	300,000 - 500,000 yds ³ yr ⁻¹
b)	Eroded from Santa Clara River delta	300,000 - 500,000 yds ³ yr ⁻¹
c)	Longshore transport by Mandalay Beach	<hr/> = (a)+(b) = ~ 800,000 yds ³ yr ⁻¹
d)	Longshore transport at Channel Islands Harbor	= ~ 1,200,000 yds ³ yr ⁻¹

and the Santa Barbara, Channel Island, and Port Hueneme Harbors. Santa Barbara Harbor traps 280,000 yd³ of sands per year. The Channel Island Harbor and Port Hueneme Harbors are located next to each other and collectively trap about 1.2×10^6 yd³ of sand annually. About 1,000,000 yd³/yr are lost down each of the Mugu and Hueneme Submarine Canyons.

7. SANTA MONICA CELL

The Santa Monica Cell extends from Point Dume to Palos Verde Point, a distance of 40 miles (see Figure 1.2-1). Including the nine miles of pocket beaches and rocky cliffs in the Dume Sub-Cell, the entire length of the extended cell is 49 miles. There are 19.5 miles of sandy beaches from Pacific Palisades to Malaga Cove. The extended cell has two natural sediment sinks, Dume and Redondo Submarine Canyons. The coastline has been extensively developed. Structures along the shore at Santa Monica Bay have essentially stabilized the beach, preventing extensive longshore transport and the loss of sand down Redondo Submarine Canyon.

7.1 COASTAL EROSION PROBLEMS, NATURAL AND MAN-MADE

USACE SPD (1971) inventories coastal shoreline characteristics related primarily to erosion produced by waves or other coastal phenomena (see Figure 7.1-1). The report systematically discusses erosion problem areas throughout the Santa Monica cell. There are areas of critical erosion at the northern end of the cell, while non-critical erosion occurs from Santa Monica to Redondo Beach. Herron (1980) briefly describes the Santa Monica Cell and mentions the erosion problems along this coastline. But as previously mentioned, the coastline has been essentially stabilized by man. Potter (1983) discusses the erosion control facilities and catch basins on local streams. He also briefly reviews local erosion problems and remedial courses of action.

7.2 SHORELINE CHANGES

Data on shoreline changes in the Santa Monica Cell contained in the reports reviewed for this study, such as surveys, beach profiles and photographs are summarized in Table 7.2-1. USACE LAD (1962b, 1963, 1966, 1969a and 1970) discuss the past data collection programs for Ventura and Los Angeles Counties. These reports summarize existing data such as aerial

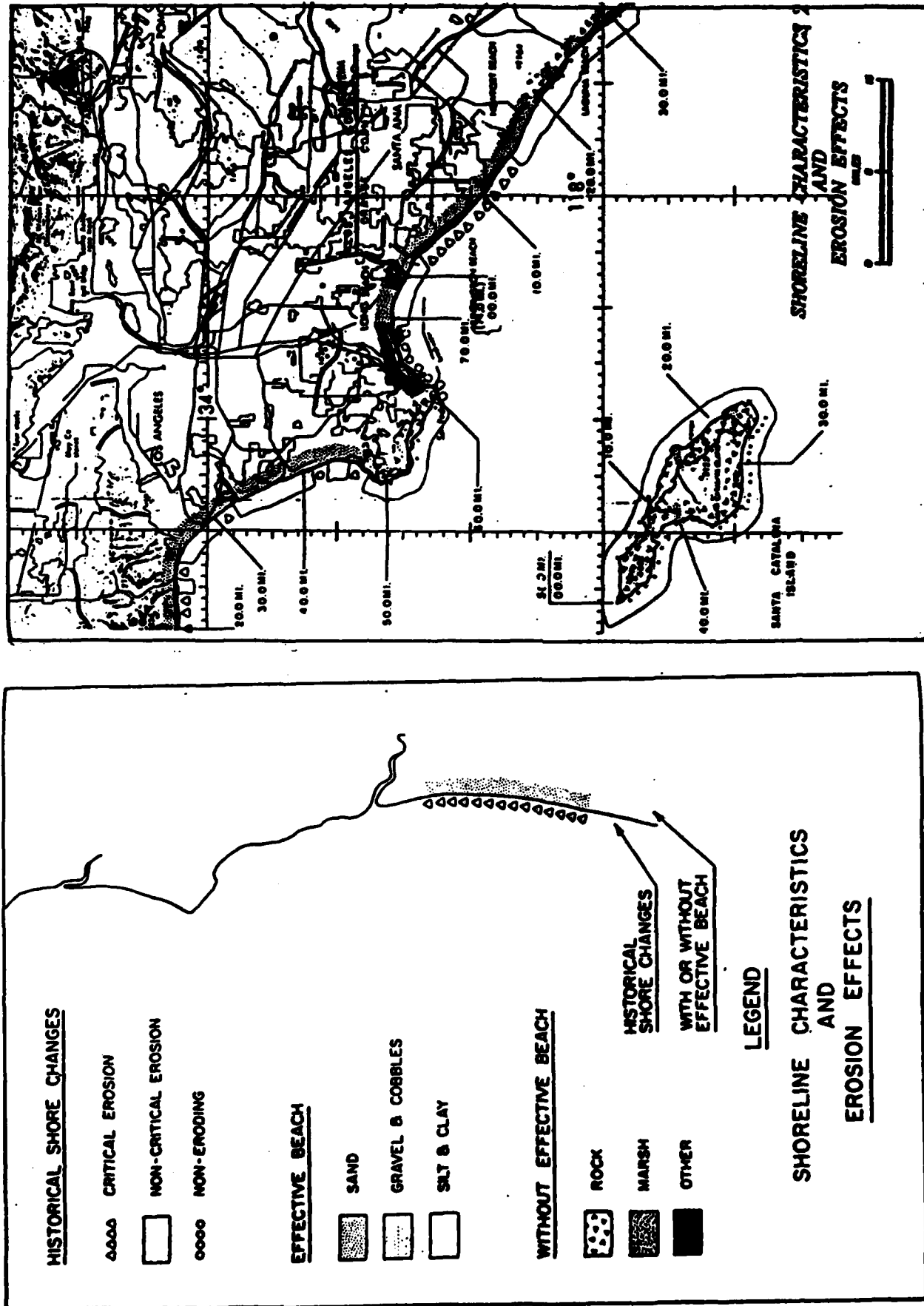


Figure 7.1-1. Shoreline characteristics and historical shore changes (from USACE SPD, 1971).

Table 7.2-1
EXISTING SURVEYS, MAPPING STUDIES, PHOTOGRAPHS

Author(s) Date	Type of Data	Location and Dates
Munk and Traylor, 1947	Aerial photography (historical)	Redondo Beach/Submarine Canyon (no date)
Handin and Ludwick, 1950	Aerial photograph	Santa Monica breakwater, 1947
USACE LAD, 1962b	Bathymetric profiles	Malibu Creek to Ballona Creek, 1961
	Beach profiles	Malibu Creek to Ballona Creek, 1949, 1961
USACE LAD, 1963	Aerial mosaics	Malibu to Santa Monica, 1963
	Offshore contours	Malibu to Santa Monica, 1963
USACE LAD, 1966	Aerial photograph	Redondo Harbor to Palos Verde Point, 1966
	Offshore contours	Redondo Beach to Malaga Cove, 1966
	Beach profiles	Redondo Beach to Malaga Cove, 1935, 1965
USACE LAD, 1967	Condition survey (bathymetric and beach profile)	Marina del Rey, 1964
		Ballona Creek to Redondo Beach, 1962

Table 7.2-1 (cont'd.)
EXISTING SURVEYS, MAPPING STUDIES, PHOTOGRAPHS

Author(s) Date	Type of Data	Location and Dates
USACE LAD, 1969a	Condition survey (bathymetric and beach profile)	Santa Monica to Redondo Beach, 1965 Marina del Rey, 1966 Redondo Beach to Malaga Cove, 1965
USACE LAD, 1970	Hydrographic surveys	Redondo Beach, 1967, 1968
Herron, 1980	Aerial photographs	Ballona Creek/Marina del Rey, 1938, 1962 Redondo Beach State Park, 1922 1968
Dames and Moore, 1983	Aerial and ground photographs	El Segundo, 1982, 1983

photographs, ground photographs and surveys, but some reports do not contain all the data sets (see Table 7.2-1). Beach profile data sets tend to show a seasonal on-offshore movement of sand. USACE LAD (1974) discusses the erosion problems and the deterioration of the local groins at Las Tunas Beach Park. Herron (1980) contains comparative historical aerial photographs of the Marina del Rey area and Redondo Beach State Park. Dames and Moore (1983) includes a thorough discussion of the shoreline history and shore erosion problems in the El Segundo area.

7.3 NEARSHORE WAVES

There are no long-term measurements of deep water waves offshore of this cell and inside the Channel Islands. Several studies (USACE LAD, 1963, 1966, 1974; Durham et al, 1981) have produced hindcasts by combining hindcast data from Marine Advisers (1961a) Station A and NMC (1960) Stations 6 and 7 (Figure 7.3.1). MII (1977) Station 5 and Marine Advisers (1961a) hindcasts were used by Hales (1978). The methodologies used in the base hindcasts are discussed in Section 3.2.2.

The base hindcasts (i.e. MA (1961a), NMC (1960b), MII (1977)) were modified to account for the particular windows open from a given site to the deep ocean. Open windows to central Santa Monica Bay as shown schematically in Figure 7.3-1. For southernmost Santa Monica Bay, the chief difference is a rotation of the southerly window to 206° - 230° (USACE LAD, 1966). Northern portions of the bay are highly sheltered from northwest swell (Figure 7.3-1).

The accuracy of the MII (1977) hindcast has been questioned (see Section 3.3.2). Nevertheless, Hales (1978a,b) hindcast for Deer Canyon ($34^{\circ}04'$, $118^{\circ}59'$) (which used MII, 1977, for northern hemisphere waves) is the only one available for the reach of this cell between Point Mugu and Point Dume. Marine Advisers (1961a) is used for southern swell. Hales (1978a,b) concludes that in 20 m depth significant wave heights exceed 6 ft only 4.6% of the time, with most of the high wave events between December and April. South swell is dominant in the summer months. Hales (1978a,b) gives many refraction diagrams for the Deer Canyon area, and detailed (i.e. monthly, directional and height distributions) wave statistics.

In a study of northern Santa Monica Bay, USACE LAD (1963) apparently considered the entire sector from 180° - 247.5° as completely open to waves, ignoring San Nicholas and Santa Barbara Islands and shoals. The methodology is not described in sufficient detail for a critical analysis; for example it is not clear in what depth of water refraction calculations were actually started. At any rate, design waves for 42 ft depth were determined as (1) 9 sec, 11-13 ft from

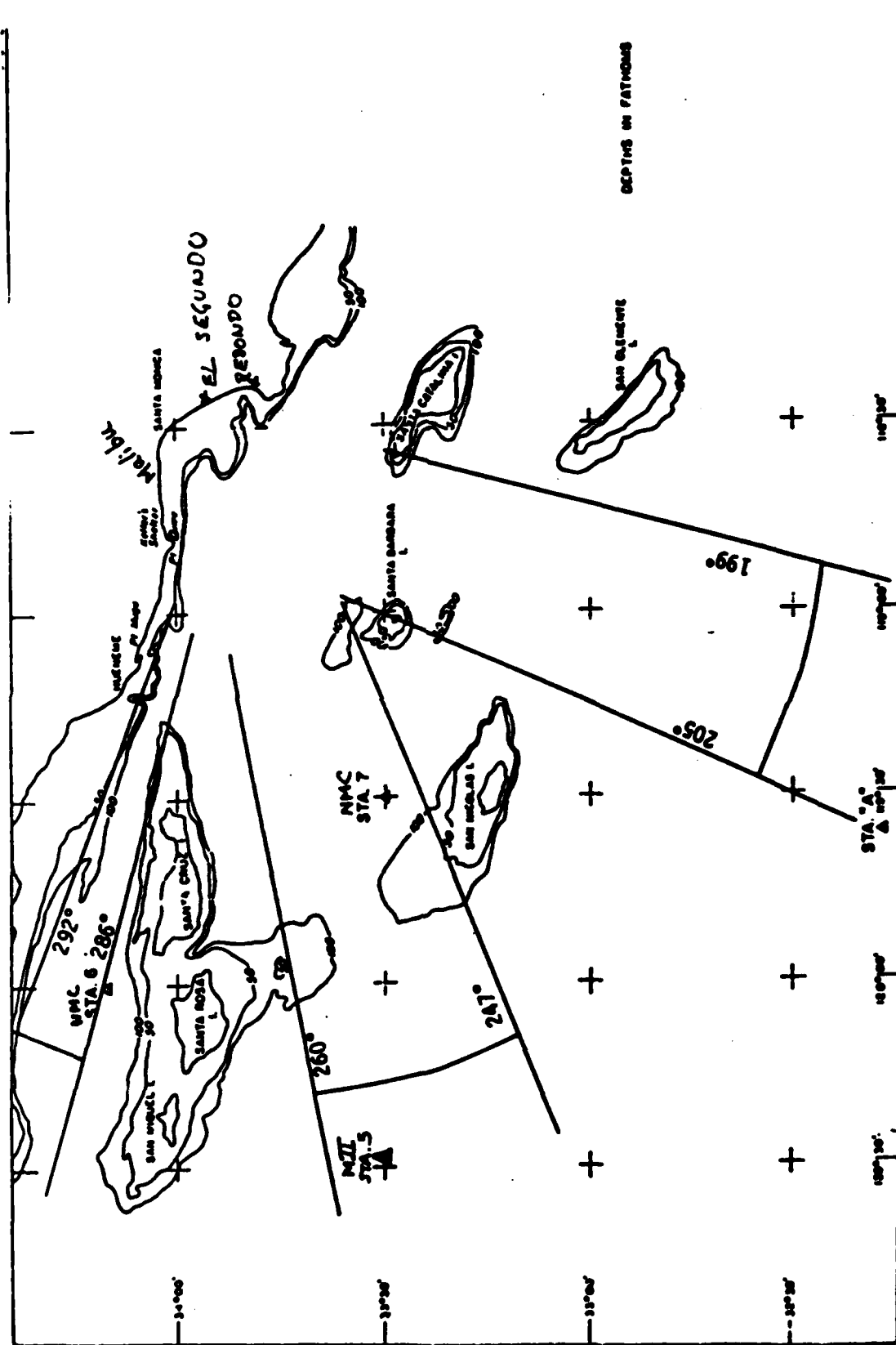


Figure 7.3-1 Schematic wave exposure diagram for Santa Monica Bay (after USACE LAD, 1966).

the south, (2) 11 sec, 6-10 ft from WSW. Many refraction diagrams are given for the reach between Malibu and Santa Monica. USACE LAD (1974) develops a wave climatology for Las Tunas Beach, midway between Malibu and Santa Monica. Open sectors are defined as 182°-192°, 205°-212° and 237°-265°. It is not clear, but apparently windows were either open or closed, no account being made for offshore banks and other refractive effects in the island vicinity. At any rate, southern swell and WSW locally generated seas are found to contain most of the energy at Las Tunas. Southern swell is very common, and typically of low height. Significant seas occur infrequently but can have large heights (> 10 ft).

Durham et al (1981) used Marine Advisers (1961b) and MII (1977) data to develop hindcasts for Redondo Beach. This site is highly sheltered. Combined sea swell heights are hindcasted as less than .5 m about 70% of the time. The 1.5 m significant height exceedance is about 0.5%. These heights are somewhat smaller than an Intersea Research hindcast for 140 ft depth off El Segundo described in Dames and Moore (1983). This 3 ft significant height exceedance is less than 20%, but heights greater than 5 ft occur about 4.7% of the time (Table 7.3-1). That is, waves greater than about 5 ft occur roughly 8 times more frequently in Dames and Moore (1983) than in Durham et al (1981). The lower waves at Redondo Beach may be associated with the strong wave divergence caused by Redondo Canyon, and a focusing of west swell at El Segundo. The hindcast base data and methodologies may also cause differences.

7.4 NEARSHORE CURRENTS

A general discussion of southern California shelf circulation is given in Section 3.1. The local current regime appears to be a combination of tidal and wind-driven currents. Short-term current meter deployments (Dames and Moore, 1983) in Santa Monica Bay indicate peak tidal current speeds of about 20 cm/sec, and relatively weak mean flows (less than 15 cm/sec). Drift card studies in Santa Monica Bay indicate onshore surface flows throughout the bay, and a southerly drift in the southern portion (Figure 7.4-1).

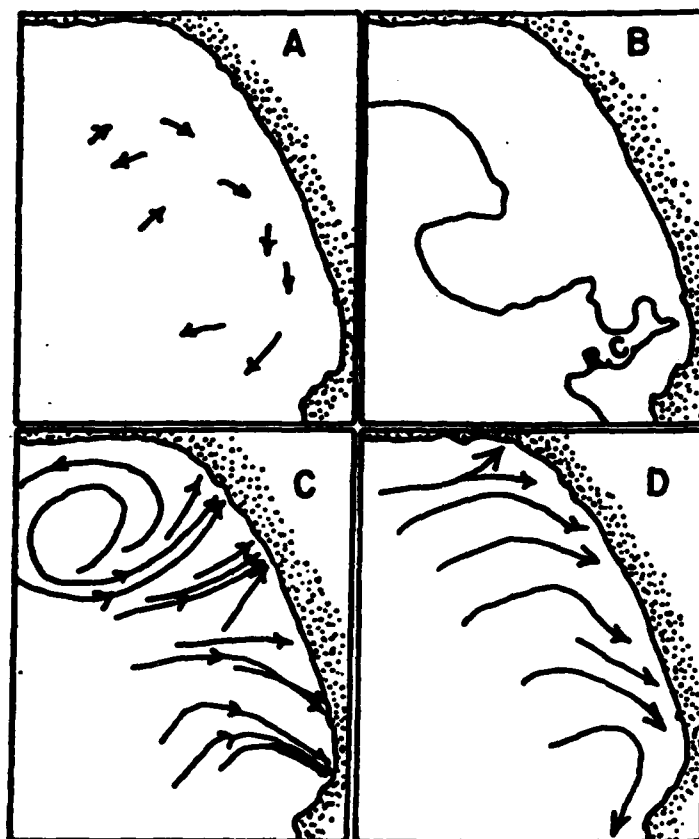


Figure 7.4-1

Surface currents from drift cards in Santa Monica Bay (A) March, 1956, (B) continental shelf area and Redondo Canyon, (C) February, 1956, (D) August, 1956 (Maloney and Chan, 1974).

Based on wave hindcast and refraction studies, USACE LAD (1974) predict a generally downcoast (eastward) flowing surf zone current for a location just east of Point Dume (Figure 7.3-1). For locations near Redondo Beach (southern Santa Monica Bay), USACE LAD (1966) predicts an upcoast surf zone flow. This agrees with 9 years of observations by lifeguards at Redondo Beach. The highest percentage of northward flows occur in July-October (USACE LAD, 1966), consistent with the increased importance of southern swell during this time.

7.5 SEDIMENT SOURCES

7.5.1 *Cliff Erosion and Relict Dunes*

Zeller (1962) briefly describes the small dune masses located along the coastline from Point Mugu to Santa Monica. He also describes the extensive dunes in the area from Playa Del Rey to Palos Verde Hills, known as the El Segundo Sand Hills. There were no reports reviewed for this study that contained any estimates of average or episodic sediment input rates from eroding cliffs or sand dunes.

7.5.2 *Sediment Discharge from Rivers and Streams*

There are no major rivers supplying sediment to this littoral cell. However, in prehistoric times the Los Angeles River at times flowed into Santa Monica Bay. Handin (1951) investigates the source, transportation and deposition of beach sediments in southern California. He includes maps of the tributary drainage areas and surface rock types for the streams in the Santa Monica Littoral Cell. He also includes information on beach sediment mineralogy and petrology, and grain size distribution plots. Averaging 372 microns, the mean grain size varied from 280 to 699 microns. The coarsest sand was found in August, but in general the grain size was fairly uniform throughout the year. Gravel was almost always present on the foreshore and gravel cusps were common.

USACE LAD (1966) contains a summary of grain size distributions for sand samples taken from Redondo Beach to Malaga Cove. Judge (1970) examines the heavy minerals contained in beach and stream sediments. He includes USGS estimates of water discharge and drainage areas for Calleguas, Malibu, Topanga and Ballona creeks (see Table 7.5-1). USACE LAD (1970) contains grain size analysis for sand samples taken at Redondo Beach. Potter (1983) discusses the erosion control facilities in this cell and how they prevent sediment from reaching the coastline (see Figure 7.5-1). Potter proposes sites for control facilities that provide effective

Table 7.5-1

River Discharge and Drainage Area

<i>Stream</i>	<i>Average Discharge</i> (acre-feet per year)	<i>Drainage Area</i> (square miles)
Malibu Creek	13,250	100
Topanga Creek	3,710	20
Ballona Creek	25,480	89

Data from topographic maps and U.S. Geological Survey Water Supply Paper 1735 (from Judge, 1970).

Discharges are averages of available years at every station, but more than five years as a minimum. Areas are by planimetric determinations to the nearest 10 square miles.

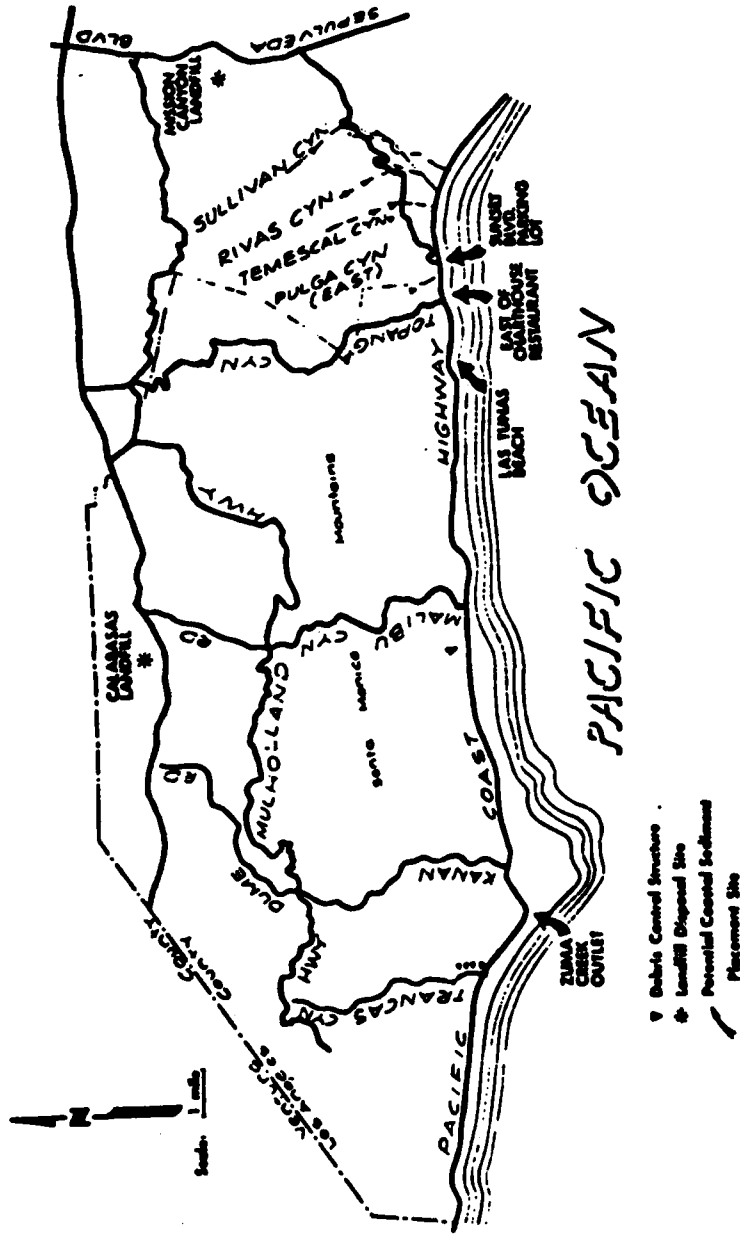


Figure 7.5-1. Locations of erosion control facilities and disposal sites (from Potter, 1983).

flood control yet allows the sand to reach and nourish the beaches.

7.5.3 *Artificial Beach Nourishment*

USACE LAD (1963) discusses alternatives for the maintenance of the beaches in the Malibu-Santa Monica area. One of the alternatives considered was sand bypassing around Malibu Point. USACE LAD (1966) examines sources of material and grain size matching for beach widening from Redondo Beach Breakwater to Malaga Cove. USACE LAD (1970) discusses the use of offshore sand sources for beach nourishment at Redondo State Beach. An offshore dredge was used to pick up deep water sands and pump them onshore. USACE LAD (1974) describes the source and placement of artificial fill to control erosion at Las Tunas Beach Park.

The California Department of Boating and Waterways compiled information on sediment transport in coastal stream basins and beach nourishment along the southern California coastline, California (1977b). This report provides order of magnitude estimates for sediment production and locations of abundant inland sources of material for beach nourishment. Herron (1980) discusses the artificial beaches in southern California. From 1938 to 1975 28 million cubic yards of sand was used for artificial beach fill in the Santa Monica Cell. Most of this came from removal of sand dunes in the vicinity of Hyperion Sewage Disposal Plant in 1938 and 1948 ($12,000,000 \text{ m}^3$) and from dredging the Marina del Rey Harbor in 1962/63 ($7,720,000 \text{ m}^3$). Shaw (1980) itemizes all the artificial beach nourishment projects in southern California. The report includes a table detailing fill location, source location, amount of fill and project dates. The report is thorough and should be used as a primary reference for this section.

Durham et al (1981) and Herron (1983) briefly describe a 1968 beach nourishment project at Redondo Beach. This was a unique nourishment project because the borrow area was located in water depths varying from 9 to 18 m and was approximately 2 km offshore of the fill project. The offshore dredge lifted the sediments off the bottom and pumped them back onto the beach.

Herron (1983) contains an aerial photograph showing the dredge in operation. Dames and Moore (1983) in a report for Chevron U.S.A., Inc., detailing the artificial beach nourishment projects from 1938 to 1981 on beaches directly downcoast of Marina del Rey. Osborne et al (1983) locates and delineates potential offshore sand and gravel resources with a combination of seismic reflection profiles and extensive vibracore data to define stratigraphic horizons, mechanical and textural properties of the material. The borrow areas between Santa Monica and Kings Harbor, located less than 6 km from shore (see Figure 7.5-2), have an estimated minimum total volume of $400 \times 10^6 \text{ yd}^3$ of sand. The report is well done, includes most of the data collected, and has an extensive reference list, most of which were not included in this study.

7.6 SEDIMENT TRANSPORT MODES

7.6.1 *Cross-shore Transport*

As is the case with most cells, little information is available on net cross-shore transport. However, Cook (1970) studied the offshore transport of sediment in rip currents at Redondo Beach. Many authors consider this to be the significant means of offshore transport (e.g. Inman, 1953). Cook (1970) noted selective sorting by rips: rip sediment is finer and less dense than beach sediment. He noted three types of rips, each with their own transport rate: large rips with $10\text{-}50\text{g}/(\text{m}^2\text{-hr})$, small rips with $2.5\text{-}7.5(\text{g}/\text{m}^2\text{-hr})$, and rips disrupted by onshore wind with $0.1\text{-}1\text{g}/(\text{m}^2\text{-hr})$. In order to translate these into volume transport rates, estimates of average rip widths, depths and spacing are required. Cook reported widths of 20 m. If we make rough guesses of 2 m depths and 1000 m spacings, then a rough estimate of transport would be 10-50 kg/day per kilometer of beach for large rips, 2-7 kg/day for small rips, and 0.1-1 kg/day for disrupted rips. Examples of seasonal profile changes at Redondo Beach may be found in Dames and Moore (1983).

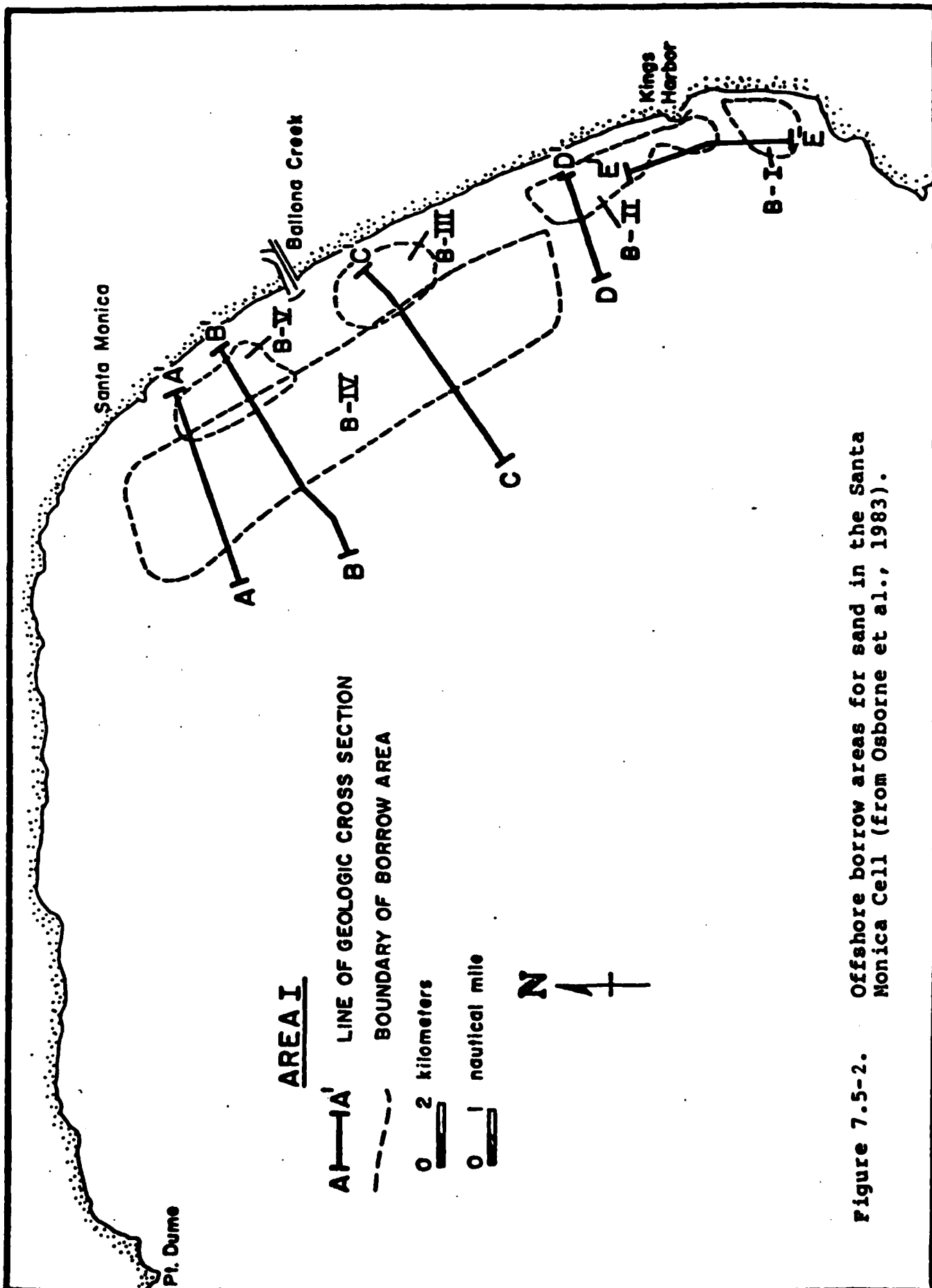


Figure 7.5-2. Offshore borrow areas for sand in the Santa Monica Cell (from Osborne et al., 1983).

7.6.2 Longshore Transport

Longshore transport rates for this cell are summarized in Table 7.6-1. "Potential" rates are obtained from application of the standard "stress-flux" equation (Section 2.4) with wave data as inputs. Both volume transport Q_1 (yd³/yr) and immersed-weight transport I_1 (newtons/second) are listed. In converting between the two measures, it was assumed that solids concentration $N_o = 0.6$ (porosity = 0.4) and sand density $\rho_s = 2.65$ g/cm³. Positive values represent downcoast transport to the south, negative to the north.

Despite the fact that there are several groups of structures in this cell at which estimates of longshore transport might be made, very few good estimates are available. The reason for this is a lack of long-term comprehensive beach profiling and incomplete dredging records. Handin (1951) and Johnson (1957) made estimates based on accumulations at coastal structures of 270×10^3 yd³/yr at the Santa Monica Breakwater, 162×10^3 yd³/yr at El Segundo, and 30×10^3 yd³/yr at the Redondo Beach breakwater. The Redondo breakwater was then much smaller than it is today. Thus the 30×10^3 yd³/yr estimate is based on profiling near a very inefficient trap and is a severe underestimate of transport. These values from Handin (1951) are probably no longer valid because of the effects of additional structures built since then.

Transport direction in this cell is apparently more subject to seasonal reversal than any of the cells further north, or the Oceanside Cell further south. Marine Advisors (1958) attempted to estimate the relative strengths of transport in both directions in the vicinity of Santa Monica. They examined the effects of different wave spectra and concluded that southerly transport is seven times greater than northerly transport. The northerly transport is more apt to occur in summer during periods of large southern Pacific swell.

Ingle (1962, 1966) measured longshore transport rates with fluorescent sand tracer at two sites in this cell during 1961-62. Values at Trancas Beach, a long beach several miles west of Point Dume, ranged from 117 to 1,671 yd³/day (43 - 610×10^3 yd³/yr.) Sand velocities were 8-21

Table 7.6-1 . Longshore Transport Rates
(Positive values indicate transport to the south, negative to the north)

Location	Notes	Reference	Potential Transport (Wave Refraction Studies)		Gross Transport (Trapping Studies)		Instantaneous Net Transport (Sand Tracer Studies)	
			Q_1 ($10^3 \text{ yd}^3/\text{yr}$)	I_1 (N/sec)	Q_1 ($10^3 \text{ yd}^3/\text{yr}$)	I_1 (N/sec)	Q_1 ($10^3 \text{ yd}^3/\text{yr}$)	I_1 (N/sec)
Santa Monica	[These estimates are out of date due to major structural changes]	Handin (1951)			270	64		
E1 Segundo		Handin (1951)			162	38		
Dume Sub-Cells	Range of values	Ingle (1966)					40 to 610	9 to 144
Dume Sub-Cells	Average of values	Ingle (1966)					333	78
Santa Monica	Range of values	Ingle (1966)					30 to 500	7 to 118
Santa Monica	Average of values	Ingle (1966)					246	58

-321-

Note: None of the measures in this cell are reliable estimates of average net transport.

ft/min (4-10 cm/s). Results at Santa Monica Beach ranged from 75 to 1,376 yd³/day (27-502 x 10³ yd³/yr) with velocities of 5-18 ft/min (2.5-9 cm/s).

Ingle did not quantify his data by balancing the tracer recovery vs the tracer injection. As a consequence his data have only quasi-quantitative value. Since these experiments were performed under a wide variety of conditions, they are estimates of the range of transport rates that can be expected from day-to-day, but they do not indicate what the annual average should be.

At the extreme southern end of the cell, between Redondo Beach and Malaga Cove, the coast orientation is so different than the rest of the cell that net transport is to the north, but has not been reliably quantified (Handin, 1951).

7.6.3 Wind Transport

No estimates of wind transport are made in the articles reviewed for this report. Santa Monica Bay has 19-1/2 miles of sandy beaches which were backed by extensive sand dune fields. This is generally an indication of active wind transport from the beach, unless the dunes are highly vegetated. However, much of this dune field has now been blocked by development. Wind transport may also be locally important at Pt. Dume. Wind transport at these two sites may be significant, but no studies have been made on this problem.

In view of the relative magnitudes of wave-induced longshore and cross-shore transports, it is probably safe to assume that wind transport's effect on the total longshore rate is small but may play a significant role in net cross-shore transport, especially at the two sites mentioned.

7.7 SEDIMENT SINKS

7.7.1 Submarine Canyons

This cell contains three submarine canyons: Dume, Santa Monica and Redondo. Dume Canyon may be an important sink for sediment moving near Pt Dume, but we are unaware of

any reports addressing this subject.

From field inspection, Inman (personal communication) concluded that most sand transported during moderate waves bypassed the head of Dume Submarine Canyon, but that during storms the canyon acts as a partial sediment sink. Santa Monica Canyon does not approach nearly close enough to the coast to have an effect on transport. (Its head is eight miles from the coast.)

Some estimates of transport down Redondo Canyon are available. Marine Advisors (1965) compared bathymetric charts revealing areas of accretion and erosion up to 7 m thick, suggesting active transport. Gorsline (1958) used radio-dating of submarine basin core samples and estimated annual transport from Redondo Canyon to deep basins at $200-400 \times 10^3 \text{ yd}^3/\text{yr}$. All of these evidences of transport must now be considered out-of-date because of the effects of Redondo Breakwater. The breakwater may now be impounding most of the sediment which formerly flowed down Redondo Canyon. This may have been an intentional result of construction (Dunham, 1965).

7.7.2 Entrapment by Harbors, Bays, and Estuaries

There are two harbors in this cell: Marina del Rey and King Harbor (Redondo Harbor). Marina del Rey structures consist of a 410 m flood-control jetty (completed in 1946), two 610 m jetties to maintain the harbor channel (completed in 1959), and a 710 m detached breakwater (completed in 1965). See Figure 7.7-1. The generally observed effect on transport is accretion to the north, erosion to the south, and shoaling between the jetties (Shaw, 1980; Hallermeier, 1983). Shaw (1980) reports a dredging history of the marina itself, but sufficient profiling has not been done in the area of the jetties and breakwater to allow quantitative estimates of longshore transport loss in the channel.

The two breakwaters establishing Redondo Harbor are illustrated in Figure 7.7-2. The 2827 m north breakwater was constructed in several stages between 1939 and 1960, and the 180

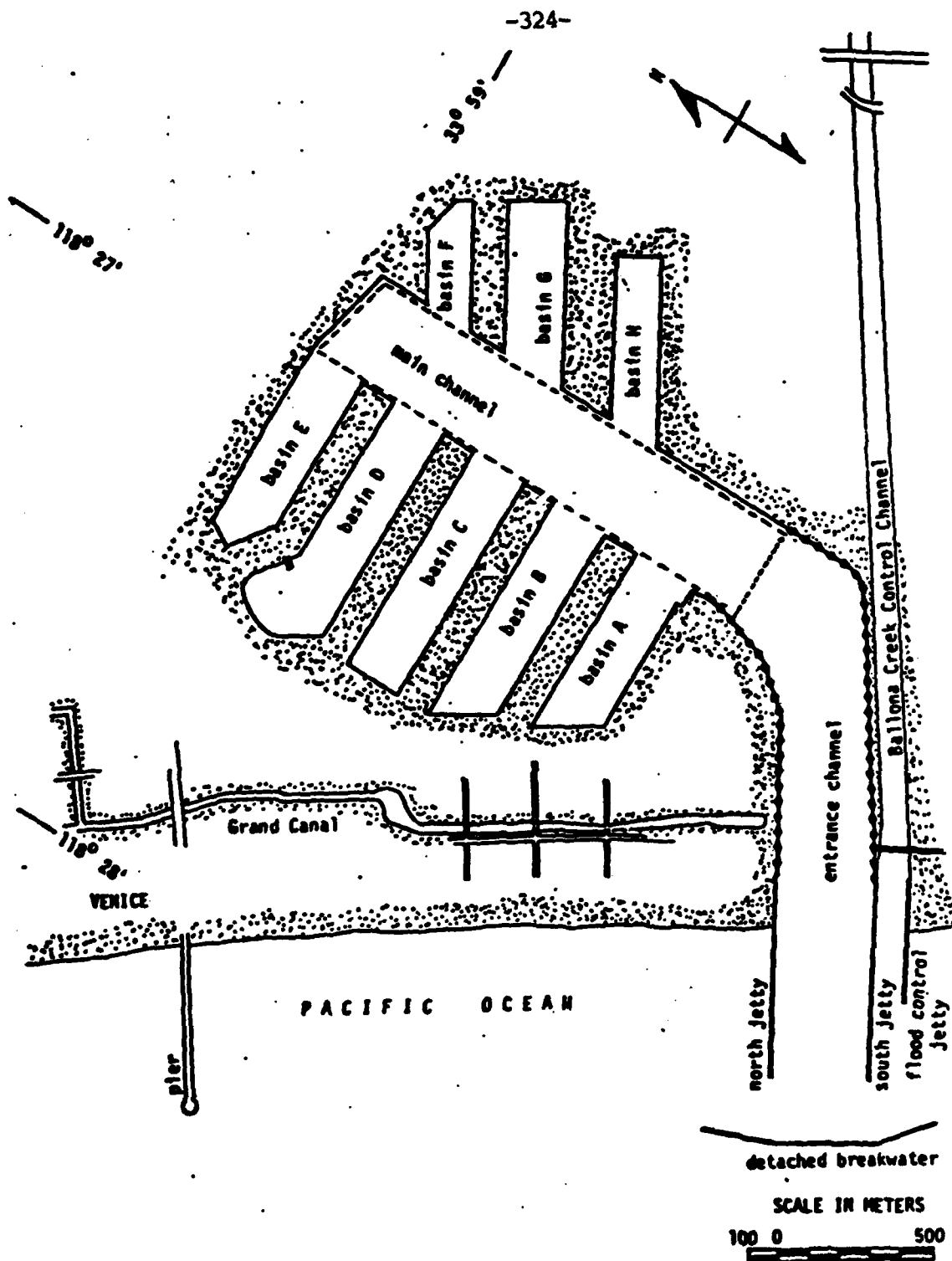


Figure 7.7-1. Marina del Rey (from Shaw, 1980).

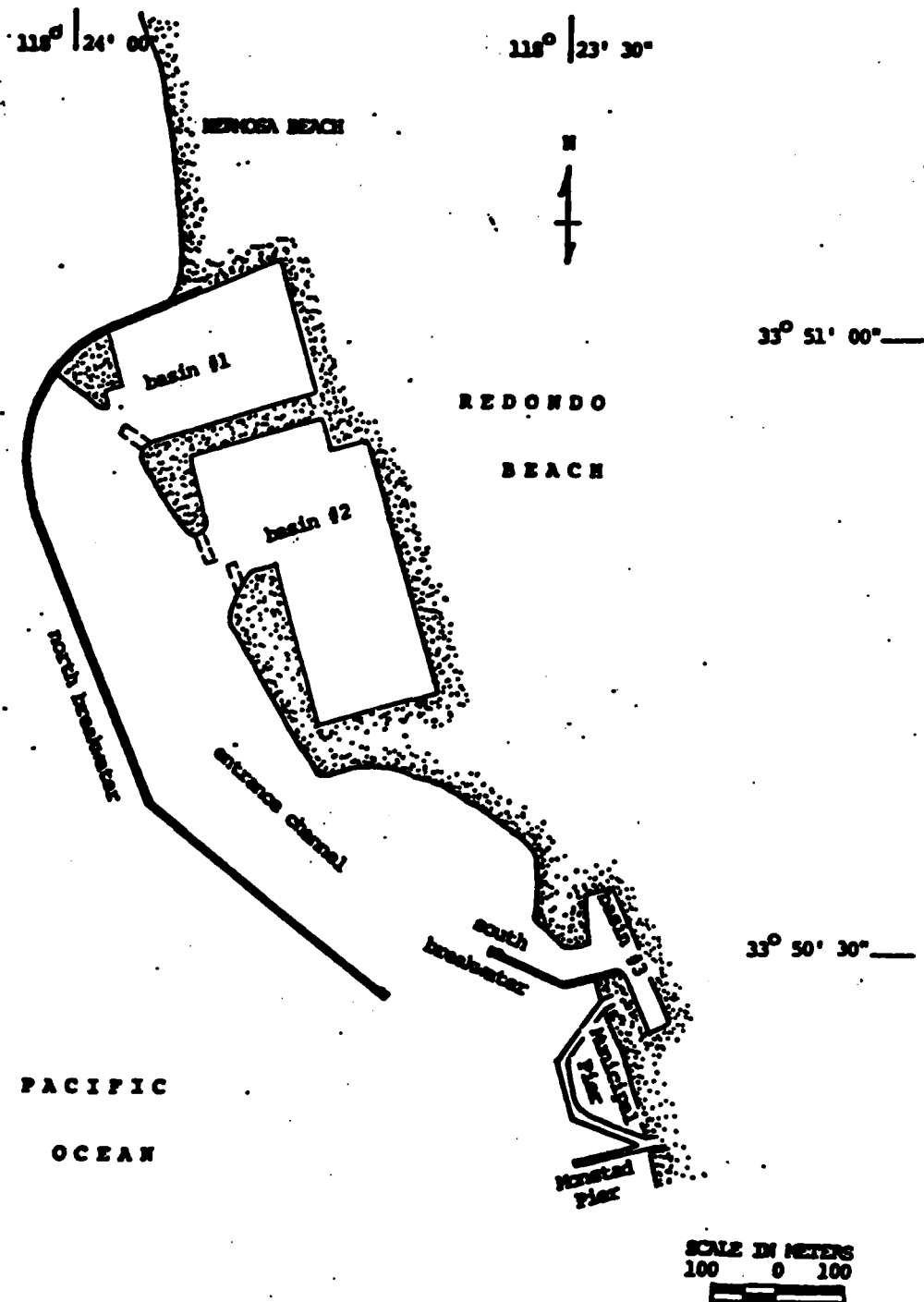


Figure 7.7-2. Redondo Beach Harbor [King Harbor] (from Shaw, 1980).

m south breakwater during 1958-64 (Shaw, 1980). Estimates of longshore transport at Redondo based on profiling were detailed in Section 7.6.2. However, these estimates were based on data from the 1930's and 1940's and are probably not now valid, since the north breakwater has been extended several times since then, and the south breakwater was built entirely after that time.

7.7.3 *Littoral Barriers*

More of the coastline in this cell consists of "artificial protection" than of "protective beach" (California, 1977a). There are a total of eight piers, three jetties, five breakwaters, and more than 60 groins (Shaw, 1980). For locations of the eight piers, see Shaw (1980). The piers in this cell have been found not to have any appreciable impact on transport (Simison et al, 1978).

The only headlands in this cell are at its ends, the Dume sub-cells from Pt. Mugu to Pt. Dume and Palos Verdes Point at the southern end. Trask (1955) examined the size distributions and mineralogy of sand near Pt. Dume. He documented some sand movement around the headland but was unable to quantify it. Various authors have speculated on motion around headlands in this sub-cell, but no quantitative data exists to our knowledge.

Proceeding from north to south, structures impeding longshore transport (groins, jetties and breakwaters) will now be listed and described. Four small groins were built on rocky outcrops at Bass Rock about halfway between Pt. Mugu and Pt. Dume to stabilize the embankment on which a highway is built (California, 1977a; Shaw, 1980). We are unaware of documentation on the success of this project.

Several steel sheetpile groins were built at Las Tunas (a few miles east of Malibu) in 1928 in an attempt to counteract erosion. The groins have now deteriorated to the point where they are ineffective (USACE LAD, 1974). In many places only the steel pilings remain, with much of the steel sheeting gone, resulting in a hazard to swimmers. Aerial photographs reveal slightly sawtooth beach orientations between groins, but most of the longshore transport appears uninterrupted (USACE LAD, 1974). (There are no large areas of erosion or accretion.)

Removal of the existing groins and construction of new groins has been proposed (USACE LAD, 1974).

At Topanga Beach, where the coast's orientation changes from east-west to northwest-southeast, a total of 33 groins of varying types and lengths have been constructed over the period 1923-58 (Shaw, 1980). Many of these have deteriorated to the point where they no longer have any effect on transport. Quantitative trapping data are not available.

Several structures have been built in the Santa Monica/Venice area (Figure 7.7-3). The three stone groins shown in the figure are 125 m, 20 m and 46 m in length, proceeding from north to south. The 600m rubble-mound Santa Monica detached breakwater and 180 m Venice breakwater were built in 1934 (Shaw, 1980). The Santa Monica breakwater was built to protect a proposed small-boat harbor channel, but functioned as a sand trap (Handin, 1951). Harbor construction was thus prevented, and Santa Monica/Venice beaches suffered considerable erosion. A dredging history behind the breakwater is presented in Shaw (1980). Longshore transport estimates enabled by dredge records and profiling at this site are presented in Section 7.6.2. Early trapping at the breakwater was estimated at $270 \times 10^3 \text{ yd}^3/\text{yr}$ (Handin, 1951), but is probably different today. Beaches have stabilized only since the breakwater began to deteriorate in the 1960's.

Several authors have described in detail the effects of the Santa Monica breakwater on currents and sand motion (Handin and Ludwick, 1950; Ingle, 1962, 1966; Hallermeier, 1983). Handin and Ludwick (1950) performed wave refractions near the breakwater and confirmed that the erosion/accretion patterns caused by the breakwater could have been at least qualitatively predicted prior to construction. Ingle (1962, 1966) performed sand-tracer experiments behind the breakwater in order to deduce sediment transport paths. He found that a significant amount of transport continues to occur in the reduced surfzone behind the breakwater. However, he confirmed an effect first deduced by Handin and Ludwick (1950). The breakwater

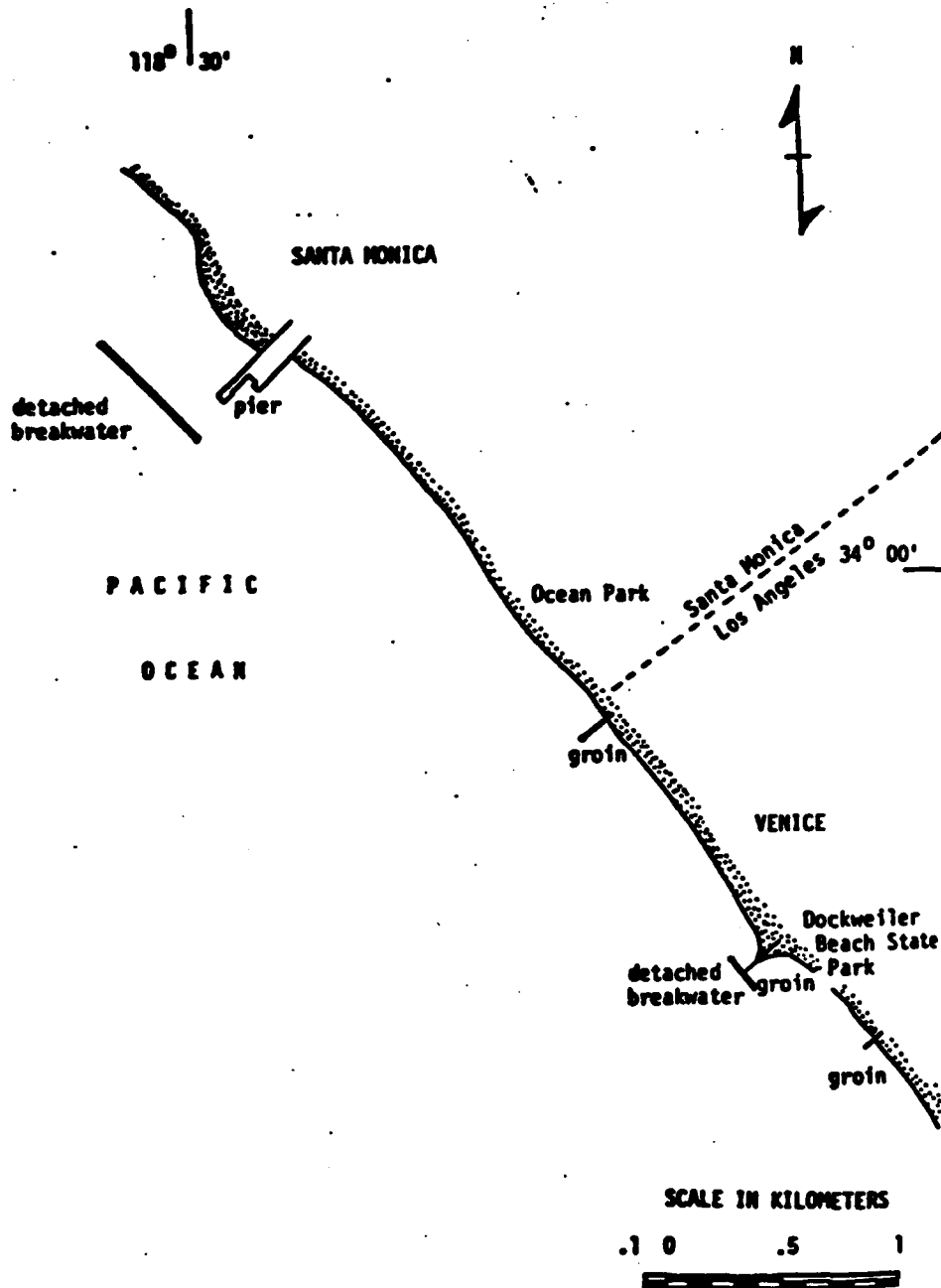


Figure 7.7-3. Santa Monica and Venice Breakwaters (from Shaw, 1980).

selectively sorts grain sizes. Coarse grains are deposited behind the breakwater and do not continue downcoast. The sand in transport becomes progressively finer as one proceeds downcoast behind the breakwater.

The effects of the three jetties and detached breakwater at Marina del Rey (Figure 7.7-1) were described in Section 7.7.2.

Four stone groins were built at Dockweiler Beach State Park (El Segundo), the last of which was completed in 1948. They were placed in order to stabilize beach fill, which was used to counteract erosion caused by the Santa Monica/Venice breakwaters (Shaw, 1980). A downcoast chain reaction of events caused by the breakwater is clear. They caused upcoast accretion, blocked the proposed small-craft entrance channel, caused downcoast erosion, necessitated beach fill, which in turn required groin construction to maintain the fill.

The breakwaters at Redondo Harbor (Figure 7.7-2) and their effects are described in Section 7.7.2.

7.7.4 *Wind Transport*

No estimates of wind transport loss have been made in this cell. This was probably a more important sink in the past than it is now, since much of the Santa Monica Bay dune fields have been blocked by development. However, wind transport may still be important enough to be included in the sand budget.

7.7.5 *Berm Overwash and Offshore Loss*

Losses to these two sinks have not been estimated in this cell. In much of the cell berm overwash is not likely to be important, since the beach is backed by either cliffs or buildings. Net offshore loss is difficult to estimate, since errors in bathymetric profiles are usually greater than accretion rates.

7.8 BUDGET OF SEDIMENT

There were no reports reviewed for this study that directly address the budget of sediment. There are no major rivers supplying sediment to this cell. The major sources of sediment are small streams and artificial beach nourishment (see Sections 7.5.2 and 7.5.3). The coastline has been extensively developed and essentially stabilized by the numerous structures impeding the longshore transport of sand. Longshore transport studies prior to 1966 are out of date because of the further addition of littoral barriers (see Table 7.6-1). Studies conducted after 1966 show a widely varying range of transport rates which illustrates the need for further study.

There are three submarine canyons in this cell: Dume, Santa Monica and Redondo. Little is known about sand transport down the Dume and Santa Monica Canyons. Prior to the construction of the Redondo Breakwater, Gorsline (1958) estimated an annual transport of $200-400 \times 10^3 \text{ yd}^3/\text{yr}$ of sediment from Redondo Canyon to deep basins. The breakwater now impounds most of this sediment (Dunham, 1965). Marina del Rey and King Harbors have required some maintenance dredging (Shaw, 1980), but insufficient profiling prevents quantitative estimates of sand entrapment by the harbors. There are numerous groins, jetties and breakwaters that intercept the longshore transport. Because of these structures and other interventions by man, the littoral budget is difficult to estimate.

8. SAN PEDRO CELL

The San Pedro Cell extends from Point Fermin to the City of Corona del Mar, a coastal length of 31 miles (see Figure 1.2-1). Including the 12 miles of rocky coast along the Palos Verde headland the extended San Pedro Cell has a coastal length of 43 miles. The cell has been extensively modified by man. Dams and catch basins on the rivers prevent sediment from reaching the coast. Most of the coast is protected from waves by the Los Angeles Outer Harbor breakwater. Because the wave energy does not reach the shore there is relatively little longshore transport of sand. As a consequence the Newport Submarine Canyon appears to be an inactive sink for littoral sand.

8.1 COASTAL EROSION PROBLEMS, NATURAL AND MAN-MADE

USACE LAD (1967b) discusses the shoreline changes and erosion problems from 1954 to 1967 in the area of Newport Beach. USACE SPD (1971) is an inventory of coastal shoreline characteristics related primarily to erosion produced by waves or other coastal phenomena. The report systematically describes the California coastline, discussing local erosion problems and historical shoreline changes (see Figure 8.1-1). The stretch of beaches to the south of Los Angeles harbor are undergoing severe erosion. California (1977a) provides an assessment and atlas of shoreline erosion along the California coast. The report proceeds from north to south detailing coastal features and erosion problems in the San Pedro Cell. Critical erosion occurs at Seal Beach, Sunset Beach, Huntington Beach and Newport Beach during high waves. However, Spencer (1985) reports that erosion at Newport beach may have stabilized in recent years.

USACE LAD (1978a) discusses the erosion problems at the Surfside-Sunset Beach area. The annual rate of erosion between the downcoast jetty at Anaheim Bay to Sunset Beach is about 300,000 cubic yards per year. Hales (1980) briefly discusses the shoreline characteristics and proposes solutions to the erosion problem in the area from Anaheim Bay to Newport Bay. Herron (1980) examines the erosion problems in the San Pedro Cell in general. Clancey (1983)

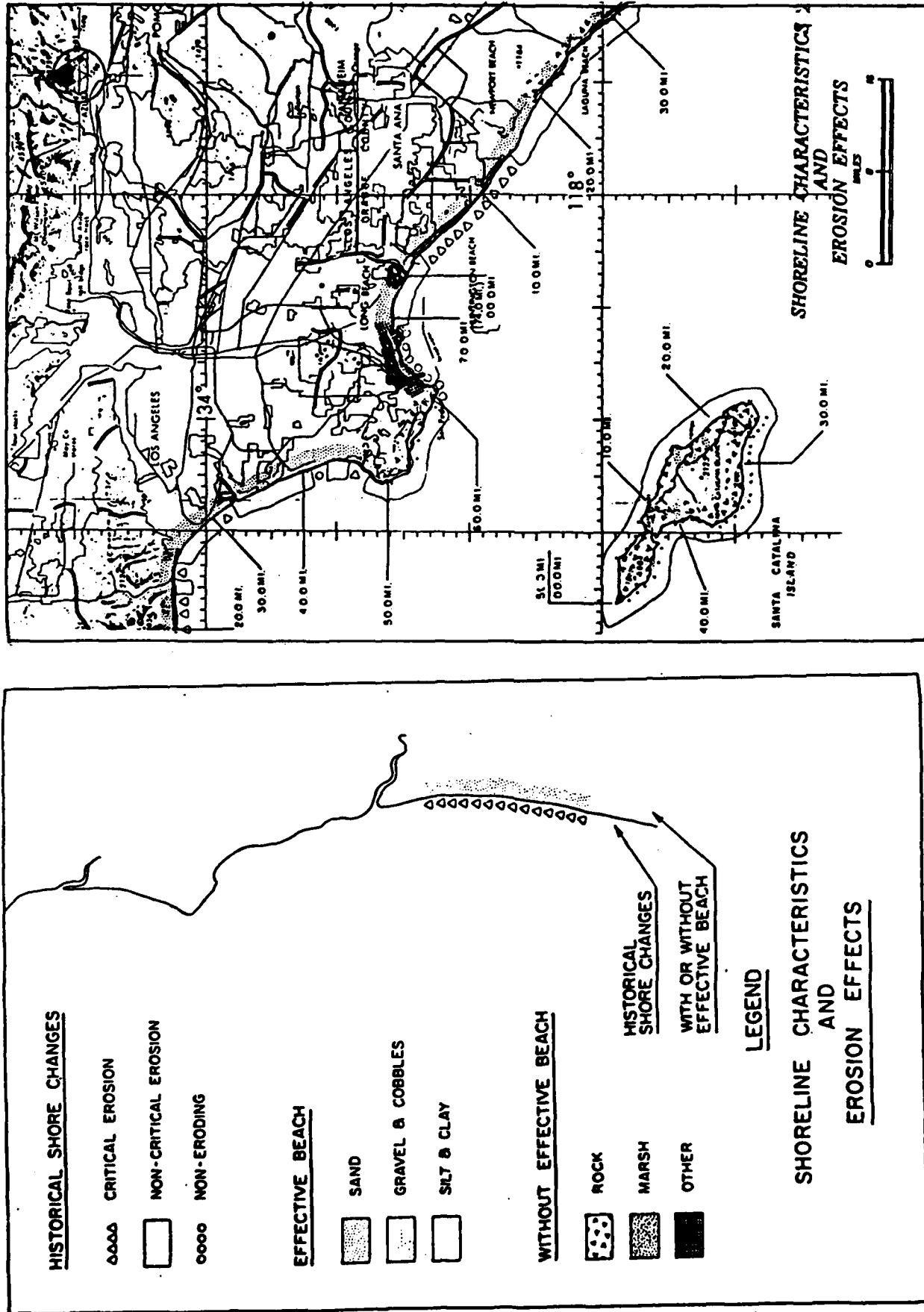


Figure 8.1-1. Shoreline characteristics and historical shore changes (from USACE SPD, 1971).

discusses erosion and accretion at the Newport Beach 48th Street Groin.

8.2 SHORELINE CHANGES

A summary of data reviewed for this study concerning shoreline changes for the San Pedro Littoral Cell is provided in Table 8.2-1. Caldwell (1956) contains historical photographs and beach profile data for the Anaheim Bay area. Inman and Frautschy (1958) examine the dynamics of the Newport Spit using historical surveys and photographs. Inman and Frautschy (1960) document the shoreline history in the Long Beach Harbor area by comparing surveys from 1859 to 1960. They include tables summarizing the littoral chronology, historical surveys and major flood events. USACE LAD (1962a) summarizes the shoreline history from the San Gabriel River to Newport Harbor. This report contains a large amount of data on shoreline changes as outlined in Table 8.2-1. USACE LAD (1967a) discusses shoreline changes, beach profile changes and volume changes for the coastline from the Santa Ana River to the Newport Pier. The report also includes historical ground and aerial photographs. USACE LAD (1967b and 1969a) contain 1960's beach and offshore profile data for Surfside-Sunset Beach continuing down the coast to Newport Bay. USACE LAD (1969b) summarizes the shoreline and beach profile changes at Newport Beach.

USACE LAD (1970) summarizes historical photograph data and hydrographic surveys but does not include the data sets. The report does include several plates of shoreline and offshore changes in the area from the San Gabriel River to Newport Bay (see Table 8.2-1). USACE SPD (1971) systematically proceeds from north to south describing coastal characteristics and shoreline changes for the entire coast of California (see Section 8.1). USACE LAD (1978a) contains a history of the beach widths from 1961-1980 at Surfside beach, along with two 1977 beach profiles at Sunset Beach. Clancy et al (1983) outlines a low cost method for measuring shoreline change. The method is simply to monitor berm widths along a set range line. The report presents data on the berm width at 48th Street, Newport Beach.

Table 8.2-1
EXISTING SURVEYS, MAPPING STUDIES, PHOTOGRAPHS

Author(s) Date	Type of Data	Location and Dates
Shepard and Grant, 1947	Aerial photographs	Pt. Fermin, 189
Caldwell, 1956	Aerial photographs	Surfside/Sunset Reach, 1947, 1948
	Volumetric changes (tables)	Anaheim Bay Area, 1948-1949
	Comparative beach profiles	Anaheim Bay Area, 1948-1949
Inman and Frautschy, 1958	Hydrographic surveys	Newport Bay, 1875
	Historical photographs	Newport Bay area
	Littoral chronology	Long Beach area, 1871-1944
	Summary of surveys	Long Beach area, 1859-1906
	Chronology of major floods	Los Angeles Basin area, 1770-1938
	Summary of erosion and accretion of sand	In the vicinity of the Wilmington breakwater, 1859-1897
Inman and Frautschy, 1960		

Table 8.2-1 (cont'd.)
EXISTING SURVEYS, MAPPING STUDIES, PHOTOGRAPHS

Author(s)	Date	Type of Data	Location and Dates
USACE LAD,	1962a	Aerial photographs	Surfside/Sunset Beach, 1947, 1948, 1957, 1961
		Ground photographs	Surfside/Sunset Beach, 1938, 1942, 1946, 1947
		Hydrographic survey	San Gabriel River to Newport Bay, 1958
		Profile analysis aid	Orange County, 1934, 1937, 1949, 1958
		Volume changes	Seal Beach, 1934-1958
			Anaheim Bay Harbor to Newport Pier, 1934-1958
			Newport Pier to Newport Harbor, 1934-1958
		Shoreline and offshore changes/Beach profiles	San Gabriel River to Newport Bay, 1878-1958

Table 8.2-1 (cont'd.)
EXISTING SURVEYS, MAPPING STUDIES, PHOTOGRAPHS

Author(s) Date	Type of Data	Location and Dates
USACE LAD, 1967a	Offshore contours	Santa Ana River to Newport Pier, 1966
	Beach profiles	Santa Ana River to Newport Pier, 1958-1966
	Aerial photographs/shoreline changes	Newport Beach, 1965-1967
	Ground photographs	Newport Beach, 1965
USACE LAD, 1967b	Condition surveys/beach profile, offshore profile	Surfside/Sunset Beach, 1963
		Polsa Chica Beach, 1963
		Huntington Beach, 1963
		Newport Beach, 1963
USACE LAD, 1969a	Hydrographic survey	Cabrillo Beach, 1965
	Condition surveys/beach and offshore profiles	Seal Beach to Huntington Beach, 1965, 1965, 1966
		San Gabriel River to Newport Bay, 1966
USACE LAD, 1969b	Aerial photograph	U.S. Naval Weapons Station, Seal Beach, 1966
		Newport Beach, 1968

Table 8.2-1 (cont'd.)
EXISTING SURVEYS, MAPPING STUDIES, PHOTOGRAPHS

Author(s)	Date	Type of Data	Location and Dates
USACE LAD, 1970		Aerial photograph	Cabrillo Beach Groin, 1967
		Ground photographs	Santa Ana River Delta, 1969
			Newport Beach, 1967, 1968, 1970
		Hydrographic survey	San Gabriel River to Newport Bay, 1969
		Shoreline and offshore changes	Newport Bay, 1968
USACE LAD, 1978a		Profiles	San Gabriel River to Newport Bay, 1878-1969
		Aerial photograph	Santa Ana River Delta, 1966-1969
		Beach width history	Surfside/Sunset Beach, 1977
		Beach profiles	Surfside Beach, 1961-1980
Clancy, et al., 1983		Beach berm widths	Sunset Beach, 1977
			Newport Beach 48th Street, 1977-1982

8.3 NEARSHORE WAVES

In situ measurement of waves in relatively deep water, but inside the Channel Islands are available from a buoy in 117 m depth at $35^{\circ}35'$, $118^{\circ}14.9'$. CDIP statistics for 2/81-3/82 (the only available period) are shown in Figure 8.3-1. The seasonal variability is similar to the CDIP Channel Islands gauge (Figure 6.3-9).

Inman and Frautschy (1960) present hindcast statistics for deep water off Long Beach. Information from a variety of sources was used, including hindcasts for 1936-1938 outside the islands (UCSD, 1947), 2 years of observations of north swell at Mission Bay, and 2 years (1952-1953) of southern swell observations at Huntington Beach and El Segundo. The hindcast statistics (Table 8.3-1) are broken down according to the wave categories shown in Figure 8.3-2. Similar to other early hindcasts, the results are very heavily influenced by observations and subjective judgments based on experience.

The Long Beach harbor area is highly sheltered from northern and even westerly swell. However, the open southern window has resulted in some unusual wave events. During the period 20-24 April, 1930, large breakers damaged the outer portion of the Long Beach harbor breakwater (the outer breakwater had not been constructed), but no unusual wave activity occurred at very nearby locations. Consideration of refraction diagrams suggested that only long-period waves from the south would be focused in the observed way (O'Brien, 1950). Figure 8.3-3 shows the intense focusing of 20 sec waves from 160° . O'Brien inferred the source to be so far south that it was in "the area not covered by available weather maps." The observed period was between 20-30 seconds, consistent with a distant southern source.

Horrer (1950) discussed waves at Long Beach associated with both the 1930 event considered by O'Brien (1950), and the 1939 tropic hurricane which caused widespread damage in southern California. Both storms generated waves with a southerly approach direction at Long Beach. Similar to O'Brien (1950), Horrer (1950) concludes that the 1930 storm waves

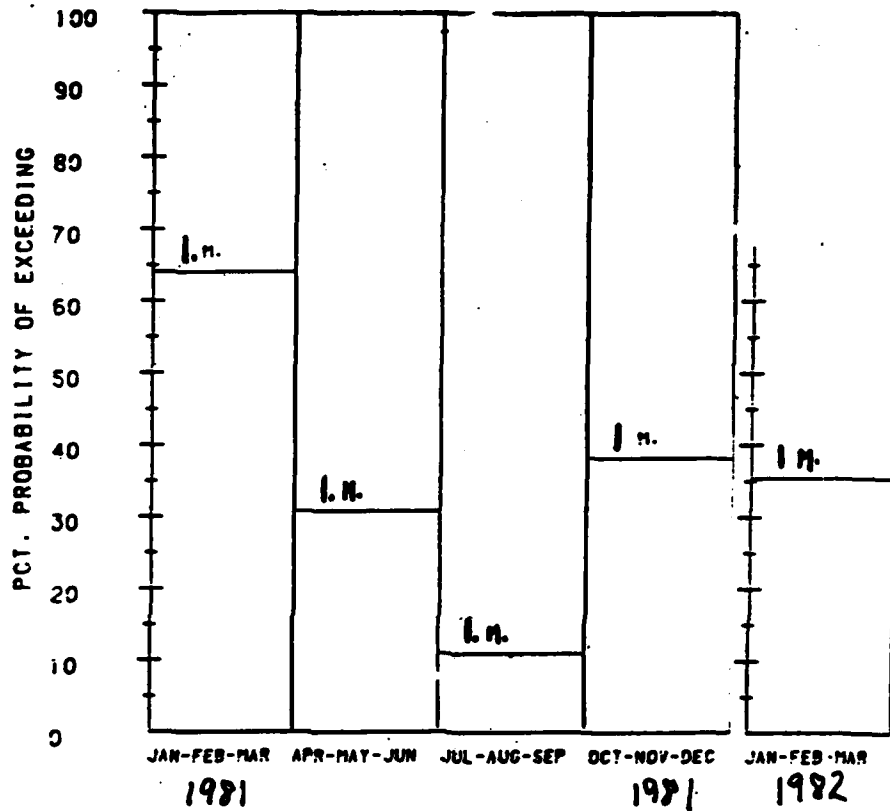
Table 8.3-1 Hindcast statistics for deep water off Long Beach (Frautschy and Inman, 1960).

WAVE TYPE	Typical Parameters		Frequency of Occurrence (days/yr)			Percent of Time	Height by Season				
	Direction	Period	Height (rms)	Winter	Summer		Transition	Winter	Summer	Transition	
Southern Hemisphere Swell	170°	15 sec	1.9 ft	--	55.1	19.5	74.6	30.2	--	1.9	1.8
Sea Breeze	210°	3½ sec	2.1 ft	19.5	42.1	26.9	88.5	35.8	1.7	2.4	1.9
Local Front, west-south-westerly	250°	7 sec	4.2 ft	20.9	18.8	18.2	57.9	23.5	4.8	3.5	4.0
Local Front, Southerly	175°	7 sec	4.3 ft	5.5	0.6	1.4	7.5	3.0	4.5	3.0	4.0
Northern Hemisphere Swell	260°	12 sec	3.5 ft	4.4	10.5	3.5	18.4	7.5	4.0	3.5	2.8

TOTAL 246.9 days

SAN PEDRO CHANNEL BUOY

SEASONAL PROBABILITY OF EXCEEDING VARIOUS SIGNIFICANT WAVE HEIGHTS.



SAN PEDRO CHANNEL BUOY FEB-DEC 1981

CUMULATIVE HEIGHT PROBABILITIES

HEIGHT (CM)	PROBABILITY
360	0.0000
330	0.0000
300	0.0000
270	0.0041
240	0.0164
210	0.0280
180	0.0576
150	0.1087
120	0.4230
90	0.8109
60	0.9984
30	0.9992

SAN PEDRO CHANNEL BUOY JAN-MAR 1982

CUMULATIVE HEIGHT PROBABILITIES

HEIGHT (CM)	PROBABILITY
360	0.0000
330	0.0000
300	0.0000
270	0.0000
240	0.0172
210	0.0401
180	0.1032
150	0.2178
120	0.3983
90	0.7421
60	0.9971
30	0.9971

Figure 8.3-1

CDIP statistics for the San Pedro Channel Buoy.

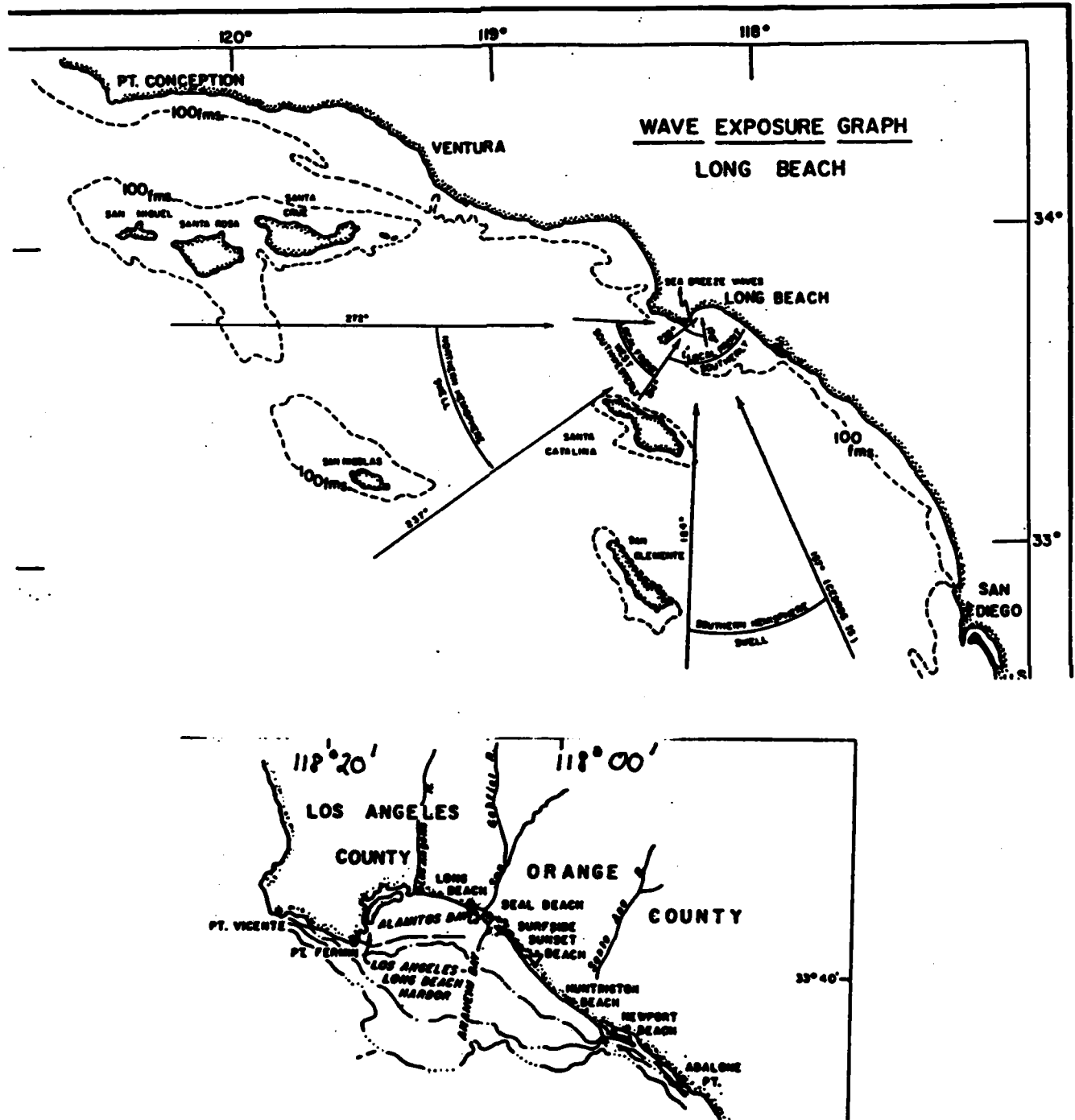


Figure 8.3-2 Schematic of wave exposure at Long Beach (Frautschy and Inman, 1960).

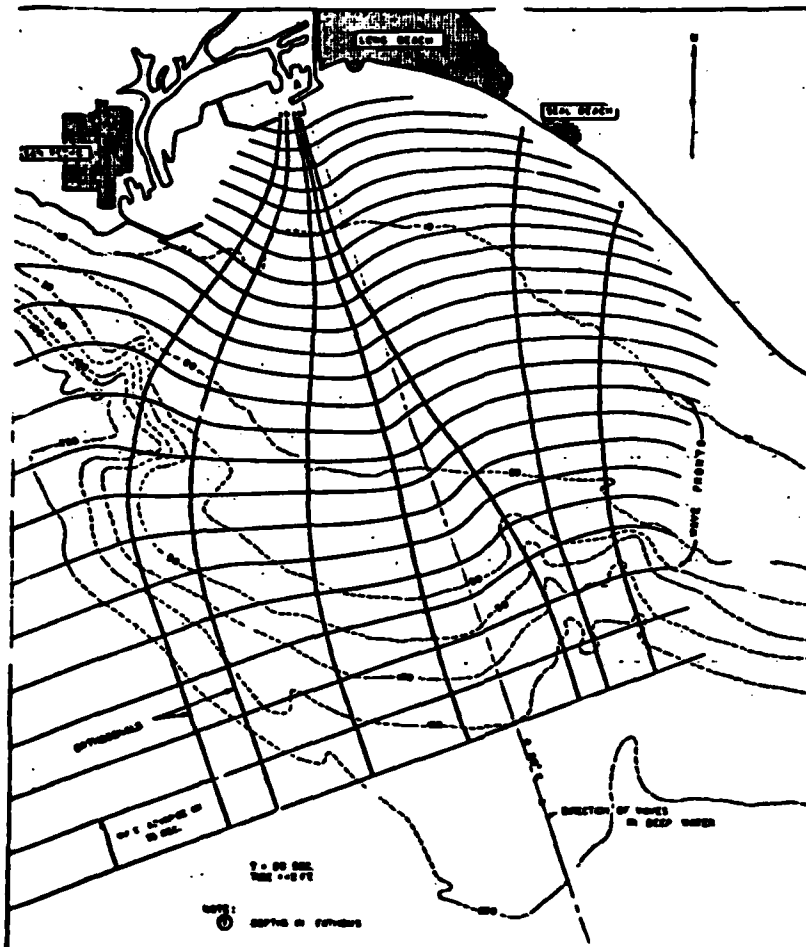


Figure 8.3-3 Refraction diagram for 20 second swell from 160° arriving at Long Beach (O'Brien, 1950).

came from about 160° , and were amplified in height by about a factor of 4 relative to just offshore. Horrer (1950) also describes the meteorological conditions of the 1939 storm, and hindcasts a maximum "height" (not further defined) of 28 feet in deep water off of San Pedro Bay. Examination of damage patterns suggests an approach direction (at Long Beach) between 175° - 185° . Horrer (1950) points out that slight changes in wave direction result in sizeable displacements of convergence zones along the Long Beach area.

Jen (1969) discusses Long Beach harbor area refraction patterns calculated by computer, as opposed to the hand drawn results in earlier studies. Jen (1969) agrees with earlier studies that show open windows due south and due west (Figure 8.3-2). He also shows that southern and southeast swell can be very highly focused within San Pedro Bay. Detailed contour maps of relative wave height are given.

Hales (1980) studied wave effects in the reach from Anaheim Bay to Abalone Point (Figure 8.3-2), essentially the southern half of this cell. Wave statistics were developed for 3 subregions; (1) Anaheim Bay to Huntington Beach, (2) Huntington Beach to Newport Beach, and (3) Newport Beach to Abalone Point. Hindcasts from Marine Advisers (1961a) Station A were used for southern swell, Station B for decayed and local seas, and NMC (1960b) Station 7 for northern hemisphere swell. The offshore swell waves were refracted through the island topography. Further refraction on detailed local bathymetry was used to obtain shallow water wave statistics for each of the 3 subareas. Typical shallow water refraction effects are shown in Figure 8.3-4. The local bathymetry causes significant divergences and convergences of these two common approach directions. Graphs are given for each subreach, which relates the *sheltered* deep water wave height, angle of approach and period to breaker height and breaker angle of approach. Unfortunately, the only wave statistics tabulated are for the unsheltered deep ocean as given by NMC (1960b) and MA (1961a). Neither the sheltered deep ocean or (further refracted) shallow water statistics are given. These statistics are reported to be available. Hales

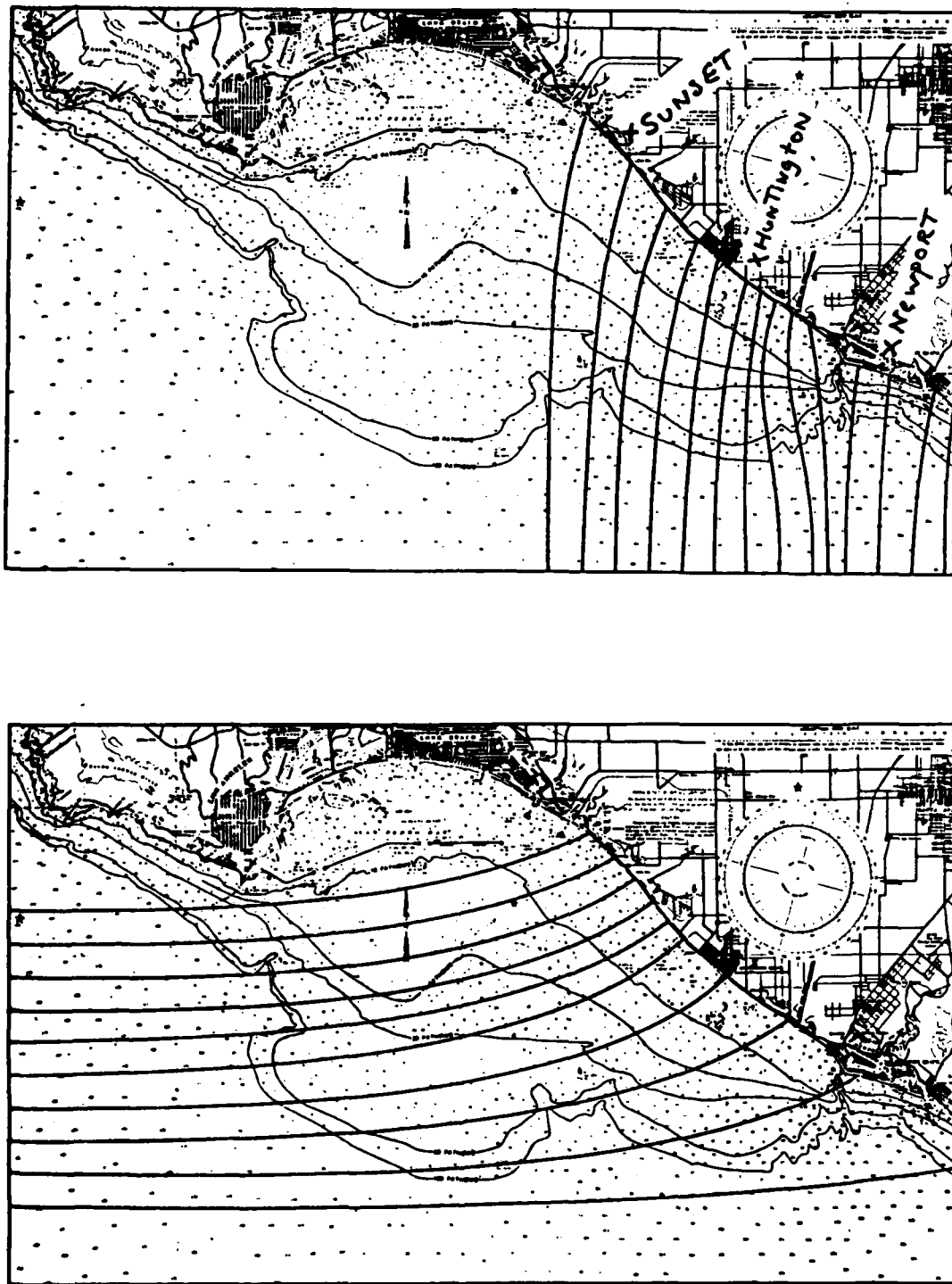


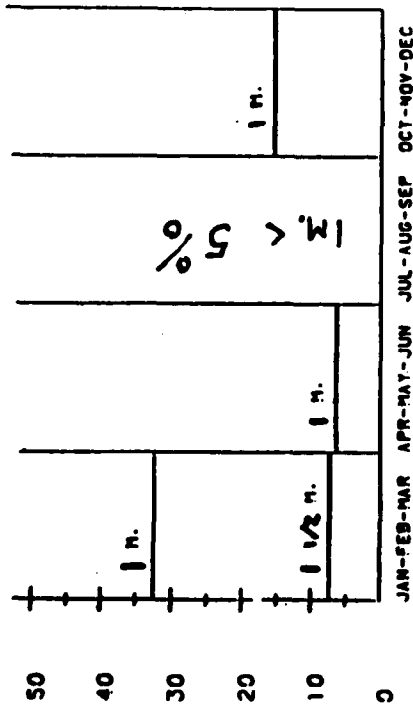
Figure 8.3-4 Refraction diagrams for 18 second swell from south (upper panel) and west (lower panel) in the vicinity of Huntington Beach (Hales, 1980).

(1978a,b) graphs of net monthly transport show a predominance of southern swell (northward transport) in summer and northern swell and sea in winter.

A CDIP slope array provides directional wave data in 8 m depth off of Sunset Beach. Wave heights are consistently low in spring and summer (Figure 8.3-5). The maximum observed significant wave height was about 13 ft, in the winter of 1983 (Seymour, 1983). Sand transport statistics calculated from directional wave data suggest southern swell (northward transport) is important in the fall (Figure 8.3-6), in agreement with Hales' (1980) hindcast calculations. Similar seasonal effects are also apparent in the Sunset Beach hindcast of Marine Advisers (1965). Figure 8.3-7 shows the winter wave rose to be dominated by westerly and southwesterly events which very rarely exceed 10 ft.

Thompson (1977) discusses data collected in about 30 ft depth at the end of the Huntington Beach fishing pier from 1948-1967 and 1972-1975. For reasons detailed in Thompson (1977), and summarized in Section 3.3.2, the 1948-1967 data are only qualitative. Figure 8.3-8 shows the 1964-1967 data to have much lower wave heights than the 1972-1975 data. The wave period data is more consistent, with longer period waves occurring in summer (southern swell) in both time periods. There is every indication that the pre-1972 data is seriously in error. Similar data from Port Hueneme (1961-1965) are probably also corrupt. Note that the early Huntington Beach data is used to develop further wave statistics in USACE LAD (1962a,b). These data are therefore also questionable. Caldwell (1956) used the Huntington Beach data for wave height and hindcasts using wind fields north of 20° N for wave direction. For the period 4/48-4/49 Caldwell (1956) finds only 11% of the deep water wave directions to be south of 270°. The large fraction of northerly waves seems to conflict with observations (Figures 6.4-5,6 and 8.3-6) which show southern swell to be dominant in summer. Of course, southern swell is not hindcast when wind fields north of 20° are considered. Caldwell (1956) actually notes the occurrence of southern swell in some spot checks between

JAN-DEC 1981

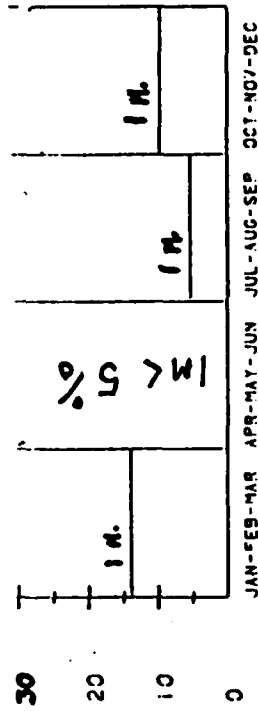


SUNSET JAN-DEC 1981

CUMULATIVE HEIGHT PROBABILITIES

HEIGHT (CM)	PROBABILITY
295	0.0000
280	0.0000
265	0.0000
250	0.0013
235	0.0022
220	0.0044
205	0.0073
190	0.0103
175	0.0147
160	0.0234
145	0.0337
130	0.0527
115	0.1055
100	0.2007
85	0.3861
70	0.6335
55	0.8945
40	0.9941
25	0.9993
10	0.9993

JAN-DEC 1982



SUNSET JAN-DEC 1982

CUMULATIVE HEIGHT PROBABILITIES

HEIGHT (CM)	PROBABILITY
250	0.0000
235	0.0000
220	0.0007
205	0.0022
190	0.0036
175	0.0072
160	0.0129
145	0.0222
130	0.0430
115	0.0667
100	0.1219
85	0.2430
70	0.5035
55	0.8345
40	0.9528
25	0.9993
10	0.9993

Figure 8.3-5 Seasonal and annual probabilities of exceeding various significant wave heights at Sunset Beach (CDIP).

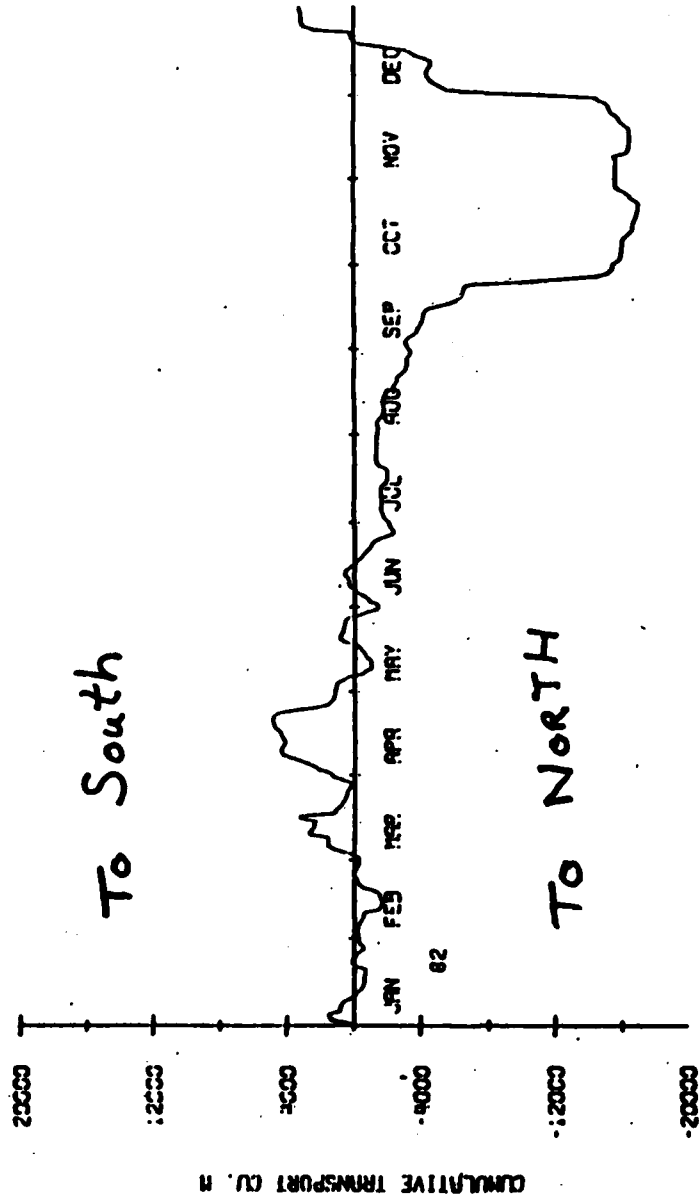


Figure 8.3-6 Cumulative transport at Sunset Beach, 1982 (CDIP).

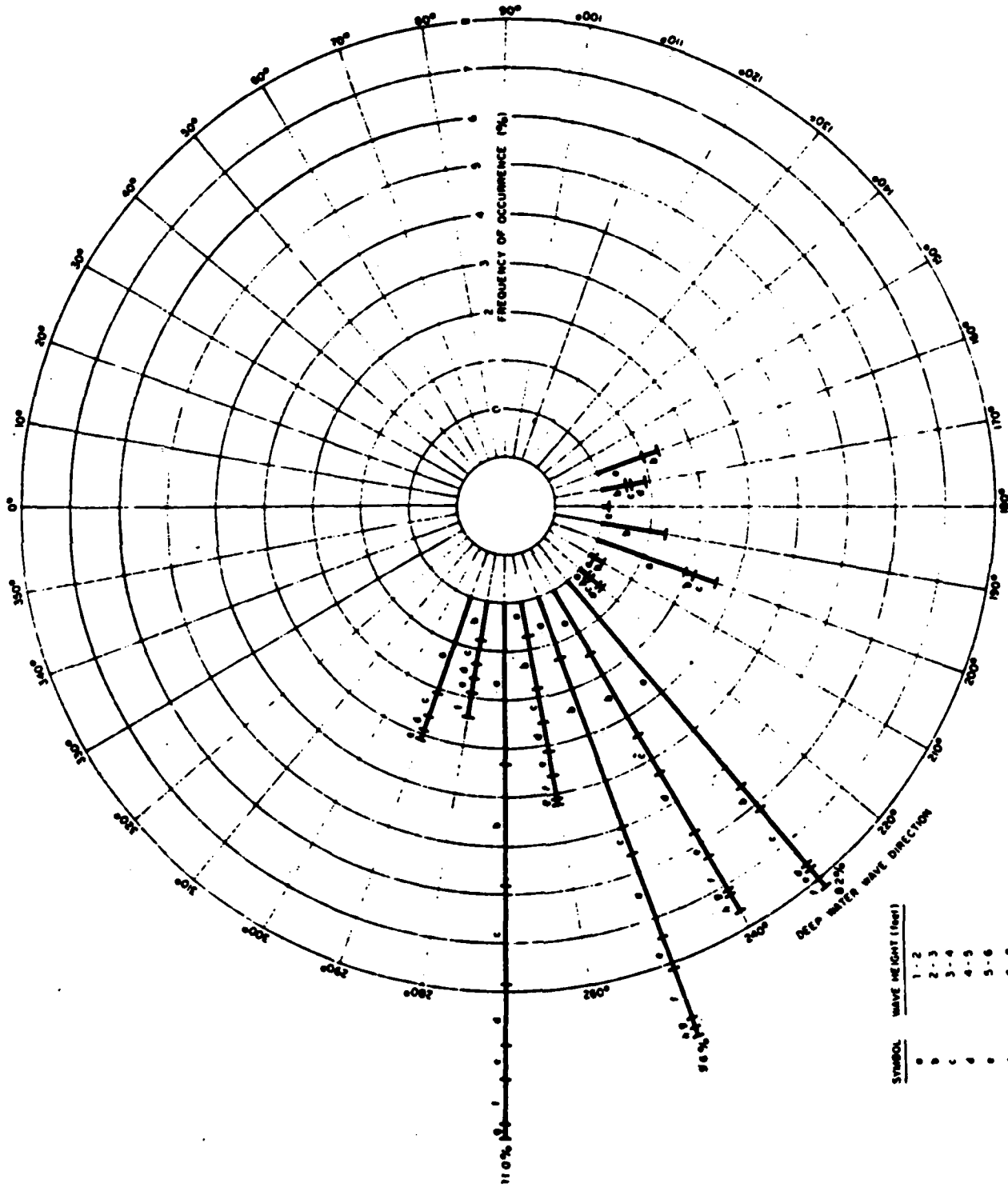


Figure 8.3-7 Hindcast wave rose for winter (Dec-Mar) in a depth of 35 ft at Sunset Beach (Marine Advisers, 1965).

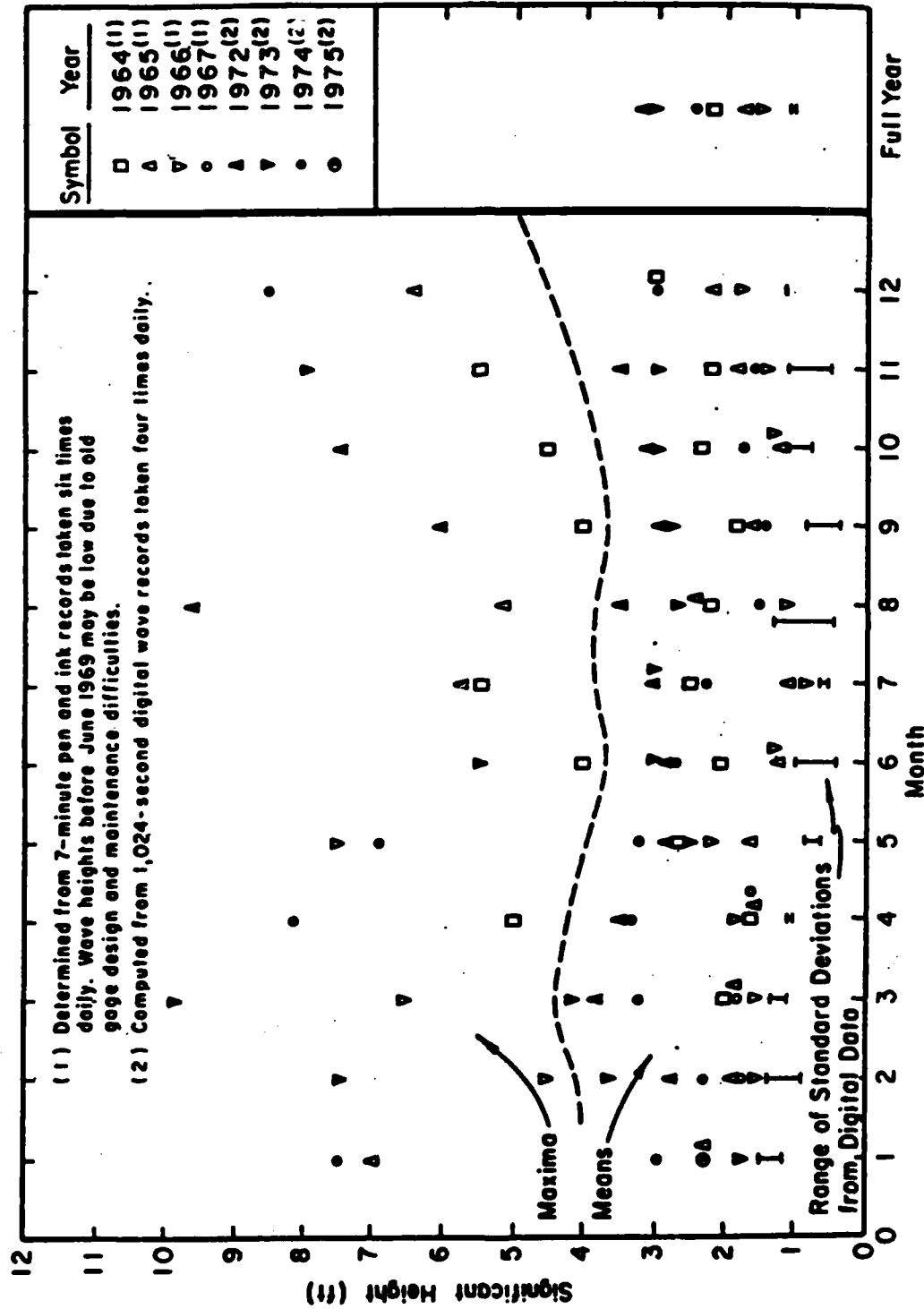


Figure 8.3-8 Maxima, means, and standard deviations of significant wave heights at Huntington Beach, California (Thompson, 1977).

hindcast and photographically determined wave directions. The combined effects of poor wave height measurements and hindcast directions probably introduce very serious errors into Caldwell's (1956) calculations of longshore wave energy flux.

Wave period and height statistics for Huntington Beach (1972-1975) are given by Thompson (1977). Seasonal variations in height similar to Sunset Beach (Figure 8.3-6) are observed. Note that 'calms' (which are not defined) are omitted in Thompson's (1977) tables so the average wave heights and height exceedance statistics refer only to noncalm conditions. The number of calm events is not given, making interpretation of the tabulations difficult. The maximum significant wave height observed was about 10 ft. Thompson (1980) discusses the spectra shapes and parameters associated with the 1972 data, and lists the 24 records (taken 4 times daily) with the maximum significant wave heights. None of these events occur during May-July, consistent with the seasonal pattern in the CDIP data (Figures 8.3-1 and 8.3-5). Nine of the 24 events (and the 294 cm height maximum) occur between 24-30 August. This may have been southern swell. The months of August 1981 and 1982 certainly were not periods of high waves at Sunset Beach (Figure 8.3-5).

8.4 NEARSHORE CURRENTS

None of the literature reviewed explicitly discussed nearshore currents. Surf zone currents are expected to vary seasonally in response to changes in the wave climate (e.g. Figure 6.4-5). Shelf currents are not expected to be dramatically different from cells to the north or south.

8.5 SEDIMENT SOURCES

8.5.1 *Cliff Erosion and Relict Dunes*

Shepard and Grant (1947) discuss wave erosion along the southern California coast. They discuss cliff erosion at Point Fermin but do not estimate the amount of material that cliff erosion delivers to the beaches. Zeller (1962) points out that a minor mass of sand at Bolsa Bay between Sunset and Huntington Beaches is the only coastal dune in this littoral cell. He does not estimate the amount of sand from the dunes that reaches the active beach zone. Norris (1964) briefly mentions the El Segundo dunes as a source of beach material.

8.5.2 *Sediment Discharge from Rivers and Streams*

USACE LAD (1962a) contains sand sample analysis for samples taken at the mouths of the San Gabriel and Santa Ana Rivers. This report also discusses the tributary drainage basins of these two rivers and the character of the littoral material they deliver to the beaches. Judge (1970) discusses the heavy mineral content in beach and stream sediments. He includes average annual discharge and drainage area for the Los Angeles, San Gabriel and Santa Ana Rivers (see Table 8.5-1). USACE LAD (1970) contains sand sample analysis at samples taken from Newport Beach. This report also contains a summary of a study of the Santa Ana River Delta.

Hales (1980) presents an extensive study of the Santa Ana River. With the exception of the Tijuana River drainage basin, the Santa Ana River is the largest river system in southern California and has been identified as one of the most significant potential flood problems in the entire State (see Figure 8.5-1). Brownlie and Taylor (1981) report on coastal sediment delivery by major rivers in southern California. They summarize water and sediment discharges for the Los Angeles and San Gabriel River basins (Figure 8.5-2); and the Santa Ana River basin, (Figure 8.5-1), (See Table 8.8-1). They estimate sediment yield from "sediment rating" curves for suspended load versus water discharge. They assume bedload to be 10% of the suspended

Table 8.5-1
River Discharge and Drainage Area

<i>Stream</i>	<i>Average Discharge</i> (Acre-feet per year)	<i>Drainage Area</i> (Square miles)
Los Angeles River	100,600	1190
San Gabriel River	23,560	540
Santa Ana River	11,000	2490

Data from topographic maps and U.S. Geological Survey Water Supply Paper 1735 (from Judge, 1970).

Discharges are averages of available years at every station, but more than five years as a minimum. Areas are by planimetric determinations to nearest 10 square miles.

load but the bedload may be more like 20% of the suspended load (see Inman and Jenkins (1983) and Section 2.5 for discussions).

8.5.3 *Artificial Beach Nourishment*

Caldwell (1956) briefly mentions the dredging of Anaheim Bay Harbor for beach nourishment material deposited at Surfside and Sunset Beaches. Dunham (1965) discusses the Cabrillo Beach Groin. When the groin was under construction in 1962, 2,000,000 yd³ of dredged material was pumped into the adjacent beach area concurrently. USACE LAD (1967a) is a design memorandum for beach stabilization between the Santa Ana River and the Newport Pier. The report describes the proposed fill and borrow area, and reports on the monitoring of 4,000,000 yd³ of sand placed on Surfside-Sunset Beach prior to 1964. USACE LAD (1969b) describes the plans for beach fill and groin construction at Newport Beach.

USACE LAD (1970) contains beach profiles and discusses beach nourishment effectiveness for the Surfside-Sunset Beach project executed in 1962. The report also discusses the Newport Beach Groin and beach nourishment project. California (1977b) is a compilation of information on sediment transport in coastal stream basins and beach nourishment along the southern California coastline. The information provides an order of magnitude estimate for sediment production and locations of abundant inland sources of material for beach nourishment. USACE LAD (1978a) is the final pre-project report describing the beach nourishment plans for Surfside-Sunset Beach. The report is thorough and the only reference reviewed for this study describing a nourishment project.

Hales (1980) describes the erosion problems at the Surfside-Sunset Beach and the determination of optimum location and temporal distribution of 1,000,000 cu yd³ of beach nourishment material dredged from the Santa Ana River flood-control channel. Herron (1980) briefly discusses the San Pedro Cell and beach nourishment from the Anaheim Bay jetties to the Newport jetties. Shaw (1980) summarizes beach nourishment projects and locations of

structures in coastal southern California. The report is well done and includes a table describing nourishment projects in terms of fill location, source location, volume of material and project dates. The report also describes all southern California man-made coastal structures, the materials they are constructed from, their sponsor, and the date of construction. Beach nourishment has also taken place at Seal Beach, Newport Beach, Cabrillo Beach and Palos Verdes.

Osborne et al (1983) locates and delineates offshore sediment resource areas with a combination of seismic reflection profiles and extensive vibracore data to define stratigraphic horizons, mechanical and textural properties of the material. This report includes an extensive reference list of reports, most of which are not included in this study.

8.6 SEDIMENT TRANSPORT MODES

8.6.1 *Cross-shore Transport*

Some examples of seasonal profile changes exist in the profiling performed by the Corps in this cell. (See Section 8.2 of this report.) However, rates of cross-shore transport, either seasonal or net, have not been computed. Volume changes for various beaches have been computed (i.e., USACE LAD, 1969a) but no differentiation is made between changes due to cross-shore transport and changes from fluctuation in the longshore rate. This cell has been developed and changed to such a large extent by man, that there are few natural beaches left on which to study cross-shore transport independent of structurally induced longshore transport variations. Inman and Frautschy (1960) examined bathymetric charts of the Los Angeles-Long Beach area from the 1800's, prior to any construction there. They found a net erosion rate for the entire area of $273 \times 10^3 \text{ yd}^3/\text{yr}$. However, it is unclear what combination of forces caused this erosion.

At the end of the cell near Newport, there is some evidence which suggests that the major sink for the cell has changed from Newport Submarine Canyon to continental-shelf deposits

carried offshore by strong rip currents. (See Section 8.7.1).

8.6.2 Longshore Transport

Longshore transport rates for this cell are summarized in Table 8.6-1. "Potential" rates are obtained from application of the standard "radiation stress" equation (Section 2.4) with wave data as inputs. Both volume transport (Q_l (yd^3/yr)) and immersed-weight transport I_l (newtons/second) are listed. In converting between the two measures, it was assumed that solids concentration $N_o = 0.6$ (porosity = 0.4) and sand density $\rho_s = 2.65 \text{ g/cm}^3$. Positive values represent transport to the south, negative to the north.

In the northern part of this cell, the Los Angeles-Long Beach Harbor area, the coastline has been almost completely blocked from waves by breakwaters (Figure 8.7-3). Also, much of the sand beach has been replaced by development. Thus in the presence of structures, it is believed that longshore transport in the area is essentially zero (Inman and Frautschy, 1960). Inman and Frautschy performed a wave refraction study in the area, assuming the structures were absent. They found that if the coastline were unprotected, the net longshore transport would be $117 \times 10^3 \text{ yd}^3/\text{yr}$ to the east.

Several estimates of longshore transport have been made in the 16-mile stretch of coast, which includes from north to south: Seal Beach, Anaheim, Sunset Beach, Huntington Beach and Newport. In 1944, Anaheim Bay was constructed which effectively halted transport to the beaches south of the bay entrance. To halt erosion beach nourishment was tried in 1945, 1947, and 1950. The Corps performed a series of beach profiles after the 1947 nourishment. Caldwell (1956) used that data to estimate net annual southerly longshore transport of $175 \times 10^3 \text{ yd}^3/\text{yr}$. Das (1971) summarizes their methods and data, and lists wave data for the same period. Marine Advisors (1965) used wave refraction to estimate transport from the radiation-stress equation and obtained $282 \times 10^3 \text{ yd}^3/\text{yr}$.

Table 8.6-1. Longshore Transport Rates
(Positive values indicate transport to the south, negative to the north)

Location	Notes	Reference	Potential Transport (Wave Refraction Studies)		Gross Transport (Trapping Studies)		Instantaneous Net Transport (Sand Tracer Studies)	
			Q_1 ($10^3 \text{ yd}^3/\text{yr}$)	I_1 (N/sec)	Q_1 ($10^3 \text{ yd}^3/\text{yr}$)	I_1 (N/sec)	Q_1 ($10^3 \text{ yd}^3/\text{yr}$)	I_1 (N/sec)
Long Beach	Natural state	Inman and Frautschy (1960)	117	28				
Long Beach	Protected state	Inman and Frautschy (1960)	none					
Anaheim to Newport	Followed sand plug	Caldwell (1956) Johnson (1957)			175 150	41 35		
Anaheim to Newport		Marine Ad- visors (1965)	282	66				
Anaheim to Newport	Range of values	Ingle (1966)					27 to 1060	6 to 249
Anaheim to Newport	Average of values	Ingle (1966)					192	45
Sunset Beach	No refraction < 10 m deep	Seymour and Castel (1984)	200	47				
*Surfside-Sunset		Hales (1980)	276	65				
*Santa Ana River		Hales (1980)	112	26				
*Newport Beach		Hales (1980)	127	30				

* "Best" estimate at the location

Ingle (1966) measured longshore transport with fluorescent sand tracer on Huntington Beach. He obtained longshore sand velocities ranging from 6 to 23 ft/min (3-12 cm/s) and transport of 75 to 2900 yd³/day (27-1060 x 10³ yd³/yr). These measurements are probably good estimates of the range of transport rates to be expected. Ingle (1966) averaged all his measurements to obtain 192 x 10³ yd³/yr.

The most complete study of longshore transport in this area was made by Hales (1980). Hales used wave refraction and calculated not only net transport but also temporal and spatial variations in the transport. In his studies at Oceanside (Hales, 1978b) and Mission Bay (Hales, 1979) he used DNOD fleet numerical data for northern swell. These data are inaccurate for southern California beaches, see Section 3.2.2. Thus his Oceanside and Mission Bay transport estimates are suspect. For the San Pedro Cell he used the Marine Advisors (1965) wave data, which is more accurate. The results of his transport calculations are presented in Figures 8.6-1 through 8.6-3. His estimates of net transport were 276 x 10³ yd³/yr at Surfside-Sunset Beach, 112 x 10³ yd³/yr at the Santa Ana River mouth, and 127 x 10³ yd³/yr at Newport Beach, all to the south. The different contributions from the three wave sources (southern swell, northern swell, and local sea waves) are shown in Figure 8.6-1. The contributions from all three sources are more important in the middle of the study area than at either end. In Figure 8.6-2 the transport both to the north and south at each of the three sites is listed by month. In general there is strong southerly transport in the winter and moderate northerly transport in the summer. This trend is even more obvious in the plot of each month's net transport in Figure 8.6-3. Transport reversals are much more common in this cell than in other southern California cells. Other investigators have confirmed this conclusion of Hales (1980). The motion of dredge spoil near Newport was monitored in the 1930's. House Document #637 (1940) revealed transport during that period of 567 x 10³ yd³/yr to the north and 160 x 10³ yd³/yr to the south.

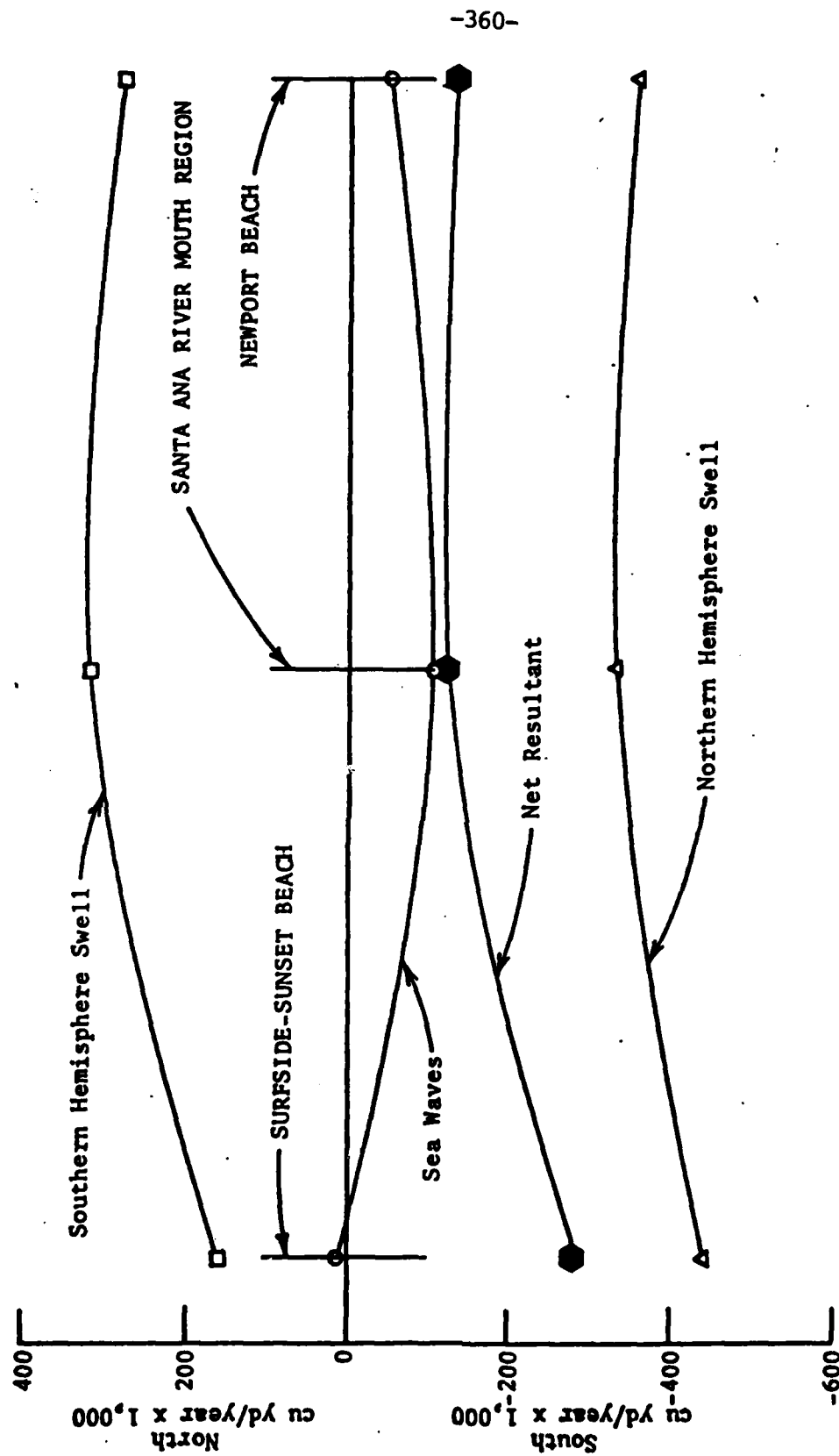


Figure 8.6-1. Net annual potential longshore transport from Surfside-Sunset Beach to Newport Beach (from Hales, 1980).

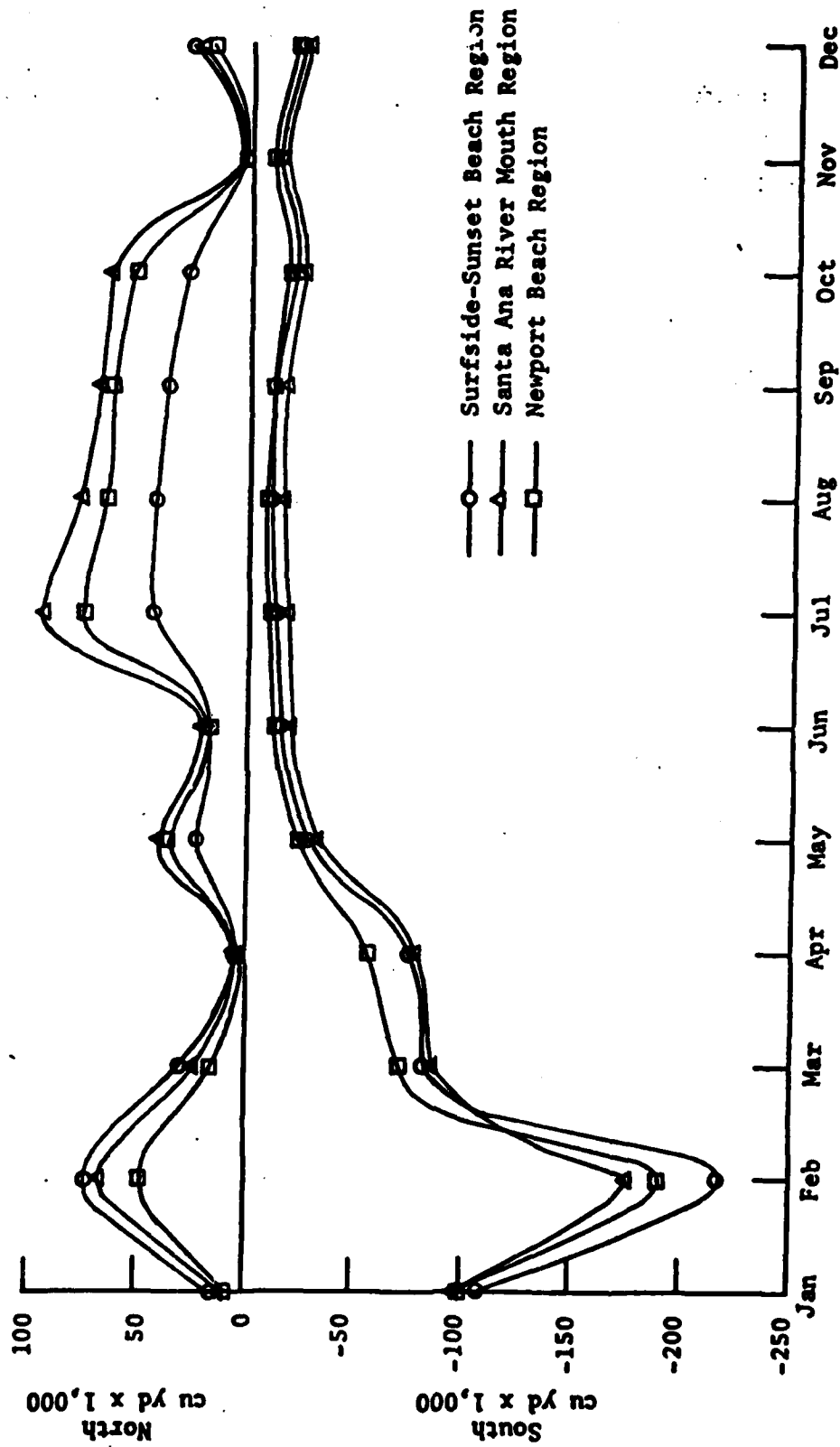


Figure 8.6-2. Monthly potential longshore transport from Surfside-Sunset Beach to Newport Beach (from Hales, 1980).

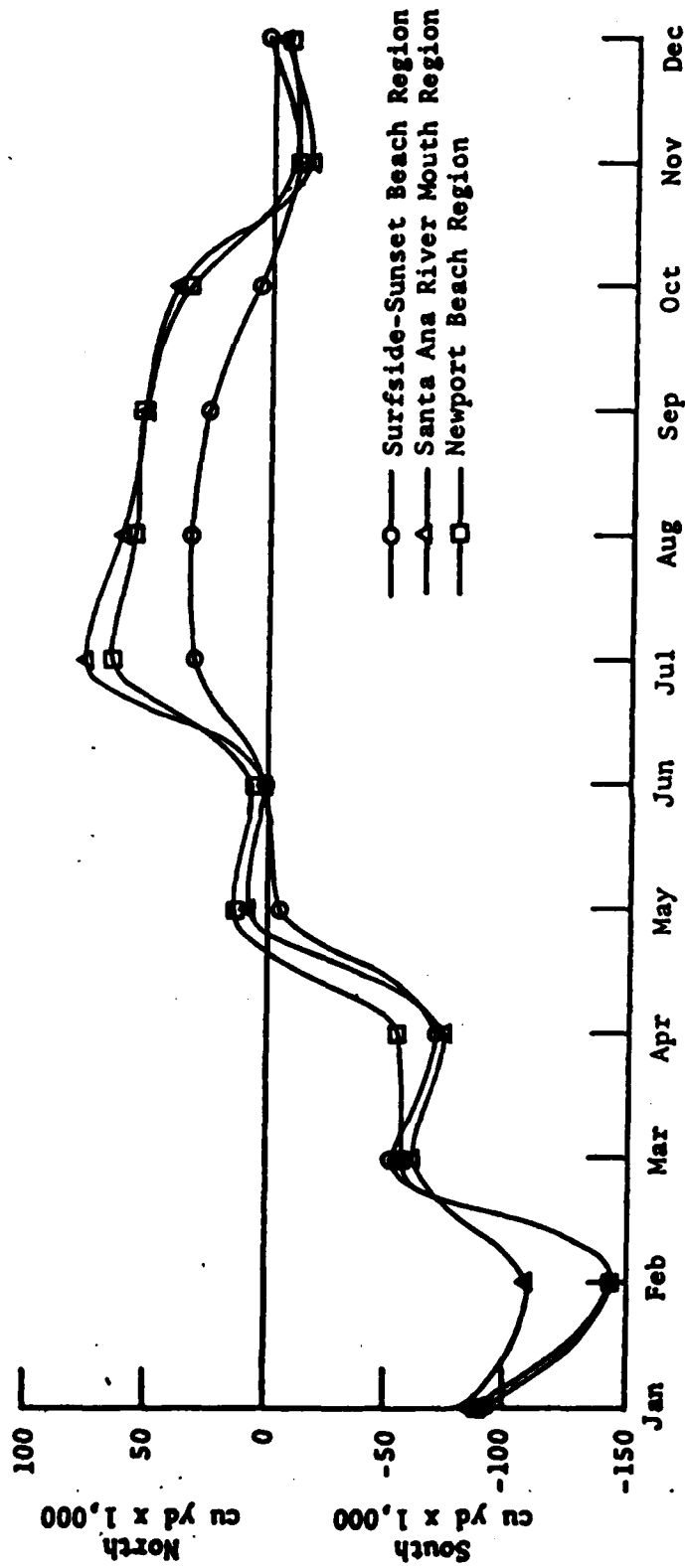


Figure 8.6-3. Net monthly potential longshore transport from Surfside-Sunset Beach to Newport Beach (from Hales, 1980).

Clancey, Camfield and Schneider (1983) estimated longshore transport from two different methods, both of which have serious drawbacks. They monitored erosion and accretion simply by monitoring the location of the beach berm. They assumed no seasonal cross-shore transport, an assumption which is clearly false for southern California beaches. Instead they assumed all berm motion to be caused by longshore transport of plugs of sand. The other method they tried was computation of longshore transport from the radiation-stress equation with visual (LEO) wave data as inputs. Such visual data are not adequate for computation of longshore transport rates.

Castel and Seymour (1982) reported on seasonal cycles of transport at Sunset Beach in 1981. As input to their calculations they used data from their array of pressure sensors at 8 m depth. They assumed no wave refraction took place shoreward of their sensors, a very dubious assumption. Thus their absolute values of transport are unreliable. Nevertheless, important relative information on seasonal cycles is available. They show exactly the same seasonal variations as Hales (1980): strong southerly transport in the winter and moderate northerly transport in the summer. In our opinion, the seasonal cycles shown in Figure 8.6-2 and 8.6-3 are reliable, since they have been confirmed from two independent sets of wave data. Seymour and Castel (1984a) report on the transport cycles at Sunset Beach in more detail. The absolute transport rates in columns 2 and 3 of Table 9.6-6 are unreliable because of the aforementioned wave-refraction problem. But the relative magnitudes of episodicity of transport in columns 4 and 5 reveal important information. The transport during one day can be as large as 9% of the total net annual transport. Half of the year's transport can occur during only 10% of the most energetic days. In building coastal structures, statistics such as these become important, in addition to the usual consideration of net annual transport.

8.6.3 Wind Transport

This area is well developed with no large dune fields, which tends to indicate that wind transport is not important. Nevertheless, some investigators (i.e. Hales, 1980) show photographs of sand that has been blown off beach berms back onto city streets. No quantitative data on wind transport are available in this cell. Longshore wind transport is probably quite small compared to the large wave-induced longshore transport. Whether onshore wind transport represents a significant portion of net cross-shore motion is unknown.

8.7 SEDIMENT SINKS

8.7.1 *Submarine Canyons*

There are two submarine canyons in this cell, San Gabriel and Newport (Figure 8.7-1). The only one close enough to the coast to have a significant impact as a beach-sand sink is Newport. Nevertheless, Karl (1980) has identified transport mechanisms for very fine beach sand to San Gabriel Canyon, 7.5 km from the coast. Karl (1980) describes the following scenario: "Overlap of inshore turbid water, transported seaward by a current system generated by surface waves, with sediment resuspended by breaking internal waves farther offshore creates a continuous cross-shelf corridor...for the transport, primarily as suspended load, of fine sediment." He does not quantify the total amount of sand transported in such a manner. Considering the distance of the canyon from the coast, it is difficult to believe that there could be significant transport down San Gabriel Canyon.

In the past it has been suggested that Newport Canyon may represent a significant sand sink (House Document # 637, 1940; Inman and Frautschy, 1965). However, these suggestions refer to the cell in its natural state. There is now evidence which suggests that Newport Canyon is no longer an active sink.

Felix (1969) finds Newport head to now be "dead" as a sand sink and attributes this to the formation of Newport Spit in 1925. However, the spit has been present during historic times

(Inman and Fratuschy, 1958). Felix fails to recognize that the most likely reasons for the death of Newport Submarine Canyon as a sand sink are: (1) the loss of sand source from the many rivers that formerly brought sediment to the coast in this area; and (2) the Long Beach/Los Angeles Harbor breakwater that cuts off wave energy that formerly carried sand to the canyon head.

Felix and Gorsline (1971) claim that most of the sand which formerly flowed down Newport Canyon is now deposited on the continental shelf northwest of the canyon head. They examined the sediment distribution in the area and found that the canyon head contains silt and clay, not sand. However, they found a large (2 x 2 mile) area of fine sand on the shelf northwest of the canyon. This is the same area that Karl (1980) was working in. Felix and Gorsline (1971) describe a scenario of beach sediment transport to the shelf very much like the one described by Karl. Their transport scenarios for the two principal wave directions are illustrated in Figure 8.7-2. They claim that wave convergence associated with the canyon and the rip currents occurs northwest of the canyon, rather than at the canyon head. Neither Felix and Gorsline (1971) nor Karl (1980) have quantified this transport. In any case, the important point to note in terms of the cell budget is that most of the sand that reaches the end of the cell is transported offshore, whether onto the continental shelf or down-canyon.

8.7.2 *Entrapment by Harbors, Bays and Estuaries*

The following channels from the Pacific Ocean to other bodies of water exist in this cell: channels behind the Los Angeles-Long Beach breakwaters, Alamitos Bay channel, Anaheim Bay, the Santa Ana River mouth, and Newport Bay channel (Shaw, 1980). The channels behind the Los Angeles-Long Beach breakwaters (Figure 8.7-3) are effectively protected from wave attack and thus do not trap longshore transport. Profiling and dredging of Alamitos Bay channel (Figure 8.7-4) have not been done on a regular enough basis to enable good trapping estimates. However, Shaw (1980) reports extensive shoaling in the channel from sediment carried in from

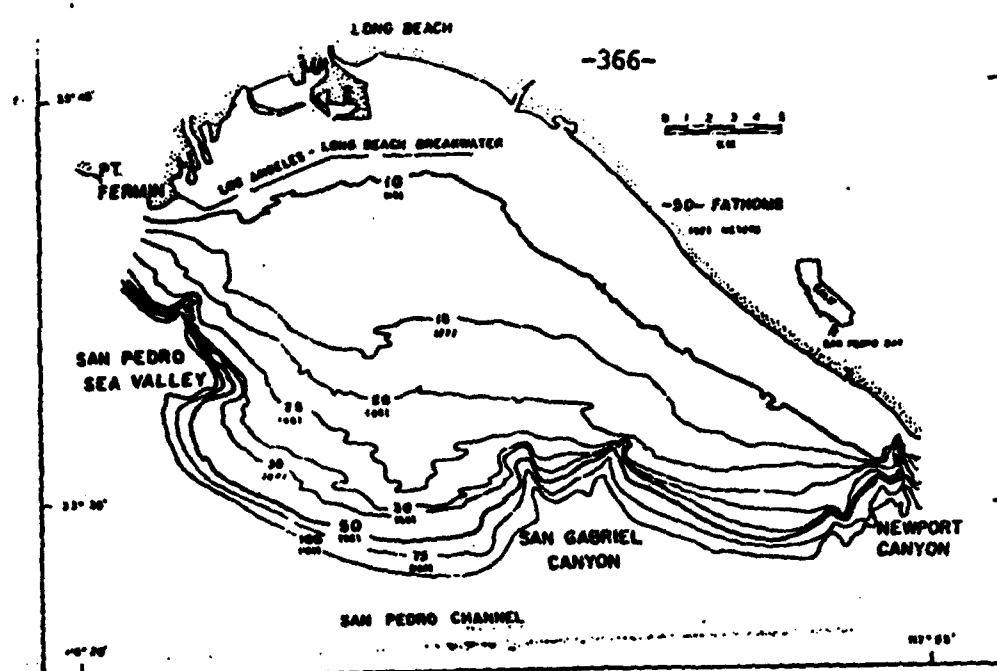


Figure 8.7-1. San Pedro Cell bathymetry and submarine canyon locations (from Karl, 1980).

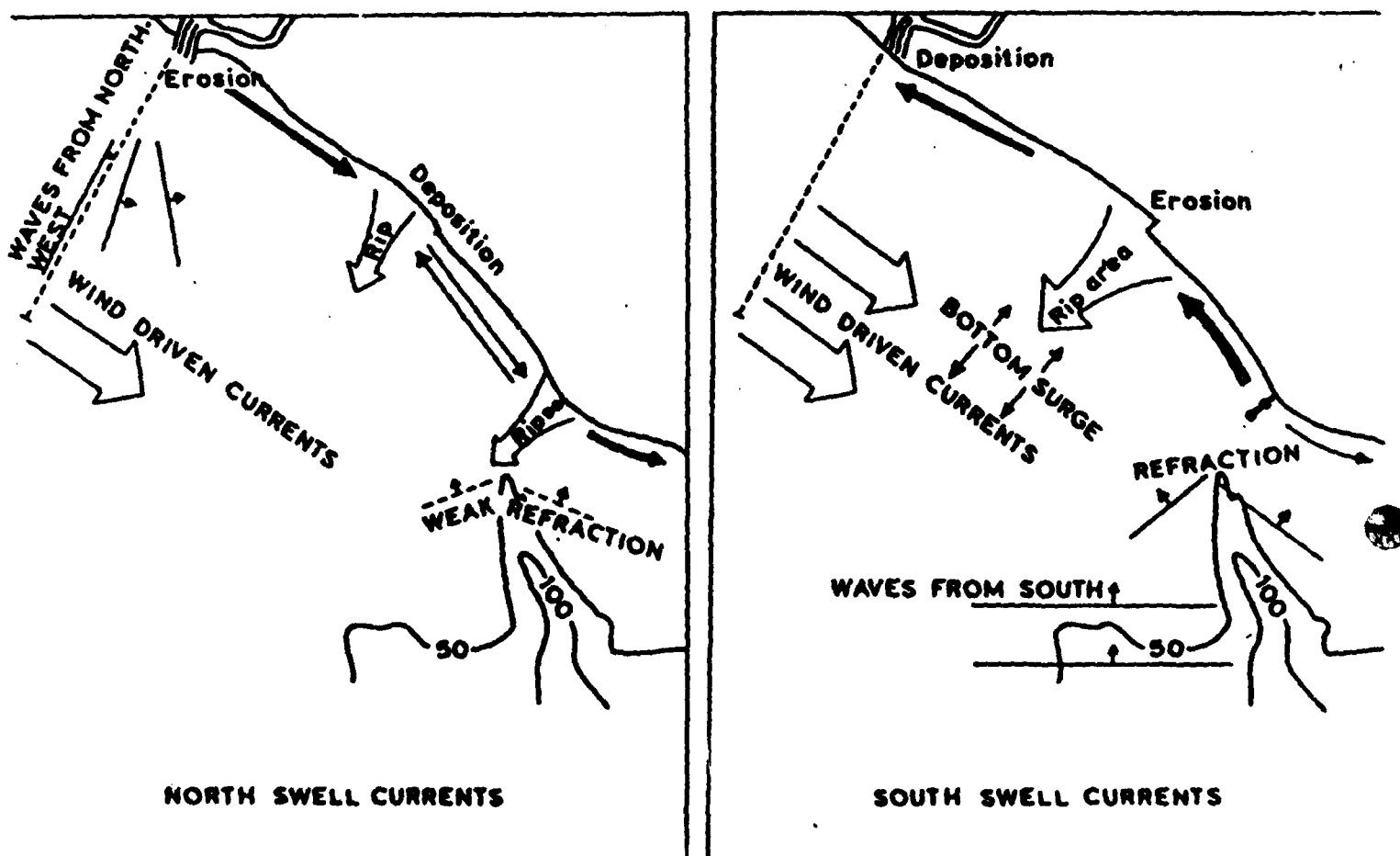


Figure 8.7-2. Longshore drift and current system for the two major local wave directions near Newport Submarine Canyon. Flow magnitudes and directions are schematically shown (from Felix and Gorsline, 1971).

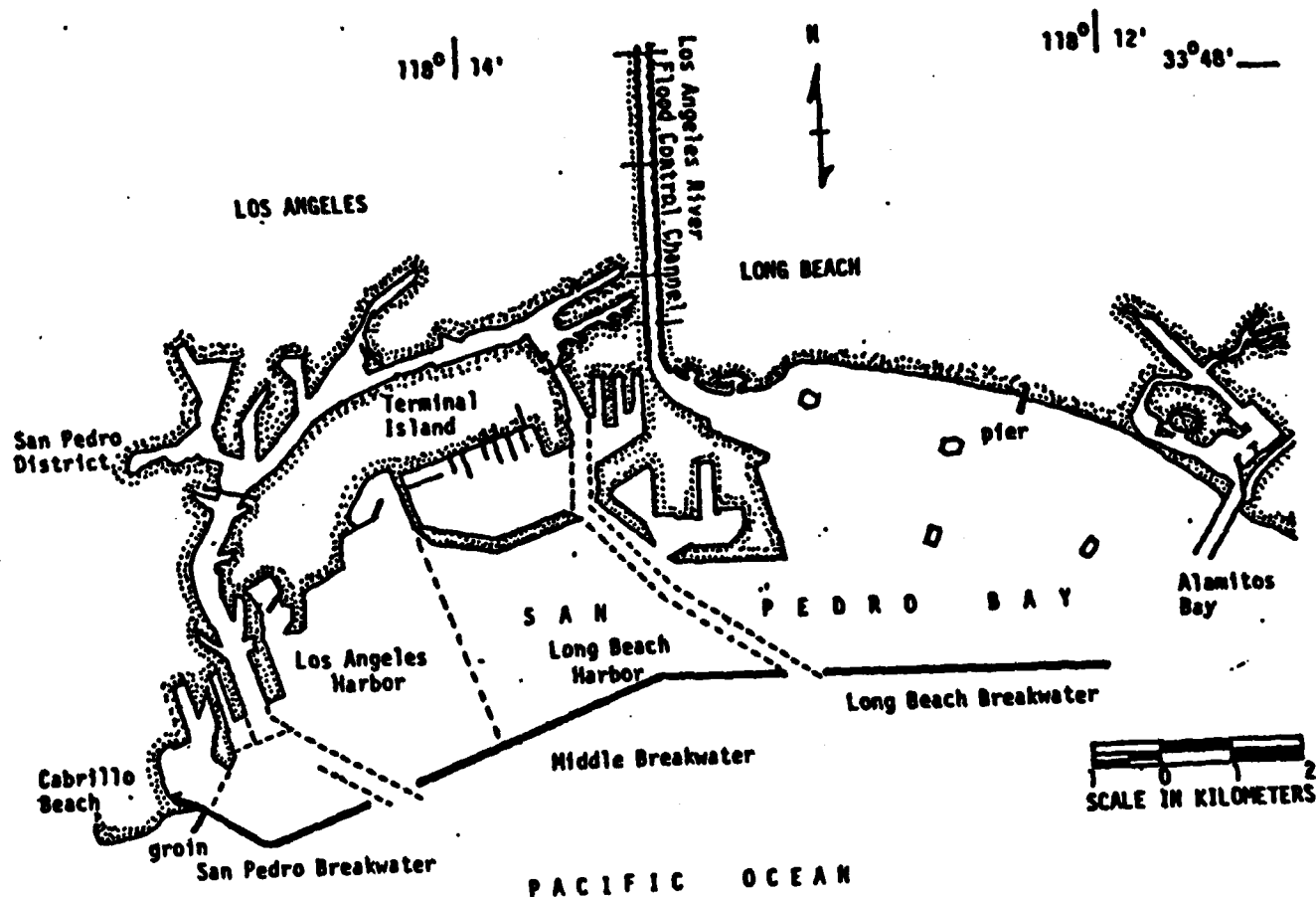


Figure 8.7-3. San Pedro Harbor [Los Angeles and Long Beach Harbors] (from Shaw, 1980).

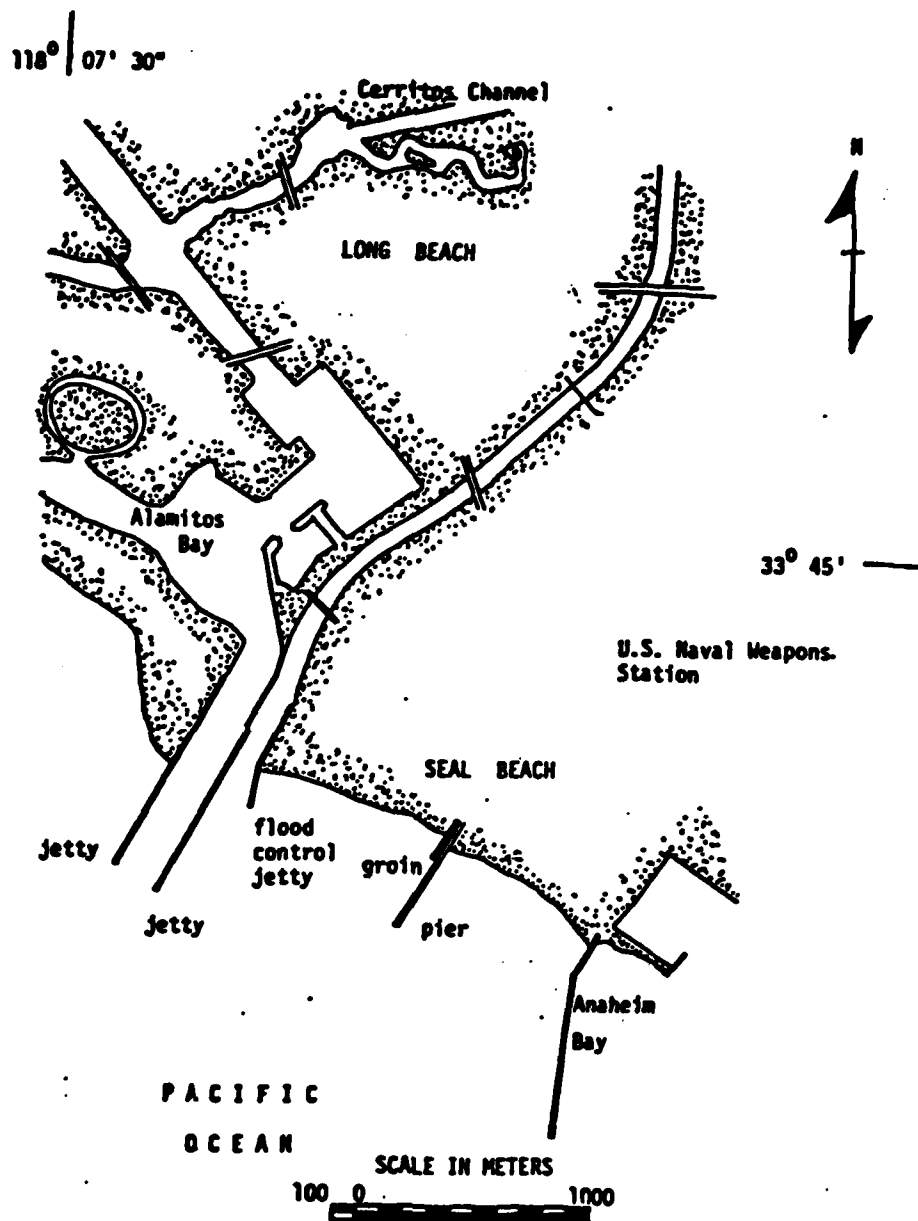


Figure 8.7-4. Alamitos Bay and Seal Beach (from Shaw, 1980).

offshore during the flood tide.

The largest interruption of longshore transport in this cell appears to be at the Anaheim Bay breakwaters (Figure 8.7-5). The rubble-mound 1160 m east breakwater and 915 m west breakwater were completed in 1944 (Shaw, 1980). Profiling south of the breakwaters documents severe erosion caused by essentially total blockage of longshore transport by the structures (Caldwell, 1956). Transport on the beach south of the bay was measured by profiling, and was found to vary between 303 and 1680 yd^3/day to the south ($111\text{--}613 \times 10^3 \text{ yd}^3/\text{yr}$) with one reversal of transport to the north at 2130 yd^3/day ($777 \times 10^3 \text{ yd}^3/\text{yr}$). Various authors have used aerial photographs to observe that transport appears to be essentially totally blocked by the breakwaters (Caldwell, 1956; Inman and Frautschy, 1960; Hales, 1980). No visible or measurable amounts of sediment appear to be bypassing the structures or entering the channel.

At the mouth of the Santa Ana River (Figure 8.7-6) four 45 m jetties were constructed in 1935 in an attempt to stabilize the flood-control channel (Shaw, 1980). Hales (1980) presents aerial photographs showing blockage of the river mouth by littoral drift. However, during periods of high river flow, photographs show removal of the mouth's sand plug by the river flow. Trapping rates at the mouth have not been measured.

The structures at Newport Bay entrance channel are two breakwaters (Figure 8.7-7). The 867 m west breakwater was completed in 1927 and the 495 m east breakwater in 1936 (Shaw, 1980). The adjacent beaches have remained relatively stable (Shaw, 1980). This must be because either there is little longshore transport here or the breakwaters are effectively bypassed by the littoral drift. At the Newport Pier (Figure 8.7-7) there is a change in orientation of the coast. There is some speculation that north of this point there is significant offshore transport, and that south of the pier there is little longshore transport (Inman and Frautschy, 1958; Felix and Gorsline, 1971; Karl, 1980). Newport Submarine Canyon is just offshore of this point. In summary, no direct evidence of longshore transport near Newport Bay entrance channel exists,

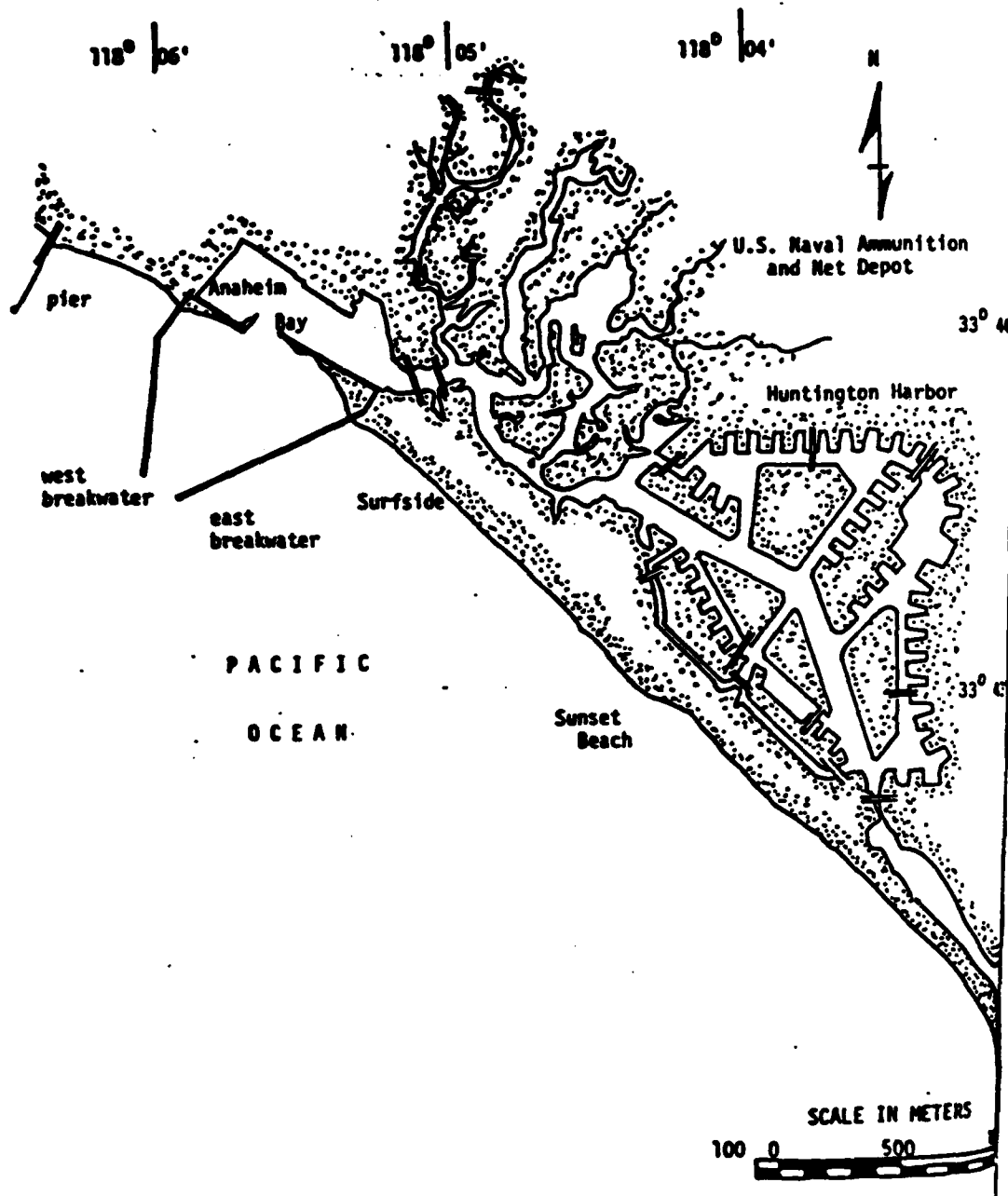


Figure 8.7-5. Anaheim Bay, Surfside and Sunset (from Shaw, 1980).

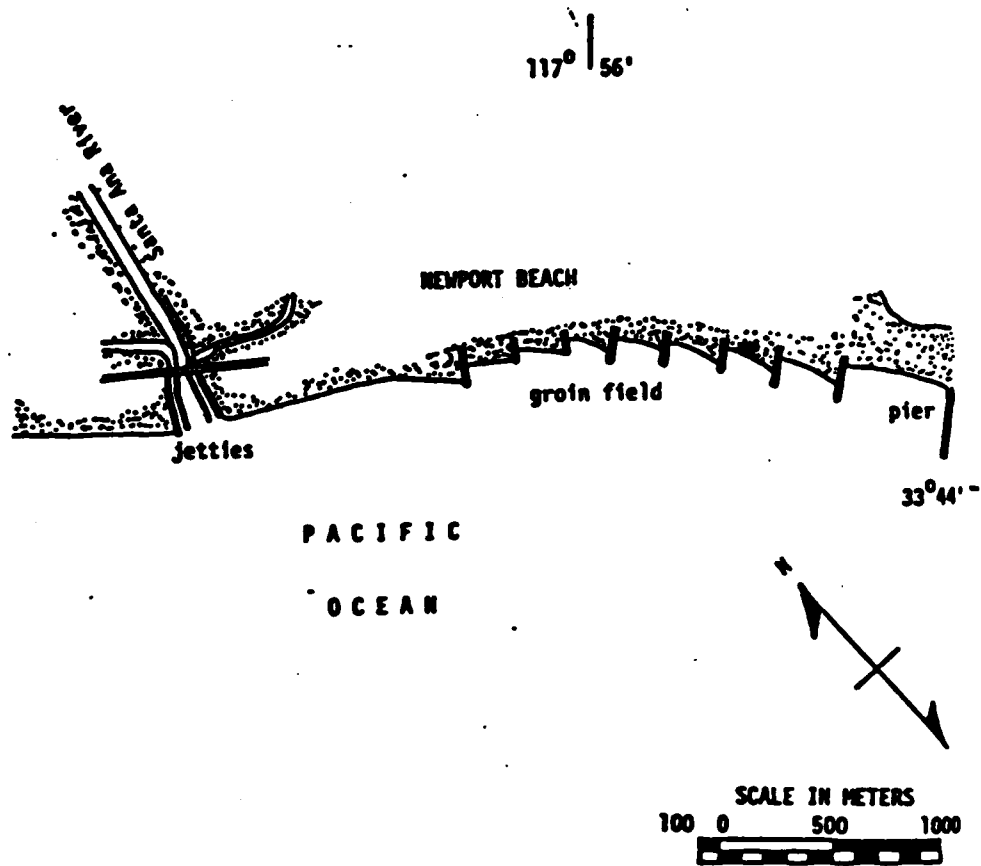


Figure 8.7-6. Newport Beach (from Shaw, 1980).

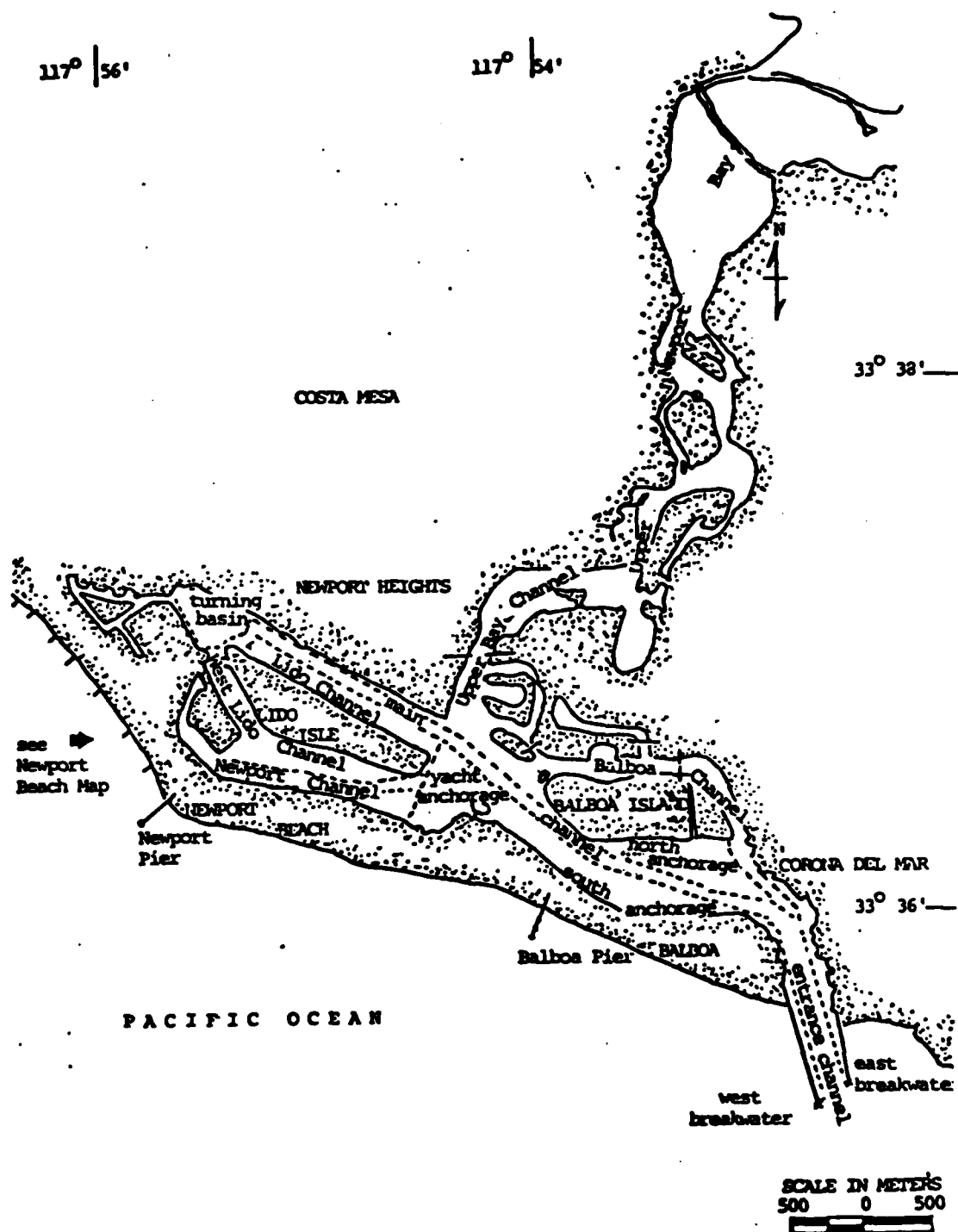


Figure 8.7-7. Newport Bay Harbor (from Shaw, 1980).

whereas some evidence of offshore motion several miles to the west exists.

8.7.3 *Littoral Barriers*

The shore structures in this cell consist of six piers, five breakwaters, nine jetties, ten active groins and 90 buried groins (Shaw, 1980). Piers are generally believed to have little effect on transport. This was confirmed with aerial photographs in this cell by Simison et al (1978). For locations of piers and other structures, see Shaw (1980). The remaining structures and their effects will be discussed in order from north to south.

A 230 m rubble-mound groin was built at Cabrillo Beach in 1962 to create a beach (Figure 8.7-3). Dunham (1965) reports that the groin has been relatively successful in retaining most of the 2×10^6 yd³ of fill placed at the time of construction. Since there are no beaches downcoast of this groin, this appears to be one of the few wise choices for coastal structure placement in this cell.

The three breakwaters of Los Angeles-Long Beach Harbor (Figure 8.7-3) and the three jetties at Alamitos Bay entrance (Figure 8.7-4) were discussed in Section 8.7.2. Since there is essentially no longshore transport in the area, the harbor structures appear to have little effect on longshore transport (Inman and Frautschy, 1960). However, there is considerable shoaling in the Alamitos Bay channel. Dredging and profiling records are not complete enough to quantify this effect or determine the source of the sediment.

In 1959 a 230 m concrete groin was built next to the pier at Seal Beach to stabilize the beach (Shaw, 1980). Dunham (1965) presents a pictorial and descriptive history of Seal Beach. USACE LAD (1970) reports upcoast drift in the summer and fall often results in erosion on the north side of the groin and accretion on the south side. When erosion becomes critical, local interests must pay for sand fill in the affected area (USACE LAD, 1970). Transport blockage has not been quantified.

AD-A166 699

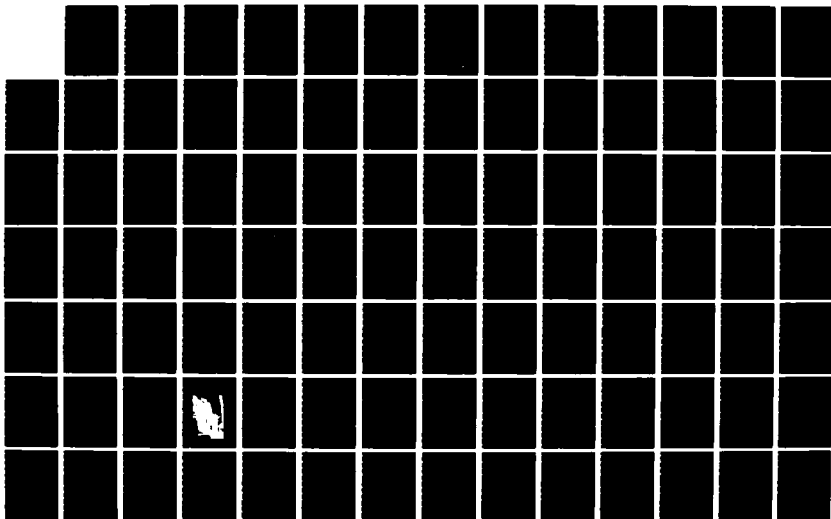
COAST OF CALIFORNIA STORM AND TIDAL WAVES STUDY
SOUTHERN CALIFORNIA COAST (U) ARMY ENGINEER DISTRICT
LOS ANGELES CA COASTAL RESOURCES BRANC
D L INMAN ET AL FEB 86 CCSTWS-86-1

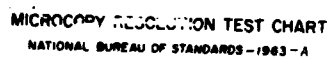
5/7

UNCLASSIFIED

F/G 8/3

NL





MICROCOPY RESOLUTION TEST CHART
NATIONAL BUREAU OF STANDARDS-1963-A

The severe erosional problems caused by the complete blockage of longshore transport by the Anaheim Bay breakwater (Figure 8.7-5) were discussed in Section 8.7.2.

In 1933 ninety stone groins were built at Surfside (Figure 8.7-5), which are now buried and therefore inactive (Shaw, 1980). The partial interference with transport caused by the four Santa Ana River jetties (Figure 8.7-6) was discussed in Section 8.7.2.

Between 1968 and 1973, a total of eight groins ranging in length from 60 to 180 m were built along Newport Beach (Figure 8.7-6) in an attempt to halt erosion (Shaw, 1980). Details of the groin construction and a subsequent 2×10^6 yd³ beach fill are outlined in USACE LAD (1969a). USACE LAD (1970) reports on the erosion history and controversy as to possible causes and solutions. The Corps proposed construction of a breakwater to halt sand flow into Newport Submarine Canyon. However, as outlined in Section 8.7.1 there is now evidence which suggests that the canyon is inactive and that sand flows offshore further north. Also the local landowners claimed that the erosion was caused by transport to the north from southern swell, not by sand flow south into the canyon (USACE LAD, 1970). The Corps paid for a fluorescent sand tracer study to determine transport directions, but the study was inconclusive. In 1968 construction of an experimental steel sheet-pile groin along with beach fill indicated erosion appeared to be caused by transport to the north. Clancey et al (1983) use beach profiles to report on erosion and accretion near the groins. But they are unable to quantify the extent to which the groins block longshore transport. Furthermore, it appears there is net offshore transport which they are unable to estimate. The pattern of erosion in this groin field reported in USACE LAD (1970) appears to have altered, starting in 1973. Spencer (1985) reports that the shoreline between the Santa Ana River and the Newport Pier appears to have stabilized during the period 1973 through 1985.

As reported in Section 8.7-2, the two Newport Bay jetties appear to have little effect on the beach, since the waves tend to approach the shore in a normal direction in this area, and

the resulting longshore transport is therefore small.

8.7.4 *Wind Transport*

The articles included in this study do not quantify wind transport loss in this cell. Photographs of occasional onshore wind-blown drifts are available (Hales, 1980), but areas which are subject to such drifts are not systematically catalogued. The topography and large extent of development would suggest that loss from wind transport is not generally significant in this cell, although it may be so in small areas.

8.7.5 *Berm Overwash and Offshore Transport*

Berm overwash has not been examined in this cell. Considering the highly developed condition of the coast, one would expect that local interests would provide for return of berm overwash to the beach on the few occasions (storm wave-high tide coincidence) when it might occur.

Net offshore transport appears to be quite important in the southern portion of this cell, as outlined in Section 8.7.1 (Felix and Gorsline, 1971; Karl, 1980). Unfortunately, this sink has not been quantified. A quantification of offshore transport in the area would contribute greatly to understanding of the cell's sediment budget in general and the erosion problems on Newport Beach in particular.

8.8 BUDGET OF SEDIMENT

There were no reports reviewed for this study that directly address the budget of sediments for the San Pedro Cell. The major sources of sediment for this littoral cell have been the Los Angeles, San Gabriel and Santa Ana Rivers, and artificial beach nourishment. In the Santa Monica Cell the river basins have been extensively developed. Brownlie and Taylor (1981) estimate a sediment yield for these rivers under "natural" and present conditions (see Table 8.8-1). The estimates may not be accurate because they assume bedload to be 10% of the

Table 8.8-1

Estimated sand deliveries under natural versus present conditions
for extensively developed basins (from Brownlie and Taylor, 1981).

<u>River</u>	<u>Area</u> <u>(km²)</u>	Natural Conditions	Present Conditions
		<u>(m³/yr)</u>	<u>(m³/yr)</u>
Los Angeles River	2,155	600,000	200,000
San Gabriel River	1,663		
Santa Ana River	4,406	330,000-500,000	140,000

Data from topographic maps and U.S. Geological Survey Water Supply
Paper 1735.

Discharges are averages of available years at every station, but
more than five years as a minimum. Areas are by planimetric
determinations to the nearest 10 square miles.

suspended load instead of the more typical 20% for southern California Rivers (see Section 2.5. and Inman and Jenkins, 1983 for discussion). Even though their estimates may not be accurate, comparing the natural and present yields clearly shows that the development of the river basins has severely diminished the average annual supply of sand to the beaches.

Beach nourishment has also been a major source of sand to the beaches. Surfside-Sunset Beach has received over 5,000,000 yd³ of sands since 1962. Shaw (1980) summarizes this nourishment project along with projects at Newport Beach, Seal Beach, Cabrillo Beach and Palos Verdes.

Longshore transport of beach sands is best summarized by Hales (1980). Hales' estimates of longshore transport rates vary from $112-276 \times 10^3$ yd³/yr along the cell and are presented in Table 8.6-1.

There are two submarine canyons in this cell, San Gabriel and Newport Canyons. The amounts of sand intercepted and transported down these canyons has not been quantified. There are several harbors and nearshore structures along this cell that act as littoral barriers (see Section 8.7.2 and 8.7.3). The largest interruption of longshore transport in this cell is at the Anaheim Bay breakwaters (Figure 8.7-5) where as much as 613×10^3 yd³/yr of sand is trapped.

9. OCEANSIDE CELL

The Oceanside Cell extends from Dana Point to Point La Jolla, a distance of 56 miles (see Figure 1.3-1). Including the Laguna Sub-Cells from Corona del Mar to Dana Point, the extended cell has a length of 70 miles (see Figure 9.6-1). The coast from Dana Point to La Jolla is primarily low semi-continuous sandy beaches backed by wave-cut sea cliffs. The coast from Corona del Mar to Dana Point consists of pocket beaches backed by sea cliffs. The extended cell includes two small craft harbors, one at Dana Point and the other at Oceanside. Portions of the Oceanside Cell are the most studied coastal segments in southern California.

9.1 COASTAL EROSION PROBLEMS, NATURAL AND MAN-MADE

A qualitative systematic summary of coastal erosion problems, both natural and man-made from Corona Del Mar to Point La Jolla, is contained in the Assessment and Atlas of Shoreline Erosion (California 1977a). The coastline from Corona Del Mar to Dana Point is a series of pocket beaches backed by cliffs. The primary natural erosion problem along this stretch of coast is wave attack undercutting at the cliff base and the subsequent cliff failure. Landscape irrigation of the housing developments has increased the natural erosion of the cliff tops and faces. Inman (1978b) discusses the beach and shoreline processes in the Laguna Niguel area. He shows how a reduction in size of the Salt Creek Beach sand reservoir from river damming subjects the beach and sea cliffs to a greater potential for erosion.

A brief summary of the beach erosion project at Doheny State Beach is contained in USACE LAD (1970). The report also summarizes some of the Corps of Engineers past projects to alleviate erosion occurring at Oceanside Beach during the 1960's. USACE SPD (1971) contains a plate showing the critical erosion, non-critical erosion, and non erosion areas of the coastline from Mussel Cove to the Mexican border (Figure 9.1-1). Nordstrom and Inman (1973) discuss the erosional nature of the San Diego County coastline. They site examples of erosion due to localized wave conditions on less resistant bedrock and, due to the presence of man-made

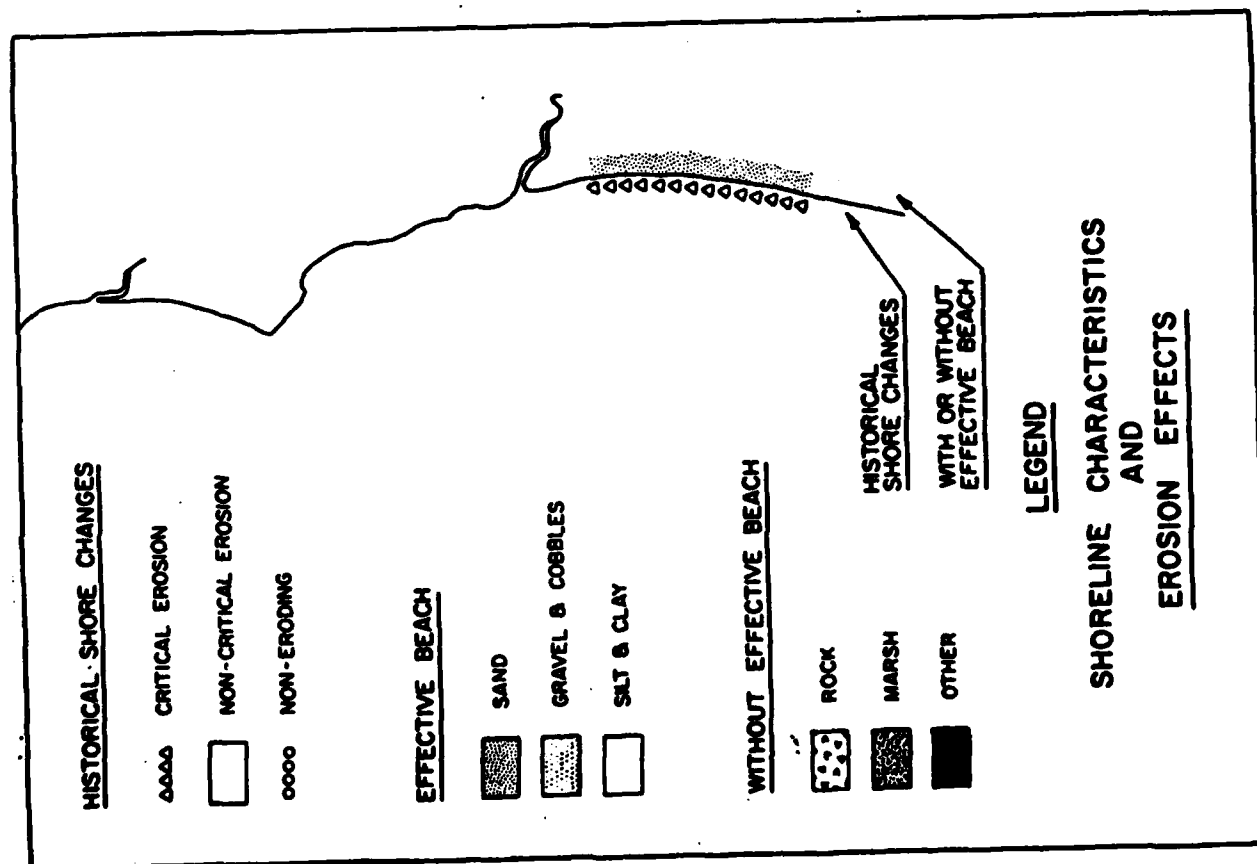


Figure 9.1-1. Shoreline characteristics and historical shore changes (from USACE SPD, 1971).

structures in the nearshore environment. Inman (1976) documents how the accretion of sand in the Oceanside Harbor is eroding the beach to the south of the harbor. He makes several recommendations to alleviate this problem, including a sand bypassing system.

The coastline from Dana Point to Point La Jolla is mostly narrow sand or cobble beaches backed by cliffs. The cliffs in the Leucadia and Torrey Pines State Beach area have active slides along the base, face and rim of the cliffs (California 1977a). Lee (1980) gives an average annual erosion rate of 0.1 to 0.7 in/yr for the Leucadia sandstone cliffs. He discusses the natural erosional processes of wave action, rain, water, and wind on sea cliffs. He also discusses the activities of man and animals that hasten the rate of cliff erosion. Inman (1983) shows photographic evidence of sea cliff erosion at Torrey Pines State Reserve and sea cliff collapse at La Jolla Shores.

USACE LAD (1980b) discusses the beach erosion problems and shore protection needs at Oceanside. It includes historical photographs illustrating storm damage and coastal erosion. Inman and Jenkins (1983) do a thorough job of summarizing the recent shoreline history of Oceanside Beach and Harbor and present an interpretation of the causes of shoreline changes. They include an extensive reference list of reports pertaining to Oceanside Beach, Harbor and cliffs. Kuhn and Shepard (1983) discuss sea cliff erosion in San Diego County. They include historical coastline surveys and several photographs showing cliff conditions before and after a catastrophic failure occurs. Kuhn and Shepard (1984) is similar to their 1983 paper. However, in this book they document with photographs, natural cliff erosion at Camp Pendleton and San Onofre State Park, and the man induced accelerated erosion of a canyon head at San Onofre State Park. USACE LAD (1984b) discusses the mineral composition of the cliffs, and the local cliff erosion problems from Dana Point to the Mexican border. Figure 9.1-2 illustrates cliff and gully erosion and shows the relative volume of sediment produced. Inman (1983), Inman and Jenkins (1983) and Inman (1985b) discuss how damming of rivers in this littoral cell has lead to

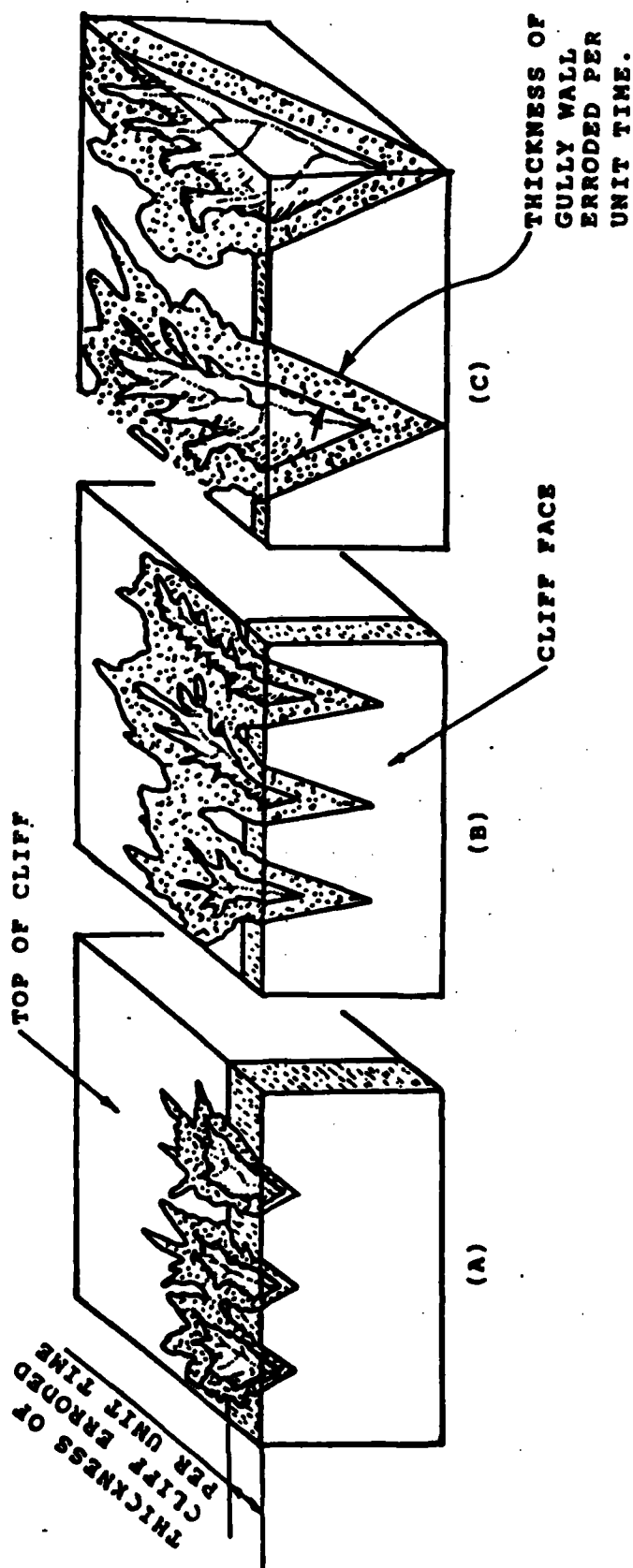


Figure 9.1-2. Schematic diagram showing relative volume of sediment produced by cliff-face retreat (shore dashed lines) and the volume of sediment produced by headward erosion (stippled area) of major gullies. (A) indicates cliff-face erosion greater than gullying. (B) cliff-face erosion about equal to gullying. (C) Gully erosion greater than cliff-face erosion. (From USACE LAD, 1984b.)

Figure 9.1-2.

beach erosion.

9.2 SHORELINE CHANGES

Table 9.2-1 lists the data contained in the reports reviewed for this study concerning shoreline change and explains the type of data available. Newton (1959) systematically discusses the history of shoreline and offshore changes from Newport Bay to San Mateo Creek. The appendices contain several plates comparing historical shorelines and beach profiles covering a 70 year period from 1887-1956. Similar to Newton (1959), USACE LAD (1960) systematically discusses the shoreline history and volumetric changes from San Clemente to Point La Jolla. The appendices contain plates comparing historical shoreline and beach profiles covering a 25 year period from 1934-1959 along with tables of shorter term volumetric beach sand changes. USACE LAD (1960) also has several historical aerial photographs of Oceanside Harbor and Beach taken from 1932 to 1959.

Nordstrom and Inman (1973) contains on-offshore beach profiles at Torrey Pines Beach from 1960 to 1973. Nordstrom and Inman (1975) has the most detailed beach profiles of Torrey Pines Beach during the period from 1972 through 1974. Aubrey et al (1976) used four years of beach profile data, measured at Torrey Pines Beach, correlated with the tides and the incident wave field, to determine short term and seasonal patterns of shoreline changes. USACE LAD (1980b) is similar to all the Corps of Engineers Beach Erosion Control reports. It contains historical aerial and ground photographs, beach profiles (1960, 1970, 1977), plates showing shoreline and offshore changes, and a table of volumetric changes, all at Oceanside. Inman and Jenkins (1983) describe the recent shoreline history of the Oceanside area and include beach profiles of both Oceanside Beach and Torrey Pines State Beach.

Waldorf and Flick (1983) performed monthly beach profiles at four range lines from May, 1980 to January, 1983 along Del Mar Beach. The sand level changes were monitored to measure seasonal variations and patterns of shoreline changes. In a similar data report Waldorf

Table 9.2-1

EXISTING SURVEYS, MAPPING STUDIES, PHOTOGRAPHS

Author(s)	Date	Type of Data	Location and Dates
Munk and Traylor,	1947	Bathymetric survey	So. Torrey Pines Beach to Point La Jolla (no date)
		Aerial photographs	Camp Pendelton and Scripps Pier, 1944
Shepard and Inman,	1951b	Volumetric changes on beach and shelf	Scripps Beach, 1949-1950
Inman,	1953	Beach profiles, volumetric changes on beach and shelf, sediment analysis	Scripps and Torrey Pines 1949-1951
Inman and Rusnak,	1956	Beach profiles	Scripps Beach, 1953-1956
Inman,	1957	Sediment analysis and type of ripples on shelf	La Jolla-Scripps Beach and various other shelf localities, 1952-1956
Newton,	1959	Summary of shoreline and offshore changes	Newport Beach to Oceanside,
		Beach profiles	Newport Bay to San Mateo Creek, 1887, 1934-1956

Table 9.2-1 (cont'd.)
EXISTING SURVEYS, MAPPING STUDIES, PHOTOGRAPHS

Author(s)	Date	Type of Data	Location and Dates
USACE LAD,	1960a	Beach profiles	San Onofre to Torrey Pines, 1934-1957
		Aerial photographs	Oceanside, 1932-1959
		Tables of volumetric change	Oceanside, 1950-1956
		Shoreline and offshore changes	San Onofre to Torrey Pines, 1934-1959
USACE LAD,	1969a	Beach survey	Doheny Beach, 1965; Oceanside Beach, 1966
USACE LAD,	1967	Beach profiles	Oceanside, March 1963; April 1963, Oct 1963, May 1964
USACE LAD,	1970	Hydrographic survey	Doheny Beach to San Clemente and Oceanside, 1969
		Shoreline and offshore changes	Mussel Cove to San Mateo Point, 1958-1969
		Delta profiles	Santa Ana River, 1966-1969
		Delta profiles	San Juan Creek, 1934-1969

Table 9.2-1 (cont'd.)
EXISTING SURVEYS, MAPPING STUDIES, PHOTOGRAPHS

Author(s)	Date	Type of Data	Location and Dates
Nordstrom and Inman,	1973	Beach profiles	Torrey Pines State Beach, 1960-1973
Nordstrom and Inman,	1975	Beach profiles	Torrey Pines State Beach, 1972-1974
Aubrey et al.,	1976	Beach profiles	Torrey Pines State Beach, 1975-1976
USACE LAD,	1980b	Historical aerial and ground photographs	Oceanside
		Table of volumetric changes	Oceanside, 1950-1972
		Beach profiles	Oceanside, 1966, 1970, 1977
		Shoreline and offshore changes	Oceanside, 1934-1972
Inman and Jenkins,	1983	Beach profiles	Oceanside, 1934-1983
Moffatt and Nichol,	1983	Beach profiles	Oceanside, 1966-1977

Table 9.2-1 (cont'd.)
EXISTING SURVEYS, MAPPING STUDIES, PHOTOGRAPHS

Author(s) Date	Type of Data	Location and Dates
Waldorf and Flick, 1983	Beach profile	Del Mar, 1980-1983
Waldorf et al., 1983	Beach profiles	Oceanside and Carlsbad, Dec 1981 - Feb 1983
Kuhn and Shepard, 1983	Historical photographs	San Onofre to Point La Jolla
Flick and Waldorf, 1984	Beach profiles (Longard Tube)	Del Mar, 1981-1983
Kuhn and Shepard, 1984	Historical aerial and ground photographs	San Diego County,
USACE LAD, 1984b	Beach profiles	Dana Point to the Mexican Border, 1983

et al (1983) measured monthly beach profiles at Oceanside and Carlsbad beaches. Weggel and Clark (1983) summarize the beach changes to the south of Oceanside Harbor due to the entrapment of sands in the harbor. Kuhn and Shepard (1983) includes qualitative descriptions of historical shoreline changes along the Encinitas and Leucadia coastline. The report also contains several aerial and ground photographs showing areas before and after catastrophic erosional events. Flick and Waldorf (1984) monitored beach profiles at the Longard Tube installation in Del Mar to determine shoreline changes and to evaluate the tube's performance. Kuhn and Shepard (1984) added additional photographs and descriptions of historical shoreline changes in the Oceanside area to their previous, 1983, report.

9.3 NEARSHORE WAVES

Measurements of waves in unsheltered waters offshore of this cell (i.e. outside the Channel Islands) are relatively sparse. Representative data from a buoy at Begg Rock (Figure 3.2.2-1) is shown in Figure 3.2.2-2. Deep ocean hindcasts are more numerous (Figure 3.2.2-6). Wave roses for Marine Advisers Station A are given in Figures 3.2.2-7,8,9; for NMC Stations 5 and 6 in Figures 3.2.2-10,11 and for MII Stations 5 and 6 in Figures 3.2.2-13,14. Like the other cells within the Southern California Bight, the coastal waves for this cell are greatly modified by propagation through the Channel Islands. Schematics of the open wave windows to the deep ocean are shown in Figure 9.3-1 for Dana Point and Oceanside (near the northern edge and center of the cell, respectively) and Figure 3.3.1-1 for Torrey Pines Beach near the southern cell boundary. Note there is considerable variation of the direction of blocked (and open) wave sectors within this cell. For example, the angle ranges blocked by San Clemente Island are roughly 221° - 240° (Dana Point), 243° - 261° (Oceanside) and 264° - 278° (Torrey Pines). The patterns of coastal wave energy spatial variability in this cell have been calculated with a refraction model which accounts for refraction by subaerial island banks and shoals, as well as simple island blocking (Pawka and Guza, 1983). The results are discussed extensively in Section 3.3-1. For example, Figure 3.3.1-7 illustrates that the importance of San Clemente Island as a block to southern swell increases with more northerly position in this cell (e.g. Dana Point is shadowed for angles between 220° - 240°).

Marine Advisers (1960b) hindcast extreme storm wave heights at Dana Point and Oceanside. Marine Advisers (1960b) scanned weather maps and researched damage reports on file with newspapers and government agencies (and other sources) for indications of high storm waves in the period 1900-1958. Guided by these qualitative reports, 49 storms were chosen for further investigation, and 15 were selected for complete hindcasting. There were also eight cases of reported high waves which occurred in the summer. No storms were apparent on northern

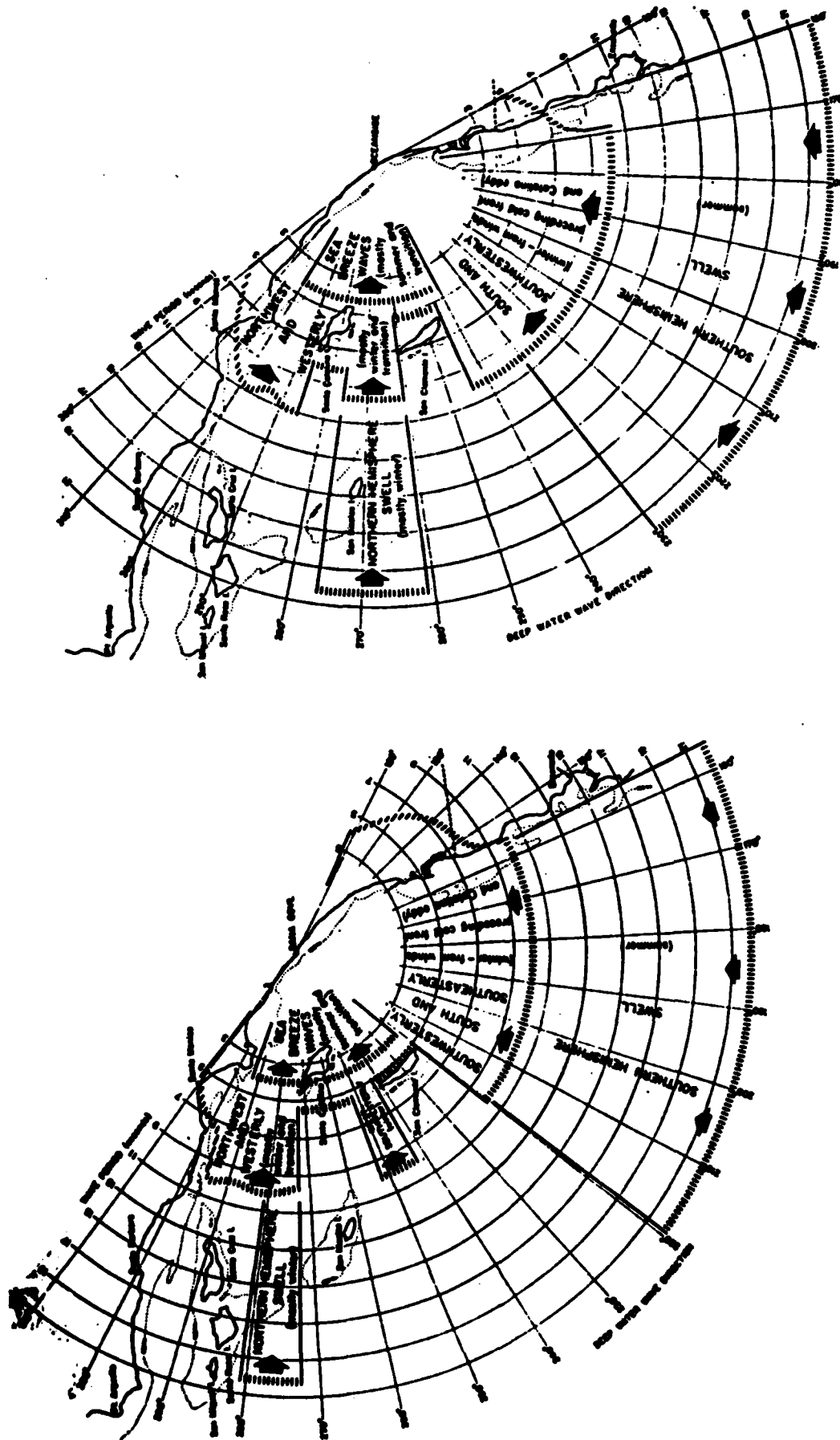


Figure 9.3-1 Schematics of island blocking effects at Dana Point (left) and Oceanside (right) (Marine Advisers, 1961).

hemisphere maps and these events are probably southern swell. Since historical southern hemisphere weather maps were not available, hindcasts for these events could not be prepared. Of the 15 hindcast events, 2 yielded rather small waves and were not considered further. Statistics for the 13 remaining storms, at an unsheltered location off of Oceanside, are given in Table 3.2.2-5. These waves were then brought through the Channel Islands with a simple blocking model. Refraction by subaerial island features was not accounted for. Using this crude model (see Section 3.3-1 for discussion of a more refined model) the reduction of coastal wave height relative to outside the islands (I/I_0) was calculated. The sheltered waves were then refracted and shoaled to shallow water (breaking wave) using Oceanside or Dana Point bathymetry. Extensive refraction diagrams for Dana Point are given in Marine Advisers (1961b). Table 9.3-1 gives the sheltered and shoaled (to the break zone) statistics for each site, for events with significant breaker heights greater than 10 ft. Note that some events at Oceanside (for example January 1953 and February 1926) do not appear at Dana Point because of blocking of 230° swell by San Clemente Island. It is prudent to note that the Marine Advisers results are based on largely outdated methodologies (see Section 3.2.2) and reflect the subjective judgments of individual forecasters.

Marine Advisers (1960a) also contains a general hindcast (i.e. not just storm waves) for Oceanside prepared by combining information from a variety of sources: northern hemisphere swell hindcast outside the islands (UCSD, 1947) and measured for 2 years at Mission Bay; offshore ship operations from 1949-1954; southern swell hindcast combined with observations at El Segundo and Huntington Beach (1952, 1953); local seas hindcast with 5 years of wind data at Oceanside. An island blocking model was used to bring the offshore data through the islands. Refraction summaries were used to "unrefract" the coastal southern swell observations to coastal deep water. Refraction at Oceanside was then used to bring all data in shallow water. The annual summary of period-height-direction distributions is shown in Table 9.3-2.

Table 9.3-1 Severe storm waves (1900-1958) hindcast at Dana Point and Oceanside (Marine Advisers, 1961).

Design significant wave data at Dana Cove.

Storm Date	Island Shelter Coeff.	Breaker Refraction Coeff.	Shoaling Coeff.	Significant Breaker Height	Significant Period	Breaker Direction
	$(I/I_0)^{1/2}$	K_b	H_b/H_0'	H_b	T_s	
15-25 Sept 1939	.90	1.00	1.00	24.2 ft.	14.0 sec.	204°
28-30 Jan 1915	.92	1.02	1.04	15.9	11.8	235
9-10 Mar 1904	.81	.92	1.12	14.9	12.0	237
20-23 Jan 1943	.93	.96	1.00	14.4	10.8	195
8-10 Mar 1912	.72	.87	1.17	12.8	11.5	243
16-17 Dec 1914	.93	.97	1.02	12.0	9.9	192
26-28 Jan 1916	.87	.97	.97	11.4	9.6	235
1-3 Feb 1915	.61	.88	1.23	10.8	12.4	244

Design significant wave data at Oceanside.

Storm Date	Island Shelter Coeff.	Breaker Refraction Coeff.	Shoaling Coeff.	Significant Breaker Height	Significant Period	Breaker Direction
	$(I/I_0)^{1/2}$	K_b	H_b/H_0'	H_b	T_s	
15-25 Sept 1939	.92	1.02	.98	24.7 ft.	14.0 sec.	219°
9-10 Mar 1904	.92	1.03	1.02	17.2	12.0	226
28-30 Jan 1915	.94	1.02	1.03	16.1	11.8	221
8-10 Mar 1912	.78	1.01	1.07	14.7	11.5	238
6-8 Jan 1953	.66	.94	1.45	14.4*	15.0*	231
1-2 Feb 1926	.66	1.01	1.59	13.3	16.0	231
20-23 Jan 1943	.79	.94	1.07	12.8	10.8	215
1-3 Feb 1915	.62	.98	1.27	12.7	12.4	238
26-28 Jan 1916	.92	1.03	.95	12.6	9.6	233
13-14 Mar 1952	.74	1.03	1.29	11.5	11.7	226
6-12 Dec 1937	.56	.86	1.90	10.6	16.4	232
16-17 Dec 1914	.80	.95	1.07	10.6	9.9	215
6-8 Apr 1926	.56	.97	1.58	10.1	13.8	235

*If hindcasted significant period of 19.2 sec. is used instead of the 15 sec. recorded by the U. S. M. C., then the calculated value of H_b is 16.9 feet.

Note that this is not the same data base used to construct the Marine Advisers (1961a) deep water hindcast at Station A outside the Channel Islands. See Section 3.2.2 for a discussion of the Station A data. Marine Advisers (1961a) brought the Station A data through the islands (blocking only) to develop a hindcast for Marine Advisers Station C in deep water off of Encinitas (10 miles south of Oceanside; station locations shown in Figure 3.2.2-6). Station C wave roses are shown in Figure 9.3-2.

Hales (1978c) constructed a hindcast for 3 locations near Oceanside using south swell hindcasts from Marine Advisers Station A and north swell and seas hindcasts from MII Station 5 and 6. An island blocking/refraction model was used to bring these unsheltered data through the islands. Hales (1978c) presents tables of sheltered deep water, and shoaled to the breaking depth, wave statistics for Oceanside, Las Flores (10 miles north of Oceanside) and Encinitas. The breaking wave statistics vary substantially between the sites because of both differential shadowing by the offshore islands and local bathymetry differences.

Inman and Jenkins (1983) constructed an Oceanside hindcast using MII Station 5 data for north swell and Marine Advisers Station C (already sheltered) for south swell and local seas. Neither Hales (1978c) or Inman and Jenkins (1983) give simple summary statistics for Oceanside. The goal of those works was to hindcast longshore energy fluxes from which sediment transports could be calculated. At first glance, the net southerly transport numbers seem substantially different; $102,000 \text{ yd}^3/\text{yr}$ (Hales, 1978c) compared to $254,000 \text{ yd}^3/\text{yr}$ (Inman and Jenkins, 1983). Marine Advisers (1960a) has previously used the hindcast data in Table 9.3-2 to calculate $216,000 \text{ yd}^3/\text{yr}$. Hales (1978c) notes that use of Marine Adviser Station C wave hindcasts for all waves results in about $250,000 \text{ yd}^3/\text{yr}$ northward transport. Presumably the differences are due largely to which wave hindcasts were used. Figure 9.3-3 shows the contributions of different components of the wave field to the net transport of Hales (1978c) and Inman and Jenkins (1983). The south swell and northwest sea components are nearly identical.

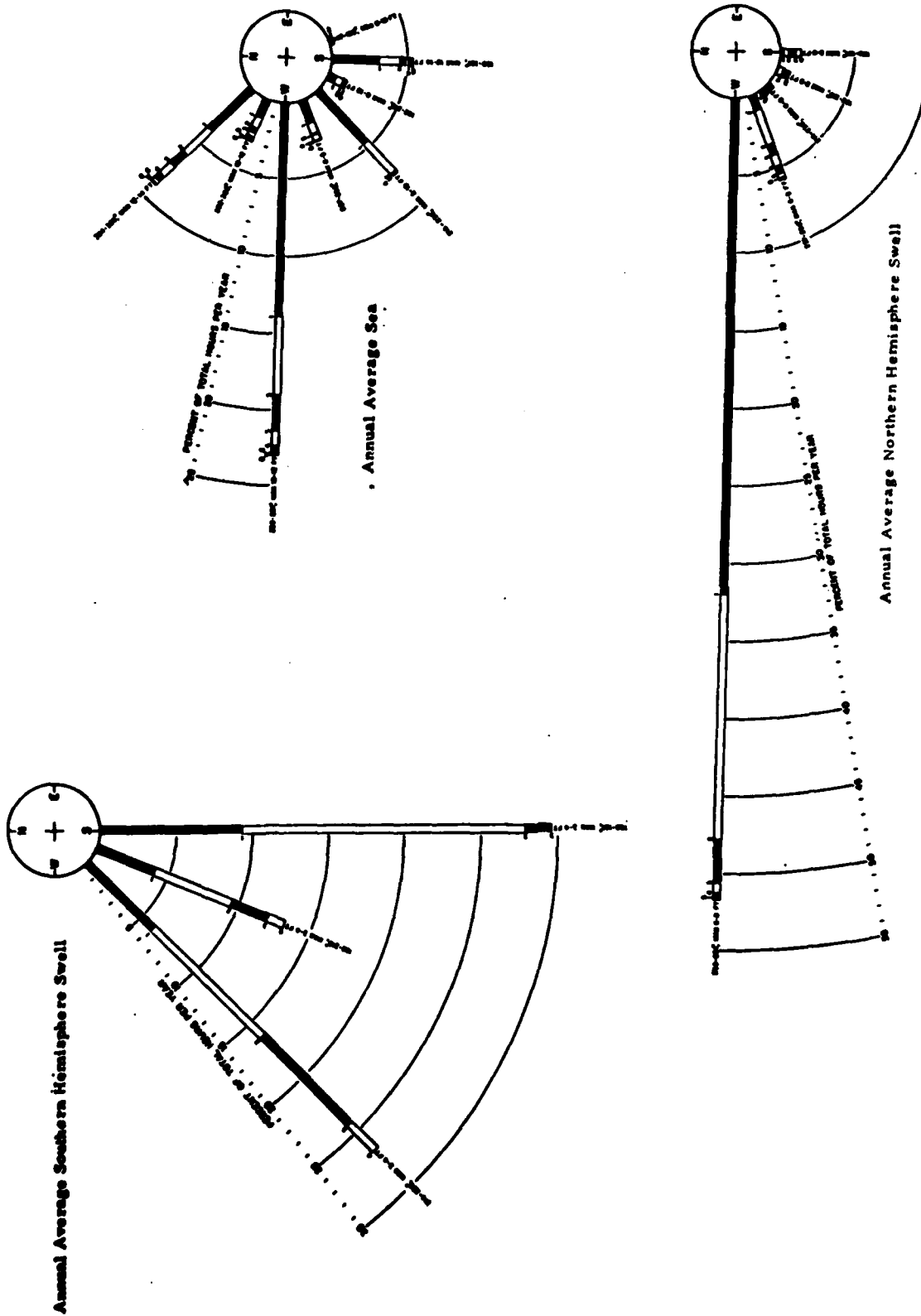


Figure 9.3-2 Marine Advisers (1961) hindcast wave roses at Station C.

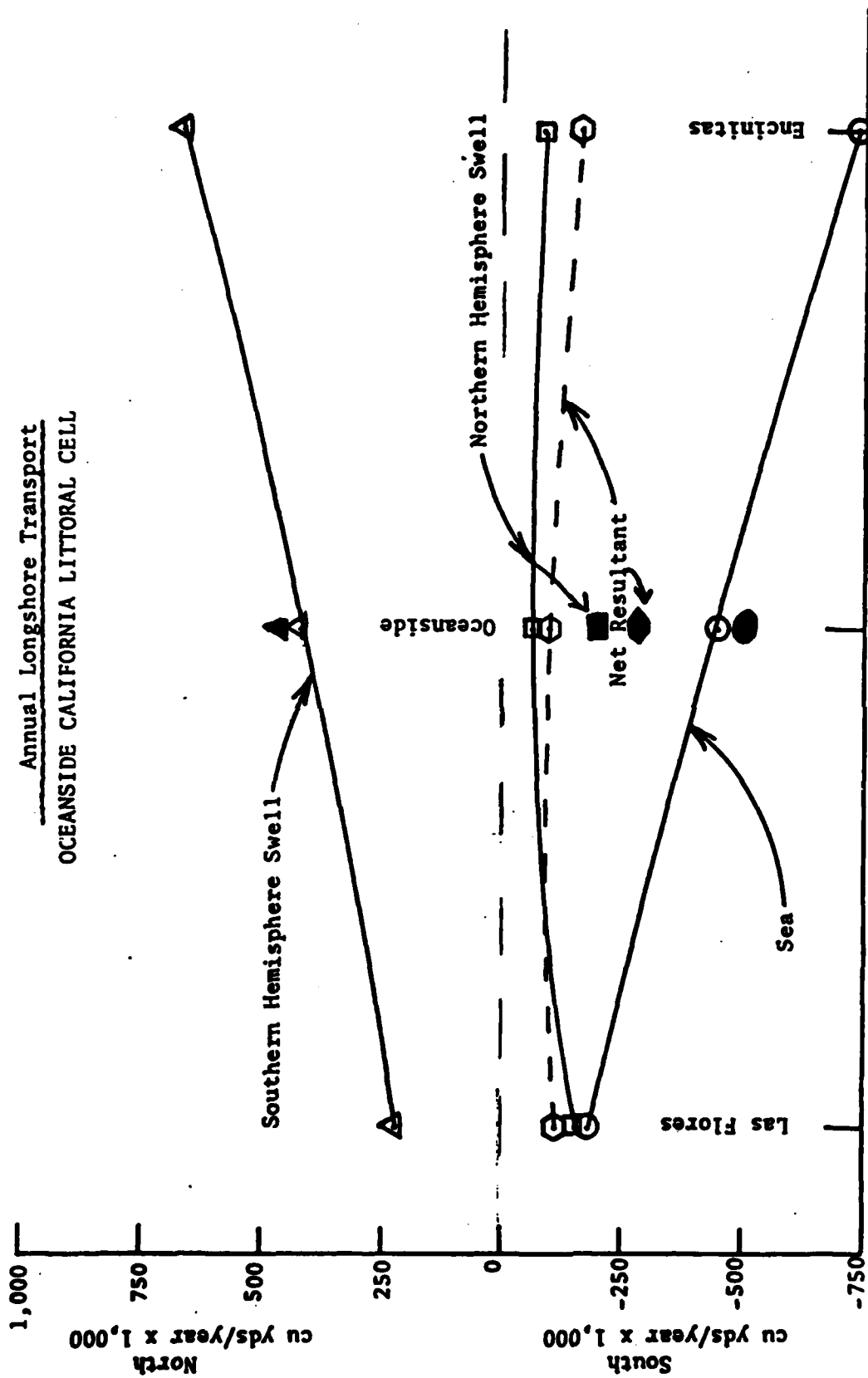


Figure 9.3-3 Annual sediment transport rates from Hales (1978, open symbols) and Inman and Jenkins (1983, filled symbols).

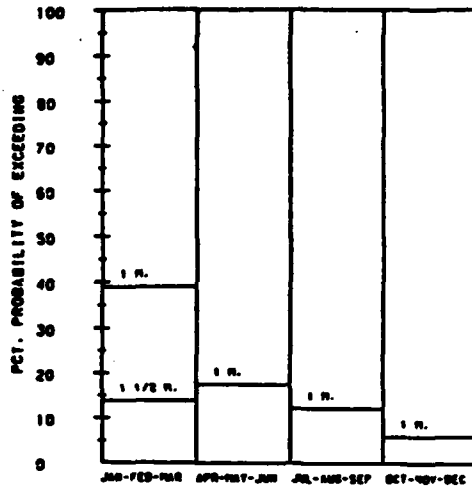
The chief difference in the net transport stems from differences in the transport due to northern swell, which is a small fraction of the gross transport. That is, the net transport is the small difference between large numbers. It is stated in Marine Advisers (1961a), and reviewed in Section 3.2.2, that the south swell energy hindcast could have been multiplied by a factor of 2 to account for measured variations in the south swell energy level between the south swell (1948-50) and north swell (1956-58) hindcast periods. If this factor were applied, the net transport would be to the north. Thus even the 250,000 yd³/yr northward value is within the plausible range predicted from wave statistics. In other words, south swell is the largest single component in the longshore energy flux and its statistics are very poorly known. It is not clear if reliable transport estimates cannot be obtained from existing wave data. Impoundment rates, etc. seem a much more reliable method at the present time.

In situ wave measurements in about 9 m depth have been made at Oceanside, Del Mar and Scripps Pier for varying lengths of time by the CDIP program. Seasonal variations, variability between stations, and annual exceedance probabilities for 1980 and 1984 are illustrated in Figures 9.3-4,5 (Del Mar was not functioning in 1980). Maximum and minimum monthly wave heights measured at Oceanside (6/76-3/81) are shown in Figure 9.3-6. Figure (9.3-7) plots extreme significant wave heights observed from 1953-1959 in 32 ft depth at the Camp Pendleton surf and weather station. A crude estimate of the 50-year maximum significant wave height is in the range 12-14 ft (in 32 ft depth). The maximum significant height observed in 7 years is 10 ft, similar to the maximum of 8 ft observed by CDIP over 5 years. A maximum value of 10 ft was observed during 9/78-4/83 at Scripps Pier (Seymour, 1983).

The CDIP gauges at Del Mar and Oceanside are directional, and are used to calculate longshore sediment transport. The 1984 data for Oceanside and Del Mar show predominantly southward transport, but with a period of northward transport in the summer associated with

OCEANSIDE BEACH JAN-DEC 1980

SEASONAL PROBABILITY OF EXCEEDING
VARIOUS SIGNIFICANT WAVE HEIGHTS

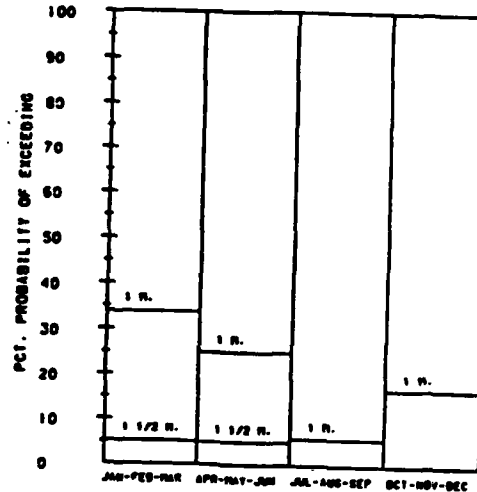


CUMULATIVE HEIGHT PROBABILITIES

HEIGHT (CM)	PROBABILITY
265	0.0000
255	0.0000
245	0.0025
235	0.0042
225	0.0067
215	0.0101
205	0.0126
195	0.0151
185	0.0176
175	0.0277
165	0.0361
155	0.0470
145	0.0613
135	0.0789
125	0.1024
115	0.1411
105	0.1921
95	0.2662
85	0.3678
75	0.5357
65	0.7053
55	0.8303
45	0.9706
35	0.9973
25	0.9992

SCRIPPS PIER JAN-DEC 1980

SEASONAL PROBABILITY OF EXCEEDING
VARIOUS SIGNIFICANT WAVE HEIGHTS



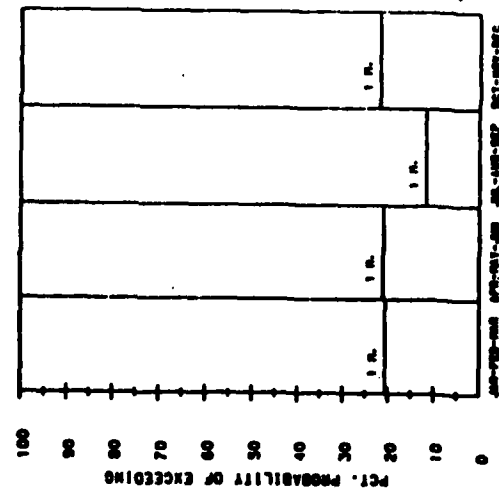
CUMULATIVE HEIGHT PROBABILITIES

HEIGHT (CM)	PROBABILITY
295	0.0000
285	0.0009
275	0.0009
265	0.0009
255	0.0018
245	0.0018
235	0.0027
225	0.0036
215	0.0036
205	0.0054
195	0.0064
185	0.0127
175	0.0145
165	0.0254
155	0.0336
145	0.0408
135	0.0681
125	0.1025
115	0.1397
105	0.2078
95	0.3049
85	0.4147
75	0.5499
65	0.6642
55	0.8094
45	0.9238
35	0.9918
25	0.9991

Figure 9.3-4 CDIP wave height statistics for Oceanside and Scripps Pier, 1980.

OCEANSIDE JAN-DEC 1984

SEASONAL PROBABILITY OF EXCEEDING
VARIOUS SIGNIFICANT WAVE HEIGHTS

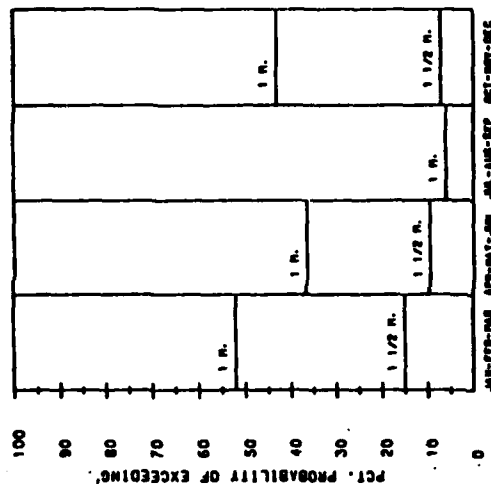


CUMULATIVE HEIGHT PROBABILITIES

HEIGHT (CM)	PROBABILITY
265	0.0000
250	0.0000
235	0.0007
220	0.0021
205	0.0043
190	0.0097
175	0.0107
160	0.0164
145	0.0341
130	0.0661
115	0.1373
100	0.2752
85	0.4915
70	0.7383
55	0.9538
40	0.9964
25	0.9992
10	0.9993

DEL MAR JAN-DEC 1984

SEASONAL PROBABILITY OF EXCEEDING
VARIOUS SIGNIFICANT WAVE HEIGHTS

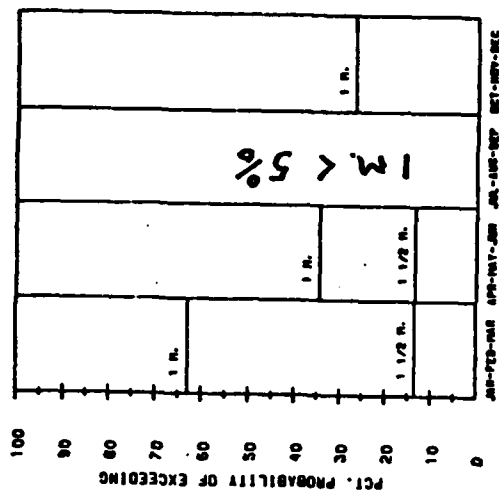


CUMULATIVE HEIGHT PROBABILITIES

HEIGHT (CM)	PROBABILITY
325	0.0000
310	0.0007
295	0.0007
280	0.0014
265	0.0028
250	0.0043
235	0.0044
220	0.0135
205	0.0177
190	0.0298
175	0.0461
160	0.0773
145	0.1234
130	0.1950
115	0.2865
100	0.4234
85	0.5901
70	0.8142
55	0.9688
40	0.9986
25	0.9993
10	0.9993

SCRIPPS PIER MAR-DEC 1984

SEASONAL PROBABILITY OF EXCEEDING
VARIOUS SIGNIFICANT WAVE HEIGHTS



CUMULATIVE HEIGHT PROBABILITIES

HEIGHT (CM)	PROBABILITY
355	0.0000
340	0.0009
325	0.0017
310	0.0017
295	0.0035
280	0.0035
265	0.0032
250	0.0078
235	0.0096
220	0.0122
205	0.0148
190	0.0227
175	0.0349
160	0.0602
145	0.1029
130	0.1491
115	0.2119
100	0.3147
85	0.4447
70	0.6469
55	0.8588
40	0.9878
25	0.9991

Figure 9.3-5 CDIP wave height statistics for Oceanside, Del Mar, and Scripps Pier, 1984.

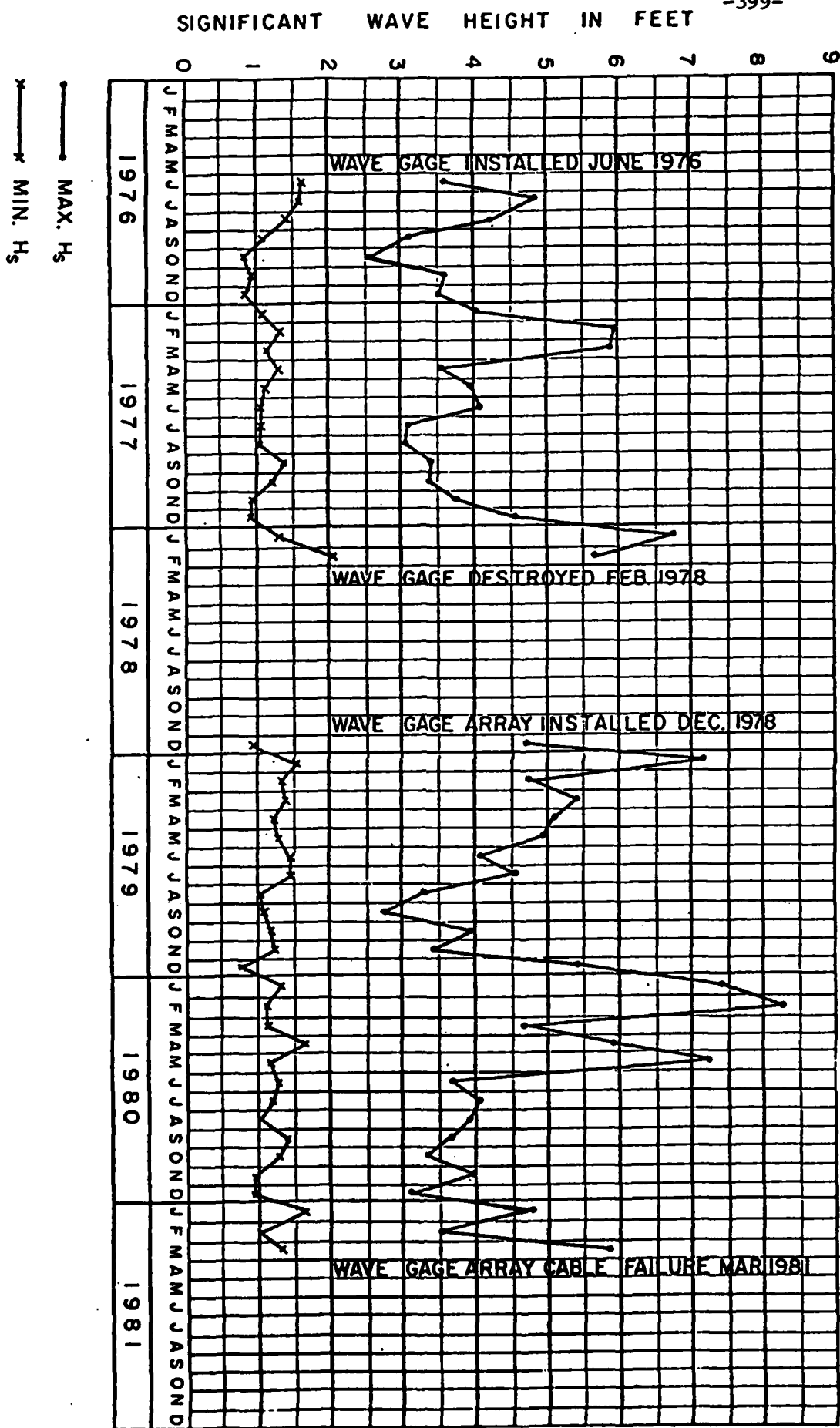


Figure 9.3-6 Monthly maximum and minimum CDIP significant wave heights at Oceanside (Moffatt and Nichol, 1983).

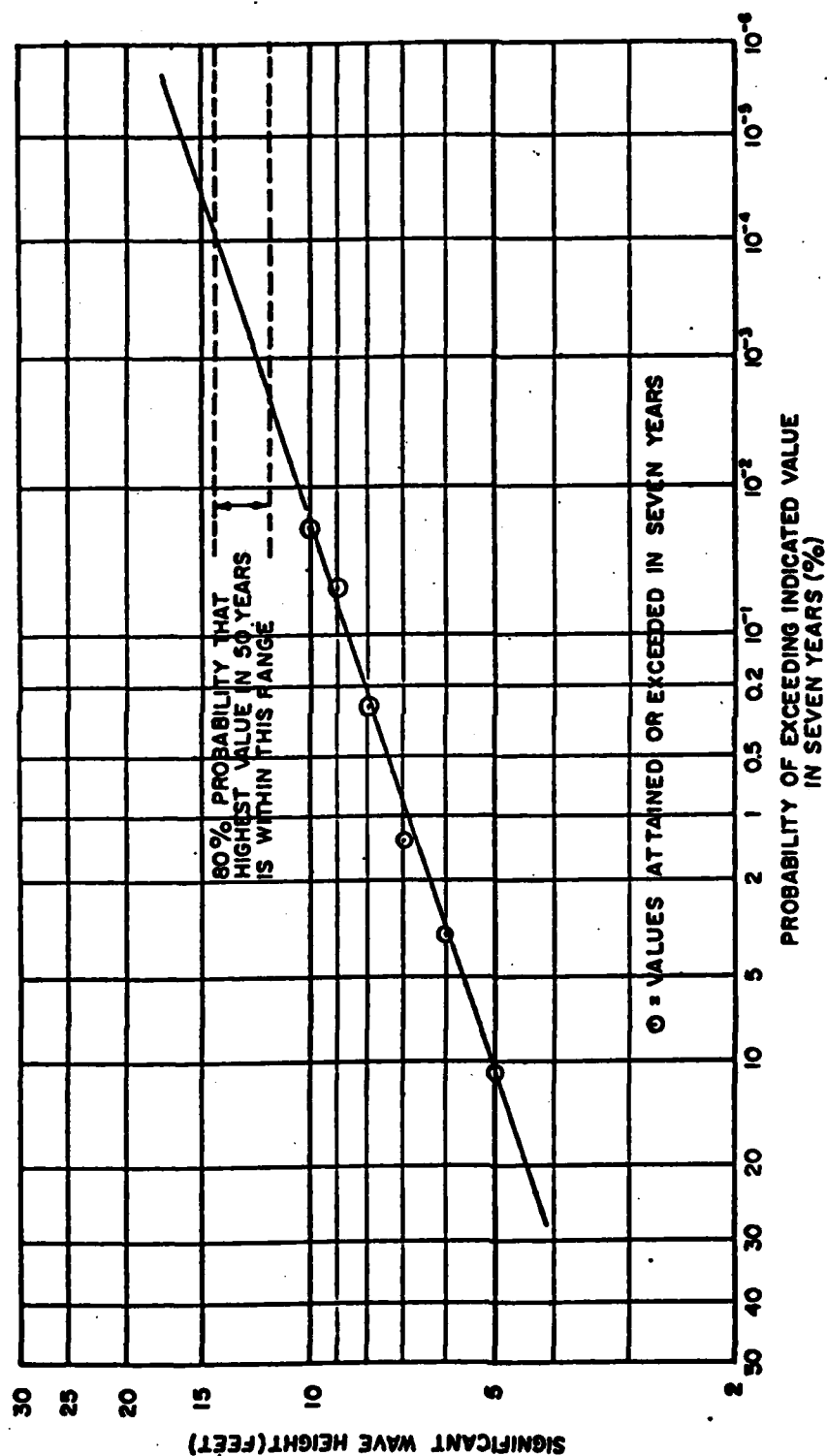


Figure 9.3-7 Significant wave height exceedances based on 1953-59 Marine Corps data at Oceanside (Moffatt and Nichol, 1983).

the southern swell season.

A directional wave array was maintained at Torrey Pines Beach, in 10 m depth, from 2/73 to 5/74 (Pawka et al, 1976). During the winter and spring months waves with 12-15 sec periods approach the beach at an angle of 5-15° north of normal to the beach. A smaller amount of wave energy, in two components, approaches the beach from the south during the winter; long period waves of 13-18 sec and shorter period waves of 5-12 sec. The latter were associated with local storms which come from the west and have wind blowing from the southwest. The summer and fall wave energy is less than half that of the winter-spring season (Figure 9.3-8). The fall wave spectrum consists of two components; low frequency southerly swell waves (10-16 sec) and locally generated northwest seas (6-10 sec). These measurements are qualitatively consistent with hindcasts and the CDIP observations. On an annual basis, the wave energy from the north at Torrey Pines Beach is greater than that from the south because of the higher energy waves during winter (Figure 9.3-8). Winter and spring storms of short duration contribute significantly to the total energy budget of the year (Pawka et al, 1976). Subsequent deployments of a linear array at Torrey Pines Beach were used to study aspects of island sheltering (see Section 3.3.1 and references therein).

A large nearshore waves experiment was conducted at Torrey Pines Beach in November 1978 as part of the NSTS program (Gable, 1979). Useful information about a variety of nearshore wave topics was obtained. Published results address the accuracy of linear wave theory in relating sea surface elevation pressure and velocity to each other, in and near the surf zone (Guza and Thornton, 1980); the connection between incident wave conditions and wave set-up at the shoreline (Guza and Thornton, 1981); the contribution of edge waves to surf beat (Huntley et al, 1981); the correlation between incident wave and surf beat energy levels (Guza and Thornton, 1982), and the relationship between fluid depth and wave height in the surf zone (Thornton and Guza, 1983). Although these experiments were scientifically productive, most

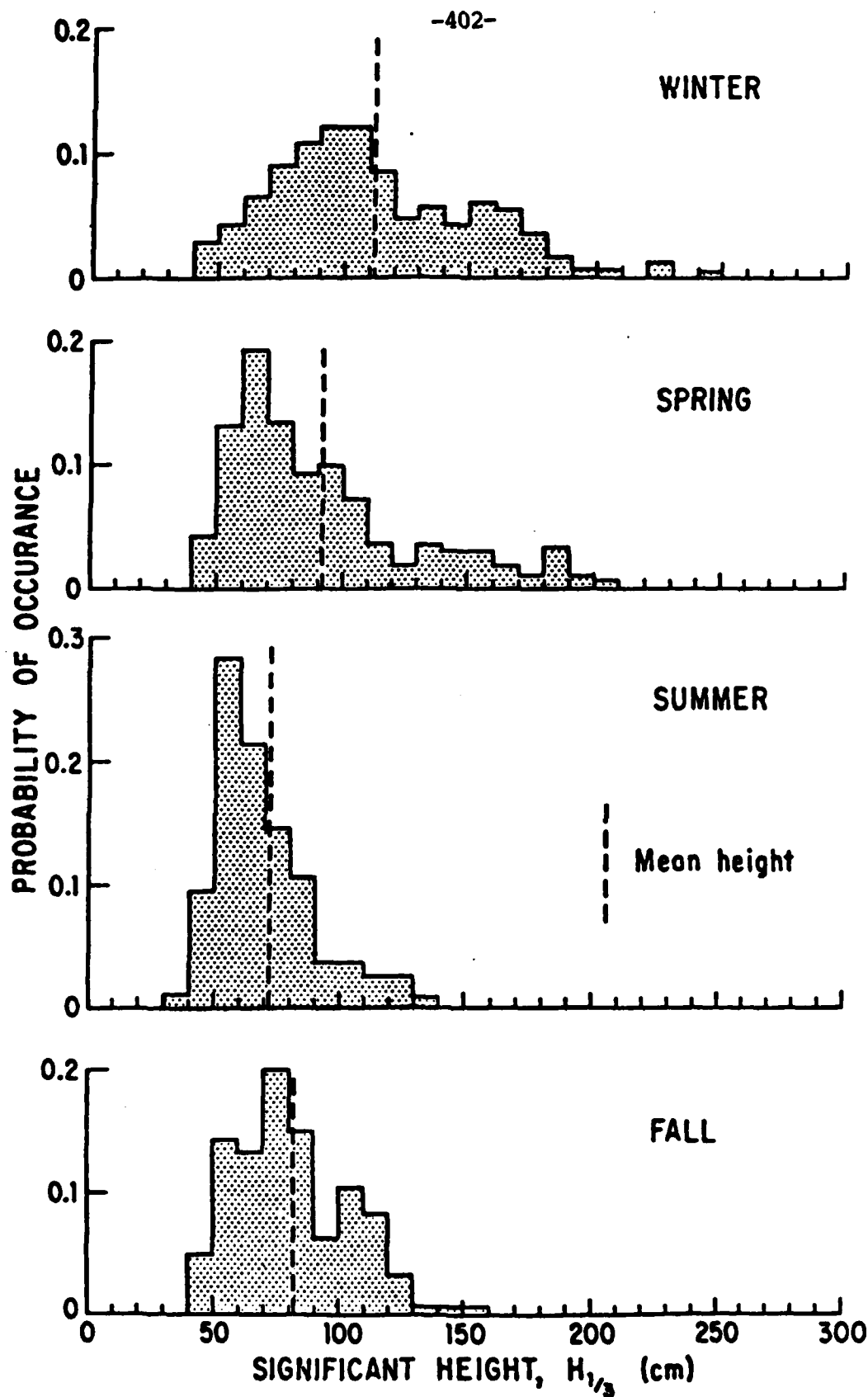


Figure 9.3-8

Seasonal distribution functions of significant wave height at Torrey Pines Beach, California (Pawka et al, 1976).

results do not have direct engineering or site specific application and are not discussed further.

9.4 NEARSHORE CURRENTS

Shelf current, temperature and bottom pressure fluctuations were measured on the shelf off of Del Mar (Figure 9.4-1) in each season during 1978. Lentz and Winant (1979) give time series plots of the data and simple statistics (means, variances, maxima, etc.) and Winant and Bratkovich (1981) discuss the dynamics of different frequency bands.

The mean currents are generally southward, and weak (Figure 9.4-2). Fluctuations about the mean are much larger than the mean (Figure 9.4-3). The tidal currents in this experiment are discussed briefly in Section 3.1.2 (see Figures 3.1.2-3,4). Current fluctuations with time scales longer than the tides obviously contribute a large fraction of the variance in Figure 9.4-3. Figure 9.4-4 shows the spatial dependence of the amplitudes of the first and second eigenvectors of subtidal longshore currents (eigenfunction analysis is briefly described in Section 3.1.2).

The time dependence of the two largest eigenfunctions is shown in Figure 9.4-5 for each deployment period. Also shown are time series of the longshore and cross-shelf components of wind stress computed from National Weather Service wind records from Lindbergh Field and a drag coefficient equal to 1.3×10^{-3} . The bottom pressure records are detided using a least-squares fit to periodic fluctuations at the dominant tidal periods before bottom pressure is formed. The resulting recording is detrended over each period, since the primary interest was in fluctuations with periods of several days rather than in the long-term trends. All the time series have been low-pass filtered with the same filter, which has a cutoff period of 36 h. The time dependence of the low-frequency current modes is presented as a dimensional quantity, so that the relative importance of the two modes is reflected in this figure. The large wind event occurring on 5 September 1978 was induced by Tropical Storm Norman. The correlation between the largest current eigenvector and bottom pressure is obvious, but the correlation between the current eigenvectors and wind stress is less clear.

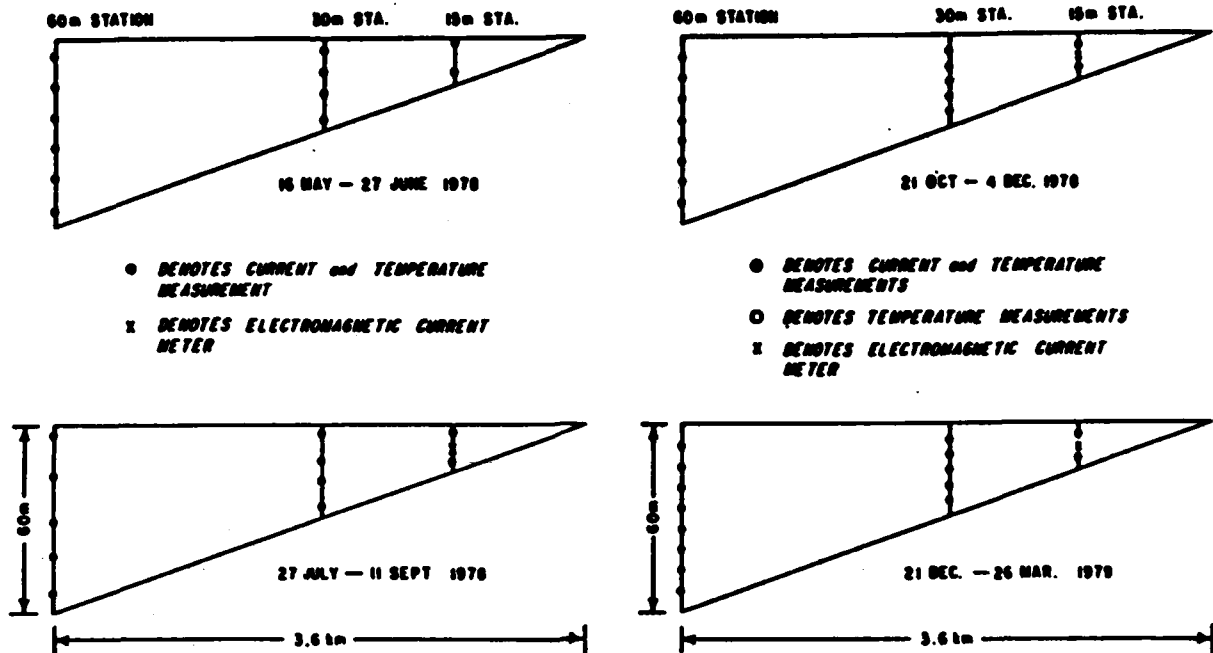


Figure 9.4-1 Instrument deployments of Winant and Bratkovich (1981) on the shelf off of Del Mar.

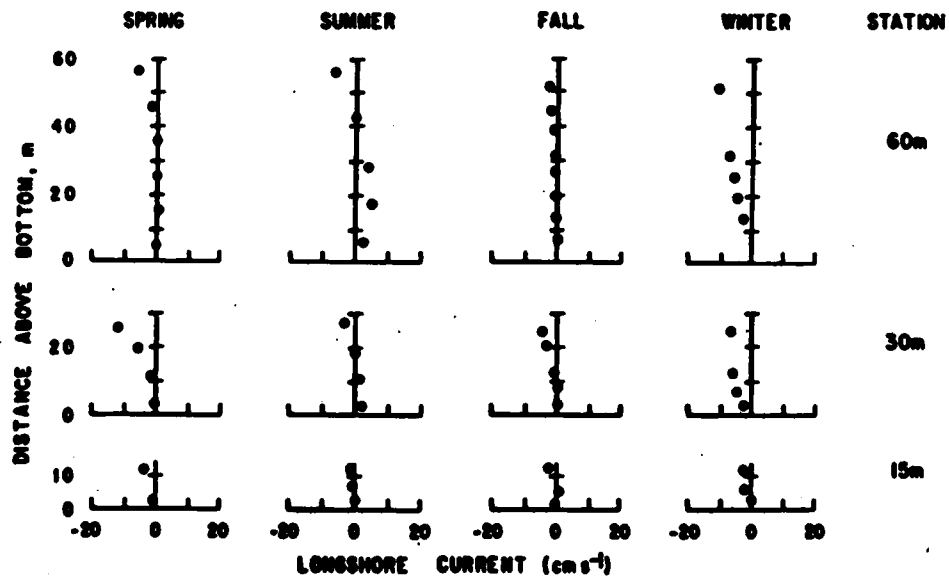


Figure 9.4-2 Distribution of mean longshore currents. A positive value corresponds to a current to the north (Winant and Bratkovich, 1981).

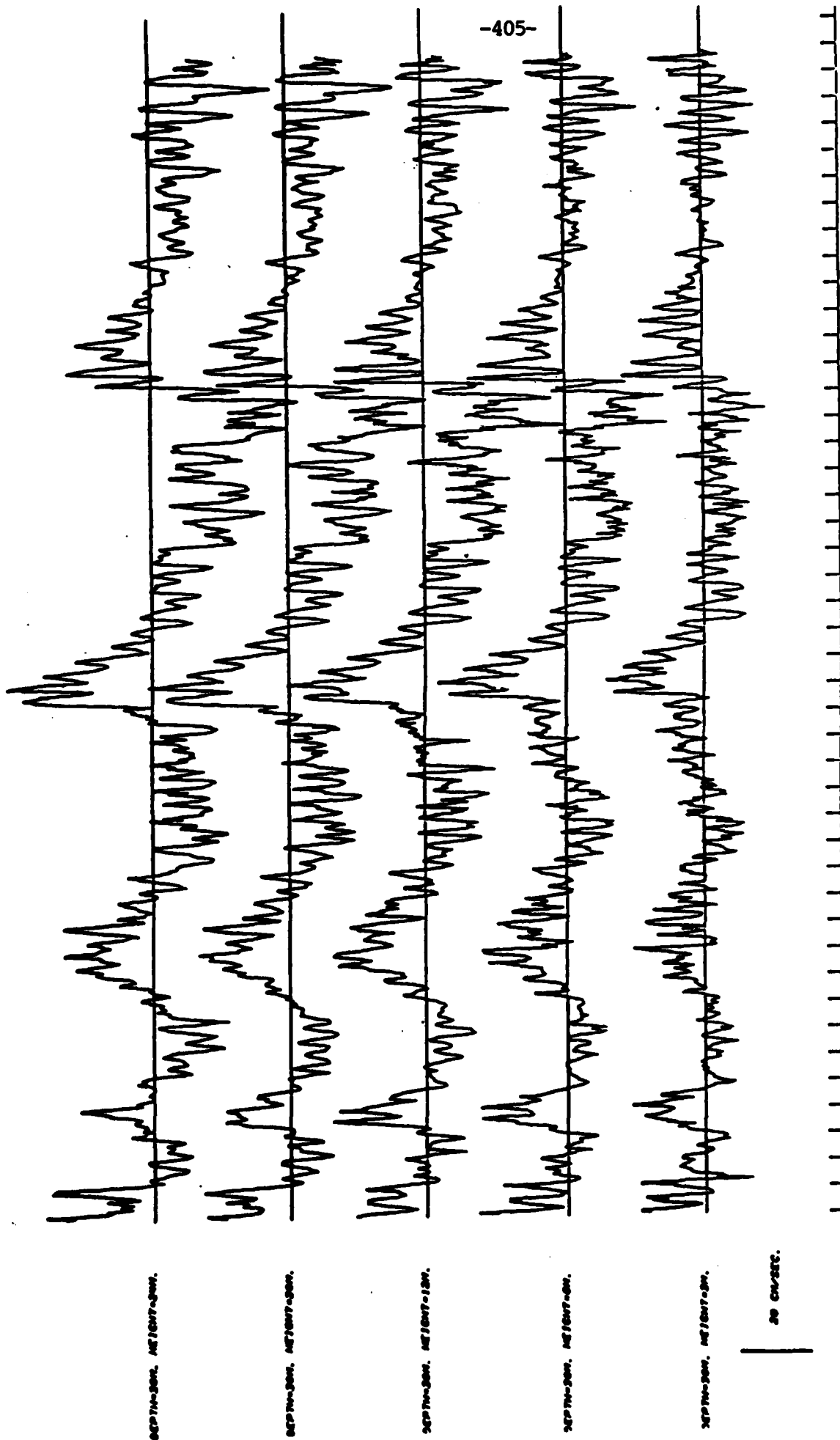


Figure 9.4-3 Longshore currents at Del Mar, 21 Oct - 8 Dec 1978 in 30 m depth at various heights above bottom. Tics are 1 day apart (Lentz and Winant, 1979).

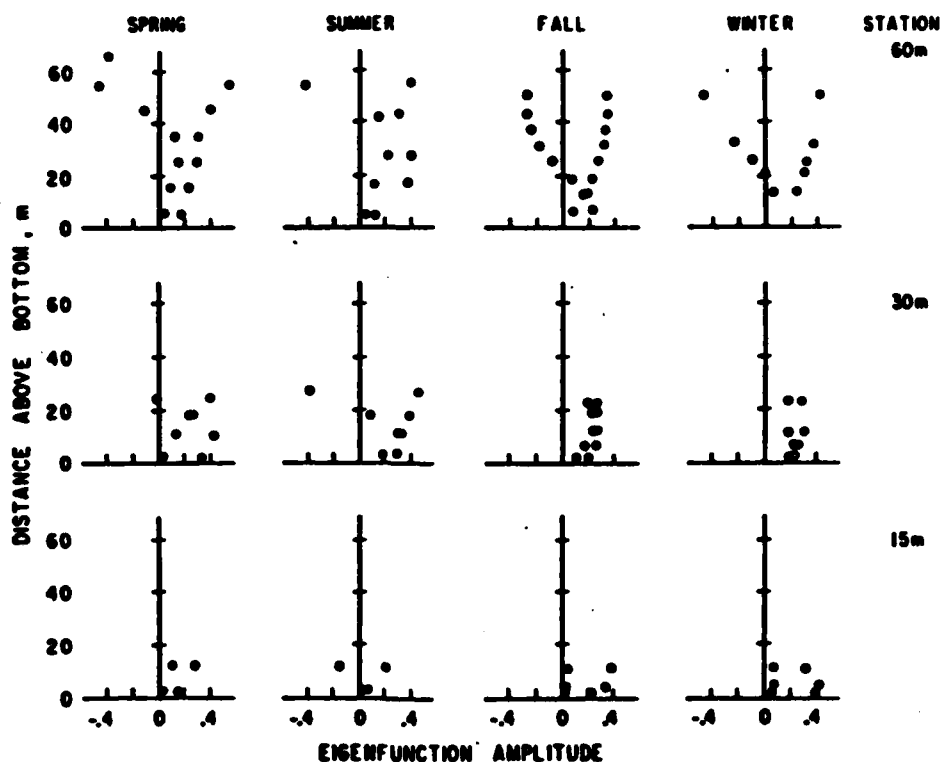


Figure 9.4-4 Distribution of the amplitude of the first (filled circle) and second (open circle) eigenvectors of low-passed (periods longer than 36 h) longshore currents (Winant and Bratkovich, 1981).

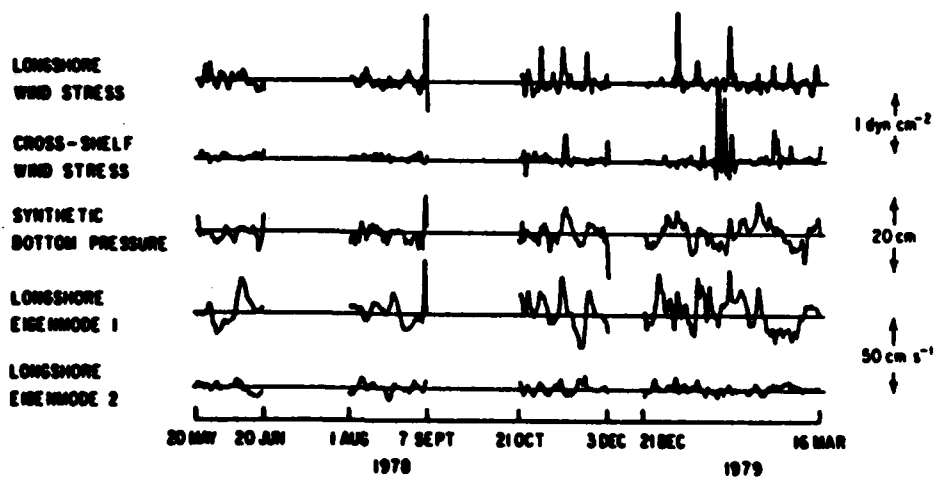


Figure 9.4-5 Time dependence of low-passed (periods longer than 36 h) longshore and cross-shelf wind stress, bottom pressure and two largest longshore current eigenvectors (Winant and Bratkovich, 1981).

Observations of temperature and current fluctuations on the shelf off of Oceanside are reported in Severance et al (1978), Winant and Holmes (1983), and Winant (1983). Winant and Holmes (1983) present time series plots and simple statistics for a current meter array deployed along the 30 m isobath (Figure 9.4-6). Each mooring had a near surface and near bottom current meter/temperature sensor. Figure 9.4-7 shows near bottom longshore current time series. The means are all small (< 6 cm/sec), similar to the surface long and cross-shore currents (Figure 9.4-8). The standard deviations of the currents are larger than the means for both current directions and all sensor locations. The surface longshore current standard deviations are at least twice as large as the surface cross-shore current deviations. This strong directional polarization is common to virtually all shelf current observations. The near bottom longshore current fluctuations have standard deviations comparable to those of the near surface cross-shore flow. Thus, the largest fluctuations are longshore near the surface. Figure 9.4-9 shows the longshore currents are not significantly correlated at rather short distances; 24 km for the subtidal band and 8 km for the tidal band. Winant (1983) used the observed scales of motion in different frequency bands to estimate the dispersive properties of the shelf motions. The dispersion coefficient was found to vary with scale, as the current variance associated with larger, lower-frequency motions becomes available to dispersion. Observations of surf zone longshore currents within the cell are discussed in Section 3.3.3.

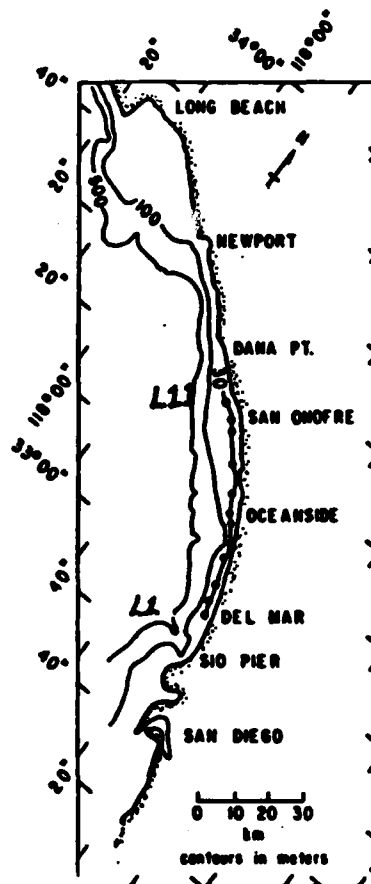


Figure 9.4-6 The dots indicate mooring locations (Winant, 1981).

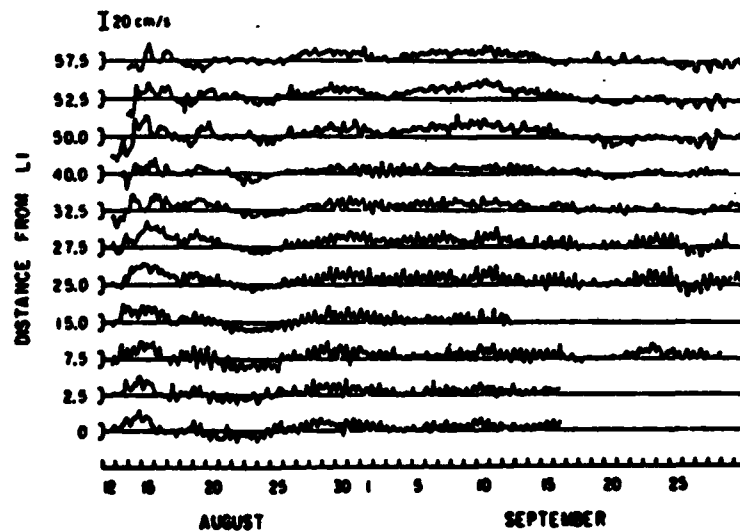


Figure 9.4-7 Near-bottom longshore-current time series. The top trace represents observations at the northernmost mooring (L11) and the bottom trace corresponds to the southern mooring (L1). The distance along the coast between each mooring and L1 is noted on the left, in kilometers (Winant, 1981).

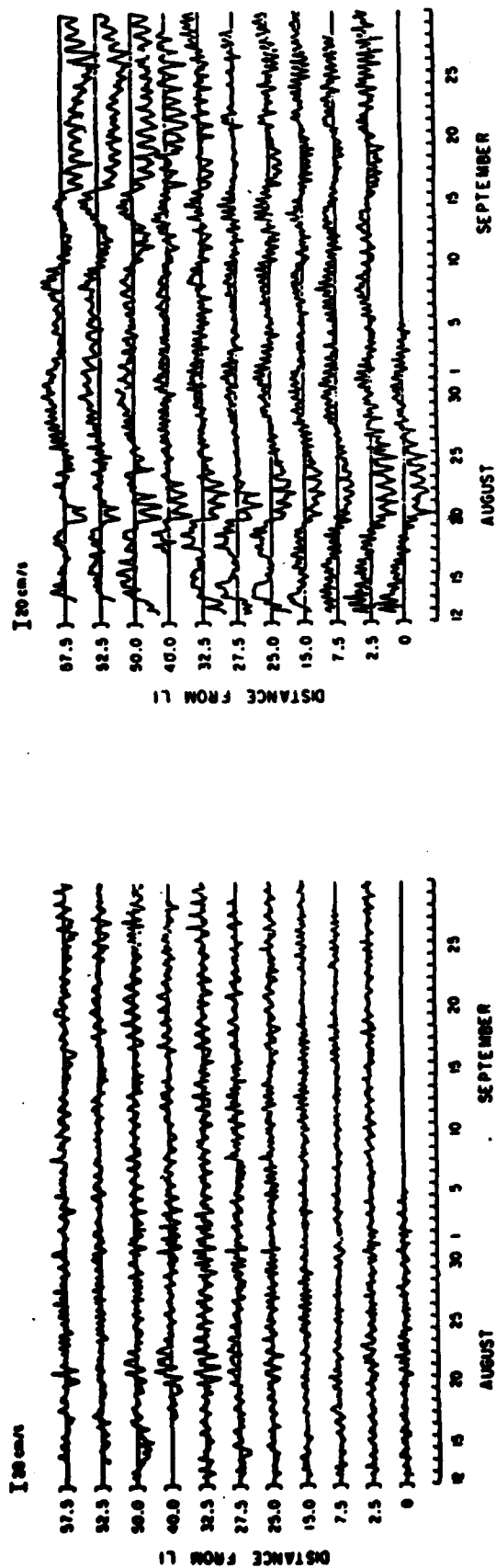


Figure 9.4-8 Near-surface cross-shore (left) and longshore (right) current time series plots and statistics (Winant, 1981).

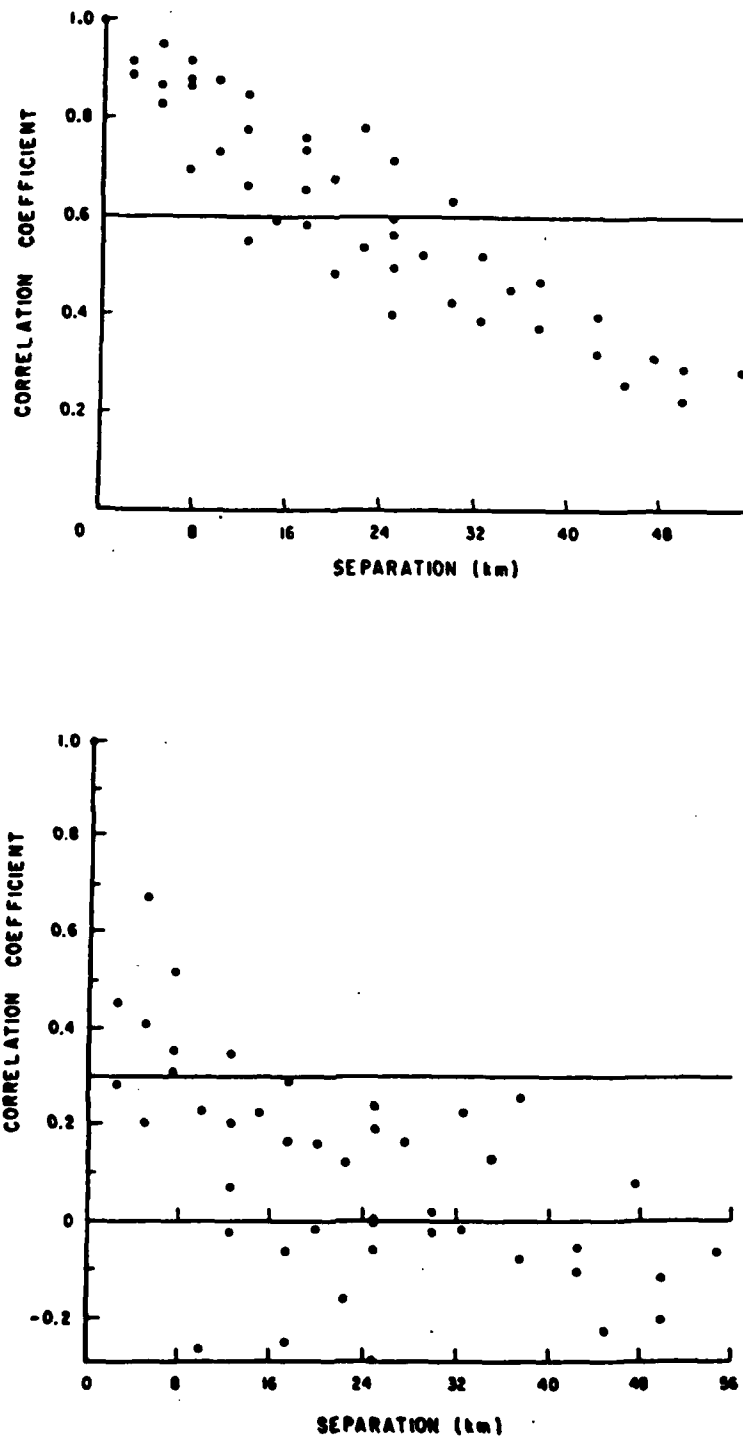


Figure 9.4-9

Correlation coefficients for low-frequency, subtidal (upper) and tidal (lower) near-surface longshore currents as a function of separation between current meter pairs. The light horizontal line represents the 95% confidence limit for no correlation (Winant, 1981).

9.5 SEDIMENT SOURCES

9.5.1 *Cliff Erosion and Relict Dunes*

Surveys taken at the unprotected sea cliffs both north and south of the Scripps Institution of Oceanography buildings during the period from 1936 to 1946 showed a maximum retreat of six feet during that 10-year period (Shepard, 1946). However, the more consolidated conglomerates and sandstone sections of cliff showed little retreat. Shepard and Grant (1947) used photograph comparisons to illustrate that over a 50 year period the high cliffs in the Torrey Pines State Park have experienced negligible erosion. This paper also contains several historical photographs of local sea cliffs dated back to 1887. Shepard and Inman (1951) estimated that the amount of sand introduced to, and transported down the Scripps submarine canyon is about 100 times as much as introduced from erosion of the land adjacent to the intercanion area. Nordstrom and Inman (1973), Inman and Jenkins (1983) and Inman (1985b) discuss how damming of rivers and the resulting beach erosion may increase the rate of sea cliff retreat.

Lee (1980) discusses the processes that erode sea cliffs. These include wave action, rain, water, and wind processes, natural or induced landslides, and animal and human activity. Erosion related to animals consists primarily of burrowing into the cliff face or behind protective structures. Man-induced erosion of sea cliffs can be attributed to foot traffic, excavation of caves, and carving of graffiti on the cliff face. He also discusses the petrology and geology of the cliffs at Solana Beach, Cardiff by the Sea, and the Encinitas-Leucadia cliffs. Lee does not directly address the quantity of material eroded or the erosion rate of these sea cliffs, but he does outline methods to measure sea cliff erosion.

Photographs of sea cliff erosion at Torrey Pines State Beach and of sea cliff collapse of La Jolla Shores Beach are shown in Inman (1983). Inman also describes the paleocoastline of the cell and their development to modern times. Kuhn and Shepard (1983, 1984) give descriptive

accounts of severe cliff erosion in San Diego North County. They discuss the correlation between volcanic activity, high annual rainfall, sea surface temperature and the occurrence of catastrophic coastal erosion events. While their hypothesis is not proven, they do point out some interesting implications. Kuhn and Shepard (1984) contain several historical ground and aerial photos which, when compared to present day photos, illustrate some catastrophic cliff failures. Simmons, Li and Associates (1984) use a simplified model to calculate the annual yield of beach sand material along 52 miles of coast in the Oceanside Cell. They use an average annual shoreline retreat over the last 5,000 years of 0.7 feet. This annual rate does not correct for the rise in sea level or any coastal uplift during the last 5,000 years. Also, the rate of shoreline retreat is not necessarily equal to the rate of cliff retreat. These reasons make their estimate for annual yield of beach sand from cliff retreat of 140,000 yds³ very questionable.

USACE LAD (1984b) contains a chapter concerning coastal cliff sediment resources. Figure 9.5-1 shows the classification of coastal cliffs from Dana Point to the Mexican Border. The report identifies the age of the various conglomerates and dense stone strata. It points out that very little work on long-term rates of cliff erosion has been completed. Table 9.5-1 lists reported rates of cliff retreat, together with estimates of the amount of sediment produced. The rates are derived from very different geologic terrains under differing conditions of erosion, but they illustrate the data gaps and the need for further investigation.

9.5.2 *Sediment Discharge from Rivers and Streams*

USACE LAD (1960a) systematically describes the drainage areas from the San Mateo Creek to the Los Penasquitos Creek. USACE LAD (1970) contains grain size analysis for sand samples taken at Newport Harbor and Oceanside Beach. The report also summarizes a study of the San Juan Creek Delta along with a description of the 1970 shoreline features throughout the littoral cell. Inman and Nordstrom (1973) estimated the total sediment contribution from streams to the Oceanside Cell to be between 230,000 and 350,000 yd³/yr. Taylor (1978)

Table 9.5-1.

Estimated rates of cliff retreat, Dana Point to
the Mexican Border (from USACE LAD, 1984 b.)

Locality	Rate of Retreat (Ft)	Volume (Yd ³)	Source
Unnamed gully, Camp Pendleton		^a 200,000 (1960-1980)	Kuhn and others (1980)
Unnamed gully, Camp Pendleton		^a 50,000 (6 days, 1978)	Kuhn and others (1980)
Solana Beach	8-10, (1972-78)		Kuhn and Shepard (1979)
Encinitas	^b 12-16 (1978)		Kuhn and Shepard (1979)
Del Mar	^b 1-12 (1973-77)		Kuhn and Shepard (1979)
La Jolla Terrace Sediments	10-20 (1923-30)		Vaughn (1932)

a. Erosion due to gullyng of cliff face.

b. Collapse of large blocks into the surf zone, usually during a storm
or a series of storms through the years indicated.

discusses the impact of sand and gravel mining, and how during the past 30 to 40 years these operations have removed and transported some 10 million yd^3/yr of sediment from the beaches.

Brownlie and Taylor (1981) summarize water and sediment discharges for Southern California rivers. The report estimates sediment yield from "sediment rating" curves for suspended load versus water discharge. The total load estimate is probably low because they assume bedload to be 10% of the suspended load instead of a more typical 20% value for southern California rivers (see Inman and Jenkins, 1983). The report discusses in some detail basin description, geologic setting, gaging stations and stream bed characteristics of the Santa Margarita River, the San Luis Rey River and the San Dieguito River. Figures 9.5-2 and 9.5-3 show the drainage basins for the Santa Margarita and San Dieguito Rivers. Osborne and Associates (1982) performed a detailed geomorphologic and sedimentologic analysis of the Oceanside area. This report contains discussions of watershed hydrology, sediment source areas, petrographic analysis and beach sand sample mineral composition and moment measures. Figure 9.5-4 shows the source areas and erosive characteristics of the drainage area in the Oceanside Littoral Cell.

Osborne et al (1983) presents extensive data on offshore sand deposits on the inter-continental shelf in the area adjacent to the Oceanside Littoral Cell. The report includes bathymetric maps, vibracores, grain size analysis, petrology, stratigraphy and lithology data for these areas. Inman and Jenkins (1983) present a thorough discussion of the sediment yield from streams in the Oceanside area for both pre-dam and present conditions (see Table 9.5-2). Weggel and Clark (1983) estimate sediment contributions from the Santa Margarita and San Luis Rey Rivers. Similar to Brownlie and Taylor (1981) they use the sediment discharge-streamflow rating curve, which may underestimate the annual sediment yield (see Inman and Jenkins, 1983 and Section 2.5 for discussion).

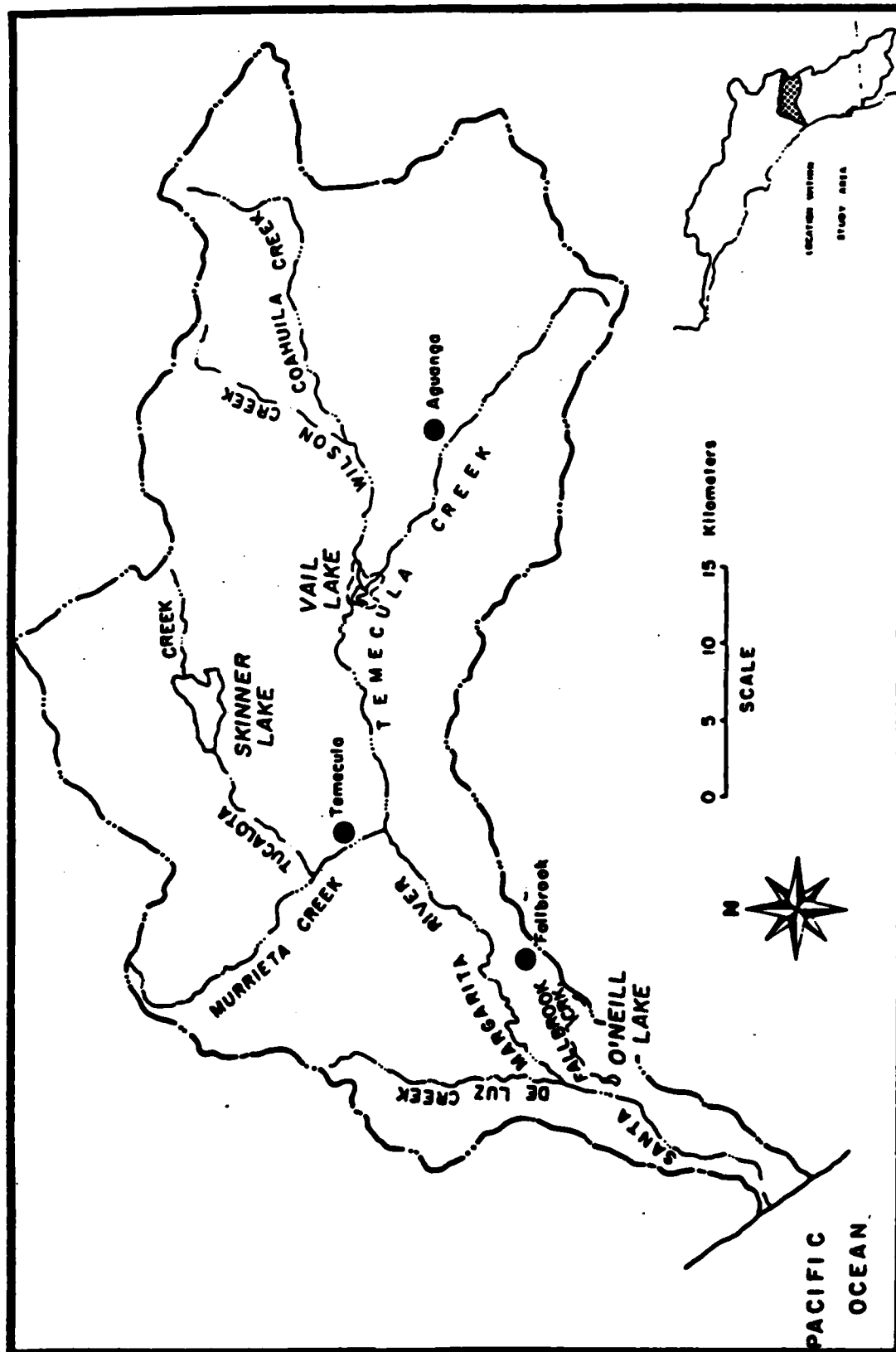


Figure 9.5-2. Santa Margarita River Basin (from Brownlie and Taylor, 1981).

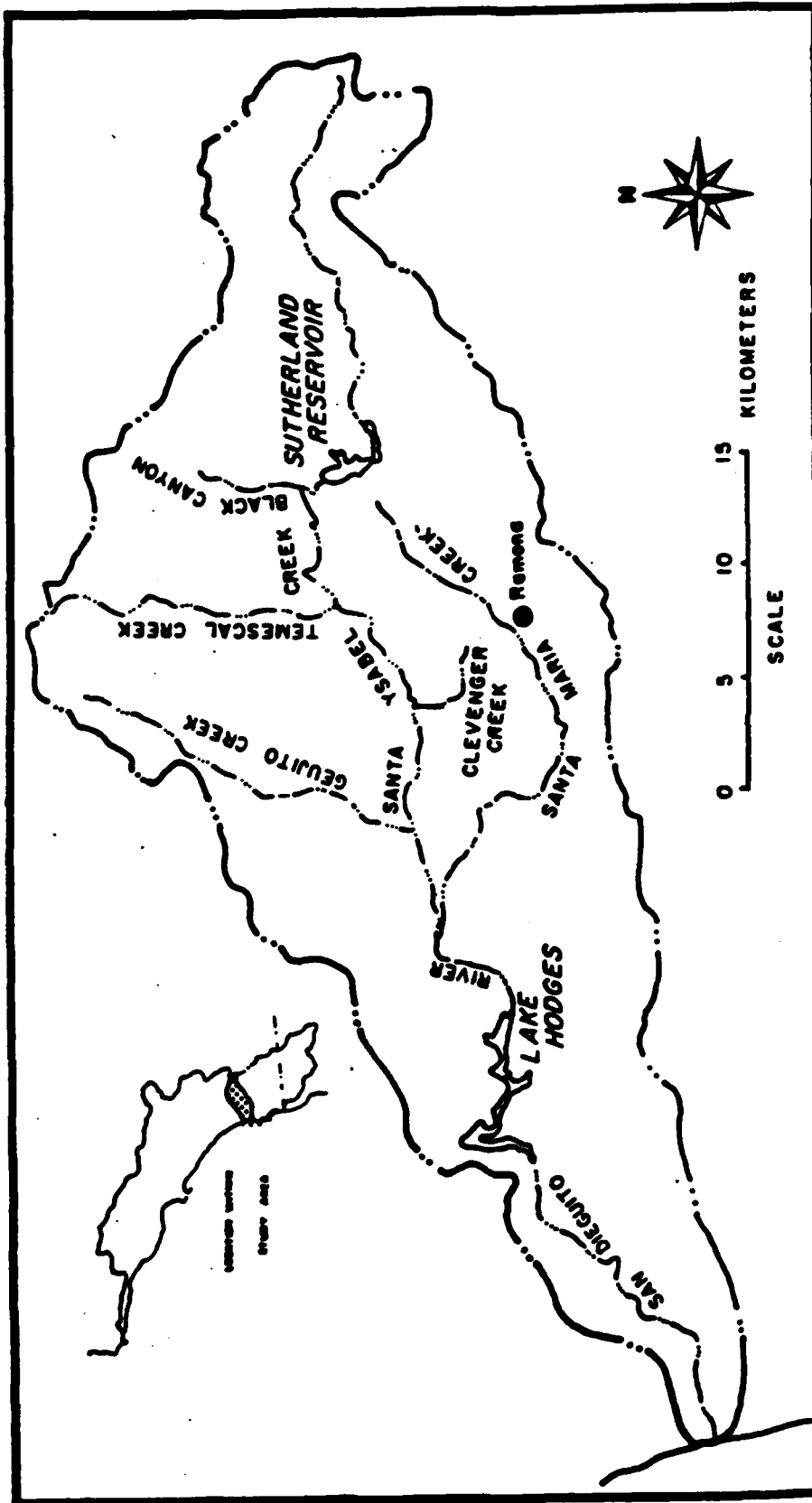


Figure 9.5-3. San Dieguito River Basin (from Brownlie and Taylor, 1981).

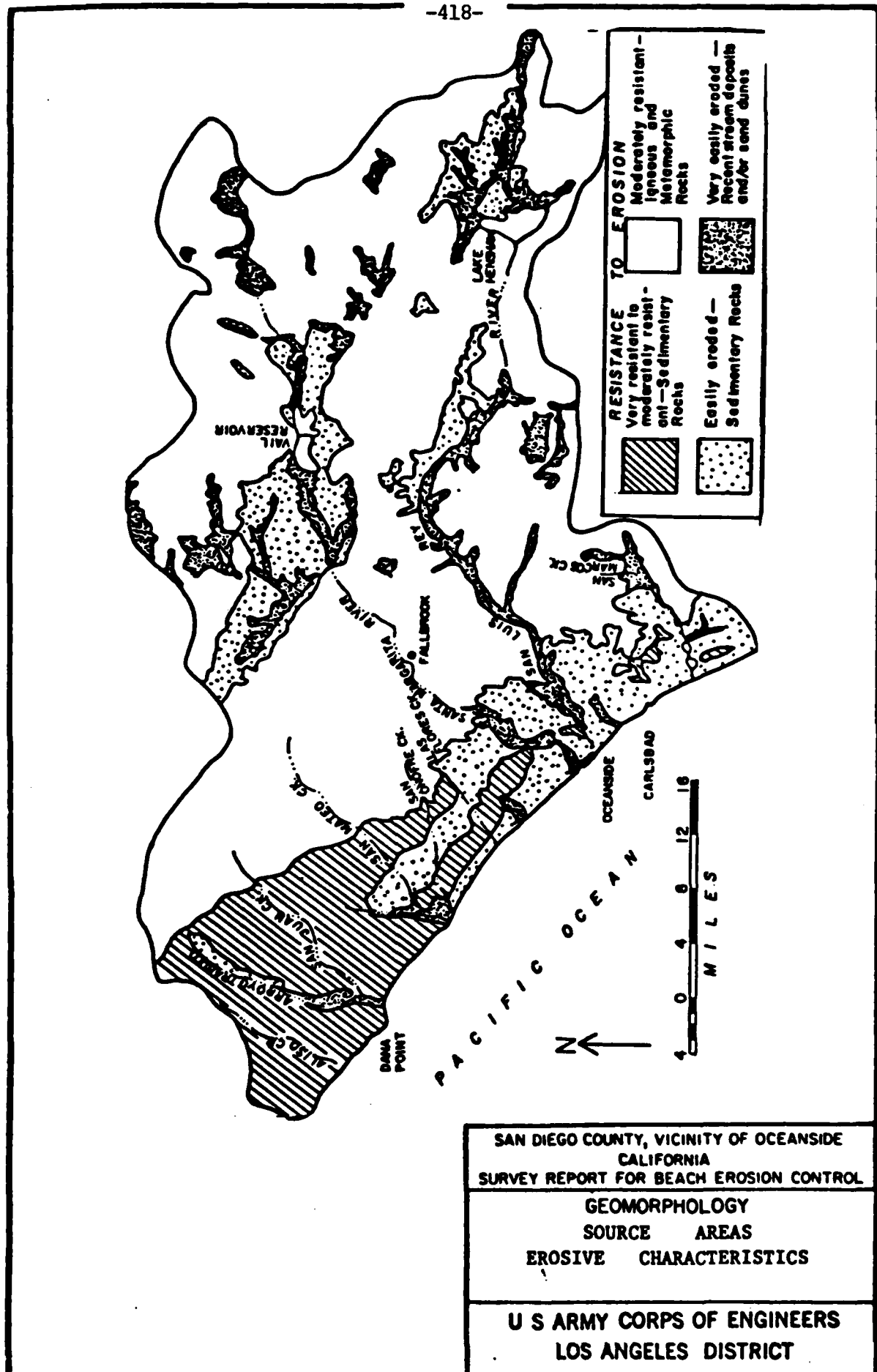


Figure 5.5-4. Source areas and erosive characteristics, Oceanside Littoral Cell (from Osborne and Associates, 1982).

Table 9.5-2. Yield to the coast of sand and gravel and total load (including fines) from the Santa Margarita and San Luis Rey River basins. Data estimated from stream gauging stations by Brownlie and Taylor (1981), but assuming bedload is 20% of suspended. Yield is in cubic meters and (cubic yards) (from Inman and Jenkins, 1983).

River Basin	Santa Margarita		San Luis Rey	
	natural	actual	natural	actual
Ave Annual Sand & Gravel	22,000 (29,000)	18,000 (24,000)	86,000 (112,000)	28,000 (37,000)
Ave Annual Total Load	57,000 (75,000)	47,500 (62,000)	229,000 (391,000)	74,000 (97,000)
Largest Event				
Year Measured				
	1969/1970		1938/1939	
Sand & Gravel	329,000 (430,000)	234,000 (306,000)	1,207,000 (1,578,000)	464,000 (607,000)
Total Load	863,000 (1,128,000)	623,000 (814,000)	3,218,000 (4,207,000)	1,233,000 (1,612,000)

* Assuming that 1 metric ton mass equals 1 cubic meter of sediment "at-rest" volume with solids concentration $H_c = 0.6$. Refer to Equation 3.3.1.

**Similar calculations give the natural yield of sand and gravel from the San Dieguito River as 32,000 m³ (42,000 yd³) per year.

Simons, Li and Associates (1984) address the effects of the proposed Santa Margarita River dam project on the delivery of beach sands to the Oceanside Littoral Cell. This report contains data on sediment yield from area streams, rainfall and runoff, and cliff erosion. But, as discussed in Section 9.5.1, they probably overestimate the sediment yield from cliff erosion and underestimate the yield from the Santa Margarita River. USACE LAD (1984b) contains an extensive summary of the Oceanside Littoral Cell basin sediment resources. The report presents data on drainage basin areas and degree of control, estimated annual sediment production for rivers and creeks, and the distribution of potential sand sources. It also includes local mineral composition and sand sample grain size analysis. Inman (1985b) discusses how the damming of rivers in this littoral cell intercept the normal flow of sand to the beaches.

9.5.3 *Artificial Beach Nourishment*

Shaw (1980) reports on artificial beach nourishment (artificial sediment transport) in coastal southern California, by systematically outlining the quantity of dredged material and beach fill material for nourishment projects in the Oceanside Littoral Cell. There is currently no sand bypassing operation in this littoral cell, although the Oceanside Harbor sand bypass project should be completed in the near future. Herron (1980) discusses a 1966 beach nourishment project at Doheny State Park where 900,000 yd³ of beach nourishment material was taken from an ancient inland beach deposit at an elevation of +200 feet MSL. Inman and Jenkins (1983) in an oceanographic report for Oceanside Beach facilities, recommend a continued beach nourishment program for Oceanside Beach, a concentrated effort to find new sources of sand, and a halt to future dam building on streams supplying the cell with sand.

Osborne et al (1983) inventories potential sand and gravel sources located within offshore coastal areas from Point Dume to the Mexican Border. Waldorf et al (1983) briefly discusses the nourishment of Oceanside's south beach and recommends a seasonal nourishment program to maximize the benefits of the beach nourishment. Kuhn and Shepard (1984) mention the Del

Mar Longard Tube and its performance as an alternative to beach nourishment. USACE LAD (1984b) outline sand and gravel resources for beach nourishment in the Oceanside Littoral Cell (see Figure 9.5-5). As part of their continuing program for the protection of the California shoreline from erosion, the California Department of Boating and Waterways compiled information on sediment transport in coastal stream basins and beach nourishment along the southern California coastline (California, 1977b).

9.6 SEDIMENT TRANSPORT MODES

9.6.1 *Cross-shore Transport*

Little information is available on cross-shore transport in the Laguna Sub-cell area north of Dana Point. Some historical beach profiles of the area's pocket beaches are available and are detailed in Section 9.2. However, these profiles were not used to compute volumetric changes or cross-shore transport rates (Newton, 1959), because the beaches were considered stable until recent housing development on the beaches. With the advent of shoreline housing development, some information on seasonal transport patterns has become available from environmental impact studies (Inman, 1978b).

A net change in beach volume can be the result of two factors: cross-shore transport or a change in the rate of longshore transport. In general, it can be expected that volume changes on long straight beaches (i.e., the southern portion of the Oceanside cell) are due principally to cross-shore transport and that changes on pocket beaches (i.e., Laguna Sub-cells) are due principally to changes in longshore transport rates. Inman (1978b) has shown from beach profiles and aerial photographs that seasonal variation in the longshore transport (to the north in summer, south in winter) causes volume changes estimated at $108 \text{ yd}^3/\text{yd}$ of beach in the Laguna Niguel Sub-cell. (For location of this sub-cell, see Figure 9.6-1). Nevertheless, there is a possibility of offshore transport in strong rip currents observed in aerial photographs (Inman,

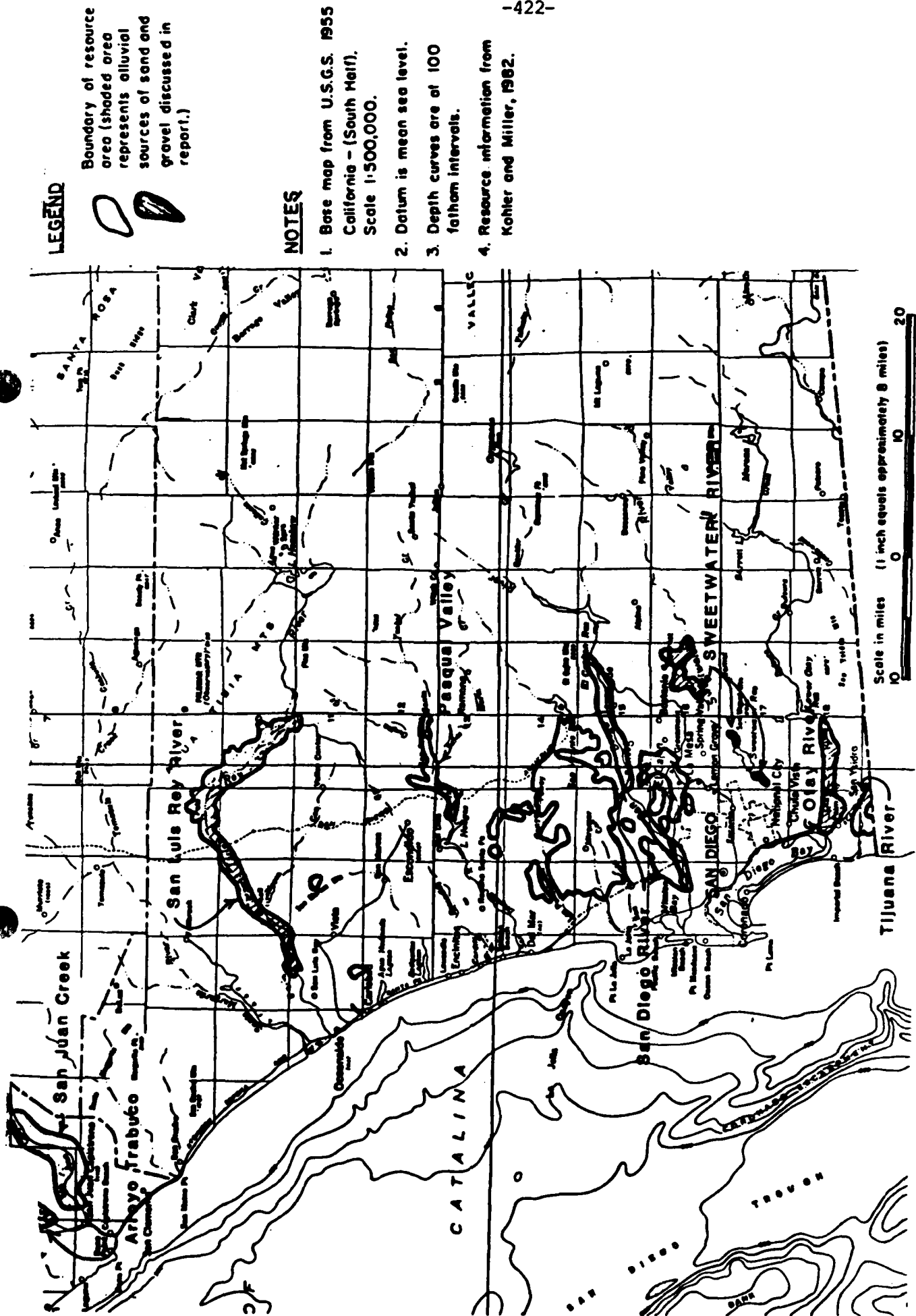


Figure 9.5-5. Major sand and gravel resource areas: Oceanside, Mission Bay and Silver Strand Cells (from USACE LAD, 1984).

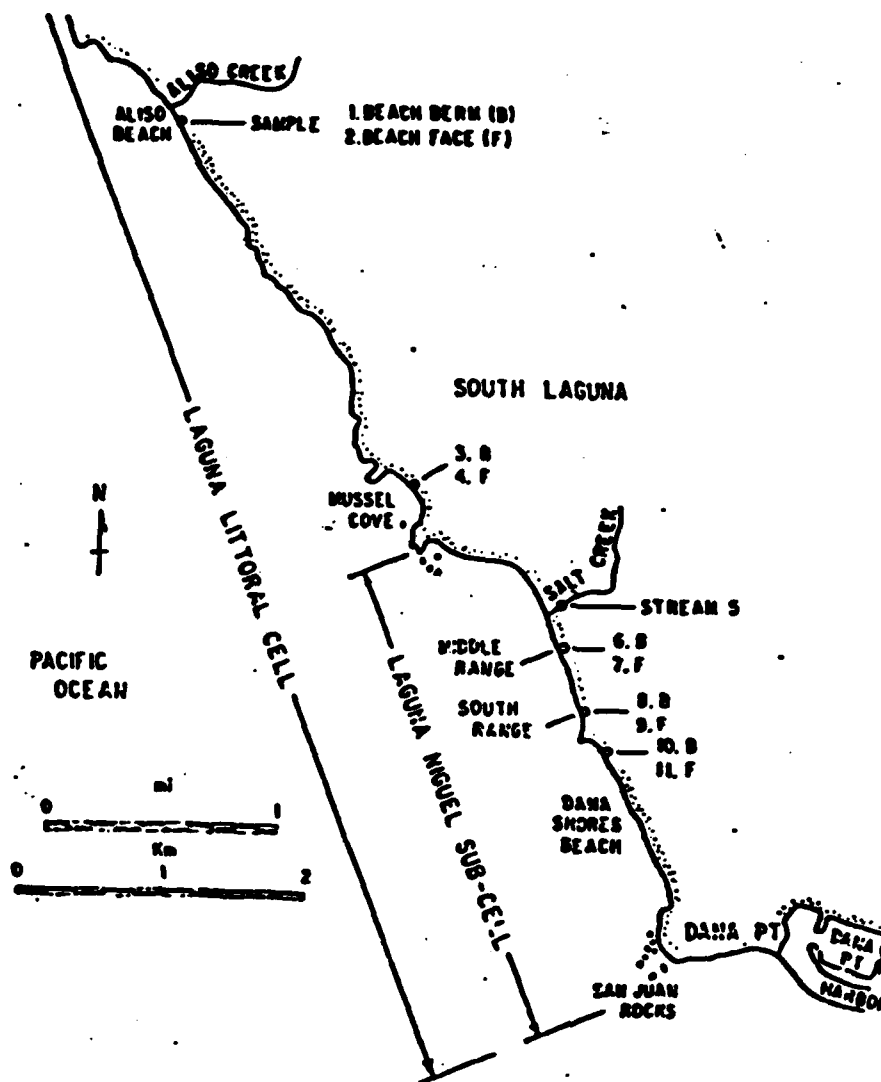


Figure 9.6-1. Laguna Niguel Littoral Sub-cell (from Inman, 1978b).

1978b).

Between Dana Point and Oceanside historical beach profiles are available (Section 9.2 and Figure 9.6-2). but the only cross-shore transport computations were made at San Onofre Nuclear Power Plant as part of various environmental impact statements not included in this study.

Numerous profiles of beaches near Oceanside have been completed in order to document effects of construction of the boat basin and harbor. Profiling consists of a long-term study by the Corps (USACE LAD 1960b, 1967b, 1969a, 1970 and 1980c) begun in 1950 and several short-duration scientific and environmental studies (Shepard, 1950c; Inman and Jenkins, 1983; Weggel and Clark, 1983). Long-term changes in beach profiles appear to be caused more by changes in longshore transport due to harbor construction than to cross-shore transport. Initial studies did not attempt to separate the two modes but simply reported the amount of erosion or accretion. (See the South Oceanside profiles in Figure 9.6-2.) Analysis of the Corps' series of profiles from 1950 to 1980 (Weggel and Clark, 1983) reveals exactly the type of erosion/accretion trends one would expect from changes in the longshore transport rate by harbor construction - accretion north of Oceanside Harbor, erosion south of the Harbor, and accretion north of the Agua Hedionda Lagoon jetties at Carlsbad. These changes are documented in Figures 9.6-3 and 4. The first figure represents cumulative volume change as one progresses away from Oceanside Harbor. The second curve is the slope of the first curve and represents actual erosion/accretion.

Weggel and Clark (1983) computed a theoretical offshore loss of sand due to rise in sea level. They assume a "standard Bruun beach profile." Bruun's profile is actually a very simplified generalized profile which can easily be described mathematically and thus has no offshore bars. However, the difference between such a simplified representation and actual Oceanside beach profiles can be quite dramatic. Furthermore, the presence of sea cliffs along

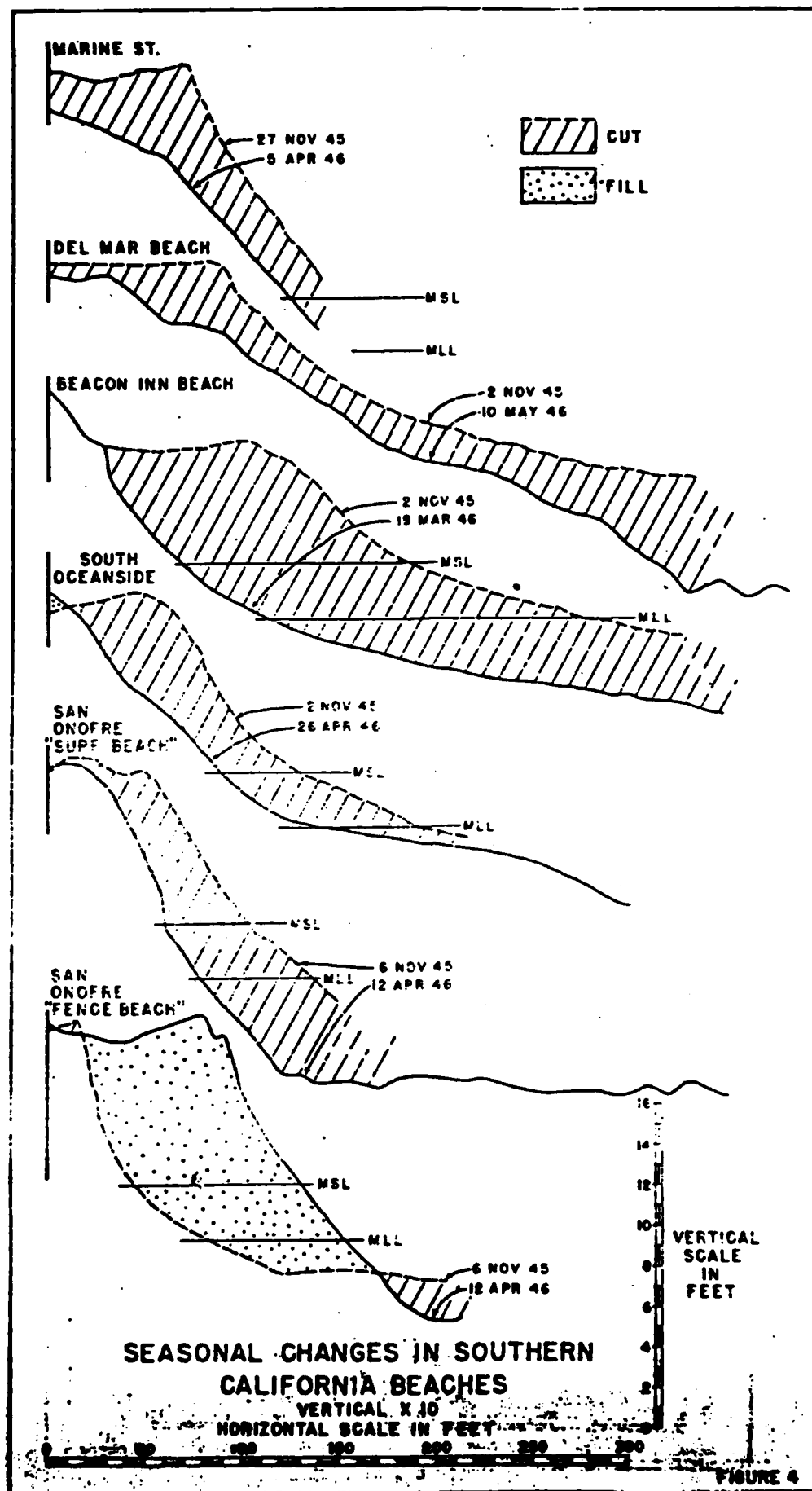


Figure 9.6-2. Seasonal changes in southern California beaches as measured by rod-and-level profiling (from Shepard, 1950c).

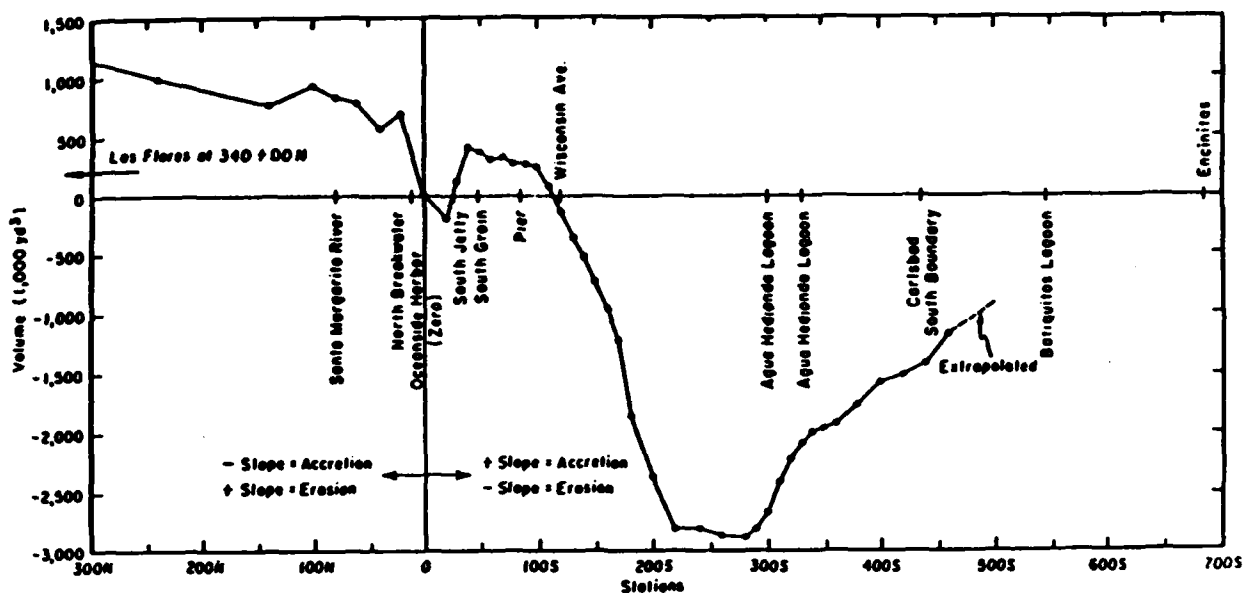


Figure 9.6-3. Cumulative volume accretion or erosion as a function of distance from Oceanside Harbor (from Weggel and Clark, 1983).

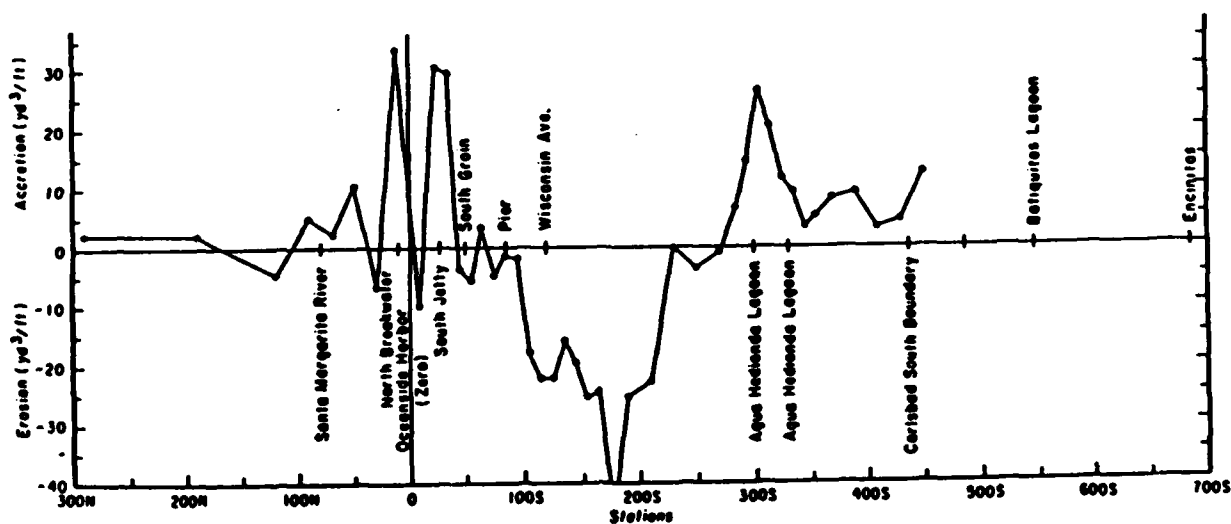


Figure 9.6-4. Erosion or accretion per unit length of beach as a function of distance longshore (from Weggel and Clark, 1983).

much of the cell means that the profile is quite variable geographically and that loss due to sea level rise is abrupt, not gradual as they assumed.

Inman and Jenkins (1983) interpreted the erosional patterns in both the Corps' 1950-80 profiles and the more recent Waldorf, Flick and Hicks (1983) profiles taken during 1982-83. Analysis of both data sets indicates erosion of the sand delta of the San Luis Rey River which formerly extended seaward to depths greater than 10 m. Rangelines near the river show erosion along the entire profile. Other ranges south of the Harbor show erosion only shoreward of 10 m depths. In general, this erosion pattern also caused steeper profiles which results in increased longshore transport, as will be described in the next section.

Occasional beach profiles and seasonal cycles were measured at Del Mar as part of scientific studies as early as the forties. (See the Del Mar profile in Figure 9.6-2.) The City of Del Mar has funded monthly beach profiling and study of its beach cycles since 1974. Waldorf and Flick (1983) and Flick and Waldorf (1984) have examined seasonal erosion/accretion cycles. The annual cycle of winter erosion and summer accretion is clearly evident in Figure 9.6-5. The dotted line indicates change from year-to-year. Clearly there are also trends (possibly cycles) which extend over several years, as well as occasional catastrophic events (early 1983). The erosional events of strong offshore transport coincide with high waves. The strongest offshore transport and most destructive erosion occur at the coincidence of high storm waves and high tides (i.e., early 1983).

Numerous scientific studies have been performed at Torrey Pines Beach between Del Mar and La Jolla. A major portion of many of these studies has been the study of cycles of cross-shore beach changes. Monthly profiling was supported by the Corps from 1972-1974. Nordstrom and Inman (1975) identified the seasonal cycles of gradual onshore transport from a submarine bar to a subaerial berm during the spring and summer; in the fall, abrupt offshore transport from the berm to the bar occurred at high wave and high tide coincidence. They

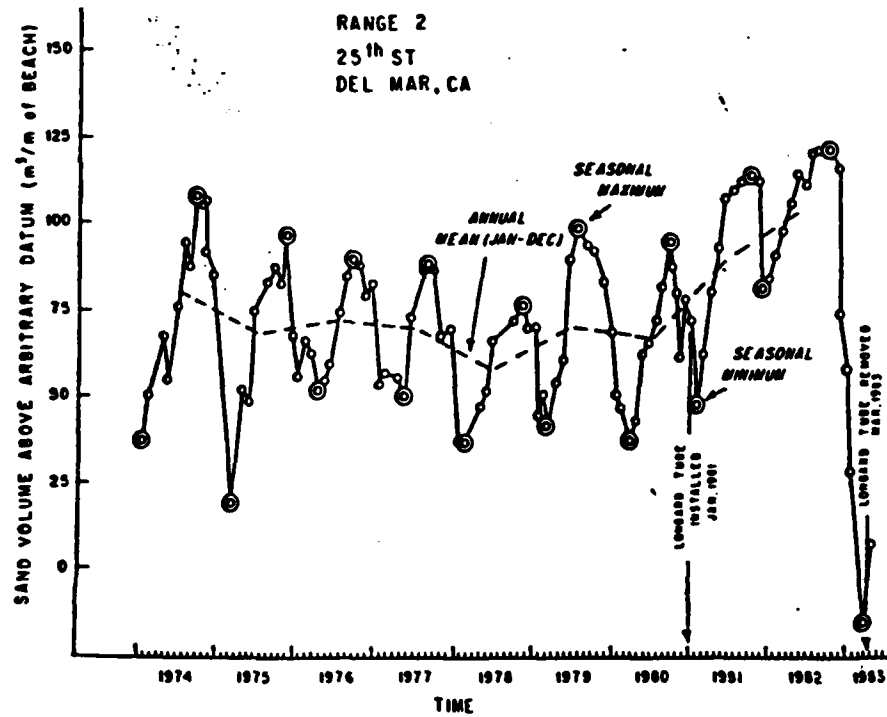


Figure 9.6-5. Beach foreshore sand volume changes at Del Mar range 2 (from Flick and Waldorf, 1984).

estimated seasonal erosion and accretion rates, which are summarized in Table 9.6-1. The source of the berm sand was the offshore region shallower than 10 m. The erosion of the summer berm in the fall resulted in accretion at depths between 3 m and 9 m. A statistical analysis that separated the temporal and spatial dependence of the profile changes is given in Winant et al (1975). This analysis, using empirical eigenfunctions, showed that the major cross-shore seasonal changes were associated with the second eigenfunction, the "bar-berm function." This function has a maximum at the location of the summer berm and a minimum at the location of the winter bar, with a cross-over or pivotal point between. A statistical correlation of these beach changes with wave and tide characteristics was demonstrated by Aubrey, Inman and Nordstrom (1976). Aubrey (1979) later identified a seasonal "pivot point" about which the cross-shore transport oscillated at 2.5 m deep and presented data suggesting the possibility of a 6 m pivot point also.

Monthly profiling continued through 1977 at Torrey Pines, along with a short weekly profiling study. From this 1972-77 data set a new technique of analyzing beach profile changes was developed, expressing beach changes in terms of "empirical eigenfunctions." Winant and Aubrey (1976) showed that the first temporal eigenfunction could be used to identify net erosion/accretion of the beach. If this function was stable, they found that even short data sets (monthly profiles for one year) could effectively be used with this analysis procedure to quantify beach cycles. Both spatial and temporal eigenfunctions are obtained. It is much easier to discern cycles in the beach behavior from the temporal functions than from raw beach profile plots. The spatial functions have physical significance. Figure 9.6-6 illustrates the spatial decomposition of the profile data into eigenfunctions. The first function represents the mean level of the beach. The second function has a large positive peak at the mean subaerial berm location and a large negative value at the mean submarine bar location and is referred to as the "bar-berm function". The third function has a broad peak at the low-tide terrace and is called

Table 9.6-1. Seasonal volume change of Torrey Pines Beach
in m^3 per meter of beach length (from Nordstrom
and Inman, 1975).

Period	Foreshore		Offshore	
	erosion	accret.	erosion	accret.
23 Oct. 1972 - 11 April 1973	121			82
11 April 1973 - 25 Oct. 1973		121	72	
25 Oct. 1973 - 4 April 1974	37.4			60

SPATIAL DEPENDENCE-EMPIRICAL EIGENFUNCTIONS SOUTH RANGE

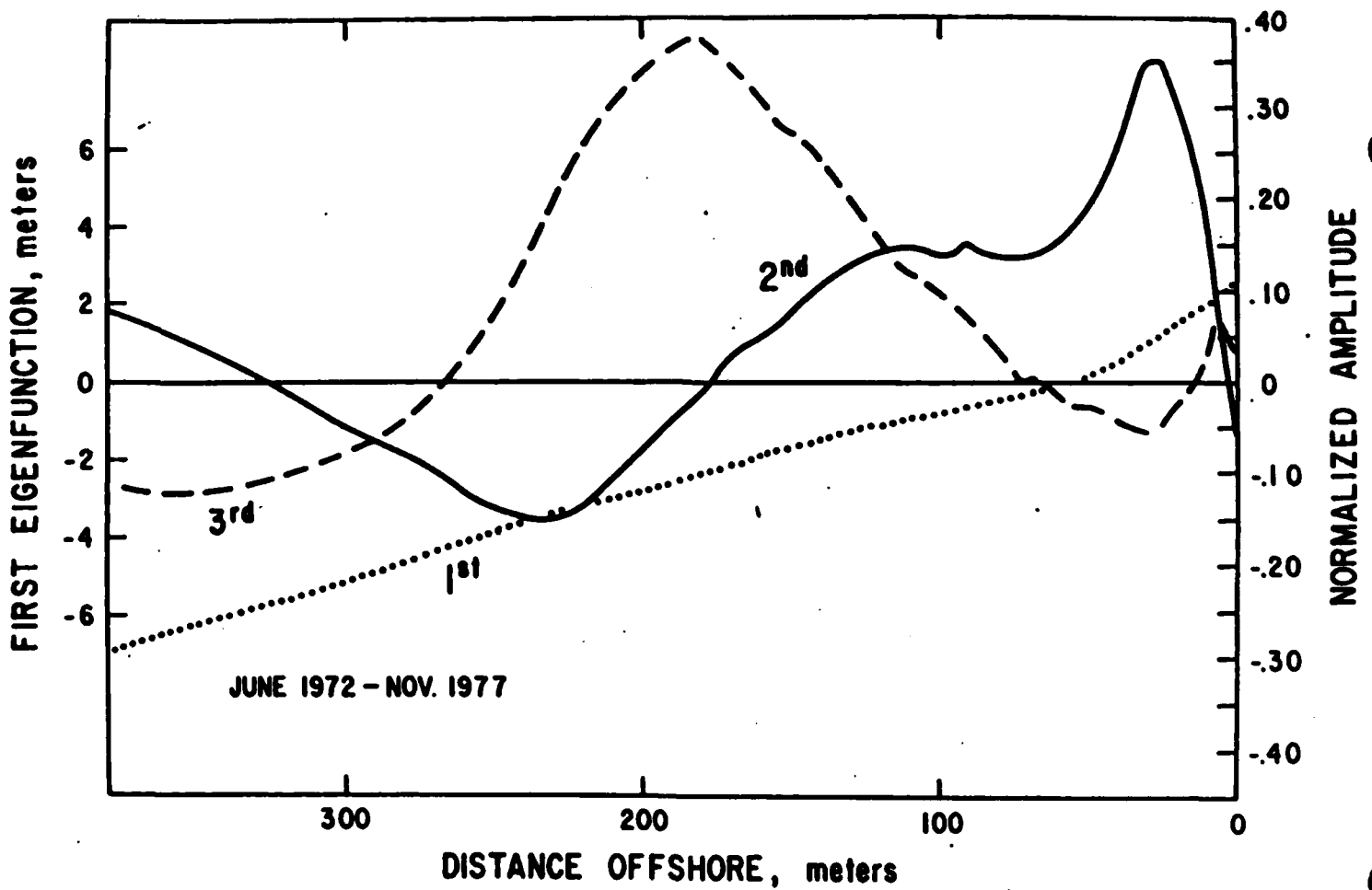


Figure 9.6-6. Spatial beach eigenfunctions at south range, Torrey Pines beach (from Aubrey, 1978).

the "terrace function". Aubrey (1978) and Aubrey, Inman and Winant (1980) extended this procedure to include decomposition of wave data into characteristic eigenfunctions. They were then able to correlate the wave eigenfunctions and beach eigenfunctions in a statistically significant cause-and-effect relationship, with possible predictive value.

In the fall of 1978 the National Sediment Transport Study was performed at Torrey Pines (Gable, 1979). A major portion of this study involved almost daily measurement of waves, currents and beach profiles. It was thus possible to test models of cross-shore transport (Seymour and King, 1982). Several models relating wind, tides and waves to beach changes were tested (Table 9.6-2). The general conclusion reached through statistical correlations (Table 9.6-3) was that wave steepness was the most important parameter in cross-shore transport. However, it appears that the more complicated models (i.e., Bailard and Inman, 1981) were not adequately tested due to incomplete understanding of the coefficients present in the models.

Many short-term studies of cross-shore transport have been performed at Scripps Beach just north of La Jolla Submarine Canyon, although much of the data remain unpublished. Shepard (1946) measured beach profiles along this coast at several sites during 1945-46, but most intensely at Scripps. He was one of the first to document the now familiar summer-winter seasonal cycles. He also recognized a correlation between beach slope and grain size. From daily measurements of beach profiles off Scripps Pier in 1937-38, Shepard (1950a) was able to document the seasonal migration of submarine bars (onshore in spring, offshore in fall). He also showed statistical correlation of bar depth and magnitude with wave height. Inman and Rusnak (1956) documented significant sand level changes to depths greater than had previously been thought possible, thus emphasizing the need to perform fathometer profiles in addition to rod-and-level profiles. Significant monthly variation was found to 70-foot depths and seasonal variations to 52-foot depths.

Table 9.6-2. Models for cross-shore transport and their significant parameters (from Seymour and King, 1980).

Model (1)	References (2)	Parameters (3)
Onshore wind	King & Williams (18)	Mean onshore component of near surface wind
Tides	Seibold (25)	Daily tide range
Wave height	Shepard (27)	Mean incident significant wave height
	Aubrey (1)	
	Hashimoto & Uda (10)	
	Shepard (25)	
	Short (29)	
Wave steepness	Dean (6)	Wave steepness, period, sand fall velocity
	Hattori & Kawamata (11)	
Wave power	Short (29)	Mean incident wave power
Velocity asymmetry	Wells (30)	Mean of cube of near bottom fluid velocity
General bedload transport	Bailard & Inman (3)	Means of: (1) Near bottom velocity squared times onshore velocity component; and (2) cube of magnitude of velocity Mean beach slope, angle of repose

* Adds beach slope.

Table 9.6-3. Maximum squared correlation coefficients between beachface volume changes and significant independent parameters of various predictive models for cross-shore transport, based on data from NSTS Field Experiment, Torrey Pines Beach, California, Nov. 3-24, 1978 (from Seymour and King, 1980).

Investigator (1)	Parameter(s) (2)	Correlation coefficient squared* (3)	Lag, in days (4)
King & Williams, Seibold	mean offshore wind	0.065	-1
Shepard	daily tidal range	0.160	0
Aubrey, Hashimoto & Uda, Shepard	mean significant wave height	0.270	-1
Dean	Dean criterion	0.353	-1
Hattori & Kawamata	Hattori & Kawamata criterion	0.352	-1
Short	mean incident wave power	0.289	-1
Wells	mean cube of velocity	0.095	0
Bailard & Inman	Bailard & Inman rate	0.023	0

* Indicates the fraction of the variance explained by the factor.

Inman and Chamberlain (1959) were the first investigators to use radioactive sand tracer and the first to attempt to directly measure sand transport velocity in the ocean. Their measurements just outside the breakers indicated onshore transport of 1-1/2 ft/min (46 cm/min) under highly erosive conditions. As yet unpublished studies at Scripps indicate cross-shore transport outside the breakers is only a few centimeters a second under near-equilibrium conditions.

9.6.2 Longshore Transport

Longshore transport rates for this cell are summarized in Table 9.6-4. "Potential" rates are obtained from application of the standard "radiation stress" equation (Section 2.4) with wave data as inputs. Both volume transport Q_l (yd³/yr) and immersed-weight transport I_l (newtons/second) are listed. In converting between the two measures, it was assumed that solids concentration $N_o = 0.6$ (porosity = 0.4) and sand density $\rho_s = 2.65 \text{ g/cm}^3$.

Along the small pocket beaches of Laguna Niguel (Figure 9.6-1), Inman (1978b) estimated a seasonal gross transport of 36,000 (to the north in the summer and to the south in the winter). These estimates were obtained from beach profiles and aerial photographs. He found that the net transport out of the sub-cell was more difficult to estimate, but made the following observations: the headlands are more effective in blocking northerly transport than southerly; the strongest waves come from the northwest and thus favor some southerly transport around headlands; in the winter more sand is available offshore where it is easier to move around the headlands; the south promontories do not extend far enough to allow a beach reorientation of zero-attack angle for winter storms. Inman (1978b) thus concludes that there must be some net transport to the south. From beach sand roundness data, he makes a very rough estimate of 15,000 yd³/yr net southerly transport out of the Laguna sub-cell.

Longshore transport estimates at San Onofre are available only in environmental impact statements not included in this study. Johnson (1957) estimated net transport as 100,000

Table 9.6-4 . Longshore Transport Rates
(Positive values indicate transport to the south, negative to the north)

Location	Notes	Reference	Potential Transport (Wave Refraction Studies)		Gross Transport (Trapping Studies)		Instantaneous Net Transport (Sand Tracer Studies)	
			Q_1 ($10^3 \text{ yd}^3/\text{yr}$)	I_1 (N/sec)	Q_1 ($10^3 \text{ yd}^3/\text{yr}$)	I_1 (N/sec)	Q_1 ($10^3 \text{ yd}^3/\text{yr}$)	I_1 (N/sec)
*Laguna Niguel Sub-Cell	Annual loss from sub-cell	Inman (1978)			15	4		
Range Within Entire Cell	Includes all historical estimates	Taylor (1978)			65 to 790	15 to 186		
Entire Cell	Data from several sources	Nordstrom and Inman (1973)			250	59		
Camp Pendleton	Out of date	Johnson (1957)			100	24		
Oceanside		Marine Advisors (1960)	216	51				
Oceanside		Hales (1978)	102	24				
Oceanside	Dredging (1942- 1963)	Inman (1976)			250	59		
Oceanside	Dredging (1963- 1970)	Inman (1976)			360	85		
Oceanside	No refraction <10 m deep	Castel and Seymour (1982)	90	21				
Oceanside		Inman and Jenkins (1983)	254	60				

* "Best" estimate at that location

Table 9.6-4 . Longshore Transport Rates (cont'd.)
(Positive values indicate transport to the south, negative to the north)

Location	Notes	Reference	Potential Transport (Wave Refraction Studies)		Gross Transport (Trapping Studies)		Instantaneous Net Transport (Sand Tracer Studies)	
			Q_1 ($10^3 \text{ yd}^3/\text{yr}$)	I_1 (N/sec)	Q_1 ($10^3 \text{ yd}^3/\text{yr}$)	I_1 (N/sec)	Q_1 ($10^3 \text{ yd}^3/\text{yr}$)	I_1 (N/sec)
Torrey Pines	Range of values on several days	Imman et al (1980)					1020- 2010	240- 473
*Torrey Pines	Down-canyon loss	Chamberlain (1964)					263	62
Scripps Inst. Oceanography	Range of values	Ingle (1966)					27 to 341	6 to 80
Scripps Inst. Oceanography	Average of values	Ingle (1966)					115	27

* "Best" estimate at that location.

yd³/yr at Camp Pendleton, but this value is now out of date because the coastline and structures have changed much since then.

Most of the studies estimating longshore transport in this cell were performed at Oceanside. The intense interest there was spawned by the severe disruption of longshore transport by the boat basin and harbor construction. The history of the construction is detailed in Section 9.7.2.

Marine Advisors (1960a) estimated potential longshore transport rates at Oceanside by refracting offshore wave data over the nearshore bathymetry. They estimated potential transport (in the absence of structures blocking transport) to be 760×10^3 yd³/yr to the south, 545×10^3 to the north, and net transport of 216×10^3 to the south. Hales (1978) used similar methods but obtained somewhat different estimates of 540, 643 and 102×10^3 yd³/yr for northerly, southerly and net transport, respectively. One explanation of the difference between the results of Marine Advisors (1960) and Hales (1978b) is the fact that Hales used DNOD data for northern swell but Marine Advisors' data for southern swell. This changes three transport values as shown in Table 9.6-5. DNOD wave data is not generally useful for Southern California transport calculations, as explained in section 3.2.2. Thus the actual values in Table 9.6-5 should not be considered reliable, but the seasonal trend of southerly transport in the spring and northerly in the fall is valid, as it was later confirmed by Castel and Seymour (1982). The transport values in Weggel and Clark's (1983) report on Oceanside use Hales' transport values and thus are subject to the same criticism (imprecise wave data).

Since Oceanside Harbor has been dredged on a regular basis, it is possible to estimate longshore transport from dredge records. Inman (1976) reports an average net transport of 250×10^3 yd³/yr from 11 dredgings between 1942 and 1969. Dredging since Oceanside Harbor completion (1963) suggests an increase in net transport to 360×10^3 yd³/yr.

Table 9.6-5. Summary of potential longshore transport at Oceanside, San Diego County, vicinity of Oceanside, California (from Hales, 1978).

Month	Sea		Northern swell		Southern swell		Sum		Net		Gross	
	North	South	North	South	North	South	North	South	North	South	North	South
Jan	35,501	25,281	1,741	9,148	0	0	37,242	34,429	2,813		71,671	
Feb	26,188	25,188	3,544	8,759	0	0	29,732	33,947		4,215	63,679	
Mar	9,788	63,737	5,977	8,080	0	0	15,765	71,817		56,052	87,582	
Apr	2,993	61,542	1,735	6,896	0	0	4,728	68,438		63,710	73,166	
May	88	90,521	180	8,265	61,979	0	62,247	98,786		36,539	161,033	
Jun	34	99,024	0	9,852	36,889	0	36,923	108,876		71,953	145,799	
Jul	9	57,129	0	7,804	112,906	0	112,915	64,933	47,982		177,848	
Aug	0	42,133	8	6,105	84,664	0	84,672	48,238	36,434		132,910	
Sep	63	33,445	375	3,472	89,151	0	89,589	36,917	52,672		126,506	
Oct	1,307	27,342	43	2,970	35,147	0	36,497	30,312	6,185		66,809	
Nov	10,389	16,959	1,127	6,541	0	0	11,516	23,136		11,620	34,652	
Dec	17,244	15,518	1,546	7,841	0	0	18,790	23,259		4,469	42,049	
Annual	103,604	557,355	16,276	85,733	420,736	0	540,616	643,088	146,086	248,558	1,183,704	
Net		453,751		69,457	420,736			102,472				102,472

Using data from offshore wave arrays and assuming no wave refraction shoreward of the sensors (obviously invalid at many sites). Castel and Seymour (1982) estimate net transport as $90 \times 10^3 \text{ yd}^3/\text{yr}$ in 1979 and 1980. Although their absolute numbers are probably not valid because of lack of refraction seaward of their sensors at 10 m deep, Seymour and Castel's (1984a) description of seasonal and other cyclical variations in longshore transport is probably the best available in Southern California. A table from their report which explains the episodicity of transport is included here as Table 9.6-6. As already indicated the absolute numbers in columns 2 and 3 are not reliable, but column 4 (the ratio of 2 and 3) is more valid and indicates strong daily variability of transport at Oceanside. On the day of greatest transport, daily gross transport can be as large as the annual net transport. At all stations, including Oceanside, half of the year's gross transport occurs during only 10% of the days of the year, as shown in column 5. The authors admit that the absolute numbers in columns 6 and 7 are not reliable. Although individual transport values for Seymour and Castel (1984a) are not valid, they have statistically confirmed what many investigators have observed for years: seasonal transport can be several times larger than the annual net transport; most transport occurs during only a few days (50% of transport during 10% of days); huge transports can be attained during even a single day. The implication of these conclusions for coastal engineers is that structures obstructing longshore transport can experience much greater sand accumulations than might be expected from knowledge of mean net transport alone.

The most complete computation to date of longshore transport in this littoral cell was performed at Oceanside by Inman and Jenkins (1983). They refracted complete wave spectra by computer, using deep-water wave climate corrected for island sheltering as input. The resulting transports due to each of the five wave sources are listed in Table 9.6-7. The net transport is $254,000 \text{ yd}^3/\text{yr}$ to the south ($194,000 \text{ m}^3/\text{yr}$) with gross transports of $807,000 \text{ yd}^3/\text{yr}$ to the south and $553,000 \text{ yd}^3/\text{yr}$ to the north. Inman and Jenkins (1983) refracted the

TABLE 9.6-6. STATISTICS OF EPISODICITY OF ESTIMATED
LONGSHORE TRANSPORT (from Seymour and Castel, 1984).

STATION NAME	(1)	(2)	(3)	(4)	(5)	(6)	(7)
	YEAR	MAX. DAILY NET m ³ /d	ANNU. NET thou. m ³	(2)AS PCT. OF(3)	PCT. TIME TO 50% GROSS	PCT. TIME <1000 m ³ /d	NET > 10%OF TIME m ³ /d
Mission Bay	1981	16700	372.0	4.5	14.9	84.0	2600
	1982	10290	395.6	2.6	15.0	72.5	2400
Oceanside	1979	4090	2.3	177	9.3	94.8	550
	1980	4420	5.8	76	9.3	95.7	700
Sunset	1981	3850	42.3	9.1	12	94.0	800
	1982	9270	152.2	6.1	10	89.8	1000
Santa Barbara	1980	2840	38.0	7.5	9.6	99.0	350
	1981	1890	46.7	4.0	16.4	99.0	290
	1982	1470	45.9	3.2	18.2	99.5	370
Santa Cruz	1981	2870	23.0	12.4	12.9	97.8	540
	1982	7040	86.4	8.1	8.7	92.6	920
Pacifica	1981	43600	86.8	50.3	7.3	50	7000
Stinson Beach	1981	6920	89.0	7.8	4.9	94.3	650

TABLE 9.6-7. SUMMARY OF LONGSHORE TRANSPORT ESTIMATES
(from Inman and Jenkins, 1983).

I) Annual Transports at Wisconsin Street
(Averaged over 5,000 m of Beach), M^3/yr :

Due to: North Swell - Island Sheltered	= + 140,000 M^3/yr to South
Due to: South Swell - Island Sheltered	= + 4,400 M^3/yr to South
Due to: Direct South Swell	= - 333,000 M^3/yr to North
Due to: Local Wind Generation Due to Northwesterlies	= + 472,500 M^3/yr to South
Due to: Local Wind Generation Due to Southwesterlies	= - 90,300 M^3/yr to North
<hr/>	
	+ 194,000 M^3/yr to South

wave data more rigorously than earlier studies (Marine Advisors, 1960a; Hales, 1978b) by refracting individual energy bands. However, their offshore wave data comes from the same sources as Hales (1978b) and thus is subject to the same large error bars (See Section 9.3). The net transport is in close agreement with the measured 261,000 yd³/yr loss of sand down Scripps Submarine Canyon at the end of the cell (Chamberlain, 1964).

These three values (from Inman and Jenkins, 1983) are averages for several years of data. The transport for any single year may be different, as explained by Inman and Jenkins (1983, p. 89): "The relative balance between these two large opposing gross transports reflects the net trend that persisted throughout the long temperate drought periods, 1945-1977. A shift away from northerly storm tracks typical of this era, as occurred during the winter of 1979-1980, will alter the relative energy flux balance between local wind generation and south swell. In fact, the more extreme southern storm tracks during the 1979-1980 winter resulted in a zero net transport at Oceanside for that anomalously wet year (Seymour, 1980)."

A large long-term net transport to the south in this cell has strong implications for any beach nourishment projects. Waldorf, Flick and Hicks (1983) document motion of 706,000 m³ of sand placed south of Oceanside Harbor. The sand first moved to the north, but in the winter of 1982-83 the fill moved offshore and then proceeded to move steadily south in the direction of net transport.

The longshore transport values described so far are wave-refraction estimates of longshore transport, not direct measurements. The most complete direct measurements in the cell were made at Torrey Pines Beach between Del Mar and La Jolla in the fall of 1978. Gable (1979) lists the tasks involved in monitoring longshore transport: an extensive fluorescent sand tracer study on several days, volume sampling of suspended sediment, optical backscatter measurements of suspended sediment, acoustic Doppler measurements of bedload, and wave and current measurements. Inman et al (1980) describe the results of the experiments. Their "best

measures" of bedload are listed in their Table 5-1 under immersed weight transport. line # 2, as 150-360 n/S (638-1530 yd³/yr) and suspended transport as 90-113 n/S (382-480 yd³/yr). The range is due to the fact that transport varies from day-to-day depending on the wave climate. Thus these total transport measurements of 240-473 n/S (1020-2010 yd³/yr) should be considered gross transport values for medium to high waves. The upper values are good measures of the maximum daily transport rates to be expected in the Oceanside cell.

Several short-term studies of longshore transport have been performed at Scripps Beach just north of the end of the cell at La Jolla Canyon. Studies began with interpretation of beach profile data to show that motion on the deeper portion of profiles (> 25 ft) is mostly longshore (Shepard and Inman, 1951a). Later Ingle (1966) performed sand-tracer studies and found longshore sand velocities of 4-18 ft/min (2-9 cm/s) and longshore transport rates of 74-934 yd³/day (27,000-341,000 yd³/yr) for low to medium wave conditions.

9.6.3 *Wind Transport*

To our knowledge there are no estimates or measurements of wind transport in this cell. This is not surprising, since the geology of the area effectively prevents wind transport. The lack of coastal sand dunes precludes a sand source for significant wind transport. The presence of high sea cliffs prevents strong winds on most beaches. Finally, strong long-duration winds are not observed in this cell.

9.7 SEDIMENT SINKS

9.7.1 *Submarine Canyons*

Scripps and La Jolla Submarine Canyons at the southern end of the cell in La Jolla are among the most important in Southern California in terms of sediment motion because they extend so close to shore. They are actually two nearshore branches of the same canyon (Figures 9.7-1 and 9.7-2). They are also among the most studied submarine canyons in the world. Much of the physics and geology of these canyons is also applicable to other canyons which approach close to shore (Redondo, Dume, Mugu, Hueneme and Monterey Canyons). Since most of the scientific studies of canyons in southern California were done in Scripps Canyon, the reader can refer to this section for general information regardless of which of the aforementioned canyons is of interest.

Study of the canyons began in the 1940's. Shepard (1951) documented with bathymetric profiles the canyon's two types of sand motion: slow small changes in topography in the canyon heads and occasional catastrophic sand loss down-canyon. At the end of 1949 Shepard (1951) documented a loss of four million cubic yards of sand down Scripps Canyon. Shepard and Inman (1951a) documented transport by profiling the sand motion all along the inter-canyon shelf and demonstrated the now classical concept of the "river of sand" flowing along beaches and then down canyons.

Several theories have been put forth over the years as to the cause of rapid motion of sand down canyons: slow creep, buildup followed by slumping, turbidity currents of dense suspension, earthquakes, tsunamis, edge waves, rip currents, etc. Shepard (1952) first recognized two important mechanisms which were suggested by the data in his 1951 paper, slumping and turbidity currents. The amounts and rates of sand motion measured suggested that there must be both slow (slumping) and rapid (turbidity currents) transport mechanisms.

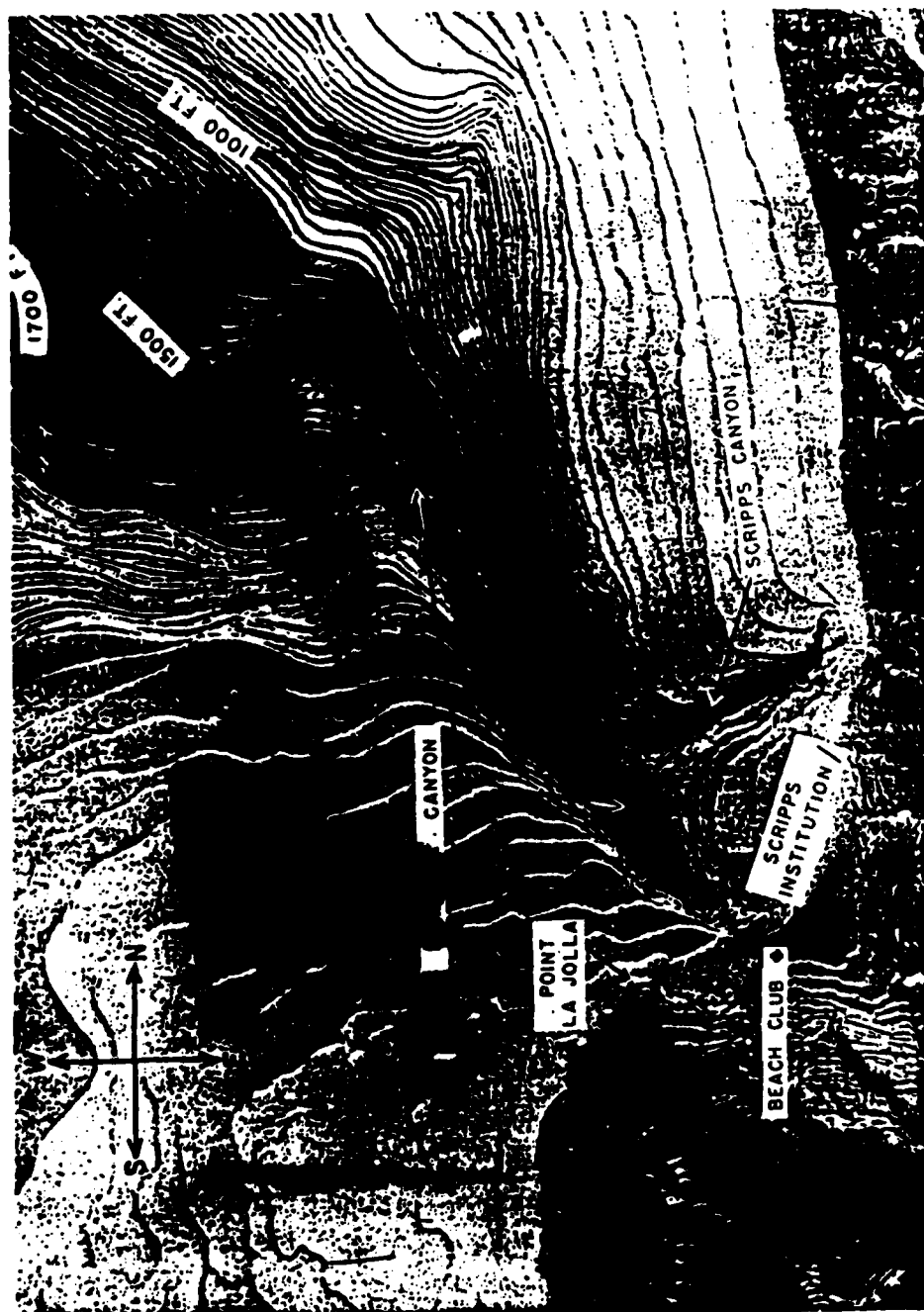


Figure 9.7-1. La Jolla and Scripps Canyons bathymetry (from Munk and Traylor, 1947).

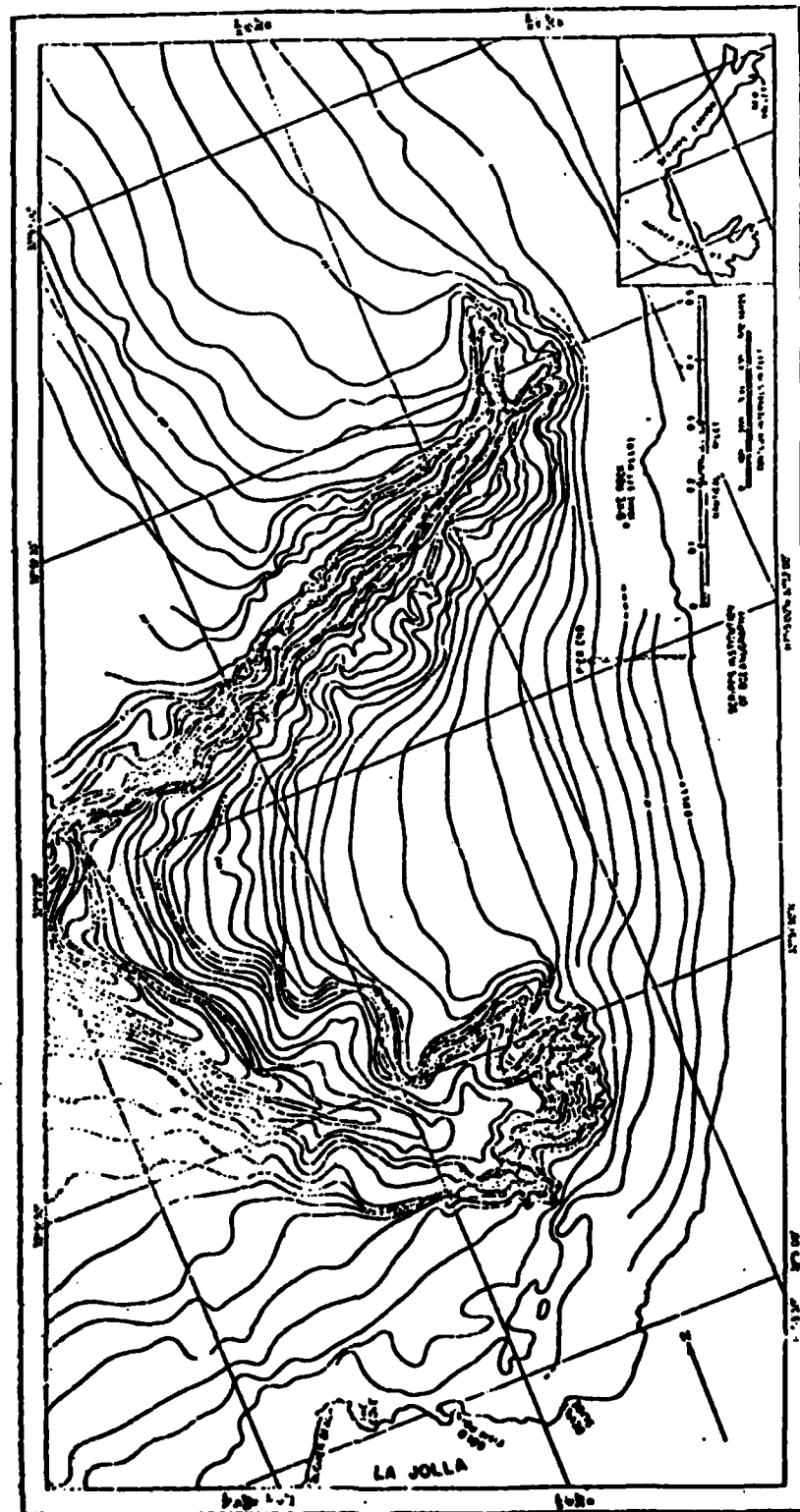


Figure 9.7-2. Contours of the heads of La Jolla and Scripps Submarine Canyons (from Shepard and Einsele, 1962).

Inman (1953) first showed that nearly all of the sand being transported along the shore in the Oceanside cell eventually travels down the canyons rather than around Pt. La Jolla. He examined the size distribution, roundness, and mineralogy of the sediments north and south of the canyons and showed that the Pt. La Jolla sand could not have originated north of the canyons.

Chamberlain (1960, 1964) completed the first thorough study of the canyons, aided by the advent of SCUBA diving. He documented the loss of sand down-canyon over several years (Table 9.7-1). The sand loss ranges from 60×10^3 to $230 \times 10^3 \text{ m}^3/\text{yr}$ ($79\text{-}303 \times 10^3 \text{ yd}^3/\text{yr}$) with a mean of $172 \times 10^3 \text{ m}^3/\text{yr}$. Chamberlain found limited evidence of long-term low-frequency losses not evident in the measured canyon head losses, suggesting the total mean sand loss to be about $200 \times 10^3 \text{ m}^3/\text{yr}$ ($263 \times 10^3 \text{ yd}^3/\text{yr}$).

Chamberlain (1964) describes the mechanisms of transport of sediment from the surfzone to the canyonheads as follows: "All of this material, however, is not deposited directly into the submarine canyon. Much of the alongshore-transported sand is deposited on the beach and just outside the surf zone during the summer months and during other extended periods of low waves. Subsequently, during periods of steep waves - e.g., the high, short-length waves that often result from local winter storms, the beaches are cut back at the head of the submarine canyon and along the coast to the north. If these waves occur during spring tides, especially active erosion takes place, both high up on the beach and offshore to depths of 1 to 2 meters below mean lower low water (m.l.l.w.). The sand, put into suspension by such erosion, is maintained in suspension by the abnormal turbulence that these waves cause within the surf zone, and the sand is passed into the littoral circulation system, also exceptionally well developed at these times.

"Because of the local submarine topography and the angle of wave approach, seaward-flowing rip currents develop over the heads of Scripps Canyon when large volumes of water are

TABLE 9.7-1. TOTAL SEDIMENT LOSSES IN SCRIPPS
SUBMARINE CANYON, 1948 - 1960
(from Chamberlain, 1964).

Flow No.	Date	Total Sediment Loss (10^3 m^3)
I	11/48	1.4
II	8/49	1.4
III	2/50	2.3
IV	3/51	2.3
V	12/51	1.2
VI	2/53	2.1
VII	11/53	0.8
VIII	11/54	2.0
IX	1/58	2.0
X	11/58	0.6
XI	12/59	1.9

Mean $1.72 \times 10^3 \text{ m}^3$
Range 0.6 to $2.3 \times 10^3 \text{ m}^3$

driven onto the adjacent beaches (Chamberlain, 1960). The result is that during local storms the large volumes of sand formerly deposited on the beaches and in the nearshore zone by alongshore currents are carried seaward and deposited in the heads of Scripps Canyon."

In addition to recognizing the importance of the two transport mechanisms of slumping and turbidity currents, Chamberlain (1960, 1964) first successfully explained the important contribution of the eel grass in the canyon to transport. The eel grass mixed with the sand partially "cements" the sand, effectively increasing the sediment's static coefficient of friction but having little effect on the dynamic coefficient. This means that it is difficult for transport to be initiated, but once begun, it increases in area and intensity rapidly. This helps explain the "catastrophic events" documented by Shepard (1951).

Inman and Nordstrom (1961) and Shepard and Einsele (1962) examined the sand at the opposite end of the canyon, the area where the canyon empties into the wide San Diego Trough (Figure 9.7-3). By examining numerous core samples including the core from the Experimental Deep-Sea Drilling in San Diego Trough (Inman and Nordstrom, 1961), they identified the source of the San Diego Trough sands as the Scripps Submarine Canyon. Mineralogical analysis of the sands identified the origin as terrigenous.

Dill (1964) performed a qualitative survey of the canyonhead with SCUBA diving. His observations confirmed Shepard's (1951) identification of two transport modes: a slow creep of organic grass/sand mats and periodic flushing during storms. His study provided many useful photographs and figures of the canyonhead and its many small tributaries (Figure 9.7-4).

Until the study of Inman, Nordstrom, and Flick (1976), only the sedimentological and geological aspects of the canyon had been studied. They measured currents in the canyon and explained the origins of the strong down-canyon currents as: "1. a pile-up of water along the shoreline caused by strong onshore winds; 2. down-canyon pulses of water associated with groups of high incident waves; 3. excitation of standing edge waves that produce long-period

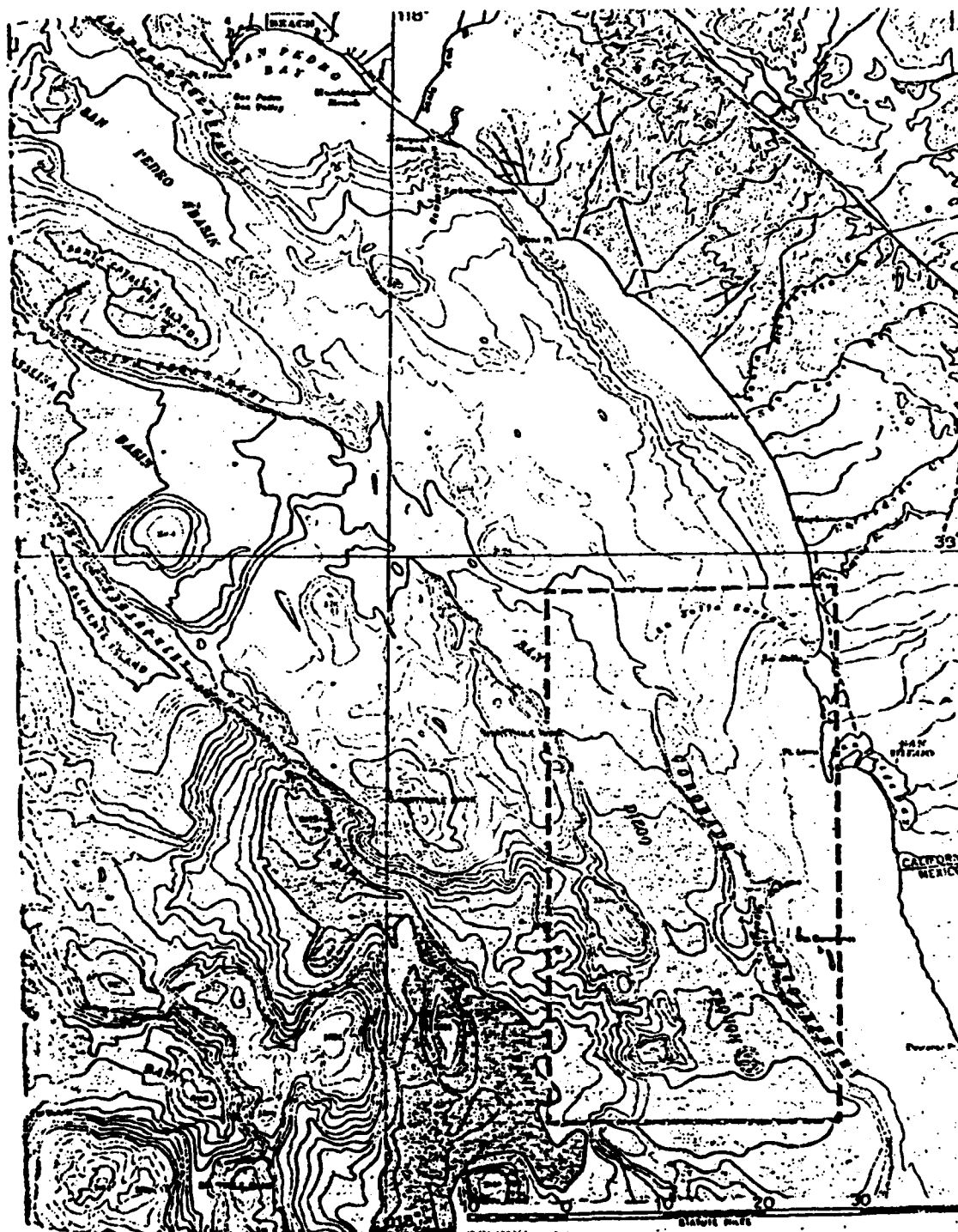


Figure 9.7-3. San Diego Trough topography (from Shepard and Einsle, 1962).

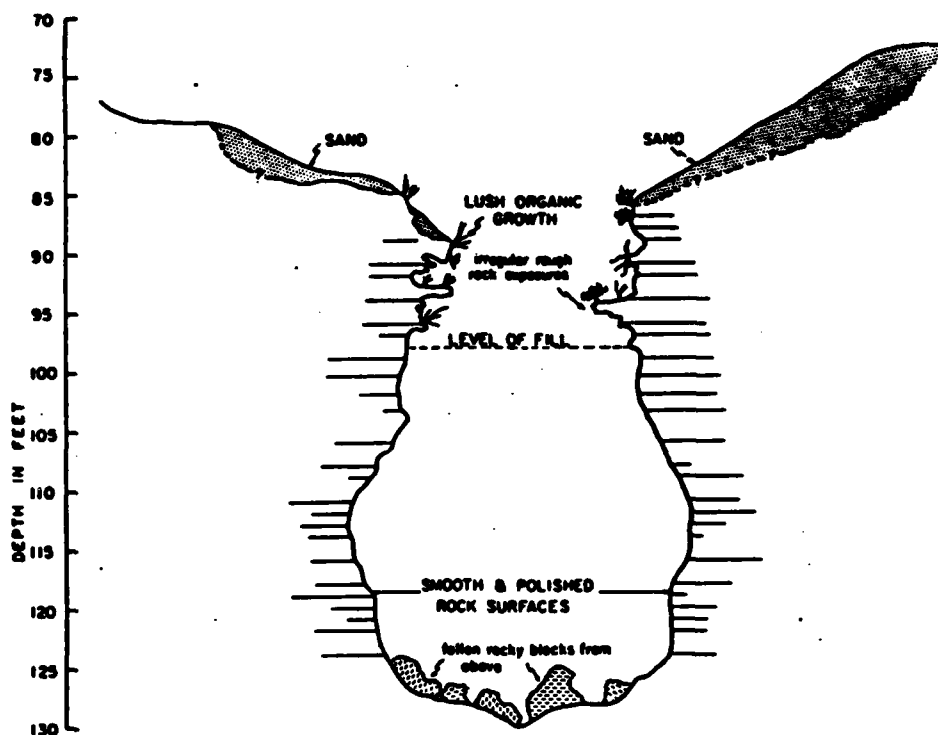


Figure 9.7-4. Schematic cross-section of a typical canyon tributary at its seaward-most extremity. "Level of fill" indicates level at which the sediment becomes unstable and moves into deeper water (from Dill, 1964).

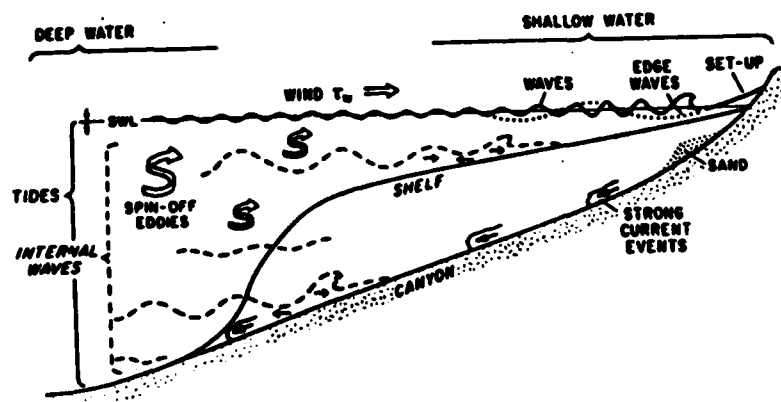


Figure 9.7-5. Schematic diagram of driving forces near submarine canyons (from Inman, Nordstrom and Flick, 1976).

up- and down-canyon oscillations; and finally, 4. the formation of discrete pulses of down-canyon motion, which become more intense and lead to sustained down-canyon currents, as the weight of the sediment suspended by the currents overcomes the density stratification of the deeper water." This combination of driving forces is schematically illustrated in Figure 9.7-5. During two different types of events, very strong currents have been measured in Scripps Canyon. Inman, Nordstrom and Flick (1976) measured a sustained current of 1.9 m/s downcanyon at 44 m deep during the passage of a storm front on 24 November 1968. The current meter was swept down-canyon and lost by higher velocities. Shepard, Sullivan and Wood (1981) measured up-canyon currents of 82 cm/s during a perigean (closest approach of moon to earth) spring tide at 48 m deep. Clearly both storms and tides are important in causing strong canyon currents, although only storms generate strong down-canyon currents associated with sediment transport.

9.7.2 *Entrapment by Harbors, Bays and Estuaries*

Dana Point Harbor was built at a unique location, the boundary between the Laguna sub-cells and the Oceanside Cell. Thus instead of interrupting a large longshore transport of sand as does Oceanside Harbor, it interrupts only the small amount of sand that "leaks" between the two cells. Dana Point Harbor was built for anchorage of small craft and to serve as refuge for light draft vessels (Shaw, 1980). It is illustrated in Figure 9.7-6. It consists of two large basins for anchorage and two channels protected by breakwaters, completed in October 1968. The east breakwater is 682 m long and the west breakwater 1666 m.

Initial dredging took place at Dana Point in 1965 and 1968 as the harbor was constructed. In 1970 $96 \times 10^3 \text{ m}^3$ ($126 \times 10^3 \text{ yd}^3$) was dredged from the harbor and deposited downcoast as a surfing reef (Shaw, 1980). This would mean that roughly $50 \times 10^3 \text{ m}^3/\text{yr}$ accumulated in the harbor. Undoubtedly some of this sand came from rearrangement of topography within the harbor.

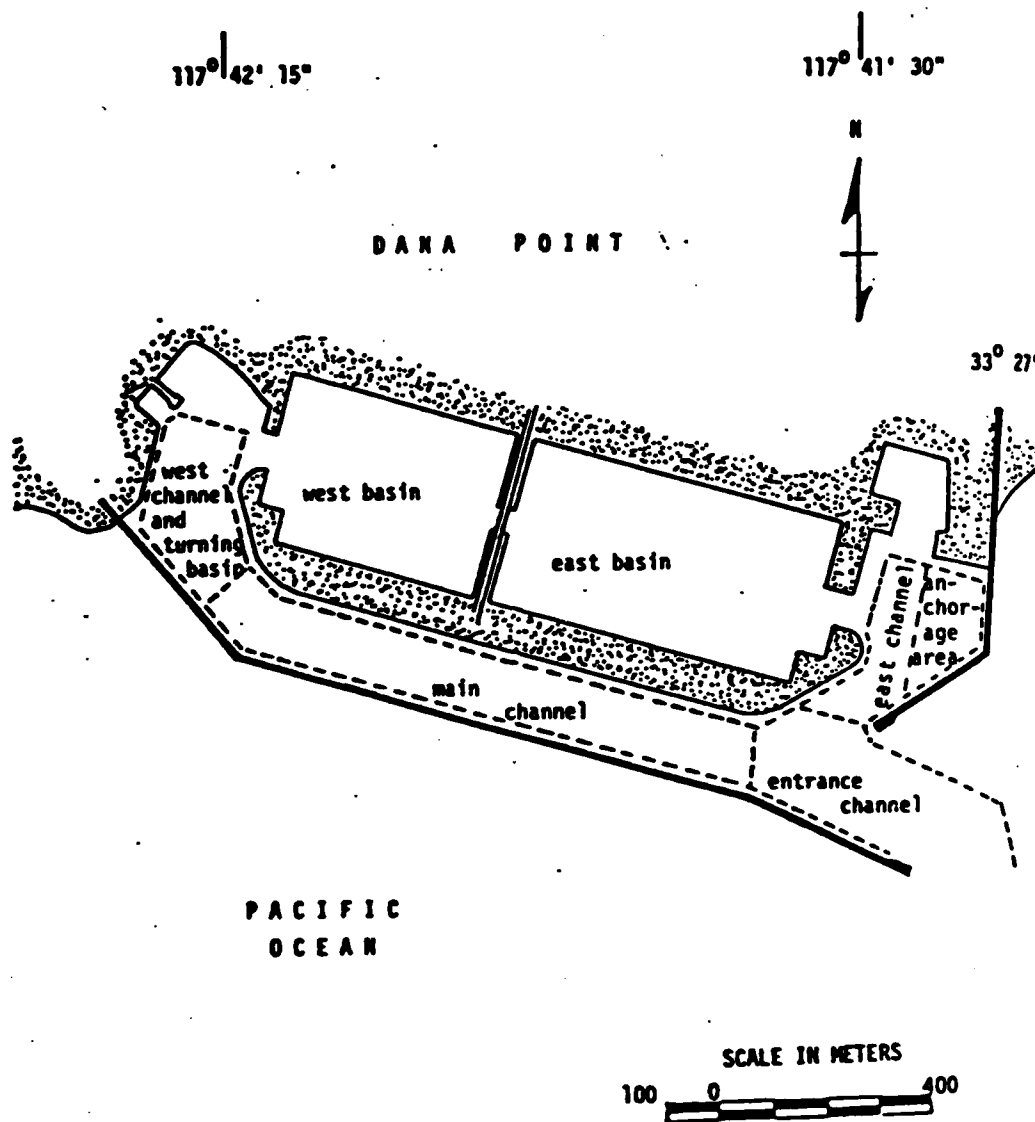


Figure 9.7-6. Dana Point Harbor (from Shaw, 1980).

Doheny State Beach is just south of Dana Point Harbor (Figure 9.7-7). Construction consists of a 30 m bulkhead levee and a 75 m groin completed in June 1964 (shown just at the west side of San Juan Creek mouth in Figure 9.7-7). The groin and bulkhead were constructed in order to maintain a flood control channel for the creek. Rather than wait for unpredictable flooding to flush the channel and bring sediment to the beach, it was decided to periodically dredge the channel. The dredging history may be found in Shaw (1980).

The Del Mar Boat Basin near Oceanside was constructed by the Navy on an "emergency" basis in 1942 and became the antecedent member of the Oceanside Harbor complex. Various groins, jetties and breakwaters were added over the years, as illustrated in Figure 9.7-8. Oceanside Harbor was completed in 1963 by federal and local authorities. The present-day harbor (Figure 9.7-9) structures consist of a south jetty and north breakwater at the boat basin, two groins and a jetty at the harbor. The effects of these structures on the topography and transport are described by Inman and Jenkins (1983), a portion of which is excerpted here: "Oceanside Harbor has caused a number of artificial changes on the beach and nearshore topography: (i) the jetties interrupt the longshore transport of sand producing a large fillet beach up coast of the structure" (Figure 9.7-10), "and during times of southern swell, a smaller fillet beach between the south jetty and the south groin by the San Luis Rey River; (ii) the north jetty intensifies transport along its seaward central portion and produced a semi-permanent rip current that transports sand offshore" (Figure 9.7-10) "and (iii) the harbor and its entrance traps large quantities of sand." The exact areas of erosion and accretion near the harbor are illustrated in detail by Inman and Jenkins (1983).

Dredging of Oceanside Harbor began at relatively small rates in the 1950's when only the boat basin was present but increased substantially in the mid-1960's after the completion of Oceanside Harbor. The dredging history is reported in Table 9.7-2. Nordstrom and Inman (1973) estimated the mean annual dredging rates for the two periods as $180 \times 10^3 \text{ yd}^3/\text{yr}$ and

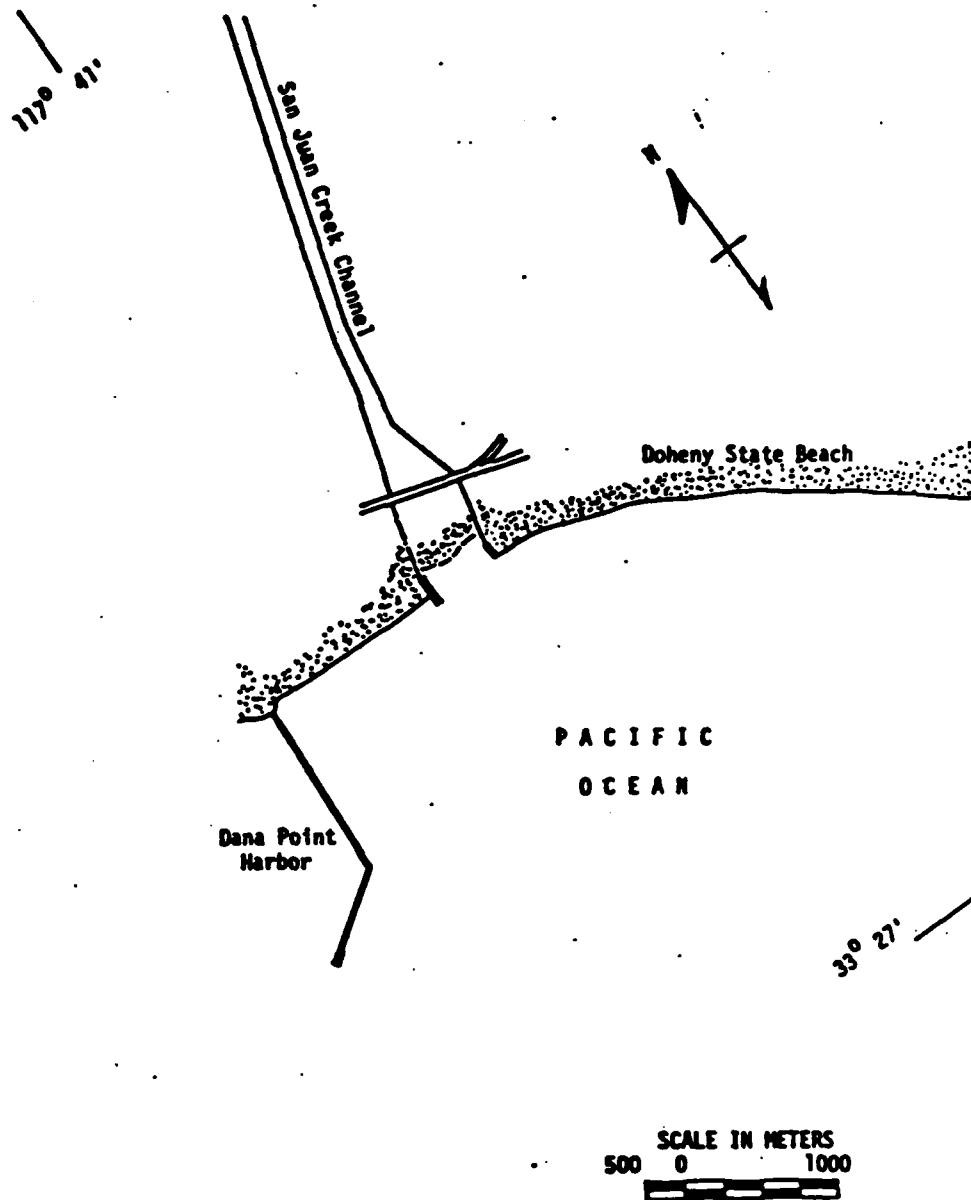


Figure 9.7-7. San Juan Creek and Doheny State Beach (from Shaw, 1980).

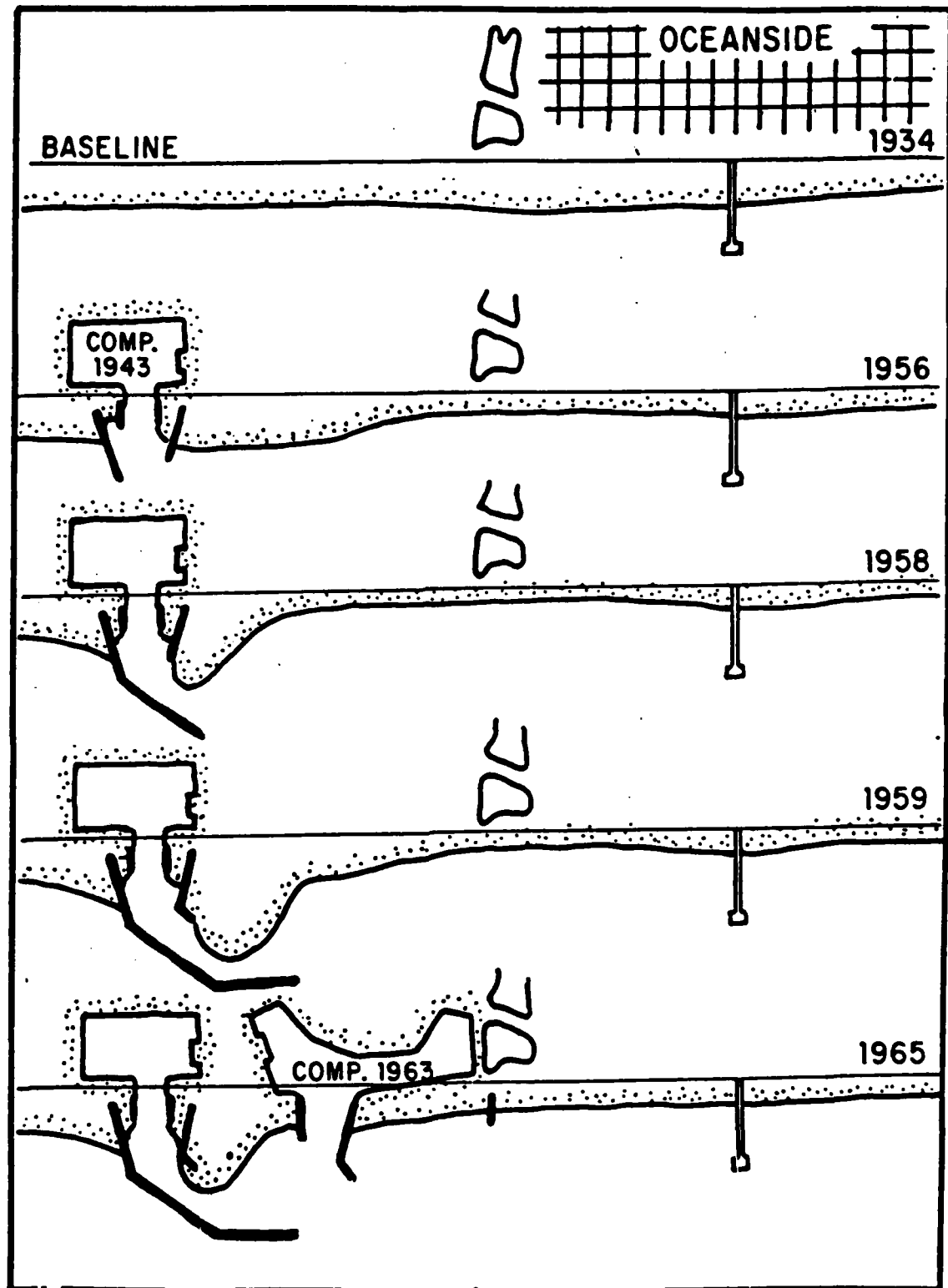


Figure 9.7-8. Stages in the development of Oceanside Harbor (from Inman, 1976).

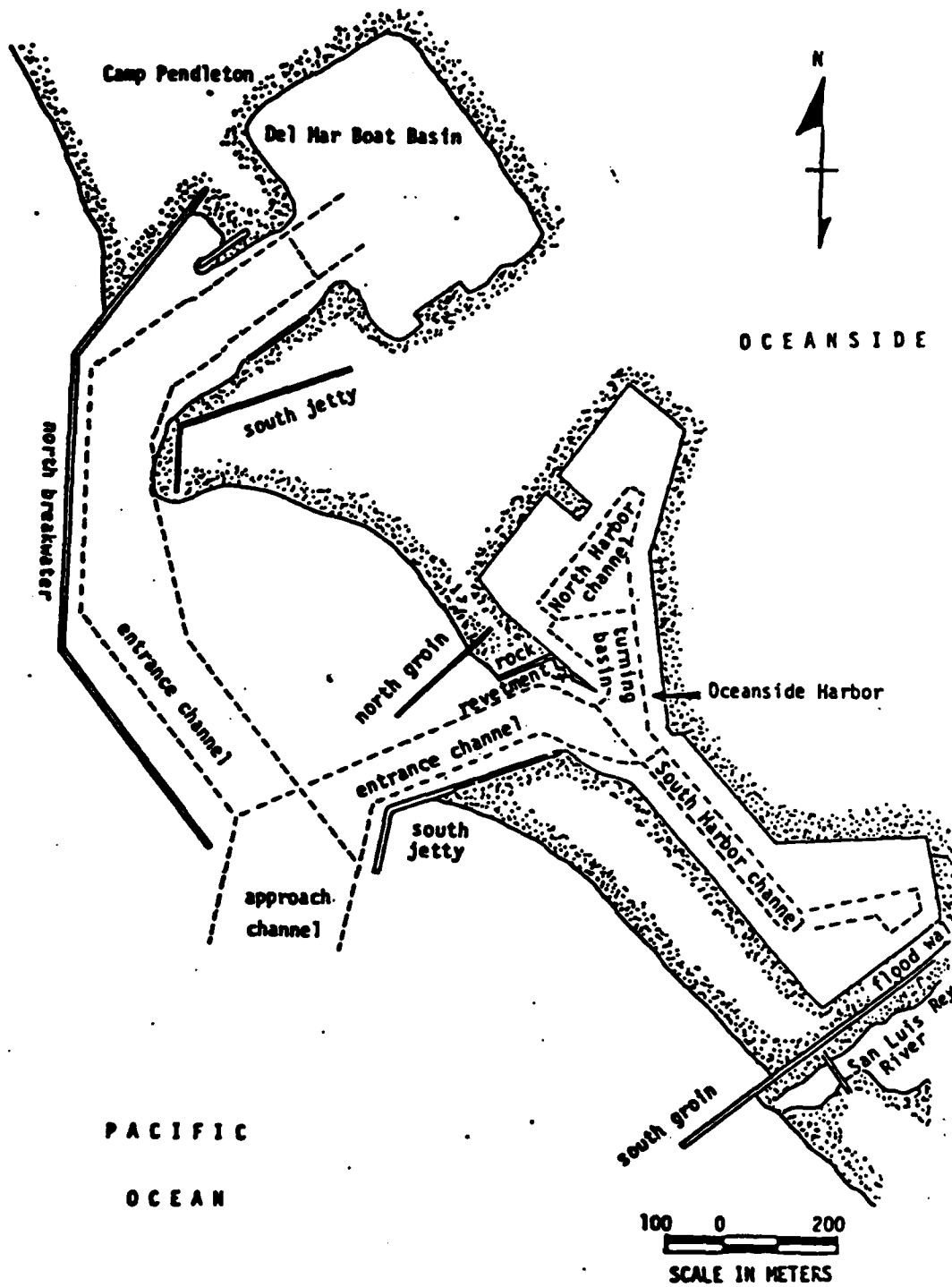


Figure 9.7-9. Del Mar Boat Basin and Oceanside Harbor (from Shaw, 1980).

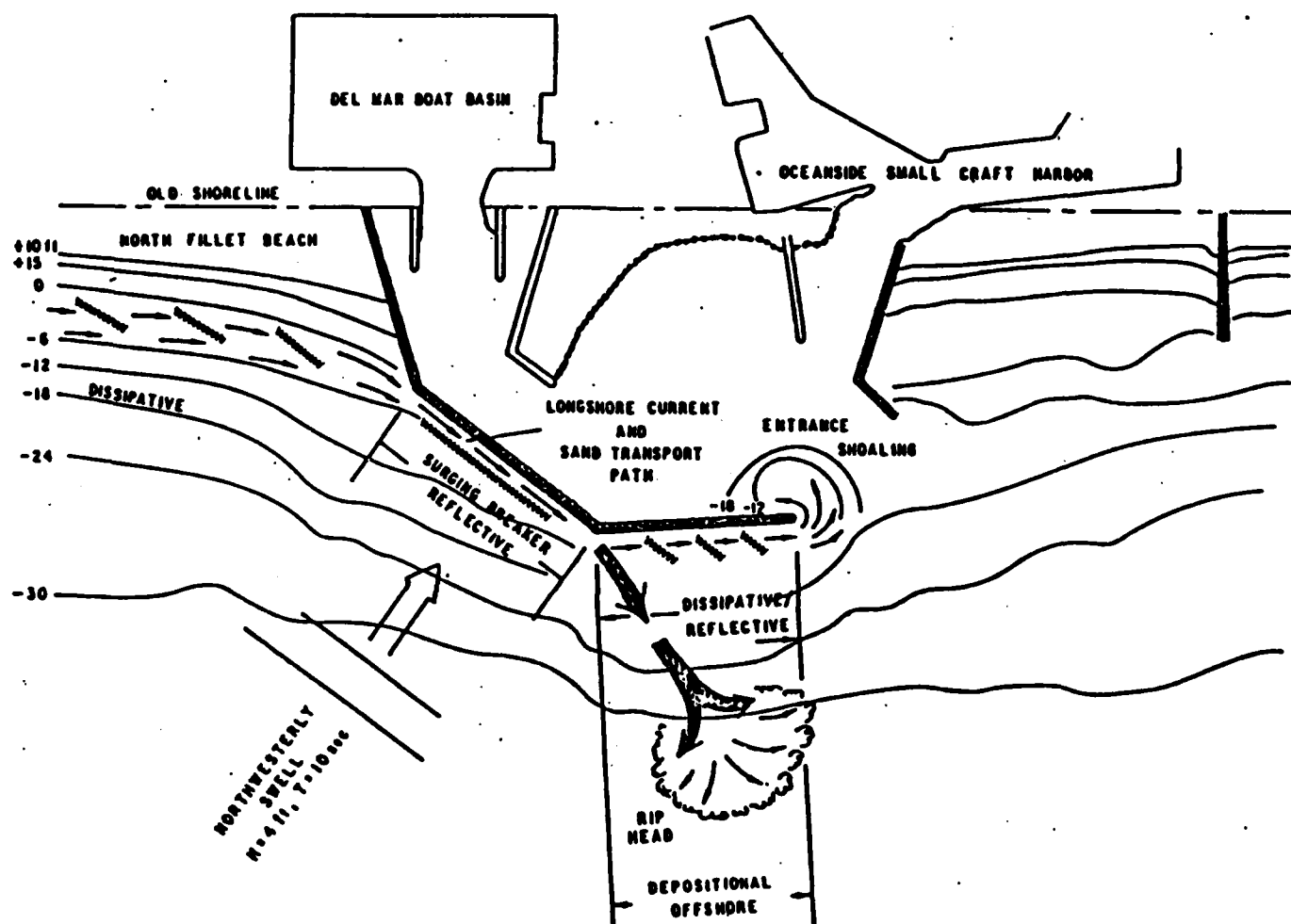


Figure 9.7-10. Typical circulation patterns near Oceanside breakwater (from Inman and Jenkins, 1983).

Table 9.7-2. Summary of quantities of dredged material for Oceanside Harbor and Beach
(from Inman and Jenkins, 1983).

Starting Date	Completion Date	Disposal Area	Approx. Dredge Quantity, yds ³	Cumulative Beach nour. 106yds ³
May 1942	August 1944	Inland fill	1,500,000.	0
April 1945	June 1945	Inland fill	219,000.	0
April 1957	May 1958	6th to 9th St.	800,000.	0.80
August 1960	August 1960	6th to 9th St.	17,500.	
September 1960	October 1960	6th to 9th St.	23,700.	0.84
January 1961	May 1961	6th to 9th St.	222,350.	
August 1961	December 1961	6th to 9th St.	258,800.	
March 1962	February 1963	9th St. to Loma Alta Creek	3,810,700.	1.32
August 1965	February 1965	9th to 3rd St.	111,400.	5.13
March 1966	April 1966	3rd St. to Minnesota Ave.	684,000.	5.24
July 1967	July 1967	3rd to Tyson St.	177,900.	5.93
March 1968	June 1968	San Luis Rey to Wisconsin Ave.	433,900.	6.11
July 1969	September 1969	San Luis Rey to 3rd St.	353,000.	6.54
April 1971	July 1971	3rd St. to Wisconsin Ave.	551,900.	6.89
June 1973	July 1973	Tyson to Hays St.	434,100.	7.44
October 1974	January 1975	Pine to Witherby St.	559,750.	7.88
May 1976	July 1976	Ash to Witherby St.	550,000.	8.44
August 1977	February 1978	Ash to Witherby St.	318,550.	8.99
February 1981	June 1981	3rd St to Buccaneer	463,000.	9.31
November 1981	May 1982*	Oceanside Beaches	920,000.	9.77
				10.69
		TOTAL in cubic yds	12,409,550	10.69
		TOTAL in cubic meters	(9,493,000)	(8.18)

*Dry hall from San Luis Rey River

$340 \times 10^3 \text{ yd}^3/\text{yr}$. Weggel and Clark (1983) obtained estimates of $66 \times 10^3 \text{ yd}^3/\text{yr}$ and $290 \times 10^3 \text{ yd}^3/\text{yr}$. Inman and Jenkins (1983) estimate the latter value at $301 \times 10^3 \text{ yd}^3/\text{yr}$. The dredging numbers from Table 9.7-2 are plotted in Figure 9.7-11, where it is illustrated how the value of $301 \times 10^3 \text{ yd}^3/\text{yr}$ was obtained.

Clearly the initial boat basin construction trapped only part of the available longshore transport. The current mean annual dredging rate is considered a good estimate of the total net longshore transport. The estimate from the Oceanside "total trap" is in good agreement with the loss down Scripps Submarine Canyon at the end of the cell ($263 \times 10^3 \text{ yd}^3/\text{yr}$, Chamberlain, 1960).

Four 150 m jetties were constructed at Agua Hedionda Lagoon in 1954 (Figure 9.7-12). These were placed to stabilize the mouth of the lagoon and power plant discharge outlet and to counteract shoaling in the lagoon, which was blocking power plant water intake (Shaw, 1980). The lagoon's natural sand level appears to be shallower than that desired for the power-plant intake. This fact, along with the partial obstruction of longshore transport by the jetties, has necessitated frequent dredging of the lagoon and nourishment of the beach. These 13 dredging events are detailed by Shaw (1980). Weggel and Clark (1983) estimate a mean annual dredging rate of $118 \times 10^3 \text{ yd}^3/\text{yr}$ (39% of the total longshore transport obtained at Oceanside). It is difficult to say just how much of the longshore transport is being blocked by the jetties, since transport is not in a natural balance in the area due to the Oceanside Harbor effects.

9.7.3 *Littoral Barriers*

The Laguna Sub-cell is composed of pocket beaches separated by rocky headlands. These headlands appear to be more effective in preventing transport to the north than transport to the south (Inman, 1978b). Inman gives a rough estimate of $15 \times 10^3 \text{ yd}^3/\text{yr}$ net southerly transport past the headland at the south end of Laguna Niguel (Figure 9.6-1). The rest of the Oceanside Cell (south of Dana Point) does not contain any headlands which effectively curb

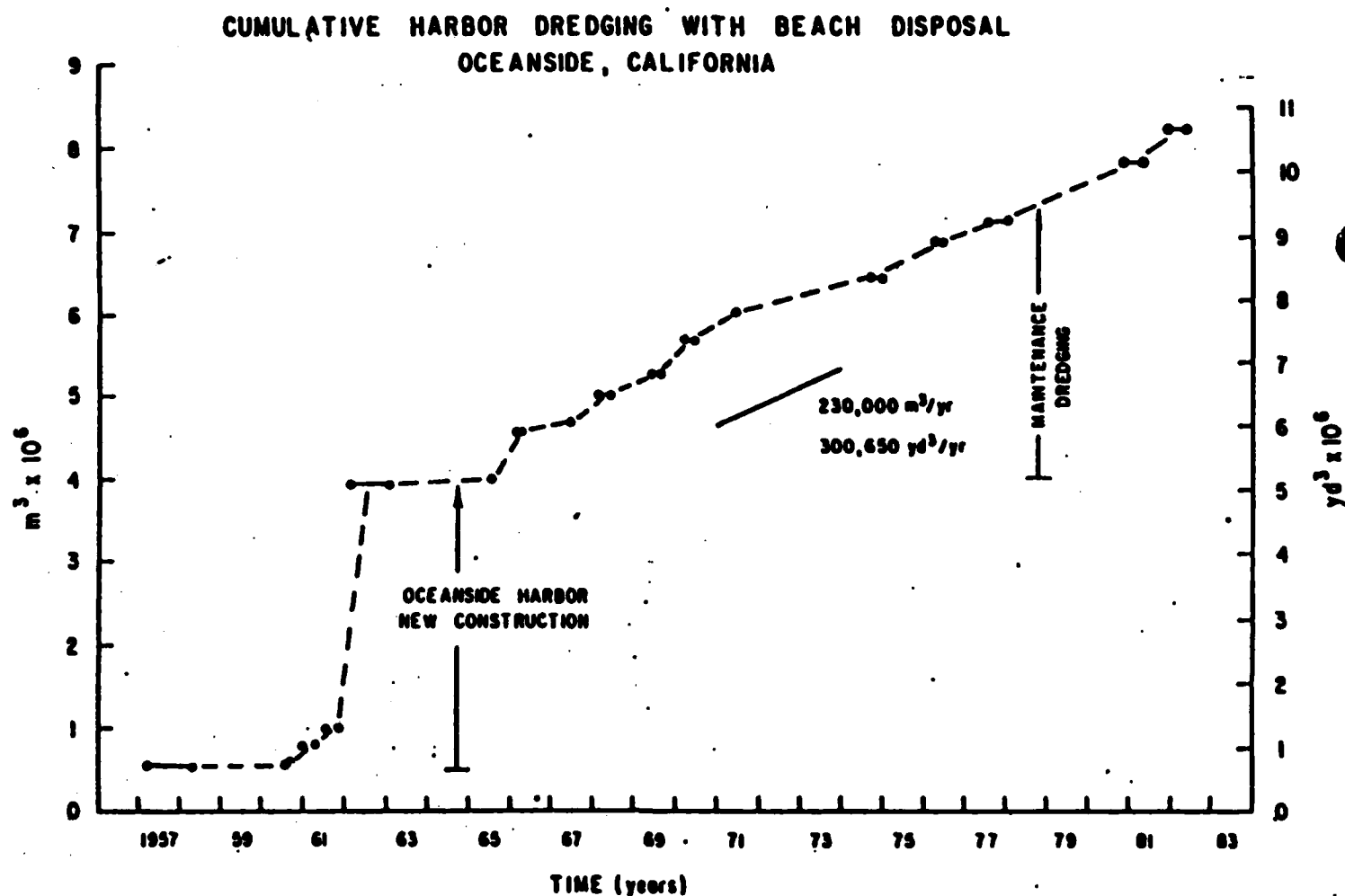


Figure 9.7-11. Cumulative volume of material dredged from Oceanside Harbor (from Inman and Jenkins, 1983).

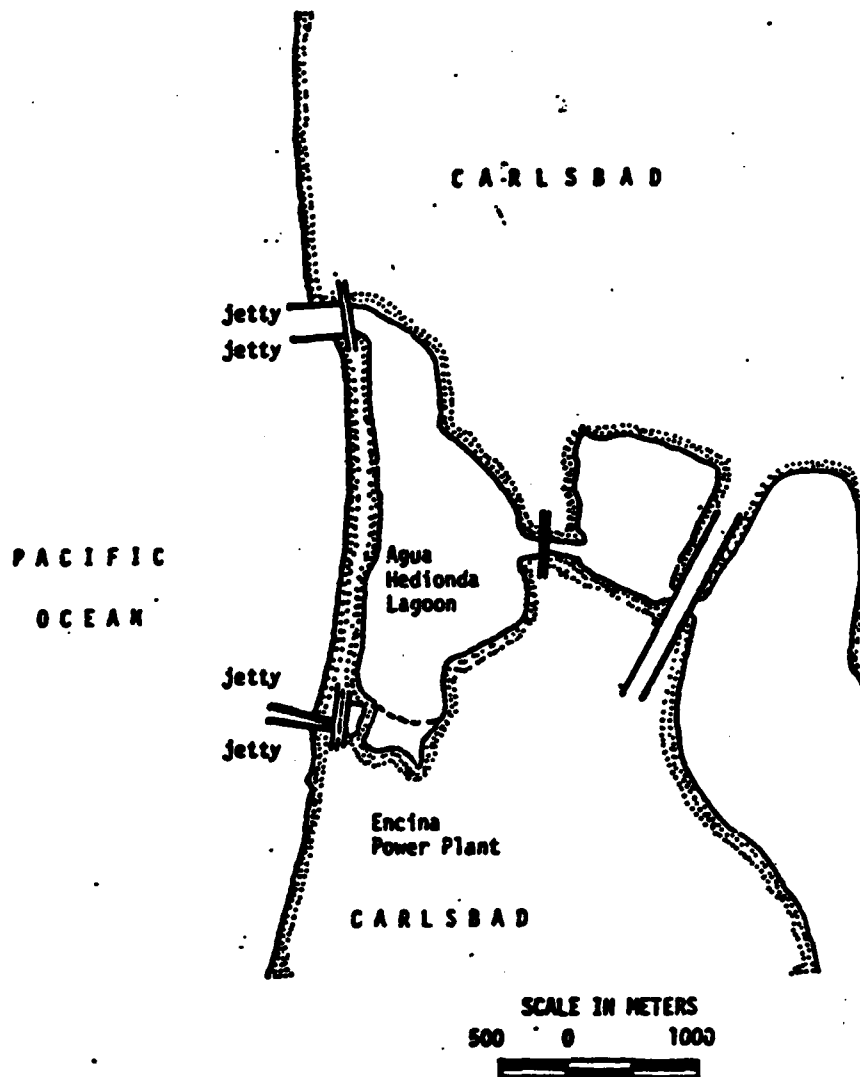


Figure 9.7-12. Agua Hedionda Lagoon (from Shaw, 1980).

longshore transport.

The shore-normal structures (piers, breakwaters, groins and jetties) will be discussed from north to south in the cell. Piers rarely interfere with the longshore transport but will be included here for completeness. For a map of seawalls and revetments in the cell, see the maps at the end of Shaw (1980). Much of the rest of this section is summarized from the tables in Shaw (1980).

A 180 m concrete open-pile pier was constructed at Dana Point in 1975. The two rubble-mound breakwaters were constructed for Dana Point Harbor in 1968 (Figures 9.7-6). The details of the harbor's effect on transport can be found in Section 9.7.2.

A 75 m groin and 30 m bulkhead levee were constructed at Doheny State Beach in 1964 in order to stabilize San Juan Creek's mouth (Figure 9.7-7). Since the groin is quite short, only a small portion of the longshore transport is interrupted. It is impossible to determine from dredging records what portion of the transport the groin interrupts, since the creek itself is a major source of sediment.

The City of Oceanside built a 590 m open-pile pier at San Clemente in 1929, which was rebuilt in 1939. A 345 m open-pile pier was built at Oceanside in 1927, but has been damaged and repaired on several occasions in 1945, 1977 and 1978 (Inman and Jenkins, 1983).

The series of groins, jetties and breakwaters at Del Mar Boat Basin and Oceanside Harbor was constructed over four decades (Figure 9.7-8). The effects of these structures today (Figure 9.7-9) on transport are discussed in great detail by Inman and Jenkins (1983), part of which is excerpted in Section 9.7.2 of this report. Shorter descriptions which omit much of the physics are in USA COE LAD (1970 and 1980b) and in Weggel and Clark (1983). Continual accretion north of the harbor and erosion south of the harbor are quite dramatic. Based on average dredging rates of about $300 \times 10^3 \text{ yd}^3/\text{yr}$ at Oceanside, the net longshore transport rate is considered to be about $250 \times 10^3 \text{ yd}^3/\text{yr}$ to the south (Inman and Jenkins, 1983).

Four 120-150 m rubble-mound jetties were built in 1954 at Agua Hedionda Lagoon (Figure 9.7-12) to stabilize the lagoon outlet and power plant intake. The portion of longshore transport trapped by the jetties is not really known since the lagoon itself is also a source of sediment. The mean annual dredging rate ($118 \times 10^3 \text{ yd}^3/\text{yr}$) is 39% of the known longshore transport in the area.

At Del Mar an experimental shore-protection device called the Longard Tube was installed along a 200 m section of beach in January 1981 (Flick and Waldorf, 1984). It remained for two years. Although it had some impounding effect on the beach, it was "not a substantial enough barrier to effectively prevent beach sand erosion during severe storm events on the Southern California coast." (Flick and Waldorf, 1984). See Figure 9.6-5 for its location in the erosion cycles.

At the southern end of the cell is a 305 m wooden open-pile pier at Scripps Institution of Oceanography constructed in 1914. It will be replaced by a concrete pier in 1986.

9.7.4 *Wind Transport*

No dune fields are present in this cell. No studies on loss of sediment due to wind transport exist to our knowledge. The geology of the area (lack of dunes, high sea cliffs, lack of sustained strong winds) effectively prevents significant wind transport.

9.7.5 *Berm Overwash and Offshore Loss*

We are unaware of any studies on permanent loss of sand from the cell by either berm overwash or transport offshore. Numerous studies have been performed in this cell on cycles of cross-shore transport (Shepard, 1946, 1950a, 1950c; Shepard and Inman, 1951; Inman and Rusnak, 1956; Inman and Chamberlain, 1959; Nordstrom and Inman, 1975; Aubrey, Inman and Nordstrom, 1976; Winant and Aubrey, 1976; Aubrey, 1978, 1979; Gable, 1979; Aubrey, Inman and Winant, 1980; Seymour and King, 1982; and Waldorf and Flick, 1983). However, all of

these papers deal with the cyclical nature of beach changes and not permanent loss to the system (except in submarine canyons). Since berm overwash is rare and transport far offshore may be small, one would expect these losses to be small in comparison to canyon and harbor losses.

9.8 SEDIMENT BUDGET

Nordstrom and Inman (1973) were the first to discuss the sediment budget for the Oceanside Cell. Weggel and Clark (1983) performed sediment budget calculations for Oceanside to predict the effect of groins and nearshore breakwaters on adjacent beaches. Their transport values are based on somewhat questionable wave data (see Section 9.6.2) and their sediment yield from the local rivers may be underestimated (see Section 9.5.2). Inman and Jenkins (1983) performed a more thorough examination of the littoral processes in the Oceanside Harbor area (see Figure 9.8-1). They also calculate a sediment budget for the entire cell as shown in Table 9.8-1.

The littoral processes along this coastline have been extensively studied. Cliff erosion apparently supplies a small percentage of the beach sands (see Section 9.5.1). The major sources of sediment for this cell are the San Luis Rey and Santa Margarita Rivers (see Section 9.5.2). Currently, Oceanside relies upon beach nourishment to supply its beaches with sand (see Section 9.6.3). Longshore transport rate estimates from various sources are summarized in Table 9.6-4, with a value of $250 \times 10^3 \text{ yd}^3/\text{yr}$ as the best estimate of the southerly net longshore transport. The two major sinks of sand in this cell are the Oceanside Harbor and the Scripps-La Jolla Submarine Canyons. Oceanside Harbor is not a true sink because it is dredged periodically with the dredge spoils being placed on the downcoast beaches. On the other hand, as much as $261,000 \text{ yd}^3/\text{yr}$ of sand is transported down the Scripps Canyon (Chamberlain, 1964 and Section 9.7.1).

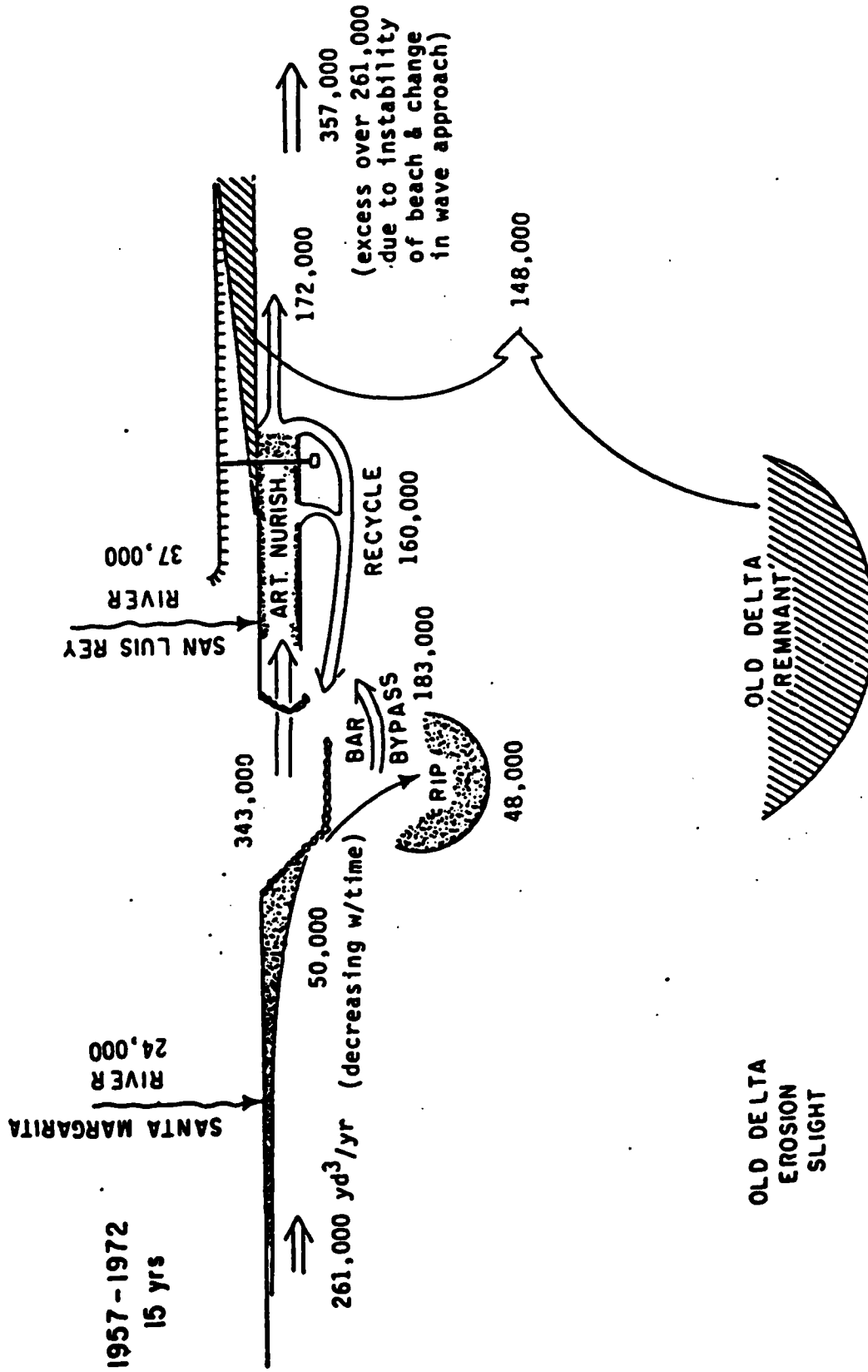


Figure 9.8-1. Budget of sediment at Oceanside Harbor, 1957-1972 (from Inman and Jenkins, 1983).

Table 9.8-1. Budget of sediment for Oceanside
Littoral Cell, 1957-1972 under
natural conditions (from Inman and
Jenkins, 1983).

Yield of sand and gravel from streams	Potential longshore transport	Loss down Scripps Submarine Canyon
273,000 yd ³ /yr	254,000 yd ³ /yr	261,000 yd ³ /yr

10. MISSION BAY CELL

The Mission Bay Sub-Cell extends from Point La Jolla to Point Loma, a distance of 15 miles (see Figure 1.3-1). It includes small pocket beaches along the La Jolla headland, 4.5 miles of sandy beach from False Point to the Municipal Pier at Ocean Beach, and rocky cliffs along the Point Loma headland. The natural source of sediment for this sub-cell was the San Diego River. However, the many dams on the river may now prevent it from being a significant source of sediment.

10.1 COASTAL EROSION PROBLEMS, NATURAL AND MAN-MADE

USACE LAD (1964) for the City of San Diego in a Beach Erosion Control Report analyzed the erosion problems from Point La Jolla to Sunset Cliffs. Both the La Jolla Cliffs and Sunset Cliffs are currently eroding due to wave undercutting and increased cliff top development. USACE SPD (1971) presents an inventory of coastal characteristics relating primarily to erosion produced by waves or other coastal phenomena (see Figure 10.1-1). Kuhn and Shepard (1984) give a descriptive account of erosion of the cliff at Point La Jolla. They include several historical and current photographic comparisons which illustrate failure of sea arches and stacks. They also discuss and document with photographs the rapid erosion of Sunset Cliffs in recent years.

10.2 SHORELINE CHANGES

USACE LAD (1960a) summarizes the shoreline, offshore and volumetric changes in the Mission Bay Cell. It includes historical survey and beach profiles. A summary of the shoreline change data contained in this report and other references is shown in Table 10.2-1. USACE LAD (1964) is similar to the previous report but contains an update on shoreline and offshore changes. It also includes plates illustrating cliff line and offshore changes, and comparative

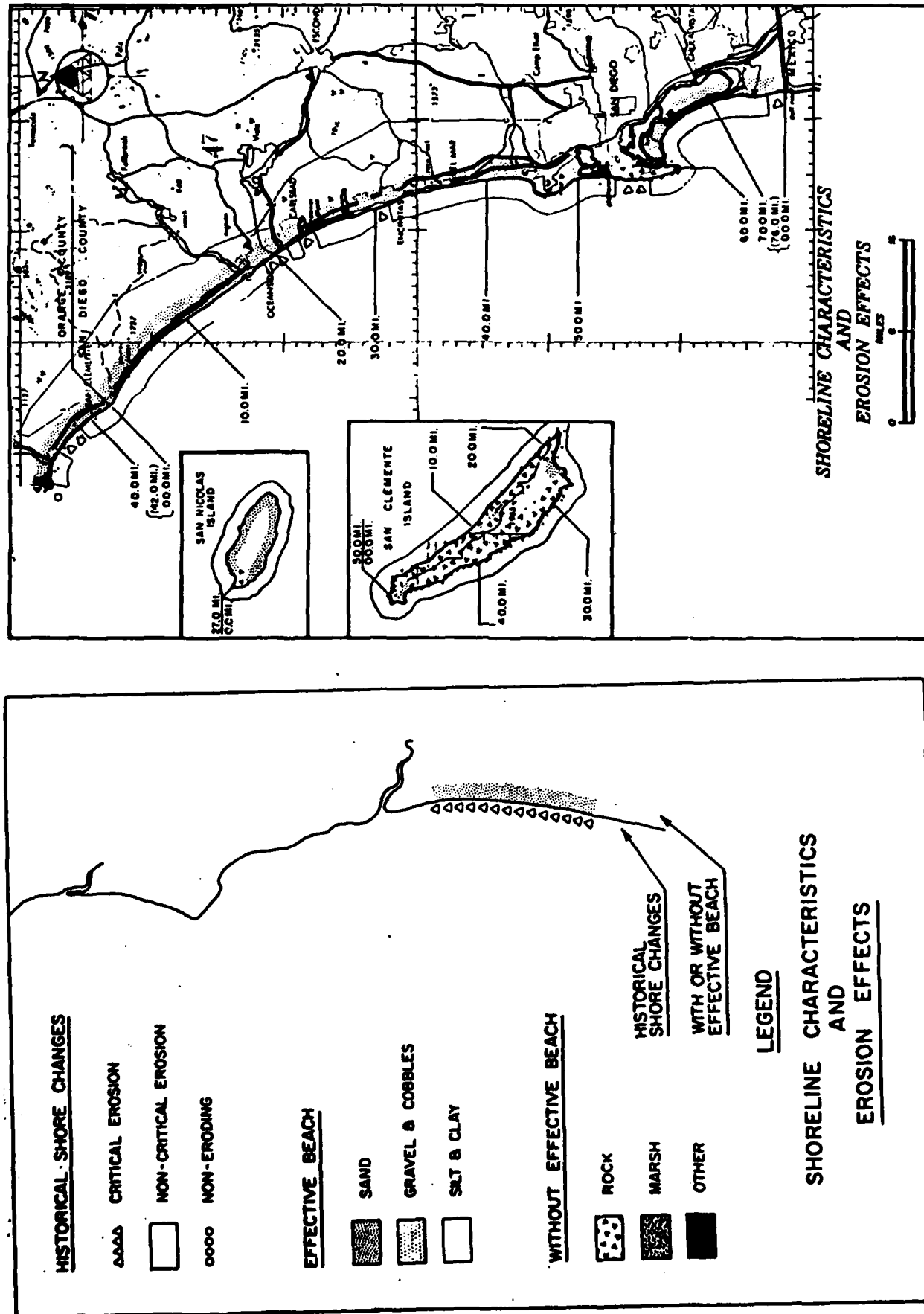


Figure 10.1-1. Shoreline characteristics and historical shore changes (from USACE SPD, 1971).

AD-A166 699

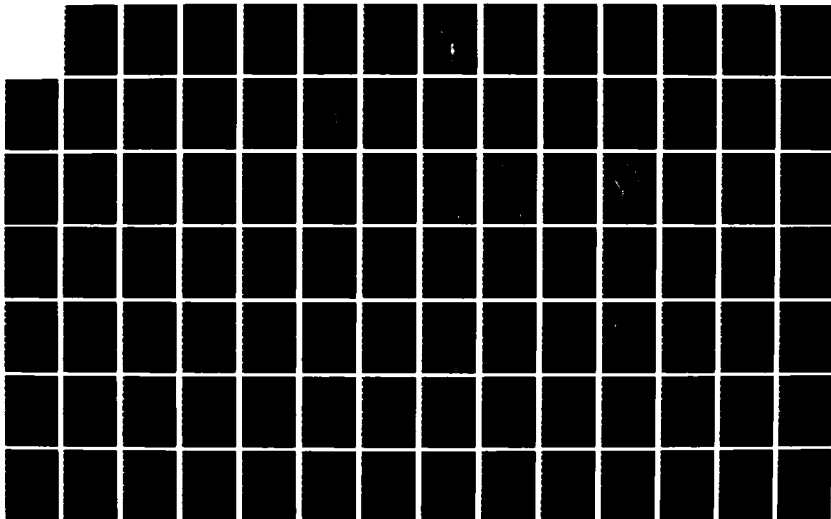
COAST OF CALIFORNIA STORM AND TIDAL WAVES STUDY
SOUTHERN CALIFORNIA COAST (U) ARMY ENGINEER DISTRICT
LOS ANGELES CA COASTAL RESOURCES BRANC
D L INMAN ET AL FEB 86 CCSTWS-86-1

6/7

UNCLASSIFIED

F/G 8/3

NL



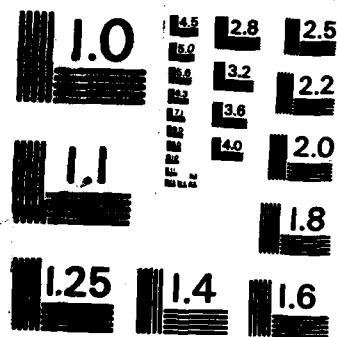


Table 10.2-1
EXISTING SURVEYS, MAPPING STUDIES, PHOTOGRAPHS

Author(s) Date	Type of Data	Location and Dates
Frautschy and Inman, 1964	Surveys of entrance channels, early photographs	Mission Bay jetties and entrance channel
USACE LAD, 1960a	History of surveys	False Point to Point Loma, 1940-1958
	Table of volumetric changes	Pacific Beach, Mission Beach and Ocean Park,
	Shoreline and offshore changes	Pacific Beach to Ocean Beach, 1857-1951
	Beach profiles	Mission Beach, 1940-1957 Ocean Beach, 1951-1957
USACE LAD, 1964	Bluffline and offshore changes	Sunset Cliffs, 1926-1961
	Comparative profiles	Sunset Cliffs, 1934-1962
USACE LAD, 1969a	Condition survey	San Diego Bay and Mission Bay, 1966
USACE LAD, 1970	Historical ground and aerial photographs	Oceanside, Sunset Cliffs
	Hydrographic survey	Oceanside, 1967

Table 10.2-1 (cont'd)
EXISTING SURVEYS, MAPPING STUDIES, PHOTOGRAPHS

Author(s) Date	Type of Data	Location and Dates
USACE LAD, 1971	Aerial photographs	Bird Rock Cliffs, 1976
Herron, 1980	Aerial photographs	Mission Bay, 1948, 1963
Kuhn and Shepard, 1984	Historical ground and aerial photographs	Point La Jolla, Mission Bay, Sunset Cliffs

profiles in the Sunset Cliffs area. USACE LAD (1969a) lists data on study items (aerial and ground photographs, beach samples, shoreline condition, etc...) in the Mission Bay Cell collected from 1964-66. It includes beach profiles (condition surveys) in San Diego Bay and the entrance to Mission Bay.

Like the previous Corps of Engineers Beach Erosion Control Reports, USACE LAD (1970) summarizes the items of information gathered during 1967-69 for the Cooperative Research and Data Collection Program. USACE LAD (1971) in a reconnaissance report of shoreline erosion at Tourmaline Surfing Park presents data on local historical shoreline changes along with several photographs of the cliffs along the Bird Rock area of La Jolla. Frautschy and Inman (1954) review the development of the Mission Bay jetties, their relation to the tidal prism of the bay and their effect on the beaches (refer to Section 10.7.2). Hales (1979) discusses the historical shoreline changes near the entrance to Mission Bay. Herron (1980) briefly discusses the development of Mission Bay and includes photographs showing the entrance area before and after dredging and inlet stabilization occurred. Kuhn and Shepard (1984) also discuss the development of Mission Bay and presents historical photographs of the area. They include discussions of shoreline changes throughout the littoral cell along with several ground and aerial photographs at selected locations.

10.3 NEARSHORE WAVES

The Channel Islands provide significant shelter to this cell, particularly from northern swell (Figure 10.3-1). A blocking/refraction model discussed in Section 3.3.1 shows that the islands reduce climatic north swell energy to about 15% of the deep ocean energy but provide little sheltering from climatic southern swell (Figure 3.3.1-5). The fraction of deep ocean energy theoretically reaching Mission Bay entrance channel from individual north and south swell events is shown in Figures 3.3.1-6,7. South swell events with deep water approach angles between 190° - 240° are not sheltered (Figure 3.3.1-7). The coastal response to north swell increases with decreasing angle (Figure 3.3.1-6). The fraction of deep ocean energy reaching the coast varies from about 10% for swell from 320° to 40% for a 280° approach angle. Refractive effects associated with shoals and banks in the island vicinity yield a rather different sheltering picture than obtained by simply assuming geometric shadows behind islands and banks. For example, Figure 10.3-1 shows waves from 280° as shadowed by San Clemente Island but Figure 3.3.1-6 shows about 40% of the deep ocean energy actually reaches the coast. Visual observations (Figure 10.3-2) in winter suggest that most of the energy approaches from directions (260° - 280°) shown as shadowed in Figure 10.3-1.

CDIP wave data collected at the Ocean Beach pier (1976-1978) and in 10 m depth just offshore of the Mission Bay entrance channel (1978-1982) were analyzed by Seymour (1982). Table 10.3-1 and Figure 10.3-3 show that the most frequently occurring waves have significant heights of about 80 cm and periods of about 5 and 15 seconds. The 5 second waves are locally generated and the long waves are remotely generated swell. Seymour (1982) developed significant height return periods based on observations with peak periods both above and below 10 seconds (Table 10.3-2). The 10-year return significant height is about 4 m (13 ft) in both cases. Inclusion of large waves which occurred in 1983 alters the 10-year return period to about 17 ft (Figure 10.3-4). The seasonal variability of wave heights, and the very stormy winter of

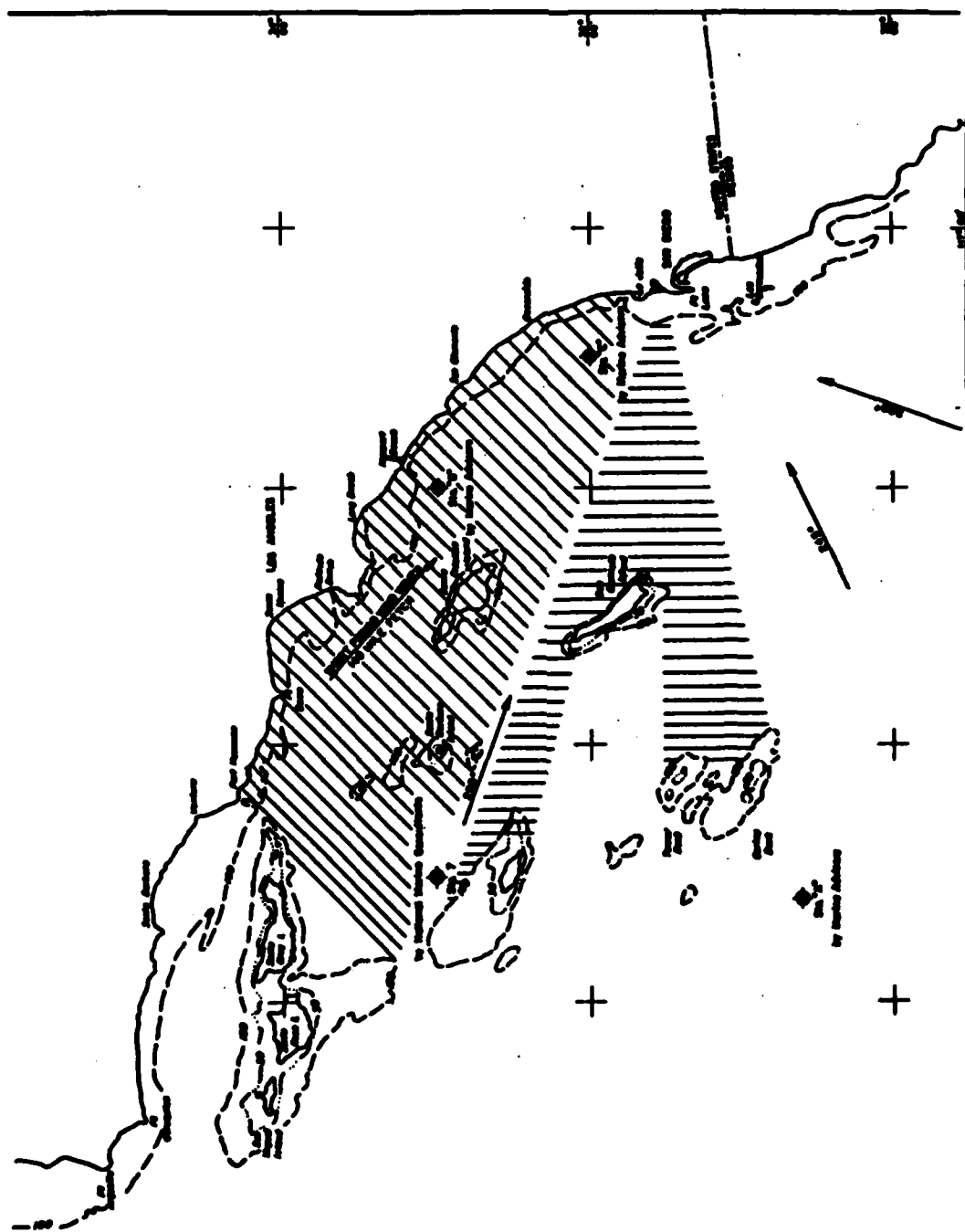


Figure 10.3-1 Schematic of island sheltering effects on 13 second waves at Mission Bay (USACE LAD, 1964).

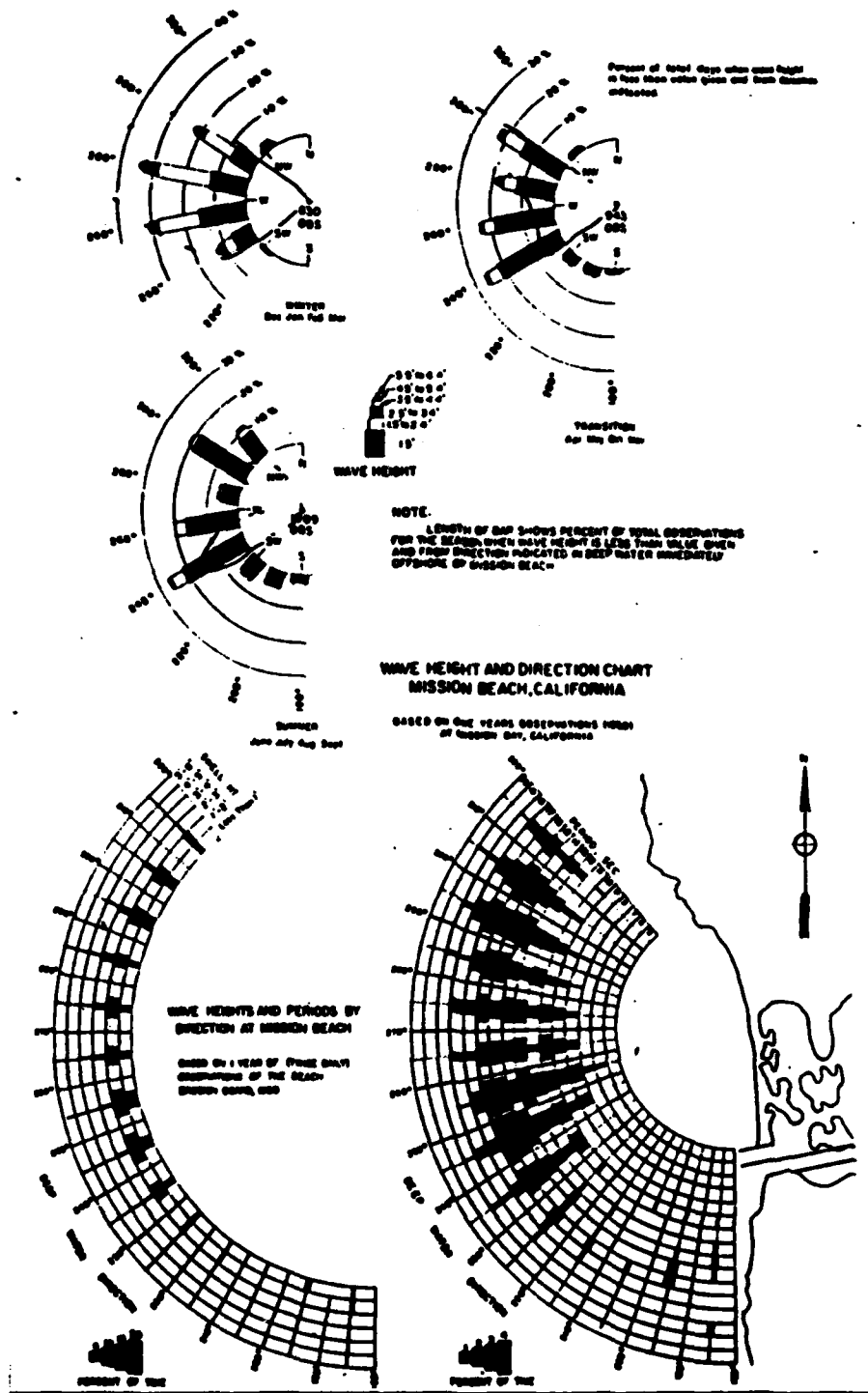


Figure 10.3-2

Summary of 1 year (1950) of visual wave observations at Mission Beach
(USACE LAD, 1964).

Table 10.3-1 Joint distributions of height and period for Mission Bay entrance channel (1/76-10/82), 5591 samples (Seymour, 1982).

HT. (CM)	PERIOD (SEC)							
	22+	19	17	15	13	11	9	7
400.	0	0	0	0	0	0	0	0
390.	0	0	0	0	0	0	0	0
380.	0	0	0	0	0	0	0	0
370.	0	0	0	0	0	0	0	0
360.	0	0	1	0	0	0	0	0
350.	0	0	0	1	0	0	0	0
340.	0	0	0	0	0	0	0	0
330.	0	0	0	0	0	0	0	1
320.	0	0	0	2	0	0	0	0
310.	0	1	2	0	0	0	0	0
300.	0	0	0	2	1	0	1	0
290.	0	0	1	2	3	0	3	0
280.	0	0	1	1	0	0	0	2
270.	0	1	2	2	2	1	3	4
260.	0	1	7	3	0	0	2	2
250.	0	1	2	2	3	2	1	6
240.	1	0	1	7	5	0	1	4
230.	0	1	3	7	4	0	1	1
220.	0	0	7	4	2	1	4	3
210.	0	0	5	9	9	6	3	2
200.	0	3	5	13	7	5	4	9
190.	1	1	7	4	14	3	6	10
180.	3	2	5	9	20	8	11	17
170.	2	6	17	14	22	7	10	8
160.	0	3	15	21	14	13	17	19
150.	1	4	20	18	25	16	13	31
140.	0	10	17	28	39	23	29	25
130.	0	8	30	24	49	28	24	53
120.	0	12	29	44	69	35	42	72
110.	0	9	41	82	72	31	46	100
100.	0	10	52	88	69	69	65	95
90.	0	19	85	83	79	59	67	101
80.	0	19	83	124	80	61	65	120
70.	0	14	65	117	84	63	73	86
60.	1	13	33	75	71	54	50	69
50.	0	6	9	41	38	22	47	28
40.	3	4	5	9	10	8	9	11
30.	1	0	0	3	1	4	1	3
20.	1	0	0	2	0	0	0	1
10.	0	0	0	0	0	0	0	0

MISSION BAY ENTRANCE JOINT PERIOD AND HEIGHT DISTRIBUTION CONTOURS

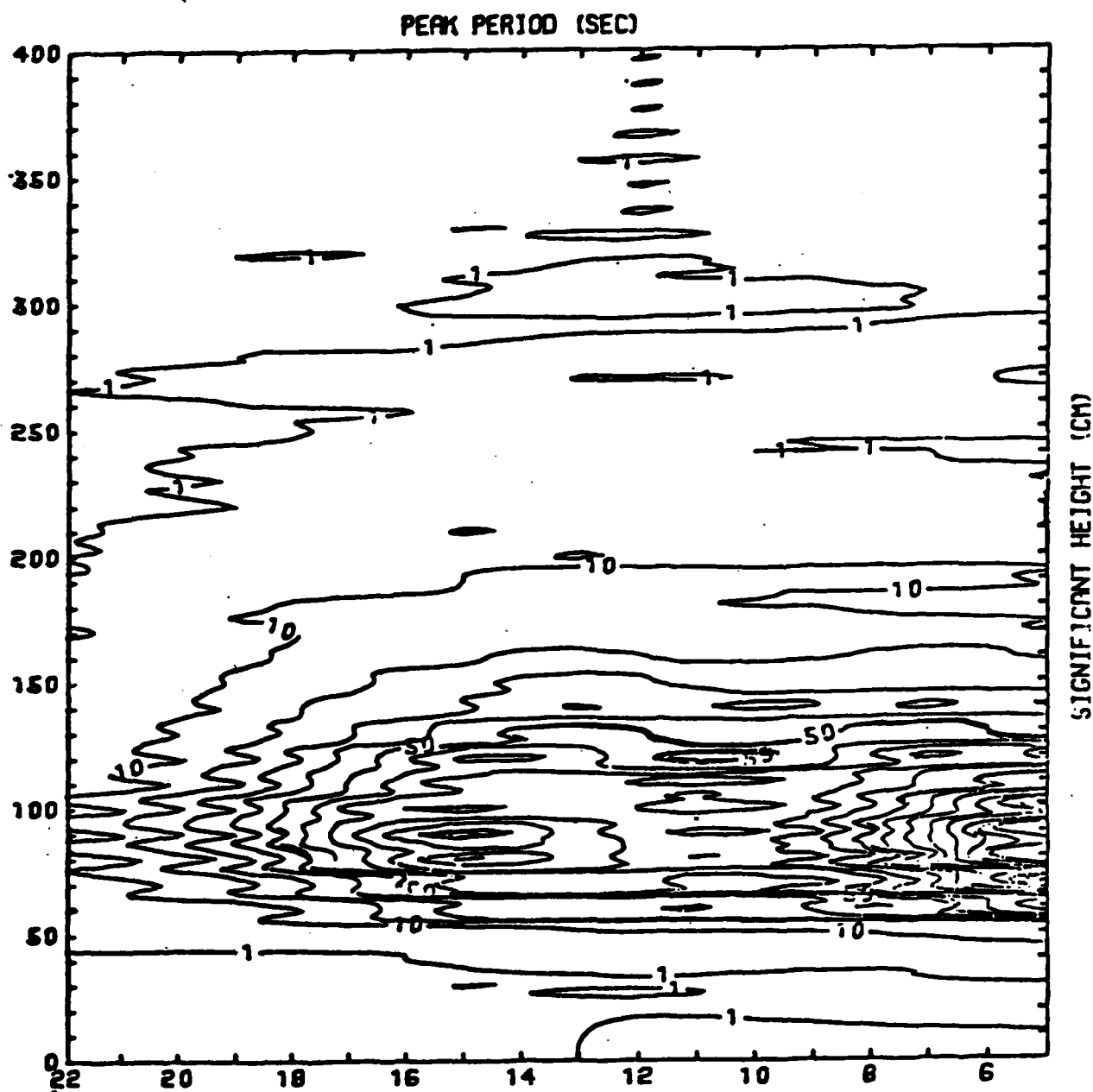


Figure 10.3-3

Contours of joint period and height distributions at Mission Bay entrance channel, 5591 samples (Seymour, 1982).

Table 10.3-2 Significant height return periods based on Mission Bay entrance channel data (Seymour, 1982).

SIGNIFICANT HEIGHTS FOR VARIOUS RETURN PERIODS
SEA-DOMINATED OBSERVATIONS

SIG. HT. (CM)	0.99 CONFIDENCE LIMITS		RETURN PERIOD (YR)
	UPPER LIM.	LOWER LIM.	
322.7	381.3	303.1	1
374.4	455.3	344.1	5
395.8	486.7	360.9	10
416.8	517.7	377.2	20
428.9	535.7	386.6	30
443.9	558.3	398.2	50
455.6	575.8	407.1	75
463.9	588.4	413.4	100

SIGNIFICANT HEIGHTS FOR VARIOUS RETURN PERIODS
WELL-DOMINATED OBSERVATIONS

SIG. HT. (CM)	0.99 CONFIDENCE LIMITS		RETURN PERIOD (YR)
	UPPER LIM.	LOWER LIM.	
344.0	393.4	328.8	1
390.8	454.7	367.4	5
409.9	480.1	383.0	10
428.5	504.9	398.0	20
439.1	519.3	406.6	30
452.3	537.0	417.2	50
462.5	550.7	425.4	75
469.7	560.6	431.2	100

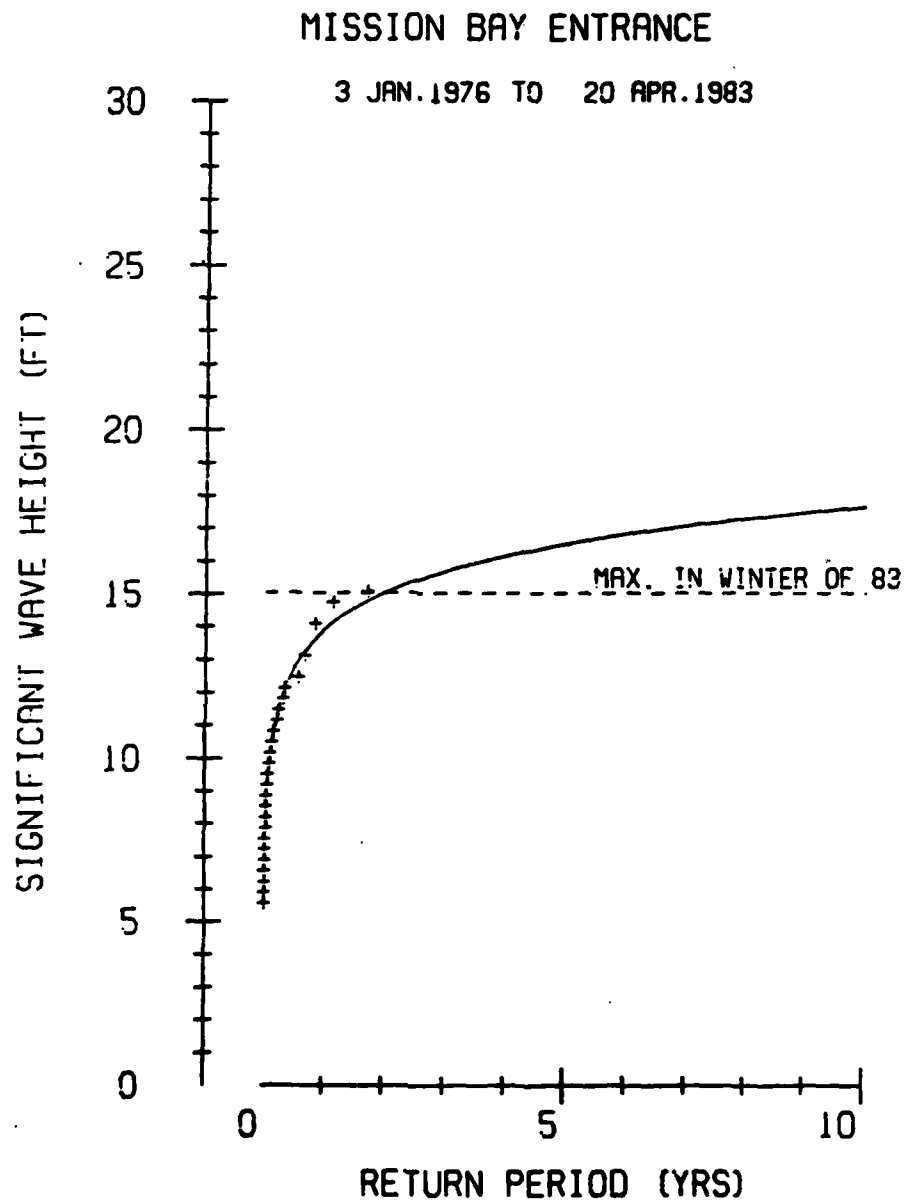


Figure 10.3-4

Significant height return period at Mission Bay entrance channel (Seymour, 1983).

1983, are evident in Figure 10.3-5.

The CDIP cumulative transports indicate that there was rarely southerly transport at Mission Bay entrance during 1982 (Figure 10.3-6). At first glance this seems inconsistent with the known importance of northerly swell during winter. However, northerly swell has been shown to have some peculiar refractive properties at Mission Bay (Figure 10.3-7). Northerly swell comes through the open window at 290° (Figure 10.3-1), but there is also a strong peak around 265° . This southerly coastal response to northern swell is probably due to Tanner and Cortez Banks (Figure 10.3-2) which act as a refractive source. Similar effects at Torrey Pines Beach are discussed in Section 3.3.1. The shore normal at Mission Bay is apparently taken as about 285° for the CDIP calculations so deep ocean northerly swell actually gives a northward transport according to Figure 10.3-7.

The nearly unidirectional transport measured by CDIP, and qualitatively supported by detailed swell refraction studies, contrasts sharply with the calculations of Hales (1978c). Hales (1978c) developed a coastal wave climatology based on unsheltered MII (1977) hindcast northern hemisphere swell at Stations 5 and 6 and Marine Advisers (1961a) Station A southern swell hindcasts (station locations shown in Figure 3.2.2-6). These offshore hindcasts were refracted through the islands but there is not sufficient description of the refraction program to deduce whether refractive effects associated with submerged banks were calculated. The sheltered statistics were shoaled to the breakpoint and the longshore energy flux used to calculate longshore sediment flux (Figure 10.3-8). The net monthly fluxes show sign reversals and a net yearly flux which is less than 10% of the gross fluxes. The differences between Figures 10.3-6 and 10.3-8 could simply stem from different definitions of the "offshore direction" used to define the coordinate system. Neither Hales (1978c) nor the CDIP reports explicitly state the coordinate frame used for the calculations (i.e. what is the longshore direction?). The differences could also result from Hales (1978c) not including the southern refractive peaks (e.g.

MISSION BAY ENTRANCE

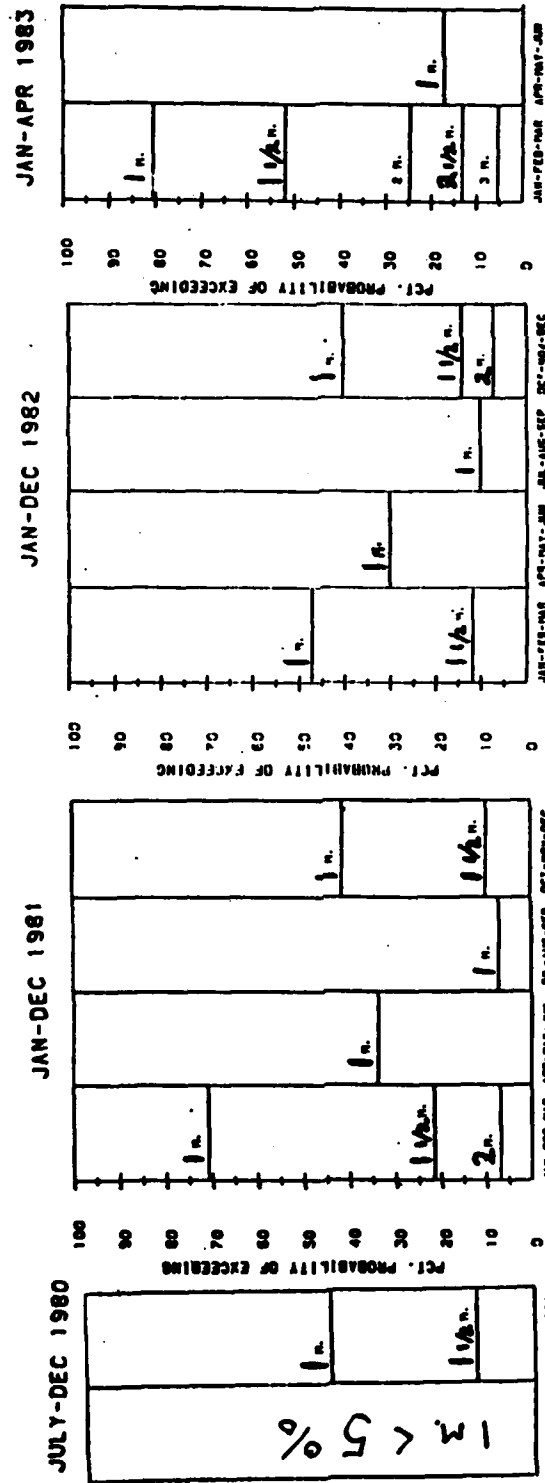


Figure 10.3-5 Seasonal probability of exceeding various significant wave heights at Mission Bay entrance channel (from CDIP annual reports).

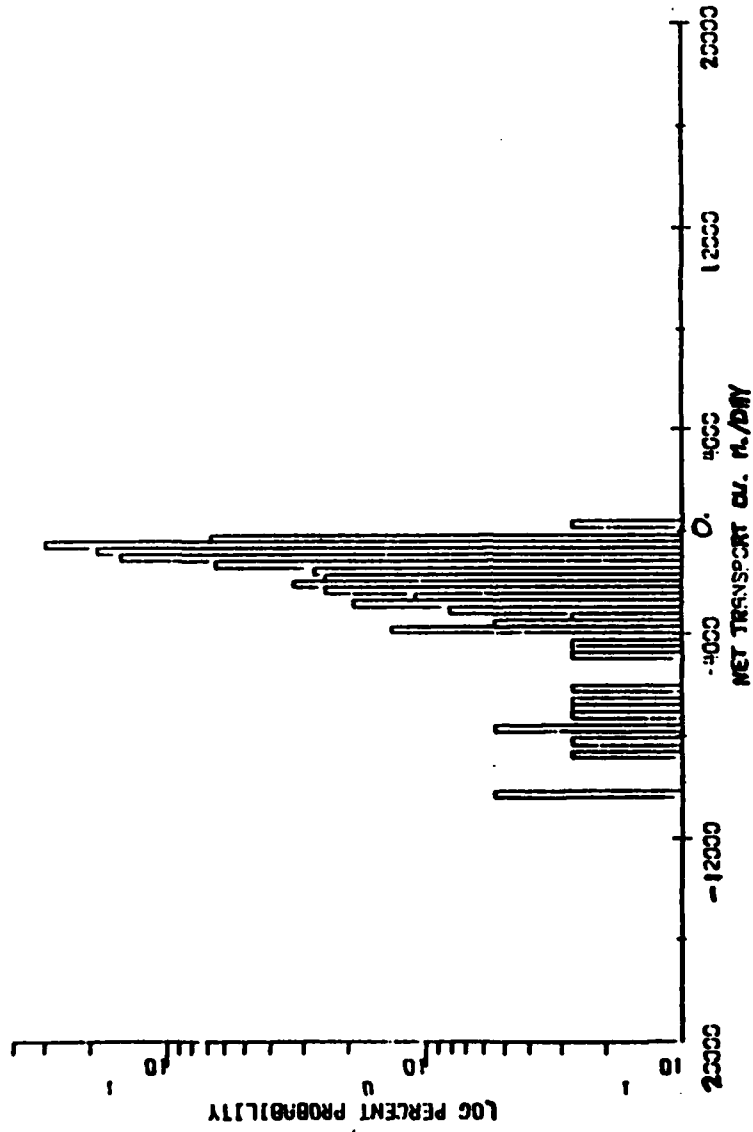


Figure 10.3-6 Percent probability (note log scale) of net daily longshore sediment transport at Mission Bay entrance channel (1982 annual CDIP report).

MISSION BAY ENTRANCE

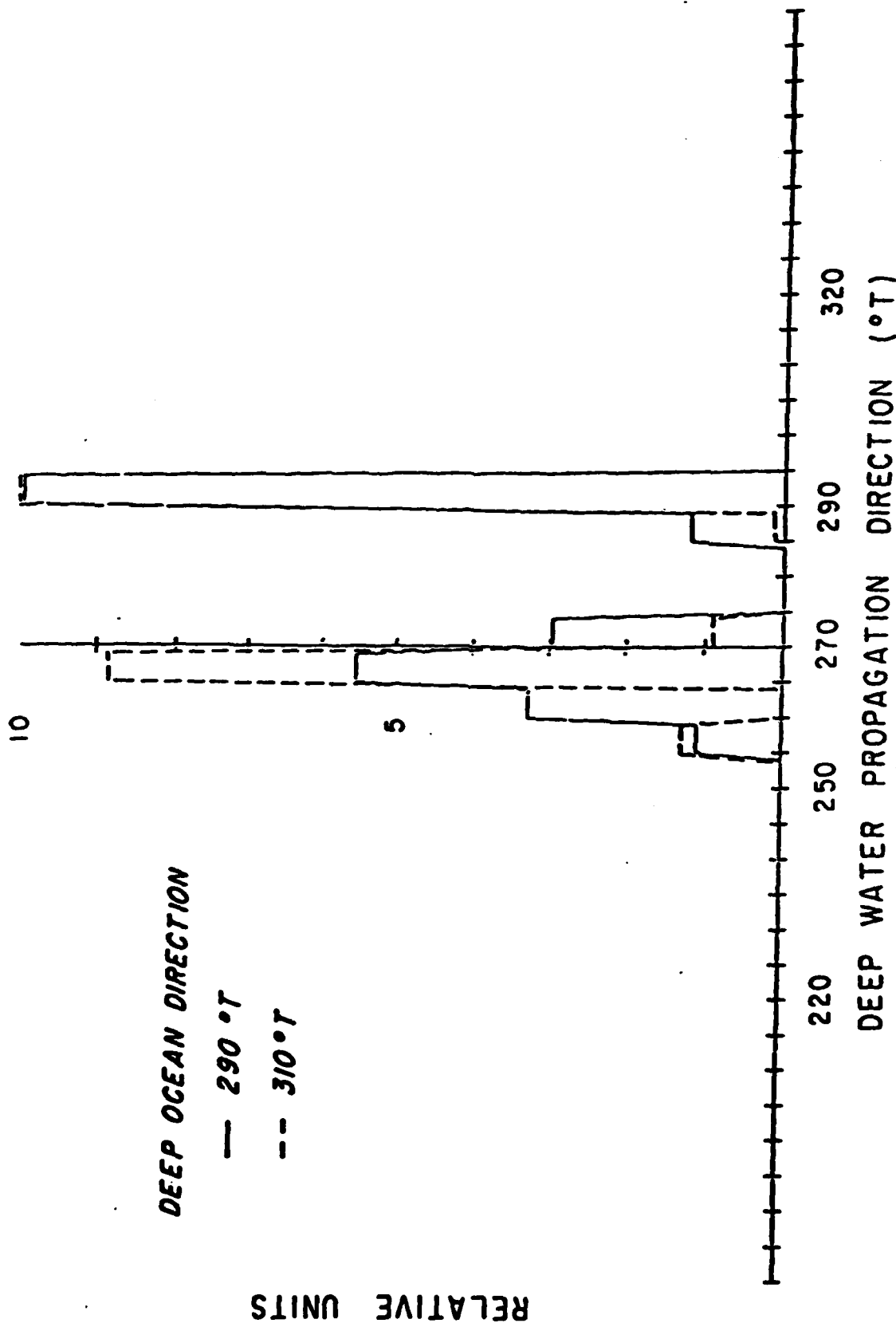


Figure 10.3-7 The local deepwater responses at Mission Bay entrance to two north swell events with 15 sec period. The directional distributions of the deep ocean events (not shown) have widths of 20° (full width at half maximum) and are smooth (cos power) functions. The responses have been block-averaged into 5° increments (Pawka and Guza, 1983).

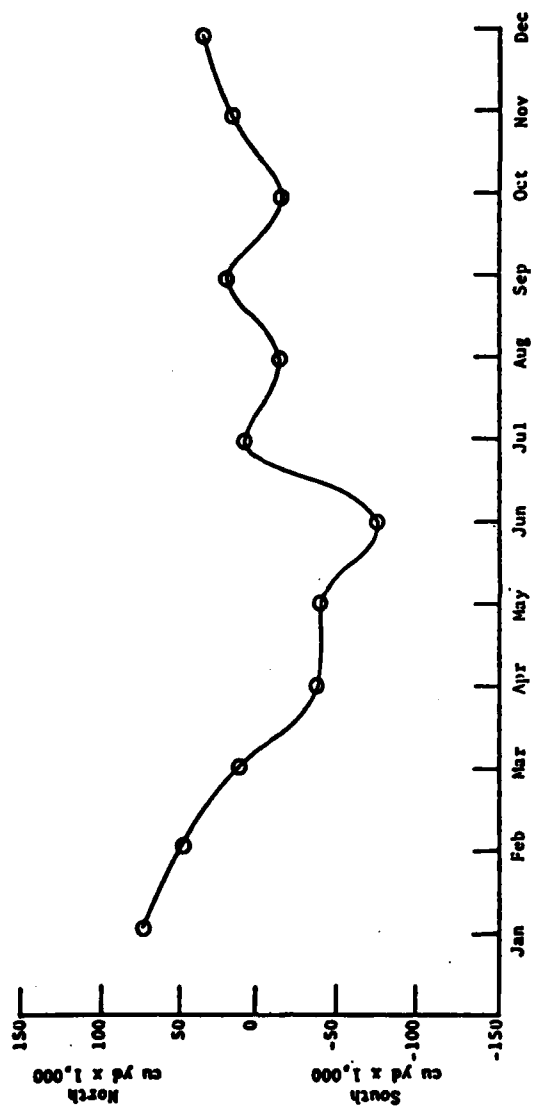


Figure 10.3-8 Potential net monthly longshore transport at Mission Beach (Hales, 1978).

Figure 10.3-7).

Marine Advisers (1961c, 1963) present results of in situ studies of sea, swell and seiches in Mission Bay. Some of the interior bays are shown to resonate at relatively long periods (100-300 seconds).

10.4 NEARSHORE CURRENTS

The shelf circulation in this cell is similar to that in the Oceanside cell (Section 9.4). Early measurements of surf zone currents are described in Section 3.3.1. Additional early measurements (methodology not described) for various locations are given in USACE LAD (1964). These indicate a predominantly northward flow.

10.5 SEDIMENT SOURCES

10.5.1 *Cliff Erosion*

Shepard and Grant (1947) discuss erosion of sea cliffs in the Point La Jolla, Ocean Beach and Sunset Cliffs areas. They compare historical photographs of these areas to illustrate rapid cliff retreat. USACE LAD (1970) reports on the Bird Rock Project to protect the cliffs in the area south of La Jolla. They also discuss the severe erosion problem in the Sunset Cliffs area, with cliff retreat rates as high as 3 ft/yr. While Shepard and Grant (1947) and USACE LAD (1970) both discuss cliff retreat, they do not directly address the erosion of sea cliffs as a source of sediment.

Nordstrom and Inman (1973) point out that modification of coastal streams by dams often block the river transport of sediment to the beach. The reduction of beach material will result in beach erosion. Without beaches to buffer wave action, wave energy will eventually dissipate in active erosion of the sea cliffs. USACE LAD (1984b) contains reported erosion rates of the coastal cliffs and observations on the potential impact that cliff retreat would have on the volume of sediment available to the littoral zone. They classify coastal cliffs by the erosive process that formed the cliff (Figure 10.5-1), such as wave attack and sheet erosion.

10.5.2 *Sediment Discharge from Rivers and Streams*

USACE LAD (1964) contains a description of the tributary drainage, and characteristics and sources of littoral material in the Mission Bay Cell. The information on tributary drainage area, though historical, is important for understanding sediment input and transport data at that time. The appendices of this report contain information on sand sample grain size distributions and figures showing the geology and drainage area of this littoral cell. Hales (1979) performed a study of the Mission Bay "littoral compartment". He describes the drainage area of the San Diego River - Mission Bay region. Brownlie and Taylor (1981) summarize water

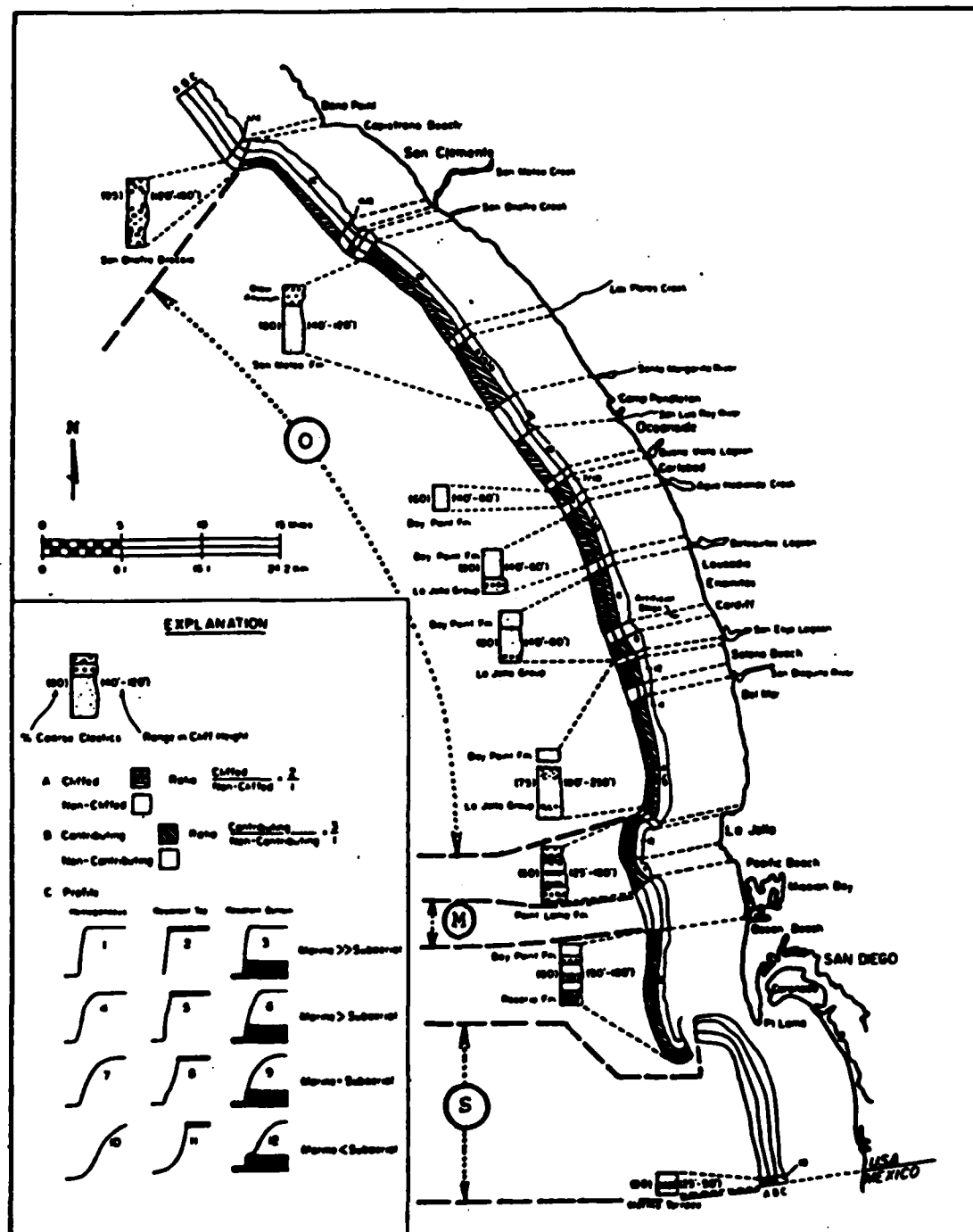


Figure 10.5-1. Classification of coastal cliffs. An "O" (Oceanside), "M" (Mission Beach), "S" (Silver Strand) denote littoral-geomorphic cells (from USACE LAD, 1984b.)

and sediment discharge for southern California rivers, including the San Diego River (see Figure 10.5-2). They estimate sediment yield from sediment rating curves which may underestimate bedload (see Inman and Jenkins, 1983, and Section 2.5 for discussion). California (1977a) is a summary of information on sediment transport in coastal stream basins and beach nourishment along the southern California coast. Like Brownlie and Taylor (1981) they use a sediment rating curve to estimate the sediment yield of the coastal streams.

USACE LAD (1984b) is a report presenting basic data on the geomorphology, the physical characteristics of the sediment, as well as concepts of sediment transport along the coast of California from Dana Point to the Mexican Border. It contains a lengthy discussion of the sediment resources in the inland basin that contribute sediments into the littoral and offshore zones. USACE LAD (1984b) estimates the annual sediment production of the San Diego River to be 100,000 cu. yds., and discusses some historic transport records. They also include grain size distribution information for both inland basin and beach sediments.

10.5.3 *Artificial Beach Nourishment*

Dunham (1965) discusses the construction of the Ocean Beach groin and the placement of 250,000 cu yds. of artificial fill along the beach. Shaw (1980) outlines the dates and quantities of artificial sediment transport and construction of beach structures in the Mission Bay area. Herron (1980) briefly discusses the development of Mission Bay and the resulting 4 million cubic yards of artificial fill that was placed along Ocean Beach and Mission Beach. Osborne et al (1983) discuss the offshore sand and gravel resources of the inner continental shelf of southern California. They devote a section of the report to the Mission Beach area complete with vibracore data, petrology studies and borrow area descriptions and maps. USACE LAD (1984b) discusses sand and gravel mining to combat the serious beach erosion problems in San Diego County. The report identifies inland borrow areas and estimates the amount of beach sand size material available.

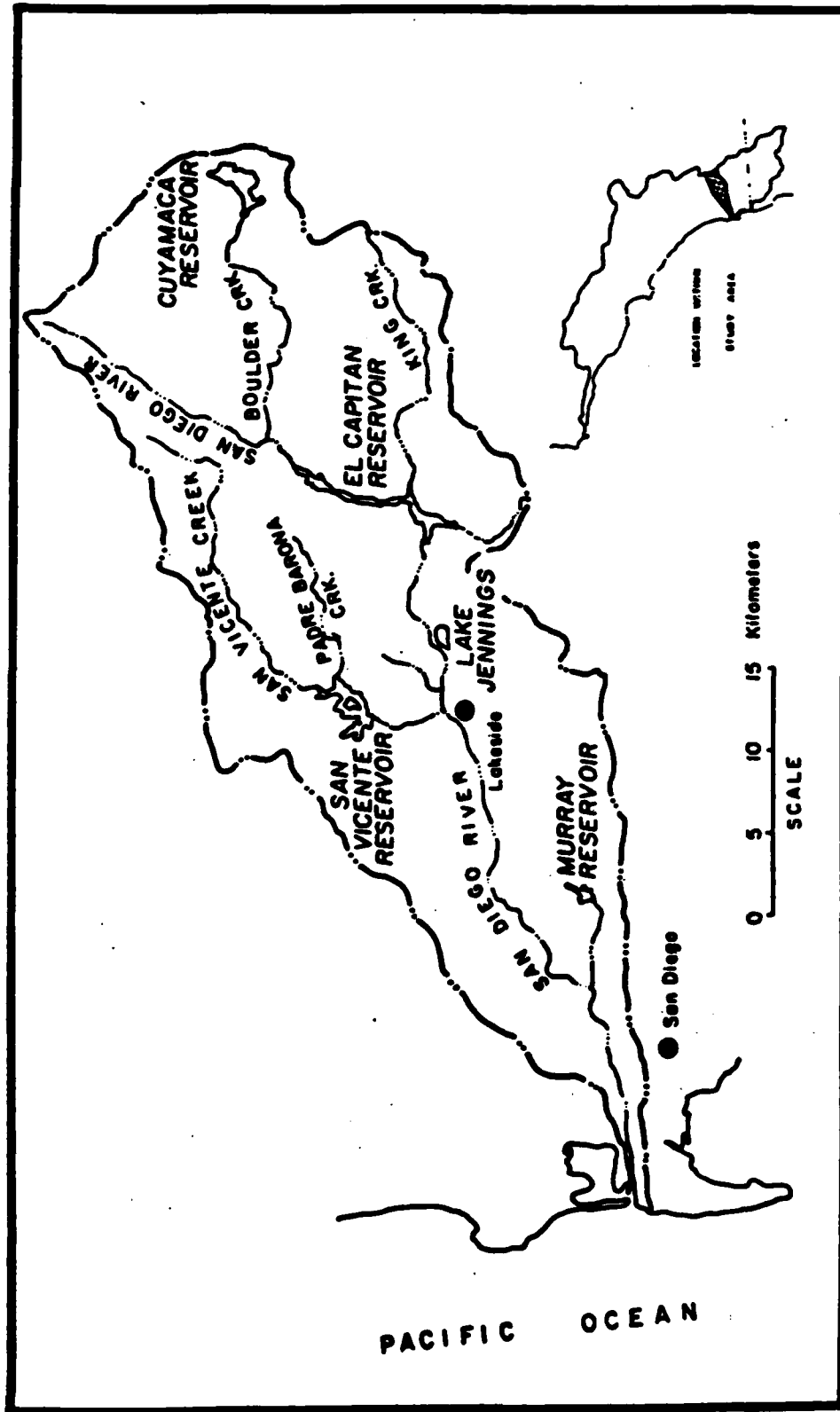


Figure 10.5-2. San Diego River Basin (from Brownlie and Taylor, 1981).

10.6 SEDIMENT TRANSPORT MODES

10.6.1 *Cross-shore Transport*

Shepard (1946, 1950c) first studied seasonal beach profile changes in the La Jolla area at Marine Street, a steep coarse-grained pocket beach. Bruun (1954) monitored seasonal changes at Mission Beach and computed typical area, width and foreshore steepnesses (Bruun's Table 39).

The Corps has computed some volume changes at Pacific Beach, Mission Beach and Ocean Beach since the 1940's (USACE LAD 1960a, 1964), but has not tried to separate the changes into cross-shore and longshore transport effects. (Profile changes may be due to either cross-shore transport or changes in the longshore transport rate.) Volume changes north of Crystal Pier in Pacific Beach (Figure 10.6-1) indicate average annual erosion of $13 \text{ yd}^3/\text{yd}$ of beach from 1940 to 1951 (USACE LAD 1960a). Seasonal beach changes in the area are simply described as "large" and extending to 50 ft. depth. Comparative surveys are presented for the Sunset Cliffs area between 1930 and 1962 in USACE LAD (1964). However, volume changes for entire beach survey regions are computed, rather than erosion per yard of beach.

Aside from the short studies at Marine Street in La Jolla by Shepard (1950c) and Mission Beach by Bruun (1954), information on seasonal cycles and long-term behavior of beach profiles is lacking.

10.6.2 *Longshore Transport*

Komar (1978) reports on a test of suspended sediment samplers at Pacific Beach by Watts in 1953 in which Watts found an average volume concentration of sand of 0.00026 in the surf zone. Komar determined from Watts' data that the maximum portion of the total longshore transport represented by suspended transport was 26% at Pacific Beach.

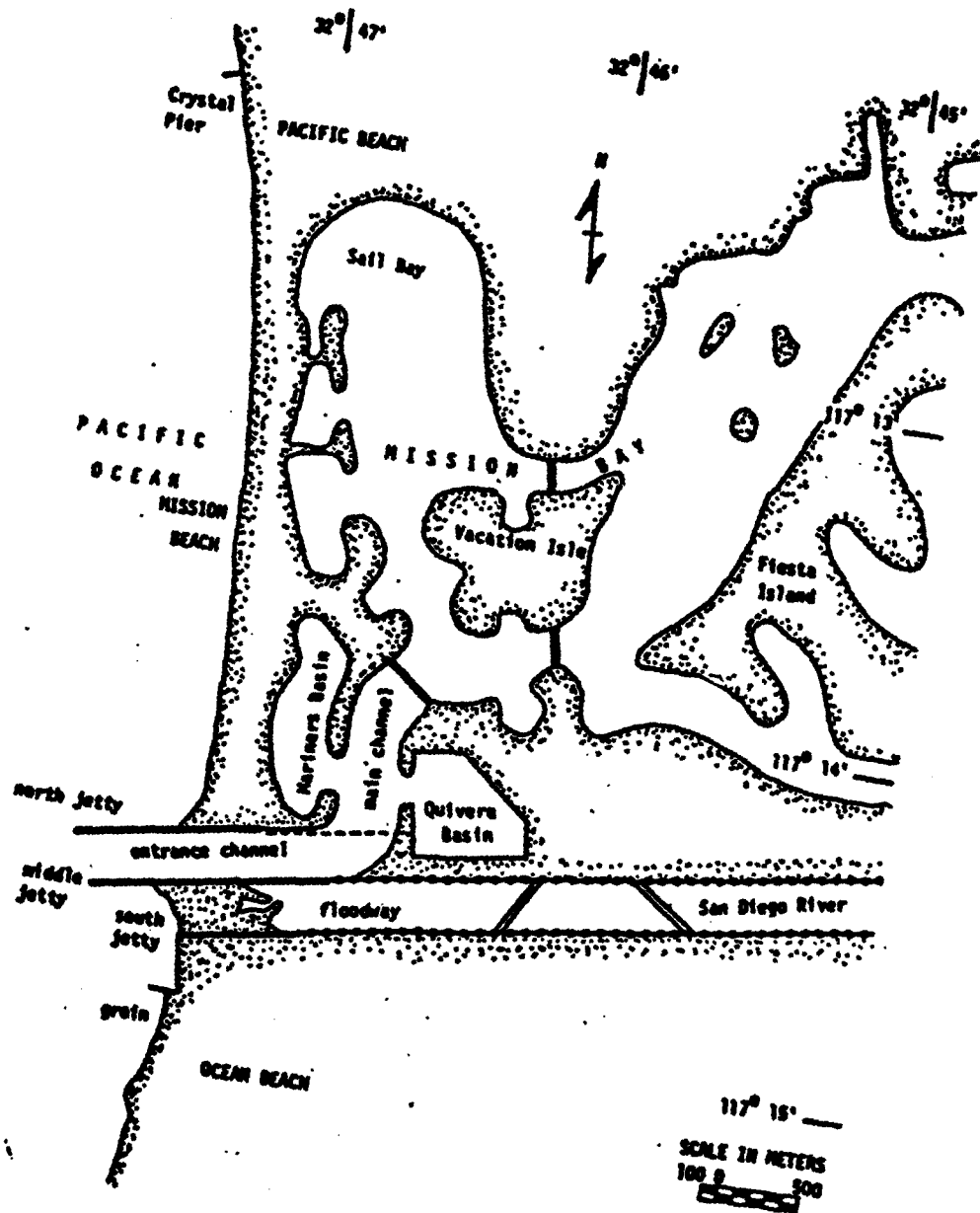


Figure 10.6-1. Mission Bay area (from Shaw, 1980).

Hales (1979) made a longshore transport study at Mission Bay in which local sea waves, northern swell and southern swell were refracted into the beach. The gross and net transport rates obtained are listed in Table 10.6-1 for each month. The rates are small relative to nearby cells (i.e., Oceanside). The general trend is for northerly transport in the winter (mostly from local sea waves rather than swell) and southerly transport in the spring (again mostly from local sea waves). The net transport of $20 \times 10^3 \text{ yd}^3/\text{yr}$ to the north represents a small difference of large numbers and thus could not be considered accurate. Hales' (1979)

study suffers from two serious deficiencies. The data source for northern swell is DNOD fleet numerical data, which is of questionable accuracy for this area. (See Section 3.2.2 of this report.) Furthermore, the island-shadowing techniques are inadequate. In general, only two pieces of data from Hales' report may be considered reliable: the trend of strong transport to the north in winter, and a gross transport rate on the order of $100 \times 10^3 \text{ yd}^3/\text{month}$.

Castel and Seymour (1982) used data from a nearshore slope-array of pressure sensors to compute longshore transport at Mission Bay. They did not refract the waves shoreward of the slope-array location (10 m deep). Because of this the location of the line of zero transport on their figures is not accurate. Nevertheless, the seasonal trends are still valid. Like Hales, they show strong northerly transport in the winter months. Seymour and Castel (1984a) examined the episodicity and cycles in the longshore transport at Mission Bay. The actual transport values listed in columns 2 and 3 of Table 9.6-6 cannot be considered reliable because of the aforementioned refraction problem. However, the episodicity measures in columns 4 and 5 are relative measures and thus reliable. These values indicate that the maximum daily net transport is 2-5% of the total annual net transport, not nearly as large as the value for Oceanside. However, 50% of the gross transport occurs during only 15% of the days. In relative terms, this means that transport during storms represents a large portion of the total transport, but that large daily transports do not occur at Mission Bay, as they do at Oceanside.

TABLE 10.6-1. SUMMARY OF POTENTIAL LONGSHORE TRANSPORT
COMPUTATIONS (from Hales, 1979).

Month	Sea		Northern Swell		Southern Swell		Sum		Net	
	North	South	North	South	North	South	North	South	North	South
	+	-	+	-	+	-	+	-	+	-
Jan	92,500	25,383	13,747	9,073	0	0	106,247	34,456	71,791	140,703
Feb	78,053	31,728	10,433	9,911	0	0	88,486	41,639	46,847	130,125
Mar	57,085	60,032	26,567	15,112	0	0	83,652	75,144	8,508	158,796
Apr	37,823	69,198	7,251	16,028	0	0	45,074	85,226		40,152
May	4,816	88,940	389	27,728	70,195	0	75,400	116,668		41,268
Jun	4,013	89,646	252	29,552	39,101	0	43,366	119,198		75,832
Jul	1,605	87,530	0	26,897	119,563	0	121,168	114,427	6,741	235,595
Aug	0	86,120	259	19,281	90,828	0	91,087	105,401		14,314
Sep	4,816	67,083	913	8,842	90,056	0	95,785	75,925	19,860	171,710
Oct	8,829	49,363	519	7,127	32,851	0	42,199	56,490		14,291
Nov	52,270	28,908	3,366	9,416	0	0	55,636	38,324	17,312	93,960
Dec	59,494	21,152	7,201	10,496	0	0	66,695	31,648	35,047	98,343
Annual	401,304	705,083	70,897	189,463	442,594	0	914,795	894,546	206,106	185,857
Net		303,779		118,566	442,594		20,249		20,249	

Only two estimates of transport in this cell are available. For the reasons already presented, neither of these estimates is reliable. Good estimates of longshore transport in this cell are lacking.

10.6.3 *Wind Transport*

To our knowledge, no studies have been made in this cell on wind transport. This is not surprising, since the geology of the area effectively prevents significant wind transport. Lack of dune fields, presence of high rocky headlands, and lack of strong sustained winds are reasons for the unimportance of wind transport in this cell.

10.7 SEDIMENT SINKS

10.7.1 *Submarine Canyons*

There are no submarine canyons in this cell. The nearest canyon is the Scripps Canyon to the north at the end of the Oceanside Cell.

10.7.2 *Entrapment by Harbors, Bays and Estuaries*

The construction of three jetties at the entrance to Mission Bay (Figure 10.6-1) has greatly affected the longshore transport of the Mission Beach and Ocean Beach coastlines. Frautschy and Inman (1954) explain in detail the effect of the jetties on the transport:

"Prior to construction of the jetties, sand was moved by waves and nearshore currents in both directions along the coast during the course of a year. It crossed the shallow bar at the mouth of Mission Bay without significant attrition (their Figure 2). Northerly flowing currents caused a loss of sand from Ocean Beach, but such loss was made up from time to time by transport of sand caused by southerly currents. The jetties have had two principal effects on the adjacent beaches: a) they impede the natural flow of sand which formerly existed between the beaches to the north and south of the channel, and b) they form wave and current shadows

which result in quiet water and the deposition of sand adjacent to the jetties, and consequently erosion of the beaches in other areas. Thus the jetties form a dam which obstructs the sand-laden southbound currents and results in the formation of a wide beach to the north of the northern jetty. In the same manner periodic northbound currents carrying sand from Ocean Beach now meet an obstruction and the sediment load is deposited in the wave shadow of the middle jetty and across the mouth of the flood channel. The net effect is that the supply of sand to Ocean Beach has been diminished while erosion, or transport out of the area, has been diminished little."

In order to quantify the effect of the jetties on the transport, periodic (at least seasonal) beach profiles would be necessary on both sides of and in the entrance channel. Although some profiles made by the Corps and Scripps Institution of Oceanography are available (Frautschy and Inman, 1954) they are not of sufficient quantity to enable calculations of transport blockage.

On several occasions the jetties allowed partial penetration of sand. The causes of the penetrations and actions taken to prevent further motion of sand into the entrance channel are detailed by Hales (1979).

Shaw (1980) presents a dredging and beach fill history of the area. But much of the fill was obtained from places in Mission Bay other than the entrance channel. Thus this information cannot be used to estimate capture rates of transport by the jetties. A total of $1251 \times 10^3 \text{ yd}^3$ of dredging and subsequent placement of fill on Ocean Beach and Pacific Beach from 1948 to 1973 are reported by Shaw (1980).

10.7.3 *Littoral Barriers*

The shore-normal structures in this cell consist of two piers, four jetties and a groin (Shaw, 1980). The two piers have essentially no impact on the transport. The privately built 275 m wooden Crystal Pier in Pacific Beach (Figure 10.6-1) was built in 1925. The concrete 660 m

Ocean Beach pier was built in 1966 by the City of San Diego. A 90 m concrete jetty was built at the La Jolla headland for recreational purposes in 1930. Its effect on transport is negligible since little sand moves between pocket beaches on the headland.

Inman (1953) showed that the sand on the pocket beaches of the La Jolla headland is locally derived and does not come from further north or south. Each pocket beach is essentially a self-contained micro-cell into and out of which there is essentially no transport. Examination of the sand size and mineralogy on the Point Loma pocket beaches suggests that the Point Loma headlands are not efficient barriers to longshore transport. Much of the sand on them appears to come from the beaches to the north. Some sand may also "leak" southward to the Silver Strand Cell. None of these transports have been quantified.

The remainder of the cell is made up of the two long sandy beaches of Pacific Beach/Mission Beach (north of the Mission Bay entrance channel) and Ocean Beach (south of the entrance channel). In 1950 the Corps built three rubble-mound jetties to stabilize the entrance to Mission Bay and provide a flood-control channel for the San Diego River. The 1005 m long north jetty effectively impounds sand on the north side. The 1160 m middle jetty and 460 m south jetty were extended to 1305 m and 630 m, respectively, in 1970. The channel between middle and south jetties is generally filled with sand. The dynamic effects of the three jetties are detailed by Frautschy and Inman (1954), part of which is excerpted in Section 10.7.2 of this report. The jetties effectively halt all longshore transport, both to the north and south (Frautschy and Inman, 1954; Hales, 1979).

After the construction of the jetties, Ocean beach became effectively a pocket beach, with its primary source of material, the San Diego River, cut off (Frautschy and Inman, 1954). The wave shadow created by the jetties resulted in accretion at the north end of the beach and erosion at the south end (Frautschy and Inman, 1954; Dunham, 1965). In order to halt this counterclockwise reorientation of the beach, a 150 m stone groin was built in Ocean Beach in

1959 (Figure 10.7-1). The Corps placed $250 \times 10^3 \text{ yd}^3$ of fill south of the groin (Dunham, 1965; USACE LAD, 1970). The groin is at least partially successful in maintaining the beach to the south. Nevertheless, Ocean Beach will continue to have erosion problems since its sand source, the San Diego River, has been cut off.

10.7.4 *Wind Transport*

Loss of sand due to transport by wind must be small, since the geology of the area effectively prevents such loss. High cliffs behind the beaches and lack of strong sustained winds prevent significant wind transport. No studies have been made on this subject in this cell.

10.7.5 *Berm Overwash and Offshore Loss*

Loss of sand out of the littoral transport regime due to onshore transport over the berm is effectively prevented by the presence of either sea cliffs or buildings.

Permanent offshore loss has not been quantified. Investigators generally assume it to be small, since transport rates offshore are much smaller than in the surfzone. It is possible for such loss to occur, but studies on this topic are lacking.

10.8 SEDIMENT BUDGET

There are no reports addressing the sediment budget for the Mission Bay Sub-Cell. The sources of sediment for this unique littoral compartment are cliff erosion at False Point and Sunset Cliffs, and sand from the San Diego River. Cliff failure being episodic in nature is not well documented, with little more than comparative "before and after" photographs for data (see Section 10.5.1). The sediment discharge from the San Diego River is about $100,000 \text{ yd}^3/\text{yr}$ (USACE LAD, 1984b). There are few longshore transport estimates. The only sink for sand is Mission Bay which has been infrequently dredged, with the spoils being placed back on the local beaches, and the probability that some sand migrates to the south around Point Loma and into the Silver Strand Littoral Cell.

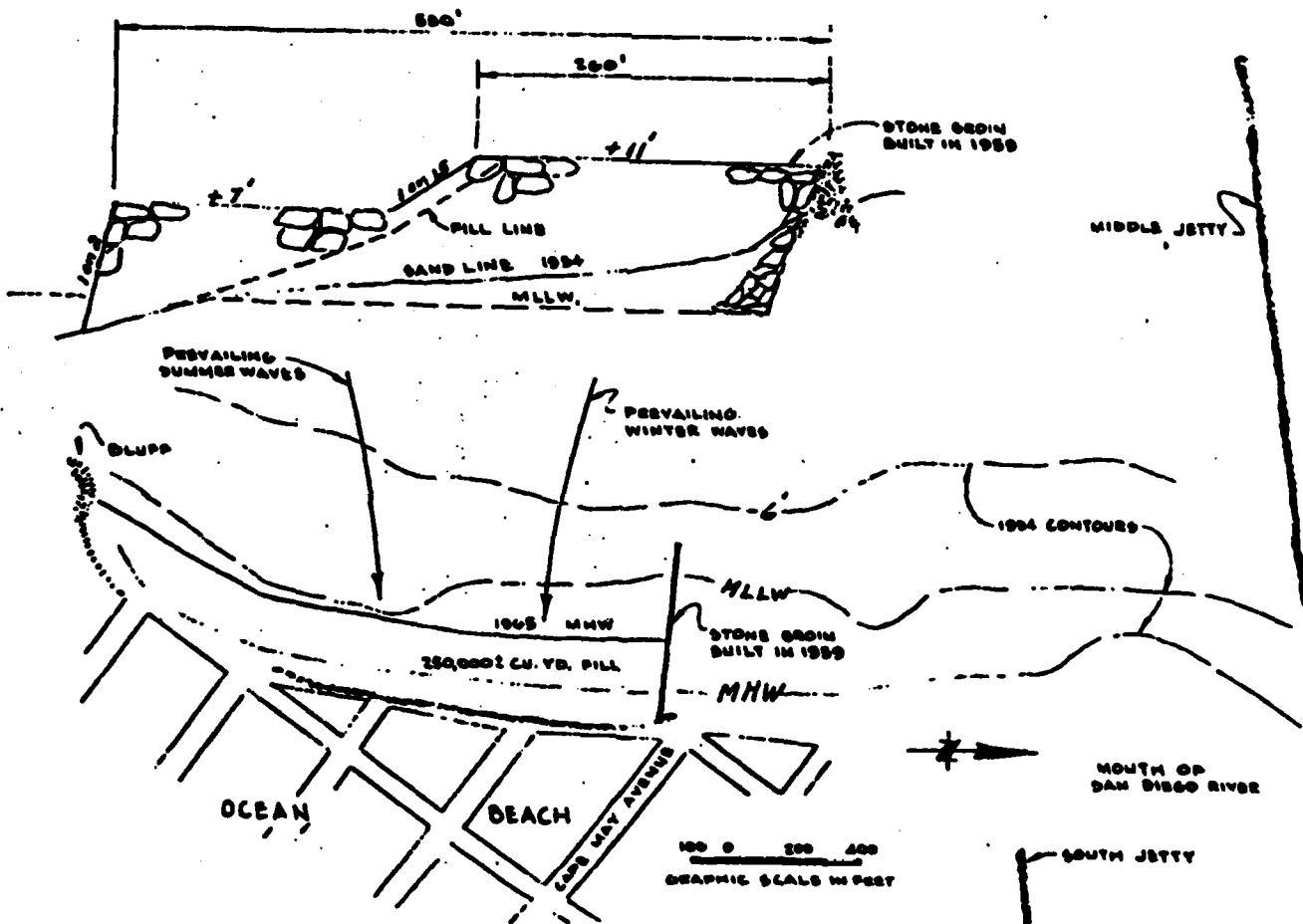


Figure 10.7-1. Ocean Beach groin and sand fill (from Dunham, 1965).

11. SILVER STRAND CELL

The Silver Strand Cell extends for 16 miles from Point Loma to the United States/Mexico Boundary, and for many miles along the coast of Baja, California, Mexico (see Figure 1.3-1). The cell includes 14 miles of sandy beaches from the Zuniga Jetty to the border. This cell is one of the few cells with a significant northerly transport of sand because of the wave shadow in the lee of Point Loma. The principal source of sediment is the Tijuana River, but the construction of dams both in the United States and Mexico has almost eliminated the Tijuana River as a source of sediment for the beaches. Imperial Beach has serious erosion problems as a result.

11.1 COASTAL EROSION PROBLEMS, NATURAL AND MAN-MADE

A qualitative systematic summary of coastal erosion problems from Zuniga Point to the Mexican border is contained in the Assessment and Atlas of Shoreline Erosion (California, 1977a). The majority of the coast in this littoral cell is sandy beaches backed by low sand dunes with sparse vegetation. *There are about three miles of small 10 foot high cliffs which are stabilized by rip-rap and rubble mound sea walls.* The main erosion problem is loss of beach sands and the resulting backshore damage. Chamberlain et al (1958) and Inman et al (1974) give histories of beach erosion from 1893, prior to construction of Zuniga Jetty, to 1974. Sonu et al (1978) discuss erosion due to man-made structures inside San Diego Harbor at the North Island Naval Air Station.

USACE LAD (1978b) discusses the problem of gradual beach erosion along Imperial Beach, caused by an inadequate natural supply of beach material. Herron (1980) briefly discusses erosion and littoral drift in the Silver Strand Cell. Kuhn and Shepard (1984) give a detailed discussion of historical shoreline erosion problems at Coronado and the Silver Strand, including comparisons of 1923 and 1934 surveys, and historical photographs. Inman (1985c) summarizes the erosion problem at Imperial Beach and presents viable approaches for remedial action as an alternative to the proposed offshore breakwater (see Section 11.5.3).

11.2 SHORELINE CHANGES

A summary of the data concerning shoreline changes contained in the reports reviewed for this study is shown in Table 11.2-1. USACE LAD (1960a) discusses shoreline, offshore and volumetric changes in this littoral cell. The appendices include historical offshore and shoreline surveys starting from 1856, and beach profile data starting from 1937. USACE LAD (1962b) includes comparative shoreline profiles at Bayview Estates, Coronado, inside San Diego Bay from 1944-1962. USACE LAD (1969a) contains surveys of the entrance channel to San Diego Bay along with a maintenance dredging condition survey. Also included in this Corps of Engineers report are 1965 beach profiles at Imperial Beach. USACE LAD (1970) contains a discussion of the shoreline changes at Imperial Beach starting from the winter of 1952, when severe wave action caused erosion, to 1968. Also included in the appendices are plates showing 1967 area hydrographic surveys and shoreline and offshore changes from 1856 to 1967.

Figure 11.2-1 from USACE SPD (1971) illustrates the historical shoreline changes in the Silver Strand Cell. Inman et al (1974) present a study of the sources, littoral transport paths, transport rates, and depositional sinks of beach sand in the Silver Strand Cell. The report examines the broad scope erosion problems along this coastline. Included are aerial photographs, offshore bathymetric map and beach profile data. USACE LAD (1978b) presents an historical analysis of shoreline changes in this cell. This design memorandum includes Inman et al (1974) along with additional reports on littoral processes, including beach profile data.

Table 11.2-1
EXISTING SURVEYS, MAPPING STUDIES, PHOTOGRAPHS

Author(s) Date	Type of Data	Location and Dates
Chamberlain et al, 1958	Shoreline and offshore changes	Tijuana River to Zuniga Jetties
USACE LAD, 1960a	Shoreline and offshore changes	Coronado to Imperial Beach, 1856-1956
	Beach profiles	Coronado to Imperial Beach, 1937-1956
	Volumetric changes	Imperial Beach, 1946-1954
USACE LAD, 1962a	Comparitive profiles	San Diego Bay, 1944-1962
USACE LAD, 1967	Condition survey	Imperial Beach, July-August, 1962
USACE LAD, 1969a	Hydrographic survey	San Diego Bay, 1969
	Beach profiles	Imperial Beach, 1965
USACE LAD, 1970	Hydrographic survey	Coronado, Silver Strand, 1967
	Aerial photographs	Imperial Beach Groins, 1967
	Shoreline and offshore changes	Coronado, Silver Strand, Imperial Beach, 1856-1967

Table 11.2-1 (cont'd).
EXISTING SURVEYS, MAPPING STUDIES, PHOTOGRAPHS

Author(s)	Date	Type of Data	Location and Dates
Inman et al.,	1974	Aerial photographs, offshore changes	Silver Strand Littoral Cell, 1945, 1967
		Offshore bathymetry	Silver Strand Littoral Cell, Entire Cell
		Beach profiles	Silver Strand Littoral Cell 1967-1974
USACE LAD,	1978b	(Includes Inman et al., 1974)	
		Beach profiles	Silver Strand Littoral Cell Entire Cell, 1937-1975

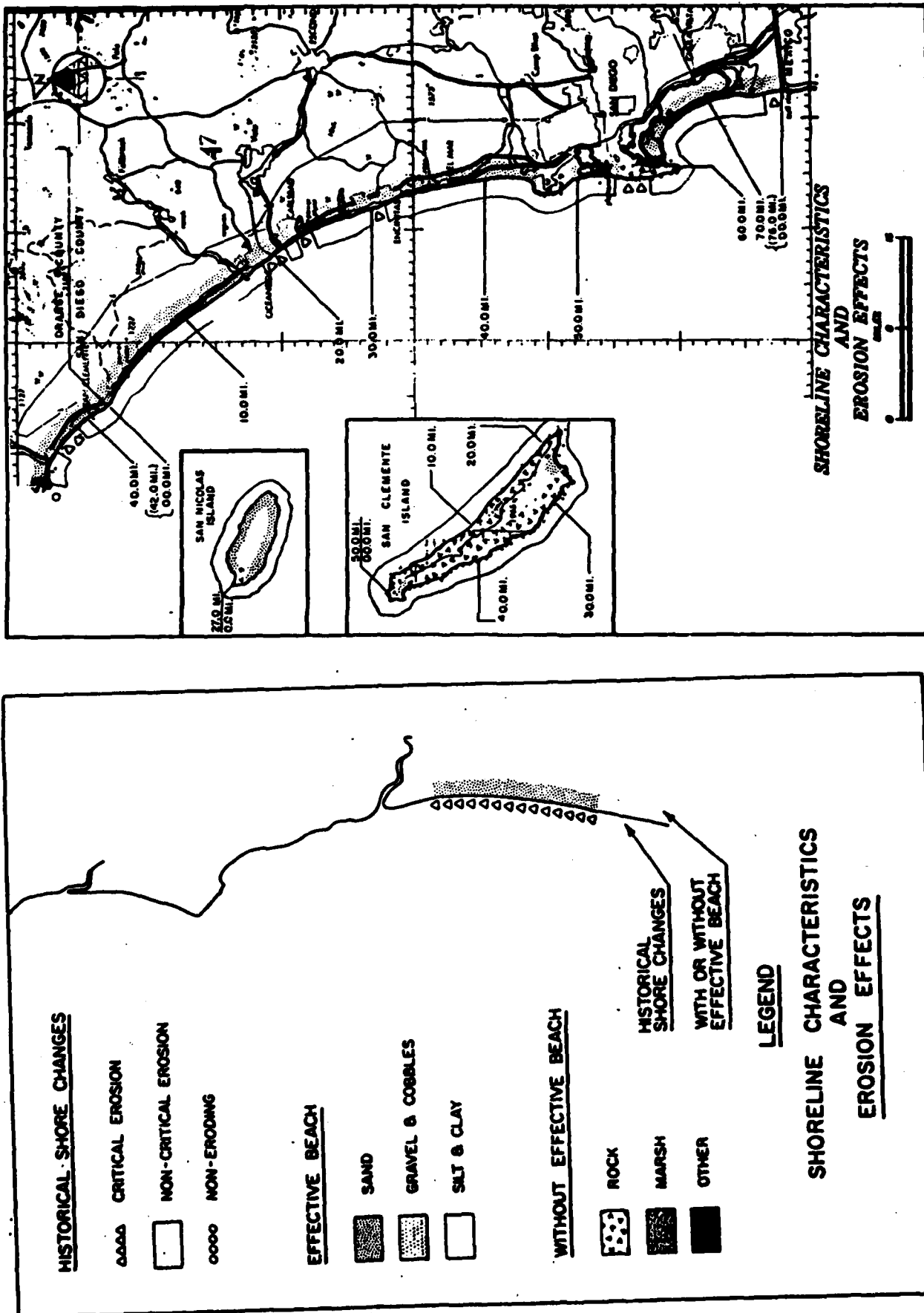


Figure 11.2-1. Shoreline characteristics and historical shore changes (from USACE SPD, 1971).

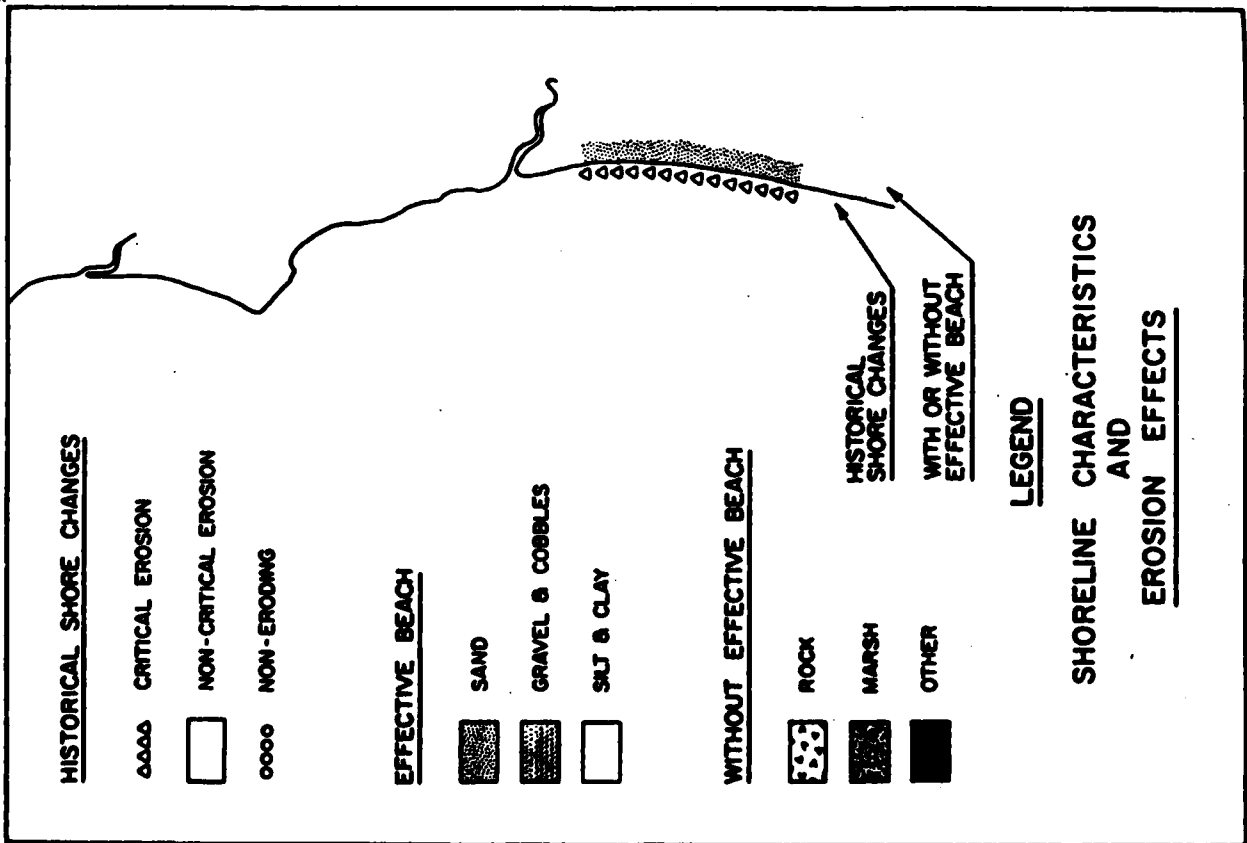
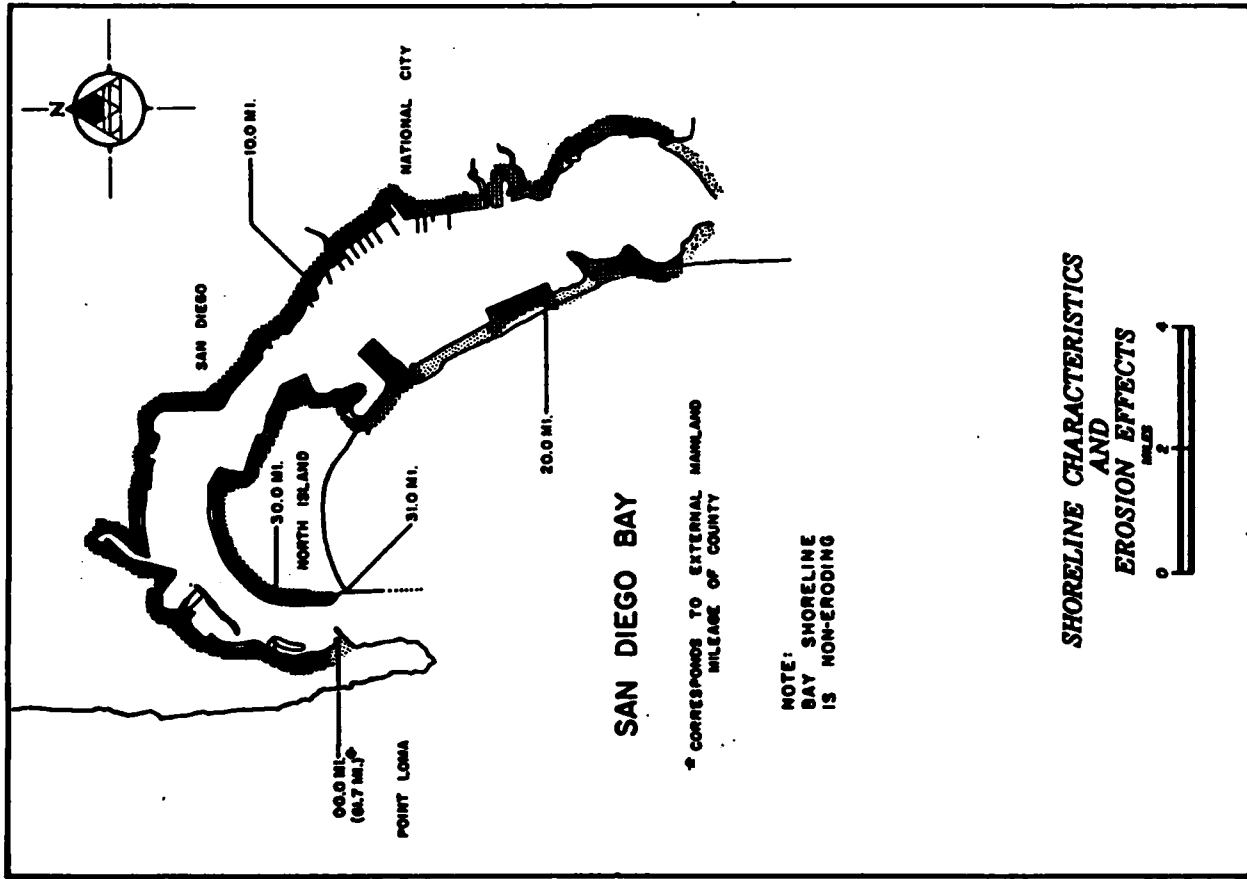


Figure 11.2-2. Shoreline characteristics and historical shoreline changes (from USACE SFO, 1971).

11.3 NEARSHORE WAVES

Waves outside the Channel Islands (Section 3.2) are highly modified upon reaching this cell. Northern swell is significantly sheltered by Point Conception and the Channel Islands (Figure 3.2.2-1) and locally by Point Loma (Figure 11.3-1). According to the blocking/refraction model of Pawka and Guza (1983), the percentage of deep ocean energy reaching deep water off Imperial Beach decreases from about 40% for swell from 280° to about 10% for 320° swell (Figure 3.3.1-6). The high angle 320° swell reaches Imperial Beach because of refraction associated with Tanner and Cortez Banks, analogous to Figure 3.2.2-1 at Torrey Pines.

The bathymetry to the south of this cell is very complex (Figure 11.3-1). The shelf width to the 100 m contour is about 4 times wider at Imperial Beach than Del Mar (Figure 11.3-1). Waves approaching Imperial Beach from the 180° - 230° sector pass through a complex of small islands, banks and shoals and are then in depths of less than 100 m for at least 20 km. Because of the exceptionally long propagation distance over rough topography (as on most nautical charts, the contours in Figure 11.3-1 are artificially smooth), Pawka and Guza (1983) doubted the results of their southern swell refraction studies at Imperial Beach and the values are not shown on any of their plots (Figures 3.3.1,5,7,9). The accuracy of linear refraction theory on this sort of topography is unknown. It is likely that a significant fraction of deep ocean southern swell reaches this cell, but there are no meaningful theoretical estimates of the amount.

CDIP wave height measurements at Imperial Beach are summarized in Figure 11.3-2. The summer months are low in energy, similar to other sites in southern California (e.g. Figure 9.3-5). The wave directional characteristics from the CDIP slope array (which began operating in July, 1983) indicate the net daily longshore energy flux is always northward (Figure 11.3-3). The direction of the offshore normal to the beach (which essentially defines the dividing direction between upcoast and downcoast transport) is not explicitly given in the CDIP annual

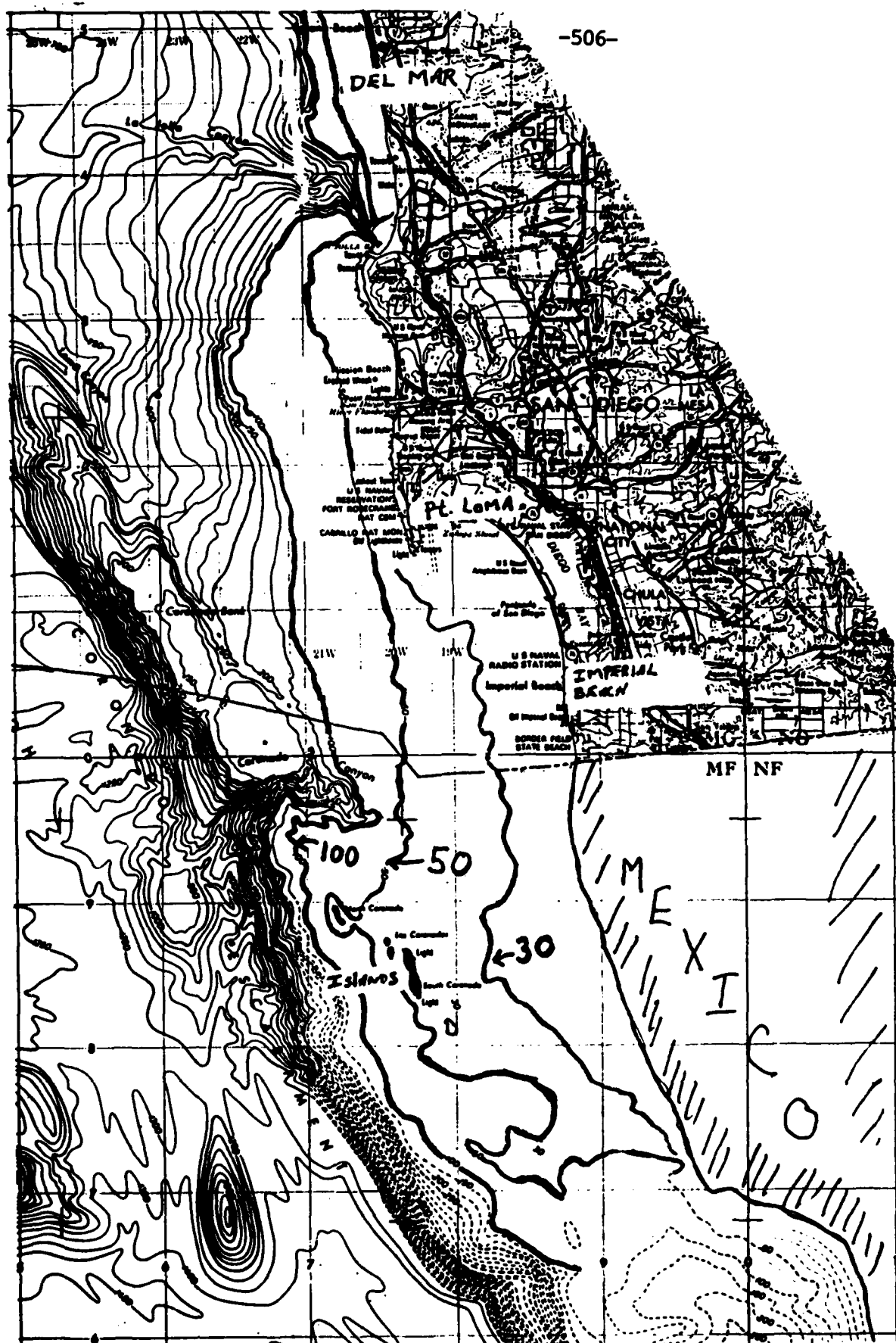


Figure 11.3-1 Bathymetry (contours in meters) in the vicinity of the Silver Strand cell.

IMPERIAL BEACH

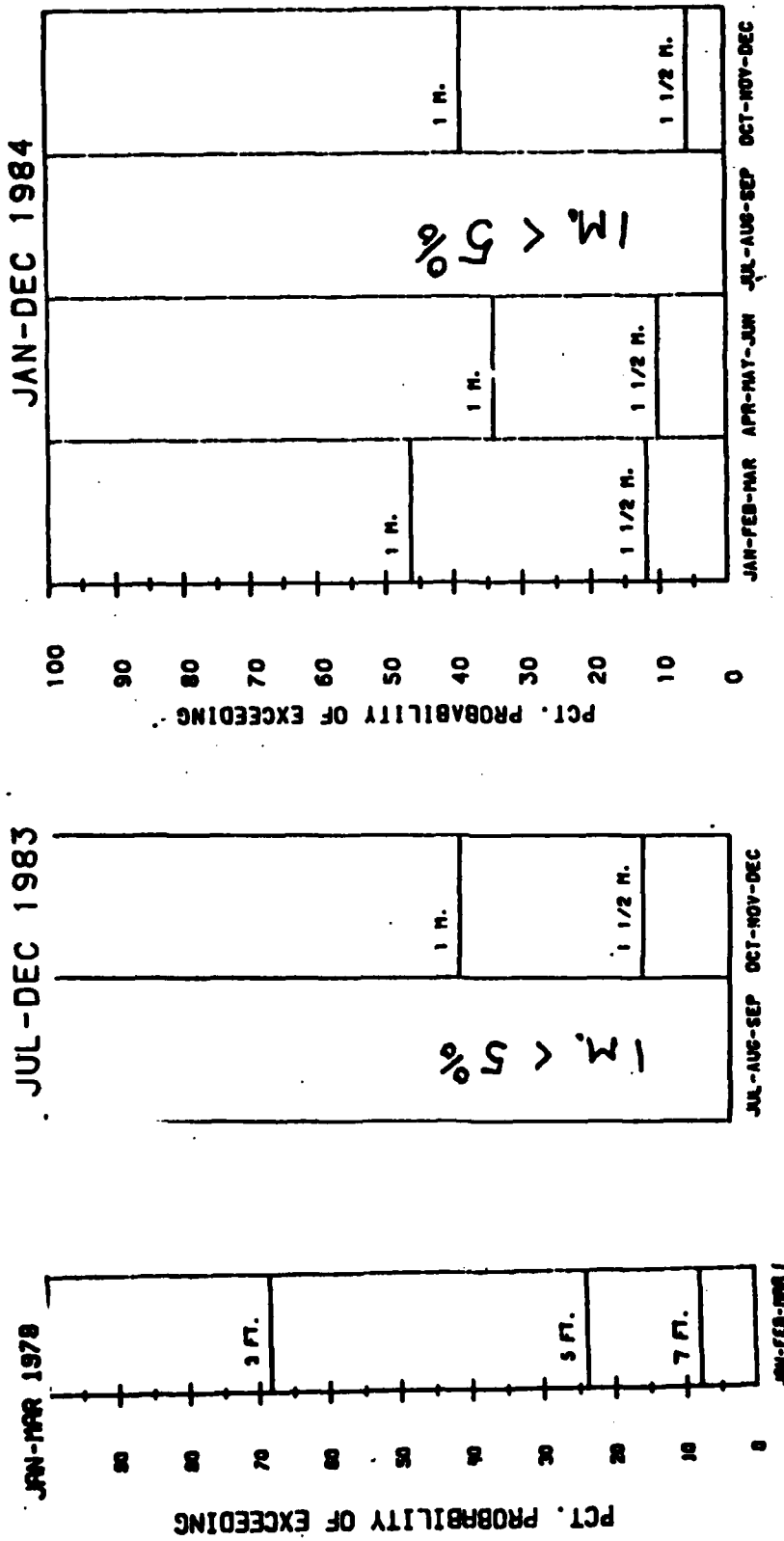
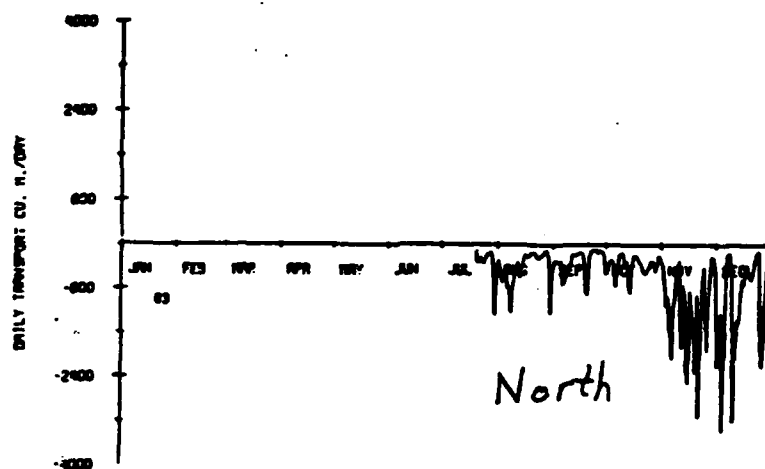


Figure 11.3-2 CDIP seasonal probabilities of exceeding various wave heights at Imperial Beach.

IMPERIAL BEACH ARRAY. DIRECTION
ANNUAL DATA 1983



IMPERIAL BEACH ARRAY. DIRECTION
ANNUAL DATA 1984

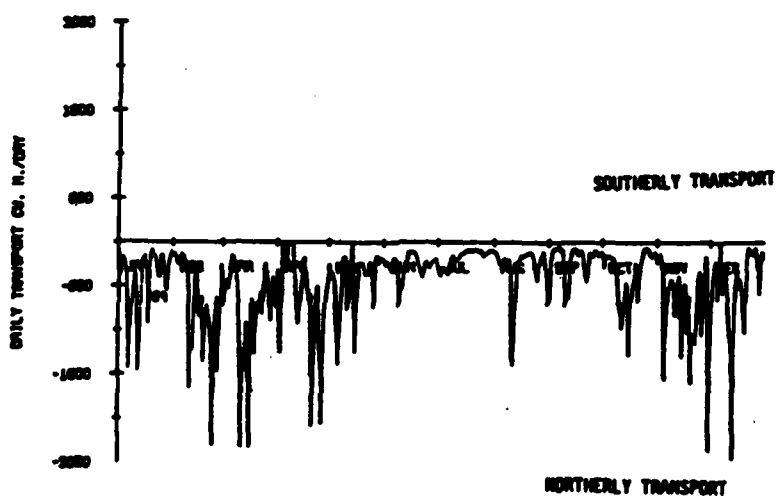


Figure 11.3-3 Net daily transports at Imperial Beach (CDIP annual reports).

reports but is apparently about 285° . A sketch from a 1985 monthly report is reproduced in Figure 11.3-4. The choice of 285° may reflect the orientation of bottom contours in the immediate vicinity of the Imperial Beach Pier, but seems an inappropriate choice for the general shoreline orientation. At any rate, the use of 285° as an offshore direction presumably explains the surprising unidirectional nature of the calculated transport. The offshore direction angles are explicitly given in the most recent monthly reports.

Inman et al (1974) used hindcast deep water wave statistics to estimate longshore sediment transport rates in the Silver Strand cell. Hindcast statistics used included UCSD (1947) and Marine Advisers (1961a) Station A. Island sheltering effects were crudely modelled as casting geometric shadows. The resulting coastal wave height statistics were believed to be "erroneously low." The resulting longshore transport values "will necessarily be lower than they should be, and perhaps indicate an erroneous direction of transport."

USACE LAD (1978b) also used Marine Advisers Station A hindcast data to estimate longshore transport rates. Island sheltering was modelled with geometric island shadows. Deep water wave directions greater than 300° were assumed to be completely shadowed; actually about 15% of this energy does reach Imperial Beach according to Figure 3.3.1-6. The refraction procedure used to propagate high angle (190° - 230°) southern swell over the complex shelf region to the south of Imperial Beach (Figure 11.3-1) is not described in detail. Apparently the southern islands were assumed to cast geometric shadows and the rest of the complex topography ignored; refraction diagrams show a homogeneous wave field directly offshore of the study site (Figure 11.3-4).

Because the same Marine Advisers Station A hindcast data that gave Inman et al (1974) unacceptably low wave height values was used by USACE LAD (1978b), the sheltered wave height statistics given in USACE LAD (1978b) (Tables C1, C2 and C3) were examined in detail. The 3 ft wave exceedance is about 16%. This compares to a 48% measured exceedance

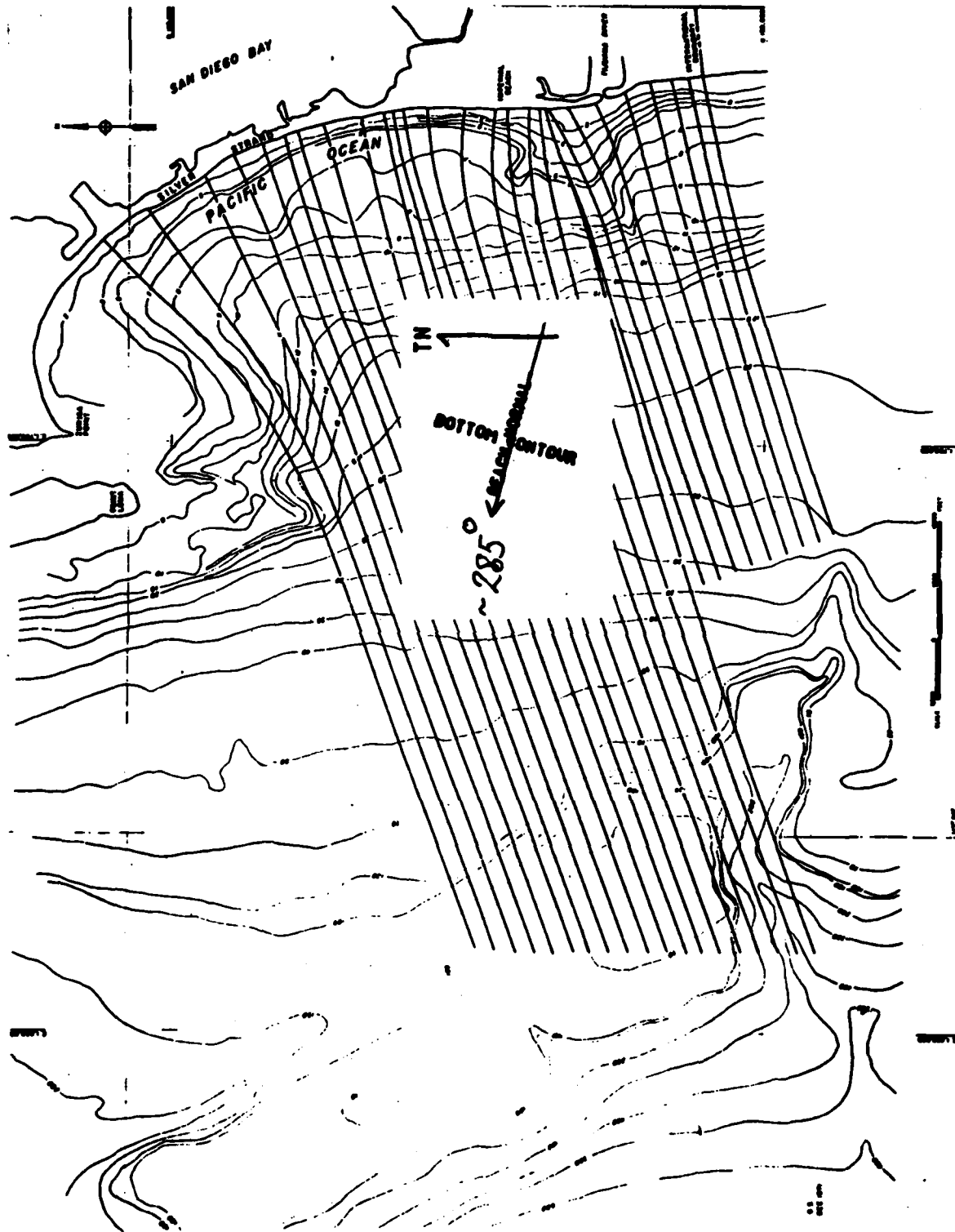


Figure 11.3-4 Refraction diagram for 12 second waves from 250° (USACE LAD, 1978b). The inset showing an approximately 285° beach normal is from a CDIP monthly report.

of 90 cm (3 ft) in the Imperial Beach CDIP data shown in Figure 11.3-2. Including the exceptionally calm 12 months of CDIP data for 1977 drops the CDIP exceedance to 30%. Note that the stormy winters of 1980 and 1983 are not included in this 30% exceedance. The basic hindcast data may be faulty (as suggested by Inman et al, 1974) or the use of a very simplified island blocking model may have resulted in substantial errors. The calculated net 100,000 yd^3/yr northward transport is only 13.5% of the gross total (USACE LAD, 1978b). The southern swell related transport is 103,000 yd^3/yr . As discussed in Section 3.2.2, Marine Advisers (1961a) explicitly state that there is at least a factor of two variability in the southern swell hindcast energies associated with their particular choice of hindcast years.

It seems clear that the combined inadequacies of the basic offshore wave hindcasts and the applied refraction methodologies result in very large error bars on the southern swell component of the USACE LAD (1978b) wave climatology. The problem is compounded by the fact that the net transport is the small difference of opposing effects. The point here is not that the 100,000 yd^3/yr net transport is necessarily wrong, but that there is not sufficient wave information to calculate meaningful longshore wave energy fluxes for this cell.

Groves (1953) developed a wave climatology for two shallow water sites near Point Loma using UCSD (1947) offshore hindcasts and observations at Mission Beach. Because of many approximations and the quality of the basic hindcasts, Groves considered his results "approximately qualitatively correct." He notes that "it would probably not be worthwhile to attempt to treat the problem with more accuracy without considering the complete two-dimensional spectrum of the waves." As yet, there are no hindcasts for this cell based on a two-dimensional spectrum.

11.4 NEARSHORE CURRENTS

Sonu et al (1978) deployed a current meter within San Diego Bay for 2 weeks. The observed currents are primarily tidal, with peak velocities of about 25 cm/sec, and are polarized

along the bay axis. Early current drogue studies conducted off the Point Loma sewage outfall are summarized by Maloney and Chan (1974). As at other shelf sites, the currents are highly variable both in speed and direction. Current monitoring projects in the vicinity of the Point Loma outfall are ongoing.

Some early references to observations of surf zone currents at Silver Strand Beach are given in Section 3.3. Inman et al (1971) used observations of the dilution of dye at Silver Strand Beach to infer the mixing and dispersion associated with both the passage of individual waves and the overall nearshore circulation system.

11.5 SEDIMENT SOURCES

11.5.1 *Cliff Erosion and Relict Dunes*

There are low active dunes along the Silver Strand Cell but there are no reports reviewed for this study which discuss the dunes as a sediment source.

11.5.2 *Sediment Discharge from Rivers and Streams*

The primary source of sediment in this littoral cell is the Tijuana River which has the largest drainage basin in southern California (4,483 km²). Nordstrom and Inman (1973) estimate that under natural conditions the Tijuana River supplies 660,000 yd³/yr of sand to the beaches. Damming of the river has apparently resulted in a 72% reduction of the available beach sand supply. USACE LAD (1970) contains sand grain size distribution for samples taken at North Island, Silver Strand and Imperial Beach. Inman et al (1974) further discuss the sources of sediment for this cell. Table 11.5-1 shows peak discharge data for the Tijuana River. This report also includes sand grain size distributions and mineral composition.

California (1977b) compiles information on sediment transport in coastal stream basins to provide order of magnitude estimates of sediment production and locations of abundant inland sources of material for beach nourishment. USACE LAD (1978) contains Inman et al (1974) along with an additional report discussing the sediment budget in the Silver Strand Cell. Brownlie and Taylor (1981) is a report summarizing water and sediment discharges for the Tijuana River. They estimate the annual sediment yield based upon the "sediment rating" curve which may lead to an underestimation of the bedload (see Inman and Jenkins, 1983, and Section 2.5). Figure 11.5-1 shows the Tijuana River drainage basin. USACE LAD (1984b) presents basic data on the geomorphology and the physical characteristics of the sediment in this littoral cell. The report discusses the inland basin sediment resources, the neotectonics and geomorphic processes of the area.

Table 11.5-1.
(from Inman et al, 1974)

Peak Discharge Data For Tijuana River

<u>Date</u>	<u>Peak Discharge</u>	
	<u>Cubic Feet/Second</u>	<u>Cubic Meters/Second</u>
February 1884	50,000	1,416
December 1889	20,000	566
February 1891	20,000	566
January 1895	38,000	1,076
24 March 1906	16,000	453
21 February 1914	5,000	142
17 January 1916	75,000	2,125
12 March 1918	16,000	453
26 December 1921	15,000	425
16 February 1927	25,000	708
18 February 1932	1,500	42
Rodriguez Dam Completed		
Summer 1936		
7 February 1937	17,700	501
3 March 1938	6,760	191
13 March 1938	1,600	45
24 December 1940	2,700	76
22 February 1941	15,000	425
15 March 1941	8,620	244
11 April 1941	10,400	295
17 March 1942	2,770	78
23 December 1944	2,100	59
7 January 1944	2,500	71
23 February 1944	13,800	391
13 January 1949	2,600	74
16 March 1952	3,560	101
7 December 1967	2,020	57

NOTE: Flood data is from Nestor gaging station on the Hollister St. Bridge. No floods less than 1,500 cubic feet/sec ($42 \text{ m}^3/\text{sec}$) are included and flood data prior to 1937 is based on historical data and information obtained from long-time residents and estimates based on data recorded from nearby streams. Table adapted from City of San Diego (1973).

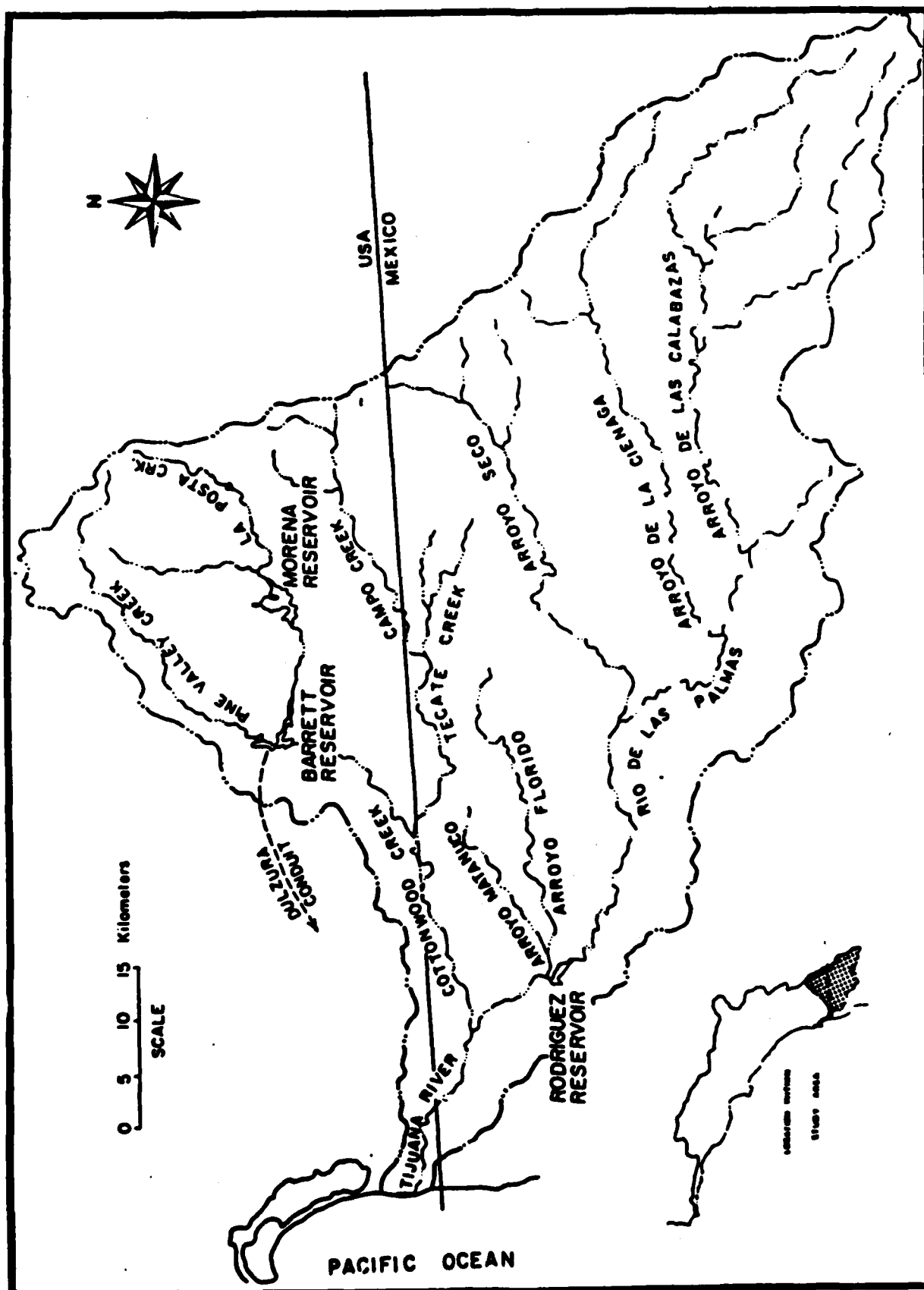


Figure 11.5-1. Tijuana River Basin (from Brownlie and Taylor, 1981).

11.5.3 *Artificial Beach Nourishment*

California (1977b) provides order of magnitude estimates of sediment production and location of abundant inland sources of material for beach nourishment. Many of the proposed borrow sites may not be available today because of changing land use. Sonu et al (1978) investigates an erosion problem inside San Diego Bay at the North Island Naval Station. The report discusses sources of fill material and grain size matching. Shaw (1980) inventories the man-made structures that intercept the sediment transport pathways along the coastline of southern California. The report describes shore protection projects, beach structures and the dates and amounts of beach fill. Herron (1980) briefly discusses the Silver Strand Cell and the placement of 33 million cubic yards of material on the beaches of the Silver Strand and the City of Coronado by the U.S. Navy during World War II. Osborne et al (1983) gives extensive data on offshore sand deposits. This report includes survey maps, vibracores and sediment petrology. Inman (1985c,d) in a letter report critiquing the proposed Imperial Beach breakwater discusses viable alternatives to the proposed remedial action. These include artificial sand nourishment, sand nourishment with a wave-absorbent seawall, adjustable groins with occasional sand nourishment and various combinations of these approaches.

11.6 SEDIMENT TRANSPORT MODES

11.6.1 *Cross-shore Transport*

Significant changes in beach profiles have been documented for beaches along the Silver Strand beaches (USACE LAD, 1960a). But it has become quite clear that these changes (principally erosional) are due primarily to the change in longshore transport caused by loss of source sand from the Tijuana River (Inman et al., 1974; Inman, 1976; USACE LAD, 1978b). Erosion is quite severe. USACE LAD (1960a) reports annual erosion of $27 \text{ yd}^2/\text{yr}$ at Imperial Beach in the 1950's and significant accretion only after beach nourishment projects.

Investigators have not attempted to separate profile changes due to longshore transport changes and offshore loss, except at the cell end, Zuniga Shoals (Figure 11.6-1), where transport must be in the offshore direction. Fortunately, most Corps profiles (USACE LAD, 1960a) extend far enough offshore that seasonal cross-shore changes are included in the profile. Thus the assumption that the noted erosion rates are due to longshore transport changes rather than cross-shore transport appears to be a safe assumption.

Sites which have been repeatedly profiled by the Corps are shown as solid dots in Figure 11.6-1. The profiles are characterized by flat backslopes, steep beach faces and gentle slopes offshore. Profiles from the five stations generally show steepest profiles at the Tijuana River mouth and along Silver Strand (Inman et al., 1974). Coronado and Imperial Beach have gentler slopes. Inman et al., (1974) show the extent of seasonal changes in the profiles, caused by offshore transport in the fall and onshore transport in the spring. It is important to note that the summer and winter profile lines do not converge until 9 m depth. It is fortunate that the Corps profiles extend to 10 m depth. If they had stopped somewhat shallower, it would be difficult to separate profile changes due to longshore transport variation from seasonal cross-shore changes.

Inman et al (1974) applied general physics of beach processes and studies from other sites to the available profile data in the Silver Strand Cell, in order to deduce patterns of cross-shore transport. They explain that deposition on a profile already in equilibrium results in onshore transport. Thus prior to the Zuniga Jetty construction in 1893-1904 the ebb tidal flow deposited sand in water sufficiently shallow (the Zuniga Shoals area in Figure 11.6-1) that it was transported back onshore to Silver Strand (Chamberlain et al., 1958). Thus net loss of sand from the cell was relatively small. Silver Strand now has beach profiles significantly steeper than areas with similar grain size. This suggests that the onshore reintroduction of sand into the cell stopped once Zuniga Jetty was constructed. The conclusive proof of this scenario is

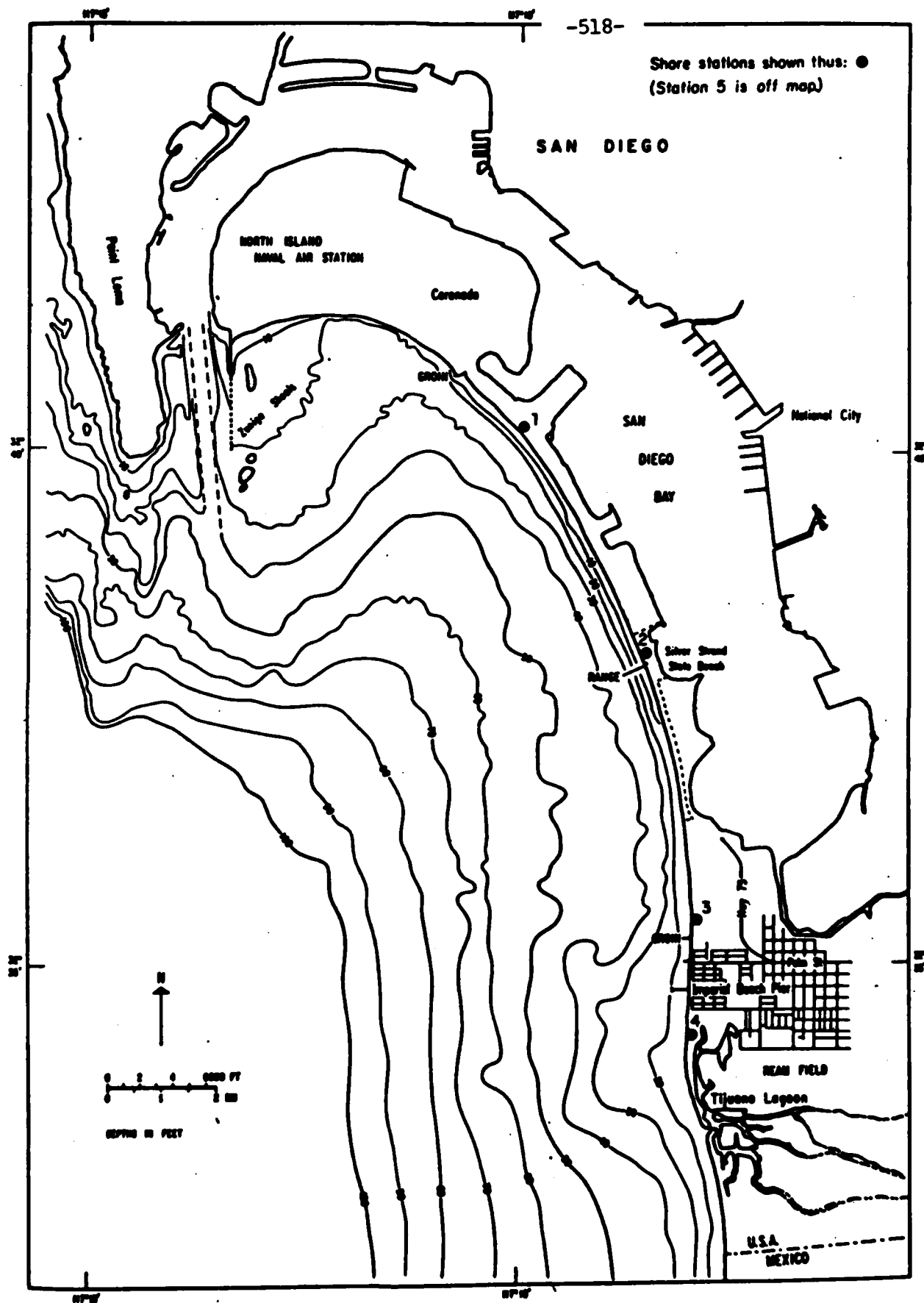


Figure 11.6-1. Silver Strand nearshore bathymetry and wave-refraction stations (from Inman et al., 1974).

the documentation by Chamberlain et al (1958) of 2×10^6 yd³/yr accretion in offshore depths of 50-100 ft between 1923 and 1937.

USACE LAD (1978b) computed volume changes from profiles taken from 1937 to 1975 from station 3 to station 4 at Imperial Beach (Figure 11.6-1). The volume between each of 15 profiling stations at each time surveyed was computed and is shown in Table 11.6-1. Because of intermittent profiling for some years, different methods of computing volumes were attempted. The average result for the two methods appears as the bottom line of the table in units of yd²/yr erosion. The numbers range from 12.4 to 13.6 yd²/yr. The total erosion is plotted in Figure 11.6-2, yielding an average annual erosion rate of 30×10^3 yd³/yr for this 9078 ft stretch of beach. It is important to note that changes at the seaward end of the profile were not observed. Thus it is more likely that erosion was due principally to longshore-transport variation, rather than cross-shore transport, despite USACE LAD's (1978b) entitling this data as "On-Offshore Transport Rates."

All studies on transport in this cell (Chamberlain et al., 1958; USACE LAD, 1960a; Inman et al., 1974; USACE LAD, 1978b) emphasize the lack of direct measurement of cross-shore transport in this cell. All information on cross-shore transport is inferred indirectly from changes in profile steepness and offshore bathymetry.

11.6.2 Longshore Transport

Longshore transport rates for this cell are summarized in Table 11.6-2. "Potential" rates are obtained from application of the standard "radiation stress" equation (Section 2.4) with wave data as inputs. Both volume transport Q_l (yd³/yr) and immersed-weight transport I_l (newtons/second) are listed. In converting between the two measures, it was assumed that solids concentration $N_o = 0.6$ (porosity = 0.4) and sand density $\rho_s = 2.65$ g/cm³. Positive values represent transport to the south, negative to the north.

Table 11.6-1. Beach cross-sectional area and computed volumes, Imperial Beach, California. (All values are $\times 10^6$ cu yds.)
(from USACE LAD, 1978b).

Station	Summer 1927	Fall 1946	Winter 1954	Winter 1956	Fall 1959	Summer 1962	Spring 1965	Summer 1967	Summer 1973	Summer 1975
515+00			31,540		32,433	32,933	33,670	33,433	33,203	28,870
520+00			31,930		32,500	33,200	35,000	34,500	34,260	
525+00			33,670		34,500	35,200	36,830	38,000	35,500	35,200
528+35						35,867			37,430	36,570
530+19	37,750	37,750	34,870	37,250	37,050	37,750	37,430	40,417	35,700	
541+00		40,450	39,167		39,850		40,767	41,850	39,834	
545+00		41,450	39,234	40,117	40,450		41,167	42,650	41,734	42,567
550+00		42,250	43,233				43,733	43,683	44,433	
560+00		43,517	43,030	42,850	47,184		42,300	43,317	44,033	
572+41		40,883	38,433					41,550	35,166	
577+74						40,000	38,334	39,667	37,567	38,067
586+23	43,533	36,433	34,067	35,167				38,600	29,233	37,900
591+00							36,333	34,783		
596+76							37,966	35,917	35,400	38,533
605+78							46,434		42,367	48,767
Weighted length V.	13.59	13.10	12.37	12.75	14.34	12.83	13.14	13.21.	12.57	12.99
Averaged area V.	13.55	13.46	12.31	12.95	12.57	11.94	13.05	13.04	12.52	12.77
Average	13.57	13.28	12.34	12.85	13.46	12.39	13.10	13.13	12.55	12.88

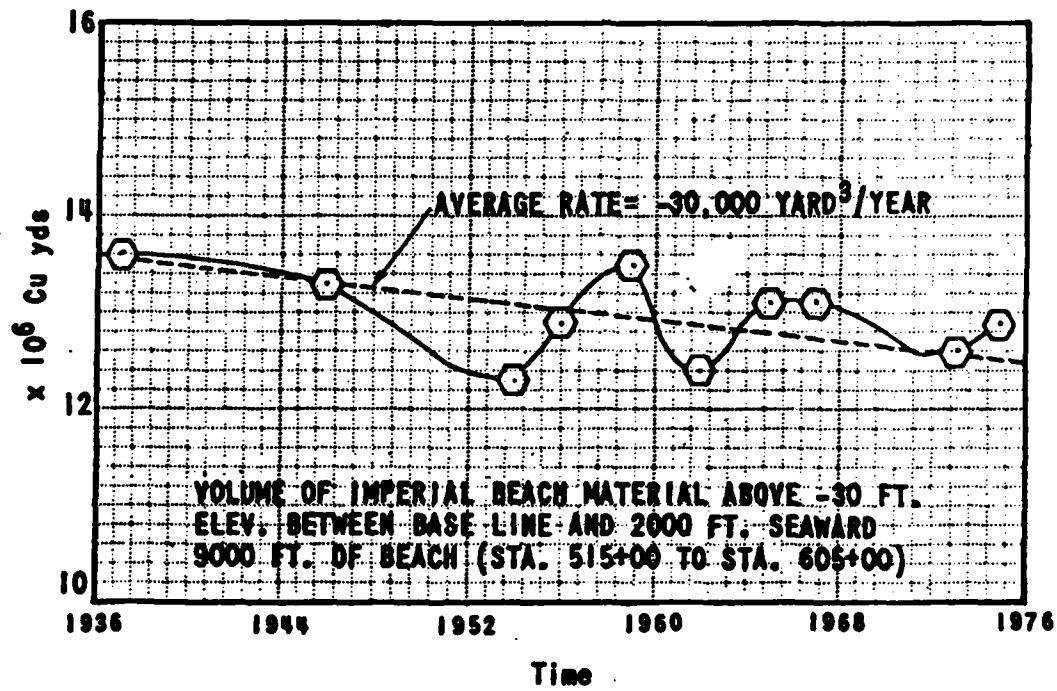


Figure 11.6-2. Imperial Beach sand volume changes (from USACE LAD, 1978b).

Table 11.6-2. Longshore Transport Rates
(Positive values indicate transport to the south, negative to the north)

Location	Notes	Reference	Potential Transport (Wave Refraction Studies)		Gross Transport (Trapping Studies)		Instantaneous Net Transport (Sand Tracer Studies)	
			Q_1 ($10^3 \text{ yd}^3/\text{yr}$)	I_1 (N/sec)	Q_1 ($10^3 \text{ yd}^3/\text{yr}$)	I_1 (N/sec)	Q_1 ($10^3 \text{ yd}^3/\text{yr}$)	I_1 (N/sec)
Silver Strand (between stations 2 and 3)	Low waves	Inman et al (1968)					55	13
	Medium waves	Inman et al (1968)					-183	-43
	High waves and large angle of incidence	Komar and Inman (1970)					-1284	-302
Station 1, Figure 11.6-1		Inman et al (1974)	-43	-10				
Station 2	Longshore cur- rents invalidate method	Inman et al (1974)	9	2				
Station 3	Longshore cur- rents invalidate method	Inman et al (1974)	98	23				
Station 5	Longshore cur- rents invalidate method	Inman et al (1974)	602	142				
Station 1	LEO visual wave observations	USACE LAD (1978b)	-384	-90				

Note: None of the measures in this cell are reliable estimates of average net transport.

Table 11.6-2. Longshore Transport Rates (Cont'd.)
(Positive values indicate transport to the south, negative to the north)

Location	Notes	Reference	Potential Transport (Wave Refraction Studies)		Gross Transport (Trapping Studies)		Instantaneous Net Transport (Sand Tracer Studies)	
			Q_1 ($10^3 \text{ yd}^3/\text{yr}$)	I_1 (N/sec)	Q_1 ($10^3 \text{ yd}^3/\text{yr}$)	I_1 (N/sec)	Q_1 ($10^3 \text{ yd}^3/\text{yr}$)	I_1 (N/sec)
Station 2	LEO visual wave observations	USACE LAD (1978b)	48	11				
Station 4	Severe topo-graphical variation	USACE LAD (1978b)	-100	-24				
Station 5	LEO visual wave observations	USACE LAD (1978b)	382	90				

Note: None of the measures in this cell are reliable estimates of average net transport.

Inman, Komar and Bowen (1968) used fluorescent sand tracers to measure the longshore transport rate at Silver Strand in 1967-68. Their study was located about halfway between stations 2 and 3 in Figure 11.6-1. They used these measurements to calibrate the "radiation stress" transport equation of Section 2.4 and obtained a value of K, the transport coefficient, of about 0.7. Komar and Inman (1970) refined this value to 0.77 and obtained the transport values listed in Table 11.6-2. The value of $183 \times 10^3 \text{ yd}^3/\text{yr}$ is probably a good estimate of net transport, except when the beach has been recently nourished. The rate of $1284 \times 10^3 \text{ yd}^3/\text{yr}$ ($3.5 \times 10^3 \text{ yd}^3/\text{day}$) is a good estimate of the maximum expected daily transport rate. Komar and Inman (1970) also obtained the only values of sand velocity and thickness of the moving sand layer available in this cell. Das (1971) reprints Komar and Inman's field data.

Nordstrom and Inman (1973) report a longshore transport rate of $1400 \times 10^3 \text{ yd}^3/\text{yr}$ to the north based on beach profiling and bathymetry off Zuniga Jetty. However, this value applies only to the very temporary nonequilibrium period of mid-1940's to mid-1950's when large plugs of beach fill were moving north. It should be considered an estimate of transport potential of large nourishment projects, not a transport under natural conditions.

Inman et al (1974) performed a wave refraction study and computed longshore transport rates with the radiation-stress equation at stations 1, 2, 3 and 5 on Figure 11.6-1. The net transport rates are reported in Table 11.6-2. The transport to the north at station 1 and to the south at station 5 (just off the southern edge of the map) were expected. The investigators did not expect the southerly transport obtained at stations 2 and 3, since it contradicts sand tracer studies (Inman, Komar and Bowen, 1968) and movement of beach fill. The authors caution that their data source underestimates southern-swell wave amplitudes, compared with data from nearshore sensors. Furthermore, station 3 is in an area of wave convergence where small errors in wave or bathymetry measurements produce large errors in transport estimates. Also strong topographically induced longshore currents are present at station 3. The radiation-stress

equation does not apply to situations where: 1) longshore currents have sources other than surface-gravity waves or 2) complex topography negates the assumption of simple relations between offshore wave energy and surfzone currents. Thus the estimates at stations 1 and 5 are reasonably accurate, but not the estimates at stations 2 and 3. The sand-tracer estimate of transport under medium wave conditions of $183 \times 10^3 \text{ yd}^3/\text{yr}$ to the north (Komar and Inman, 1970) is probably a better measure of longshore transport for those middle stations 2 and 3 than Inman et al's (1974) refraction-based estimates.

Table 11.6-3, taken from Inman et al (1974), details the seasonal variability of transport in the area. Inman et al (1974) point out that the area is in approximate equilibrium. (Roughly the same amounts of material are moved north in the summer and south in the winter.) This near-balance of transport rates illustrates two problems of interest to coastal engineers. First, the system is extremely sensitive to changes made in the coastline (beach nourishment, groins, etc.) In addition to manmade changes, it is important to remember that natural changes may occur. The wave climate varies from year-to-year, as does the Tijuana River flow and sediment discharge. Any of these changes could drastically alter net transport. Second, the wave refraction estimates of net transport are small differences between large gross transports.

USACE LAD (1978b) report the results of two longshore-transport studies at Silver Strand. The LEO program used visual estimates of wave heights and breaker angles as inputs to the radiation-stress equation. Their observations were made at three stations: "Yellow One" near Inman et al's (1974) station 1, Silver Strand (station 2) and the border (station 5). The observational durations were one year at stations 1 and 5, six years at station 2. Their estimates of net transport were $384 \times 10^3 \text{ yd}^3/\text{yr}$ to the north at station 1, $48 \times 10^3 \text{ yd}^3/\text{yr}$ to the south at station 2, and $382 \times 10^3 \text{ yd}^3/\text{yr}$ southerly transport at station 5. Since these estimates are all based on visual rather than measured wave data, they may be very inaccurate and are included here only for purposes of comparison.

Table 11.6-3. Longshore Transport Estimates Based on Longshore Component of Energy Flux (from Inman et al, 1974).

Longshore Transport Estimates Based on Longshore Component of Energy Flux, $I_L = K(E\cos\alpha)_b \sin\alpha \cos\alpha$ and Converted to Volume Transport by the Relation $S_L = I_L / (\rho_s - \rho) g N_o$.

SEASON	STATIONS			
	1	2	3	5
Winter (Dec-Mar)	- 10.9 (- 8.3)	-113.9 (- 87.1)	-167.2 (-127.8)	-305.4 (-233.5)
Transition (April-May)	- 6.7 (- 5.1)	- 0.3 (- 0.2)	- 37.1 (- 28.4)	-126.4 (- 96.6)
Summer (June-Sept)	+ 60.4 (+ 46.2)	+112.4 (+ 85.9)	+138.0 (+105.5)	- 89.5 (- 68.4)
Transition (Oct-Nov)	+ 0.3 (+ 0.2)	- 7.6 (- 5.8)	- 31.8 (- 24.3)	- 80.4 (- 61.5)
Net	43.1 (+ 33.0)	- 9.4 (- 7.2)	- 98.1 (- 75.0)	-601.7 (-460.0)

All values are $\times 10^3$ cubic yards per season, with $\times 10^3$ cubic meters in parentheses.

Negative values indicate southerly transport.

Positive values indicate northerly transport.

A longshore-transport study by the Corps Experimental Station (WES) is also included in USACE LAD (1978b). Their wave data is from Marine Advisors' (1961) deep-water wave measurements. They applied island-sheltering corrections and refracted the waves to the beach near station 4 (Figure 11.6-1). Their estimate of mean net annual transport is $100 \times 10^3 \text{ yd}^3/\text{yr}$ to the north, a value consistent with impoundment rates and tracer studies (Komar and Inman, 1970). Note that Inman et al (1974) did not compute transport at station 4. They state that "No longshore transport calculations were done for station 4 because of the very complex ridge topography offshore, which would invalidate calculations that in general require that there be little gradient in the breaker height along the shore." The WES longshore-transport estimates violate this assumption of small-breaker-height variation. Their estimates may not be accurate for this reason, and their estimates' agreement with other studies may be coincidental.

Both LEO and WES estimates of transport (USACE LAD, 1978b) were computed on a monthly basis and express seasonal variation. These numbers are not reprinted here, because they are subject to the same criticisms already mentioned. The "best" estimates of seasonal variation of transport are in columns 1 and 5 of Table 11.6-3.

Komar (1978) estimated a maximum ratio of suspended transport to total transport of 0.25 for Silver Strand from sand tracer studies of Inman, Komar and Bowen (1968). Komar's estimates of suspended load velocities for the area may be faulty, however, since he assumed that dyed sand did not leave the suspension sampling grid and further assumed that tracer would be of sufficiently high concentration to be detectable in the suspension samplers.

Sonu et al (1978) used wave and current measurements at the northern edge of North Island inside San Diego Bay to estimate longshore transport rates at that location. They estimate net longshore transport at that location to be $3 \times 10^3 \text{ yd}^3/\text{yr}$ inside the surfzone and $3 \times 10^3 \text{ yd}^3/\text{yr}$ outside the surfzone, both to the east. Note that the rate inside the surfzone is only a "potential" rate, since there usually is little sand there. Furthermore, the transport

equation used by the investigators is not the radiation-stress equation. It is a suspended-load equation based on unidirectional threshold-of-motion criteria and is only considered to be accurate within an order of magnitude.

11.6.3 *Wind Transport*

On the long stretch of Silver Strand beach between Coronado and Imperial Beach there are portions of the beach which are not obstructed by buildings or cliffs. These stretches of beach represent topographical bumps on a Pacific Ocean/San Diego Bay cross-section and thus present themselves as areas subject to wind erosion. We are unaware of any studies attempting to quantify such wind transport at Silver Strand. It is possible for such transport to represent a significant portion of net cross-shore sand transport, since net cross-shore transport by waves is small. However, the longshore component of wind transport is probably not significant compared with longshore transport by waves, since the latter is so large.

Wind transport should be small at North Island, Coronado and Imperial Beach due to the presence of structures and sea cliffs blocking the wind.

11.7 SEDIMENT SINKS

11.7.1 *Submarine Canyons*

Shepard and Einsele (1962) report on Coronado Submarine Canyon, the head of which is 12 statute miles offshore of the California-Mexico border (Figure 9.7-3). Their core samples indicate that some sand has been transported from the nearshore to Coronado Canyon. The size distribution of sand indicates that at some time sand flowed through the canyon. (Medium size sand is in the canyon channel and fine sand on the levees.) The most plausible explanation of sand presence there is that transport from the southern end of the Silver Strand Cell to Coronado Canyon was active during a time of lowered sea level when the canyonhead was close to the coast. Because the canyon is now so far from the coast, it is doubtful that any transport

from the coast has occurred in recent times.

11.7.2 *Entrapment by Harbors, Bays and Estuaries*

The two breaks in the coastline in this cell are the entrance to Tijuana Lagoon and San Diego Bay. The estuary at the Tijuana River mouth extends about 1.5 miles inland from the beach and occupies nearly the full width of the Tijuana River Valley (Inman et al., 1974). About one quarter of the lagoon is a salt marsh which is flooded by daily tides, and about one half of the estuary is flooded by spring tides.

Inman et al (1974) describe the stability of the lagoon entrance: "The tidal prism in the lagoon appears to be sufficient to maintain a natural opening since the lagoon has a history of open circulation with the ocean. Comparison of recent aerial photographs with others taken in 1956 and 1928 indicate that the lagoon entrance has changed very little in position or size. It appears that the location of the entrance along the barrier beach is affected by wave refraction over a shoal area just offshore. Refraction of most waves over this shoal creates a zone of convergence just to the north of the entrance. The presence of abnormally high waves in this area probably prevents the continued migrations of the entrance along the barrier beach."

Since the Tijuana Lagoon is in a natural state and the entrance is quite stable, presumably whatever sand reaches the inlet from the river is carried through the entrance and deposited on the beaches to the north and south. Since no significant sand deposits are visually evident in the estuary, most of the sand entrained downstream of the dams must reach the beaches. Inman (1976) describe the three different transport paths of the boulder/cobble, sand and silt/clay size fractions: "Once the fluvial sediment reaches the shoreline it comes under the influence of waves and currents which dominate the nearshore environment. These driving forces sort the sediment into specific size fractions that follow different transport paths in the coastal zone. The sediment load carried by the Tijuana River especially under flood conditions involves material ranging in size from boulders and cobbles, many cm in diameter, down to silt

and clay size material. Much of the coarsest material is deposited in the Tijuana Lagoon and at the mouth of the river where it has been slowly accumulating. These residual deposits consist almost entirely of cobbles and boulders too large to be moved by waves and nearshore currents so they remain as a vestigial delta at the mouth of the lagoon.

"The silt and clay fraction brought to the coast by the river stays in suspension as it flows into the ocean where it is distributed over a large area by the local currents. This fine material is often carried considerable distances offshore and along shore before it finally settles to the bottom.

"Sand sized material 2 mm to 0.064 mm is easily transported by the waves and becomes the source of sediment for the local beach. Upon reaching the beach the sand is then redistributed along the shoreline by the prevalent longshore currents."

Frautschy and Inman (1954) and Inman et al (1974) report on the self-scouring capability of the San Diego Bay entrance channel at the northern end of the cell. The volume of the tidal prism of a bay and the tidal range determine the head differential at the entrance. The scouring actions of the resulting tidal currents keep the channel open, while the transport of sand tends to close the channel. If the channel cross-section is constant, then these forces are in equilibrium. This is the case at San Diego Bay entrance channel. Channels which exhibit this balance fall on the straight line of Figure 11.7-1. If either the tidal prism or the channel cross-sectional areas are changed for San Diego Bay, then the channel could change from self-scouring to one needing dredging.

Since the channel is self-scouring, this means that any sand which leaks through or around Zuniga Jetty will not deposit in the channel, but in the harbor (on flood tide) or offshore (on ebb-tide). Bathymetric profiles confirm that nearly all the loss is offshore rather than into the bay (Chamberlain et al., 1958).

11.7.3 *Littoral Barriers*

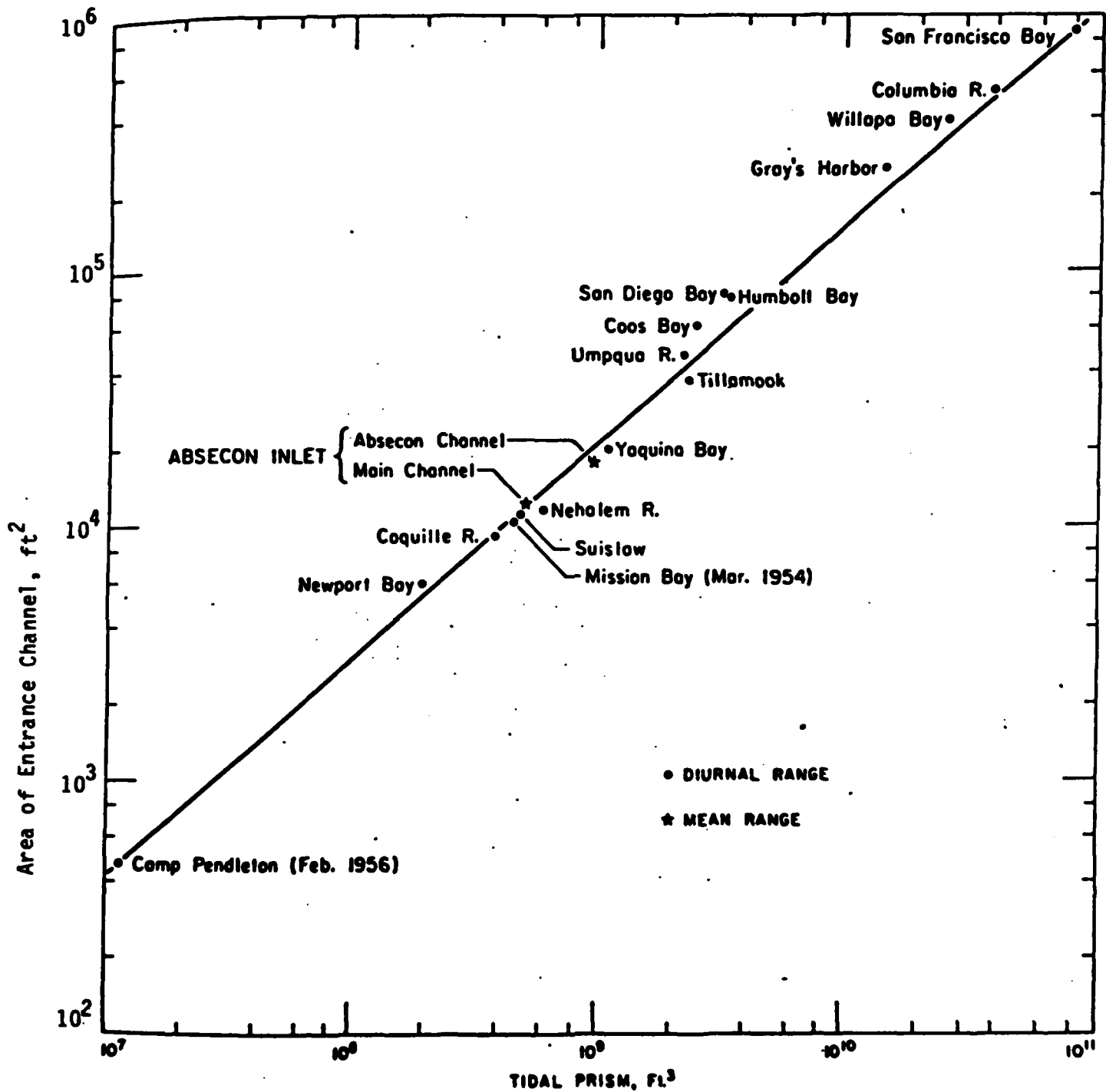


Figure 11.7-1. Plot of relationship between area of entrance channel and tidal prism for self-scouring inlets (from Inman, 1976).

The headland of Point Loma is a large natural feature that influences waves, currents and sand transport and forms the northern boundary of the cell. No other headlands are present in this cell to interrupt transport paths. The shore-normal structures consist of a pier, two groins, a breakwater and a jetty (Shaw, 1980). The 365 m wooden Imperial Beach pier was built in 1963 (Figure 11.6-1) and has essentially no effect on transport.

The Imperial Beach area has experienced continued erosion problems primarily due to the reduction of sand supply to Imperial Beach through damming of the Tijuana River. In an attempt to stop sand at Imperial Beach and prevent its further motion north, the federal, state and city governments financed the construction of two groins, with the possible later addition of up to seven more (USACE LAD, 1978b). The northern stone groin was built to 180 m in 1959 and extended to 220 m in 1963. The southern 120 m stone groin was built in 1961 (Figure 11.6-1). Predictably, the initial effect was accretion to the south and erosion to the north. However, erosion apparently now continues in the area due to inadequate source material.

Several plans have been considered to alleviate the erosion problem at Imperial Beach (USACE LAD, 1978b). They are seven groins, nine groins, a rubblemound revetment, beach nourishment, an offshore surface-piercing breakwater, and an offshore submerged breakwater. The plan selected for construction consists of a submerged breakwater and two terminal groins.

A 425 m rock breakwater was built at Hotel del Coronado in 1900 (Figure 11.6-1). It was originally intended to be used as a small boat anchorage, but instead functioned as a groin, trapping sand on the north side. It traps to the north rather than the south because it curves to the north, creating a wave shadow on the north side but not on the south. None of the reports reviewed for this study estimate the amount of trapped sand.

Zuniga Jetty is a 2285 m rubble-mound jetty completed in 1904. It was intended to stabilize the location of the harbor entrance. It has dramatically altered the transport paths of the northern portion of the Silver Strand Cell. Chamberlain et al (1958) estimated 2×10^6

yd³/yr of accretion was occurring in the offshore area of Figure 11.7-2. Inman (1985d) points out that this value is not a longshore transport rate. It is mostly deposition resulting from tidal scour. Prior to jetty construction, sand was deposited in the Zuniga Shoals area of Figure 11.7-2. It then was transported by waves back onto the Coronado Beach. This sand is now permanently lost to the cell offshore. In addition to this permanent sand loss, Inman et al (1974) explain the other beach changes induced by the jetty construction: "The construction of Zuniga Jetty altered the natural sand transport pattern at the north end of the cell in several ways. The most obvious effect of the jetty is to impound sand in the nearshore area on its east side. This has caused the beach to increase in width at the base of the jetty and seaward extension of the shoal area along its east side. Since the jetty is a porous structure, some sand continues to enter the entrance channel where it is carried seaward by tidal currents. The jetty constricts the tidal flow in the channel out beyond the tip of Point Loma so that sand is transported into deeper water where it is not returned to the beach."

11.7.4 *Wind Transport*

As explained in Section 11.6.3, it is possible for cross-shore wind transport to act as a significant sediment sink in the Silver Strand area. In that area the winds are not blocked by cliffs or structures. The significance of loss due to wind transport is conjecture at this point, since no studies on this topic have been performed in this cell.

11.7.5 *Berm Overwash and Offshore Loss*

Inman et al (1974) discuss the effect of tsunami waves on the Silver Strand. They point out that Silver Strand Beach is only 3 m in elevation along much of its length and thus subject to berm overwash and loss of sediment into San Diego Bay. This possibility of overwash may also occur at storm-wave high-tide coincidence in addition to the tsunami situation discussed by Inman et al (1974). Whalin et al (1970) relate the results of model studies of wave runup on

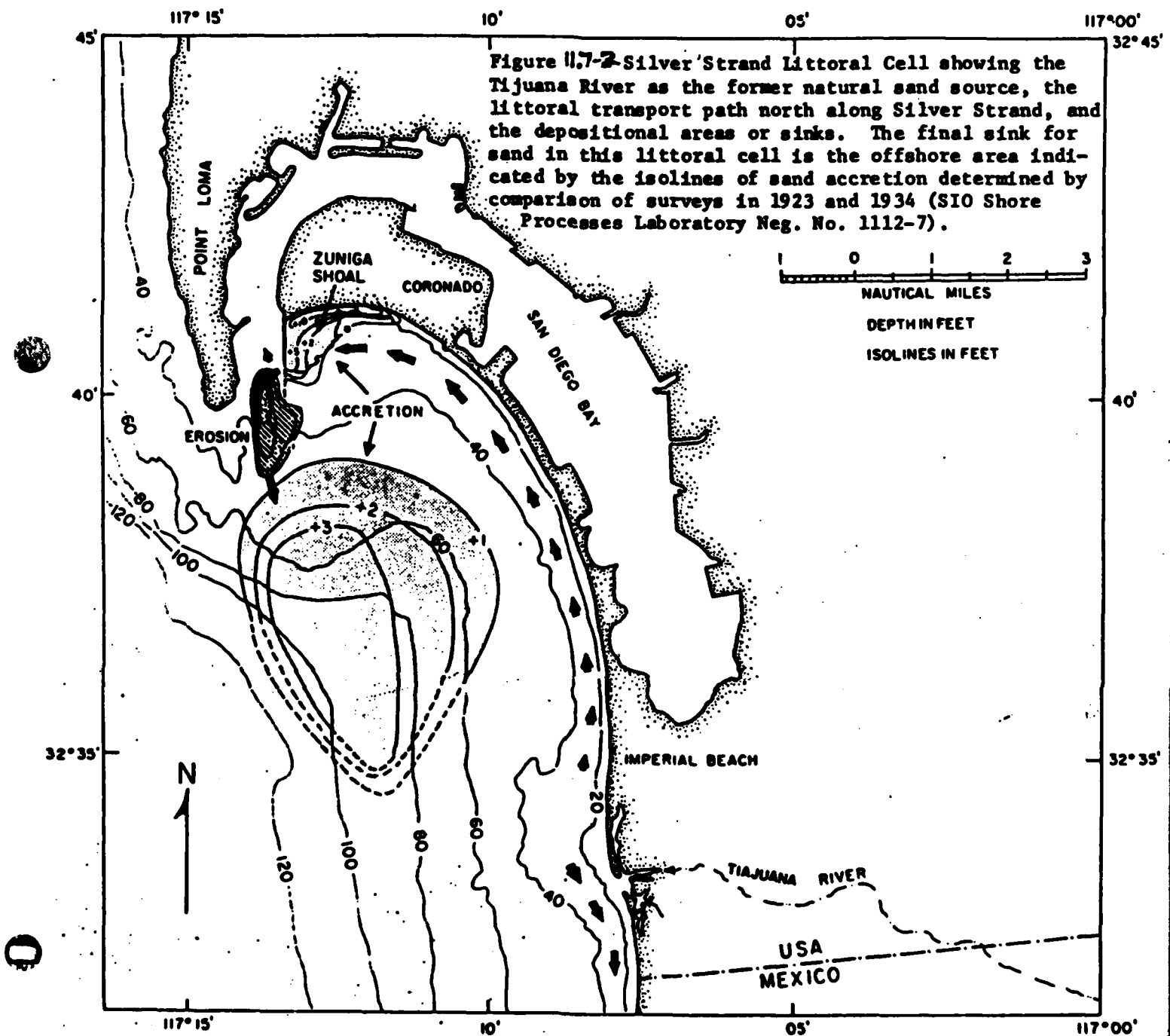


Figure 11.7-2. Silver Strand Littoral Cell transport paths and sinks (from Inman et al., 1974).

Silver Strand and Coronado, conducted at the Waterways Experiment Station. In these studies of low-frequency waves, overtopping of Silver Strand Beach occurred with considerable destruction. Silver Strand beach is clearly more subject to sediment loss by overwash than most southern California beaches, because of its topography.

The Silver Strand Cell is one of the few cells where offshore loss of sediment is well documented. The study of bathymetric records by Chamberlain et al (1958) documenting changes caused by Zuniga Jetty clearly shows continuing accretion offshore in water too deep for the waves to return the sediment to the beach (Figure 11.7-2). Chamberlain's study was performed at a time when much more sediment was available for transport, at both the northern end of the cell and in the San Diego Bay entrance channel. Today's rate of offshore loss is undoubtedly lower than Chamberlain's estimate of 2×10^6 yd³/yr, but must still be significant.

11.8 BUDGET OF SEDIMENTS

Nordstrom and Inman (1973) were the first to apply the concept of sediment budget to the Silver Strand Cell. This report was followed by Inman et al (1974), which was re-distributed as USACE LAD (1978b). The report is the only complete sediment budget study of this littoral cell to date. It is estimated that currently only about 185,000 yd³/yr of sand reaches the coast from this cell's only source of sediment, the Tijuana River. Longshore transport rates are summarized in Table 11.6-2, which shows the varying rates and directions.

Core samples show that some sand has been transported down the Coronado Submarine Canyon (Shepard and Einsele, 1962), but there is currently no other evidence that the canyon is an active sink for sands. The Zuniga Jetty at the entrance to San Diego Bay is the primary littoral barrier in this cell. Chamberlain et al (1958) estimated 2×10^6 yd³/yr of accretion was occurring in the offshore area just south of the jetty. Inman (1985d) points out that this is not

a longshore transport rate. Rather this is mostly deposition resulting from tidal scour caused by the construction of Zuniga Jetty. True this deposit is the ultimate sink of Silver Strand littoral drift, but that littoral drift is only a small part of the net deposition. Further, the rate of entrapment of sand behind Zuniga Jetty is not a net littoral transport either. This is because the jetty protects the area from west and northwesterly waves, so that this is an entrapment rate rather than the net longshore transport rate. There is both southerly and northerly transport of sand elsewhere along the Silver Strand, and the difference is the net transport. Figure 11.7-2 illustrates the source, transport path and sink for the sediments in the Silver Strand Cell. Table 11.8-1 provides order of magnitude estimates of the amount of sediment introduced to this cell, the net rate at which it moves along the shore, and the amount lost from the cell.

Table 11.8-1. Summary of sediment budget, Silver Strand
Littoral Cell.

Sources of Sediment

A. Tijuana River (from Inman et al, 1974)

- | | |
|-----------------------|-----------------------------|
| 1. Natural conditions | 660,000 yd ³ /yr |
| 2. Present conditions | 184,800 yd ³ /yr |

Net Longshore Transport Rate (from Komar and Inman, 1970)

- A. 183,000 yd³/yr to the north

Sediment Sinks

A. Zuniga Shoals (from Chamberlain et al, 1958)

2×10^6 yd³/yr

12. REFERENCES

- Abdelrahman, S. M., 1983, "Longshore Sand Transport Distribution Across the Surf Zone Due to Random Waves," M.S. Thesis, *Naval Postgraduate School*, Monterey, Calif., 87 pp. COE Ref # 1
- Allen, J. S., 1980, "Models of wind driven currents on the continental shelf," *Annual Review of Fluid Mechanics*, v. 12, p. 389-433.
- Allen, J. S. and R. L. Smith, 1981, "On the dynamics of wind-driven shelf currents," *Phil. Trans. Royal Soc. London A*, v. 302, p. 617-634.
- Armstrong, G. A., 1980, "Coastal Winter Storm Damage, Malibu, Los Angeles County, Winter 1977-78," p. 423-452 in *Floods and Debris Flows in Southern Calif. and Ariz., 1978-1980, Proc. of Symp.*, Sept. 17-18, 1980, Nat'l. Res. Council and C.I.T., Nat'l. Academy Press, Washington, D.C. COE Ref # 3
- Arthur, R. S., 1951, "The Effect of Islands on Surface Waves," Bulletin of Scripps Inst. of Ocean., *Univ. of California Press*, Berkeley, Calif., v. 6, n. 1, p. 1-26; and *Univ. of Calif.*, Scripps Inst. Oceanography, Reference Series 51-23, 28 pp. COE Ref # 4
- Artim, E. R., 1981, "Sea cliff retreat: a case study at Oceanside, California," p. 84-96 in P. L. Abbott and S. O'Dunn (ed.) *Geologic Investigations of the Coastal Plain, San Diego County, California*, San Diego Assn. of Geologists, 166 pp.
- Asquith, D. O., 1983, "Rates of Coastal Bluff Retreat, Pismo Beach, California," p. 1195-1207 in *Coastal Zone 1983, Symposium*, San Diego, California, June 1-4, 1983, ASCE, N.Y., Vol. II. COE Ref # 236
- Aubrey, D. G., 1978, "Statistical and dynamical prediction of changes in natural sand beaches," Ph.D. Thesis, *Univ. of California at San Diego*, 194 pp.
- Aubrey, D. G., 1979, "Seasonal Patterns of Onshore/Offshore Sediment Movement," NOAA Office of Sea Grant Report No. WHOI-CONTRIB-4354; NOAA-79122615, 9 pp.; and *Jour. of Geophysical Research*, v. 84, n. C10, 20 October, 1979, p. 6347-6354. COE Ref # 7
- Aubrey, D. G. and K. O. Emery, 1983, "Eigenanalysis of recent United States sea levels," *Cont. Shelf Research*, v. 2, n. 1, p. 21-33.
- Aubrey, D. G., D. L. Inman and C. E. Nordstrom, 1976, "Beach Profiles at Torrey Pines, California," p. 1297-1311 in *Proceedings of 15th Coastal Engineering Conference*, Honolulu, Hawaii, July 11-17, 1976, ASCE. COE Ref # 6
- Aubrey, D. G., D. L. Inman and C. D. Winant, 1980, "The statistical prediction of beach changes in southern California," *Jour. of Geophysical Research*, v. 85, n. C6, p. 3264-3276. COE Ref # 8

- Bagnold, R. A., 1941, *The physics of blown sand and desert dunes*, Wm. Morrow and Co., New York. 265 pp.
- Bagnold, R. A., 1963, "Mechanics of marine sedimentation," p. 507-528 in M. N. Hill (ed.) *The Sea*, v. 3, *The Earth Beneath the Sea*, Interscience Publ., New York, London, 963 pp.
- Bagnold, R. A., 1966, "An approach to the sediment transport problem from general physics," *U.S. Geological Survey*, Professional Paper 422-I, 37 pp.
- Bailard, J. A. and D. L. Inman, 1981, "An energetics bedload model for a plane sloping beach: local transport," *Jour. of Geophysical Research*, v. 86, n. C3, p. 2035-2043. COE Ref # 11
- Bailard, J. A. and S. A. Jenkins, 1982, "City of Carpinteria beach erosion and pier study," City of Carpinteria, CA., 292 pp.
- Balsillie, J. H., 1975, "Surf observations and longshore current predictions," *U.S. Army Corps of Engineers*, Coastal Engineering Research Center, Technical Memo 58, Vicksburg, MS, 49 pp. COE Ref # 15
- Barber, N. F., M. J. Tucker, 1962, "Wind Waves," in M. N. Hill (ed.) p. 664-699, v. 1, *Physical Oceanography, The Sea, Ideas and Observations on Progress in the Study of the Seas*, Interscience Publishers, John Wiley & Sons, N. Y. COE Ref # 16
- Barber, N. F. and F. Ursell, 1948, "The generation and propagation of ocean waves and swell," *Phil. Trans. Royal Society London, A*, v. 240, p. 527-560.
- Barnett, T. P., 1983a, "Recent changes in sea level and their possible causes," *Climate Change*, v. 5, p. 15-38.
- Barnett, T. P., 1983b, "Long term changes in dynamic height," *Jour. Geophysical Research*, v. 88, n. C14, p. 9547-9552.
- Barnett, T. P., 1984, "The estimation of 'global' sea level changes: a problem of uniqueness," *Jour. Geophysical Research*, v. 89, n. C5, pp. 7980-7988.
- Basco, D. R., 1982, "Surf zone currents, Volume I, State of Knowledge," *U.S. Army Corps of Engineers*, Coastal Engineering Research Center, Technical Paper 82-7(1), Vicksburg, MS, 243 pp. COE Ref # 18
- Bascom, W. N., 1951, "Investigation of coastal sand movements near Santa Barbara, California, Part I," *Univ. of California, Berkeley*, Inst. Engineering Research, Ser. 14, Issue 8, Pt. 1, 38 pp. COE Ref # 22
- Battjes, J. A., 1974, "Surf similarity," *Proc. 14th Coastal Engineering Conference*, Amer. Society of Civil Engineers, New York, p. 466-479.
- Belly, P-Y, 1964, "Sand movement by wind," *U.S. Army Corps of Engineers*, Coastal Engineering Research Center, Technical Memo No. 1, 80 pp.

- Bloom, A. J. (compiler). 1977. *Atlas of sea-level curves*, IUGS, UNESCO, Intl. Geological Correlation Program, Project 61, 100 pp.
- Borgman, L. E. and N. N. Pannicker, 1970, "Design Study for a suggested wave gage array off Point Mugu, California," *Univ. of California, Hydraulic Engineering Laboratory, Berkeley*. Technical Report HEL-1-14, 23 pp. COE Ref #355
- Bowen, A. J. and D. L. Inman, 1966, "Budget of littoral sands in the vicinity of Point Arguello, California," *U.S. Army Corps of Engineers, Coastal Engineering Research Center*, Technical Memo 19, Vicksburg, MS, 55 pp. COE Ref #30
- Bowen, A. J. and D. L. Inman, 1969, "Rip currents, Part 2: Laboratory and field observations," *Jour. Geophysical Research*, v. 74, p. 5479-5490.
- Bowen, A. J. and D. L. Inman, 1971, "Edge waves and crescentic bars," *Jour. Geophysical Research*, v. 76, p. 8662-8671.
- Bowen, A. J., D. L. Inman and V. P. Simmons, 1968, "Wave set-down and set-up," *Jour. Geophysical Research*, v. 73, n. 8, p. 2569-2577.
- Bretschneider, C. L., 1957, "Revisions in wave forecasting: deep and shallow water," *U.S. Army Corps of Engineers, Beach Erosion Board, Hydraulic Engineering Research*.
- Brink, K. H., D. Chausse and R. E. Davis, 1985, "Moored current meter and wind recorder measurements near Point Conception, California: The 1983 OPUS Observations," *Woods Hole Oceanographic Inst.*, Technical Report WHOI-85-1.
- Brown, A. J., 1983, "Space and time relationships on Ventura County Beaches, California," Ph.D. Thesis, *Univ. of California at Los Angeles, Calif.*, Geology Department, 163 pp. COE Ref #34
- Brown, G. M. and P. W. Leftwich, 1982, "Compilation of eastern and central north Pacific tropical cyclone data," *U.S. Department of Commerce, NOAA Technical Memo 82080613*, National Hurricane Center, Coral Gables, Florida, 21 pp. COE Ref #237
- Brownlie, W. R. and W. R. Brown, 1978, "Effects of Dams on Beach and Sand Supply," p. 2273-2287 in *Coastal Zone '78*, v. I, ASCE, N.Y. COE Ref #35
- Brownlie, W. R. and B. D. Taylor, 1981, "Sediment management of southern California mountains, coastal plains and shoreline - Part C, Coastal Sediment Delivery by major rivers in So. Calif.," *California Inst. of Technology, Environmental Quality Lab Report No. 17-C*, Pasadena, Calif., 314 pp. COE Ref #36
- Bruno, R. O., R. G. Dean and C. G. Gable, 1981, "Longshore sand transport study at Channel Islands Harbor, California," *U.S. Army Corps of Engineers, Coastal Engineering Research Center*, Technical Paper 81-2, Vicksburg, MS, 48 pp. COE Ref #39
- Bruno, R. O. and C. G. Gable, 1976, "Longshore transport at a total littoral barrier," *Proceedings, 15th Coastal Engineering Conference, ASCE, NY*, p. 1203-1222. COE Ref #37.

- Bruno, R. O., G. M. Watts and C. G. Gable, 1978. "Sediments impounded by an offshore barrier," *U.S. Army Corps of Engineers*, Coastal Engineering Research Center. Reprint 78-8, Vicksburg, MS, 20 pp. COE Ref # 38
- Bruun, P., 1954, "Coast erosion and the development of beach profiles," *U.S. Army Corps of Engineers Beach Erosion Board*, Technical Memo 44. Washington, D. C. COE Ref # 42
- Burdette, E. L. and W. W. Howard, 1982, "Intercomparison of directional wave spectra from an NDBO discus-hulled buoy and a wavestaff array," *Proceedings, Oceans '82 Conference*, p. 1282-1287.
- Caldwell, J. M., 1956, "Wave action and sand movement near Anaheim Bay, California," *U.S. Army Corps of Engineers, Beach Erosion Board*, Technical Memo 68, Washington, D. C. COE Ref # 44
- California, 1977a, "Assessment and Atlas of Shoreline Erosion along the California Coast," *State of California*, Dept. of Navigation and Ocean Development, The Resources Agency, Sacramento, 69 pp. COE Ref # 50
- California, 1977b, "Study of Beach Nourishment along the Southern California Coastline," *State of California*, Dept. of Navigation and Ocean Development, The Resources Agency, Sacramento, 150 pp. COE Ref # 51
- Cardone, V. J., W. J. Pierson and E. G. Ward, 1976, "Hindcasting the directional spectra of hurricane-generated waves," *Jour. Petrol. Tech.*, v. 25, p. 385-394.
- Cardone, V. J., H. Carlson, J. A. Ewing, K. Hasselmann, S. Lazanoff, W. McLeish and D. Ross, 1981, "The surface wave environment in the GATE B/C scale - Phase III," *Jour. Geophysical Oceanography*, v. 11, p. 1280-1293.
- Castel, D. and R. J. Seymour, 1982, "Longshore Sand Transport Report, February 1978 through December 1981," *Univ. of California*, Scripps Institution of Oceanography, Nearshore Research Group, Institute of Marine Resources, La Jolla, Calif., 216 pp. COE Ref # 55
- Cayan, D. R. and R. E. Flick, 1985, "Extreme sea levels in San Diego, California, Winter 1982-83," *Univ. of California, San Diego*, Scripps Inst. of Oceanography, Reference Series 85-3, 58 pp.
- Chamberlain, T. K., 1960, "Mechanics of Mass Sediment Transport in Scripps Submarine Canyon," *Univ. of California at San Diego*, Ph. D. Dissertation in Oceanography, Scripps Inst. of Oceanography, La Jolla, Calif., 200 pp. COE Ref # 58
- Chamberlain, T. K., 1964, "Mass Transport of Sediments in Head of Scripps Submarine Canyon, California," p. 42-64 in R. I. Miller (ed.), *Papers in Marine Geology*, Shepard Commemorative Volume, Macmillan & Co., N.Y. COE Ref # 59
- Chamberlain, T. K., P. L. Horrer and D. L. Inman, 1958, "Analysis of littoral processes for dredge fill, Carrier Berthing Facilities, Naval Air Station, North Island, San Diego,

- California," unpublished report, *Marine Advisors, Inc.*, La Jolla, CA. 41 pp - figs. tbl., pl.
- Chatham, C. E., D. E. Davidson and R. W. Whalin, 1973. "Study of beach widening by the perched beach concept, Santa Monica Bay, California," *U.S. Army Corps of Engineers*, Waterways Experiment Station. Technical Report H-73-8, Vicksburg, MS, 100 pp. COE Ref # 61
- Chelton, D. B., 1983, "Effects of sampling errors in statistical estimation," *Deep-Sea Research*, v. 30, n. 10a, p. 1083-1103.
- Chelton, D. B. and R. E. Davis, 1982. "Monthly mean sea-level variability along the west coast of North America," *Jour. Physical Oceanography*, v. 12, n. 8. p. 757-784.
- Clancy, R. M., R. E. Camfield and C. Schneider, 1983, "Low-cost measurements of shoreline change," p. 717-726 in *U.S. Army Corps of Engineers*, Coastal Engineering Research Center, Reprint 83-11, Vicksburg, MS, 10 pp. COE Ref # 63
- Colby, B. R. and C. H. Hembree, 1955, "Computations of total sediment discharge," *U.S. Geological Survey*, Water Supply Paper No. 1357, 187 pp.
- Collins, J. I., 1972, "Prediction of shallow-water spectra," *Jour. Geophysical Research*, v. 77, n. 15, p. 2693-2707.
- Cook, D. O., 1970, "The occurrence and geological work of rip currents off Southern California," *Marine Geology*, v. 9, n. 3, p. 173-186. COE Ref # 68
- Cramer, A. J. and R. D. Pauly, 1979, "Shore processes at a man-made headland," *Shore and Beach*, v. 47, n. 3, p. 2-7. COE Ref # 96
- Crease, J., 1956, "Propagation of long waves due to atmospheric disturbances in a rotating sea," *Proc. Royal Society London, A*, v. 233, p. 556-569.
- Cross, Ralph H., 1980, "Ocean wave statistics for San Francisco," *Jour. of the Amer. Shore and Beach Preservation Assoc.*, v. 48, n. 3, p. 26-29.
- Crouch, J. K., 1981, "Northwest margin of California continental borderland: marine geology and tectonic evolution," *Amer. Assoc. Petroleum Geologists Bulletin*, v. 65, n. 2, p. 191-218.
- Curray, J. R., 1960, "Sediments and history of Holocene transgression, continental shelf, northwest Gulf of Mexico," p. 221-226 in F. P. Shepard, F. B. Phleger and T. H. van Andel (eds.) *Recent Sediments, Northwest Gulf of Mexico, 1951-1958*, Amer. Assn. of Petroleum Geologists, Tulsa, OK, 394 pp.
- Curray, J. R., 1961, "Late Quaternary sea level: a discussion," *Geological Society of America Bulletin*, v. 72, n. 11, p. 1707-1712.
- Curren, C. R. and C. E. Chatham, 1977, "Imperial Beach, California, Design of Structures for Beach Erosion Control," *U.S. Army Corps of Engineers*, Waterways Experiment

Station. Technical Report H-77-15. Vicksburg, MS, 161 pp. COE Ref # 72

- Curren, C. R and C. E. Chatham, 1980, "Oceanside Harbor and Beach. California, Design of Structures for Harbor Improvement and Beach Erosion Control. Final Report." *U.S. Army Corps of Engineers*, Waterways Experiment Station. Technical Report HL-80-10, Vicksburg, MS. 350 pp. COE Ref # 73
- Darnes & Moore, 1982, "Environmental report (production). Supporting Technical Data. Environmental Setting, Santa Ynez Unit Development, Unit Operations, v. 2, Exxon Co., U.S.A., *Darnes & Moore, Inc.*
- Darnes & Moore, 1983, "El Segundo Marine Terminal (ESMT) Protection Project, El Segundo Refinery. Initial Study," *Darnes & Moore* for Chevron U.S.A., Inc., Job No. 00113-668-15. Marine Services, Los Angeles, California, 100 pp. COE Ref # 75
- Dana, R. H., Jr., 1909. *Two Years Before the Mast*, P. F. Collier & Son, New York, 405 pp.
- Das, M. M., 1971, "Longshore Sediment Transport Rates; A Compilation of Data," *U.S. Army Corps of Engineers*, Coastal Engineering Research Center, Misc. Paper 1-71, Vicksburg, MS. COE Ref # 76
- Dean, R. G., E. P. Berek and C. G. Gable, 1982, "Longshore transport determined by an efficient trap," *Proceedings, 18th Coastal Engineering Conference, ASCE, NY*, p. 954-968. COE Ref # 79.
- Dickinson, W. R., 1981, "Plate tectonics and the continental margin of California," p. 1-28 in W. G. Ernst (ed) *The Geotectonic Development of California*, Prentice-Hall, Inc., Englewood Cliffs, NJ, 706 pp.
- Dill, R. F., 1964, "Sedimentation and Erosion in Scripps Submarine Canyon Head" pp. 2-41 in *Papers in Marine Geology*, Shepard Commemorative Volume, R. I. Miller, Ed., Macmillan & Co., N. Y.
- Disney, L. P., 1955, "Tide heights along the coasts of the United States," *Proceedings, Hydraulics Division, ASCE*, v. 81, n. 666, p. 1-9.
- Dobson, R. S., 1967, "Some applications of digital computer to hydraulic engineering problems," *Stanford Univ., Dept. of Civil Engineering*, Technical Report 80.
- Dolan, R., B. Hayden, S. May, 1983, "Erosion of the U. S. Shorelines," pp. 285-299 in Paul D. Komar (ed.), *Handbook of Coastal Processes and Erosion*, CRC Press, Boca Raton, Florida. COE Ref # 81
- Domurat, G. W., 1978, "Winter Storm Damage Along the California Coast 1977-78," *U. S. Army Corps of Engineers*, San Francisco District, 75 pp., and *Shore and Beach*, v. 46, n. 3, p. 15-20. COE Ref # 82
- Douglas, A. and H. C. Fritz, 1972, "Tropical cyclones of eastern north Pacific and their effects on climate of the western United States," *Univ. of Arizona, Tucson*, Laboratory of Tree Ring Research, Final Report to NOAA Contract 1-35741.

- Drake, D. E., R. L. Kolpak and P. J. Fischer, 1972, "Sediment Transport on Santa Barbara-Oxnard Shelf, Santa Barbara Channel, California," p. 307-332 in D.B. Duane and O. H. Pilkey (eds.). *Shelf Sediment Transport*, Dowden, Hutchinson and Ross, Inc., Stroudsburg, PA. COE Ref # 85
- Duane, D. B. and W. R. James. 1980, "Littoral transport in the surfzone elucidated by an Eulerian sediment tracer experiment," *Jour. Sedimentary Petrology*, v. 50, n. 3, p. 929-942.
- Duane, D. B. and C. W. Judge, 1969, "Radioisotopic Sand Tracer Study, Point Conception, California. Preliminary Report on Accomplishment, July 1966-June 1968," *U.S. Army Corps of Engineers, Coastal Engineering Research Center, Misc. Paper 2-69*, Vicksburg, MS, 81 pp. COE Ref # 87
- Dunham, J. W., 1965, "Use of groins as artificial headlands," p. 755-762, Chapter 32, in *Coastal Engineering Specialty Conference*, Santa Barbara, October 1965, ASCE, NY, 1006 pp. COE Ref # 89
- Durham, D. L., L. Z. Hales and T. W. Richardson, 1981, "Beach Nourishment Techniques, Report 4; Wave Climates for Selected U.S. Offshore Beach Nourishment Projects, Main Text," *U.S. Army Corps of Engineers, Waterways Experiment Station, Technical Report H-76-13*, Vicksburg, MS., 27 pp. COE Ref # 91
- Earle, M. D., 1979, "Storm Surge Conditions for the California Coast and Continental Shelf," *Marine Environments Corp.*, Rockville, MD, 56 pp. COE Ref # 94
- Eckart, C., 1951, "Surface waves on water of variable depth," *Univ. of California, San Diego, Scripps Inst. of Oceanography, Wave Report 100*, La Jolla, CA., 99 pp.
- Einstein, H. A., 1942, "Formulae for transportation of bed-load," *Transactions, ASCE*, v. 107, p. 561-577.
- Einstein, H. A., 1950, "The bed-load function for sediment transport in open channel flows," *U.S. Dept. of Agriculture, Technical Bulletin No. 1026*, Soil Conservation Service, Washington, D. C.
- Elgar, S. and R. T. Guza, 1985a, in press, "Shoaling gravity waves: comparisons between field observations, linear theory, and a nonlinear model," *Jour. Fluid Mechanics*.
- Elgar, S. and R. T. Guza, 1985b, in press, "Bispectral analysis of shoaling surface gravity waves," *Jour. Fluid Mechanics*.
- Elgar, S., R. T. Guza and R. J. Seymour, 1984, "Groups of Waves in Shallow Water," *Jour. of Geophysical Research*, v. 89, n. C3, p. 3623-3634. COE Ref # 97
- Emery, K. O., 1980, "Relative sea levels from tide gauge records," *Proc. Nat'l. Academy of Science*, v. 77, n. 12, p. 6969-6972.
- Emery, W. J. and K. Hamilton, 1985, "Atmospheric forcing of interannual variability in the Northeast Pacific Ocean: connections with El-Nino," *Jour. Geophysical Research*, v.

90, n. C1, p. 857-868.

Environment Research & Technology. 1984. "Oceanography and Marine water quality technical appendix for proposed Getty Gaviota Facility. Santa Barbara County Document No. 84-EIR-15, *Environment Research and Technology*.

Ernst, W. G. (ed.), 1981, *The Geotectonic Development of California*, Prentice-Hall, Inc., Englewood Cliffs, NJ, 706 pp.

Esteve, D. C., 1977, "Evaluation of the Computation of Wave Direction with Three-Gage Arrays," *U.S. Army Corps of Engineers*, Coastal Engineering Research Center, Technical Paper 77-7, Vicksburg, MS, 123 pp. COE Ref # 104

Everts, C. H., 1983, "Shoreline Changes Downdrift of a Littoral Barrier," *U.S. Army Corps of Engineers*, Coastal Engineering Research Center, Reprint 83-10, Vicksburg, MS, p. 673-689. COE Ref # 125

Felix, D., 1969, "Origin and Recent History of Newport Submarine Canyon, California Continental Borderland," *University of Southern California, Los Angeles*, Dept. of Geological Sciences Report 69-3, Technical Report for Office of Naval Research, Contract No. NONR228(17)NRO83-144, 116 pp. COE Ref # 108

Felix, D. W. and D. S. Gorsline, 1971, "Newport submarine canyon, California: an example of the effects of shifting loci of sand supply upon canyon position," *Marine Geology*, v. 10, p. 177-198.

Finkel, J. H., 1959, "The barchans of southern Peru," *Journal of Geology*, v. 67, p. 614-647.

Flick, R. E. and D. R. Cayan, 1984, "Extreme Sea Levels on the Coast of California," *Coastal Engineering, 19th Int'l. Conf.*, Houston, Texas, 3-7 Sept 1984, ASCE, N.Y., 13 pp. COE Ref # 116

Flick, R. E. and B. W. Waldorf, 1984, "Performance documentation of the Longard Tube at Del Mar, California, 1980-1983," p. 199-217 in v. 8, *Coastal Engineering*, Elsevier Science Publishers, Amsterdam. COE Ref # 117

Forristall, G. Z., E. G. Ward, V. J. Cardone and L. E. Borgmann, 1978, "The directional spectra and kinematics of surface gravity waves in tropical storm Delia," *Jour. Physical Oceanography*, v. 8, p. 888-909.

Frautschy, J. D. and D. L. Inman, 1954, "Review of the effects of the Mission Bay jetties upon sand migrations," unpublished letter to the Beach Erosion Board, 11 pp.

Freeman, J. C., Jr., L. Baer and C. H. Jung, 1957, "The bathystrophic storm tide," *Jour. Marine Research*, v. 16, n. 1.

Friehe, C. and C. D. Winant, 1982, "Observation of wind and sea surface temperature structure off of the northern California coast," *Proceedings, First Int'l Conference on Meteorology and Air/Sea Interaction of the Coastal Zone*, 10-24 May, 1982, The Hague, Netherlands.

- Gable, C. G. (ed.). 1979, "Report on Data from the Nearshore Sediment Transport Study at Torrey Pines Beach, California, November-December, 1978," *Univ. of California, San Diego*. Scripps Inst. of Oceanography, Reference Series 79-8. La Jolla, CA.. 90 pp. COE Ref # 126
- Gable, C. G. (ed.), 1981, "Report on Data from the Nearshore Sediment Transport Experiment at Leadbetter Beach, Santa Barbara, California, January-February, 1980." *Univ. of California, San Diego*. Scripps Inst. of Oceanography, Reference Series 80-5, La Jolla, CA., 314 pp. COE Ref # 127
- Galvin, C. J., 1964, "Resonant edge waves on laboratory beaches," Abstracts volume, *EOS*, Amer. Geophysical Union, v. 46, p. 112.
- Galvin, C. J., 1967, "Longshore Current Velocity: A Review of Theory and Data," p. 287-304 in *U.S. Army Corps of Engineers*, Coastal Engineering Research Center, Reprint 2-68, Vicksburg, MS. COE Ref # 128
- Galvin, C. J., 1972, "Waves breaking in shallow water, p. 413-456 in R. E. Mayer (ed.) *Waves on Beaches*, Academic Press, New York. 462 pp.
- Garcia, A. W. and Cpt. F. C. Perry, 1976, "Beach Nourishment Techniques, Report 2; A Means of Predicting Littoral Sediment Transport Seaward of the Breaker Zone." *U.S. Army Corps of Engineers*, Waterways Experiment Station, Technical Report H-76-13, Vicksburg, MS, 58 pp. COE Ref # 130
- Garrett, C., 1977, "Predicting changes in tidal regime: the open boundary problem," *Jour. Physical Oceanography*, v. 7, p. 171.
- Garrett, C. and B. Toulany, 1982, "Sea level variability due to meteorological forcing in the northern Gulf of St. Lawrence," *Jour. Geophysical Research*, v. 87, n. C3, p. 1968-1978.
- Gaul, R. D. and H. B. Stewart, 1960, "Nearshore Ocean Currents off San Diego, California," *Jour. of Geophysical Research*, v. 65, n. 5, p. 1543-1556. COE Ref # 132
- Godshall & Williams, 1981, "A climatology and oceanographic analysis of the California Pacific outer continental shelf region," *U.S. Dept. of Commerce*, NOAA, Environmental Data and Information Services, Washington, DC, 250+ pp. COE Ref # 549
- Gornitz, V., S. Lebedeff and J. Hansen, 1982, "Global Sea Level Trend in the Past Century," *Science*. v. 215. p. 1611-1614. COE Ref # 133
- Gorsline, D. S., 1958, "Marine geology of San Pedro and Santa Monica Basins and vicinity, California," Ph.D. Thesis, *Univ. of Southern California*, Los Angeles, CA.
- Gorsline, D. S. and D. J. Grant, 1972, "Sediment Textural Patterns on San Pedro Shelf, California (1961-1971); Reworking and Transport by Waves and Currents," p. 575-600, in D. J. Swift, D. B. Duane and O. H. Pilkey (eds.), *Shelf Sediment Transport: Process and Pattern*, Dowden, Hutchinson & Ross, Inc., Stroudsburg, PA. COE Ref # 137

- Groves, G. W., 1953. "The Statistical Description of Average Wave Conditions Near the Entrance of San Diego Bay." *Univ. of California, San Diego*. Scripps Inst. of Oceanography. Reference Series 53-63, Wave Report No. 102, La Jolla, CA., 18 pp. COE Ref # 139
- Groves, G. W. and E. J. Hannan. 1968. "Time series regression of sea level on weather." *Rev. Geophys.*, v. 6, n. 2, p. 129-174.
- Gunther, E. G., 1978. "Eastern North Pacific Tropical Cyclones, 1977," p. 157-166 in *U.S. Dept. of Commerce*, NOAA National Weather Service, Eastern Pacific Hurricane Center, Mariner's Weather Log No. 22(3). Redwood City, CA. COE Ref # 244
- Gunther, H., W. Rosenthal and K. Richter, 1980, "Application of the parametrical wave prediction model to rapidly varying wind fields during JONSWAP. 1973, *Jour. Geophysical Research*, v. 84, p. 4855-4864.
- Guza, R. T. and A. J. Bowen, 1976, "Resonant interaction for waves breaking on a beach," *Proceedings 15th Coastal Engineering Conference*, p. 560-572, Amer. Society of Civil Engineers, New York.
- Guza, R. T. and A. J. Bowen, 1981. "On the Amplitude of Beach Cusps," *Jour. of Geophysical Research* v. 86, n. C5, p. 4125-4132. COE Ref # 292
- Guza, R. t. and R. Davis, 1974, "Excitation of edge waves by waves incident on a beach," *Jour. Geophysical Research*, v. 79, p. 1285-1291.
- Guza, R. T. and D. L. Inman, 1975, "Edge Waves and Beach Cusps," *Jour. of Geophysical Research*, v. 80, n. 21, p. 2997-3012. COE Ref # 141
- Guza, R. T. and E. B. Thornton, 1978, "Variability of Longshore Currents," p. 756-775 in *Proceedings of the 16th Coastal Engineering Conference*, Hamburg, W. Germany, Aug 28-Sept 1, 1978. ASCE, N.Y. COE Ref # 142
- Guza, R. T. and E. B. Thornton, 1980, "Local and Shoaled Comparisons of Sea Surface Elevations, Pressures and Velocities," *Jour. of Geophysical Research*, v. 85, n. C3, p. 1524-1530. COE Ref # 143
- Guza, R. T. and E. B. Thornton, 1981, "Wave Set-Up on a Natural Beach," *Jour. of Geophysical Research*, v. 86, n. C5, p. 4133-4137. COE Ref # 144
- Guza, R. T. and E. B. Thornton, 1982, "Swash oscillations on a natural beach," *Jour. Geophysical Research*, v. 87, n. C1, p. 483-491.
- Guza, R. T. and E. B. Thornton, 1985, "Observations of surf beat," *Jour. Geophysical Research*, v. 90, n. C2, p. 3161-3172.
- Hagstrum, J. T., M. McWilliams, D. G. Howell and S. Gromme, 1985, "Mesozoic paleomagnetism and northward translation of the Baja California Peninsula," *Geological Soc. Amer.*, Bulletin, v. 96, n. 8, p. 1077-1090.

- Hales, L. Z., 1978a, "Preliminary evaluation of wind and wave effects at potential LNG terminal sites, State of California. Appendix A: An evaluation of the relative wave climate at five offshore LNG sites considering island influences and topographic effects." *U.S. Army Corps of Engineers, Waterways Experiment Station, Misc. Paper H-78-2*, Vicksburg, MS.
- Hales, L. Z., 1978b, "Coastal Processes Study of the Oceanside, California Littoral Cell, Final Report." *U.S. Army Corps of Engineers, Waterways Experiment Station, Misc. Paper H-78-8*, Vicksburg, MS, 464 pp. COE Ref # 149
- Hales, L. Z., 1979, "Mission Bay, California, Littoral Compartment Study, Final Report," *U.S. Army Corps of Engineers, Waterways Experiment Station, Misc. Paper HL 79-4*, Vicksburg, MS, 225 pp. COE Ref # 150
- Hales, L. Z., 1980, "Littoral Processes Study, Vicinity of Santa Ana River Mouth from Anaheim Bay to Newport Bay, Final Report." *U.S. Army Corps of Engineers, Waterways Experiment Station. Technical Report HL-80-9*, Vicksburg, MS, 107 pp. COE Ref # 151
- Hallermeier, R. J., 1983, "Sand Transport Limits in Coastal Structure Designs," p. 703-716 in *U.S. Army Corps of Engineers, Coastal Engineering Research Center, Reprint 83-8*, Vicksburg, MS COE Ref # 157
- Handin, J. W., 1951, "The source, transportation and deposition of beach sediments in Southern California," *U.S. Army Corps of Engineers Beach Erosion Board, Technical Memo 22*, Washington, D. C., 113 pp. COE Ref # 161
- Handin, J. W. and J. C. Ludwick, 1950, "Accretion of beach sand behind a detached breakwater," *U.S. Army Corps of Engineers Beach Erosion Board, Technical Memo 16*, Washington, D. C., 14 pp. COE Ref # 160
- Harris, D. L., 1973, "Characteristics of wave records in the coastal zone," *U.S. Army Corps of Engineers, Coastal Engineering Research Center, Reprint 2-73*, Vicksburg, MS, and p. 1-51 in *Waves on Beaches and Resulting Sediment Transport*, Academic Press, Inc., N.Y., 1972. COE Ref # 164
- Harris, T. F. W., 1967, "Field and model studies of the nearshore circulation," *Univ. of Natal, South Africa, Ph. D. Dissertation, Dept. of Physics*.
- Hasselmann, D. E., M. Dunkel and J. A. Ewing, 1980, "Directional wave spectra observed during JONSWAP 1973," *Jour. Physical Oceanography*, v. 10, p. 1264-1280.
- Hasselmann, K., D. B. Ross, P. Muller and W. Sell, 1976, "A parametric wave prediction model," *Jour. Physical Oceanography*, v. 6, p. 200-228.
- Heaps, N. S., 1965, "Storm surges on a continental shelf," *Phil. Trans. Royal Society London, A*, v. 257, p. 351-383.
- Helle, J. R., 1958, "Surf Statistics for the Coasts of the United States," *U.S. Army Corps of Engineers Beach Erosion Board, Technical Memo 108*, Washington, D. C., 22 pp.

COE Ref # 170

- Herron, W. J., 1980, "Artificial beaches in Southern California," *Shore and Beach*, v. 48, n. 1, p. 3-12. COE Ref # 172
- Herron, W. J., 1983, "The influence of man upon the shoreline of Southern California," *Shore and Beach*, v. 51, n. 3, p. 17-27. COE Ref # 173
- Herron, W. J. and R. L. Harris, 1966, "Littoral bypassing and beach restoration in the vicinity of Port Hueneme, California," *Proceedings of the 10th Conf. on Coastal Engineering*, ASCE, N.Y. COE Ref # 171
- Hickey, B. M., 1979, "The California current system-hypothesis and facts," *Progress in Oceanography*, v. 8, n. 4, p. 191-279.
- Hicks, S. D., 1981, "Long period sea level variations for the United States through 1978," *Shore and Beach*, v. 49, n. 2, p. 26-29.
- Hicks, S. D., H. A. Debaugh and L. E. Hickman, Jr., 1983, "Sea level variations for the United States, 1855-1980," *U.S. Dept. of Commerce, NOAA*, 170 pp.
- Hileman, J. A., C. R. Allen and J. M. Nordquist, 1973, "Seismicity of the southern California Region, 1 January 1932 to 31 December 1972," *Calif. Inst. of Technology*, Division of Geological and Planetary Sciences, Contribution 2385.
- Hobson, R. D., 1982, "Performance of a sand trap structure and effects of impounded sediments, Channel Islands Harbor, California," *U.S. Army Corps of Engineers*, Coastal Engineering Research Center, Technical Report 82-4, Vicksburg, MS, 38 pp. COE Ref # 178
- Hoffman, J. S., D. Keyes and J. G. Titus, 1983, "Projecting future sea level rise, Methodology estimates to the year 2100, and research needs," *U.S. Environmental Protection Agency*, n. 230-09-007, 121 pp.
- Horrer, P. L., 1950, "Southern hemisphere swell and waves from a tropical storm at Long Beach, California," p. 1-18 in *U.S. Army Corps of Engineers Beach Erosion Board*, Bulletin v. 4, n. 3 Washington, D. C., 51 pp. COE Ref # 180
- House Document # 277, 1954, "Appendix II, Coast of California, Point Mugu to San Pedro breakwater, Beach Erosion Control Study," 178 pp.
- House Document # 637, 1940, "Beach erosion study, Orange County, California," 26 pp.
- Houston, J. R., 1978, "Tsunami run-up predictions for the west coast," p. 2885-2896 in *Coastal Zone '78*, v. IV, ASCE, N.Y. COE Ref # 183
- Houston, J. R., 1980, "Tsunami predictions for Southern California, Type 19 Flood Insurance Study, Final Report," *U.S. Army Corps of Engineers*, Waterways Experiment Station, Technical Report HL-80-18, Vicksburg, MS, 32 pp. COE Ref # 185

- Houston, J. R. and A. W. Garcia. 1978. "Tsunami predictions for the West Coast of the Continental United States. Type 16 Flood Insurance Study." *U.S. Army Corps of Engineers*, Waterways Experiment Station, Technical Report H-78-26, Hydraulics Laboratory, Vicksburg, MS, 35 pp. COE Ref # 184
- Hsiao, S. V., J. F. Vesecky and O. H. Shemdin, 1980. "An investigation of wave sheltering by islands." *Coastal Engineering Conference*, 1980, Ch. 52, ASCE, NY, p. 840-849. COE Ref # 557
- Hubert, W. E. and B. R. Mendenhall, 1970, "The FNWC singular sea/swell model," Fleet Numerical Weather Central, Technical Note 59, Monterey, CA.
- Huntley, D. A., R. T. Guza and A. J. Bowen, 1977, "A universal form of shoreline run-up spectra." *Jour. of Geophysical Research* v. 82, n. 18, p. 2577-2581. COE Ref # 188
- Huntley, D. A., R. T. Guza and E. B. Thornton, 1981, Field observations of surf beat, 1. Progressive edge waves," *Jour. of Geophysical Research* v. 86, n. C7, p. 6451-6466. COE Ref # 189
- Huyer, A., R. L. Smith and R. D. Pillsbury, 1974, "Observation in a coastal upwelling region during a period of variable winds (Oregon coast, July 1972)," *Tethys*, v. 6, p. 391-404.
- Huyer, A., E. J. C. Sobey and R. L. Smith, 1979, "The spring transition in currents over the Oregon continental shelf," *Jour. Geophysical Research*, v. 84, n. C11, p. 6995-711.
- Ingle, J. C., 1962, "Tracing beach sand movement by means of fluorescent dyed sand," *Shore and Beach*, Reprint, 6 pp. COE Ref # 193
- Ingle, J. C., Jr., 1966, "The movement of beach sand," v. 5 in *Developments in Sedimentology*, Elsevier, NY, 221 pp.
- Inman, D. L., 1950a, "Report on beach study in the vicinity of Mugu Lagoon, California," *U.S. Army Corps of Engineers Beach Erosion Board*, Technical Memo 14, Washington, D. C., 47 pp. COE Ref # 195
- Inman, D. L., 1950b, "Submarine topography and sedimentation in the vicinity of Mugu Submarine Canyon, California," *U.S. Army Corps of Engineers Beach Erosion Board*, Technical Memo 19, Washington, D. C., 45 pp. COE Ref # 196
- Inman, D. L., 1953, "Areal and seasonal variations in beach and nearshore sediments at La Jolla, California," *U.S. Army Corps of Engineers, Beach Erosion Board*, Technical Memo 39, 134 pp.
- Inman, D. L., 1954, "Beach and nearshore processes along the southern California coast," *Geology of Southern California*, State of California Division of Mines, Bulletin, n. 170, ch. 5, p. 29-34.
- Inman, D. L., 1957, "Wave generated ripples in nearshore sands," *U.S. Army Corps of Engineers, Beach Erosion Board*, Technical Memo 100, 65 pp.

- Inman, D. L., 1963, "Ocean waves and associated currents," p. 49-80, Chapter III, in F. P. Shepard (ed.), *Marine Geology*, Harper and Row, N.Y. COE Ref # 209
- Inman, D. L., 1973, "Shore processes," p. 317-338 in R. C. Vetter (ed.) *Oceanography: The Last Frontier*, Basic Books, Inc., New York, 399 pp.
- Inman, D. L., 1976, "Summary report of man's impact on the California coastal zone," *California Dept. of Navigation and Ocean Development*, Scripps Inst. of Oceanography, La Jolla, CA., 150 pp. (reissued 1980 by *Calif. Dept. Boating and Waterways*) COE Ref # 222
- Inman, D. L., 1978a, "The impact of coastal structures on shorelines," p. 2265-2272 in *Coastal Zone '78, Proceedings of the Symposium on Aspects of Coastal Zone Management*, San Francisco, California, ASCE, N.Y. COE Ref # 224
- Inman, D. L., 1978b, "A study of the sedimentation, sand replenishment, urban runoff and marine ecological effects related to development of Arco subunits A, B, C and D, Laguna Niguel, Orange County, California," unpublished consulting report with Larry Seeman Associates, Newport Beach, CA, p. 64-84.
- Inman, D. L., 1978c, "Status of surf zone sediment transport relations," p. 9-20 in *Univ. of Delaware, Proceedings of Workshop on Coastal sediment transport with emphasis on the National Sediment Transport Study*, Sea Grant College Program DEL-SG-15-78. COE Ref # 223
- Inman, D. L., 1981, "Beach and dune stability in the vicinity of Mandalay Beach," letter report submitted to Union Oil Co. via Intersea Research Corporation, 8 January 1981, 12 pp.
- Inman, D. L., 1983a, "Application of coastal dynamics to the reconstruction of paleocoastlines in the vicinity of La Jolla, California," p. 1-49 in P. M. Masters and N. C. Flemming (eds) *Quaternary Coastlines and Marine Archaeology: Toward the Prehistory of Landbridges and Continental Shelves*, Academic Press, London, 641 pp.
- Inman, D. L., 1983b, "The Santa Margarita River, a sand source for the Oceanside Littoral Cell, California," testimony presented to the Subcommittee on Water and Power Resources, House Committee on Interior and Insular Affairs in San Diego, 4 Nov '83, 9 pp., 2 tbls., 5 figs.
- Inman, D. L., 1985a, "Dynamics of migrating inlets," *Estuaries*, v. 8, n. 2B, p. 114A.
- Inman, D. L., 1985b, "Damming of rivers in California leads to beach erosion," p. 22-26 in *Oceans 85: Ocean Engineering and the Environment*, Marine Tech. Society and IEEE, v. 1, 674 pp.
- Inman, D. L., 1985c, "A critique of the proposed Imperial Beach Breakwater..." a letter report to Michael Fisher of the California Coastal Commission dated 26 April 1984, 14 pp.
- Inman, D. L., 1985d, letter report to Kristin Johnson, Staff Analyst, Calif. Coastal Commission, letter dated 27 June 1985, Re: Imperial Beach Preliminary Staff Report, dated 11

June 1985. 4 pp.

- Inman, D. L. and R. A. Bagnold. 1963. "Littoral processes," p. 529-553 in M. N. Hill (ed) *The Sea* v. 3 of *The Earth Beneath the Sea*. Interscience, John Wiley and Sons, New York. London. 963 pp.
- Inman, D. L. and B. M. Brush, 1973, "The Coastal Challenge," *Science*, v. 181, n. 4094, p. 20-32.
- Inman, D. L. and T. K. Chamberlain, 1959, "Tracing beach sand movement with irradiated quartz," *Jour. of Geophysical Research* v. 64, n. 1, p. 41-47. COE Ref # 206
- Inman, D. L. and T. K. Chamberlain, 1960, "Littoral sand budget along the southern California coast," p. 245-246 in Volume of Abstracts, *Report of the 21st Int'l. Geological Congress*, Copenhagen, Denmark. COE Ref # 208
- Inman, D. L. and J. D. Frautschy, 1958, "Dynamics of Newport Spit," and "Preliminary Precis of an Evaluation of References bearing on the County of Orange vs. State of California, Orange No. 70717," 3 pp + chart vicinity of Newport Bay circa 1875 + 8 pp of notes.
- Inman, D. L. and J. D. Frautschy, 1960, "Determination of the last natural shoreline in the Long Beach Harbor area," unpublished report.
- Inman, D. L. and J. D. Frautschy, 1965, "Littoral processes and the development of shorelines," p. 511-553 in *Coastal Engineering*, Amer. Soc. Civil Engin., New York, 1006 pp.
- Inman, D. L. and R. T. Guza, 1976, "Application of nearshore processes to the design of beaches," *Amer. Society of Civil Engin.*, Abstracts, 15th Coastal Engin. Conference, p. 526-529.
- Inman, D. L. and R. T. Guza, 1982, "The origin of swasp cusps on beaches," p. 133-148, v. 49, *Marine Geology*, Elsevier Scientific Publishing Co., Amsterdam, Netherlands. COE Ref # 228
- Inman, D. L. and D. M. Hanes, 1980, "Field measurements of bed and suspended load motion in the surf zone," p. 217-218 in *Proceedings, 17th Intl. Conference on Coastal Engin.*, abstracts volume, 456 pp.
- Inman, D. L. and P. L. Horrer, 1958, "Santa Monica slide bypass - oceanographic aspects," unpublished report prepared for the Dept. of Public Works, Division of Highways, State of California by *Marine Advisors, Inc.*, La Jolla, CA., 8 pp.
- Inman, D. L. and S. A. Jenkins, 1983, "Oceanographic report for Oceanside Beach facilities," prepared for City of Oceanside, CA., 206 pp. COE Ref # 229
- Inman, D. L. and S. A. Jenkins, 1984, "The Nile Littoral Cell and man's impact on the coastal zone of the southeastern Mediterranean," p. 1600-1617 in *Proceedings, 19th Intl. Conference on Coastal Engin.*, v. 2, Amer. Society of Civil Engin., New York.

- Inman, D. L. and S. A. Jenkins, 1985, "Erosion and accretion waves from Oceanside Harbor." p. 591-593 in *Oceans 85: Ocean Engineering and the Environment*. IEEE. v. 1. 674 pp.
- Inman, D. L., P. D. Komar and A. J. Bowen, 1968, "Longshore transport of sand," p. 298-300 in *Proceedings of the 11th Conference on Coastal Engineering*, London, England. v. 1. ASCE, N.Y. COE Ref # 215
- Inman, D. L. and C. E. Nordstrom, 1961, "Scientific work: La Jolla Site: Experimental drilling in deep water at La Jolla and Guadalupe sites," *National Acad. Sciences*, National Research Council, Publication 914, p. 123-126.
- Inman, D. L. and C. E. Nordstrom, 1971, "On the tectonic and morphologic classification of coasts," *Journal of Geology*, v. 79, n. 1, p. 1-21.
- Inman, D. L., C. E. Nordstrom and R. E. Flick, 1976, "Currents in submarine canyons: an air-sea-land interaction," *Annual Review of Fluid Mechanics*, v. 8, p. 275-310.
- Inman, D. L., C. E. Nordstrom, S. S. Pawka, D. G. Aubrey and L. C. Holmes, 1974, "Nearshore processes along the Silver Strand Littoral Cell," *Intersea Research Corp.*, La Jolla, CA., prepared for the U.S. Army Corps of Engineers, Los Angeles District, 72 pp. COE Ref # 232
- Inman, D. L. and W. H. Quinn, 1952, "Currents in the surf zone," *Proceedings, 2nd Coastal Engineering Conference*, Univ. of California, Council on Wave Research, p. 24-36.
- Inman, D. L. and G. S. Rusnak, 1956, "Changes in sand level on the beach and shelf at La Jolla, California," p. 106-127 in *U.S. Army Corps of Engineers Beach Erosion Board*, Technical Memo 82, Washington, D. C. COE Ref # 202
- Inman, D. L., R. J. Tait and C. E. Nordstrom, 1971, "Mixing in the surf zone," *Jour. of Geophysical Research* v. 76, n. 15, p. 3493-3514. COE Ref # 216
- Inman, D. L., J. A. Zampol, T. E. White, D. M. Hanes, B. W. Waldorf and K. A. Kastens, 1980, "Field measurements of sand motion in the surf zone," p. 1215-1234 in *Proceedings of the 17th Int'l Coastal Engineering Conference*, Sydney, Australia, March 23-28, 1980, ASCE, N.Y. COE Ref # 225
- Jansen, L., 1976, "A study of longshore sand transport at Mission Beach," *San Diego State Univ.*, San Diego, CA., 45 pp. COE Ref # 246
- Jelesnianski, C. P., 1972, "SPLASH - Special program to list amplitudes of surges from hurricanes," *National Weather Services*, NOAA, Rockville, MD.
- Jen, Y., 1969, "Wave refraction near San Pedro Bay, California," *Journal of Waterways and Harbors Division*, ASCE, N.Y., v. 95, n. WW3, p. 379-393; and *Discussion*, v. 97, n. 1, Feb., 1971, p. 209-211. COE Ref # 248
- Johnson, J. W., 1953, "Sand transport by littoral currents," *State Univ. of Iowa*, Proceedings Fifth Hydraulics Conference, Bulletin 34, Studies in Engineering, p. 89-109.

- Johnson, J. W., 1957. "The littoral drift problem at shoreline harbors." *Jour. of Waterways and Harbors Div.* Proceedings ASCE, v. 83, n. WW1, 37 pp.
- Johnson, J. W., 1965. "Sand movement on coastal dunes." p. 747-755 in *Federal Interagency Sediments Conference Proceedings*, U.S. Dept. of Agriculture. Misc. Publication No. 970, 933 pp.
- Johnson, J. W., J. T. Moore and F. B. Ovet, 1971, "Summary of annual wave power for ten deep water stations along the California, Oregon and Washington Coasts," *Univ. of California, Berkeley*, Hydraulic Engineering Laboratory Report HEL-24-9. Berkeley, CA., 241 pp. COE Ref # 253
- Judge, C. W., 1970, "Heavy minerals in beach and stream sediment as indicators of shore processes between Monterey and Los Angeles, California," *U.S. Army Corps of Engineers*, Coastal Engineering Research Center. Technical Memo 33, Vicksburg, MS, 44 pp. COE Ref # 255
- Julian, P. R. and R. M. Chervin, 1978, "A study of the southern oscillation and Walker circulation phenomena." *Monthly Weather Review*, v. 106, n. 10, p. 1433-1451.
- Kadib, A.-L., 1964, "Calculation procedure for sand transport by wind on natural beaches," U.S. Army Corps of Engineers, *Coastal Engin. Research Center*, Misc. Paper n. 2-64, 25 pp.
- Karl, H. A., 1980, "Influence of San Gabriel submarine canyon on narrow-shelf sediment dynamics, Southern California," *Marine Geology*, v. 34, n. 1-2, p. 61-78. COE Ref # 257
- Karl, T. R., R. E. Livezey and E. S. Epstein, 1984, "Recent unusual mean winter temperatures across the contiguous United States," *Amer. Meteorological Soc., Bulletin*, v. 65, n. 12, p. 1302-1309.
- Kaufman, W. and O. H. Pilkey, 1983, *The beaches are moving: The drowning of America's shoreline*, Duke University Press, Durham, N.C., ISBN 0-8223-0-575-7, 336 pp. COE Ref # 259
- Kerr, R. A., 1983, "Fading El Nino broadening scientists' view," *Science*, v. 221, p. 940-941.
- Kolpack, R. L., 1971, "Oceanography of the Santa Barbara Channel," in K. L. Kolpack (ed.) *Biological and Oceanography Survey of the Santa Barbara Channel Oil Spill, 1969-1970*, v. 2.
- Komar, P. D., 1976a, "Nearshore currents and sediment transport, and the resulting beach configuration," p. 241-254 in D. J. Stanley and J. P. Swift (eds.), *Marine Sediment Transport and Environmental Management*. COE Ref # 270
- Komar, P. D. 1976b, *Beach Processes and Sedimentation*, Prentice-Hall, Inc., Englewood Cliffs, N.J., 429 pp.
- Komar, P. D., 1977, "Beach sand transport: Distribution and total drift," *Jour. of Waterways*,

- Ports, Coastal and Ocean Div., ASCE, N.Y., v. 103, n. 2, p. 225-239. COE Ref # 271*
- Komar, P. D., 1978, "Relative quantities of suspension versus bed-load transport on beaches," *Jour. Sedimentary Petrology*, v. 48, n. 3. COE Ref # 272
- Komar, P. D. and D. L. Inman, 1970, "Longshore sand transport on beaches," *Jour. of Geophysical Research* v. 75, n. 30, p. 5914-5927. COE Ref # 269
- Komen, G. J., D. E. Hasselmann and K. Hasselmann, 1985, "On the existence of a fully developed wind-sea spectrum," *Jour. Physical Oceanography*, v. 14, p 1271-1285.
- Kuhn, G. G. and F. P. Shepard, 1983, "Beach processes and sea cliff erosion in San Diego County, California," p. 267-284, Chapter 13, in P. D. Komar (ed.), *Handbook on Coastal Processes and Erosion*, CRC Press, Inc., Boca Raton, FL. COE Ref # 281
- Kuhn, G. G. and F. P. Shepard, 1984, *Sea cliffs, beaches and coastal valleys of San Diego County*, Univ. of California Press, Berkeley and Los Angeles, CA.; London, England, 193 pp. COE Ref # 282
- Kundu, P. K. and J. S. Allen, 1976, "Some three-dimensional characteristics of low frequency current fluctuations near the Oregon coast," *Jour. Physical Oceanography*, v. 6, p. 181-199.
- Kundu, P. K., J. S. Allen and R. L. Smith, 1975, "Modal decomposition of the velocity field near the Oregon coast," *Jour. Physical Oceanography*, v. 5, p. 683-704.
- Lambech, K. and S. M. Nakibogler, 1984, "Recent global changes in sea level," *Geophysical Research Letters*, v. 11, n. 10, p. 959-961.
- Langbein, B. and S. A. Schumm, 1958, "Yield of sediment in relation to mean annual precipitation, *Amer. Geophysical Union Transactions*, v. 39, p. 1076-1084.
- Lawson, L. M. and R. B. Long, 1983, "Multimodal properties of the surface-wave field observed with pitch-roll buoys during GATE," *Journal Physical Oceanography*, v. 13, p. 474-486.
- Lazanoff, S. M. and N. M. Stevenson, 1975, "An evaluation of a hemispheric operational wave spectral model, " *Fleet Num. Weather Cent.*, Technical Note 75-3.
- LeBlond, P. H. and L. A. Mysak, 1978, *Waves in the Ocean*, Elsevier, Oceanography Series 20, 602 pp.
- Legg, M. R., 1980, "Seismicity and tectonics of the inner continental borderland of southern California and northern Baja California, Mexico," M.S. Thesis, Oceanography, *Univ. of California, San Diego*, 60 pp.
- Lee, L. J., 1980, "Sea cliff erosion in Southern California," p. 1919-1938, v. III in *Coastal Zone '80, Symposium*, Nov. 17-20, 1980, Hollywood, Florida, ASCE, N.Y. COE Ref # 301
- Lentz, S. J., 1984, "Subinertial motions on the southern California continental shelf," Ph. D.

- Thesis. *Univ. of California, San Diego*. Scripps Inst. of Oceanography. La Jolla. CA., 145 pp.
- Lentz, S. J. and C. D. Winant, 1979, "Ocean station Del Mar current meter campaign, 1978-1979 data report," *Univ. of California, San Diego*, Scripps Inst. of Oceanography. La Jolla, CA. SIO Reference Series 79-27.
- Lisitzen, E., 1974. *Sea Level Changes*, Elsevier, NY, 286 pp.
- Littler, M. M. and D. S. Littler, 1980, "Mainland rocky intertidal aerial survey from Point Arguello to Point Loma, California," *U.S. Dept. of the Interior*, Bureau of Land Management Contract No. YN010-CT9-4, 47 pp. COE Ref # 308
- Longuet-Higgins, M. S., 1952, "On the statistical distribution of the heights of sea waves," *Jour. Marine Research*, v. 11.
- Magoon, O. T., 1965, "Structural damage by tsunamis," *Coastal Engineering, Santa Barbara Specialty Conference*, ASCE, p. 35-68.
- Maloney, N. and K. M. Chan, 1974, in *A Summary of Knowledge of the Southern California Coastal Zone and Offshore Areas*, v. I, Report to the Bureau of Land Management, Dept. of the Interior, Washington, D. C.
- Marine Advisors, 1960a, "Design Waves for proposed small craft harbor at Oceanside, California," prepared for U.S. Army Corps of Engineers, Los Angeles District, *Marine Advisors, Inc.*, La Jolla, CA. COE Ref # 314
- Marine Advisors, 1960b, "Design waves for a proposed small craft harbor at Dana Point, California," prepared for U.S. Army Corps of Engineers, Los Angeles District, *Marine Advisors, Inc.*, La Jolla, CA., 20 pp. COE Ref # 315
- Marine Advisors, 1961a, "A statistical survey of ocean wave characteristics in Southern California waters," prepared for U.S. Army Corps of Engineers, Los Angeles District, *Marine Advisors, Inc.*, La Jolla, CA., 30 pp. COE Ref # 316
- Marine Advisors, 1961b, "Design wave for proposed small craft harbor at Dana Point, California, Appendix 1 - Refraction Diagrams," prepared for U.S. Army Corps of Engineers, Los Angeles District, *Marine Advisors, Inc.*, La Jolla, CA., 27 pp. COE Ref # 317
- Marine Advisors, 1961c, "A study of sea-swell and seiches in Mission Bay," prepared for U.S. Army Corps of Engineers, Los Angeles District, *Marine Advisors, Inc.*, La Jolla, CA., 24 pp. COE Ref # 318
- Marine Advisors, 1963, "Wave study at Mission Bay, California," prepared for U.S. Army Corps of Engineers, Los Angeles District, *Marine Advisors, Inc.*, La Jolla, CA., 15 pp. COE Ref # 319
- Marine Advisors, 1964, "Longshore component of seasonal wave power calculated for four locations near Point Arguello, California," *Marine Advisors, Inc.*, La Jolla, CA.

- Marine Advisors, 1965, "Oceanographic factors pertinent to the MWD combined desalination and power plant feasibility and site study." prepared for Bechtel Corporation Power and Industrial Division by *Marine Advisors, Inc.*, La Jolla, CA., 53 pp.
- Marine Advisors, 1969, "Summary report of San Onofre oceanographic surveys - July 1963 to December 1968," prepared for U.S. Army Corps of Engineers, Los Angeles District. *Marine Advisors, Inc.*, La Jolla, CA., 168 pp. COE Ref # 320
- Marine Biological Consultants (MBC), 1984, "Monitoring Program for Texaco's Anita South exploratory drill site: Draft interim report prepared for Texaco, U.S.A.." *Marine Biological Consultants*.
- Mason, M. A., 1950, "The wind element in beach erosion," *Symposium on Hydrometeorological Problems*, American Geophysical Union, p. 19-23.
- Mattie, M. G., S. V. Hsiao and D. D. Evans, 1981, "Wave direction measured by four different systems," *U.S. Army Corps of Engineers*, Coastal Engineering Research Center, Reprint 81-5, Vicksburg, MS; and *IEEE Journal of Oceanic Engin.*, v. OE-6, n. 3, p. 87-93. COE Ref # 321
- Mei, C. C., 1983, *The Applied Dynamics of Ocean Surface Waves*, John Wiley & Sons, NY, 740 pp.
- Meteorology Int'l., Inc., 1977, "Deep-water wave statistics for the California coast. Stations 1-6," *California Dept. of Navigation and Ocean Development*, Resources Agency, Sacramento, CA; six volumes, each station report is 200+ pp. COE Ref # 325
- Meyer-Peter, E., H. Favre and A. Einstein, 1934, "Neuere Versuchsergebnisse über den Geschiebetrieb," *Schweiz. Bauzeitung*, v. 103, n. 13.
- Miller, G. R., W. H. Munk and F. E. Snodgrass, 1962, "Long-period waves over California continental borderland, Part II: Tsunamis," *Jour. of Marine Research*, v. 20, p. 31-41. COE Ref. # 327
- Mineral Management Service, 1983, "Santa Barbara channel circulation and modeling study," prepared for the U.S. Dept. of the Interior, Pacific OCS Region, *Mineral Management Service*, MMS Contract 14-12-0001-29123.
- Mitsuyasu, H. and K. Rikiishi, 1978, "The growth of duration limited wind waves," *Jour. Fluid Mechanics*, v. 85, p. 705-730.
- Moffatt & Nichols, 1983, "Experimental sand bypass system at Oceanside Harbor, California. Phase 1 Report: Data Collection and Analysis," prepared for U.S. Army Corps of Engineers, Los Angeles District, *Moffatt & Nichols, Engineers*, Long Beach, CA., 100+ pp. COE Ref # 535
- Munk, W. H., 1947, "Tracking storms by forerunners of swell," *Jour. Metrology*, v. 4, p. 45-57.
- Munk, W. H., 1951, "Origin and generation of waves," *Univ. of Calif., San Diego*, Scripps Inst. of Oceanography, Reference Series 51-57, Wave Report No. 99, La Jolla, CA., 4 pp.

COE Ref # 336

- Munk, W. H., 1962a, "Long period waves over California's Continental borderland." *Jour. of Marine Research*, v. 20, n. 2, p. 119-120. COE Ref # 339
- Munk, W. H., 1962b, "Long ocean waves," p. 647-663 in M. N. Hill (ed.), *The Sea, Ideas and Observations on Progress in the study of the Seas*, vol. 1, Physical Oceanography, Interscience Publ., Div., John Wiley & Sons, N.Y. COE Ref # 340
- Munk, W. H. and R. S. Arthur, 1952, "Forecasting ocean waves," *Univ. of Calif., San Diego*. Scripps Inst. of Oceanography, Reference Series 52-19. (Reprinted from Compendium of Meteorology, American Meteorological Society, Boston. MA, p. 1082-1089). COE Ref # 337
- Munk, W. H., G. R. Miller, F. E. Snodgrass and N. F. Barber, 1963, "Directional recording of swell from distant storms," p. 505-584 in *Philosophical Transactions of the Royal Society of London*, Series A, Mathematical and Physical Sciences, v. 55, n. 1062, COE Ref # 341
- Munk, W. H. and F. E. Snodgrass, 1957, "Measurements of southern swell at Guadalupe Island," *Deep Sea Research*, v. 4, p. 272-286.
- Munk, W. H., F. Snodgrass and F. Gilbert, 1964, "Long waves on the continental shelf: An experiment to separate trapped and leaky modes," *Jour. Fluid Mechanics*, v. 20, p. 529-554.
- Munk, W. H., F. E. Snodgrass and M. J. Tucker, 1959, "Spectra of low-frequency ocean waves," *Univ. of California San Diego*, Scripps Inst. of Oceanography, SIO Bulletin, v. 7, p. 283-361.
- Munk, W. H., F. Snodgrass and M. Winbush, 1970, "Tides offshore: Transition from California coastal to deep sea waters," *Geophysical Fluid Dynamics*, v. 1, n. 1,2, p. 161-236. COE Ref # 342
- Munk, W. H. and M. A. Traylor, 1947, "Refraction of ocean waves, a process linking underwater topography to beach erosion," *Jour. of Geology*, v. 55, n. 1. COE Ref # 335
- Munk, W. H. and M. Wimbush, 1969, "A rule of thumb for wave breaking over sloping beaches," *Oceanology*, v. 9, p. 56-59.
- Mysak, L. A., 1980, "Topographically trapped waves," *Annual Review of Fluid Mechanics*, v. 12, p. 45-76.
- Namias, J., 1980, "Causes of some extreme Northern Hemisphere climate anomalies from summer 1978 through the subsequent winter," *Monthly Weather Review*, v. 108, p. 1333-1346.
- Namias, J. and D. R. Cayan, 1984, "El Nino: implications for forecasting," *Oceanus*, v. 27, n. 2, p. 41-47.

- Namias, J. and J. C. Huang, 1972. "Sea level at southern California - a decadal fluctuation." *Science*, v. 177, n. 4046, p. 351-353. COE Ref # 347
- National Marine Consultants, 1959a, "Oceanography Study. Port San Luis, California," prepared for U.S. Army Corps of Engineers, Los Angeles District. *National Marine Consultants*, Santa Barbara, CA., 21 pp. COE Ref # 348
- National Marine Consultants, 1959b, "Oceanography Study. Morro Bay, California," *National Marine Consultants*, Santa Barbara, CA.
- National Marine Consultants, 1960a, "Oceanography Study. Santa Barbara, California," prepared for U.S. Army Corps of Engineers, Los Angeles District, *National Marine Consultants*, Santa Barbara, CA., 17 pp. COE Ref # 349
- National Marine Consultants, 1960b, "Wave statistics for seven deep water stations along the California coast," prepared for U.S. Army Corps of Engineers, Los Angeles and San Francisco Districts. *National Marine Consultants*, Santa Barbara, CA. COE Ref # 351
- Nekton, Inc., 1984, "Interim Report: An ecological study of discharged drilling fluids on a hard bottom community in the western Santa Barbara Channel," prepared for Texaco, U.S.A., *Nekton, Inc.*
- Newberger, P. N., 1982, "Physical oceanography and meteorology of the California outer continental shelf," *U.S. Dept. of the Interior*, POCS Region, Minerals Management and Service, Technical Paper 82-2, BLM-YN-P/T-82-002-1792, Los Angeles, CA., 308 pp. COE Ref # 558
- Newton, C. T., 1959, "Beach Erosion Control Report on Cooperative Study of Orange County, California - Appendix V, Phase I," *U.S. Army Corps of Engineers*, Los Angeles District, CA., 44+ pp. COE Ref # 693
- Noble, M. and B. Butman, 1979, "Low-frequency wind induced sea level oscillations along the east coast of North America," *Jour. Geophysical Research*, v. 84, n. C6, p. 3227-3236.
- Nordstrom, C. E. and D. L. Inman, 1973, "Beach and cliff erosion in San Diego County, California," p. 125-131 in A. Ross and R. J. Dowlen (eds.), *Studies in the geology and geologic hazards of the greater San Diego area*, San Diego Assn. of Geologists, San Diego, CA. COE Ref # 357
- Nordstrom, C. E. and D. L. Inman, 1975, "Sand level changes on Torrey Pines Beach, California," *U.S. Army Corps of Engineers*, Coastal Engineering Research Center, Misc. Paper 11-75, Vicksburg, MS, 166 pp. COE Ref # 358
- Norris, R. M., 1964 "Dams and beach sand supply in southern California," p. 154-171 in R. I. Miller (ed), *Papers in Marine Geology*, Shepard Commemorative Volume, McMillian & Co., NY. COE Ref # 510
- O'Brien, M. P., 1950, "Wave refraction at Long Beach and Santa Barbara, California," *U.S. Army Corps of Engineers*, Beach Erosion Board, Bulletin v. 4, n. 1, 49 pp.

Washington, DC. COE Ref # 363

- Oceanographic Services, 1969, "Storm wave study, Santa Barbara Channel," unpublished supplemental plan of operations, Santa Ynez Unit, Humble Oil and Refining Co., *Oceanographic Services, Inc.*, Report No. 166-2.
- Oceanographic Services, 1971, "Study of ocean currents affecting proposed pipeline in Santa Barbara Channel - Westerly Route." *Oceanographic Services, Inc.*, Report No. 238-2.
- Oltman-Shay, J. and R. T. Guza, 1984, "A data-adaptive ocean wave directional-spectrum estimator for pitch and roll type measurements," *Jour. Physical Oceanography*, v. 14, n. 11, p. 1800-1810.
- Orme, A. R. and A. J. Brown, 1983, "Variable sediment flux and beach management, Ventura County, California," *Coastal Zone '83, Symposium*, San Diego, Calif., June 1-4, 1983, v. III, ASCE, NY, p. 2328-2342. COE Ref # 365
- Osborne, R. H. and Associates, 1982, "Geomorphic and sedimentologic analysis for Oceanside project, Phase II," prepared by U.S. Army Corps of Engineers, Los Angeles District, *Robert H. Osborne & Assoc.*, Los Angeles, CA., 81 pp. COE Ref # 540
- Osborne, R. H., N. J. Darigo and R. C. Scheidemann, 1983, "Report of potential offshore sand and gravel resources of the inner continental shelf of southern California," prepared for Calif. State Dept. of Boating and Waterways, Sacramento, *Univ. of Southern California*, Dept. of Geological Services, Los Angeles, CA., 302 pp. COE Ref # 367
- Pacific Weather Analysis, 1983, "Preparation of wave hindcasts," for Moffatt and Nichol Engineers.
- Pawka, S. S., 1982, "Wave directional characteristics on a partially sheltered coast," *Univ. of California, San Diego*, Scripps Inst. of Oceanography, Ph.D. Dissertation in Oceanography, La Jolla, CA., 279 pp. COE Ref # 379
- Pawka, S. S., 1983, "Island shadows in wave directional spectra," *Jour. Geophysical Research*, v. 88, n. C4, p. 2579-2591.
- Pawka, S. S. and R. T. Guza, 1983, "Coast of California waves study - site selection," *Univ. of California, San Diego*, Scripps Inst. of Oceanography, Reference Series 83-12, La Jolla, CA., 51 pp. COE Ref # 380
- Pawka, S. S., S. V. Hsiao, O. H. Shemdin and D. L. Inman, 1980, "Comparison between wave directional spectra from SAR pressure sensor arrays," *Jour. Geophysical Research*, v. 85, n. C9, p. 4987-4995. COE Ref # 378
- Pawka, S. S., D. L. Inman and R. T. Guza, 1984, "Island sheltering of surface gravity waves: model and experiment," *Continental Shelf Research*, v. 3, n. 1, Pergamon Press, p. 35-53. COE Ref # 381
- Pawka, S. S., D. L. Inman, R. L. Lowe and L. Holmes, 1976, "Wave climate at Torrey Pines beach, California." *U.S. Army Corps of Engineers, Coastal Engineering Research*

Center, Technical Paper 76-5, Vicksburg, MS. 372 pp. COE Ref # 376

- Perlin, M. and R. G. Dean, 1983, "A numerical model to simulate sediment transport in the vicinity of coastal structures," *U.S. Army Corps of Engineers, Coastal Engineering Research Center, Misc. Report 83-10*, Vicksburg, MS. 117 pp. COE Ref # 384
- Pierson, W. R., G. Neumann and R. James, 1953, "Practical methods for observing and forecasting ocean waves by means of wave spectra and statistics." *New York Univ. Research Division, College of Engineering*, New York.
- Pollard, D., 1979, "The source and distribution of beach sediments, Santa Barbara County, California." *Univ. of California, Santa Barbara*, Ph. D. Dissertation. COE Ref # 388
- Potter, D. M., 1983, "Erosion control facilities - mitigating their effect on coastal sediment supplies," *Coastal Zone '83, Symposium*, San Diego, CA., June 1-4, 1983, v. III, ASCE, NY, p. 2317-2327 COE Ref # 389
- Putnam, J. A., W. H. Munk and M. A. Traylor, 1949, "The prediction of longshore currents," *Transactions. Amer. Geophysical Union*, v. 30, p. 337-345.
- Raudkivi, A. J., 1976, *Loose Boundary Hydraulics* (2nd ed), Pergamon Press, Oxford, New York, etc., 397 pp.
- Reid, J. L., 1965, "Physical oceanography of the region near Point Arguello," *Univ. of California, San Diego*, Scripps Inst. of Oceanography, Inst. of Marine Research, Report 65-19, La Jolla, CA. COE Ref # 394
- Reid, J. L. and A. W. Mantyla, 1976, "The effect of the geostrophic flow upon coastal sea elevations in the north Pacific Ocean," *Jour. Geophysical Research*, v. 81, n. 18, p. 3100-3110.
- Rod Lundin & Assoc., 1978, "Ventura harbor sand bypass development project, partial report," prepared for Ventura Port District, *Rod Lundin & Assoc.*, Northridge, CA., 38 pp. COE Ref # 399
- Rosenfeld, L. K. (ed.), 1983, "Code-1: Moored array and large-scale data report," *Woods Hole Oceanographic Inst.*, CODE Technical Report No. 21, Woods Hole, MA.
- Sallenger, A. H., 1979, "Beach-cusp formations," *Marine Geology*, v. 29, p. 23-37.
- Saur, J. F. T., 1962, "The variability of monthly mean sea level at six stations in the eastern north Pacific Ocean," *Jour. Geophysical Research*, v. 67, n. 7, p. 2781-2790.
- Schneider, C. and J. R. Weggel, 1981, "Visually observed wave data at Point Mugu, California," *U.S. Army Corps of Engineers, Coastal Engineering Research Center*, Reprint 81-12, Vicksburg, MS.; and *Proc. of 17th Int'l Coastal Engin. Conference*, Mar 23-28, 1980, ASCE, NY, p. 23-28. COE Ref # 407
- Schwalbach, J. R., 1982, "A sediment budget for the southern California continental borderland," *Univ. of Southern California*, M.S. Thesis, Los Angeles, CA. COE Ref

408

- Schwartzlose, R. A., 1963, "Nearshore currents of the western United States and Baja California as measured by drift bottles," *CalCOFI Report*, v. 9, p. 15-22.
- Schwartzlose, R. A. and J. L. Reid, 1972, "Nearshore circulation in the California current," *State of Calif., Marine Res. Comm., Calif. Coop. Oceanic Fisheries Investigation*, Cal COFI Report No. 16, p. 57-65. COE Ref # 410
- Science Applications, 1984, "Revised draft Environmental impact statement report, Technical Appendix II, Santa Ynez/Los Flores Canyon Development and Production Plan," *Science Applications, Inc.*, La Jolla, CA.
- Severance, R. W., C. D. Winant and R. E. Davis, 1978, "A study of physical parameters in coastal waters off San Onofre, California, final report," *Univ. of California, San Diego*, Scripps Inst. of Oceanography, Reference Series 78-22, La Jolla, CA., 19 pp. COE Ref # 431
- Seymour, R. J., 1982, "Analysis of extreme wave statistics, Mission Bay entrance, January 3, 1976 to October 29, 1982," *Univ. of California, San Diego*, Scripps Inst. of Oceanography, Nearshore Research Group, Inst. of Marine Resources, La Jolla, CA., 5 pp. COE Ref # 443
- Seymour, R. J., 1983a, "The nearshore sediment transport study," *Jour. of Waterway, Port, Coastal and Ocean Engineering*, v. 109, n. 1, p. 79-85; and discussion and closure, Feb. 84, v. 110, n. 1, p. 130-133. COE Ref # 445
- Seymour, R. J., 1983b, "Extreme waves in California during winter, 1983," *California Dept. of Boating and Waterways*, Sacramento, CA., 17 pp. COE Ref # 446
- Seymour, R. J. and D. Castel, 1984a, "Episodicity in longshore sediment transport," *Jour. Waterway, Port, Coastal and Ocean Engin.*, COE Ref # 448
- Seymour, R. J. and D. Castel, 1984b, "A historical evaluation of north Pacific storms during the winter of 1983," *Abstracts of the 19th Int'l. Conference on Coastal Engineering*, Sept. 3-7, 1984, Houston, TX, ASCE, NY, p. 344-345. COE Ref # 449
- Seymour, R. J. and A. L. Higgins, 1977, "A slope array for measuring wave direction," *Proceedings of a workshop on coastal processes instrumentation*, Univ. of California, San Diego, Sea Grant Publication No. 62, IMR Ref. No. 78-102, p. 133-142.
- Seymour, R. J. and A. L. Higgins, 1979, "Deepwater wave direction from an intensity array," *Proceedings of 16th Coastal Engineering Conference*, Aug 27-Sept 2, 1978, Hamburg, Germany, ASCE, NY, p. 305-311. COE Ref # 437
- Seymour, R. J. and D. B. King, 1982, "Field comparisons of cross-shore transport models," *Jour. of Waterway, Port, Coastal and Ocean Engineering*, v. 108, n. WW2, p. 163-179, ASCE, NY. COE Ref # 442

- Seymour, R. J. and M. H. Sessions, 1976, "A regional network for coastal engineering data," *Proceedings, 15th Intl. Conf. on Coastal Engineering*, ASCE, p. 60-71.
- Seymour, R. J., R. R. Strange, D. R. Cayan and R. A. Nathan, 1984, "Influence of El Ninos on California's wave climate," *Proceedings, 19th Coastal Engineering Conf.*, ASCE, NY, v. 1, p. 577-592. COE Ref # 450
- Seymour, R. J., J. O. Thomas, D. Castel, A. E. Woods, M. H. Sessions, 1985, "Coastal Data Information Program - Ninth Annual Report, January 1984 - December 1984," prepared for U.S. Army Corps of Engineers and Calif. Dept. of Boating and Waterways, *Univ. of California, San Diego*, Scripps Inst. of Oceanography, IMR Reference No. 84-5, La Jolla, CA., 161 pp. COE Ref # 514
- Shaw, M. J., 1980, "Artificial sediment transport and structures in coastal Southern California," *Univ. of California, San Diego*, Scripps Inst. of Oceanography, Reference Series 80-41, 109 pp. COE Ref # 451.
- Shaw, M. J., 1982, "Coastal response of Leadbetter Beach, Santa Barbara to Southern California storm of February 16-21, 1980," p. 437-452 in *Storms, Floods and Debris Flows in Southern California and Arizona, 1978-1980, Proceedings of Symposium*, Sept. 17-18, 1980, Nat'l Res. Council and C.I.T., National Academy Press, Washington, DC. COE Ref # 452
- Shepard, F. P., 1946, "Beaches and Wave Action," *Univ. of California, San Diego*, Scripps Inst. of Oceanography, Reference Series 46-4, Wave Project Report 56, La Jolla, CA., 13 pp. COE Ref # 417
- Shepard, F. P., 1950a, "Longshore bars and longshore troughs," *U.S. Army Corps of Engineers*, Beach Erosion Board, Technical Memo 15, Washington, DC. COE Ref # 457
- Shepard, F. P., 1950b, "Longshore current observations in southern California," *U.S. Army Corps of Engineers*, Beach Erosion Board, Technical Memo 13, Washington, DC. COE Ref # 456
- Shepard, F. P., 1950c, "Beach cycles in southern California," *U.S. Army Corps of Engineers*, Beach Erosion Board, Technical Memo 20, Washington, DC, 26 pp. COE Ref # 459
- Shepard, F. P., 1951, "Mass movements in submarine canyon heads," *Univ. of California, San Diego*, Scripps Inst. of Oceanography, Reference Series 51-26; and *Transactions, Amer. Geophysical Union*, v. 32, n. 3, p. 405-418. COE Ref # 461
- Shepard, F. P., 1952, "Transportation of sand into deep water," *Univ. of California, San Diego*, Scripps Inst. of Oceanography, Reference Series 52-17, La Jolla, CA. (Reprinted from Soc. of Economic Paleontologists and Mineralogists, Special Publ. No. 2, Nov. 1951, p. 53-65.) COE Ref # 464
- Shepard, F. P. and G. Einsele, 1962, "Sedimentation in San Diego Trough and contributing submarine canyons," *Sedimentology*, v. 1, p. 81-133. COE Ref # 466
- Shepard, F. P. and U. S. Grant, 1947, "Wave erosion along the Southern California coast,"

Geological Soc. of America, Bulletin. v. 58, p. 919-926. COE Ref # 455

- Shepard, F. P. and D. L. Inman. 1950, "Nearshore water circulation related to bottom topography and wave refraction." *Transactions, Amer. Geophysical Union*, v. 31, n. 2, p. 196-212. COE Ref # 458
- Shepard, F. P. and D. L. Inman, 1951a, "Sand movement on the shallow inter-canyon shelf at La Jolla, California," *U.S. Army Corps of Engineers*, Beach Erosion Board, Technical Memo 26, Washington, DC, 29 pp. COE Ref # 462
- Shepard, F. P. and D. L. Inman, 1951b, "Nearshore circulation," *Proceedings of 1st Conference on Coastal Engineering*, Ch. 5., p. 50-59, Long Beach, CA; and *Univ. of California., San Diego*, Scripps Inst. of Oceanography, Sub. Geol. Report 14, La Jolla, CA., 12 pp. COE Ref # 463
- Shepard, F. P. and E. C. LaFond, 1940, "Sand movements along the Scripps Institution pier," *Amer. Jour. Science*, v. 238, p. 272-285.
- Shepard, F. P. and D. B. Saylor, 1953, "Longshore and coastal currents at Scripps Institution Pier," *U.S. Army Corps of Engineers*, Beach Erosion Board, Bulletin v. 7, n. 1, Washington, DC. COE Ref # 465
- Shepard, F. P., G. G. Sullivan and F. J. Wood, 1981, "Greatly accelerated currents in submarine canyon head during optimum astronomical tide-producing conditions," *Shore and Beach*, v. 49, n. 1, p. 32-34. COE Ref # 476
- Simison, E. J., K. C. Leslie and R. M. Noble, 1978, "Potential shoreline impacts from proposed structures at Point Conception, California," *Coastal Zone '78, Symposium*, v. III, ASCE, NY, p. 1639-1652. COE Ref # 480
- Simons, Li and Assoc., 1984, "Effect of the Santa Margarita Project on beach nourishment, draft report," prepared for U.S. Dept. of the Interior, Bureau of Land Mgmt., *Simons, Li and Assoc., Inc.*, Fort Collins, CO, 100+ pp. COE Ref # 479
- Simons, R. S., 1977, "Seismicity of San Diego, 1934-1974," *Seismological Society of America Bulletin*, v. 67, p. 809-826.
- Simons, R. S., 1979, "Instrumental seismicity of the San Diego area: 1934-1978," in Abbott, P. L. and W. J. Elliott (eds.) *Earthquakes and Other Perils - San Diego Region*, Geological Society of America Annual Meeting Guidebook, p. 101-105.
- Skogsberg, T., 1936, "Hydrography of Monterey Bay, California thermal conditions, 1929-1933," *American Phil. Soc. Transactions*, v. 29, 152 pp.
- Smith, R. A. and R. J. Leffler, 1980, "Water level variations along California coast," *Jour. Waterway, Port, Coastal and Ocean Division*, v. 106, n. WW3, ASCE, NY, p. 335-348. COE Ref # 484
- Snodgrass, F. E., G. W. Groves, K. F. Hasselmann, G. R. Miller, W. H. Munk and W. H. Powers, 1966, "Propagation of ocean swell across the Pacific," *Philosophical*

Transactions of the Royal Society of London, Series A, n. 1103, v. 259, p. 431-497.

- Snodgrass, F. E., W. H. Munk and G. R. Miller, 1962. "Long period waves over California's continental borderland, Part I: Background Spectra." *Jour. Marine Research*, v. 20, n. 1, p. 3-30. COE Ref # 485
- Sonu, C. J., D. R. Patterson and M. T. Czerniak, 1978. "Littoral Transport Study, Naval Air Station, North Island, San Diego, CA., Final Report," prepared for Ferver Engineering Co., San Diego, CA., Contract TC-3206, *Tetra Tech*, Pasadena, CA., 38 pp. COE Ref # 519
- Spencer, D. G., 1985, "The Newport Beach groin field, Orange County, California," p. 151-201 in J. McGrath (ed), *California's Battered Coast*, Proc. Conference on Coastal Erosion, Calif. Coastal Commission, San Diego, February 6-8, 1985, 403 pp.
- Steele, K. E., 1982, "Accuracy of XERB measurements of wave directionality," *NDBO Engineering Note*.
- Steele, K. E., 1984, "Buoy measuring directional wave spectra deployed off southern California," *NOAA Data Buoy Center*, Technical Bulletin, v. 10, n. 2.
- Sternberg, R. W., N. C. Shi and J. D. Downing, 1984, "Field investigations of suspended sediment transport in the nearshore zone," *Proceedings, 19th Conf. on Coastal Engineering*, ASCE, NY, p. 1782-1798. COE Ref # 491
- Stevenson, R. E., 1961, "The oceanography of southern California mainland shelf," *Univ. of Southern California*, Allan Hancock Foundation, Los Angeles, CA. COE Ref # 493
- Strange, R. R. and N. E. Graham, 1983, "Wind and wave environment of the Santa Barbara Channel," unpublished report submitted to Woodward-Clyde Consultants.
- Straughan, D., 1981, "Inventory of the natural resources of sandy beaches in southern California," *Univ. of Southern California*, Allan Hancock Foundation, Technical Report 6, Los Angeles, CA., 447 pp. COE Ref # 495
- Sverdrup, H. U. and F. H. Fleming, 1941, "The waters off the coast of southern California, March to July 1937," *Univ. of California, San Diego*, Scripps Inst. of Oceanography, Bulletin 4, p. 271-378.
- Sverdrup, H. U. and W. H. Munk, 1947, "Empirical and theoretical relations between wind, sea and swell," *Transactions*, American Geophysical Union, v. 27, n. 6.
- Sverdrup, H. U. and W. H. Munk, 1947, "Wind, sea and swell: theory of relations for forecasting," *U.S. Hydrographic Office*, Publication No. 601, Technical Report No. 1.
- Sverdrup, H. U., M. W. Johnson and R. H. Fleming, 1942, "The Oceans: Their physics, chemistry and general biology," *Prentice-Hall*, New York, 1087 pp.
- Taylor, B. D., 1978, "Sediment management for southern California," *Coastal Zone '78, Symposium*, v. III, ASCE, NY, p. 2259-2264. COE Ref # 516

AD-A166 699

COAST OF CALIFORNIA STORM AND TIDAL WAVES STUDY
SOUTHERN CALIFORNIA COAST (U) ARMY ENGINEER DISTRICT
LOS ANGELES CA COASTAL RESOURCES BRANC
D L INMAN ET AL FEB 86 CCSTWS-86-1

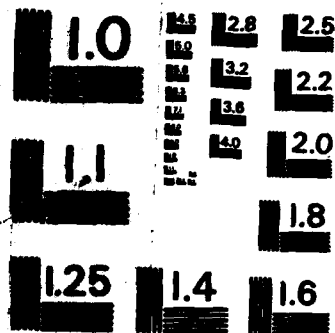
7/7

UNCLASSIFIED

F/G 8/3

NL





MICROCOPY RESOLUTION TEST CHART
NATIONAL BUREAU OF STANDARDS-1963-A

- Tetra Tech, 1976, "An investigation of coastal factors and processes relating to harbor siting at Ocean Beach," *Dept of the Air Force Space and Missile System Org. Headquarters*, 79 pp.
- Thompson, E. F., 1977, "Wave climate at selected locations along U.S. coasts," *U.S. Army Corps of Engineers, Coastal Engineering Research Center, Technical Report 77-1*, Vicksburg, MS. 364 pp. COE Ref # 521
- Thompson, E. F., 1980, "Energy spectra in shallow U.S. coastal waters," *U.S. Army Corps of Engineers, Coastal Engineering Research Center, Technical Report 80-2*, Vicksburg, MS, 149 pp. COE Ref # 522
- Thompson, E. F. and D. L. Harris, 1972, "A wave climatology for U.S. coastal waters," *U.S. Army Corps of Engineers, Coastal Engineering Research Center, Reprint 1-72*, Vicksburg, MS. COE Ref # 520
- Thornton, E. B. and R. T. Guza, 1981, "Longshore currents and bed shear stress," *Proceedings of the Conf. on Directional Wave Spectra Applications*, Sept. 14-16, 1981, Berkeley, CA., ASCE, NY, p. 147-164. COE Ref # 526
- Thornton, E. B. and R. T. Guza, 1983, "Transformation of wave height distribution," *Jour. of Geophysical Research*, v. 88, n. C10, p. 5925-5938. COE Ref # 527
- Thornton, E. G. and R. T. Guza, in press, "Surf zone longshore currents and random waves: models and field data," *Jour. Physical Oceanography*.
- Trask, P. D., 1952, "Source of beach sand at Santa Barbara, California, as indicated by mineral grain studies," *U.S. Army Corps of Engineers, Beach Erosion Board, Technical Memo 28*, Washington, DC., 24 pp. COE Ref # 532
- Trask, P. D., 1955, "Movement of sand around southern California promontories," *U.S. Army Corps of Engineers, Beach Erosion Board, Technical Memo 76*, Washington, DC, 66 pp. COE Ref # 534
- Tsuchiya, M., 1975, "California undercurrent in the southern California bight," *CalCOFI Report*, n. 18, p. 155-158.
- Tsuchiya, M., 1980, "Onshore Circulation in the southern California bight," *Deep-Sea Research*, v. 27a, p. 99-118.
- USACE CERC, 1977, "Shore Protection Manual, Vols. I and II," *U.S. Army Corps of Engineers, Coastal Engineering Research Center*, 3rd edition.
- USACE LAD, 1960a, "Beach Erosion Control Report on Cooperative Study of San Diego County, California - Appendix IV, Phase 2," *U.S. Army Corps of Engineers, Los Angeles District, Beach Erosion Control Report*, 60 pp. COE Ref # 697
- USACE LAD, 1960b, "Beach Erosion Control Report on Cooperative Study of Coast of Southern California, Point Conception to Mexican Boundary - Appendix VII, Interim Report," *U.S. Army Corps of Engineers, Los Angeles District, California*,

60+ pp. COE Ref # 725

USACE LAD, 1960c, "GDM for Rehabilitation of North Breakwater and Continuing Maintenance of Morro Bay Harbor, California," *U.S. Army Corps of Engineers*, Los Angeles District, CA., 100+ pp. COE Ref # 625

USACE LAD, 1961a, "Beach Erosion Control Report on the Coast of Southern California, Special Interim Report on Ventura Area - Appendix VII," *U.S. Army Corps of Engineers*, Los Angeles Division, Contract W-04-193-ENG-5196, CA., 77 pp. COE Ref # 640

USACE LAD, 1961b, "River and Harbor Improvement, Review Report for Navigation, Santa Barbara County, California," *U.S. Army Corps of Engineers*, Los Angeles District, CA., 100+ pp. COE Ref # 635

USACE LAD, 1962a, "Beach Erosion Control Report on Coast of Southern California, Cooperative Study of Orange County, California - Appendix V, Phase 2," *U.S. Army Corps of Engineers*, Los Angeles District, CA., 250+ pp. COE Ref # 674

USACE LAD, 1962b, "Beach Erosion Control Report on Cooperative Study of Coast of Southern California, Point Conception to Mexican Boundary - Appendix VII, Second Interim Report," *U.S. Army Corps of Engineers*, Los Angeles District 18+ pp. COE Ref # 737

USACE LAD, 1963, "Report on Cooperative Beach Erosion Investigation, Malibu, Santa Monica Area, California," prepared for the California Dept. of Water Resources and Dept. of Public Works, Div. of Highways, *U.S. Army Corps of Engineers*, Los Angeles District, CA., 100+ pp. COE Ref # 664

USACE LAD, 1964, "Beach Erosion Control Report on Cooperative Study of Coast of Southern California, Special Study of the City of San Diego - Appendix VII," *U.S. Army Corps of Engineers*, Los Angeles District, 53+ pp. COE Ref # 717

USACE LAD, 1966, "Beach Erosion Control Report on Cooperative Study of Coast of California, Shore Protection Improvement, Point Mugu to San Pedro Breakwater: GDM for Beach Protection and Widening from Redondo Beach Breakwater to Malaga Cove, Los Angeles County, California - Appendix II," *U.S. Army Corps of Engineers*, Los Angeles District, 50+ pp. COE Ref # 669

USACE LAD, 1967a, "Beach Erosion Control Report, GDM for beach stabilization, stage 2 construction in the segment from Santa Ana River to Newport Pier, Orange County, California," *U.S. Army Corps of Engineers*, Los Angeles District, 50 pp. COE Ref # 669

USACE LAD, 1967b, "Beach Erosion Control Report on Cooperative Study of Coast of Southern California, Cape San Martin to Mexican Border - Appendix VII, Final Report," *U.S. Army Corps of Engineers*, Los Angeles District, CA., 100+ pp. COE Ref # 726

USACE LAD, 1969a, "Beach Erosion Control Report, Shore Protection Improvement Design

- Memo for Stage 3 Construction, Beach Stabilization with Groins and Beach Fill at Newport Beach, Orange County, California," *U.S. Army Corps of Engineers*, Los Angeles District, CA., 50+ pp. COE Ref # 688
- USACE LAD, 1969b, "Navigation improvement, GDM No. 1 for Port San Luis, California," *U.S. Army Corps of Engineers*, Los Angeles District, CA., 100+ pp. COE Ref # 628
- USACE LAD, 1970, "Cooperative research and data collection program, coast of southern California, Three year report, 1967-1969," *U.S. Army Corps of Engineers*, Los Angeles District, CA., 21 pp. COE Ref # 729.
- USACE LAD, 1971, "Shoreline erosion at Tourmaline Surfing Park in the vicinity of False Point, San Diego, California, Reconnaissance Report," *U.S. Army Corps of Engineers*, Los Angeles District, CA., 27+ pp. COE Ref # 714
- USACE LAD, 1972, "Detailed project report for shore protection at Point Loma Light Station, San Diego County, California," prepared for the 11th Coast Guard District, *U.S. Army Corps of Engineers*, Los Angeles District, CA., 198 pp. COE Ref # 716
- USACE LAD, 1974, "Beach erosion control, DPR for small beach erosion project, Las Tunas Beach Park, Los Angeles County, California," *U.S. Army Corps of Engineers*, Los Angeles District, CA., 100+ pp. COE Ref # 662
- USACE LAD, 1976, "Navigation improvement supplement No. 1 to GDM No. 1 for Port San Luis, California (Main Report), *U.S. Army Corps of Engineers*, Los Angeles District, CA., 125+ pp. COE Ref # 632
- USACE LAD, 1978a, "Periodic Beach nourishment at Surfside-Sunset Beach, Orange County, California, Shore Protection Improvement Design Analysis for Stage 7 Construction," *U.S. Army Corps of Engineers*, Los Angeles District, CA., 40 pp. COE Ref # 685
- USACE LAD, 1978b, "Imperial Beach Erosion Control Project, San Diego County, California, GDM No. 4," *U.S. Army Corps of Engineers*, Los Angeles District, CA., 150+ pp. COE Ref # 654
- USACE LAD, 1979, "Ventura County, California, Survey Report for Beach Erosion Control - Main Report and Appendices," *U.S. Army Corps of Engineers*, Los Angeles District, CA., 150+ pp. COE Ref # 654
- USACE LAD, 1980a, "Ventura County, California," Survey Report for Beach Erosion Control, Main Report," *U.S. Army Corps of Engineers*, Los Angeles District, CA., 52 pp. COE Ref # 655
- USACE LAD, 1980b, "Ventura County Survey Report for Beach Erosion Control - Appendices," *U.S. Army Corps of Engineers*, Los Angeles District, CA., 210 pp. COE Ref # 656
- USACE LAD, 1980c, "San Diego County, Vicinity of Oceanside, California, Survey Report for Beach Erosion Control - Draft," *U.S. Army Corps of Engineers*, Los Angeles District, CA., 129+ pp. COE Ref # 706

- USACE LAD, 1984a, "Coastal Storm Damage, Winter 1983," *U.S. Army Corps of Engineers*, Los Angeles District: and State of California. Sacramento. CA., 51+ pp. COE Ref # 735
- USACE LAD, 1984b, "Geomorphology Framework Report. Dana Point to the Mexican Border," *U.S. Army Corps of Engineers*, Los Angeles District, CCSTWS 84-4, CA, 75+ pp. COE Ref # 736
- USACE SPD, 1971, "National Shoreline Study, California Regional Inventory," *U.S. Army Corps of Engineers*, South Pacific Division, San Francisco California; and *Dames & Moore*, San Francisco, CA., 200+ pp. COE Ref. 619
- USDOC NOAA, 1984, "Tide Tables 1985, high and low water predictions, west coast of north and south America including the Hawaiian Islands," *U.S. Dept. of Commerce*, Nat'l. Oceanic and Atmospheric Admin., National Ocean Service, Rockville, MD, 232 pp. COE Ref # 556
- USGS DOI, 1974, "Final environmental statement, proposed plan of development, Santa Ynez Unit, Santa Barbara Channel, off California," 3 volumes, *U.S. Geological Survey*.
- USN NOC, 1981, "Summary of synoptic meteorological observations (SSMO)," *U.S. Navy*, Naval Oceanography Commend Detachment, Asheville, NC., 405 pp. COE Ref # 563
- Univ. of California, San Diego, 1945a, "Longshore Currents," *Univ. of California, San Diego*, Scripps Inst. of Oceanography, Reference Series 45-11, Wave Project Report 40, La Jolla, CA., 18 pp. COE Ref # 412
- Univ. of California, San Diego, 1945b, "Effect of wave refraction on breaker heights - a comparison between computed and observed changes along the beach to the north of La Jolla," *Univ. of California, San Diego*, Scripps Inst. of Oceanography, Reference Series 45-12, Wave Project Report 38, La Jolla, CA., 27 pp. COE Ref # 413
- Univ. of California, San Diego, 1947, "A statistical study of wave conditions at five open sea localities along the California coast," *Univ. of California, San Diego* by *Scripps Inst. of Oceanography*, SIO Wave Report 68, 34 pp + figs. + appen. COE Ref # 418
- Univ. of California, San Diego, 1985, "El Nino," *Univ. of California, San Diego*, Scripps Inst. of Oceanography, Annual Report 1984, v. 18, n. 1, p. 4-7. COE Ref # 430
- Vesecky, J. R., S. V. Hsiao, C. C. Teagye, O. H. Shemdin and S. S. Pawke, 1980, "Radar observations of wave transformations in the vicinity of islands," *Jour. Geophysical Research*, v. 85, n. C9, p. 4977-4986.
- Viera, M., 1974, "Time-series study of sanding in Ventura Harbor, California," M.S. Thesis, *U.S. Navy Postgraduate School*, Monterey, CA. COE Ref # 547
- Waldorf, B. W. and R. E. Flick, 1983, "Beach profile changes at Del Mar, CA., May 1980 to January 1983, Data Report," *Univ. of California at San Diego*, Scripps Inst. of Oceanography, Reference Series 83-3, 23 pp. COE Ref # 567

- Waldorf, W. B., R. E. Flick and D. M. Hicks, 1983, "Beach sand level measurements, Oceanside and Carlsbad, California. December 1981 to February 1983, Data Report," *Univ. of California at San Diego*, Scripps Inst. of Oceanography. Reference Series 83-6, 37 pp. COE Ref # 568
- Walker, J. R., R. A. Nathan and R. J. Seymour, 1984, "Coastal Design Criteria in southern California," *Abstracts, 19th Int'l. Conference of Coastal Engineering*, Sept. 3-7, 1984. Houston, TX, ASCE, NY, p. 186-187; and *Moffatt & Nichol*, Long Beach, CA., Preprint, 17 pp. COE Ref # 569
- Weggel, J. R. and G. R. Clark, 1983, "Sediment budget calculations, Oceanside, California, Final Report," *U.S. Army Corps of Engineers*, Los Angeles District, Coastal Engineering Research Center, Misc. Paper 83-7, Vicksburg, MS., 55 pp. COE Ref # 574
- Whalin, R. W., D. R. Bucci and J. N. Strange, 1970, "A model study of wave run-up at San Diego, California," p. 427-452 in W. M. Adams (ed.), *Tsunamis of the Pacific*, East-West Center Press, Honolulu, Hawaii.
- White, T. E. and D. L. Inman, in press,a, "Application of tracer theory to NSTS Experiments," Ch. 6B in R. J. Seymour (ed.), *Nearshore Sediment Transport*, Plenum, N.Y.
- White, T. E. and D. L. Inman, in press,b, "Measuring longshore transport with tracers," Ch. 13 in R. J. Seymour (ed.) *Nearshore Sediment Transport*, Plenum, N.Y.
- Wickham, J. B., 1975, "Observations of the California countercurrent," *Jour. Marine Research*, v. 33, n. 3, p. 325-340.
- Wiegel, R. L., 1959, "Sand bypassing at Santa Barbara, California," *Jour. Waterways and Harbors Division*, v. 8, WW2, n. 1, ASCE, NY. COE Ref # 578
- Wiegel, R. L. and H. L. Kimberly, 1950, "Southern swell observed at Oceanside, California," *EOS, Transactions, Amer. Geophysical Union*, v. 31, n. 5, p. 717-722. COE Ref # 577
- Williams, R. G., R. W. Reeves, F. A. Godshall, S. W. Fehler, P. J. Pytlowany, G. R. Halliwell, K. C. Vierra, C. N. K. Mooers, M. D. Earle, K. Bush, 1981, "A climatology and oceanographic analysis of the California Pacific outer continental shelf region," Final report, prepared for U.S. Dept. of Interior, Bureau of Land Management, Center for Environmental Studies, U.S. Dept. of Commerce, NOAA, Environmental Data and Information Services, Washington, DC, 500+ pp. COE Ref # 548
- Wilson, B. W., J. Yuan, J. A. Hendrickson and H. Soot, 1968, "Wave and surge-action study for Los Angeles-Long Beach harbors, Volume 1, Final Report," prepared for U.S. Army Corps of Engineers, Los Angeles District, *Science Engineering Assoc.*, San Marino, CA., 362+ pp. COE Ref # 607
- Winant, C. D., 1979, "Coastal current observations," *Reviews of Geophysics and Space Physics*, v. 17, n. 1, p. 89-98. COE Ref # 594

- Winant, C. D., 1980, "Coastal circulation and wind induced currents," *Annual Review of Fluid Mechanics*, v. 12, p. 271-301.
- Winant, C. D., 1983, "Longshore coherence of currents on the southern California shelf during summer," *Jour. of Physical Oceanography*, v. 13, n. 1, p. 54-64. COE Ref # 597
- Winant, C. D. and D. G. Aubrey, 1976, "Stability and impulse response of empirical eigenfunctions." Chapter 77, *Proceedings 15th Coastal Engineering Conference*, Honolulu, Hawaii, ASCE NY, p. 1312-1325. COE Ref # 590
- Winant, C. D. and A. W. Bratkovich, 1981, "Temperature and currents on the southern California Shelf: a description of the variability," *Jour. of Physical Oceanography*, v. 11, n. 1, p. 71-86. COE Ref # 596
- Winant, C. D. and R. C. Holmes, 1983, "The longshore coherence of currents on the southern California shelf during winter, a data report," *Univ. of California, San Diego*, Scripps Inst. of Oceanography, Reference Series 83-22, 44 pp.; and *Jour. of Physical Oceanography*, v. 13, n. 1, p. 54-64. COE Ref # 598
- Winant, C. D., D. L. Inman and C. E. Nordstrom, 1975, "Description of seasonal beach changes using empirical eigenfunctions," *Jour. Geophysical Research*, v. 80, n. 15, p. 1979-1986.
- Winston, J. S., 1982, "The climate of spring 1982. A season of abnormally strong subtropical westerlies," *Monthly Weather Review*, v. 110, n. 11, p. 1729-1744.
- Winzler & Kelly, 1977, "A summary of knowledge of the central and northern California coastal zone and offshore areas," v. I-IV, prepared for Dept. of Interior, BLM Contract AA550-CT6-52; Winzler & Kelly, Consulting Engineers, Eureka, CA., 400+ pp. each part (4 parts).
- Wood, F. J., 1978, "The strategic role of perigean spring tides in nautical history and North American coastal flooding, 1635-1976," *U.S. Dept. of Commerce*, NOAA, Nat'l. Oceanic Survey, Washington, DC, 539 pp. COE Ref # 601
- Wood, F. J., 1981, "Astronomical and tidal analysis of unusual currents in a submarine canyon during proxigee-syzygy alignment," *Shore and Beach*, v. 49, n. 1, p. 35-36. COE Ref # 602
- Wooster, W. D. and J. H. Jones, 1970, "California undercurrent off northern Baja California," *Jour. Marine Research*, v. 28, n. 2, p. 235-250.
- Wooster, W. D. and J. L. Reid, Jr., 1963, "Eastern boundary currents," in *The Sea*, vol. 2, John Wiley and Sons, N.Y., p. 253-276.
- Wright, L. D., R. T. Guza and A. D. Short, 1982, "Surf zone dynamics on a high energy dissipative beach," *Marine Geology*, v. 45, p. 41-62.
- Wu, C-S, E. B. Thornton and R. T. Guza, 1985, "Waves and longshore currents: comparison of a numerical model with field data," *Jour. Geophysical Research*, v. 90, n. C3, p.

4951-4958.

- Wunsch. C., 1972, "Bermuda sea level in relation to tides, weather and baroclinic fluctuations," *Rev. Geophysical and Space Physics*, v. 10, n. 1, p. 1-49.
- Wyllie, J. G., 1966, "Geostrophic flow of the California current at the surface and at 200 meters," *CalCOFI*, Atlas No. 4. 228 pp.
- Zampol. J. A., in press, "Discrete measurements of suspended sediment," Ch. 11B in R. J. Seymour (ed.) *Nearshore Sediment Transport*, Plenum, N.Y.
- Zeller, R. P., 1962, "A general reconnaissance of coastal dunes of California," *U.S. Army Corps of Engineers*, Beach Erosion Board, Misc. Paper 1-62, Washington, DC, 38 pp. COE Ref # 604
- Zetler, B. D., 1982, "State of the art in tide predictions," *Proc. 18th Conference on Coastal Engineering*, American Soc. of Civil Engineering, v. 1, p. 192-202.
- Zetler, B. D. and R. E. Flick, 1985a, "Predicted extreme high tides for mixed tide regions," submitted to *Jour. of Physical Oceanography*, 9 pp. COE Ref # 605
- Zetler, B. D. and R. E. Flick, 1985b, "Predicted extreme high tides for California, 1983-2000," *Jour. Waterways, Port, Coastal, Ocean Division*, ASCE, NY, 14 pp. (in press). COE Ref # 606
- Zingg, A. W., 1953, "Wind-tunnel studies of the movement of sedimentary material," *Proceedings, 5th Hydraulics Conference*, State Univ. Iowa, Studies in Engineering, Bulletin 34, p. 111-135.

END

DTIC

5-86